Author:
Hazell, Georgina Grace Joan

Title:
Deorphanising G protein-coupled receptors : the search for fast steroid receptors

Deorphanising G Protein-Coupled Receptors: The Search For Fast Steroid Receptors

University of BRISTOL

Georgina Grace Joan Hazell

A dissertation submitted to the University of Bristol in accordance with the requirements for the degree of Doctor of Philosophy in the Faculty of Medicine and Dentistry, School of Clinical Sciences.
September 2011.

Word count: 79,886

Abstract

G protein coupled receptors (GPCRs) are the largest family of transmembrane receptors in the genome and are activated by a multitude of ligands including neuropeptides, hormones and sensory signals. The paraventricular nucleus (PVN) and supraoptic nucleus (SON) of the hypothalamus are important mediators in homeostatic control. Many modulators of PVN/SON activity, including neurotransmitters and hormones act via GPCRs - in fact over 100 non-chemosensory GPCRs have been detected in either the PVN or SON. The introduction to this thesis begins with a comprehensive summary of GPCR expression within the PVN/SON, with a critique of the detection techniques used within the literature. Also discussed are some aspects of the regulation and known roles of GPCRs in the PVN/SON, as well the possible functional significance of orphan GPCRs. Particular interest is paid to the recently 'deorphanised' G protein-coupled oestrogen (E2) receptor, GPER, which is the first receptor to be acknowledged as a steroid binding GPCR (although there are conflicting studies regarding its affinity for E2) and is expressed in the PVN and SON. Steroids are known to have fast non-genomic effects that are thought to be mediated in-part by membrane-associated forms of the traditional steroid receptors (members of a family of transcription factors). However, the possible discovery of a fast E2 GPCR has raised speculation regarding the existence of other steroid binding GPCRs. Thus the experimental Chapters were undertaken to explore the concept of fast steroid receptors, with particular emphasis on their possible roles in neuroendocrine systems. Firstly, the distribution of the putative E2 receptor was investigated to give further insight into its possible *in vivo* roles. In the rodent, high levels of GPER gene and protein expression were detected in the oxytocin and vasopressin neurones in the PVN and SON, the anterior and intermediate lobe of the pituitary, adrenal medulla and renal medulla and pelvis, suggesting roles for GPER in multiple functions including hormone release. To clarify the controversy surrounding GPER as an E2 receptor, we investigated GPER function *in vitro* using a series of cell signalling assays. However, E2 did not stimulate GPER-mediated signalling, suggesting that either GPER remains an orphan GPCR, or the cell lines used in this study lacked a vital component for E2 activation of GPER. As the rapid effects of glucocorticoid have been reported in numerous brain regions (including the PVN and SON), endocrine, and other tissues, the second part of this thesis focussed on the search for a possible fast glucocorticoid receptor. We compared the tissue distribution gene expression profiles of approximately 125 orphan GPCRs common to human and rodent with tissues that are known to exhibit fast effects of steroids (e.g., hippocampus, PVN, SON, thymus, kidney, etc.). Of the 125 orphans, 3 GPCRs (GPR108, GPR146, and TMEM87B) had distribution profiles that closely matched the regions/tissues of interest. These orphans were tested for glucocorticoid activation using a universal deorphanisation assay. However, the identity of the fast glucocorticoid receptor remains unknown, as none of the candidate orphan GPCRs responded to glucocorticoids.

Dedication and Acknowledgements

Firstly, I would like to thank my supervisor Dr Stephen Lolait who invested many hours in my tuition over the last four years. His teachings have provided me with excellent foundations for a future in science, for which I am extremely grateful. I would also like to thank my co-supervisor Dr Anne-Marie O'Carroll who often praised 'my enthusiasm for science,' and whose coffee breaks offered light relief from some of the pressures that one experiences during a PhD.

I would also like to thank the members of the Lolait/O'Carroll/Murphy groups of which I shared lab space with, and who supplied endless support (and entertainment), namely George Pope, Emma Roberts, Lesley Stewart, Mike Greenwood, and especially James Roper – who taught me so much.

Thank you also to all the PhD students. I enjoyed all of our chats in the write-up room, our Friday night drinks, and various house parties. I would particularly like to thank Andrew Collins for getting as ridiculously excited about Fridays as me and Jason Pont for endless statistical/IN CELL advice. I would like to thank Professor Craig McArdle also for his guidance and help with the IN CELL. In addition, I am so grateful to Allison Fulford, Karen Dawe and David Hodson, who encouraged me to do a PhD in the first place, and have been supportive ever since.

Greatest thanks obviously go to my parents John and Penny. Dad, you taught me that you never get anything unless you work extremely hard for it. Mum, you thought I could do anything I wanted. Together you provided me with unconditional love and support throughout my education. Thank you also to all of my large Hazell/Thynne family, especially my big sisters Diane, and Julia, their partners and children, and to my little bro Steve. Special thanks also to Auntie Sarah and Uncle Tom – you've always been so proud. And a huge thank you to my partner James for his constant encouragement and assistance outside of work – I don't know what I would have done without you.

To my 33 Longmead Avenue housemates, Amy Colman, Rachael Coulson and Dave McFetridge – thank you for all of the support and fun times. Particularly Amy - I couldn't ask for a more wonderful friend. Thank you to Ellie Waite and Rosie Lees and the 'Up and Running' runners for keeping me sane. I would also like to acknowledge the main members of the Glastonbury crew, James, Robbie, Kui and Dave, and also Sophie and Chris, who made my annual holiday as hilarious and eventful as possible.

And finally, thank you to Professor Stafford Lightman and Dr Carmine Pariante, who took the time to read my thesis and examine me. You made my 'viva experience' unexpectedly enjoyable, and this has left me with extremely fond memories of my last day as a PhD student.

Authors' Declaration

"I declare that the work in this dissertation was carried out in accordance with the requirements of the University's Regulations and Code of Practice for Research Degree Programmes and that it has not been submitted for any other academic award. Except where indicated by specific reference in the text, the work is original. Any views expressed in the dissertation are those of the author.

SIGNED: ..... DATE: 7/2/12

Contents

Tables and Figures

Chapter 1

Tables

Figures

Chapter 2

Figures

Chapter 3

Tables

Figures

Chapter 4

Tables

Figures

Chapter 5

Tables

Figures

Chapter 6

Tables

Figures

Chapter 7

Figure

Abbreviations

αMEM	Minimum Essential Media (MEM), α medium 1 x
αMSH	α-melanocyte stimulating hormone
A	Adenine
ACTH	Adrenocorticotrophin releasing hormone
AFU	Arbitrary fluorescence units
AG1478	N-(3-chlorophenyl)-6,7-dimethoxy-4-quinazolinamine (EGFR inhibitor)
ALD	Aldosterone
AMP	Ampicillin
AR	Androgen receptor
ARG	Autoradiography
ATP	Adenosine 5'-triphosphate
β-Gal	Beta-galactosidase
BES	N,N-Bis(2-hydroxyethyl)-2-aminoethanesulfonic acid, N,N-Bis(2 hydroxyethyl)taurine
bp	Base pairs
BSA	Bovine serum albumin
C	Cytosine
cAMP	Cyclic adenosine monophosphate
c-Fos	Cellular proto-oncogene
CHO	Chinese hamster ovary cells
C/I	Chloroform/isoamyl alcohol
CNS	Central nervous system
CORT	Cortisol in humans, corticosterone in rodents
COS-7	Transformed kidney fibroblast cells of the African green monkey
cpm	Counts per minute
CREB	cAMP response element binding protein
CRF	Corticotrophin releasing factor
cpm	Counts per minute
DAB	3,3'-diaminobenzidine
DAPI	4',6-diamidino-2-phenylindole
DBD	DNS binding domain
DEPC	Diethylpyrocarbonate
DMEM	Dulbecco's modified Eagle's medium
DMEM/F12	Dulbecco's Modified Eagle's Medium: Nutrient Mixture F-12
dNTPs	Deoxyribonucleotides
DMSO	Dimethyl sulphoxide
DTT	Dithiothreitol
E2	Oestrogen or 17β-oestradiol
E2-BSA	Oestrogen covalently linked to BSA
E.coli	*Escherichia coli.*
EC50	Half-maximal effector concentration
EL	Extracellular loop
EDTA	Ethylenediaminetetraacetic acid
EGF	Epidermal growth factor
EGFR	Epidermal growth factor receptor
ERα	Oestrogen receptor alpha
ERβ	Oestrogen receptor beta
ERE	Oestrogen response elements
ERK	Extracellular signal-regulated kinases
EST	Expression sequence tag

FCS	Foetal calf serum
G	Guanine
G-1	GPER agonist
G-15	GPER antagonist
G418	Geneticin®
GHRH	Growth hormone-releasing hormone
GnRH	Gonadotrophin-releasing hormone
GPCR	G protein-coupled receptor
GPER	G protein-coupled oestrogen receptor 1
GR	Glucocorticoid receptor
GRK	GPCR kinase
GTP	Guanosine-5'-triphosphate
HA tag	Influenza hemagglutinin epitope tag
HEK293	Human embryonic kidney 293 cells
HeLa	Human cervical adenocarcinoma cells
hnRNA	Heteronuclear RNA
HNS	Hypothalamo-neurohypophsial system
HPA	Hypothalamic-pituitary-adrenal axis
HRP	Horseradish peroxidase
Hygro	Hygromycin B
IgG	Immunoglobulin G
IP_3	Inositol trisphosphate
ir	Immunoreactivity
IHC	Immunohistochemistry
ISHH	*In situ* hybridization histochemistry
KO	Knock out (mouse)
LB	Lysogeny broth
LBD	Ligand binding domain
M	Molar
MAPK	Mitogen-activated protein kinase
mEST	Mouse oestrogen sulphotransferase
min	Minute(s)
miR	microRNA
MR	Mineralocorticoid receptor
mPVN	Magnocellular portion of the PVN
mRNA	Messenger ribonucleic acid
ms	Millisecond(s)
NaCl	Sodium Chloride
NMDA	N-methyl-D-aspartate
NPY	Neuropeptide Y
NR	Nuclear receptor
OT	Oxytocin
PBS	Phosphate-buffered saline
P/C/I	Phenol/chloroform/isoamyl alcohol
PCR	Polymerase chain reaction
PFA	Paraformaldehyde
PIP_2	Phosphatidylinositol 4,5-bisphosphate
PKA	Protein kinase A
PKC	Protein kinase C
PLC	Phospholipase C
ppERK	Phosphorylated extracellular signal-regulated kinases
POMC	Proopiomelanocortin
PR	Progesterone receptor
P/S	Penicillin and Streptomycin antibiotics

PVN	Paraventricular nucleus of the hypothalamus
pPVN	Parvocellular portion of the PVN
Q	L-glutamate
RNA	Ribonucleic acid
RNase	Ribonucleases
rpm	Rotations per minute
^{35}S-UTP	^{35}S labelled uridine triphosphate
s	Second(s)
SCN	Suprachiasmatic nucleus
SDS	Sodium dodecyl sulphate
shRNA	Small hairpin RNA
siRNA	Small interfering RNA
SKBR3	Human breast carcinoma cells
SON	Supraoptic nucleus of the hypothalamus
T	Thymine
TE	Tris-EDTA
Tm	Melting temperature
TM	Transmembrane domain
TRH	Thyrotropin-releasing hormone
TX-100	Triton-X 100/ t-Octylphenoxypolyethoxyethanol
U	Uracil
VIP	Vasoactive intestinal peptide
VP	(Arginine) Vasopressin
WS-E2	Water soluble oestrogen
xg	Times gravity
X-Gal	5-bromo-4-chloro-3-indolyl-β-D-galactopyranoside

Note: Abbreviations for non-chemosensory GPCRs are the standard nomenclature for these receptors as advocated by NC-IUPHAR (the International Union of Basic and Clinical Pharmacology Committee on Receptor Nomenclature and Drug Classification). Please note that generic family names are used rather than the individual receptor gene names given to each species (e.g., as in the case of the oestrogen receptor GPER (family name), it has been assigned the human gene name GPER, rat gene name Gper, and the mouse gene name Gpr30). For simplicity, nuclear receptors will be referred to once by their official names agreed by NC-IUPHAR and the Nuclear Receptor Nomenclature Committee, 1999, and from then on by their trivial names (e.g., oestrogen receptor alpha's official nomenclature is NR3A1 and trivial name is ERα). Abbreviations for the endogenous ligands of the non-chemosensory GPCRs and steroid receptors will be in keeping with the family names or trivial names, respectively.

Chapter 1: General Introduction

The hypothalamo-neurohypophseal system (HNS) responds to dehydration by increasing vasopressin (VP) and oxytocin (OT) gene transcription and translation, and releasing large amounts of VP and OT into the systemic circulation. Similarly, acute and chronic stress, pregnancy, and lactation are all associated with phenotypic changes in the paraventricular (PVN) and/or supraoptic (SON) nuclei of the hypothalamus that include elevations in VP, OT and/or corticotropin-releasing factor (CRF) gene expression (Aguilera *et al.*, 2008; Burbach *et al.*, 2001). Alterations in the pattern and/or level of modulating inputs (e.g., receptor-driven signals) that impinge on the PVN and SON have important functional implications in the control of the HNS and the hypothalamic-pituitary-adrenal (HPA) axis response to stress. The activity of such inputs may drive changes in the PVN/SON VP and OT signature associated with a number of neuroendocrinological disturbances (Swaab, 1998), and contribute to the dysregulation of the HPA axis implicated in many conditions including the classical psychosomatic disorders, cardiovascular disease, diabetes and affective disorders such as depression. Receptor function in the PVN/SON may also be altered in immunologically-related disturbances such as immunosuppression and autoimmune, allergic, and inflammatory states (Charmandari *et al.*, 2005; Raison and Miller, 2003).

By virtue of their expression in the PVN and SON, many receptors are key targets for regulating hypothalamic-HNS and -HPA axis activity. There are four major classes of receptors in the central nervous system (CNS) – (1) the ionotropic receptors such as the excitatory glutamate (e.g., N-methyl-D-aspartate (NMDA)) or inhibitory $GABA_A$ receptors that create a membrane pore to allow the flow of ions, and have a very rapid response time; (2) receptor tyrosine kinases such as tyrosine kinase receptor type B (TrkB) and the epidermal growth factor receptor (EGFR), which upon stimulation activate intracellular signalling networks like the extracellular signal-regulated kinase (ERK) pathway; (3) nuclear receptors including glucocorticoid, sex steroid and thyroid hormone receptors that regulate transcriptional activation; and (4) G protein-coupled receptors (GPCRs), or seven transmembrane (TM) receptors, occasionally termed heptahelical or 'serpentine' receptors. GPCRs constitute the largest superfamily of transmembrane signalling molecules, estimated to comprise about 1,900 members (not including pseudogenes) in the rat and mouse genomes, and at least 800 members in the human genome (Gloriam *et al.*, 2007). The proportion of one-to-one GPCR orthologues is approximately 60% between rats and humans, primarily due to divergence in chemosensory receptors that are activated by sensory signals of external origin such as odors, pheromones or tastes. Olfactory receptors make up about 60% of all GPCRs in the rat and mouse genome and 50% in the human genome (Gloriam *et al.*, 2007). Most other GPCRs are activated by a diverse array of endogenous,

extracellular (and perhaps intracellular) signals that include photons, biogenic amines, neuropeptides, amino acids, ions, hormones, chemokines, lipid-derived mediators and proteases. Upon ligand binding, GPCRs primarily transduce these signals via the heterotrimeric G proteins into rapid intracellular responses that regulate cell function (e.g., increases in protein kinase C (PKC) and/or protein kinase A (PKA) activity, intracellular calcium and cyclic adenosine monophosphate (cAMP)). It is estimated that 80% of all known hormones and neurotransmitters activate cellular signal transduction mechanisms via GPCRs (Birnbaumer *et al.*, 1990), and a substantial portion (estimates vary between 30 and 60%) of current pharmaceutical agents directly or indirectly act on these receptors (Hopkins and Groom, 2002; Lundstrom, 2006) - angiotensin II and aminergic (adrenoceptor, dopamine, 5-hydroxytryptamine (5-HT)) receptor subtypes feature as prominent drug targets (Insel *et al.*, 2007). There are still 120-130 non-chemosensory 'orphan' GPCRs for which the corresponding ligands have not yet been identified (Gloriam *et al.*, 2007; Harmar *et al.*, 2009).

The current Chapter will highlight efforts to examine GPCR expression and regulation in the rat PVN and SON by receptor autoradiography (ARG), immunohistochemistry (IHC) and *in situ* hybridization histochemistry (ISHH) methods, in conjunction with more recent transcriptomic approaches (e.g., DNA microarrays) to present an overall estimate of the GPCR repertoire expressed in the PVN and SON. Data has been collated on all of the known non-chemosensory GPCRs documented in the on-line International Union of Basic and Clinical Pharmacology Committee on Receptor Nomenclature and Drug Classification database (NC-IUPHAR; http://www.iuphar-db.org/) (Harmar *et al.*, 2009) including orphan GPCRs. These data will be discussed in the context of the regulation and function (and possible redundancy) of GPCRs in the PVN and SON as revealed by current pharmacological/physiological approaches in rats, the species in which the vast majority of studies on the HNS and HPA axis have been conducted. With respect to GPCR localisation in the PVN and SON efforts have been made to cite as many of the original reference sources as possible - apologies are made in advance if some citations have inadvertently been omitted. The architecture of the PVN/SON, GPCR structure/function studies, and the function of many neurotransmitters/neurohormones in the PVN and/or SON have been extensively reviewed and we shall refer to these papers throughout. The GPCR subfamily nomenclature will be used thoughout this Chapter (e.g., 5-HT_{1A}; rather than rat gene name (e.g., Htr1a)) as per NC-IUPHAR recommendations (Harmar *et al.*, 2009).

1.1 Anatomy and function of the rat PVN and SON

The hypothalamus is essential for maintaining homeostatic equilibrium, integrating signals from other brain regions to regulate an assortment of functions including temperature regulation, appetite and

fertility. Within the hypothalamus the PVN and SON are two of the most exhaustively studied nuclei and are fundamental in the control of fluid homeostasis, lactation, cardiovascular regulation, feeding behaviour, nociception, behaviour and the response to stress. The PVN is located either side of the third ventricle, and can be subdivided into five parvocellular (pPVN) (periventricular, anterior, medial, dorsal and lateral parts) and three magnocellular (mPVN) (anterior, medial and posterior parts) divisions (Simmons and Swanson, 2009; Swanson and Sawchenko, 1983). The main neuronal populations in the mPVN and pPVN subdivisions are intermingled with interneurons and supporting cells such as glia. The SON straddles the lateral border of the optic chiasm and contains a 'homogeneous' population of magnocellular neurons (Poulain and Wakerley, 1982). The large magnocellular neurons in the PVN and SON secrete mainly VP and OT as part of the HNS whereas the smaller parvocellular neurons elaborate primarily CRF, VP and OT as part of the HPA axis and/or regulate autonomic activity. Elegant, detailed studies on the mapping of the spatial organization of major neuroendocrine and non-neuroendocrine neurons in the rat PVN have revealed that although neuroendocrine neuron clusters display a unique distribution pattern, there is extensive overlap between different phenotypes (Simmons and Swanson, 2009). For instance, there is some intermixing of magnocellular and parvocellular neurons particularly at the mPVN/pPVN border (Simmons and Swanson, 2009), and isolated magnocellular cells in the pPVN have been noted (Engelmann *et al.*, 2004). Moreover, there is evidence that the HNS and HPA axis may functionally overlap but the extent of this interaction is not fully understood (Engelmann *et al.*, 2004).

Magnocellular neurons of both the PVN and SON project via the internal zone of the median eminence to the posterior pituitary, and upon appropriate stimulation secrete VP and/or OT into the peripheral blood. Magnocellular VP is released mainly in response to dehydration, hypovolemia and hypotension, while magnocellular OT is primarily involved in the milk ejection reflex during lactation, and uterine contraction at the later stages of parturition (Gimpl and Fahrenholz, 2001; Poulain and Wakerley, 1982; Renaud and Bourque, 1991; Stricker and Sved, 2002). Parvocellular neurons project from the periventricular, anterior, and medial (dorsal portion) parts of the PVN to the external zone of the median eminence, and release their peptides into the hypophysial portal system, a series of blood vessels that bathe the anterior lobe of the pituitary. In response to stressful stimuli, CRF and VP from the dorsomedial pPVN stimulate the release of adrenocorticotrophin releasing hormone (ACTH) from the corticotrope cells of the anterior pituitary, which in turn induces the secretion of cortisol (corticosterone (CORT) in rodents) from the adrenal glands. CORT exerts a negative feedback action on the pituitary, PVN and other brain regions such as the hippocampus to restrict the dramatic initial release of ACTH and CORT (Antoni, 1988). OT can either potentiate or inhibit ACTH and/or CORT responses by binding to the pituitary VP V_{1B} receptor or by an action on central OT receptors, respectively (Roper *et al.*, 2011; Windle *et al.*, 2006). In addition, OT stimulates the release of

luteinising hormone from gonadotropes, and prolactin from lactotropes in the anterior pituitary (Gimpl and Fahrenholz, 2001). Other parvocellular neuroendocrine cells include those that express growth hormone-releasing hormone (GHRH), somatostatin, dopamine and thyrotropin-releasing hormone (TRH) (Simmons and Swanson, 2009). Parvocellular neurons from the dorsal, lateral, and medial (ventral portion) regions of the PVN also project to other regions of the brain, in particular to the brain stem and spinal cord (Swanson and Sawchenko, 1983). Here the parvocellular neurotransmitters/neuropeptides modulate somatomotor-behavioural and autonomic circuitry; for example, CRF axons terminate in regions such as the locus coeruleus, where the peptide is reported to interact with noradrenergic neurons (Dunn *et al.*, 2004; Valentino *et al.*, 1992), VP neurons project to autonomic nuclei in the brainstem and spinal cord, and are involved in cardiovascular control (Benarroch, 2005; Pyner, 2009; Sofroniew, 1980), while parvocellular OT released in the hindbrain/spinal cord influences nociception, gastric reflexes, cardiovascular responses, yawning and penile erection (Gimpl and Fahrenholz, 2001; Kita *et al.*, 2006; Ludwig and Leng 2006; Pyner, 2009). Moreover, dendritically released neuropeptides from magnocellular perikarya may act locally or diffuse away from the PVN/SON, contributing to the central OT and VP pool (Ludwig and Leng 2006). It has been proposed that centrally released OT and VP from dendrites and/or parvocellular projections modulates behaviour e.g., maternal and affiliative behaviour, sexual behaviour, and social recognition (Guastella *et al.*, 2010; Ludwig and Leng 2006, Strom and Tecott, 2005).

The PVN and SON are subject to regulation by many brain regions including the hindbrain/brainstem, limbic regions, lamina terminalis system, and other hypothalamic nuclei, and also from chemicals/hormones such as oestrogen (E2) and CORT that can pass the blood brain barrier (Cunningham and Sawchenko, 1991; Hatton, 1990; Michael, 1965; Sladek, 2000; Swanson and Sawchenko, 1983). As such the PVN/SON is modulated by a considerable array of neurotransmitters and hormones. For example, neurons of the PVN/SON are immersed in glutamatergic and GABAergic terminals that provide major stimulatory and inhibitory tone, respectively. Input from the hindbrain to the PVN and SON includes catecholamine and serotonergic afferents from the ventral medulla, and catecholamine projections from the nucleus of the solitary tract and locus coeruleus, all of which may co-express additional neurotransmitters or neuropeptides (Sladek, 2000; Swanson and Sawchenko, 1983; Ulrich-Lai and Herman, 2009). The PVN and SON also receive efferents from the subfornical organ, and those projecting to the PVN have been shown to contain angiotensin II (Ferguson, 2009), while neuropeptide Y (NPY)- and proopiomelanocortin (POMC)-expressing neurons projecting to the PVN from the arcuate nucleus (Sawchenko, 1998) are essential for the complex control of feeding behaviour (Schwartz *et al.*, 2000). Further, parvocellular and magnocellular neurons of the PVN/SON coexpress many neuroactive substances (e.g., CRF, galanin, cholecystokinin, enkephalin, and vasoactive intestinal peptide (VIP) that may have a paracrine/autocrine action on PVN/SON neurons

(Bundzikova *et al.*, 2008, Ceccatelli *et al.*, 1989). Importantly, in response to various physiological conditions the PVN and SON exhibit a considerable degree of morphological (e.g., glial cell remodeling (Hatton, 2002)) and functional plasticity. This can manifest itself by changes in neuronal excitability (Flak *et al.*, 2009; Tasker *et al.*, 2002) that may be accompanied by enhanced co-expression of certain neuropeptides (e.g., VP in CRF pPVN neurons after stress exposure (Aguilera *et al.*, 2008; Bundzikova *et al.*, 2008) and/or altered neuro-transmitter/peptide release (Burbach *et al.*, 2001; Ludwig, 2002).

The defined cytoarchitecture of the rat PVN and SON and the features of the neurons contained within and projecting from these nuclei (e.g., large size of magnocellular cells; accessibility to experimental manipulation with reference to the SON in particular; physiologically defined outputs) make these brain regions excellent models to investigate GPCR function. As shown in Figure 1.1, GPCRs can modulate PVN/SON activity at a number of levels.

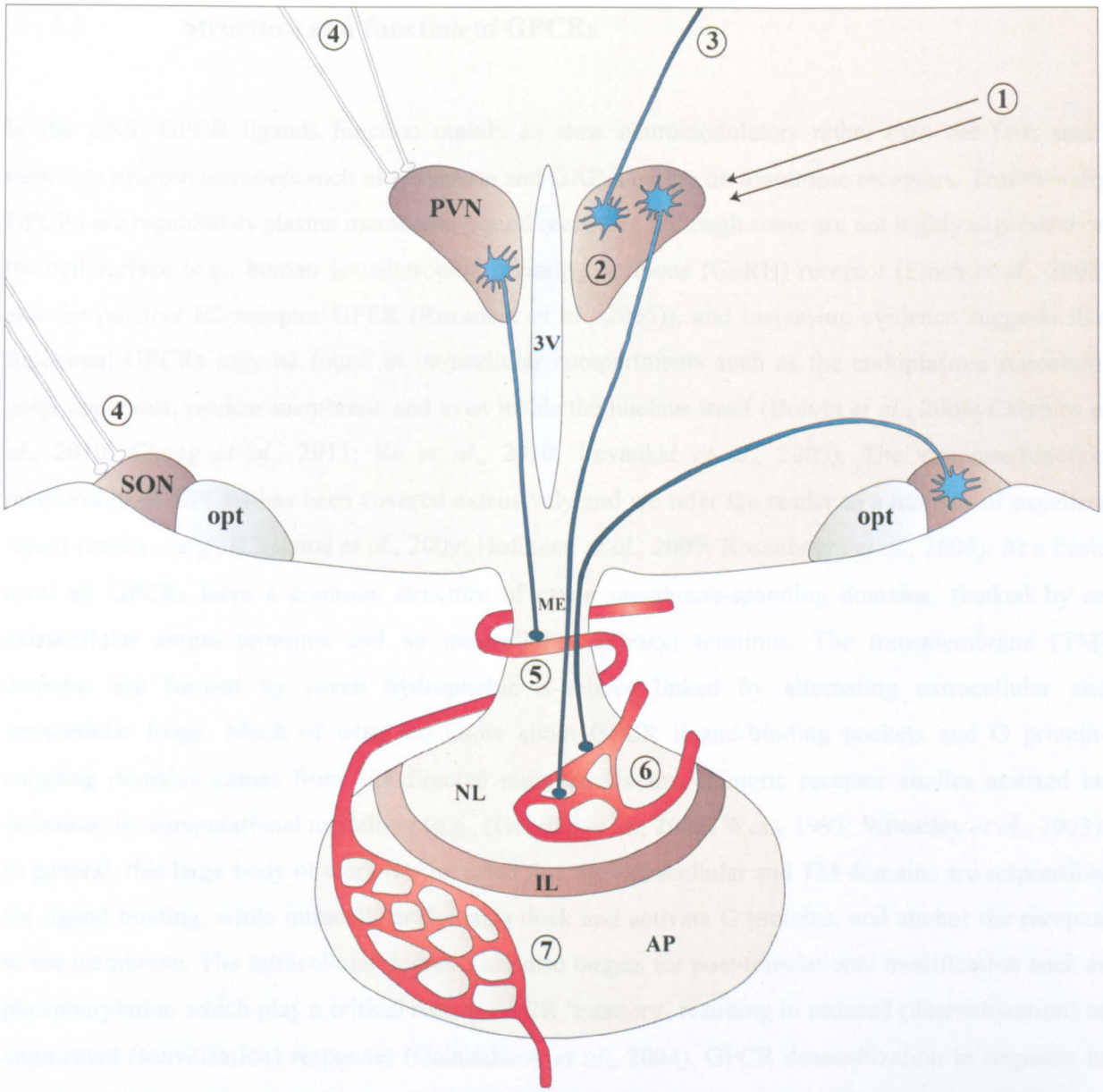

Figure 1.1. Schematic diagram representing the possible roles of GPCRs in modulating PVN/SON activity.

1) Hormonal signals from peripheral blood may regulate PVN/SON activity directly (substances such as neuropeptide Y and orexin A (Kastin and Akerstrom, 1999a,b) that can pass through the blood brain barrier activating GPCRs), or indirectly (e.g., activation of GPCRs in the circumventricular organs by humoral factors like cytokines, or neuropeptides such as angiotensin II (Ganong, 2000) can regulate neurotransmitter/neuropeptide-expressing neurons projecting to the PVN/SON). 2) Local release of neurotransmitters from within PVN/SON (e.g., from dendrites) that act on GPCRs may have potential autocrine/paracrine effects on PVN/SON neurons e.g., priming of OT neurons by dendritically released OT in parturition/lactation (Ludwig and Leng, 2006). In addition, neurotransmitters (e.g., melatonin, gonadotrophin releasing hormone (Veening and Barendregt, 2010)) released from alternate (ventricular bordering) brain regions may reach the PVN via the ventricular system, and act to regulate neuronal activity via GPCRs. Similarly, dendritically released OT and VP from PVN neurons may permeate into the cerebrospinal fluid of the third ventricle and diffuse to, and act on, GPCRs in distant brain regions (Veening and Barendregt, 2010). 3) GPCRs may modulate the activity of neurons that project away from the PVN/SON (e.g., parvocellular PVN projections to the hindbrain), acting directly on perikarya within the PVN/SON and/or at the nerve terminals in different brain regions. 4) GPCRs may be present on/or near the nerve terminals of interneurons (e.g., GABAergic and glutamatergic) within the PVN/SON and/or neurons originating from other regions (e.g., alternate areas of the hypothalamus, hippocampus, amygdala, brainstem), that synapse with PVN/SON soma, possibly regulating postsynaptic neurotransmitter release or acting directly to stimulate/inhibit PVN/SON neuronal activity. 5) GPCRs present in the external zone of the median eminence could modulate the secretion of CRF/OT/VP from parvocellular neurons into the portal blood stream, and GPCRs in the pituitary could have a direct effect on hormone release e.g., regulate VP/OT release from the neural lobe (6) and ACTH (amongst other neuroendocrine hormones) from the anterior lobe (7). PVN, paraventricular nucleus; SON, supraoptic nucleus; ME, median eminence; NL, neural lobe; IL, intermediate lobe; AP, anterior pituitary; opt, optic tract; 3V, third ventricle.

1.2 Structure and function of GPCRs

In the CNS, GPCR ligands function mainly as slow neuromodulators rather than the fast, small molecule neurotransmitters such as glutamate and GABA acting on ionotropic receptors. Traditionally GPCRs are regarded as plasma membrane-bound receptors, although some are not highly expressed on the cell surface (e.g., human gonadotrophin releasing hormone (GnRH) receptor (Finch *et al.*, 2008) and the putative E2 receptor GPER (Revankar *et al.*, 2005)), and increasing evidence suggests that functional GPCRs may be found in intracellular compartments such as the endoplasmic reticulum, golgi apparatus, nuclear membrane and even inside the nucleus itself (Boivin *et al.*, 2008; Calebiro *et al.*, 2010; Cheng *et al.*, 2011; Re *et al.*, 2010; Revankar *et al.*, 2005). The structure/function relationship of GPCRs has been covered extensively and we refer the reader to a number of excellent recent reviews (e.g., (Costanzi *et al.*, 2009; Hofmann *et al.*, 2009; Rosenbaum *et al.*, 2009). At a basic level all GPCRs have a common structure of seven membrane-spanning domains, flanked by an extracellular amino terminus and an intracellular carboxyl terminus. The transmembrane (TM) domains are formed by seven hydrophobic α-helices linked by alternating extracellular and intracellular loops. Much of what we know about GPCR ligand-binding pockets and G protein-coupling domains comes from site-directed mutagenesis and chimeric receptor studies assisted on occasions by computational modelling (e.g., (Gearing *et al.*, 2003; Wess, 1993; Wheatley *et al.*, 2003). In general, this large body of work has revealed that the extracellular and TM domains are responsible for ligand binding, while intracellular domains dock and activate G proteins, and anchor the receptor to the membrane. The intracellular domains are also targets for post-translational modification such as phosphorylation which play a critical role in GPCR 'memory' resulting in reduced (desensitization) or augmented (sensitization) responses (Gainetdinov *et al.*, 2004). GPCR desensitization in response to agonist stimulation is common to nearly all GPCRs, and typically involves GPCR kinase (GRK) - or other kinase-induced phosphorylation of the activated GPCR, and recruitment of β-arrestins to uncouple the receptor from its associated G protein (s), and target the GPCR for endocytosis by linking it to 'adaptor' molecules such as clathrin (Gainetdinov *et al.*, 2004; Tobin *et al.*, 2008a). The amino terminus invariably contains N-linked glycosylation sites involved in intracellular receptor trafficking, membrane expression and ligand binding (Wheatley and Hawtin, 1999), and the carboxyl terminus hosts sites for palmitoylation to facilitate interaction with the membrane, and together with phosphorylation sites have roles in receptor dimerisation and internalisation, and intracellular signalling (Huynh *et al.*, 2009).

GPCRs can be grouped into four main classes based on shared sequence motifs: (1) Class A (rhodopsin-like), the largest GPCR class that includes the earliest GPCRs cloned (β_2-adrenoceptor

(Dixon *et al.*, 1986), acetylcholine M_1 (Kubo *et al.*, 1986)) and the aminergic, olfactory and majority of neuropeptide GPCRs; (2) Class B (secretin-like), comprising calcitonin, glucagon, CRF and parathyroid hormone receptors that have a characteristic long amino-terminus tail containing three conserved disulphide bonds; (3) Class C (metabotropic glutamate-like) with an amino terminus consisting of two lobe-like structures that resemble that of a 'venus flytrap' (e.g., metabotropic glutamate, calcium-sensing, and $GABA_B$ receptors); and (4) Frizzled/Smoothened receptors, which are the sole members of the fourth group. Frizzled receptors have a large amino terminus, and are important in embryonic development and adult tissue homeostasis, while Smoothened receptors contribute to the hedgehog signalling system, and are involved in embryogenesis and tumorigenesis (Harmar *et al.*, 2009; Oldham and Hamm, 2008).

For many years the prototypical reference for GPCR organization in the lipid bilayer has been based on rhodopsin and its high-resolution X-ray crystallographic structure (Palczewski *et al.*, 2000). The successful crystallography of hormone-binding GPCRs is a significant breakthrough in GPCR research that has required the recombinant generation of high levels of GPCR protein, enhancing their stability (e.g., using stabilizing ligands) and structural modifications to encourage crystal formation. The structures of a number of Class A GPCRs (e.g., β_1- and β_2-adrenoceptors (Cherezov *et al.*, 2007; Rasmussen *et al.*, 2007); adenosine A_{2A} receptor (Jaakola *et al.*, 2008) and the minimally active conformation of opsin (the ligand-free form of rhodopsin) (Park *et al.*, 2008) have now been elucidated, confirming that essentially all Class A (and by extension Classes B and C) GPCRs possess seven membrane-spanning helical domains arranged in a bundle with a cytoplasmic eighth helix immediately following TM7. One insight from the small number of X-ray crystallography studies to date is that each subfamily of GPCRs possesses its own unique mode of natural ligand binding reflecting their unique structure. In the rat genome there are a total of 356 non-chemosensory GPCRs of which 132 are classified as orphans (Harmar *et al.*, 2009).

GPCRs are coupled to G proteins that are comprised of three subunits: Gα, Gβ and Gγ. Stimulation from physiological, environmental or experimental signals provokes a conformational change in the receptor-7TM structure, catalysing the replacement of GDP for GTP on the Gα subunit. Subsequently, Gα detaches from Gβγ to create two separate components that can activate a multitude of intracellular signalling pathways e.g., Gα may increase adenylyl cyclase activity, whilst Gβγ can independently act to stimulate phospholipases and ERKs, and activate ion channels. Heterotrimeric G proteins are encoded by a family of related genes that comprises 21 Gα, 5 Gβ and 12 Gγ mammalian genes, giving rise to a variety of G protein combinations (Downes and Gautam, 1999). They are categorised into four main groups according to the structure and function of the α subunit: $G\alpha_s$, $G\alpha_{q/11}$, $G\alpha_i$, and $G\alpha_{12/13}$ (Oldham and Hamm, 2008). $G\alpha_s$ typically activates adenylate cyclases that catalyse the production of

cAMP from ATP, stimulating PKA activity. $G\alpha_{q/11}$ couples to and activate phospholipase Cβ (PLCβ), and increases intracellular calcium and PKC activity. $G\alpha_i$ often inhibits adenylate cyclase activity, impeding cAMP synthesis, as well as activating G protein-coupled potassium channels. The remaining group of G proteins is the $G\alpha_{12/13}$ family that regulate the small G protein Rho through Rho-specific guanine nucleotide exchange factors (Pierce *et al.*, 2002).

A typical feature of GPCR signalling is that by activating a cascade of signal transduction mediators the signals can be amplified. Cross-talk between GPCRs, or GPCRs and other proteins at the cell surface (e.g., via oligomerization) and in the cytoplasm (e.g., via convergent signalling pathways such as $G_s/G_q/G_i$- and receptor tyrosine kinase-activation of ERKs) can modify GPCR-mediated signalling. In addition, GPCRs vary in their specificity for activating/coupling to the G protein subtypes with some activating only one Gα subtype while others are more promiscuous and couple to a number of Gα proteins to activate multiple intracellular signalling cascades. The ability of GPCRs to activate more than one class of G proteins can depend on receptor density, the nature of the ligand (different responses to two ligands can confer 'functional selectivity'), tissue distribution, and on its localisation within specialized compartments of the plasma membrane which may depend on whether the GPCR is active in a monomeric or oligomeric form (Kenakin and Miller, 2010; Maudsley *et al.*, 2005; Woehler and Ponimaskin, 2009; Zheng *et al.*, 2010a). One facet of GPCR intracellular signalling that should not be overlooked is that some GPCRs can activate both G protein-dependent and G protein-independent pathways. For example, angiotensin II AT_{1A} receptor-triggered transactivation of the EGFR, and β-arrestin-dependent and -independent AT_{1A} receptor internalization can take place independently of G protein activation (Feng *et al.*, 2005). In addition, AT_{1A}-mediated activation of ERK features both G_q- and β-arrestin-dependent pathways (Lefkowitz and Shenoy, 2005), while β_2-adrenoceptor stimulation of the ERK pathway is G_s-coupled and Gα-independent/tyrosine kinase Src-dependent at low and high concentrations of stimulating agonist, respectively (Sun *et al.*, 2007). Overall it is apparent that GPCRs dynamically interact with numerous associated proteins as part of a tightly regulated signalling network, and this interaction in different tissues reflects the types of signalling components within a given cell and the receptor's physiological role.

1.3 GPCR expression in the PVN and SON

Over 90% of non-chemosensory GPCRs are expressed in the mouse brain with a large proportion (82% of those examined by RT-PCR) expressed in the hypothalamus (Vassilatis *et al.*, 2003). The profiles of the vast majority of GPCRs are unique, and when combined with brain region-specific intracellular signalling component expression (see Section 1.3.1), yield thousands of GPCR signalling combinations for the modulation of physiological processes. Some GPCRs even appear to be relatively

confined to the CNS, although it is rare to find evidence of CNS exclusivity if techniques such as reverse-transcription (RT)-PCR or EST profiling (e.g., see http://www.ncbi.nlm.nih.gov/UniGene/) are used.

After a flourish of research in the 1980's/early 1990's localizing GPCRs by receptor ARG, more recent developments in IHC, ISHH, transcriptome approaches such as DNA microarrays, and *ex vivo/in vivo* electrophysiological methods have greatly contributed to our understanding of the regulation of the PVN/SON activity by GPCR-based signalling. The PVN and SON are highly vascularized and blood vessel elements and 'supporting' cells such as glial cells express GPCRs. In the following sections we focus on the expression of GPCRs in neurons of the rat PVN and SON, although it should be emphasized that this has not been conclusively demonstrated in all studies, e.g., receptor ARG and DNA microarray experiments.

1.3.1. Intracellular signalling components in the PVN/SON

We would expect that cells in the PVN and SON are equipped with the appropriate sets of receptors and various intracellular signalling components to sense and respond to perturbations in homeostasis. Regulation of both GPCR signalling molecules and GPCRs themselves (see Section 1.4) will contribute to the adaptive responses of the PVN and SON. The distribution of various GPCR cytoplasmic signalling components in the PVN/SON has not been extensively studied, although the function of various G proteins and other intracellular signal transduction mediators involved in GPCR-mediated effects has been implicated in a number of studies. Immunoreactive (ir)-Gβ1-5 and γ3 are expressed at low levels in the rat PVN and the expression of the various β subunits is increased by repeated restraint (Lee *et al.*, 2006; Liang *et al.*, 1998). While ISHH studies suggest that there are very low levels of PKC subunit mRNAs in the rat PVN and SON (Brandt *et al.*, 1987), other studies point to the expression of ir-PKC-δ in neuronal cell bodies in the PVN/SON, and ir-PKC-ϕ in PVN fibres (Irani *et al.*, 2010), and phosphatidylcholine specific phospholipase C-mediated VP release from the hypothalamus *in vitro* appears to involve PKC activation (Wayte *et al.*, 1997). Osmotic stimulation increases $G\alpha_i$ and $G\alpha_s$ mRNAs in the magnocellular PVN and SON, and cAMP in the SON (Young *et al.*, 1987), while $G\alpha_q$ appears to participate in high-salt induced VP secretion in Dahl salt-sensitive rats (Wainford and Kapusta, 2010). Of the nine adenylate cyclase isoforms only type 2 appears to be strongly expressed in the PVN and SON (Mons and Cooper, 1994). Elevated cAMP within PVN/SON neurons may stimulate cAMP response elements in gene promoters to alter neuropeptide (or GPCR) gene transcription, exemplified by studies showing cAMP-driven CRF and VP gene expression in the PVN (Arima *et al.*, 2001; Burbach *et al.*, 2001; Itoi *et al.*, 1996; Wong *et al.*, 2003). The PVN and SON also express mRNAs for numerous members of the regulators for G protein signalling (RGS) family including RGS4, 5, 7, 8 and 9 (Gold *et al.*, 1997) - these proteins modulate the function of the

Gα and Gβ subunits, and the gene expression of at least one member (RGS4) in the PVN has been shown to be downregulated by repeated stress (Ni *et al.*, 1999). Other studies suggest that the spatial distribution of some signalling molecules within the PVN may be functionally relevant, e.g., RGS4 and $G\alpha_{q/11}$ mRNAs are found in both pPVN and mPVN neurons while RGS7 gene expression is confined to the mPVN (Shuey *et al.*, 1998).

Gene expression profiling (Hindmarch *et al.*, 2006) considerably extends early studies (Lightman, 1988) cataloguing some GPCR-related signalling molecules in the PVN and SON. A plethora of gene transcripts relevant to GPCR signal transduction has been revealed (see Supplementary Tables 1 and 2), including those encoding the relatively abundantly expressed calcium-binding calmodulins, endocytosis adaptor molecules dynamin and clathrin, various RGS and G proteins, and a number of PKC, phospholipase C and D, and cAMP isoforms. While the presence and anatomical distribution of the majority of these transcripts has not been validated by other criteria (e.g., IHC, ISHH, RT-PCR), the data indicates that the PVN and SON express a considerable network of intracellular signalling proteins that could potentially be enlisted upon GPCR activation.

1.3.2. Detection of GPCR proteins by receptor autoradiography (ARG)

The advent of molecular biological techniques that resolved the genetic fingerprint of GPCRs led to the popular use of GPCR antibodies - generated from predicted protein sequences of cloned GPCR DNA sequences - to visualize GPCR protein expression by techniques such as IHC. Prior to this receptor ARG was a popular tool to delineate GPCR binding sites in brain and peripheral tissues since it provided the ability to anatomically resolve receptor protein expression and to quantitate receptor levels. The method can give higher (cellular) resolution if tissue sections are apposed against emulsion-coated coverslips (Young and Kuhar, 1979) rather than against X-ray film. A major consideration when using receptor ARG is that not all pharmacologically defined binding sites necessarily represent physiologically active receptors - in a famous 'caveat' to those undertaking receptor studies, Cuatrecasas and Hollenberg described how iodinated insulin appears to bind with high affinity to non-biological surfaces like talc with characteristics - except 'biological activity' - that are commonly attributed to specific hormone-receptor interactions (Cuatrecasas and Hollenberg, 1975). Moreover, while radiolabelled ligands may bind 'functional' (capable of binding an agonist) GPCRs they may not bind to the entire receptor pool. For example, they may only bind to high affinity binding sites, receptor-G protein interactions critical for agonist binding may be disrupted during the receptor ARG procedure, and 'immature' GPCRs that have not been post-translationally modified and/or possess the requisite tertiary structure, or degraded GPCRs may not bind the ligand. Other limitations of the technique include the masking of binding sites by endogenous ligand, although this is usually minimized by buffer pre-washes prior to ligand incubation. Receptor binding studies on

tissue homogenates (infrequently if ever used for GPCR expression in the PVN/SON) or receptor ARG are critically dependent on the specificity and selectivity of the radiolabelled ligand employed - high affinity radioligands selective for a particular GPCR subclass are not always available. Specific binding is defined as for receptor binding assays on tissue homogenates, and includes diminution of bound radioactivity by the addition of excess cold ligand and establishing a pharmacological profile using closely- and distantly- related compounds. Knockout (KO) mice (providing the distribution of GPCRs in rat and mouse are the same) are an invaluable addition in validating radioligands for a specific receptor. Detection of low amounts of protein also depends on the sensitivity and specific activity of the radioligand, e.g., iodinated versus tritiated ligands can be used for shorter exposure times against film but offer lower resolution.

The list of the 25 GPCR subfamilies detected in the PVN/SON by receptor ARG is shown in Supplementary Table 3. The number is likely incomplete since not all the literature covering GPCR receptor ARG in the brain encompasses the pertinent hypothalamic levels, and even when the relevant brain levels have been included in some studies it is often difficult to ascertain if binding is above background levels. Critically receptor ARG (and other receptor protein or RNA detection techniques) does not directly inform about GPCR function. This can be addressed in part by 'functional' ARG with [^{35}S]GTPγS to map region-specific, GPCR ligand-dependent activation of G proteins (Harrison and Traynor, 2003; Sóvágó *et al.*, 2001). Although it has not used extensively in the PVN and SON, [^{35}S]GTPγS binding ARG has demonstrated 'active' neuropeptide Y_1 and Y_2 (Shaw *et al.*, 2003), and cannabinoid CB_1 (Hesketh *et al.*, 2008) binding sites in the PVN. Positron emission topography (PET) is an alternative imaging technique to visualize GPCRs non-invasively in the PVN and SON *in vivo*; while the technique is relatively low resolution and there is a dearth of suitable GPCR ligands for such studies, there are a few publications (e.g., 5-HT_{1A} receptors in the rat PVN (Aznavour *et al.*, 2009) indicating that this approach may be a useful adjunct to receptor ARG studies in the future. Receptor ARG rarely has the sensitivity or resolution of IHC. Moreover, in the absence of selective ligands to define a GPCR family in the PVN/SON, IHC and/or ISHH with subtype-selective antibodies and DNA/RNA probes, respectively, can elaborate a specific GPCR receptor subtype.

1.3.3. Immunohistochemistry (IHC) to visualize GPCR expression

Since GPCR-specific and -selective ligands are not available for all GPCRs, antibodies have been a popular option to detect many GPCRs. IHC employing primary GPCR antibodies traced with secondary antibodies to permit fluorescent or chromogenic detection of ir- proteins is a valuable technique to localise GPCR expression in sections of the PVN and SON, offering a far greater lateral and axial resolution than receptor ARG. A major consideration in all GPCR protein and mRNA detection techniques is specificity. The GPCR field is awash with reports of GPCR antibodies that

don't 'work' between laboratories, those that have stopped working after new batches were purchased, and those that give no staining. For antibodies in particular and the IHC method in general, the evaluation of specificity has provoked numerous comments in the past with many concluding that antibody specificity is a difficult criterion to fulfil (Swaab *et al.*, 1977). There are well-established controls for IHC procedures, including the absence of staining when the antibody is pre-absorbed with the immunizing antigen (although this only proves that the antibody bound the added antigen and not that the antibody is 'specific' for the GPCR), and the presence by Western blotting of the appropriate GPCR molecular sizes which may correspond to post-translationally modified and/or oligomeric forms. However, other points related to antibody use and storage (e.g., possibility of 'carrier' antibodies contributing to staining patterns; tendency of antibodies to form aggregates at 4°C; potential instability of immunoglobulin fractions or affinity-purified antisera; prolonged storage times between fixation, sectioning and staining; inefficient blocking of immunoglobulin Fc receptors (which are present in the PVN/SON (Hindmarch *et al.*, 2006) - e.g., see (Wendelboe and Bisgaard, 2009) tend to be under-appreciated and often overlooked, and can lead to increased non-specific, or variable or complete absence of specific staining. Alterations in IHC staining patterns between different antibody batches (either from different animals or different bleeds from the same animal) can often be explained by the inherent characteristics of the normal immune response, e.g., decreasing antibodies titres, or high-affinity antibodies present in an early bleed may be replaced by high-avidity antibodies (perhaps with a lower relative concentrations of specific versus 'less-specific' immunoglobulins) as the immune response proceeds. The majority of GPCR antibodies for IHC are raised to short, synthetic GPCR peptides ('haptens') usually coupled to a carrier (e.g., keyhole limpet hemocyanin or sometimes bovine serum albumin (BSA)) to enhance the anti-hapten antibody response, or less frequently to partially purified native or recombinant GPCRs. Invariably the antibodies are a polyclonal mixture (monoclonal antibodies have only been used occasionally (e.g., see (Rosin *et al.*, 1998; Shi *et al.*, 1999; Zhang *et al.*, 2004) and directed to regions that are most divergent between different GPCR subclasses, N- or C-terminus moieties being the most attractive targets. Most GPCRs are post-translationally modified (Chini and Parenti, 2009; Tobin *et al.*, 2008a; Wheatley and Hawtin, 1999), a crucial point in GPCR antibody production since regions that can be potentially glycosylated, phosphorylated or acylated *in vivo* may mask an epitope to hinder antibody recognition. On the flip side, phosphospecific GPCR antibodies can be made (e.g., (Tran *et al.*, 2004)). Antibodies can also conceivably differentially react to ligand-activated versus unoccupied GPCR conformations, and antibodies raised against denatured GPCR proteins may not recognize the 'native' (usually fixed) GPCR in tissue sections.

For GPCRs, serious specificity concerns have been raised in a number of articles contesting the reliability of many GPCR antibodies for IHC (e.g., (Michel *et al.*, 2009)). In contrast the specificity of

antibodies to neuropeptides and other cellular constituents are rarely indicted to the same degree, commensurate with the diverse, largely structurally non-conserved nature of GPCR ligands compared with the often, high amino acid homology between different GPCR subtypes. A recent review of studies using antibodies against 19 α_1- and β_1-adrenoceptor, acetylcholine, dopamine and galanin receptor subtypes for immunoblotting and IHC concluded that apparent lack of specificity of GPCR antibodies appears to be the rule rather than the exception (Michel *et al.*, 2009). Some sensible suggestions for improving GPCR antibody validation have been made (Jositsch *et al.*, 2009; Michel *et al.*, 2009). These include the reduction of immunostaining following GPCR knockdown using RNA interference (although a lack of knowledge of GPCR mRNA and protein turnover may make this problematic - see Section 1.4) and obtaining similar staining patterns with antibodies against different GPCR epitopes, although it is rare to find studies using two or more antibodies to detect GPCRs by IHC in the PVN and SON (exceptions include the dopamine D_4 (Defagot *et al.*, 1997) and glutamate $mGlu_1$ (Kiss *et al.*, 1996) GPCRs). Similarly, the absence of GPCR immunostaining in GPCR KOs has also been advocated as a desired IHC control (Michel *et al.*, 2009). Assuming that an antibody is truly GPCR-specific in both rats and mice, and there are no species differences in the GPCR distribution between those animals, the absence of immunostaining in tissues from a KO animal in which the entire GPCR protein coding sequence has been eliminated should serve as an excellent 'negative' control in IHC on rat tissues. However, if the KO targeting construct does not include the relevant protein region to which the antibody was raised, it is possible that the antibody could react to a protein translated in-frame from the targeting construct *in vivo*, and lack of staining is not a foregone conclusion. While we do not necessarily share the outlook that the specificity of most GPCRs is suspect, a review of the literature emphasizes that caution is warranted, especially when using some commercially prepared antibodies (Grimsey *et al.*, 2008; Pradidarcheep *et al.*, 2008). We have not endeavoured to evaluate the specificity of antibodies used to detect GPCRs in the PVN and SON. However the expression of many GPCRs detected by IHC (see Supplementary Table 4) has been validated by other methods (which also have their own specificity issues).

Individual GPCR numbers per cell are usually quite low in the brain, with lower estimates ranging from 100-300 receptors per cell (very low copy number) to upwards of 2,000-6,000 receptors per cell (around physiological levels for many GPCRs - e.g., see (Kasai *et al.*, 2011) and refs therein)). By way of comparison, cells engineered to express recombinant GPCRs can achieve levels of greater than 100,000 receptors in each cell. The threshold of detection for a 'good' antibody in IHC is probably in the order of 10-1,000 receptors per cell depending on the staining and microscopical method used (e.g., see (Chung *et al.*, 2005; Eberwine and Bartfai, 2011)). The detection of ir-GPCRs in cell bodies, axons, dendrites and terminals, and in intracellular organelles such as endosomes, endoplasmic reticulum and the nucleus by IHC with conventional light microscopy can be facilitated by the use of

high-resolution optical imaging techniques like confocal microscopy. GPCRs are highly mobile and traffic between different subcellular compartments in the PVN and SON, and are probably dendritically sorted as in other brain regions (Ritter and Hall, 2009). For example, IHC has revealed that the tachykinin NK_3 receptor translocates to the nucleus of VP and non-VP PVN neurons in a stimulus-dependent manner, where it may play a role in transcriptional regulation (Haley and Flynn, 2006; Howe *et al.*, 2004).

CNS GPCRs are not particularly abundant proteins and their signals (and non-specific staining) can be enhanced by using modified IHC protocols incorporating tyramide signal amplification (TSA) (Bobrow *et al.*, 1989). Even with improvements in IHC detection, however, it is often difficult to discern whether GPCR staining is associated with the cell surface in detergent (e.g., Triton X-100)-treated sections of fixed tissue, although there are some examples of uniform or punctate staining closely apposed to the plasma membrane (e.g., tachykinin NK_3 (Howe *et al.*, 2004); PTH2 parathyroid hormone (Wang *et al.*, 2000) receptors). In most cases in the PVN and SON GPCR-ir staining is quite nondescript and apparently found mainly intracellularly, which has important functional implications for some GPCRs that are thought to be active inside the cell (Revankar *et al.*, 2005). For the majority of GPCRs, an intracellular versus plasma membrane distinction may 'simply' reflect the detection of mature GPCRs in the endocytic pathway and/or immature GPCR pools (presumably functionally inactive) yet to be presented to the plasma membrane. In a few instances light microscopic studies have been reinforced by higher magnification immuno-electron microcopy, e.g., in the PVN and SON ir-$GABA_{B1}$ is mainly associated with the endoplasmic reticulum, golgi apparatus and large membrane-bound vesicles, while a small amount of staining is found close to the plasma membrane (Richards *et al.*, 2005). The possible functional relevance of ir-GPCR localisation in PVN and SON neurons is supported by other studies, e.g., staining for the CB_1 cannabinoid receptor, a GPCR that inhibits the release of excitatory and inhibitory neurotransmitters in the brain (Pertwee *et al.*, 2010), is clearly present in GABAergic terminals and fibres surrounding OTergic PVN neurons (Castelli *et al.*, 2007). The CB_1 receptor appears to be synthesized in the PVN and SON (Matsuda *et al.*, 1993) but other GPCRs such as the prostanoid EP_3 receptor (Nakamura *et al.*, 2000) appear to be confined to fibre terminals presumably as part of afferent projections to the PVN/SON. So IHC can give some idea of the pre/post-synaptical localisation of GPCRs in the PVN and SON.

Strong indirect evidence that GPCRs in the PVN and SON may be functionally important also comes from studies where ir-GPCRs have been localised to phenotypically-identified neurons. For example, α_{1D}-adrenoceptor (Sands *et al.*, 1990) and angiotensin AT_{1A} (Oldfield *et al.*, 2001) receptors are both located in pPVN CRF-expressing neurons, the 5-$HT_{1A/2A}$ (Zhang *et al.*, 2004), apelin APJ (Tobin *et al.*, 2008b), chemokine CXCR4 (Callewaere *et al.*, 2006), $GABA_{B1/B2}$ (Richards et al., 2005), κ opioid (Smith and Wise, 2001) and tachykinin NK_3 (Haley and Flynn, 2006) receptors are expressed in VP

and/or OT neurons, whereas the glutamate $mGlu_1$ receptor has been identified in both CRF and VP neurons (Kocsis *et al.*, 1998). VP, OT and CRF (and TRH, dopamine, GHRH and somatostatin) neurons in the PVN and SON also express additional neuropeptides that could be co-regulated (Bundzikova *et al.*, 2008). The presence of VP V_{1A} receptors on VP neurons (Howe *et al.*, 2004) and OT receptors on OT neurons (Marroni *et al.*, 2007) suggests that these receptors may act in an autocrine fashion to regulate the release of their own cognate ligands. Moreover, the demonstration that some GPCRs (e.g., apelin APJ (Tobin *et al.*, 2008b), E2 GPER (see Chapter 3), and parathyroid hormone PTH2 (Wang et al., 2000) receptors) are present on both PVN and SON neuronal cell bodies, fibres and terminals (e.g., in the median eminence or in the posterior pituitary) suggests that GPCRs may act at different locations to alter neuropeptide or neurotransmitter synthesis and/or release. Based on its intracellular, and to a minor degree cell surface localisation, the E2 GPER receptor is an example of a GPCR that may be functionally active on or in neuronal cell bodies in the PVN and SON, dendrites, and axonal projections through the internal zone of the median eminence and posterior pituitary nerve terminals (see Chapter 3). Given the breadth of ir-GPCR distributions in the PVN and SON, and the estimated number of neurons in the PVN and SON (e.g., there are about 1,000 and 3,000 VP neurons in the rat PVN and SON, respectively, and approximately 1,250 OT neurons in both nuclei – (Rhodes *et al.*, 1981), it would be extremely likely that many GPCRs are co-expressed in individual neurons. In fact, the possible co-existence of two (or more) different GPCRs in the same neuron would support the concept that GPCRs may physically interact (see Section 1.5) in the PVN and SON. However, demonstrating co-expression of two or more proteins in a cell is difficult, although not impossible (see (Brouns *et al.*, 2002; Negoescu *et al.*, 1994) using antibodies raised in the same species to detect non-abundant proteins. In the SON and elsewhere in the brain GPCR co-expression appears to be the case for the two subunits (each a 7TM 'receptor') of the $GABA_B$ receptor, $GABA_{B1}$ and $GABA_{B2}$ (Richards *et al.*, 2005), which must heterodimerize for functional $GABA_B$ responses (Marshall and Foord, 2010).

There are a number of mismatches between GPCR protein and mRNA as determined by receptor ARG and/or IHC and ISHH, respectively. For example, binding studies with an iodinated glucagon GLP-1 receptor agonist detect dense labelling in the median eminence and posterior pituitary where there is no GLP-1 receptor mRNA (Göke *et al.*, 1995; Shughrue *et al.*, 1996). Conversely, GLP-1 receptor mRNA is concentrated in the PVN where only weak binding is observed and where ir-GLP-1 fibre terminals are closely associated with OT- and CRF-expressing neurons (Tauchi *et al.*, 2008). The apparent discrepancies between GPCR protein and mRNA localisations may highlight technical issues (e.g., sensitivity). Alternative it may be a product of transportation e.g., GPCR transcript from cell bodies is translated (either in the cell bodies themselves or perhaps in the axons and/or dendrites), and is transported along the axonal and dendritic fibres of the PVN and SON.

1.3.4. In situ hybridization histochemistry (ISHH) localisation of GPCR mRNA

ISHH was introduced in 1969 (Buongiorno-Nardelli and Amaldi, 1970; Gall and Pardue, 1969; John *et al.*, 1969) as a method to detect specific mRNAs within cells by hybridizing labelled RNA, cDNA, or short oligonucleotide DNA probes to target sequences in tissue samples. Employing IHC in concert with ISHH can provide converging anatomical evidence to form testable hypotheses and support data on GPCR function in the PVN and SON. High throughput ISHH as advocated for mapping high-resolution gene expression in the brain ((Lein *et al.*, 2007) - see Allen Brain Atlas at http:/brain-map.org) is usually satisfactory for abundant genes. Apart from a few notable exceptions such as the cannabinoid CB_1 receptor gene that is highly expressed in many brain regions (Matsuda *et al.*, 1993), most GPCR mRNA(s) are not as abundant as those encoding ionotropic receptors and are visualized usually after a short exposure (weeks-months) against X-ray film or photographic emulsion. However, refinements in the ISHH method permit the detection of as few as 10-20 mRNA copies per cell (Siegel and Young, 1985), sensitive enough to visualize the majority of the rarest GPCR transcripts, and to compare changes in GPCR gene expression at the cellular level by counting silver grains or at the macroscopic level by image analysis and densitometry with reference to the appropriate autoradiographic standards (as for receptor ARG). ISHH detection sensitivity can also be enhanced by using multiple oligonucleotide probes to different regions of the designated mRNA, or by a number of amplification methods such as TSA (see Section 1.3.3).

Cloning of the mammalian GPCR cDNAs, or identification of GPCR DNA sequences using homology-based searching tools, has provided the platform to map GPCR transcript expression in the brain by ISHH. More often than not ^{35}S-labelled antisense RNA probes targeting a large part of the GPCR mRNA (e.g., approx. 300-600 base pairs (bp) RNA probes (riboprobes) for proteins whose coding regions average about 1,000-1,500bp in length) are used for optimal GPCR transcript detection: these can be labelled to a higher specific activity, and bind more strongly to target mRNA sequences, than oligonucleotide probes. The use of long riboprobes and even short oligonucelotides (typically 40-48bp) introduces its own set of problems since hybridization to closely related GPCR subtypes may occur if probes are designed to a relatively well-conserved part of the GPCR mRNA sequence. GPCR-subtype specificity is usually increased if regions such as the 3'-untranslated (UTR) of GPCRs are targeted (providing the G/C content of the probe is not so low to preclude high stringency washes). However, specificity concerns may also be compounded if sense probes used as negative controls for antisense probe binding label the tissue of interest (one definition of 'non-specific' hybridization), which is not implausible since over 50% of the mammalian genome can produce transcripts from both DNA strands (Katayama *et al.*, 2005). Evidence that the complementary DNA strand of a GPCR gene can code for another gene is provided by the study of Foletta and coworkers (Foletta *et al.*, 2002), where a sense VP V_2 receptor probe which does not hybridize to the

V_2 receptor-expressing kidney (Ostrowski *et al.*, 1993), detected transcripts for a Rho GTPase activating protein in the brain. It is generally advised to use well-characterized probes (e.g., ones that has been validated by Northern blots, and gives appropriate hybridization patterns in control tissues), or more than one probe (and corresponding sense 'control') against a target sequence to minimize erroneous interpretations of ISHH labelling patterns. Our experience and that of many other laboratories using ISHH is that, as in the case of antibodies and IHC, there is often significant variability in the signal/noise ratios for different probes directed to the same GPCR mRNA target.

As outlined in Supplementary Table 4, a large number of GPCR mRNAs have been detected in the cell bodies of PVN and SON neurons. By and large there is general agreement on steady-state GPCR gene expression in the PVN and SON between laboratories but some exceptions are apparent in the literature. For example, while Hurbin and coworkers (Hurbin *et al.*, 1998; Hurbin *et al.*, 2002) detected VP V_{1B} receptor mRNA and protein expression in the mPVN and SON using short oliognucleotide probes and receptor antibodies, respectively, others found only occasional V_{1B} receptor mRNA-expressing cells in the pPVN using riboprobes directed against the 3'UTR of the receptor (Young *et al.*, 2006). Studies such as these emphasize the importance of probe specificity and the limits of ISHH, and raise questions of mRNA and protein turnover (see Section 1.5).

Like IHC, ISHH is also amenable to co-expression studies, whether combined with IHC or alternatively used alone to investigate the expression of two distinct transcripts in neuronal cell bodies. For example, 5-HT_{2C} (Heisler *et al.*, 2007), adrenoceptor α_{1B} (Day *et al.*, 1999), CRF_1 (Imaki *et al.*, 2001) and melanocortin MC_4 (Lu *et al.*, 2003) receptor mRNAs are predominantly found in CRF neurons, neuromedin U NMU2 receptor mRNA is mainly present in OT neurons (Qiu *et al.*, 2005), and neuropeptide Y Y1 receptor transcripts are co-expressed with TRH mRNA in pPVN cells (Kishi *et al.*, 2005). Of the 52 GPCRs with known ligands detected in the PVN by IHC, 34 of the corresponding mRNAs have also been detected in the same or independent studies (see Supplementary Table 4). The great majority of GPCRs are expressed in both the pPVN and mPVN (e.g., 5-$HT_{1A/2A}$ (Zhang *et al.*, 2004); α_{1D}-adrenoceptor (Sands and Morilak, 1999); apelin APJ (O'Carroll, *et al.*, 2000; Tobin *et al.*, 2008b); calcium-sensing CaS (Rogers *et al.*, 1997); CRF_1 (Imaki *et al.*, 2001); melanocortin MC_4 (Lu *et al.*, 2003); prostanoid $EP_{1/4}$ (Oka *et al.*, 2000) receptors). Some GPCRs appear to be preferentially expressed in the pPVN (e.g., consistent with regulating stress or autonomic responses), or mPVN (e.g., compatible with regulating water homeostasis or reproductive status) by either IHC and/or ISHH (pPVN: 5-HT_{2C} (Heisler *et al.*, 2007); angiotensin AT_{1A} (Oldfield *et al.*, 2001); prolactin-releasing peptide PRRP (Lin *et al.*, 2002) receptors; mPVN: chemokine CXCR4 (Callewaere *et al.*, 2006); neuromedin U NMU2 (Qiu *et al.*, 2005); κ opioid (Smith and Wise, 2001) receptors). One GPCR (neuropeptide FF/neuropeptide AF NPFF1) seems to be PVN-specific in rats (Goncharuk *et al.*, 2002), although ir-NPFF1 fibres found just dorsal to the SON, as in humans (Goncharuk *et al.*, 2004), may

project to the SON (Jhamandas *et al.*, 1989) and be responsible for the inhibitory effects of centrally administered NPFF on hypovolemia-induced VP secretion into the blood (Arima *et al.*, 1996).

1.3.5. Transcriptomic analysis of GPCR expression in the PVN/SON

RT-PCR-based methods have been used to delineate a partial GPCR transcriptome in a number of tissues including mouse heart (Moore-Morris *et al.*, 2009) and brain (Vassilatis *et al.*, 2003). Only the odd study has used PCR to detect the expression of an individual GPCR gene in dissected PVN/SON (Coppola *et al.*, 2004; Lu *et al.*, 2009; Shrestha *et al.*, 2009; Stofkova *et al.*, 2009). Large-scale transcriptome analysis of enriched genes, including some GPCR transcripts, has been performed in a number of mouse brain regions including striatum, frontal cortex, hippocampus and amygdala (Becker *et al.*, 2008; Ghate *et al.*, 2007; Lein *et al.*, 2004). Recently DNA microarray-based transcriptomal analysis of the rat PVN, SON, subfornical organ and area postrema, and mouse SON was reported from our laboratories (Hindmarch *et al.*, 2006; Hindmarch *et al.*, 2008; Hindmarch *et al.*, 2011; Stewart *et al.*, 2011). There are some limitations associated with such 'global' studies in rats as highlighted previously (Hindmarch *et al.*, 2006). For example, manual rather than laser dissection of PVN and SON was used so a small amount of surrounding tissue such as the third ventricle could have been included in the samples. In addition, most but not all GPCRs with known ligands, or orphan GPCRs are represented on the Affymetrix 230 2.0 rat genome chip interrogated - examples of some 'missing' GPCRs include the bombesin BB_3 receptor and the orphan GPCRs GPR101 and GPR165. Furthermore, some rare GPCR transcripts in the PVN and SON may escape detection, or some probe sets may have failed in some or all of the replicates, thus excluding them from the analysis - examples of this are the apelin APJ, E2 GPER, and VP V_{1A} receptors which are readily detected by receptor ARG, IHC and/or ISHH in the PVN and SON. Bearing these points in mind, we have constructed a list of the GPCRs genes considered present by DNA microarrays in the PVN and SON (Supplementary Tables 4, 5, 6). The relative abundance of GPCR transcripts in both hypothalamic nuclei varies from those that are highly expressed such as various $GABA_B$ subunits, and neurotensin NTS_2 and endothelin ET_B receptors, to the less highly expressed purinergic $P2Y_{13}$, adenosine A_3, and metabotropic glutamate $mGlu_4$ and $mGlu_7$ receptors.

About 80% of GPCR transcripts in the PVN are also present in the SON, and approximately 70% and 50% of transcripts for GPCRs with known ligands in the PVN and SON, respectively, has been validated by receptor ARG, IHC and/or ISHH. This includes some GPCR transcripts (e.g., parathyroid hormone PTH_1 and neuropeptide Y Y_5 in the PVN/SON) that are towards the lower limits of detection. The GPCR gene lists include 14-16 'new' GPCRs with known ligands, such as adenosine A_{2B}, chemokine CXCR3 and CXCR7, lysophospholipid LPA_1 and S_1P_1, metabotropic glutamate $mGlu_4$, purinergic $P2Y_{13}$ and protease-activated PAR1 receptors, and 17-21 'new' orphan GPCRs (see

Supplementary Table 7) whose localisation in the PVN and SON is unvalidated on review of the literature, and which may represent novel targets for future physiological studies. Another interesting feature of the transcriptomic data is that by virtue of multiple oligonucleotide probe sets representing some genes on the array chip, a number of GPCR splice variants appear to be present in the PVN and SON. Alternate splicing of pre-mRNAs is one mechanism for increasing diversity in the transcriptome. Although approximately half of GPCR genes are devoid of introns within their coding sequence, those that possess introns can theoretically undergo alternative splicing and this may have consequences on GPCR functions such as altered pharmacological profiles, constitutive activity and subcellular localisation (Markovic and Challiss, 2004). Examples of GPCRs that exhibit varying degrees of alternate splicing include the $GABA_{B1}$ subunit (Wei *et al.*, 2001), NOP opioid (Xie *et al.*, 1999), metabotropic glutamate (Niswender and Conn, 2010) endothelin ET_A (Hatae *et al.*, 2007) and parathyroid hormone PTH1 (Joun *et al.*, 1997) receptors, all of which have potential isoforms identified by DNA microarrays in the PVN and SON. Transcriptome analysis of the PVN and SON also reveals four $GABA_{B1}$ subunit isoforms (a, f, g, j) - and IHC and ISHH studies indicate that at least two $GABA_{B1}$ subunits (B1a and B1b) are expressed in the PVN and SON (Fritschy *et al.*, 1999; Bischoff *et al.*, 1999). There are twelve $GABA_{B1}$ variants (a-k including c-a and c-b) in total, the majority of which are secreted forms that may confer functional differences to the $GABA_{B1/B2}$ heterodimer (Tiao *et al.*, 2008).

It is very likely that the number of GPCR genes expressed in the PVN and SON in the DNA microarray studies outlined above is an underestimate, and would be expanded further by transcriptomic experiments on single neurons. High throughput, deep/next generation sequencing (e.g., RNASeq (Wang *et al.*, 2009a) of single cell cDNA libraries from pPVN, mPVN and SON neurons, similar to that reported for electrophysiologically identified warm sensitive neurons from the anterior hypothalamic pre-optic area (Eberwine and Bartfai, 2011), would reveal GPCR splicing complexity, rare GPCR transcripts and also those GPCR genes that are co-expressed (and thus are candidates for heterodimerization) in PVN/SON neurons.

1.3.6. Numbers of GPCRs in the PVN and SON: an overview

Embracing the data from the various detection methods outlined above we have arrived at a conservative estimate of the number of GPCRs expressed in the PVN and SON (Table 1.1). Of the 224 known non-chemosensory GPCRs in the rat genome 101 are present in the PVN (with a further 14 from unvalidated DNA microarrays), and 80 are present in the SON (excluding another 16 from unvalidated DNA microarrays). Interestingly, of the 132 orphan non-chemosensory GPCRs in the rat genome 22 (9 validated) and 24 (9 validated) are present in the PVN and SON, respectively. The GPCRs encompass the vast majority (33 that are activated by different peptide classes from 46 GPCR

families in total) of GPCR families excluding chemosensory and orphan GPCRs present in the rat genome (Table 1.2). The estimate includes a few instances where GPCR ligands appear to have functional effects (e.g., anaphylatoxin, formyl peptide, kisspeptin, leukotriene, melatonin, motilin, platelet-activating factor and trace amine receptors; see Supplementary Table 9) in the PVN/SON but their presence has not been confirmed by any of the detection criteria reviewed. It should also be emphasized that, as far as we are aware, none of the GPCR cDNAs/genes in the PVN and SON have been sequenced. Variations in GPCR sequences and/or potential splicing patterns may have an impact on the function of PVN/SON GPCRs.

GPCRs expressed in the PVN and SON	
Total number of known GPCRs*	224
Number of orphan GPCRs*	96 (class A), 29 (class B) & 7 (class C) = 132
Known GPCRs in rat PVN	94 + 7 based on functional criteria + 14 unvalidated arrays
Orphan GPCRs in rat PVN	9 by ISHH + 17 unvalidated arrays
Known GPCRs in rat SON	74 + 6 based on functional criteria + 16 unvalidated arrays
Orphan GPCRs in rat SON	9 by ISHH + 21 unvalidated arrays

Table 1.1. Summary of GPCRs expressed in the rat PVN and SON.

*Numbers based on lists in the on-line IUPHAR Database of Receptors and Ion Channels (http://www.iuphar-db.org/index.jsp) (Harmar *et al.*, 2009) excluding chemosensory (e.g., olfactory, vomeronasal, taste) receptors and possible spliced (see Supplementary Tables 5 and 6) GPCR variants.

GPCR families expressed in the PVN	
5-HT	***Melanocortin***
Acetylcholine muscarinic	Metabotropic glutamate
Adenosine	***Neuromedin U***
Adrenoceptor	***Neuropeptide FF***
Angiotensin	***Neuropeptide S***
Apelin	***Neuropeptide W***
Bombesin	***Neuropeptide Y***
Bradykinin	***Neurotensin***
Calcitonin	***Opioid***
Calcium-sensing	***Orexin***
Cannabinoid	P2Y
Chemokine	***Parathyroid hormone***
Cholecystokinin	***Peptide P518 (QRFP)***
Corticotropin-releasing factor	***Prokineticin***
Dopamine	***Prolactin-releasing peptide***
Endothelin	Prostanoid
E2	***Relaxin***
$GABA_B$	***Somatostatin***
Galanin	***Tachykinin***
Ghrelin	***Thyrotropin-releasing hormone***
Glucagon	***Urotensin***
Histamine	***VIP & PACAP***
Melanin-concentrating hormone	***Vasopressin and oxytocin***

Table 1.2. GPCR families expressed in the PVN

There are 46 GPCR families expressed in the PVN, including 33 different peptide classes (***in bold italics***). Notably absent are lipid-like GPCRs (e.g., lysophospholipids) which were detected in DNA microarrays but whose presence in the PVN (or SON) has not been validated, and the anaphylatoxin, formyl peptide, kisspeptin, leukotriene, melatonin, motilin, platelet-activating factor, and trace amine GPCRs for which there are functional responses in the PVN following central or peripheral administration of agonists, or in HNS cultures *in vitro*. The vast majority of GPCRs expressed in the PVN are also present in the SON- the exceptions are members of anaphylatoxin, formyl peptide, leukotriene, platelet-activating factor, and trace amine GPCRs which have not been demonstrated in the SON to our knowledge. To date members of the bile acid, free fatty acid, glycoprotein hormone, gonadotrophin-releasing hormone and hydroxyl acid GPCRs families do not appear to be expressed in either the PVN or SON.

1.4 Regulation of GPCR expression in the PVN and SON

There is ample evidence that GPCR expression can be regulated by, and contribute to changes in PVN and SON neuronal plasticity. Levels of GPCRs are determined in part by the rate of receptor protein synthesis, which can be regulated by either transcriptional or post-transcriptional mechanisms. Unless a reserve of "spare" receptors exists, alterations in cell surface or cytoplasmic GPCR levels can significantly influence receptor signalling capacity. GPCR signalling components (e.g., G proteins) themselves are also dynamically regulated (Kohout and Lefkowitz, 2003; Morris and Malbon, 1999), and ultimately GPCR expression and function is dependent on a host of factors that influence GPCR desensitization (e.g., following chronic activation of many GPCRs), redistribution and degradation. The role of many intracellular signalling molecules (such as GRKs and arrestins) is critical in

regulating these processes. RNA regulation is also very complex, with small RNA molecules like microRNAs (miRs) and piwi-interacting RNAs linked to transcriptional silencing, and long non-coding RNAs involved in transcriptional, post-transcriptional (e.g., RNA alternate splicing, translation) and epigenetic regulation (Licatalosi *et al.*, 2010).

The apparent absence, or low levels of GPCR expression does not preclude the possibility that some GPCRs may be induced by perturbations of PVN and/or SON neuronal function (e.g., change in osmolality, lactation, stress) as in the case of the CRF_1 receptor (Luo *et al.*, 1994). Changes in mRNA levels are usually easier to detect by ISHH compared to changes in protein as measured by IHC, but this obviously depends on when the mRNA is assayed after experimental manipulations, since GPCR mRNA turnover may vary considerably. GPCR mRNA and protein turnover has been primarily established in cell lines expressing native or cloned GPCRs and could be quite different in the PVN/SON microenvironment. Half-lives are highly variable and often cell context-dependent, ranging from around 2-20 hours for both GPCR mRNA (e.g., acetylcholine m_1 (Lee *et al.*, 1994), α_1-adrenoceptor (Izzo *et al.*, 1990), α_1-adrenoceptor (Sakaue and Hoffman, 1991), β_2-adrenoceptor (Hadcock *et al.*, 1989), leukotriene BLT_1 (Stankova *et al.*, 2002) receptors) and GPCR protein at the cell surface (adenosine $A_{1/2A/2B/3}$ (Klaasse *et al.*, 2008), $\alpha_{2A/2B/2C}$-adrenoceptor (Saunders and Limbird, 1997; Wilson and Limbird, 2000), β_2-adrenoceptor (Drake *et al.*, 2006), calcium-sensing CaS (Cavanaugh *et al.*, 2010), cannabinoid CB_1 (McIntosh *et al.*, 1998) receptors). The mRNA turnover for a number of GPCRs is also decreased by agonist stimulation (Coon *et al.*, 1997; Hadcock *et al.*, 1989; Izzo *et al.*, 1990; Lee *et al.*, 1994), emphasizing the importance of local agonist levels in the PVN and SON in regulating both GPCR mRNA and protein levels. In a few of these studies, in contrast to research on GPCR mRNA expression in the PVN and SON, nuclear run-on experiments (requiring a million cell nuclei or more) were used to confirm that changes in mRNA levels were the result of changes in GPCR gene transcription. Nuclear run on experiments provide a measure of the frequency of transcription initiation and are largely independent of the effects of RNA stability. Interestingly, other studies using hybridization of DNA microarrays with steady-state mRNA versus newly transcribed (nuclear run on) RNA have shown that approximately half of stress-regulated genes in H1299 lung carcinoma cells are due to changes in gene transcription with a similar fraction due to changes in mRNA turnover (Fan *et al.*, 2002). A point that may be relevant to possible GPCR co-expression and cross-talk in the PVN and SON is that the angiotensin AT_1 receptor induces bradykinin B_2 receptor transcription activation via the phosphorylation of cAMP response element binding protein (CREB) and assembly of p-CREB on the B_2 receptor promoter in kidney collecting duct cells (Shen *et al.*, 2007).

An alternative method to look at gene transcription rates, and one that is particularly amenable to tissue sections of PVN and SON, is to examine heteronuclear (hn)RNA levels. The binding of probes specific for introns in RNA-coding region of genes can be used to quantify hnRNA levels as an indirect measurement of the transcription rate of genes in response to a particular stimulus. For GPCR genes that contain multiple introns care must be exercised in choosing which introns to target because they can be excised from the nascent pre-mRNA at different rates (Lang and Spritz, 1987). ISSH with intron-specific probes has been successfully used to measure hnRNA changes for relatively abundant neuropeptide (e.g., VP, OT and to a lesser extent CRF (Herman *et al.*, 1991; Kovács and Sawchenko, 1996; Yue *et al.*, 2008)) mRNAs, but has not proved particularly useful to assess GPCR transcriptional activity. One exception is the dopamine D_2 mRNA distribution in the brain where hnRNA levels are (as expected) a fraction of steady-state mRNA levels (Fox *et al.*, 1993).

There are numerous studies showing that the expression of PVN/SON neuropeptides, in particular VP, OT and CRF, are developmentally regulated (Altstein *et al.*, 1988; Baram and Lerner, 1991; Szarek *et al.*, 2010), and that their expression can be altered by experimental manipulations (Burbach *et al.*, 2001; Aguilera *et al.*, 2008). In comparison, reports of ontogenetic variations in GPCR expression in the PVN/SON are scarce, with the transcript or protein level, and/or function of a few GPCRs including the angiotensin II AT_{1a} (mRNA present in PVN E19 onwards (Nuyt *et al.*, 2001)), neuropeptide Y_1 (mRNA present in PVN P2 onwards coincident with a significant increase in NPY-containing fibres innervating the nucleus (Grove *et al.*, 2003)), and melanocortin MC_4 (mRNA present in PVN and SON at E18 and P27, respectively, approximating the appearance of melanocortin binding sites (Kistler-Heer *et al.*, 1998; Lichtensteiger *et al.*, 1996)) changing developmentally. At least one GPCR in the PVN and SON is also diurnally regulated - α_2-adrenoceptor expression in the PVN peaks at the onset of dark (when CORT levels are highest) whereas in the SON the reverse diurnal pattern is observed (Jhanwar-Uniyal *et al.*, 1986).

There have been many studies using receptor ARG, IHC or ISHH to demonstrate alterations in GPCR expression by pharmacological or physiological manipulations. More recently, transcriptome approaches have established that dehydration alters the levels of transcripts encoding the cannabinoid CB_1, $GABA_{B1j}$, melanocortin MC_4, protease-activated PAR1 and somatostatin sst_3 receptors in the rat SON (Hindmarch *et al.*, 2006). Changes in GPCR protein and mRNA levels in the PVN/SON in response to agonist or antagonist administration, or physiological perturbations such as adrenalectomy, salt-loading, dehydration, lactation, gestation and stress are commonly less than two-fold, but 8-10-fold or higher increases in GPCR mRNA have been reported in some instances - e.g., for the apelin APJ receptor (O'Carroll *et al.*, 2003) (see Supplementary Table 8). Invariably gene or protein expression has been imaged over the entire PVN and/or SON, so any change in cell-to-cell GPCR

expression is often obscured. Importantly, since the vast majority of studies investigate a single experimental time point, it is surprising to note how often it is assumed that changes in GPCR mRNA reflect changes in GPCR protein levels and perhaps receptor function. That this may not always be the case is emphasized in studies where the correlation between mRNA and protein levels has been investigated using transcriptomic- in conjunction with proteomic- approaches. For example, in kidney inner medullary duct cells a large number (approx.1/3) of proteins that showed significant changes in abundance in kidney inner medullary collecting duct cells following challenge with dDAVP (desmopressin; a VP V_2 receptor agonist) did not show any changes in the corresponding mRNA species (measured by interrogating DNA microarrays) (Khositseth *et al.*, 2011). While this result relies heavily on the quantitative accuracy of the methods used, it conceivably highlights an important role in post-transcriptional regulation of protein abundance, and also obviously reflects the dynamics of mRNA versus protein turnover. Impressively, given that the half-life of GPCR mRNA or protein is usually not known, a number of studies have combined receptor ARG (or in some cases IHC) with ISHH to show that alterations in GPCR mRNA levels in the PVN/SON are associated with changes in the corresponding GPCR protein. A few examples of this are the increases in angiotensin AT_{1A} receptor after antagonist administration (Macova *et al.*, 2009; Wei *et al.*, 2009), and cholecystokinin CCK_1 and CCK_2 (Hinks *et al.*, 1995; Meister *et al.*, 1994), and galanin GAL_1 (Burazin *et al.*, 2001) receptors following osmotic perturbations.

There are other, largely unexplored and speculative ways in which GPCRs in the PVN and SON could possibly be regulated. One such mechanism is miR-mediated post-transcriptional regulation. There is substantial evidence that the 3'-UTR of proteins can affect mRNA stability and is involved in regulating gene expression at the post-transcriptional level, and in the case of some GPCRs such as the opioid receptors the length of the 3'-UTR influences receptor protein level (Wu *et al.*, 2008). MiRs are short, single-stranded non-protein coding RNAs that tend to suppress target gene expression by binding to their complementary mRNA sequences usually in introns or exons of the 3'-UTR, and have emerged as crucial modulators of gene expression especially in synaptic plasticity. The feasibility of mIR-mediated GPCR mRNA regulation has been demonstrated by miR-23b inhibition of opioid μ receptor expression (Wu *et al.*, 2008). Conversely, opioid μ receptor agonists regulate miR-190 activity (Zheng *et al.*, 2010b). Scanning individual GPCRs for consensus miR binding sites that are conserved between species would be a starting point for studies on the potential role of miRs in regulating PVN/SON GPCRs. It is also becoming increasingly clear that epigenetic control of gene (especially CRF and VP) expression in the PVN is important in the HPA axis response to stress (e.g., see (Elliott *et al.*, 2010; Murgatroyd *et al.*, 2009). DNA methylation and histone modifications have been shown to coincide with the differential expression of the opioid μ receptors in the brain (Hwang *et al.*, 2007).

As noted previously, some GPCRs have very low expression levels (e.g., <1000 receptor copies/cell) and ultimately the demonstration of a ligand-specific function is paramount. For those GPCRs investigated, a functional response has generally been observed where GPCR binding sites, ir-protein and/or mRNA have been detected in the PVN/SON.

1.5 Functions of GPCRs in the PVN and SON

The actions of numerous neurotransmitters, neuropeptides and hormones in the PVN and SON have been well documented (e.g., (Bealer *et al.*, 2010; Cunningham and Sawchenko, 1991; Hatton, 1990; Ludwig, 1998; Ludwig and Leng, 2006; Renaud and Bourque, 1991; Sladek, 2000; Swanson and Sawchenko, 1983) and only some salient features will be described here. The tonic and stimulated activity of the PVN and SON is regulated by a number of excitatory and inhibitory neurotransmitters and neuromodulators, including glutamate and GABA, the main excitatory and inhibitory neurotransmitters, respectively, as well as a host of other effectors including angiotensin II, catecholamines, histamine and numerous other neuropeptides that activate GPCRs, and mediators such as humoral factors and nitric oxide (e.g., (Brunton *et al.*, 2008a; Brunton *et al.*, 2008b; Engelmann and Ludwig, 2004; Itoi *et al.*, 2004; . Kalra and Kalra, 2004; Li *et al.*, 2010; Sladek, 2000; Ulrich-Lai and Herman, 2009). This regulation can occur directly in the PVN or SON via the effects of neurotransmitters/neuropeptides synthesized within the two nuclei and/or indirectly by interactions with glutamatergic or GABAergic interneurons or afferent projections from other hypothalamic or extrahypothalamic areas that innervate the PVN or SON (Ferguson, 2009; Joëls and Baram, 2009; Sladek, 2000). Apparent mismatches between neurotransmitters/neuropeptides and their receptors that are prevalent in the brain (Herkenham *et al.*, 1987) may not be such an issue in the PVN and SON where GPCR ligands are available from a number of sources within the nuclei or extra-PVN/SON locations.

In addition to their peptidergic or neurotransmitter phenotypes, neurons in the pPVN, and mPVN and SON have defined electrophysiological characteristics. Classically, under basal conditions OT magnocellular cells are continuously active, whereas the activity of VP magnocellular cells ranges from continuously active to robust phasic to relatively silent (Brown *et al.*, 2007; Ludwig and Leng, 2006). Early studies indicated that mPVN and SON neurons have similar electrophysiological properties (Armstrong *et al.*, 1994; McKenzie *et al.*, 1995; Tasker and Dudek, 1991) whereas pPVN cells exhibited electrophysiological heterogeneity (Tasker and Dudek, 1991). Neurosecretory neurons concentrated in the medial pPVN have no low threshold spike (LTS) and small T-type calcium currents while in non-neurosecretory cells in the dorsal and ventral pPVN the converse is true (Luther

et al., 2002). In magnocellular cells bursts of activity often characterize periods of enhanced neuropeptide release. For example, during suckling in the lactating rat and in pregnant animals OT magnocellular neurons discharge synchronously to release large amounts of OT into the systemic circulation which is dependent on dendritic OT release (Lincoln and Wakerley, 1974; Ludwig and Leng, 2006), and VP magnocellular cells increase their firing (and may switch to phasic activity) to release VP following dehydration (Leng *et al.*, 2008; Wakerley *et al.*, 1978) and hemorrhage (Wakerley *et al.*, 1975).

The effects of GPCR ligands on PVN and SON neuronal function can be direct or indirect depending upon whether they are administered peripherally, centrally via the circumventricular organs, or intra-nuclei by injection or iontophoretic application. It should be borne in mind that high doses of GPCR agonists may give 'pharmacological' rather than physiological responses, especially when compounds are applied in the vicinity of their presumed site of action. GPCR activation in the PVN/SON has been demonstrated in a number of ways. These include increases in neuronal immediate early gene (e.g., c-Fos) activation, changes in electrophysiological characteristics or neuropeptide mRNA or protein levels (e.g., by ISHH, IHC or content of push-pull perfusates or microdialysates), and alterations in any number of physiological end-points such as plasma VP, OT, CRF and ACTH release, water and energy homeostasis, cardiovascular parameters, nociception and behaviour (see Supplementary Table 9 for some examples). The specificity of the ligand-GPCR interaction is usually demonstrated by the inhibition of responses with GPCR-selective antagonists or, as in a few cases, by immunoneutralization with neuropeptide/GPCR antibodies (e.g., for NPFF effects on VP release (Yokoi *et al.*, 1998)), and more recently by RNA interference-driven gene silencing that has the added advantage over acute administration of synthetic small interfering (si)RNAs of long-term (days-months) GPCR knockdown if viral, GPCR-specific small hairpin (sh)RNA constructs are employed. The sustainable expression of such constructs obviates some of the problems that may be encountered with long GPCR mRNA turnover rates.

1.5.1. General features of GPCR function in the PVN and SON

With amplification procedures used in various GPCR detection techniques, an important question is what level of GPCR mRNA or protein is physiologically relevant? Radioligand- or fluorescent-ligand binding assays can detect as few as about 50-100 GPCRs per cell (e.g., see Mahan and Insel, 1986) which is sufficient to elicit (although higher levels are probably required to sustain) a signal transduction response in some *in vitro* systems (Sklar *et al.*, 1985). In PVN and SON neurons *in vivo* some GPCRs may be clustered to concentrate their levels at pre- or post-synaptic sites. A number of studies underscore the differences in the sensitivity/specificity of detection techniques used between laboratories, and highlight the importance of obtaining (specific) functional GPCR responses. For example, while VP V_2 receptor mRNA was not detected in the PVN or SON by nested PCR in one

study (Hurbin *et al.*, 1998), V_2 receptor mRNA (by PCR on RNA obtained from 20 neurons), and V_2 receptor protein and apparent functional responses have recently been reported in isolated cells from the SON (Sato *et al.*, 2011). Similarly, the lack of angiotensin II AT_{1A} receptor gene expression in the mPVN by ISHH in some studies (e.g., (Lenkei *et al.*, 1998) appears at odds with the AT_1-type pharmacological responses observed by electrophysiology in PVN slices (Latchford and Ferguson, 2004. Furthermore, prostanoid EP_3 receptor electrophysiological responses have been observed in the SON (Shibuya *et al.*, 2002) where no ir-EP_3 receptor cell bodies or fibres have been found (Nakamura *et al.*, 2000).

It is possible that some of the GPCR effects in the PVN or SON are spurious or redundant in nature, since it is difficult to envisage that every GPCR we have listed (see Tables 1.1 and 1.2) has an important role in co-ordinating control of PVN and/or SON function. We are reminded of a comment attributed to Alfred Gilman a number of years ago: "A typical cell has perhaps 50 different receptors, and the cell doesn't pay attention to just one receptor at a time. How does it know how to interpret the signal from one hormone when it's listening to 45 other ones at the same time? How does the whole signalling system work as a network? That's what we want to find out" (Lemonick *et al.*, 2001). Functional studies of GPCRs indicate that they do have individual roles in the PVN and SON and are probably key to neurones intergrating multiple functions as outline below (see Supplementary Table 9).

Change in the levels of intracellular signal transduction molecules (see Section 1.3.1) and immediate early gene activation (Ho *et al.*, 2009; Hoffman *et al.*, 1993) are frequently used as indices of neuronal activity in the PVN and SON, and are particularly amenable to cell imaging techniques. For example, agonist-induced increases in intracellular calcium or ERK activation have been shown for 5-HT_{1A} (Crane *et al.*, 2007), α_{1A}-adrenoceptor (Song *et al.*, 2010), dopamine D_4 (Bitner *et al.*, 2006), melanocortin MC_4 (Sabatier and Leng, 2006), purinergic $P2Y_1$ (Song *et al.*, 2007), OT (Blume *et al.*, 2008; Lambert *et al.*, 1994; Sabatier and Leng, 2006), VIP/PACAP (Dayanithi *et al.*, 2000) and VP V_{1A} (Gouzénes *et al.*, 1999) receptors. These are often accompanied by increases in PVN or SON c-Fos expression, as demonstrated for many GPCRs such as the 5-$HT_{2A/2C}$ (Lee *et al.*, 2009), CRF_1 (Parkes *et al.*, 1993), dopamine D_4 (Bitner *et al.*, 2006), glucagon GLP-1 (Larsen *et al.*, 1997), melanocortin MC_4 (Kawasaki *et al.*, 2009), motilin (Wu *et al.*, 2005), neuropeptide FF/neuropeptide AF NPFF1 (Jjamandas and MacTavish, 2003), prolactin-releasing peptide PRRP (Matsumoto *et al.*, 2000; Yamada *et al.*, 2009) and tachykinin NK_3 (Kawasaki *et al.*, 2009) receptors. One of the most extensively studied functional aspects of GPCRs in pPVN presympathetic, mPVN and SON neurons, is their often profound affects on neuronal excitability, examples of which are shown in Supplementary Table 9, and include presynaptic effects mediated via metabotropic glutamate receptors (Boudaba *et al.*, 2003a,2003b; Schrader and Tasker, 1997) and endocannabinoids (acting through

cannabinoid CB_1 receptors) (Di *et al*, 2005; Sabatier and Leng, 2006) in the SON, and GABA release in presympathetic pPVN neurons (Chen *et al.*, 2006; Li *et al.*, 2005).

GPCR activation in the PVN/SON can alter neuropeptide or GPCR gene synthesis (e.g., see (Al-Barazanji *et al.*, 2001; Fekete *et al.*, 2001, 2002; Konishi *et al.*, 2003; Morris *et al.*, 2000; Wei *et al.*, 2001)) and/or the release of neurotransmitters/neuropeptides from dendrites and/or axon terminals. Local dendritic release of neuropeptides acting in an autocrine or paracrine fashion are likely to be important factors in determining the sensitivity and plasticity of PVN and SON neurons to their multitude of inputs (Landgraf and Neumann, 2004; Ludwig, 1998; Ludwig and Leng, 2006; Morris *et al.*, 2000). Dendritic peptides may also regulate local blood flow (Alonso *et al.*, 2008) and have local (e.g., OT is anxiolytic via the PVN OT receptor (van den Burg and Neumann, 2011) and distant effects on behaviour (Ludwig and Leng, 2006). Examples of GPCRs that modulate neuropeptide release, typically performed in studies measuring VP and/or OT release from large magnocellular cells, rather than CRF release from the smaller pPVN neurons, include the α_1-adrenoceptors (inhibit intra-PVN hypoxia-induced CRF release) (Chen *et al.*, 2004)), apelin APJ (increases firing rate of VP neurons and VP dendritic release) (Tobin *et al.*, 2008b)), histamine $H_{1/2}$ (increases dendritic release of OT via stimulating noradrenaline release) (Bealer and Crowley, 1999), melanocortin MC_4 (increases calcium in OT neurons; stimulation of dendritic, and inhibition of terminal OT release) (Ludwig and Leng, 2006; Sabatier *et al.*, 2003), κ opioid (locally released dynorphin inhibits VP neurons and is essential for expression of VP neuron phasic activity; inhibits VP terminal release) (Brown and Bourque, 2004; Brown *et al.*, 2007), VIP/PACAP (stimulates somatodendritic and terminal VP release (Lutz-Bucher *et al.*, 1996; Shibuya *et al.*, 2008)), VP V_{1A} (acting on autoreceptors to excite and inhibit quiescent and phasic VP neurons, respectively (Brown *et al.*, 2004; Ludwig and Leng, 1997, 2006)), and OT (stimulates dendritic OT release via OT receptor; inhibits OT neurons by increasing endocannabionoid inhibition of glutamate release (Ludwig and Leng, 2006)) receptors.

The release of neurohypophysial hormones from posterior pituitary nerve terminals, and CRF and other pPVN products from the median eminence into the anterior pituitary portal circulation is often reflected by increased circulating levels of VP and OT, ACTH (due to the action of CRF, VP and other ACTH secretagogues) and CORT, and thyroid hormones, and in changes in water homeostasis (principally brought about by altered VP secretion) (Supplementary Table 9 gives some examples). GPCRs can also modulate autonomic functions by activating secretory and non-secretory pPVN neurons. For example, central or intra-PVN administration of a number of GPCR ligands results in orexigenic (e.g., ghrelin (Shrestha *et al.*, 2009), galanin (Kyrkouli *et al.*, 1990), and NPY agonists via Y_1 and Y_5 (Kalra and Kalra, 2004) receptors) or anorexigenic (e.g., via CRF_1 (Heinrichs *et al.*, 1993), melanocortin MC_4 (Garza *et al.*, 2008), neuropeptide S NPS (Fedelli *et al.*, 2009), and neuromedin U (Wren *et al.*, 2002) receptors) effects, and alter cardiovascular parameters (e.g., angiotensin AT_1

(Bains *et al.*, 1992), CRF_2 (Li *et al.*, 2010), tachykinin NK3 (Takano *et al.*, 1993), and urotensin II UT (Watson *et al.*, 2008) receptors), nociception (e.g., α-adrenoceptors (Zhou *et al.*, 2010)), body temperature (e.g., acetylcholine muscarinic receptors (Takahashi *et al.*, 2001), and penile erection (e.g., dopamine receptors (Succu *et al.*, 2007).

1.5.2. Possible GPCR co-expression in the PVN and SON

We do not know how many GPCRs are co-expressed in PVN/SON neurons, and different complements of GPCRs may be expressed in subsets of neurons such as magnocellular VP cells with different basal electrical activity, magnocellular neurons with different neuropeptidergic phenotypes, mPVN versus pPVN neurons, or pPVN endocrine versus non-endocrine neurons. However, extrapolating from the study on single warm-sensitive neurons (transciptomic analysis gave 168 non-olfactory GPCRs of which 27 are orphans (Eberwine and Bartfai, 2011) suggests that the number of co-expressed GPCRs is likely to be larger than the number of co-expressed neuropeptides. At least 20 different neuropeptides are co-expressed in magnocellular VP or OT neurons (Bundzikova *et al.*, 2008) but the extent of the total overlap is unknown. The co-expression of GPCRs raises the question of possible functional consequences of receptor oligomerization in the PVN and SON. The formation of functional $GABA_B$ receptors from two $GABA_B$ subunits is an example of GPCR heterodimerization that we know occurs in the PVN and SON (Zhong *et al.*, 2008). Of the GPCRs listed in Supplementary Table 4, there is also a high degree of colocalisation of $5HT_{1A}$ and $5HT_{2A}$ in OT and CRF neurons in the PVN where activation of one receptor subtype may induce the desensitization of the other (Zhang *et al.*, 2004). There are many examples of apparent GPCR homodimerization and heterodimerization in the literature (Milligan, 2009), and a number of consequences of GPCR oligomerization such as changes in receptor expression, compartmentalization, recycling, turnover and degradation have been noted mainly in *in vitro* studies (Franco *et al.*, 2009; Springael *et al.*, 2007). Assuming that oligomerization is relatively stable, co-expressed GPCRs may allow graded regulation of a population of functionally equivalent neurons in the PVN and SON, as receptor ratios and the levels of their corresponding ligands vary as a function of the physiological and pharmacological state. This could mean that with oligomerization between GPCRs of the same subclass it is possible that the heterodimer acts as a 'concentration-dependent switch' where one GPCR is activated by low agonist concentrations whereas the other is activated by higher agonist concentrations (e.g., see co-expressed adenosine $A_{1/2A}$ receptors (Ciruela *et al.*, 2006); note that the four adenosine receptor subtypes are all possibly expressed in the PVN (see Supplementary Table 4)). The signalling of one GPCR could be shut down while the other is active, e.g., by internalization of the 'inactive' GPCR. Moreover, the heterodimer may have new signalling modalities e.g., switching to coupling to a new G protein to activate a new signalling pathway (e.g., see co-expressed dopamine receptors (Lee *et al.*, 2004). To add to the complexity, GPCRs may also physically associate with non-GPCRs e.g., the dopamine D_5

receptor and the $GABA_A$ γ2 ligand-gated ion channel subunit appear to complex leading to an attenuation in D_5 receptor-mediated cAMP accumulation and $GABA_A$-mediated current (Liu *et al.*, 2000).

1.5.3. Possible function of orphan GPCRs

Some orphan GPCRs, or indeed some GPCRs with known endogenous ligands, may be constitutively active in the PVN and SON. This is not as far-fetched as it may seem since constitutive activity in GPCRs is a relatively well-known phenomenon that can be signalling pathway-dependent, and can result from the overexpression of receptors in native tissue or heterologous systems, and/or by changes in the DNA (introduced or somatic mutations) or RNA (*visa vi* RNA editing as in the 5-HT_{2C} receptor (Marion *et al.*, 2004) sequence of GPCRs. For example, isoforms of the histamine H_3 receptor are constitutively active pre- and post-synaptically in native brain cortical tissue (Morisset *et al.*, 2000), and in cell lines α_{1A}- and α_{1B}-adrenoceptors (which can heterodimerize) (Cotecchia, 2010), bradykinin B_2 (Quitterer *et al.*, 1996), ghrelin (Holst *et al.*, 2004), melanocortin MC_4 (Nijenhuis *et al.*, 2001) and neurotensin NTS_2 (Holst *et al.*, 2004) receptors exhibit constitutive activity, and co-expression of the constitutively active histamine H_1 receptor with the 5-HT_{1B} receptor confers constitutive activity on the latter receptor (Bakker *et al.*, 2004). All these GPCRs are expressed in the PVN and SON. The orphan GPCRs GPR3, 6, 12, 20, 26 (present in SON by DNA microarrays), 39, 61 (present in PVN and SON by DNA microarrays) and 78 also alter basal signal transduction activity when expressed *in vitro* (Holst *et al.*, 2004; Jones *et al.*, 2007; Tanaka *et al.*, 2007; Toyooka *et al.*, 2009). Although we may be able to predict changes in GPCR activity based on altered GPCR sequences, the demonstration of constitutive activity in the PVN and SON needs to be functionally-based. A component of the high, basal [^{35}S]GTPγS labelling in the rat PVN (Aaltonen *et al.*, 2008) may reflect constitutive basal activity of known and/or orphan GPCRs. Highly expressed, constitutively active GPCRs may account in part for the molecular mechanisms regulating signal transduction effectors in PVN/SON neurons. Some of these molecules e.g., cAMP, calcium, have key roles in axonal growth of developing or regenerating neurons (e.g., (Ming *et al.*, 1997)). Constitutive activity may also underlie ligand-independent functions of orphan GPCRs such as involvement in GPCR heterodimerization and altering target GPCR function - an example of this is the orphan GPCR GPR50 heterodimerizing with the melatonin MT_1 receptor to inhibit its activity (see (Levoye *et al.*, 2006)). In fact, constitutive activity is observed in the PVN and SON. For example, nitric oxide (whose generation is enhanced by many GPCR agonists, and is generally considered to be an inhibitor of PVN and SON activity (Stern *et al.*, 2004)), constitutively restrains ongoing firing in SON neurons (Stern and Zhang, 2005). As to GPCR-'specific' effects, very recently the melanocortin MC_4 receptor was shown to be constitutively active in the mouse PVN (Ghamari-Langroudi *et al.*, 2011).

There are a number of candidate substances that may be ligands for orphan GPCRs expressed within the PVN and SON. These include peptides that modulate PVN/SON function and/or are perhaps expressed in mPVN and SON, or pPVN neurons. Various peptides derived from larger precursor molecules (and isolated by proteomic methods) are expressed in the PVN/SON, such as: (1) the neuroendocrine regulatory peptides (NERPS-1/2), which are products of the VGF gene that colocalise with VP in the storage granules of the PVN and SON of both rats and humans, and suppress basal, hypertonic saline- or angiotensin II-induced VP release (Toshinai *et al.*, 2009; Yamaguchi *et al.*, 2007); (2) neuronostatin, a product of the somatosatin gene that depolarizes or hyperpolarizes PVN magnocellular, parvocellular or preautonomic neurons and administered centrally increases blood pressure and decreases food intake and water drinking (Samson *et al.*, 2008); (3) nesfatin-1, an amino-terminal fragment derived from NEFA/nucleobindin 2 (NUCB2) (García-Galiano *et al.*, 2010) that is present in VP and OT neurons (Brailoiu *et al.*, 2007), elevates intracellular calcium in dissociated hypothalamic (Brailoiu *et al.*, 2007) and isolated PVN (Maejima *et al.*, 2009) neurons, alters the electrophysiological properties of PVN neurons (Price *et al.*, 2008a), increases OT release from PVN tissue slices (Maejima *et al.*, 2009) and administered centrally increases c-Fos in the PVN/SON and decreases food intake via an OT-dependent, leptin-independent melanocortin pathway (Maejima *et al.*, 2009; García-Galiano *et al.*, 2010) (note that it has been reported that nesfatin activates GPR12 (Mori and Eguchi, 2009), an orphan GPCR which exhibits constitutive activity (Tanaka *et al.*, 2007)); and (4) augurin, a product of the c2orf40 gene which encodes the oesophageal cancer-related gene 4 (ECRG4) protein) (Tadross *et al.*, 2010) that is present in PVN and SON OT and VP neurons (Robertson *et al.*, 2009), increases VP and CRF release from hypothalamic explants and elevates plasma ACTH levels when administered centrally or intra-PVN (Tadross *et al.*, 2010). It is interesting to note that peptidomics of the rat SON has identified 20 unique peptides from known pro-hormones (Bora *et al.*, 2008). Candidate orphan GPCR ligands are not restricted to peptides and their by-products and post-translationally modified counterparts, but could also include compounds such as steroids (e.g., glucocorticoids) that are known to interact with the PVN/SON. There are a number of 'fast', apparently non-genomic effects of steroids (Losel *et al.*, 2003) and their metabolites (e.g., see (Neuhaus *et al.*, 2009)) that may be mediated by GPCRs, including chemosensory receptors, in the PVN/SON and other brain regions.

1.6 Steroids

1.6.1 Steroids, nuclear receptors, and genomic interactions

Steroids are hormones derived from a common cholesterol backbone. There are two major classes of steroid hormones: the sex steroids (progestogens, E2s, androgens) and adrenal steroids (glucocorticoids, and mineralocorticoids). Sex steroids reaching the circulation are mainly synthesised and released from the gonads (progestogens and E2s from the ovaries, and androgens from the testis), but they (particularly androgens) and/or their precursors (which are converted into active forms in central and peripheral tissues) are also excreted by the adrenal glands (de Ronde, 2003; Feder *et al.*, 1967; Beato and Klug, 2000). Sex steroids are imperative in the differentiation of the embryonic reproduction system, and brain gender assignment at birth, and dictate adult secondary sexual characteristics, and control reproduction and reproductive behaviour (Evans, 1988). The adrenal steroids are synthesised and released from the adrenal cortex and are heavily implicated in maintaining homeostasis, regulating for example, the neuroendocrine stress response, metabolism, water and solute secretion, and the immune system (Evans, 1988).

The effects of steroid are mediated by nuclear receptors which are part of a family of evolutionary-related, DNA-binding transcription factors that also respond to other signalling molecules including vitamin D3, retinoids, and thyroid hormones (Germain *et al.*, 2006; Huang *et al.*, 2010). The structure of nuclear receptors are characterised by an N-terminal which contains the ligand-independent activation function (AF-1; a transcriptional activation surface), a highly conserved DNA binding domain (DBD), followed by a hinge region, and then a moderately conserved ligand binding domain (LBD) which contains the C-terminus and the ligand-dependent transactivation function (AF-2; a second transcriptional activation region) (Beato and Klug, 2000; Wierman, 2007). The receptors are also split up into seven regions (A-F) which is reminiscent of the original nomenclature assigned following comparisons between the first cloned nuclear receptors (the human E2 receptor α (ERα/NR3A1), human glucocorticoid receptor (GR/NR3C1), and chicken ERα) - subsequent functional and structural analysis revealed that these regions were components of the functional domains described above (see Figure 1.2) (Beato and Klug, 2000; Wierman, 2007).

Nuclear receptors have been classified into six evolutionary groups of which steroid receptors are members of the third group – hence each official receptor name (as annotated by NC-IUPHAR and the Nuclear Receptor Nomenclature Committee, 1999) begins with nuclear receptor 3 (NR3) e.g., androgen receptor's official name is NR3C4 (trivial name AR) (note: for simplicity, nuclear receptor will be referred to by their trivial names henceforth in this dissertation). The remaining nomenclature is representative of the three subgroups within the nuclear receptor 3 group: (A), NR3A1 (ERα) and NR3A2 (E2 receptor β (ERβ)); (B), NR3B1 (E2-related receptor alpha (ERRα) and NR3B2 (E2-

related receptor alpha (ERRβ); and (C) NR3C1 (GR), NR3C2 (mineralocorticoid receptor (MR)), NR3C3 (progesterone receptor (PR)), and NR3C4 (AR).

In their inactive state, the steroid receptors are associated with a multimeric complex of proteins that include heat shock proteins (e.g., heat shock protein 90) and immunophilins (e.g., Hsp56) (Pratt and Toft, 1999). Subsequent to ligand interaction, steroid receptors typically form homodimers (although the orphan receptors ERRα/β also bind DNA as monomers, ERα and ERβ possibly form heterodimers, and GR has been shown to form heterodimers with unrelated transcription factors e.g., nuclear factor kappa B), and translocate to the nucleus where they bind to two specific palindromic genomic sequences (hormone response elements) within the promoters of target genes (Beato and Klug, 2000; Falkenstein *et al.*, 2000). Whether steroid receptors activate or silence gene transcription is dependent on the recruitment of co-activators (e.g., steroid receptor co-activator-1 (SRC-1), and CREB) or co-repressors (e.g., nuclear receptor co-repressor 1 (NCOR1), and silencing mediator for retinoid and thyroid hormone receptors (SMRT/NCOR2)) (Beato and Klug, 2000).

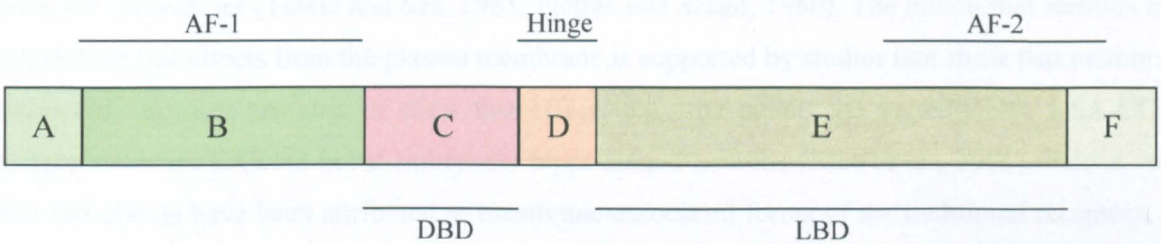

Figure 1.2. Schematic diagram representing the modular structure of steroid receptors.

The structure of nuclear receptors are characterised by: 1) an N-terminal which contains the ligand-independent activation function (AF-1; a transcriptional activation surface); 2) a highly conserved DNA binding domain (DBD); 3) followed by a hinge region (D); 4) and then a moderately conserved ligand binding domain (LBD) which contains the C-terminus and the ligand-dependent transactivation function (AF-2; a second transcriptional activation region). The LBD may bind ligands, co-activators and co-repressors, and along with the DBD and hinge region, dock to the multimeric complex of proteins such as heat shock proteins etc, when in the inactivated state. The receptors are also split into seven regions (A-F) which is reminiscent of the original nomenclature assigned following comparisons between the first cloned nuclear receptors.

1.6.2 Fast effects of steroids

In addition to their genomic effects, it is well recognised that steroids also have rapid non-genomic actions (Falkenstein *et al.*, 2000). Non-genomic effects are typically characterised by a rapid onset, insensitivity to inhibitors of transcription (e.g., actinomycin D) and translation (e.g., cycloheximide), and interaction with transduction cascades e.g., mobilisation of intracellular calcium, increase in adenylyl cyclase activity, and stimulation of the ERK1/2, phosphoinositide 3-kinase (P13K), and PLC pathways. Fast non-genomic effects have been described for all of the main steroid groups, for example: progesterone induces a rapid increase in intracellular calcium in frog oocytes, E2 hyperpolarises the postsynaptic membranes of rat medial amygdala neurones, testosterone increases ERK1/2 phosphorylation in rat muscle fibres within 5 min of administration, aldosterone (ALD) rapidly stimulates inositol triphosphate (IP_3) generation in human leukocytes, and CORT rapidly reduces mouse leydig cell cAMP content (Wasserman *et al.*, 1980; Nabekura *et al.*, 1986; Estrada *et al.*, 2003; Christ *et al.*, 1993; Dong *et al.*, 2004).

There are numerous reports of steroid binding sites on the plasma membrane e.g., [^{3}H]-testosterone binds to synaptic plasma membranes prepared from rat brain, and [^{3}H]-E2 binding sites are found on hepatocyte membranes (Towle and Sze, 1983; Pietras and Szego, 1980). The notion that steroids may mediate their fast effects from the plasma membrane is supported by studies that show that membrane impermeable steroids are able to elicit fast effects e.g., the membrane impermeable BSA-CORT conjugate activates ERK1/2 in rat embryonic hippocampal neurons (Xiao *et al.*, 2005). Indeed some of the fast effects have been attributed to membrane-associated forms of the traditional receptors, for example ERβ agonists increase cAMP production in immortalized GnRH neuronal cells (Hu *et al.*, 2008). These extranuclear receptors are thought to be localised to isolated caveolae rafts which are also part of a much larger signalsome complex consisting of many other signal proteins including G proteins, growth factor receptors (EGFR, Insulin-like growth factor 1 receptor), non-growth factor tyrosine kinases (Src, Ras), linker proteins (modulator of non-genomic actions of steroid receptors, striatin), and GPCRs (Hammes and Levin, 2007). On the other hand, there are also instances where fast effects of steroids appear to occur independently of the nuclear receptors. For example, the MR antagonist spironolactone does not inhibit an ALD-mediated increase in cAMP in rat inner medullary collecting ducts (Sheader *et al.*, 2002). This suggests that there may be other non-nuclear, membrane-bound steroid receptors.

The fast effects of steroids are often dependent on G protein activation e.g., the CORT-mediated suppression of nicotine-induced calcium influx in PC-12 adrenal chromaffin tumour cells, is inhibited by pertussis toxin, a $G\alpha_i$ inhibitor (Qiu *et al.*, 1998). Therefore, it is unsurprising that GPCRs have been implicated in steroid signalling. Recent developments in steroid research have revealed three putative G protein-coupled steroid receptors: the once orphan GPER has been shown to bind E2 with

high (nanomolar) affinity, the odorant receptor PSGR has been reported to be activated by testosterone metabolites, and the calcium sensing receptor $GPRC_6$ has also been implicated in testosterone signalling (Thomas *et al.*, 2005; Revankar *et al.*, 2005; Neuhaus et al., 2009; Pi *et al.*, 2010). While little is known regarding the role of PSGR and $GPRC_6$ in rapid testosterone signalling, there has been a considerable amount of research on GPER, since its deorphanisation in 2005. Officially regarded as an E2 receptor, GPER marks a new age in steroid research.

1.6.3 The G protein-coupled oestrogen (E2) receptor

In 1996 a GPCR with low homology to the chemokine family of receptors was first cloned by Dr Stephen Lolait and colleagues from a human B-cell lymphoblast cDNA library (Owman *et al.*, 1996). Subsequently named G protein-coupled E2 receptor 1 (GPER), the endogenous ligand for the GPCR was not initially identified although Northern blot analysis revealed high expression in both central and peripheral tissues (O'Dowd *et al.*, 1998; Owman *et al.*, 1996). In 2000, Filardo and co-workers identified a link between GPER and E2 signalling. They demonstrated that: (1) E2 activates ERK1/2 in SKBR3 cancer cells that do not express ERα and ERβ, yet express GPER (Filardo *et al.*, 2000); and (2) MDA-MB-231 breast cancer cells (ERα-/ERβ+/GPER-) that are generally unresponsive to E2-mediated ERK1/2 phosphorylation, become E2-responsive following transfection with GPER (Filardo *et al.*, 2000). In addition, the (EGFR) kinase inhibitor, tyrphostin AG-1478, blocks E2-induced ERK-1/2 phosphorylation, suggesting that GPER requires EGFR to activate ERK1/2 signalling in MDA-MB-231 breast cancer cells (Filardo *et al.*, 2000). Further studies revealed that E2 stimulation of GPER activates a modest increase in adenylyl cyclase and cAMP mediated signalling, and early c-Fos expression in SKBR3 cancer cells (Filardo *et al.*, 2002; Maggiolini *et al.*, 2004).

In 2005, two studies provided direct evidence for E2 activation of GPER. Thomas and colleagues demonstrated high affinity binding of radiolabelled E2 ($[^3H]$ E2) to membranes of SKBR3 cancer cells and human embryonic kidney 293 (HEK293) cells transfected with human GPER, with a dissociation constant of approximately 3nM; an effect abolished in cells pre-treated with GPER siRNA (Thomas *et al.*, 2005). Revankar and co-workers performed competition binding assays using fluorescent E2 derivatives along with E2 in COS-7 monkey kidney fibroblast cells transfected with human GPER, and obtained an inhibitory constant for E2 of approximately 6.6 nM for the receptor (Revankar *et al.*, 2005). They further demonstrated that flourescent E2 binding to GPER occurred predominantly in the endoplasmic reticulum, a finding confirmed using an antibody directed against GPER (Revankar *et al.*, 2005). The same group later found that only membrane-permeable E2 derivatives are capable of stimulating GPER and activating rapid calcium mobilisation and PI3K signalling in transfected COS-7 cells, indicating that the GPCR functions intracellularly (Revankar *et al.*, 2007). While this is a controversial finding considering that many GPCRs are localised and function on the plasma membrane, the cellular compartmentalisation is not unique amongst GPCRs

e.g., the proportion of human GnRH receptors at the cell surface in some cells is less than 1% (Finch *et al.*, 2008). In addition, studies on GPER have revealed that the partial and pure ER antagonists, tamoxifen and ICI182,780 respectively, are capable of binding and activating the receptor (Revankar *et al.*, 2005; Thomas *et al.*, 2005). Tamoxifen is often used to treat breast cancer patients to block the proliferative actions of ERα and ERβ on tumour growth, and hence GPER provides a potential target for therapeutic intervention (Filardo and Thomas, 2005).

1.7 Aims

The main aim of this thesis was to investigate the concept of whether GPCRs act as fast steroid receptors, focussing on steroids that have prominent roles in neuroendocrine systems (e.g., E2s and glucocorticoids). This is initially addressed in results Chapters 3 and 4 by examining the first GPCR to be identified as a putative steroid receptor, the E2 receptor GPER. Chapter 3 attempts to map GPER mRNA and protein distribution throughout central and peripheral rodent tissue, to provide insight into the roles of GPER as a fast E2 receptor - with particular interest paid to GPER distribution in the OT and VP neuroendocrine systems. Amidst controversy surrounding the E2 binding capabilities of GPER (with some arguing that GPER still remains an orphan receptor) and its unusual intracellular localisation, Chapter 4 attempts to characterise GPER (and verify the activation of GPER by E2) *in vitro*.

Results Chapters 5 and 6 address the possibility that there may be other steroid-binding GPCRs, with emphasis on a fast glucocorticoid receptor. Chapter 5 endeavours to identify some orphan GPCRs as candidates for fast glucocorticoid receptors, by matching the distribution of candidate orphan receptors with tissues that have been implicated in rapid glucocorticoid responses (hypothalamus, hippocampus, heart, thymus, etc.). Orphans with transcripts detected in the majority of target tissues were further investigated in Chapter 6, in an attempt to uncover a fast acting CORT receptor.

Chapter 2: General Methods

2.1 *In vivo* procedures

2.1.1 Animals

Adult male and female Sprague-Dawley rats, weighing 200-250g (Harlan), and adult (10-12 week) male and female wildtype mice (25-30g) from our VP V_{1B} receptor KO colony (Wersinger *et al.*, 2002), were used in this studies. Animals were housed under a constant temperature (21± 2°C), light (lights on from 0700 to 1900 h) and humidity (45-50%) regimens with food and water *ad libitum*. Animal care, maintenance and surgery were performed in accordance with the Animal Scientific Procedures Act (1986) United Kingdom and the appropriate University of Bristol ethical review process.

2.1.2 Collection of tissue for ISHH

Animals were sacrificed by decapitation rather than cervical dislocation to avoid damage to the brain and pituitary. Removal of tissues from head-to-toe took approximately 15-20 min.

Brain

Following tissue removal, a shallow midline cut was made with fine micro-dissecting scissors from the back of the skull to an approximate point of bregma, with care taken not to damage the brain. Two cuts were performed at the back of the skull either side of the first midline, allowing the caudal part of the skull to be prised back with fine micro-dissecting forceps. Another shallow cut was made from bregma to the rostral side of the skull, and both sides of this cut were peeled back to reveal the complete brain. With a fine micro-dissecting spatula, the brain was gently detached from surrounding membranes, with close attention paid when removing the olfactory bulb. The brain was lifted from skull and the optic nerves severed to liberate the brain.

Pituitary gland

Surrounding membranes were removed from the pituitary gland with fine micro-dissecting forceps. The pituitary gland was then lifted from the base of the skull.

Peripheral tissues.

Skin was removed from rodent thoracic and abdominal region and a midline incision made though the muscle layers to expose the underlying organs. All peripheral organs were dissected using micro-dissecting scissors and forceps, with care taken to remove excess connective tissue and fat. Skeletal muscle was removed from the hind leg, and fat from the abdominal region following hair and skin removal using a scalpel.

Freezing

All above tissues were wrapped in aluminium foil apart from the pituitary gland, adrenal gland and ovary which were submerged in tissue freezing medium-filled (Leica Microsystems, Germany) aluminium foil boats (mounting for sectioning). Tissues were snap frozen on dry ice and stored at -80°C until processing for ISHH.

2.1.3 Perfusion fixation and collection of tissue for IHC

Perfusion of rodents with 4% paraformaldehyde (PFA) was performed prior to IHC, to preserve cells and tissue structure, and provide mechanical strength to sections during the subsequent processing: a failure to properly fix tissue can lead to fragile sections and an increase in background staining. The method is essentially the same for both rat and mouse, although slight modifications were made to accommodate for the differences in animal size.

Animals received a lethal injection of sodium pentobarbital (100mg/kg i.p.). Once reflexes (check eye and pain reflexes by touching the eye and tail/paw pinching, respectively) were absent, rodents were transferred to a fume-hood and paws pinned to a polystyrene base to keep the animal in place during the procedure. A midline cut was made from neck to abdomen, from which skin and muscle were pulled back to expose the ribcage. A surgical cut was made along the diaphragm with blunt micro-dissecting scissors avoiding the heart and lungs. Lateral edges of the ribcage were cut with blunt micro-dissecting scissors, allowing the ribcage to be pulled upwards and away (and clamped/pinned) exposing the heart and lungs. Firstly, to reduce clotting, heparin (100 units/300g) (Sigma, UK) was injected into the left ventricle. A surgical needle attached to a peristaltic pump (Harvard Apparatus, UK) (for rats), or an AutoMate *In Vivo* Perfusion System (AutoMate Scientific, USA; for mice), was inserted into the left ventricle (and positioned up into the aorta in rats, and positioned into left ventricle in mice) and clamped. Pumps were turned on/valve turned to 'on' position and the right atrium was nicked with sharp micro-dissecting scissors. 300ml (rats) or 30ml (mice) of 1x phosphate-buffered saline (PBS) was infused into the cardiovascular system followed by an equal volume of 4% PFA in 1x PBS (see Appendix II for preparation of 4% PFA in 1x PBS). The peristaltic pump infused at a rate of 10-15ml per min whereas the AutoMate *In Vivo* Perfusion System relied on gravity (perfusate was placed into large 140ml syringes which were attached to the surgical needle by plastic tubing- the force of gravity pushed the perfusate through the mouse cardiovascular system).

If successfully perfused (as determined by blanching of tissues), tissues were removed as in section 2.1.2 and were post fixed overnight in 20% sucrose/4% PFA in 1x PBS solution at 4°C. Tissues were then frozen rapidly over liquid nitrogen in plastic weigh boats, wrapped in aluminium foil (apart from pituitary glands, adrenal glands and ovaries, which were placed in tissue freezing medium-filled aluminium foil boats) and stored at -80°C until sectioning for IHC.

2.2 Analysis of receptor mRNA distribution by ISHH

ISHH is a method of mRNA detection that allows insight into tissue (and cellular) specific gene expression. The use of riboprobes rather than oligonucleotide probes offers greater sensitivity (RNA: RNA hybrids are more stable that DNA: RNA hybrids, allowing for greater stringency washes and potentially higher signal: noise ratio). This ISHH protocol used in this thesis is described at:

http://intramural.nimh.nih.gov/lcmr/snge/Protocols/ISHH/ISHH.html

2.2.1 Tissue sectioning

12μm sections of brain and peripheral tissues were cut using a cryostat (Leica, Germany) and thaw-mounted onto polylysine slides (VWR International, UK). Slides were rapidly dried on a heat mat warmed to approximately 37°C, and stored at -80°C until use.

2.2.2 Riboprobe design

Probes of approximately 300-600bp in length were designed against the genes of interest. As GPCRs are part of a highly homologous family of receptors, every attempts were made to either direct the riboprobes towards the 3'-untranslated region (as the non-translated regions tend to have less sequence homology with other mRNA strands) or to non-conserved sequences within the translated region of the gene. For each mRNA of interest, antisense and sense riboprobes were synthesised to correspond to the sense strand of mRNA and antisense strand of mRNA (as a control), respectively. Riboprobes were checked for sequence homology against other mRNA sequences in the NCBI blast search engine (http://blast.ncbi.nlm.nih.gov/Blast.cgi) to verify that the riboprobes only potentially recognised the target transcript.

Melting temperature (Tm) is the temperature at which 50% of the duplexes have dissociated, and a measure of the stability of hybrids. The optimum hybridisation temperature is approximately 15-25°C below Tm, while the high stringency wash temperature is approximately 5-15°C below Tm (Wilkinson, 1999). Therefore, to predict whether the riboprobes could withstand the 55°C hybridisation incubation and the stringent low salt 65°C wash (see section 2.2.6 and 2.2.7 for hybridisation and wash steps), the Tm of each probe was calculated. If the Tm for a riboprobe was unavoidably low, the hybridisation and wash temperatures were adjusted accordingly (for each riboprobe, the Tm and corresponding hybridisation and wash temperatures are given in Chapters 3 and 5). The following formula was used to calculate Tm for RNA: RNA hybrids:

$$\mathbf{Tm = 79.8 + 18.5\log(Na^{+}) + 58(\%\ G+C)/100 + 11.8(\%\ G+C/100)^{2} - 1.2(\%\ mismatched\ pairs) - 820/ribonucleotide\ length - 0.35(\%\ formamide).}$$

(% G+C), represents the total guanine-cytosine content of the riboprobe; Na^+, incorporates the molarity of monovalent cations within the hybridisation buffer; (% mismatched pairs, takes into consideration any unmatched nucleotides within the hybrid duplex (all of the riboprobes in this chapter were designed to match the target mRNA sequence); % formamide, is the amount of formamide in the hybridisation buffer.

As the formula highlights Tm is proportional to G+C content. This is a product of three hydrogen bonds formed between guanine and cytosine (as opposed to the two hydrogen bonds form between adenine (A) and uracil ((U) or thymine (T) for DNA probes)). Hence, riboprobes with a high (% G+C) are more stable and form a much stronger bond within the RNA:RNA duplexes. As a result probes with high (% G+C) have higher Tms and those with low (% G+C) have reduced Tms. However, it is important that (% G+C) is not too high as it increases the possibility that nonspecifically bound riboprobes may remain bound throughout the stringent wash steps, thus increasing background signal. For this reason, riboprobes were not directed to the 5' untranslated region of the gene as it has a tendency to be G/C rich. Within this protocol it was found that a probe G+C content of approximately 50 % was optimal. As previously explained, if (% G+C)/Tm was unavoidably low for certain riboprobes (e.g., if a 3'untranslated region was too A/T rich) then the hybridisation/wash temperatures were reduced.

2.2.3 Riboprobe templates

Rat probe templates were generated by PCR from 125-150ng rat genomic DNA. The genomic DNA template for the rat orphan probes was extracted from rat testis, while genomic DNA for the GPER probe was purchased from Promega, UK (Promega no. G313A). The mouse GPER probe was generated by PCR from 20ng mouse GPER cDNA from an AtT-20 pituitary tumour cDNA library. PCR reactants included 5µl 10x HotStar buffer (Qiagen, UK), 8µl deoxyribonucleotides (dNTPs) (final concentration 200µM) (Applied Biosystems, UK), 10µl 'Q' solution (a liquid of unknown composition that according to the manufacturers reduces non-specific primer annealing – we suspect 'Q' is a DMSO solution) (Qiagen, UK), 0.5µl 2.5 U amplitaq DNA polymerase (Applied Biosystems, UK), 2µl 20µM primers (final concentration 200nM) (Invitrogen, UK), and made up to 50µl with distilled H_2O. The standard PCR run consisted of an initialization step for 45 seconds (s)-1 minute (min) at 95°C; 45s denaturation step at 94°C, 1 min annealing step at 45-50°C, 30s elongation step for at 72°C, for 20-40 cycles; followed by a 10 min final elongation at 72°C and a 4°C soak. However, not all primers amplified a product of threshold size, and changes to annealing temperature were made accordingly (see Appendix I for PCR conditions). Primers contained recognition sequences for restriction endonucleases, details of which are outlined in experimental Chapters 3 and 5.

To check the PCR product was the correct size 10µl of the reaction was run on a 1.6% ethidium bromide agarose gel, and then the ends of the remaining product were filled in to ensure that the 5'- and 3'- terminal bp were 'flushed' (no overhangs so that restriction endonuclease recognition sequences were intact (see Appendix I)). Riboprobes were digested with restriction endonucleases (see the experimental Chapters 3 and 5) and run on a 1.6% ethidium bromide agarose gel. Bands corresponding to riboprobes were removed from the gel, and the DNA extracted using a Qiagen gel extraction kit (see Appendix I for gel extraction protocol). Riboprobes were digested with restriction endonucleases (see Chapters 3 and 5 for details) and subcloned into the RNA expression vector pGEM4z (see Appendix I for ligation protocol). Vectors were transformed into DH5α *Escherichia coli (E.coli;* Invitrogen, UK) and spread onto lysogeny broth (LB)-agar plates containing 50µg/ml ampicillin (AMP) (Sigma, UK) and left to grow overnight at 37°C (pGEM4z contains an AMP resistant gene) (see Appendix I). Colonies were picked, grown overnight in LB-AMP, and DNA extracted using a DNA miniprep protocol (see Appendix I). 10µl of DNA was digested with corresponding restriction enzymes and run on a 3% agarose (microsieve; Severn Biotech Ltd, UK) gel to check the vector contained the correct insert. A colony containing the appropriate construct was grown overnight in 100ml AMP-LB at 37°C (rocked at 225rpm), and plasmid DNA obtained from lysed bacteria cells using a Qiagen plasmid maxiprep protocol (Qiagen, UK; see Appendix I for protocol). DNA concentration was measured using a spectrophotometer (at a 260nm wavelength).

2.2.4 Radioactive labelling and synthesis of riboprobe

The pGEM4z vector contains SP6 and T7 RNA polymerase promoters flanking the multiple cloning sites, thus enabling the use of RNA polymerases SP6 or T7 to transcribe the antisense and sense probe (Chapters 3 and 5 outline the polymerases used to transcribe each probe). Prior to transcription vectors were linearised (see Appendix I for linearising vectors protocol) using the restriction endonuclease which recognised the incorporated restriction enzyme sequence 3' downstream of the insert (details of which restriction endonucleases were used are summarised in Chapters 3 and 5). 500ng DNA starting template was labelled with S^{35}-UTP using the Ambion MAXIscript® transcription kit (Ambion, UK; see Appendix I for protocol).

The synthesised probe was precipitated overnight at -20°C, and centrifuged (16,000xg) for 10-15 min at 4°C. Supernatant was removed and pellet washed with 70% ethanol and resuspended in 97µl tris-ethylenediaminetetraacetic acid (Tris-EDTA or TE), 2µl 10% sodium dodecyl sulphate (SDS) and 1µl 5M dithiothreitol (DTT) (all performed on ice). 1µl of riboprobe was placed into 5ml scintillation fluid and radioactivity measured in a scintillation counter (Wallac model 1410), to give the counts per minute (cpm). Throughout the ISSH procedure, all aqueous radioactive waste was disposed of into an appointed radioactive sink. Solid waste with radioactivity above background (>2 counts per second

determined by a beta counter) was collected and stored with the departmental radioactive waste, until deemed no longer radioactive.

2.2.5 Preparing tissue sections for hybridisation

The ISHH protocol was carried out in a RNase-free environment in an attempt to minimise degradation of riboprobes/tissue mRNA. All buffers were diluted in diethylpyrocarbonate (DEPC)-treated water (see Appendix II), cylinders and tanks were pre-treated with RNase-AWAY™ (Invitrogen, UK) prior to autoclaving, and pipette tips were filter plugged and RNase/DNase free. The prehybridisation steps were as follows:

1) Slides were removed from -80°C storage and allowed to equilibrate to room temperature for 10-20 min.

2) Slides were placed into coplin jars and immediately submerged in 4% formaldehyde in 1x PBS for 5 min.

3) 2 x brief washes with 1x PBS

4) Slides were immersed in 0.25% acetic anhydride/0.42% concentrated hydrochloric acid/ 1.5 % triethanolamine in 1x PBS. Acetic anhydride acetylates positive charge residues to help reduce nonspecific binding of the negatively charged riboprobes.

5) Sections were dehydrated with ascending alcohol washes: 70%/80%/95%/100% each for 1 min.

6) Chloroform for 5 min to de-fat and permeabilise sections.

7) Sections rehydrated with descending alcohol washes: 100%/95% each for 1 min.

8) Slides air dried for approximately 20 min.

9) And finally sections were placed on top of 3M paper (that had been pre-soaked in 50% formamide/4x SSPE) within a paper container.

2.2.6 Hybridisation of sections

Hybridisation of sections was performed behind a Perspex shield to protect from beta radiation emitted from ^{35}S-UTP. 50µl of hybridisation solution, containing approximately 1-2 cpm of ^{35}S-probe, was applied to each section and covered with a 22 x 22mm cover slip (light pressure was applied to each cover slip to remove any residual air bubbles that could mask the tissue from hybridisation buffer).

50µl Hybridisation solution consisted of:

1) ^{35}S-probe + DEPC-H_2O, 4µl total.

2) 2µl ribonucleic acid mix† (reduces nonspecific binding. N.B., ribonucleic acid mix was a mixture of ^{35}S-probe and DEPC-H_2O which was then melted at 65°C for 5 min to denature the probe. This was cooled on ice, prior to adding it to the rest of the hybridisation solution).

3) 42µl Hybridisation buffer† (constituents in this buffer amongst other things aid probe dispersion, and control the stringency and efficiency of the hybridisation).

4) 1µl 5M DTT (is a reducing agent and protects ^{35}S from oxidation, as well as reduce background).

5) 0.5µl 10% sodium thiosulphate (aids probe dispersion and reduces nonspecific ionic and non-ionic absorption of the probe).

6) 0.5µl 10% SDS (permeabilises tissue and increases signal: noise ratio).

† Reagent composition described in Appendix II

7) Sections complete with hybridisation solution were incubated at 55°C overnight (however, this temperature was altered depending on the riboprobe Tm - see Chapters 3 and 5 for hybridisation temperatures for each probe).

2.2.7 Post hybridisation processing of sections

Sections underwent a variety of descending salt (SSPE) washes to remove 'nonspecific' and weakly bound ^{35}S-probe (mismatched hybrids are more stable at high salt concentrations), and reduce background signal. The most stringent of these is the 0.1x SSPE wash performed at 65°C (see below). DTT was included in washes to protect the ^{35}S from oxidation.

1) Cover slips were gently removed from sections by dipping 4x SSPE/1mM DTT in DEPC-H_2O. Slides were transferred to a slide rack and placed into a dish containing 4x SSPE/1mM DTT in DEPC-H_2O.

2) 4 x 5 min wash in 4x SSPE/1mM DTT in DEPC-H_2O at room temperature with gentle rocking.

3) 30 min incubation in RNase A solution (see Appendix II) for 30 min at 37°C. This step degrades single stranded mRNA (i.e., unbound probe).

4) 2 x 5 min wash in 2x SSPE/1mM DTT in DEPC-H_2O at room temperature with gentle rocking.

5) 1 x 5 min wash in 0.1x SSPE/1mM DTT in DEPC-H_2O at room temperature with gentle rocking.

6) 2 x 30 min wash in 0.1x SSPE/1mM DTT in DEPC-H_2O at 65°C without agitation (depending on the riboprobe Tm this temperature may have been changed - see experimental Chapters 3 and 5 for hybridisation temperatures for each probe).

7) 1 x 5 min wash in 0.1x SSPE/1mM DTT in DEPC-H_2O at room temperature with gentle rocking.

8) Finally sections are dehydrated with ascending ethanol washes that contain 300mM ammonium acetate: 70%/80%/90%/95%/100%, each for one min. Ammonium acetate was included in the ethanol washes to reduce the denaturation of hybrids.

9) Sections are air dried before exposure to film (Amersham Hyper film MP) or emulsion dipped (see Appendix I for protocol).

2.3 Analysis of protein distribution by IHC

IHC is the localisation of a protein of interest within *ex vivo* tissue, using antibodies that are directed towards that protein (such as a GPCR). The following protocols were used to investigate the distribution of GPER in rat and mouse tissue, and possible co-localisation of GPER with OT and VP neurones (Yao *et al.*, 2000; Yao *et al.*, 2001). The GPER antibody was a kind gift from Professor Eric Prossnitz from the University of New Mexico, and was a rabbit polyclonal antibody directed against the last 18 amino acids of the human C-terminus GPER (AVIPDSTEQSDVRFSSAV). The specificity of this antibody has previously been confirmed in human cancer cell lines that endogenously express the receptor, and COS-7 cells transfected with GPER-GFP, and has also been used to determine the central protein distribution of the rat GPER (Revankar *et al.*, 2005; Brailoiu *et al.*, 2007). The use of the human antibody in rodent tissue is only made possible by the high sequence homology between the human and rodent C-terminals (see Figure 4.29).

2.3.1 Tissue sectioning

Free floating brain sections

Rat and mouse brains were sectioned on a cryostat to a thickness of 40μm for rat or 35μm for mouse (as the mouse brain is smaller, thinner sectioning produces more slices per region of interest). Using a fine paint brush (slightly dampened with 1x PBS (see Appendix II for PBS recipe)) each brain slice was transferred from cryostat to a 12-well tissue culture dish. A maximum of 4 sections/well for rat brain and 8 mouse sections/well were used.

Peripheral tissues

12μm sections of rat and mouse peripheral tissues were cut and thaw-mounted onto Superfrost Plus slides (VWR International, UK). Slides were allowed to dry on a heat mat and sections were drawn around using an ImmEdge™ Pen (Vector, UK). Slides were then placed into slide mailers containing 1x PBS.

2.3.2 Single staining with 3,3'-diaminobenzidine (DAB)

This protocol was used for both free-floating mouse brain and slide-mounted peripheral sections to detect GPER-immunoreactivity (ir). The optimum dilution of GPER antibody was determined in preliminary experiments. For all steps (excluding PBS washes) sections were incubated in 400μl of solution/well and 200μl/ slide, and were subject to light agitation on a rocking platform. Slides underwent 1x PBS washes within slide mailers (this was not agitated), and free-floating sections were washed in approximately 500μl 1x PBS with agitation. Unless otherwise stated, each step was performed at room temperature.

1) 1 x 5 min wash in 1x PBS.

2) Endogenous peroxidase activity was quenched with 3% hydrogen peroxide in 1x PBS for 10 min.

3) 3 x 10 min wash with 1x PBS.

4) Incubation in 10% normal goat serum (NGS)/0.3% t-Octylphenoxypolyethoxyethanol (Triton-X 100 or TX-100; Sigma, UK) in 1x PBS for 15 min to reduce non-specific antibody binding and permeabilise tissue sections.

5) 3 x 10 min wash with 1x PBS.

6) Sections were incubated overnight in an affinity-purified rabbit antiserum against GPER diluted (1:1000 for rat tissue; 1:2000 for mouse) in 1% NGS/0.3% TX-100 in 1x PBS at 4°C (not on a plate rocker). Normal rabbit immunoglobulin G (IgG) serum (Vector Laboratories) was used as a control at the same concentration as the antibody.

7) 3 x 10 min wash with 1x PBS.

8) 1 hour incubation at room temperature in secondary biotinylated affinity purified goat anti-rabbit (1:500, Vector laboratories), in 1% NGS/0.3% TX-100 in 1x PBS.

9) 3 x 10 min wash with 1x PBS.

10) 1 hour incubation in horseradish peroxidise streptavadin (1:500, Vector laboratories) in 1% NGS/0.3% TX-100 in 1x PBS for a further hour.

11) The GPER signal was visualised with 3,3'-diaminobenzidine (DAB) in peroxidase buffer (10 min at 1:10, Roche Diagnostics).

12) Mouse brain sections were mounted onto Superfrost Plus slides with 0.5% gelatin solution, and left to air-dry.

13) Slides were coverslipped with DPX mounting medium (VWR, UK).

14) Sections were viewed under a light microscope (Leica DM IRB, Germany), and permanently stored at room temperature.

2.3.3 Double immunofluorescence

For double immunofluorescence staining, hypothalamic free floating sections (40μm for rats; 35μm for mice) were processed to either detect GPER-ir and OT-ir localisation, or GPER-ir and VP-ir

localisation, see below points 1-10. Unless otherwise stated, each step was performed at room temperature on a rocking platform. The optimum dilution of GPER/OT/VP antiserum was determined in preliminary experiments.

1) 1 x 5 min wash in 1x PBS.

2) Nonspecific ir blocked with 10% NGS/0.3% TX-100 in 1x PBS for 15 min.

3) 3 x 10 min wash in 1x PBS.

4) Sections were incubated overnight at 4°C (not on a plate rocker) with rabbit antiserum against GPER (diluted 1:1000) and guinea pig antiserum against OT or VP (diluted 1:2000 (OT), 1:500 (VP); Peninsula Laboratories).

5) 3 x 10 min wash in 1x PBS.

6) 1 hour incubation at room temperature in biotinylated goat anti-rabbit antibody (to detect GPER protein), and Alexa Fluor 488 goat anti-guinea pig antibody (diluted 1:500, Invitrogen) to detect OT or VP protein.

7) 3 x 10 min wash in 1x PBS.

8) Sections are incubated for an hour in streptavadin-conjugated Alexa Fluro 594 (diluted 1:500, Vector Laboratories) to fluorescently label the biotinylated goat anti-rabbit secondary antibody.

9) Sections were mounted onto Superfrost Plus slides, coverslipped with an antifade mounting medium (Vectashield Hard Set, Vector Laboratories, UK) and stored at 4°C (or at -20°C for long term-term storage).

10) Sections were viewed under a confocal laser-scanning microscope (Leica TCS-NT microscope housing a Leica DM IRBE inverted epifluorescence with a two-line krypton/argon laser) and processed with Adobe Photoshop CS3 extended computer software.

2.4 Molecular cloning of receptors and enzymes

2.4.1. Rodent GPER

Tagged and untagged rat GPER

Epitope tagged and untagged rat GPER receptors were generated by PCR using 250ng rat genomic DNA as a template. PCR reagents included 10µl 5x Herculase II Fusion DNA buffer (Agilent Technologies, UK), 200µM dNTPs, 1µl Herculase II fusion DNA polymerase (Agilent Technologies, UK), 2µl 10mM primers, and the reaction volume was made up to 50µl with distilled H_2O. Each PCR cycle consisted of 95°C for 2 min; then 45 s at 94°C, 1 min at 65°C, and 1 min at 72°C for 40 cycles; followed by 10 min at 72°C, and a 4°C soak.

For the untagged receptor, primers were directed to 5' and 3'-untranslated regions of the receptor (upstream: 5'- AGCTT*AAGCTT*GAAGCCATGGCTGCAACTACT -3'; downstream: 5'-AGAGC*CTCGAG*GTGGTTTGTTAAAGGGCC -3') and corresponded to 15718643-15720408bp of the rat GPER gene (Genbank Accession number NC_005111), generating a 1765bp product. Primers for the tagged receptor were again directed to 5' and 3'-untranslated regions of the receptor, but the 5' primer contained an additional 27 bp which coded for the Influenza hemagglutinin (HA) epitope tag (upstream: 5'-AAGCTT*AAGCTT*GAAGCCATG**TATCCATATGATGTTCCAGATTATGCT**GCTGCAACTAC TCCAGC -3' (bold underlined letters highlight the additional HA tag sequence); downstream: 5'-AGAGC*CTCGAG*GTGGTTTGTTAAAGGGCC -3'), and gave rise to a 1793bp product corresponding to 15718642-15718643bp of the rat GPER gene. Primers for both tagged/untagged receptors contained recognition sequences for the restriction endonucleases HindIII and XhoI (represented by underlined italics). Primer restriction endonuclease sites allowed subcloning into the vector pcDNA3.1(+) (containing AMP and neomycin resistance genes) for expression in mammalian cells.

Untagged mouse GPER

The untagged mouse GPER receptor was generated by PCR using 7.5ng mouse GPER cDNA (cloned from a mouse AtT-20 pituitary tumour cDNA library; Dr Lolait unpublished data) as a template. PCR reaction mix contained 10µl 5x Herculase II Fusion DNA buffer, 200µM dNTPs, 1µl Herculase II fusion DNA polymerase, 2µl 10mM primers, and the reaction volume was made up to 50µl with distilled H_2O. PCR cycling comprised of 95°C 2min; 94°C 45sec, 65°C 1min, 72°C 1min for 30 cycles; 72°C 10min; 4°C soak. Primers were directed to 5' and 3'-untranslated regions of the receptor (upstream: 5'- ACTG*GGATCC*GAAGCCATGGATGCGACTACC -3'; downstream: 5'-GCATC*CTCGAG*CAGGAAGGCGTTTTGTTA -3') and corresponded to 595-2323bp of the mouse

GPER gene (Genbank Accession number NM_029771), generating a 1728bp product, and contained recognition sequences for the restriction endonucleases BamHI and XhoI (represented by underlined italics). Incorporation of restriction endonuclease sites into primers allowed subcloning into the vector pcDNA3.1(+) (containing AMP and neomycin resistance genes) for expression in mammalian cells.

2.4.2. Mouse E2 sulphotransferase

A mouse E2 sulphotransferase cDNA clone was purchased from Geneservice (IMAGE clone: 1479883; SourceBioscience, UK), and supplied as pre-streaked bacterial colonies on a LB-agar slope. The mEST clone had been subcloned into pT7T3D-Pac vector which contains an AMP resistant gene. Bacterial colonies were re-spread on LB-agar plates containing 50μg/ml AMP and grown overnight at 37°C. Colonies were picked and grown overnight in LB-AMP and bacteria were lysed and DNA extracted using the DNA miniprep protocol. 10μl of DNA was digested with EcoRI and NotI restriction endonucleases, and the product run on a 1% ethidium bromide agarose gel to check the insert was the correct size. A colony containing the correct insert was grown overnight in 100ml AMP-LB at 37°C (rocked at 225rpm), and plasmid DNA obtained using the Qiagen plasmid maxiprep protocol (Appendix I).

For transfection of the mEST cDNA into a mammalian cell line, it was necessary to subclone the mEST cDNA into a mammalian expression vector. In this instance the vector pcDNA3.1 Hygromycin (Hygro) (+) was preferred as it contained a Hygro B resistance gene (as well as AMP resistance gene). Hygro resistance enabled mEST to be stably transfected into an already established stable line that had been selected with an alternative antibiotic (i.e., mGPER-expressing HEK293 cells that had been selected with the antibiotic Geneticin® (G418)). However, as there is an absence of an EcoRI site from the pcDNA3.1(+)Hygro multiple cloning sites, the mEST clone could not be directly inserted into the vector. The mouse E2 sulphotransferase plasmid DNA was therefore used as a template in PCR to amplify mouse E2 sulphotransferase DNA with the appropriate linkers for subcloning.

A new mEST clone with suitable restriction enzyme linkers was generated by PCR using 20ng of cDNA retrieved from the previous plasmid maxiprep as a template. PCR reaction mix contained 10μl 5x Herculase II Fusion DNA buffer, 200μM dNTPs, 1μl Herculase II fusion DNA polymerase, 2μl 10mM primers, and the reaction volume was made up to 50μl with distilled H_2O. PCR cycling comprised of 95°C 2min; 94°C 45sec, 60°C 1min, 72°C 1min for 30 cycles; 72°C 10min; 4°C soak. Primers were directed to the 5' and 3'untranslated of the enzyme (upstream: 5'-ACAGT*GGATCC*TTTGAGATGGAGACTTCTATGCC -3'; downstream: 5'-CAGGC*CTCGAG*TTATTTTTACTAGAAATC -3'), and corresponded to 97-1212bp of the mEST gene (Genbank Accession number NM_023135.1), generating a 1115bp product. Primers contained

recognition sequences for the restriction endonucleases BamHI and XhoI (represented by underlined italics).

2.4.3. Human orphan receptors GPR108, GPR146, TMEM87B

Orphan GPCR cDNA clones were purchased from Geneservice, and supplied as pre-streaked bacterial colonies, on LB-agar slopes. The GPR108 cDNA was subcloned into a pCR4-TOPO vector (IMAGE clone: 9056837; vector contained kanamycin and AMP resistance genes); GPR146 cDNA was inserted into a pOTB7 vector (IMAGE clone: 4563636; vector had a chloramphenicol resistance gene); and TMEM87B cDNA was inserted into a pCR-BluntII-Topo vector (IMAGE clone: 40026807; vector contained a kanamycin resistance gene). For each orphan, bacterial colonies were re-spread onto LB-agar plates containing the appropriate antibiotic (30μg/ml kanamycin sulphate (Sigma, UK) or 34μg/ml chloramphenicol (Sigma, UK)) and grown overnight at 37°C. Colonies were picked and grown overnight at 37°C in LB containing antibiotics (30μg/ml kanamycin sulphate or 34μg/ml chloramphenicol), and DNA extracted using the DNA miniprep protocol (see Appendix I). 10μl of DNA was digested with restriction endonucleases and the product run on a 0.8% ethidium bromide agarose gel (GPR108/pCR4-TOPO vector was digested with the restriction endonucleases SpeI and Not I; GPR146/pOTB7 vector was digested with EcoRI and XhoI; and TMEM87B/pCR-BluntII-Topo vector was digested with BamHI and XhoI). Bands corresponding to the inserts were removed from the gel and the DNA extracted (see Appendix I for gel extraction).

To allow transfection into mammalian cells, the orphans were subcloned into the mammalian expression vector pcDNA3.1(+). Following gel extraction GPR146 cDNA was ligated into pcDNA3.1(+) that had previously been digested with EcoRI and XhoI (see Appendix I). Unlike the GPR146 cDNA, the GPR108 and TMEM87B cDNAs could not be directly subcloned into pcDNA3.1(+) as both clones were originally inserted into their Geneservice expression vectors by blunt-end ligation. Instead, the DNAs extracted from the previous DNA minipreps were used as PCR DNA templates to re-amplify the orphan GPCRs by PCR. For both GPR108 and TMEM87B the PCR reactants included 10μl Herculase II Fusion DNA buffer, 200μM dNTPs, 1μl Herculase II fusion DNA polymerase, 1μl miniprep DNA (diluted 1:10 to give a DNA concentration of ~15-20ng), 2μl 10mM primers, and the reaction volume made up to 50μl with distilled H_2O. For GPR108 each PCR cycle consisted of 95°C for 2 min; then 45 s at 95°C, 1 min at 62°C, and 1 min at 72°C for 25 cycles; followed by 10 min at 72°C, and a 4°C soak. PCR conditions remained the same for TMEM87B apart from the annealing temperature which was at 60°C.

For GPR108 primers were also directed to the 5' and 3' untranslated regions of the receptor (upstream: 5'- GGAG*GGATCC*CCAGAGATGGCAGTGAGC- 3'; downstream: 5'-CTGG*CTCGAG*GAAGGGACTCTTCTTCC- 3'), and corresponded to 5-1828bp of the human

GPR108 gene (Genbank Accession number BC146909), generating a 1823bp product. For TMEM87B primers were directed to the 5' and 3-untranslated regions of the receptor (upstream: 5'-CAGC*GGATCC*ATCAAGATGGTCGCCGCC- 3'; downstream: 5'-AAAC*CTCGAG*GCCTGCCACCTATCAGCT- 3'), giving rise to a 1969bp product corresponding to 158-2127bp of the human TMEM87B gene (Genbank Accession number BC115373). Primers for both receptors contained recognition sequences for restriction endonucleases BamHI and XhoI (shown with bold italics). Primer restriction endonucleases sites allowed subcloning into pcDNA3.1(+) (containing AMP and neomycin resistance genes) in a 5'→ 3' direction.

2.4.4. Amplifying cDNA clones

The ends of the PCR products were filled-in (see Appendix I), digested with appropriate restriction endonucleases (see previous sections 2.4.1-2.4.3 for individual digests), and run on 0.8-1.2% agarose gels. Bands corresponding to the cDNAs were gel extracted and ligated into vector that had previously been digested with restriction enzymes corresponding to the insert (all cDNAs were inserted into the pcDNA3.1(+) vector (containing a neomycin resistance gene) except for mEST which was inserted into pcDNA3.1(+)Hygro vector) (see Appendix I for vector restriction endonucleases digests).

Following the subcloning of cDNA inserts into pcDNA3.1(+)/pcDNA3.1(+)Hygro, vectors were transformed into DH5α *E.coli,* spread onto LB-agar plates containing 50μg/ml AMP (both vectors contain the AMP resistance gene), and left to grown overnight at 37°C (see Appendix I). Colonies were picked, grown overnight and the DNA extracted (as per section 2.2.3). 10μl of DNA was digested with corresponding restriction enzymes and run on a 0.8-1.2% ethidium bromide agarose gel to check the vector contained the correct sized insert. DNA from a colony containing the appropriate construct was amplified and extracted as described in section 2.2.3.

2.5 Cell culture techniques

2.5.1 Cell lines

A variety of cells types were used during the *in vitro* studies including African green monkey transformed kidney fibroblast cells (COS-7), Chinese hamster ovary cells (CHO-K1), Human embryonic kidney 293 cells (HEK293), Human cervical adenocarcinoma cells (HeLa), endometrial adenocarcinoma cells (Ishikawa cells), and Human breast carcinoma cells (SKBR3).

2.5.2 Cell maintenance

All cell lines were grown in 10cm diameter culture dishes (Appleton Woods, UK). COS-7, HEK293, HeLa, Ishikawa and SKBR3 cells were maintained in high glucose Dulbecco's Modified Eagle's Medium (DMEM; Sigma, UK) supplemented with 10% inactivated foetal calf serum (FCS; Invitrogen, UK), 500 units/ml Penicillin (Sigma, UK), 0.5mg/ml Streptomycin (Sigma, UK) (collectively abbreviated to P/S) and 2mM L-glutamate (Q; Sigma, UK), and maintained at 37 °C in a 5% CO_2 atmosphere. CHO-K1 cells were cultured in Minimum Essential Medium (MEM), α Medium (1x) (αMEM, Invitrogen, UK), supplemented with 10% FCS and P/S, and kept at 37°C in 5% CO_2. Cells were passaged (see Appendix I for passaging cells) approximately 1:40 once a week (excluding COS-7 and SKBR3 cells which were passages 1:20 twice a week), and media was changed every 3-4 days (see Appendix II for media change). Earlier passages were frozen down in freezing-down media, for long-term storage in liquid nitrogen (see Appendix I for freezing down and thawing cells)).

2.5.3 Transiently transfecting cells

COS-7 and HeLa cells were seeded at 10,000 or 15,000 cells per well, respectively, in Costar plain black-wall 96-well plates (Corning, UK) for 24 hours. Cells were transiently transfected with cDNA and Nanofectin (PAA: The Cell Culture Company, UK) as shown:

1) Media was changed 2 hours prior to transfection with 200µl DMEM, 10% FCS, P/S and Q.

2) For each well of a 96-well plate, 0.25µg DNA was made up to a total volume of 10µl with Nanofectin diluent (PAA, UK), and mixed with gentle vortexing.

3) Nanofectin solution was prepared by diluting 0.8µl Nanofectin in 9.2µl Nanofectin diluent (for each well), with gentle vortexing.

4) Nanofectin solution was combined with the DNA solution, mixed immediately by vortexing, and incubated at room temperature for 30 min.

5) 20µl DNA-Nanofectin solution was added dropwise to each well (with gentle rocking backwards and forwards of the plate), and plate incubated at 37°C/5% CO_2 for 3.5 hours.

6) Cells were washed with 100µl 1x PBS and replaced with 200µl DMEM with 10% FCS, P/S and Q and incubated at 37°C/5% CO_2 overnight.

Alongside each transfection, transfection efficiency was estimated using a 5-bromo-4-chloro-3-indolyl-β-D-galactopyranoside (X-gal) staining assay. Control cells were transfected with a mammalian vector inserted with a LacZ gene (pSV-β-Galactosidase control vector; Promega, UK), and subsequent beta-galactosidase (β-gal) activity estimated from the percentage of blue cells (as shown in Figure 2.1; see Appendix I for detailed protocol).

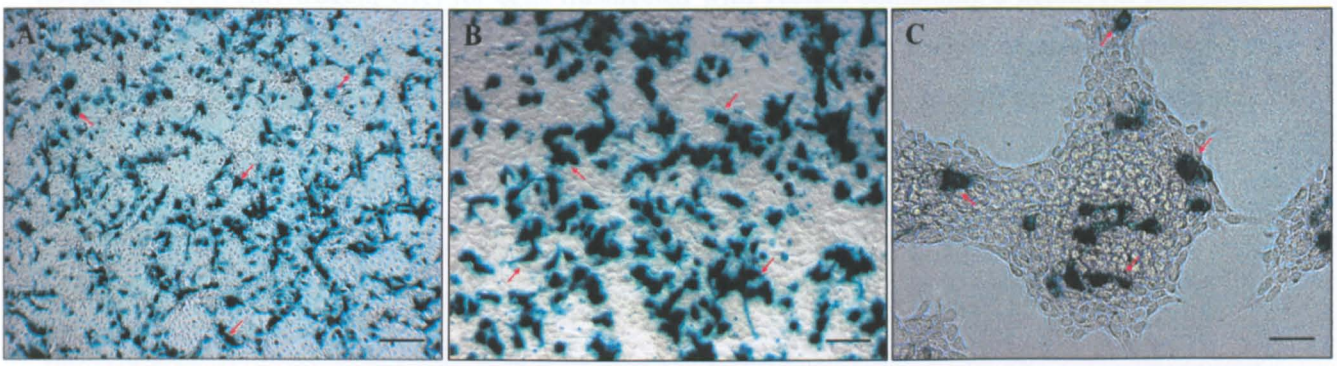

Figure 2.1. X-gal staining assay.

COS-7 (A), HeLa (B), and HEK293(C) cells were transiently transfected with pSV-β-Galactosidase control vector using Nanofectin transfection reagent. Transfection efficiency was estimated using the Xgal staining assay: cells successfully transfected with the LacZ gene developed a blue colour (red arrows highlight a few, out of many positive cells in A and B, but out of few in C). Scale bars, 200µm in (A); 100µm in (B); 50µm in (C).

2.5.4 Constructing stable cell lines

HEK293 cells were seeded at approximately 5 x 10^5 cells per well of a 6-well plate (or such that on day of transfection cells were no more than 50% confluent), and incubated for 18-24 hours in 2ml DMEM supplemented with 10% FCS, P/S and Q and maintained at 37°C/5% CO_2. Media was changed two hours prior to transfection. Cells were transfected with cDNA using a calcium phosphate protocol (Chen *et al.*, 1988) and a range of DNA concentrations were evaluated to achieve optimal transfection efficiency.

1) 1-6µg DNA was made up to 54µl with sterile H_2O.

2) 6µl 0.25M calcium chloride dihydrate (Sigma, UK; Appendix II) was mixed into each DNA solution, followed by dropwise addition of 60µl 2x BES (Appendix II), accompanied by gentle vortexing. The solution was left for 20 min at room temperature.

DNA-calcium phosphate solutions were added dropwise to the wells, and the plate was slightly agitated to facilitate mixing.

3) Plates were incubated overnight at 35°C in a 3% CO_2 atmosphere.

Grains of DNA-calcium phosphate precipitate were observed in each well. These DNA-calcium phosphate complexes (grains) form slowly under conditions of low pH, and precipitate gradually onto cells when in a low CO_2 atmosphere. Grains ranged from course to fine depending on the DNA concentration used (see Figure 2.2). Optimal transfection is usually obtained where a transition is observed between coarse and fine grains (usually occurred between 2-4μg). Wells were washed twice with media and left in media for 24 hours at 37°C/5% CO_2. Media was removed and replaced with media containing antibiotics for selection (DMEM plus 10% FCS, P/S, Q and supplemented with 800μg/ml G418 (Invitrogen, UK) for cells transfected with vectors containing a neomycin resistance gene, or 500μg/ml Hygro B (Invitrogen, UK) for cells transfected with vectors containing a Hygro B resistance gene (cells transfected with both vectors were exposed to both antibiotics for selection)). Cells were maintained in selection media for 17-18 days before creation of clonal cell lines.

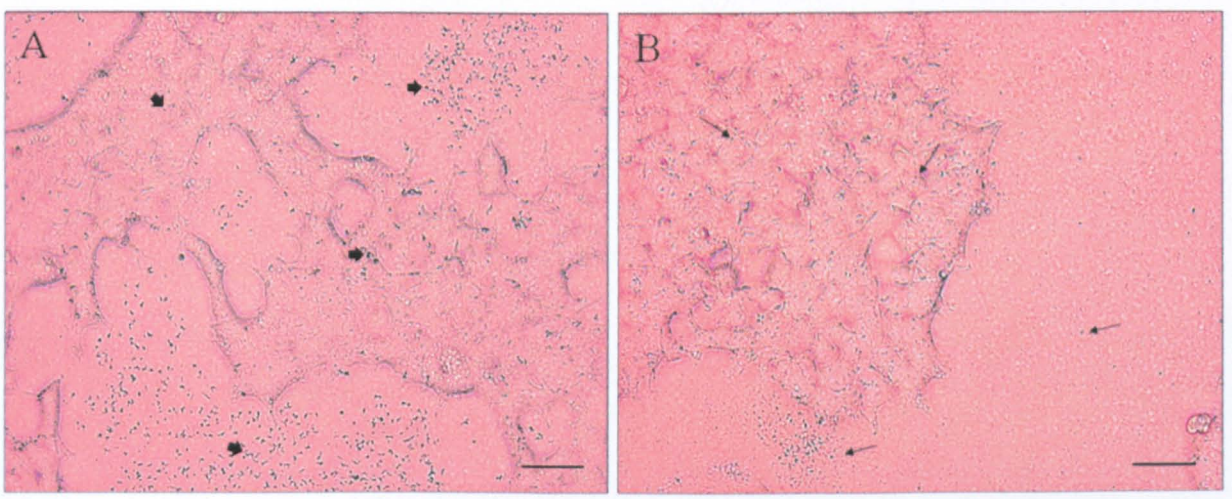

Figure 2.2. DNA-calcium phosphate precipitate.

Example of the transition between coarse and fine grains following the transfection of mEST cDNA into HEK293 cells with calcium phosphate. In this instance the transition occurred between 4μg cDNA/well (A; coarse grains shown with arrow heads) and 5μg cDNA/well (B; fine grains shown with thin arrows). Pictures appear pink due to phenol red in the DMEM medium. Scale bars, 100μm in (A) and (B).

To create clonal lines, cells were plated by limiting dilution to approximately 1 cell/well into 96-well plates and grown to near confluency in 200μl selection media. During this period (approximately 4-5 days) plates were not moved to ensure that any dividing cells did not set up separate colonies. Only wells with one colony were chosen for subsequent study - any wells with colonies with an ambiguous shape, which may have suggested two independent colonies had expanded, were not included in the

study. Clones were then trypsinised, and split, with 1:10 cells remaining on the master plate (and replenished with new selection media) and 1:4 transferred to a sister 96-well plate and grown in 200µl selection media. The sister plate was grown to 80-90% confluency ready for Northern blotting (see section 2.6), whilst the clones on the master plate were maintained in selective media and passaged if confluency was reached.

Clones that expressed high levels of mRNA of interest, as identified by Northern blotting (see section 2.6), were transferred to a 6-well plate and grown-up in maintenance media (DMEM, 10% FCS, P/S, Q and supplemented with 400µg/ml G418 and/or 250µg/ml Hygro). Once confluent, clones were further cultured in 10cm diameter petri dishes containing 10ml maintenance media (early passages were frozen down in DMSO as liquid nitrogen stocks (see Appendix I)).

2.6 Analysis of mRNA expression in cultured cells by Northern 'dot' blot hybridisation

2.6.1 Designing and labelling oligonucleotide probes

To determine the endogenous transcript expression of some genes of interest or cDNAs introduced into cells by transfection we performed northern 'dot' blot hybridisation. Two oligonucleotides approximately 48bp in length were designed against individual target genes. As some genes code for more than one transcript splice variant (that may be physiologically active) oligonucleotides were designed against regions of the gene common to all known variants. This also included homologues (and variants) from other species (e.g., human, hamster, and monkey) as expression was investigated in a variety of cells lines (human (HEK293/HeLa), hamster (CHO-K1), or monkey (COS-7) cells)).

To reduce potential hybridisation to other mRNA sequences, attempts were made to direct the oligonucleotides to the 5'- or 3'-untranslated regions (as the non translated regions tend to be less well conserved than protein-coding regions). As with designing riboprobes the Tm of each oligonucleotide was calculated to estimate whether the probe would remain bound during the high temperature/low salt washes. Optimum hybridisation temperature for oligonucleotides is between 37-45°C in a hybridisation solution containing 50% formamide, while the high stringency wash temperature is approximately 5-20°C below Tm (Wilkinson, 1999). Below is the formula used to calculate the Tm of oligonucleotides in Chapters 4 and 6:

To calculate the Tm of DNA: RNA hybrids:

Tm = 81.5 – 820/oligonucleotide length + 16.6log(Na^+) + 41(% G+C) – 1.2(% mismatched pairs) – 0.38(% formamide)

(% G+C), represents the total guanine/cytosine content of the riboprobe; Na^+, incorporates the molarity of monovalent cations within the hybridisation buffer; % mismatched pairs, takes into consideration any unmatched nucleotides within the hybrid duplex (all of the probes in Chapters 4 and 6 were designed to exactly match the target mRNA sequence); % formamide, is the percentage of formamide in the hybridisation buffer.

As highlighted in section 2.2.2 Tm is related to probe (% G+C). At times it was difficult to achieve an optimum G+C content (Within this protocol it was found that a probe G+C content of approximately 50-70% was optimal) in the 5' and 3' untranslated regions (as often is the case that the 3' untranslated region of a gene has a low (% G+C) and the 5' untranslated region has high (% G+C)). In instances where untranslated regions had inadequate G+C content, or where the transcript splice variants of the gene were only homologous in the translated region, the oligonucleotides were directed to the translated region of the mRNA, with maximum effort made to aim for non-conserved regions of the gene. Similarly, in instances where the (% G+C) could not be increased (e.g., when an oligonucleotide

had to be directed to an A/T rich region of the gene) the temperatures of the hybridisation and wash steps were reduced. To check that the oligonucleotides only potentially recognised the target transcript(s), each oligonucleotide was checked for sequence homology against other mRNA sequences in the NCBI blast search engine (http://blast.ncbi.nlm.nih.gov/Blast.cgi). Individual oligonucleotide sequences used in this thesis are summarised in Chapters 4 and 6.

Oligonucleotides were purchased from Invitrogen, UK and ~3.5μM was end labelled with α-P^{32}-ATP using the Roche Terminal Transferase tailing method (see Appendix I for protocol). Following tailing the reaction was made up to 200μl with TE with the addition of 1μl tRNA, and cleaned up by P/C/I (200μl P/C/I; see Appendix II) and C/I (200μl; see Appendix II) extraction. 10μl 4N NaCl and 550μl absolute ethanol were added to the top phase of the C/I extraction and the labelled probe was precipitated on dry ice for 10-15 min, and centrifuged (16,000xg) at 4°C for 10-15 min. The pellet was washed with ice cold absolute ethanol and resuspended in 12.5μl TE. 1μl of labelled oligonucleotide was placed into 5ml scintillation fluid and radioactivity measured in a scintillation counter, to give the cpm. Throughout the northern blot procedure, all radioactive waste was disposed of as described in section 2.2.4.

2.6.2 Blotting cells

Once the sister plate (from section 2.5.4), or a plate containing other cells of interest, had reached 80-90% confluency, the medium was removed and cells washed with 100μl 1x PBS at room temperature, and trypsinised with 50μl trypsin (Appendix I) for 10-15 min at 5% CO_2/37°C. After the addition of 50μl media, cells were transferred to a 96-well vacuum manifold lined with a nitrocellulose membrane (WHATMAN, Germany) pre-soaked in 10x SSC buffer (Invitrogen, UK)). Wells were washed through with 100μl 10x SSC and the nitrocellulose membrane removed and exposed to ultraviolet light (UV;1200 joules) in a Stratalinker® 1800 UV crosslinker (Agilent Technologies UK Ltd), for 1 min, to cross-link the RNA to the nitrocellulose membrane. The membrane was air dried for 15 min, baked for 2 hours at 80°C (to maximise RNA binding to the membrane), and stored at room temperature until hybridisation.

2.6.3 Northern 'dot blot' hybridisation

Pre-hybridisation: The nitrocellulose membrane was placed into a tub pre-treated with RNase-AWAY™ and washed with 4x SSPE for 10 min at room temperature. To pre-hybridise, the membrane was put into a plastic bag and filled with 5-10ml pre-hybridisation buffer (see Appendix II). The bag was sealed with a foot operated heat sealer (Hulme Martin, UK) and placed at 37°C for approximately 4 hours.

Hybridisation: The blot was transferred to a new plastic bag and filled with 3-10ml hybridisation buffer containing two α-^{32}P-ATP labelled oligonucleotide probes (1-2 x 10^{-6} cpm/ml per probe), and incubated at 37°C overnight.

Wash: Blot was washed twice (2-3 min wash) in 1x SSPE/0.2% SDS in DEPC-H_2O with gentle agitation, at room temperature, then 4 times at 54-56°C (temperature was altered for oligonucleotides with lower Tm's, see Chapter 4 and 6 for individual temperatures) for 15 min in a shaking water bath (45rpm). The blot was then briefly blotted on 3M paper, wrapped in cling-film, exposed to film (Amersham Hyper film MP) (in a cassette sandwiched between two enhancing screens), and stored at -80°C for 4-10 days.

2.7 Visualising HA-tagged receptor protein expression in transfected cell lines

2.7.1 Immunocytochemistry

Localisation of HA-tagged rat GPER receptors in stably transfected HEK293 was detected by an immunocytochemistry protocol using an anti-HA antibody, and visualised in a semi-automated system for image acquisition (IN CELL Analyser 1000, GE Healthcare, UK; Finch *et al.*, 2008). HA-tagged and untagged GPER HEK293 stables were cultured in poly-l-lysine-coated Costar plain black-wall 96-well plates at 10,000-15,000 cells per well (poly-l-lysine was necessary to maximise cell adherence during wash procedures: the coating of plates is described in (Appendix I). Percentage of cell surface vs whole cell HA-tagged-GPER expression was determined as follows:

Cell Surface imaging

1) Media was removed by pipetting and washed with 100µl/well of ice cold 1% BSA (Sigma, UK) in 1x PBS.

2) 1% BSA/1x PBS was replaced with 40µl/well 1:200 dilution of mouse monoclonal anti-HA.11 (Cambridge Bioscience, UK) in ice cold 1% BSA in 1x PBS and incubated at 4°C for one hour on a plate rocker.

3) 1 wash with 100µl/well ice cold 1x PBS.

4) Cells were fixed with ice cold 2% PFA in 1x PBS for 30 min at room temperature.

5) PFA was removed and cells permeabilised with 100µl/well 0.1% TX-100 in 1x PBS for 10 min at 4°C (binding of anti-HA.11 in step 2 may have caused receptor internalisation; therefore, the cells were permeabilised to allow penetration by the secondary antibody).

6) 3 x washes with 100µl/well 1x PBS for 1-2 min on a rocker.

7) Non-specific secondary antibody binding blocked with 100µl/well 0.1% TX-100/1% BSA in 1x PBS, and placed on a rocker for 1 hour at room temperature.

8) Cells were incubated in 40µl/well 1:500 dilution of Alexa Fluor 488 goat anti-mouse IgG (H+L) secondary antibody (Invitrogen, UK) in 0.1% TX-100/0.1% BSA/1x PBS, for 1 hour at room temperature with constant agitation.

9) 2 x washes with 100µl/well 1x PBS for 1-2 min on a rocker.

10) Nuclei were fluorescently labelled with 100µl/well 300nM 4',6-diamidino-2-phenylindole (DAPI; Sigma, UK) in 1x PBS for 15 min at room temperature.

11) 1 wash with 100µl/well 1x PBS.

12) Finally 100µl 1x PBS was added to each well, and plates were either imaged immediately, or were wrapped in tin foil and stored at 4°C until imaging (in the latter case the plate was left for at least 20 min at room temperature before acquiring images).

Whole cell imaging

1) Media was removed by pipetting and washed with 100µl/well of ice cold 1x PBS.

2) Cells were fixed with ice cold 2% PFA in 1x PBS for 30 min at room temperature.

3) PFA was removed and cells permeabilised with 100µl/well 0.1% TX-100 in 1x PBS for 10 min at 4°C.

4) 3 x washes with 100µl/well 1x PBS for 1-2 min on a rocker.

5) Nonspecific primary antibody binding blocked with 100µl/well 0.1% TX-100/1% BSA in 1x PBS, and placed on a rocker for 1 hour at room temperature[†].

6) Cells were incubated in 40µl/well 1:200 dilution of mouse monoclonal anti-HA.11 in 0.1% TX-100/1% BSA in 1x PBS and incubated for one hour at 4°C on a plate rocker.

7) 3 x washes with 100µl/well 1x PBS for 1-2 min on a rocker.

8) 40µl of Alexa Fluor 488 goat anti-mouse IgG (H+L) secondary antibody (1:500) in 0.1% TX-100/0.1% BSA/1x PBS was added to each well and rocked for 1 hour at room temperature.

9) 2 x washes with 100µl/well 1x PBS for 1-2 min on a rocker.

10) Cells were incubated in 100µl/well of 300nM DAPI in 1x PBS on rocker for 15 mins.

11) 1 x wash with 100µl/well 1x PBS

12) Finally 100µl 1x PBS was added to each well, and plates were either imaged immediately, or were wrapped in tin foil and stored at 4°C until imaging.

[†] *It was possible to reprocess the cell surface plate to achieve whole cell HA staining. In this instance the whole cell staining began at stage 5 as the cells had already been fixed and permeabilised in the previous cell surface protocol.*

2.7.2 Acquiring images

Cell surface and whole cell HA-GPER expression were measured by the IN CELL Analyser 1000. In brief, each plate was placed into the IN CELL Analyser microscope, and fluorescent images were taken using a 10x objective, excitation filters 475-nm (HA) and 360-nm (DAPI), and monitored through emission filters 535-nm (detecting Alexa 488, green fluorescence: HA signal) and 460-nm (detecting blue fluorescence: DAPI signal), with a 61002 trichroic mirror (GE Healthcare, UK). 2-3 fields were acquired per well (each field capturing a 0.602mm^2 area with a 10x objective), obtaining digital images of approximately 150-2500 cells per well.

2.7.3 Image analysis

Analysis of HA-GPER localisation was performed using the IN Cell 1000 Analysis Software (GE Healthcare, UK). Within each cell the software used green channel images (535-nm emission filter) to measure HA fluorescence intensity and defined the cytoplasm; while blue channel images (460-nm emission filter) measured DAPI intensity and defined the nucleus. For each field the average total amount of HA fluorescence in the cytoplasm was calculated. This value, following the subtraction of background florescence (normally measured in regions of the field absent of cells), was expressed as arbitrary fluorescence units (AFU). As HEK293 cells grow in epithelioid sheaths, a background reading was often difficult to obtain; as such, AFU was calculated from the fluorescence intensity in green channel images for each field, minus the average fluorescence intensity in green channel images from wells without primary antibody.

2.8 *In vitro* calcium stimulation assay

2.8.1 Live cell imaging

Calcium activation was determined using the green-fluorescent calcium indicator, fluo-4 AM (fluo-4; Invitrogen, UK), and measured in the IN CELL Analyser 1000 (Armstrong *et al.*, 2009). Cells were plated out at varying concentrations in Costar plain back-wall 96-well plates: CHO-K1 cells were seeded at 9,000 cells/well; SKBR3 cells 15,000 cells/well; and HEK293 cells 12,500-15,000 cells/well (into previously poly-l-lysine-coated plates). The following day, cells that were to be treated with steroids in the calcium stimulation assay were serum-starved overnight with phenol-red free DMEM with P/S, Q, 0.44mM calcium chloride dihydrate and 100μg/μl BSA (HEK293 cells), or phenol red/serum free Dulbecco's Modified Eagle's Medium: Nutrient Mixture F-12 (DMEM/F12) with P/S (SKBR3 cells).

Prior to stimulation cells were loaded with 80μl/well 2.5μM (HEK293) - 5μM (CHO-K1 and SKBR3) Fluo-4 and 0.5μM Hoechst nuclear stain (GE Healthcare, UK) in the same media used for serum starving (as above) or PSS for CHO-K1 cells (see Appendix II for PSS recipe) and incubated at 37°C/5% CO_2 for 1 hour (SKBR3) - 1.5 hours (CHO-K1 and HEK293 cells). Cells were stimulated and imaged in the IN CELL Analyser 1000 environmental control chamber, at 37°C in a 5% CO_2 humidified atmosphere. Treatment was loaded into an equivalent compound plate and inserted into the IN CELL Analyser 1000. The automated sampling system stimulated each well in turn with 20μl of 5x ligand/treatment at 12000 milliseconds (ms) (final volume in well is 100μl, as such ligands/treatments underwent a 1:5 dilution). Fluorescence images of one field per well were acquired every 12000ms ranging from 0ms to 72000ms using a 10x objective, excitation filters 475-nm (fluo-4) and 360-nm (Hoechst), and monitored through emission filters 535-nm (detecting green fluorescence; fluo-4 signal) and 460-nm (detecting blue fluorescence; Hoechst signal) with a 61002 trichroic mirror. Each field captured approximately 50-1500 cells over a 0.602mm^2 area.

2.8.2 Image analysis

Analysis was performed using the IN Cell 1000 Analysis Software. Within each cell the software used green channel images (535-nm emission filter) to measure fluo-4 fluorescence intensity to define staining in the cytoplasm, while blue channel images (460-nm emission filter) measured Hoechst intensity to define the nucleus. For each field the average total amount of fluo-4 in the cytoplasm was calculated. This value, following the subtraction of background florescence (measured in regions of the field absent of cells), was expressed as AFU. For sheathing HEK293 cells, a background reading was difficult to obtain, as such, AFU was calculated from the fluorescence intensity from the green channel images for each field, minus the fluorescence intensity from a manually selected background reading (free of cells). Data was presented as fold change over time point 0ms.

2.9 *In vitro* ERK phosphorylation assay

2.9.1 Immunocytochemistry

Cell expression of total (tERK) and phosphorylated ERK (ppERK) was detected by an immunocytochemistry protocol using antibodies against tERK and ppERK, and imaged in the IN CELL Analyser 1000 (Caunt *et al.*, 2008). Cells were seeded in Costar plain black-wall 96-well plates in varying concentrations overnight (which as previously determined reached approximately 50% confluency on the day of stimulation): CHO-K1 and Ishikawa cells were seeded at 10,000 cells/well; HEK293 cells 10,000-15,000 cells/well (HEK293 cells were seeded into poly-l-lysine-coated wells); SKBR3 cells 15,000-20,000 cells/well; and transiently transfected COS-7 and HeLa cells were set up as in section 2.5.3. The next day, cells were serum starved in either 90µl phenol-free DMEM with 0.1% charcoal stripped FCS, P/S and Q (HEK292, HeLa, COS-7, Ishikawa cells), 90µl phenol free αMEM with 0.1% FCS and P/S (CHO-K1 cells), or 90µl phenol- and serum-free DMEM/F12 and P/S (SKBR3), and left overnight at 37°C/5% CO_2. Cells were stimulated with 10µl of 10x desired agonist/antagonist concentration (agonist/antagonist undergo a 1:10 dilution when 10µl is added to the 90µl of media) for the required incubation period. Stimulation was quenched with 150µl/well ice cold 1x PBS and incubated on ice for 3-5 min. tERK and ppERK expression was visualised using the subsequent protocol:

1) 1x PBS was removed by pipetting and cells fixed with ice cold 4% PFA in 1x PBS and placed on a rocking platform for 10 min at room temperature.

2) The fixative was discarded and cells permeabilised by adding 50µl/well of absolute methanol (pre-cooled to -20°C) and incubated for 5 min at -20°C.

3) 1 x wash with 150µl 1x PBS

4) To block for immunostaining 40µl of 5% normal goat serum in 1x PBS was added to each well and plates were incubated at room temperature on a rocking platform for 2 h.

5) 1 x wash with 150µl 1x PBS.

6) 40µl Primary mouse anti-ppERK1/2 antibody (Sigma, UK) and primary rabbit anti-ERK1/2 in 1% normal goat serum (Cell Signalling Technology, UK)/1x PBS were added to each well (each primary antibody was titrated to give the optimal antibody concentration for each cell type: CHO-K1, COS-7 and HeLa cells 1:800 dilution mouse anti-ppERK1/2 antibody, 1:400 primary rabbit anti-ERK1/2; HEK293 and Ishikawa cells 1:1600 dilution mouse anti-ppERK1/2 antibody, 1:800 primary rabbit anti-ERK1/2; SKBR3 cells 1:6400-12000 dilution mouse anti-ppERK1/2 antibody, 1:3200 primary

rabbit anti-ERK1/2). 40µl 1% normal goat serum/ice cold 1x PBS was added to the no primary antibody control wells. The plate was incubated overnight on a rocking platform at 4°C.

7) 3 x washes with 150µl 1x PBS.

8) 40µl of 1:500 dilution of Alexa labelled 488 goat anti-mouse (Invitrogen, UK) and 1:500 Alexa labelled 546 goat anti-rabbit secondary antibody (Invitrogen, UK) in 1% normal goat serum/1x PBS was added to each well, and placed on a rocking platform at room temperature for 90 min.

9) 2 x washes with 150µl 1x PBS.

10) 100µl of 300nM DAPI in 1x PBS was added to each well and incubated on rocker for 15 mins.

11) 1 x wash with 150µl 1x PBS.

12) Finally 100µl 1x PBS was added to each well, and plates were either imaged immediately, or were wrapped in tin foil and stored at 4°C until imaging (if the latter the plate was left for at least 20 min at room temperature before acquiring images).

13) Images were obtained by the IN CELL Analyser 1000. Immunofluorescence was detected using a 10x objective, excitation filters 535-nm (tERK), 475-nm (ppERK) and 360-nm (DAPI), and emission filters 620-nm (detecting Alexa 546, red fluorescence: total ERK signal), 535-nm (detecting Alexa 488, green fluorescence: ppERK signal) and 460-nm (detecting blue fluorescence: DAPI signal) with a 61002 trichroic mirror. 2-4 fields were acquired per well (each field capturing a 0.602mm^2 area), obtaining digital images of approximately 150-3000 cells per well.

2.9.2 In cell image analysis

Analysis of total ERK and ppERK activity was performed using the IN Cell 1000 Analysis Software. Within each cell the software used red channel images (620-nm emission filter) to measure tERK fluorescence intensity and define the cytoplasm perimeter; green channel images (535-nm emission filter) to measure ppERK fluorescence intensity and also define the cytoplasm perimeter; while the blue channel images (460-nm emission filter) measured DAPI intensity and defined the nucleus. For each field the average total amount of tERK and ppERK in the whole cell was calculated. These values following the subtraction of background florescence (measured in regions of the field absent of cells) were expressed as AFU. In the case of sheathing HEK293 cells and confluent COS-7 and HeLa

cells (that had been transiently transfected), the IN Cell 1000 Analysis Software was unable to accurately measure background fluorescence (see Figure 2.3) – thus the background reading was taken from wells without primary antibody. Data was normalised to vehicle to allow pooling of independent experiments (fluorescence intensity can vary between experimental plates/purchased antibody aliquots).

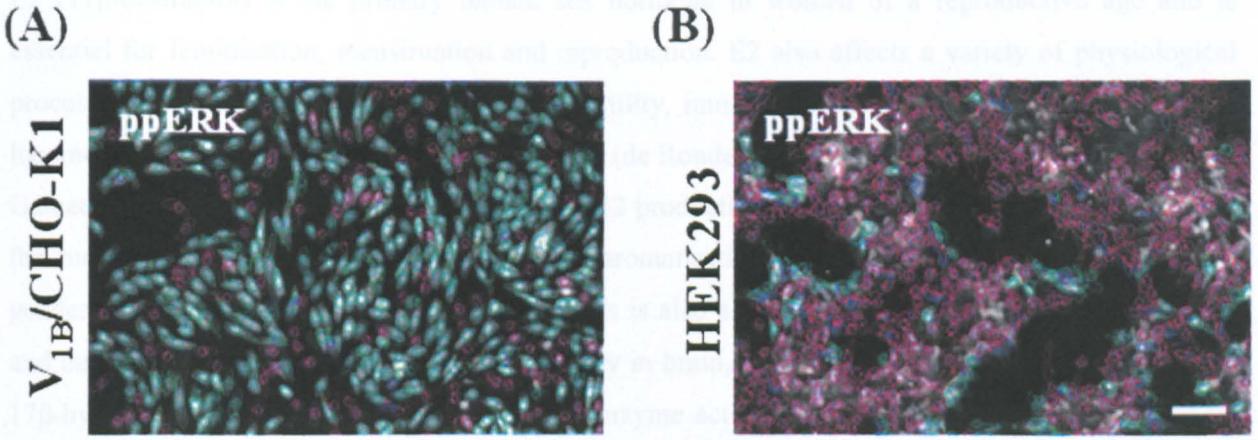

Figure 2.3. Examples of segmentation by the IN Cell 1000 Analysis Software.

(A) CHO-K1 cells stably transfected with V_{1B} receptor cDNA were treated with VP (100nM) for 10 min and processed for the ERK phosphorylation assay. Images of tERK, ppERK and DAPI fluorescence were obtained in the IN CELL Analyser 1000. An example image of ppERK fluorescence that has been analysed using the IN Cell 1000 Analysis Software is shown. Cytoplasmic and nuclear compartments are clearly demarcated. Cells outlined in green are deemed responsive as the ppERK fluorescence is above background threshold (background threshold is set for each cell type and/or antibody concentration by using a cell/background intensity filter), and cells outlined in red are unresponsive (ppERK is similar to background levels). (B) ppERK fluorescence in HEK293 cells treated with 0.01% ethanol for 5 min. As HEK293 cells grow in sheaths, the IN Cell 1000 Analysis Software is unable to clearly define the cell perimeter – therefore the software cannot obtain a background reading adjacent to each cell. Instead background is taken as the ppERK fluorescence measure in well absent of primary antibody. Scale bar, 100μm.

Chapter 3: Localisation of GPER, a novel G protein-coupled E2 receptor, suggests multiple functions in rodent brain and peripheral tissues

3.1 Introduction

3.1.1. E2

E2 (17β-oestradiol) is the primary female sex hormone in women of a reproductive age and is essential for feminisation, menstruation and reproduction. E2 also affects a variety of physiological processes in both men and women including fertility, immune function, the cardiovascular system, locomotion, neuroprotection, mood and cognition (de Ronde *et al.*, 2003; McEwen, 2002; Watson and Gametchu, 2001). The ovary is the main site of E2 production in premenopausal women, and in men the majority of E2 (a product of testosterone aromatisation) is excreted from the testis. In both genders, the zona reticularis of the adrenal glands is also a source of E2 precursors (e.g., androgens and oestrone) which are converted into E2 locally in brain, fat, and skeletal muscle by aromatase or 17β-hydroxysteroid dehydrogenase (17β-HSD) enzyme action (de Ronde *et al.*, 2003). It should be emphasised that E2s are also formed by the action of steroid sulphatases acting for example, on dehydroepiandrosterone sulphate or oestrone sulphate (Reed *et al.*, 2005), and these processes may also contribute to the E2 pool. Furthermore, testosterone and E2 metabolites and other derivatives, some of which may be biologically active (e.g., 5α-dihydrotestosterone, 3α-diol or 3β-diol bind E2 receptors (Pak *et al.*, 2007)), may dramatically influence the biology of E2 at the local tissue level.

E2s effects are typically mediated by two structurally related receptors, the alpha and beta subtypes (ERα and ERβ), that belong to the steroid/retinoid receptor gene superfamily (Weihua *et al.*, 2003). Within the cell the inactivated ERs bind to heat shock proteins within the cytoplasm. Upon ligand activation, the ERs translocate to the nucleus and bind to E2 response elements (ERE) present in the promoter region of a target gene, where they modulate transcription. The genomic actions of the ERs generally occur slowly (hours-days). ERα is found in the brain - predominantly in the bed nucleus of the stria terminalis, hypothalamus, and amygdala (Merchenthaler *et al.*, 2004), and also in bone (Lee *et al.*, 2003), uterus and mammary gland (Pelletier and El-Alfy, 2000). ERβ is most abundant in tissues such as the brain - e.g., bed nucleus stria terminalis and hypothalamus (Merchenthaler *et al.*, 2004), lung (Morani *et al.*, 2006), prostate, testis, mammary gland, and ovary (Pelletier and El-Alfy, 2000). Transgenic models clearly illustrate the contrasting roles of the individual ERs. For example, the ERα KO mouse is typically infertile, displays disrupted mating behaviour, and stunted bone growth. The ERβ KO is fertile although it exhibits reduced litter sizes, and adult females have increased bone density, while adult males are prone to prostatic hyperplasia (Pettersson and Gustafsson, 2001; Walker and Korach, 2004).

Besides the 'slow' genomic effect of E2 it is well documented that E2 can also evoke fast non-genomic effects in variety of tissues e.g., rapid release of intracellular calcium in granulosa cells of the ovary, and stimulation of uterine intracellular cyclic AMP (Morley *et al.*, 1992; Szego and Davis, 1967). These effects may be mediated by the ERs, as a subpopulation of the receptors can be found near the cell membrane and on activation stimulate second messenger pathways (Levin, 2005; Zhang and Trudeau, 2006). However several lines of evidence indicate the existence of a novel ER - e.g., E2 rapidly stimulates c-Fos protein accumulation in area 2 of cingulate cortex and the olivary pretectal nucleus in brains of ERαβ KO mice (Dominguez-Salazar *et al.*, 2006), and the ER antagonist ICI 182,780 potentiates, rather than attenuates, the stimulatory effects of E2 on ERK1/2 signalling in human neuroblastoma cells (Watters *et al.*, 1997)

3.1.2. Fast E2 receptor and possible presence in the hypothalamo-neurohypophseal system

GPER a GPCR, specifically binds E2 with high (nanomolar) affinity and evokes rapid effects (Revankar *et al.*, 2005; Thomas *et al.* 2005), including stimulating calcium mobilisation from intracellular stores directly or via EGFR transactivation, c-Fos expression, adenylyl cyclase and cAMP mediated signalling and ERK-1/2 in a variety of cell types (Prossnitz *et al.*, 2008). Intriguingly, only a small fraction of total cellular GPER appears to be expressed on the cell surface with most of the receptor is located intracellularly in the endoplasmic reticulum (Revankar *et al.*, 2007). GPER acts as an atypical GPCR, in that it is activated intracellularly by E2 which readily diffuses across cell membranes (Revankar *et al.*, 2007).

Transgenic models have enabled further insight into possible roles for GPER *in vivo*. Martensson and colleagues have shown that the female GPER KO mouse has decreased insulin expression with associated hyperglycemia, and impaired glucose tolerance. The females also exhibit reduced skeletal development, lower serum insulin-like growth factor-1 levels and elevated blood pressure (Martensson *et al.*, 2009). Additional KO models have revealed that both male and female GPER KOs have increased body weight and visceral obesity, but remain fertile and reproduce normally (Haas *et al.*, 2009; Otto *et al.*, 2009). In fact, the development of the female reproductive organs (mammary gland, uterus and ovary) in the GPER KO are unimpaired and remain E2 responsive (Otto *et al.*, 2009).

Only a few studies have investigated the distribution of GPER. Northern blot analysis has revealed wide GPER transcript distribution in human and rat central and peripheral tissues (Owman *et al.*, 1996; Bonini *et al.*, 1997; Carmeci *et al.*, 1997; Fung & Gregor, 1997; Kvingedal & Smeland, 1997). An immunohistochemical study of GPER in the rat brain revealed high protein expression in regions

such as the Islands of Calleja, striatum, olfactory tubercle, and the hypothalamic PVN and SON (Brailoiu *et al.*, 2007).

Other studies have also detected GPER-ir in the rat PVN/SON, with reports that GPER is expressed in OT neurones, implicating a role for GPER in the fast, non-genomic actions of E2 on OT release (Wang *et al.*, 1995; Brailoiu *et al.*, 2007). It is interesting to note that stimulation of the ERK1/2 (as is associated with GPER activation) pathway has been shown to modulate OT gene transcription (Koohi *et al.*, 2005). Whether or not GPER is expressed in vasopressin (VP) neurones remains unclear. One recent study found co-expression of GPER with VP (Brailoiu *et al.*, 2007), while another did not (Sakamoto *et al.*, 2007), even though both studies used the same GPER primary antibody. A role for E2 in regulating OT and/or VP release is supported by studies showing that administration of E2 to post menopausal women increases circulating levels of OT and VP (Bossmar *et al.*, 1995), and E2 rapidly stimulates intrahypothalamic and peripheral OT and possibly VP release (Wang *et al.*, 1995; Burbach *et al.*, 2001).

As GPER provides an alternative model for E2 signalling, and possibly E2-stimulated release of OT and VP, the present study was undertaken to clarify the distribution of GPER in the rodent. The aims within this chapter were to 1) clarify whether or not GPER is co-expressed in rat and mouse OT/VP neurones; 2) map the distribution of GPER in the mouse brain to determine whether there are differences to that shown in the rat; and 3) identify and highlight regions that express high levels of GPER mRNA and protein in the rodent periphery providing additional insights into the role of GPER.

3.2 Materials and Methods

3.2.1 Animals

Adult male and female Sprague-Dawley rats, weighing 200-250g (Harlan), and adult (10-12 week) male and female wildtype mice (25-30g) from our VP V_{1B} receptor KO colony (Wersinger *et al.*, 2002) were used in this study. For each separate experiment (IHC, double immunofluorescence, or ISHH) three mice or rats of each gender were used. Animals were anaesthetised with sodium pentobarbital (100mg/kg i.p.) and intracardially perfused as outlined in section 2.1.3 for IHC, and sacrificed by decapitated for ISSH.

3.2.2 IHC

Tissues were post-fixed overnight in 20% sucrose/4% PFA in 1x PBS solution. Following overnight fixation the tissues were rapidly frozen over liquid nitrogen and stored at -80°C until processed. In single staining, rat and mouse peripheral cryostat sections (12 μm) were cut and thaw-mounted onto Superfrost Plus slides, or free-floating (40 μm) mouse brain sections were cut and processed for GPER-ir. Tissues were first washed in 1x PBS, endogenous peroxidase activity was quenched with 3% H_2O_2 for 10 min, washed (3 x 10 min with 1x PBS), and then blocked with 10% normal goat serum (NGS)/0.3% Triton-X 100 (TX-100) in 1x PBS for 15 min. After washing (3 x 10 min with 1x PBS) sections were incubated overnight in an affinity-purified rabbit antiserum against GPER diluted (1:1000-1:2000) in 1% NGS/0.3% TX-100 in 0.1M PBS at 4°C. The specificity of GPER antiserum has previously been confirmed (Revankar *et al.*, 2005; Brailoiu *et al.*, 2007), and normal rabbit IgG serum was used as a control at the same concentration as the antibody. After washing (3 x 10 min with 1x PBS), sections were incubated at room temperature in secondary biotinylated affinity purified goat anti-rabbit (1:500), in 1% NGS/0.3% TX-100 in 0.1M PBS for 1 hour, washed (3 x 10 min with 1x PBS) and incubated in horseradish peroxidise streptavadin (1:500) in 1% NGS/0.3% TX-100 in 0.1M PBS for a further hour. The GPER signal was visualised with DAB in peroxidase buffer (10 min at 1:10). Mouse brain sections were mounted onto Superfrost Plus slides with 0.5% gelatin solution, and along with the pre-mounted peripheral sections were cover-slipped and viewed under a light microscope.

For double immunofluorescence staining, hypothalamic free-floating sections (40μm) were rinsed in 1x PBS, and then blocked with 10 % NGS/0.3% TX-100 in 1x PBS for 15 min. After washing (3 x 10 min in 1x PBS) sections were incubated overnight at 4°C with rabbit antiserum against GPER (diluted 1:1000) and guinea pig antiserum against OT or VP (diluted 1:2000 (OT), 1:500 (VP)). Sections were washed and incubated for an hour at room temperature in biotinylated goat anti-rabbit antibody (as above), and Alexa Fluor 488 goat anti-guinea pig antibody (diluted 1:500) to detect OT or VP protein. Sections were further washed and incubated for an hour in streptavadin-conjugated Alexa Fluro 594

(diluted 1:500). Sections were mounted onto Superfrost Plus slides, coverslipped with an antifade mounting medium and viewed under a confocal laser-scanning microscope and processed with Adobe Photoshop CS3 extended computer software.

3.2.3 ISSH

Coronal cryostat sections (12μm) were cut, thaw-mounted onto polylysine-coated slides and stored at -80°C until use. The mouse GPER riboprobe was generated by PCR using approximately 20ng mouse GPER cDNA (cloned from a mouse AtT-20 pituitary tumour cDNA library; SJL unpublished data) as a template. Primers (upstream: 5'-GAGAGGATCCGGTCAGGGGCGCAGGC-3'; downstream 5'-AAACAAGCTTTGTGAGAGGAGCATC-3') corresponding to bp1739-2344 of a mouse GPER mRNA (Genbank Accession number NM_029771) were used to generate a 606bp product. The primers contain the recognition sequences for the restriction endonucleases BamH1 and HindIII. The rat GPER riboprobe was generated using approximately 150ng rat genomic DNA (Promega #G313A, UK) as a template. PCR primers (upstream: 5'-GAGAGGATCCTCCTAGAGGAAAACGGA-3'; downstream 5'-AAACAAGCTTTGTGAGAGGAGCATC-3') corresponding to bp15718722-15718072 of a rat GPER gene (Genbank Accession numbers NM_133573 and NC_005111) were used to generate a 651bp product. The primers contain the recognition sequences for the restriction endonucleases BamH1 and HindIII. Primer restriction endonuclease sites allowed subcloning into the RNA generating vector pGEM4Z (Promega, WI, USA), and sense and antisense probes were generated using T7 and SP6 polymerases (mouse and rat antisense: linearised with BamHI and generated with T7 polymerase; sense: linearised with HindIII and generated with SP6 polymerase) with ^{35}S-UTP and the MAXIscript *in vitro* transcription kit. The integrity of each probe was verified by DNA sequencing (Geneservice, UK). All ISHH experiments were performed as explained in section 2.2. Hybridised sections were exposed to film (Amersham HyperfilmTM MP) for 8 weeks, or emulsion dipped (Ilford K5) for 24 weeks and then counterstained with toluidine blue.

3.3 Results

3.3.1 Distribution of GPER-immunoreactivity (ir) in the adult mouse brain

The data presented here are semi-quantitative assessments based on subjective judgement of three independent observers. No apparent gender differences were observed in the distribution of GPER in the adult mouse brain. In most brain regions GPER-ir was expressed in cell bodies and fibres; in some regions mostly cell bodies (e.g., paraventricular nucleus of the thalamus, hypothalamic ventromedial nucleus) or fibres (e.g., lateral mammillary nucleus) expressed GPER-ir (see Table 3.1 and Figures 3.1-3.3).

In the forebrain GPER-ir expression was high in the cingulate, motor (Figure 3.1A) and somatosensory regions of the isocortex, piriform cortex (Figure 3.1B), entorhinal cortex, the dentate gyrus hilus (Figure 3.2A), and subiculum of the dorsal hippocampus formation, and the zona incerta (Figure 3.2B). Moderate to high expression was identified in the mitral layer of the olfactory bulb, dorsal endopiriform nucleus, CA1-3 of the ventral hippocampal formation, the medial habenular nucleus of the thalamus, and anteroventral periventricular nucleus, and the medial preoptic nucleus. The retrosplenial granular region of the isocortex, the lateral nucleus of the septal complex, the nucleus of the horizontal limb of the diagonal band of broca, the olfactory tubercle, the anterior amygdaloid area of the amygdala, and the paraventricular nucleus of the thalamus (Figure 3.1D), all demonstrated moderate expression of GPER. Low to moderate staining was noted in the granular insular, perirhinal and retrosplenial agranular regions of the isocortex, medial nucleus of the septal complex, and the CA2 of the dorsal hippocampal formation. Expression of GPER was low in many areas including the glomerular layer of the olfactory bulb, islands of Calleja, claustrum, caudate putamen of the striatum, shell of the accumbens nucleus, subfornical organ, CA1 and CA3 of the dorsal hippocampal formation, bed nucleus of the stria terminalis, and amygdalohippocampal nucleus and medial nucleus of the amygdala. The data are summarised in Table 3.1.

In the hypothalamus intense GPER expression was found in the arcuate nucleus, PVN (Figure 3.1E), periventricular hypothalamic nucleus, SON (Figure 3.1C), dorsomedial, central and ventrolateral divisions of the ventromedial hypothalamic nucleus with moderate to high expression in the suprachiasmatic nucleus (SCN), and lateral mammillary nucleus. GPER-ir was low in the dorsal medial nucleus, medial mammillary nucleus and ventral tuberomammillary nucleus and GPER expression was sparse in the lateral hypothalamic area, posterior hypothalamic nucleus, subthalamic nucleus, and supramammillary nucleus.

In the midbrain and pons distinct GPER-ir could be seen in the pontine nuclei, anterior tegmental nucleus, medioventral periolivary nucleus and superior paraolivary nucleus of the superior olive, and

the locus coeruleus (Figure 3.3B). A moderate to high expression was noted in the interpeduncular nucleus, compact region of the substantia nigra (Figure 3.2E) and the reticulotegmental nucleus of pons. The dorsal medial periaqueductal gray, inferior colliculus, caudal linear raphe nuclei, oral pontine reticular nucleus, the rostal, dorsal, caudal periolivary regions and the lateral superior olivary nucleus of the superior olive, nucleus of trapezoid body, lateral nucleus of the parabrachial region and the medial vestibular nucleus all expressed moderate levels of GPER. On the other hand, low levels were found in areas such as the lateral and reticular regions of the substantia nigra, superior colliculus, dorsal raphe, and the lateral vestibular nucleus.

In the hindbrain high expression of GPER was found in the oral and dorsomedial region of the spinal trigeminal nucleus (Figure 3.3C-D). GPER-ir was also high in the Purkinje cells of the cerebellum. Moderate expression was seen in the facial motor nucleus, principal nucleus of the inferior olive and the dorsal motor nucleus of vagus with low to moderate expression in the middle cerebellar peduncle, nucleus ambiguous and nucleus of the solitary tract. Low to moderate to staining was also found in the internal granule layer and molecular layers of the cerebellum. Low expression was detected in other regions including the posterodorsal tegmental nucleus, supratrigeminal, parapyramidal, intermediate reticular, gigantocellular, lateral reticular and the rosteroventrolateral reticular nuclei and the area postrema.

Brain Region	*GPER*
Forebrain	
Olfactory bulb	
Glomerular layer	+/c
Mitral layer	++/+++/c
External plexiform layer	-
Granule layer	-
Islands of Calleja	+/c
Cortex	
Allocortex	
Piriform	+++/c
Dorsal endopiriform nucleus	++/+++/f
Isocortex	
Agranular insular	-
Cingulate	+++/c
Dorsal peduncular	-/+/c
Granular insular	+/++/c
Infra-limbic	-/+/c
Prelimbic	-/+/c
Motor	+++/c
Somatosensory	+++/c
Perirhinal	+/++/c
Retrosplenial agranular	+/++/c
Retrosplenial granular	++/c
Visual	-/+/c
Dorsal tenia tecta	-
Claustrum	+/f
Striatum	
Caudate putamen	+/f
Globus Pallidus	-
Septal complex	
Lateral nucleus	++/c
Medial nucleus	+/++
Septohippocampal nucleus	-
Diagonal band of broca	
Horizontal limb diagonal band	++
Vertical limb diagonal band	+/c
Accumbens nucleus	
Shell	+/c
Core	-/+/c
Ventral Pallidum	-/+/c
Subfornical organ	+/c
Hippocampal formation- dorsal	
CA1	+
CA2	+/++
CA3	+
Dentate gyrus hilus	+++
Subiculum	+++/c
Hippocampal formation-ventral	
CA1-CA3	++/+++
Entorhinal cortex	+++/c
Internal capsule	-
Bed nucleus of the stria terminalis	+
Interstitial nucleus post limb anterior commisure	+
Olfactory tubercle	++/c
Substantia innominata	+
Amygdala	
Anterior amygdaloid area	++
Amygdalohippocampal nucleus	+/c
Basolateral nucleus	-
Basomedial nucleus	-
Cortical amygdaloid nucleus	-
Central nucleus	-
Medial nucleus	+
Thalamus	
Anterodorsal nucleus	-
Mediodorsal nucleus	-
Central medial nucleus	-/+/c
Paraventricular nucleus	++/c

Brain region	*GPER*
Rhomboid nucleus	-
Medial habenular nucleus	++/+++/c
Precommisural nucleus	-
Pretectal nucleus	-
Lateral posterior thalamic nucleus	-
Ventral medial thalamic nucleus	-
Zona incerta	+++
Subincertal nucleus	+/c
Preoptic area	
Anteroventral periventricular nucleus	++/+++/c
Lateral preoptic nucleus	+/c
Medial preoptic nucleus	++/+++/c
Magnocellular preoptic area	-
Hypothalamus	
Anterior commissural nucleus	-
Anterior hypothalamic nucleus	-
Arcuate nucleus	+++
Dorsomedial nucleus	-
Lateral hypothalamic area	-/+/c
Paraventricular hypothalamic nucleus	+++
Periventricular hypothalamic nucleus	+++/c
Posterior hypothalamic nucleus	-/+
Subthalamic nucleus	-/+
Suprachiasmatic nucleus	++/+++
Supraoptic nucleus	+++
Ventromedial hypothalamic nucleus	
Dorsomedial	+++/c
Cental	+++/c
Ventrolateral	+++/c
Lateral mammillary nucleus	++/+++
Medial mammillary nucleus	+
Supramammillary nucleus	-/+
Ventral tuberomammillary nucleus	+
Midbrain/ pons	
Deep mesencephalic nucleus	-
Edinger-Westphal nucleus	-/+
Interfascicular nucleus	-/+
Interpeduncular nucleus	++/+++
Suprageniculate thalamic nucleus	-/+
Substantia nigra (caudal)	
Compact	++/+++
Lateral	+/c
Reticular	+/c
Ventral tegmental area	-
Nucleus brachium inferior colliculus	-/+
Parabrachial pigmented nucleus	-/+/c
Periaqueductal gray	
Dorsal medial	++/c
Superior colliculus	+
Inferior colliculus	++
Raphe nuclei	
Rostal linear	-/+
Caudal Linear	++
Medial/paramedian	-/+
Dorsal raphe	+
Pontine nuclei	+++/c
Pontine reticular nucleus	
Oral	++/c
Caudal	-
Intercollicular nucleus	-
Lateral lemniscus	-/+
Parabigeminal nucleus	-
Dorsal tegmental nucleus	+/++
Pedunculopontine tegemental nucleus	-
Reticulotegmental nucleus pons	++/+++
Anterior tegmental nucleus	+++
Superior Olive	

Table 3.1. GPER distribution in the adult mouse brain.

Summary of GPER-ir distribution in the adult mouse brain, determined using three males and three females. Data presented here are of semi-quantitative assessments and the intensity of staining is based on the subjective judgement of three observers. No apparent gender differences were detected. Intensity of label: +++ intense; ++ moderate; + low; - absent; cells (c); fibres (f)- all other regions contain both immunoreactive cells and fibres.

Brain Region	*GPER*
Medioventral periolivary nucleus	+++/c
Rostral periolivary region	++
Dorsal periolivary region	++/c
Superior paraolivary nucleus	+++/c
Caudal periolivary nucleus	++
Lateral superior olivary nucleus	++
Nucleus of trapezoid body	++
Locus coeruleus	+++/c
Subcoeruleus nucleus	-/+
Parabrachial	
Medial nucleus	-
Lateral nucleus	++
Medial Vestibular nucleus	++
Lateral Vestibular nucleus	+
Hindbrain/ Cerebellum	
Raphe nuclei	
Magnus	-/+
Pallidus	-/+
Obscurus	-/+
Middle cerebellar peduncle	+/++/f
Posterodorsal tegmental nucleus	+
Supratrigeminal nucleus	+
Facial motor nucleus	++
Parapyramidal nucleus	+
Intermediate reticular nucleus	+
Gigantocellular reticular nucleus	+
Lateral reticular nucleus	+
Paragigantocelluar reticular nucleus	-/+
Rostoventrolateral reticular nucleus	+
Nucleus ambiguus	+/++/c
Prepositus nucleus	++
Nucleus solitary tract	+/++
Area postrema	+
Inferior olive, principal nucleus	++
Dorsal motor nucleus of vagus	++
Trigeminal nucleus, sensory	+++/c
Spinal trigeminal nucleus	+++/c
Spinal trigeminal nucleus, oral	+++/c
Cerebellum	
Molecular layer	-/+
Purkinje cell layer	+++/c
Internal granule layer	+/++

Table 3.1. Continued.

Summary of GPER-ir distribution in the adult mouse brain. Intensity of label: +++ intense; ++ moderate; + low; - absent; cells (c); fibres (f)- all other regions contain both immunoreactive cells and fibres.

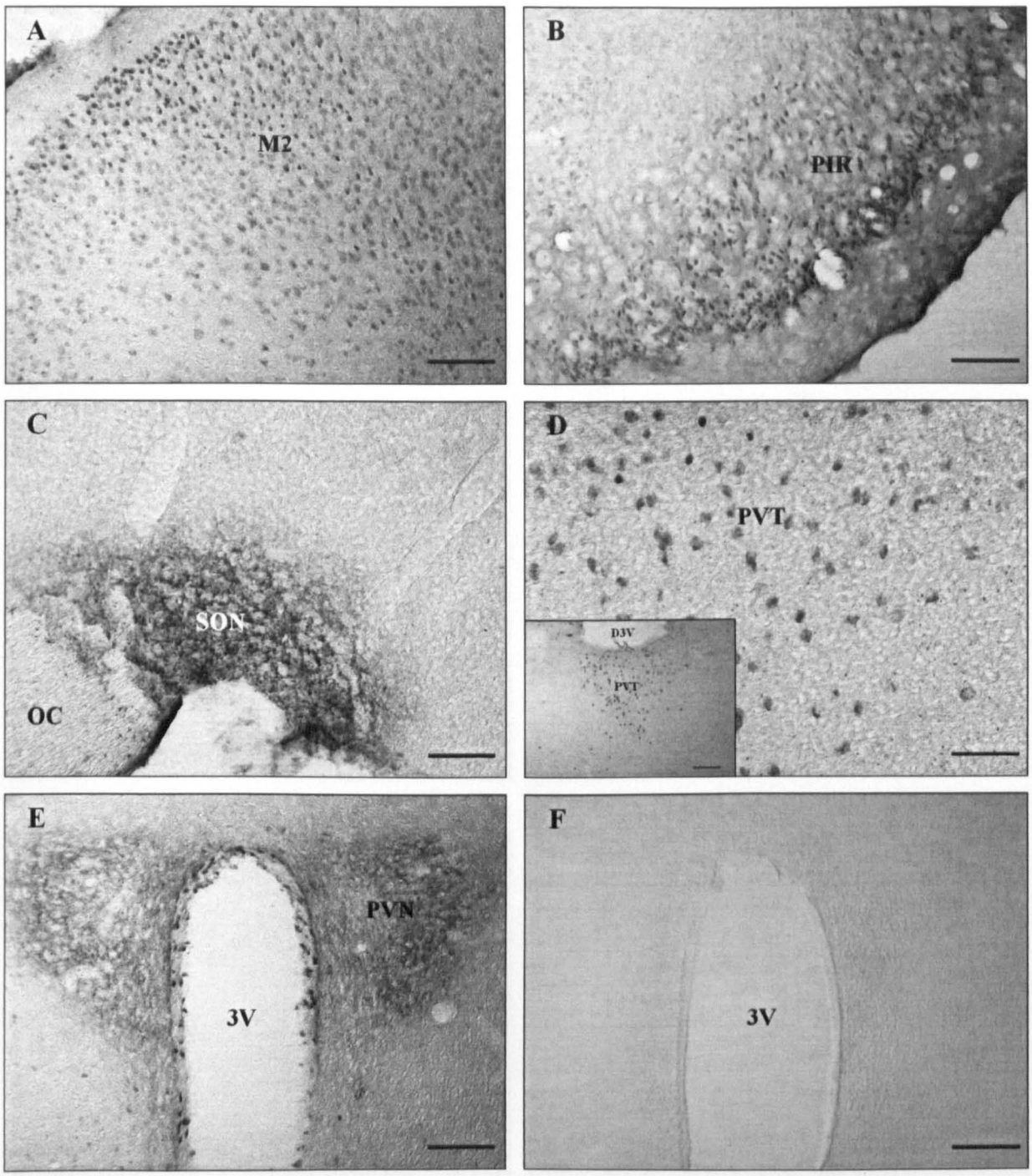

Figure 3.1. Immunoreactivity for GPER in the adult male or female mouse brain.

Labelled cells in the supplementary motor cortex (A), piriform cortex (B), labelled cells and fibres in the SON (C), with moderate labelling of cells in the paraventricular nucleus of the thalamus (D), labelled cells and fibres in the PVN (E) with an absence of labelling in the PVN with a section incubated with IgG in place of GPER antiserum (F). M2, supplementary motor cortex; PIR, piriform cortex; PVT, paraventricular nucleus of the thalamus; OC, optic chiasm; 3V, third ventricle. Scale bars, 100 μm in (A-B,E-F); 50 μm in (C-D). A lower magnification of the PVT is inserted in (D) (Scale bar = 100μm). D3V, dorsal third ventricle.

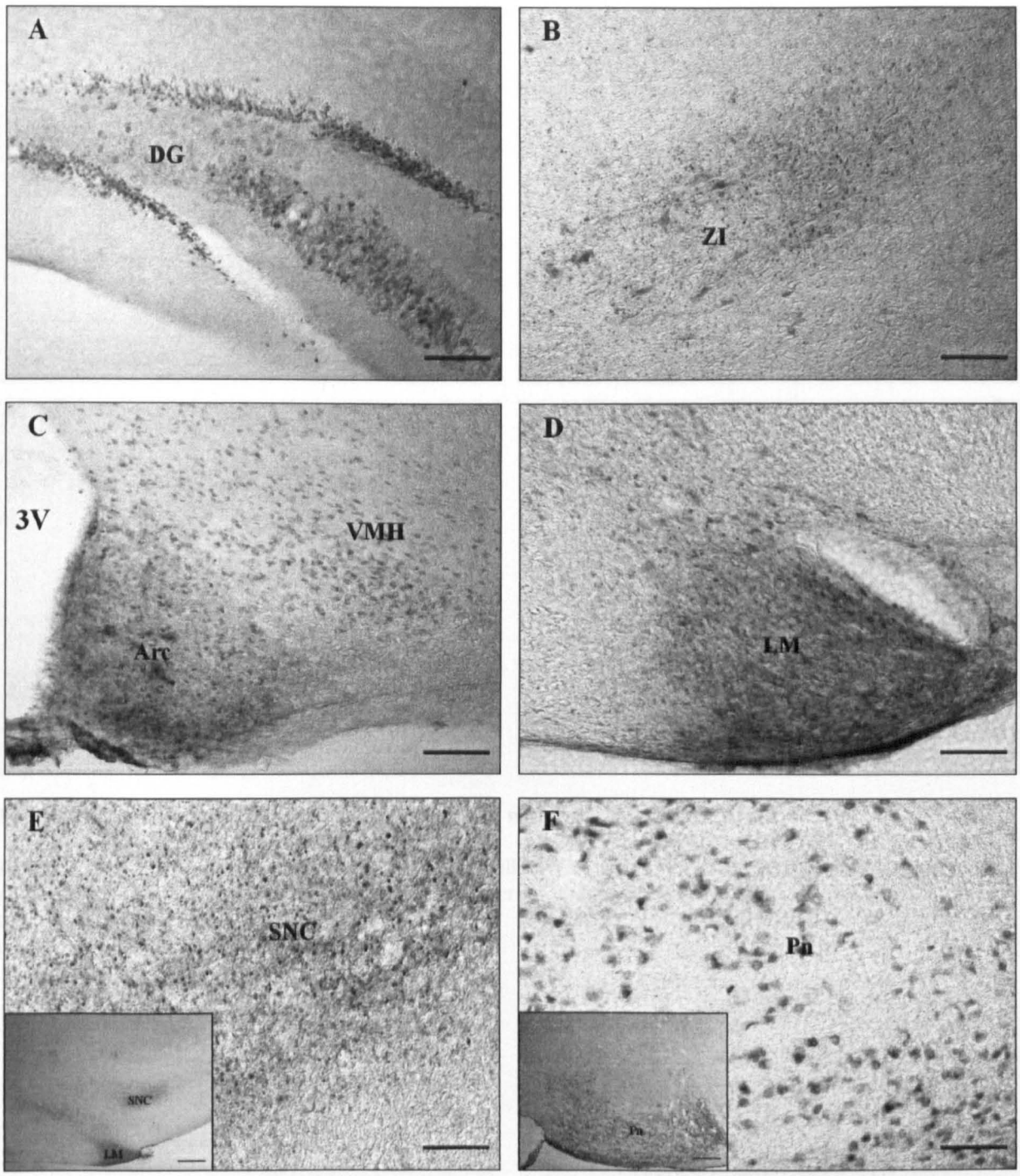

Figure 3.2. Immunoreactivity for GPER in the adult male or female mouse brain.

Labelled cells and fibres in the dentate gyrus of the hippocampus (A), zona incerta (B), arcuate nucleus and cell bodies of the ventromedial hypothalamic nucleus (C), GPER-ir in cells and fibres of the lateral mamillary nucleus of the hypothalamus (D), labelled cells and fibres of the pars compacta of the substantia nigra (E) and labelled cells of the pontine nuclei (F). DG, dentate gyrus of the hippocampus; ZI, zona incerta; Arc, arcuate nucleus of the hypothalamus; VMH, ventromedial hypothalamic nucleus; LM, lateral mamillary nucleus of the hypothalamus; SNC, pars compacta of the substantia nigra; Pn, pontine nuclei; 3V, third ventricle. Scale bars, 100 μm in (A-D); 50 μm in (E-F). In E and F, lower magnifications of the SNC and Pn, repectively, are shown (scale bars = 200μm).

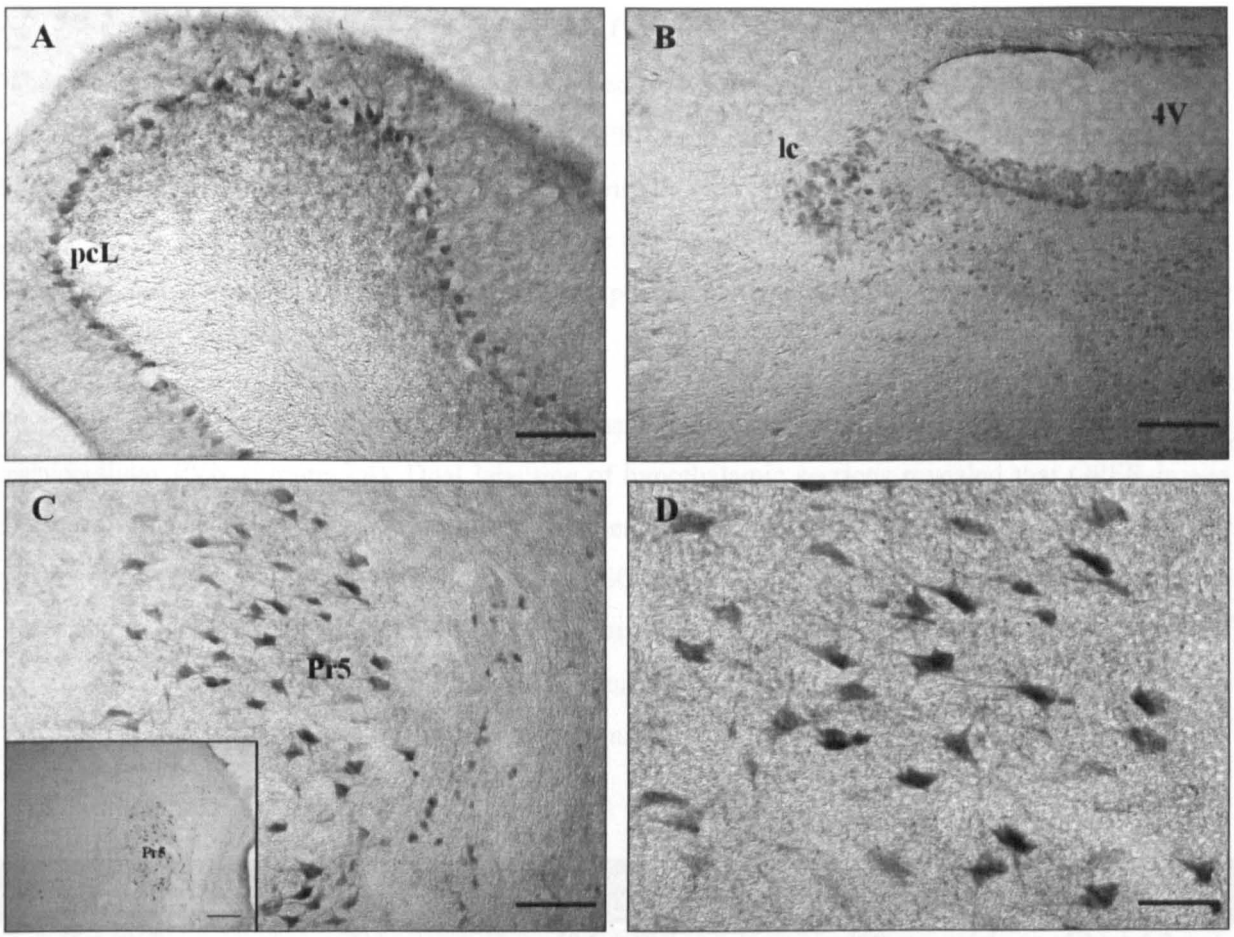

Figure 3.3. Immunoreactivity for GPER in the adult male or female mouse brain.

Labelled cells of the Purkinje cell layer of the cerbellum (A), locus coeruleus (B), and sensory trigeminal nucleus (C) enlarged in (D). pcL, Purkinje cell layer of the cerbellum; lc, locus coeruleus; Pr5, sensory trigeminal nucleus; 4V, fourth ventrcle. Scale bars, 100 μm in (A-C); 50 μm in (D). In (C), a lower magnification of Pr5 is shown (scale bar = 200μm).

3.3.2 GPER co-localises with oxytocin (OT) and vasopressin (VP) neurones

The results for this part of the study were obtained from three male and three female rat and mouse brains, double labelled with antibodies to GPER and either OT or VP. Pictures of GPER immunofluorescence were acquired and merged with the corresponding immunofluorescence pictures of OT or VP. Neurones containing both GPER-ir (red) and OT-ir or VP-ir (green) appeared yellow (merged) and were counted, and a co-expression percentage was calculated against the total number of OT-ir or VP-ir neurones.

In the rat PVN, GPER-ir is prominent in the magnocellular PVN with low level labelling in the parvocellular PVN (Figure 3.4). Dual labelling of hypothalamic sections revealed that GPER-ir was present in both OT and VP magnocellular neurones and 40-60% of OT neurones and 50-70% of VP neurones co-expressed GPER-ir in the PVN and SON (see Table 3.2 and Figures 3.4 and 3.5). In the PVN and SON of the mouse both OT and VP neurones were positive for GPER-ir, with 60-80% of OT and VP neurones expressing the receptor (Figures 3.4 and 3.5). Co-localisation of GPER-ir with OT and VP was also observed in fibres in the internal zone of the median eminence of both species.

	OT neurons	% co-localised with GPER	VP neurons	% co-localised with GPER
Rat PVN	223	50.6 ± 10.4	160	59.1 ± 6.3
Rat SON	148	54.6 ± 8.3	181	62.1 ± 7.4
Mouse PVN	191	70 ± 6.5	152	70.6 ± 8.2
Mouse SON	219	74.6 ± 8.9	131	64.2 ± 7.8

Table 3.2. Summary of GPER co-localisation with OT and VP neurones in the rodent PVN and SON.

Values represent the total number of OT and VP neurones counted in sections of PVN and SON obtained from three male and three female animals, and the average percentage (± SD) that also express GPER-ir. There was no apparent difference in the number of co-expressing neurones between the anterior, middle and posterior PVN in either rat or mouse.

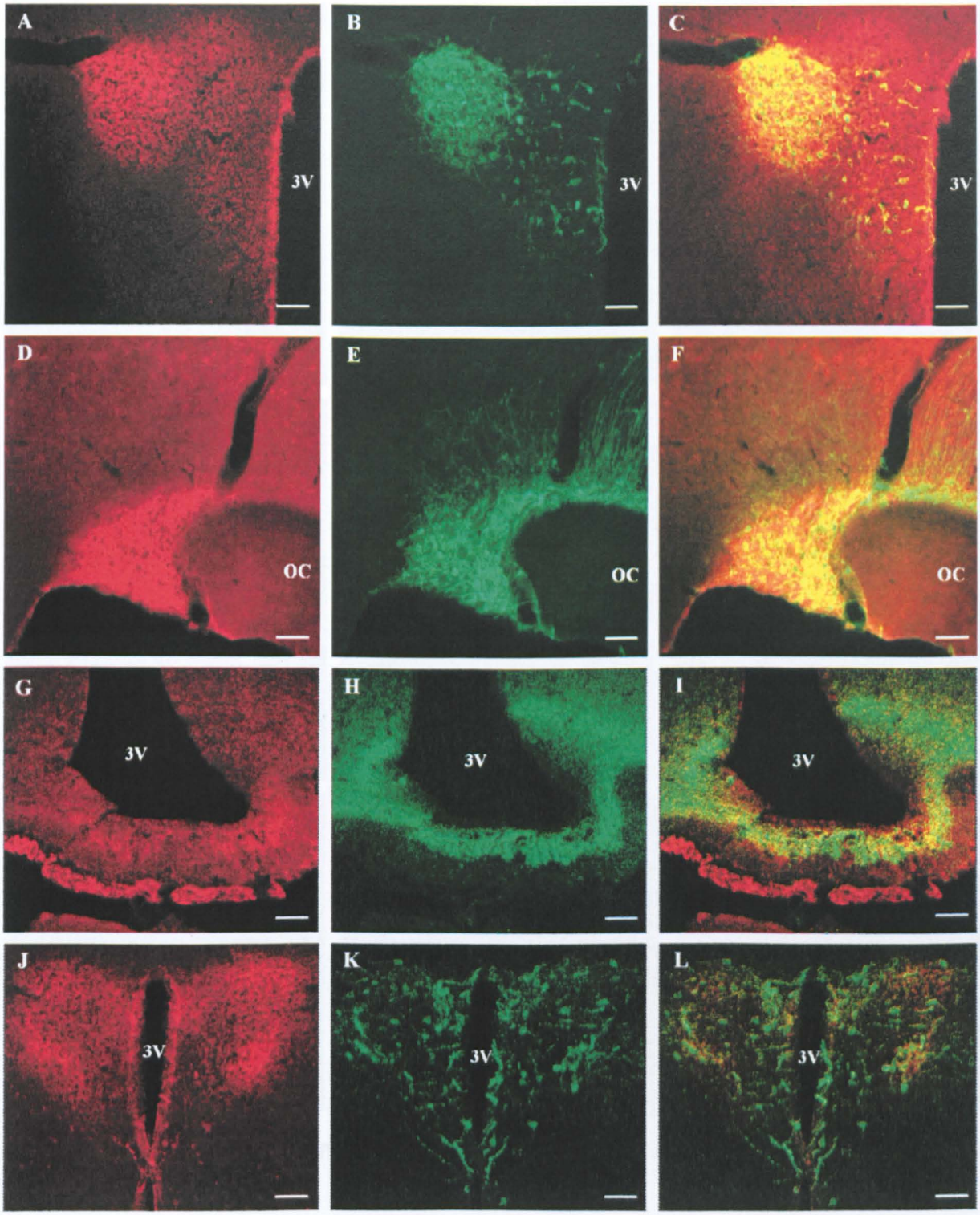

Figure 3.4. GPER is present in rodent OT and VP neurones.

Double label immunofluorescence for GPER and VP in the adult rat PVN (A-C), SON (D-F) and median eminence (G-I), and GPER and OT in the adult mouse PVN (J,K and L). Immunoreactivities against GPER (A, D, G and J; red) and VP (B, E and H; green) or OT (K; green) were merged in each right panel (C, F, I and L; overlap yellow), respectively. G-L were captured using a laser confocal microscope. 3V, third ventricle; OC, optic chiasm. Scale bars, 100 μm in (A-F); 80 μm in (G-L).

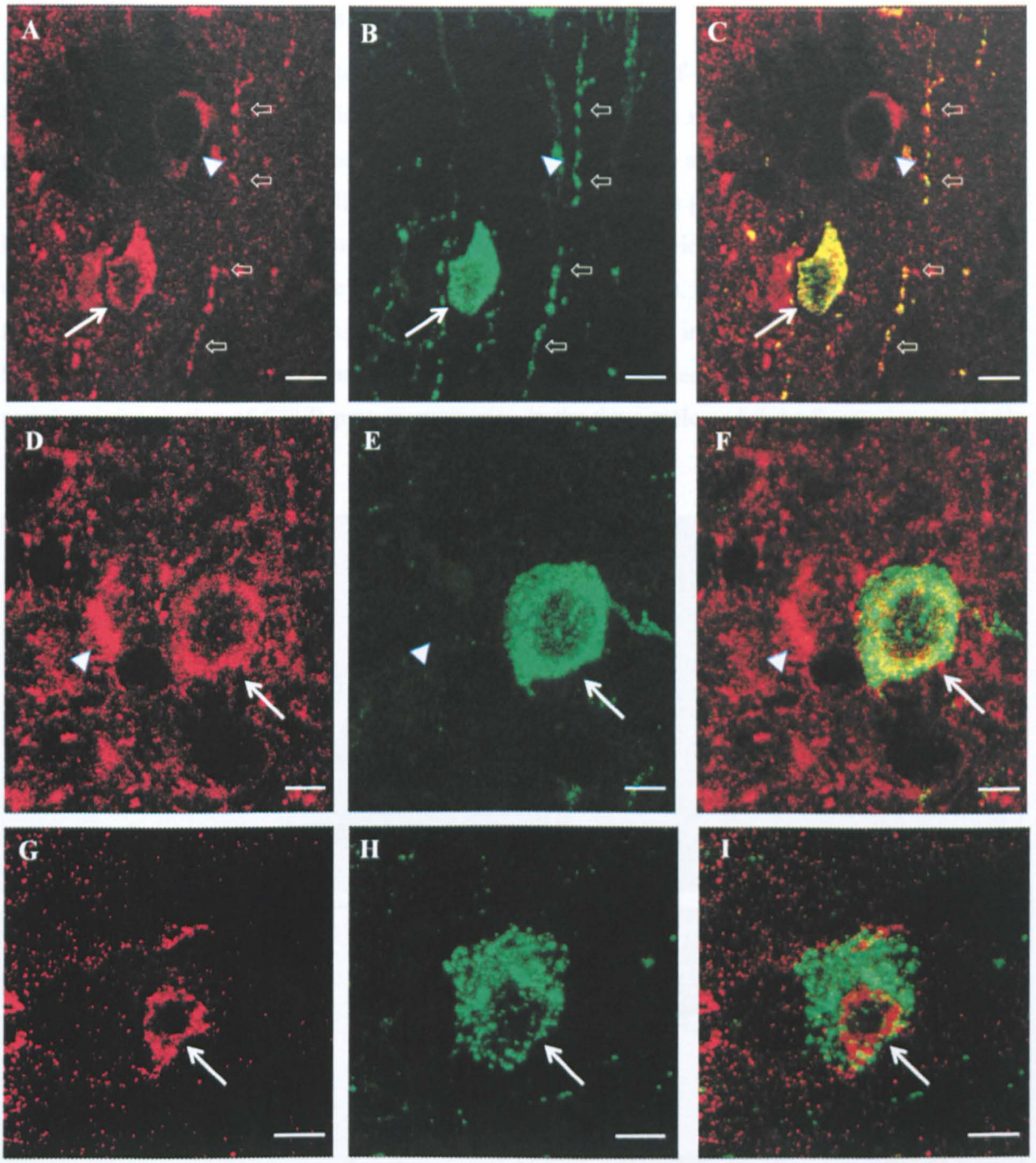

Figure 3.5. Double label immunofluorescence for GPER, OT and VP in the adult rat SON and mouse PVN.

Immunoreactivities against GPER (A, D and G; red) and OT (B; green) or VP (E, H; green) were merged in each right panel (C, F and I; overlap yellow), respectively. Arrows indicate OT or VP immunoreactive cell bodies that also contain GPER-ir. Note that some GPER-ir cells (arrowhead) do not express OT-ir or VP-ir. In addition to staining of cell bodies, there also appears to be co-expression of GPER-ir and OT-ir in processes (that may be axons or dendrites), suggesting that the receptor may be axo-dendritically transported, as has been well-established for the neuropeptide (see open arrows). The presence of possible intracellular staining of GPER within OT and VP neurones which is consistent with the predominantly cytoplasmic distribution of GPER that has been observed in various cell types *in vitro* (see discussion for details). Pictures captured at the same low magnification using a laser confocal microscope. Scale bars, 10μm in (A-I).

3.3.3 Peripheral distribution of GPER

In the anterior lobe of the pituitary gland approximately 50% of cells were intensely stained for GPER-ir. The majority of cells in the pituitary intermediate lobe stained positively and there was prominent staining of fibres in the neural lobe (Figure 3.6A). The adrenal medulla displayed strong GPER-ir; occasional GPER-ir cells were also observed in the zona glomerulosa of the cortex. In the kidney, GPER-ir was present in the smooth muscle cells of the pelvic region and to a lesser extent the medulla, with only a few positive cells in the cortex (Figure 3.6B). In the ovary, dense staining was found within the granulosa cells with moderate to low staining in the theca cells (Figure 3.6C). Staining was absent in corpora lutea. There were no species or gender differences observed in the peripheral distribution of GPER protein expression in the three male and three female rats and mice analysed.

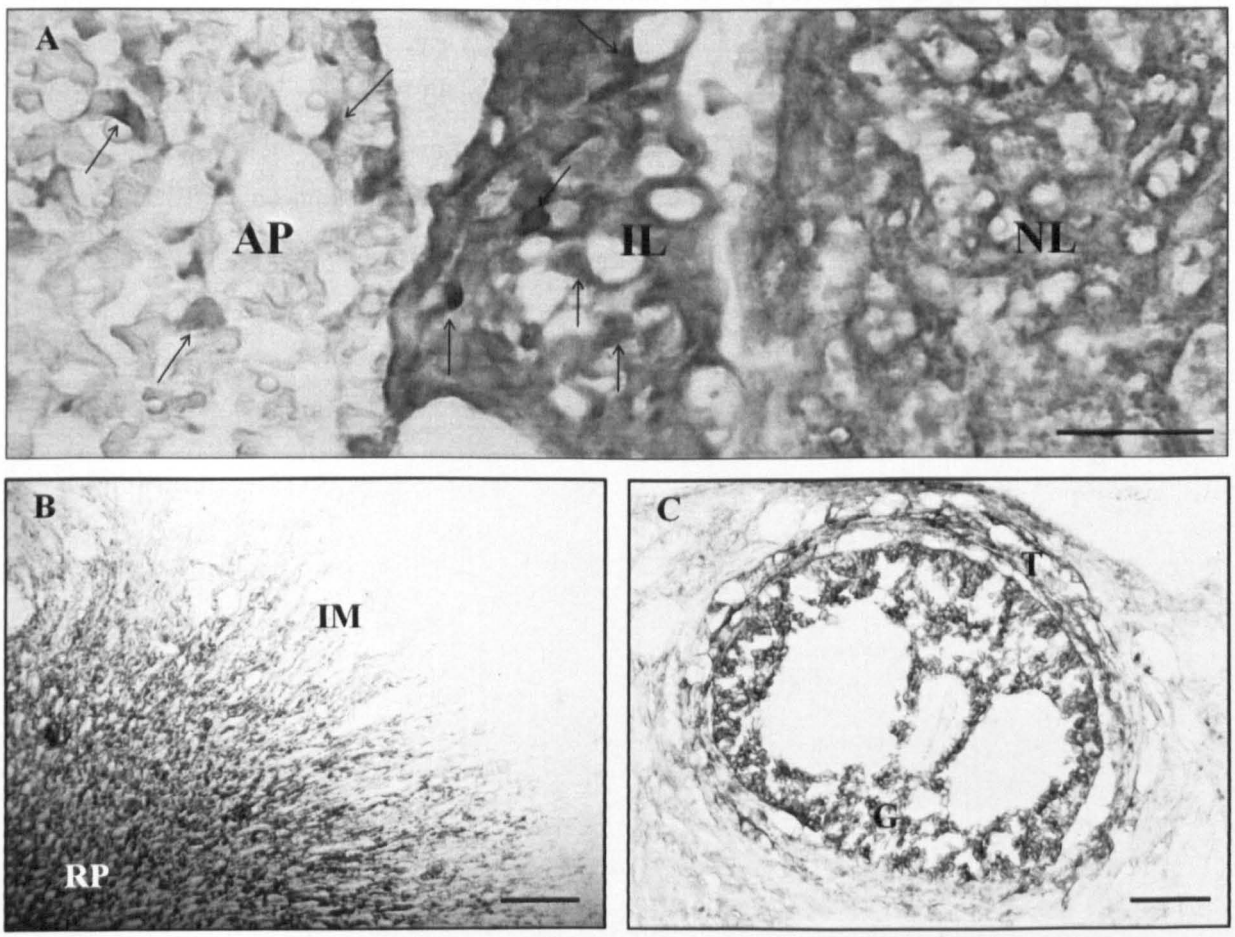

Figure 3.6. Immunohistochemical analysis of GPER in rodent peripheral tissues.

(A) GPER-ir in rat pituitary is prominent in the nerve terminals of the neural (posterior) lobe (NL) and is present in most melanotrophs of the intermediate lobe (IL) (e.g. indicated by arrows). GPER-ir is also found in scattered (approximately 50%) cells in the anterior pituitary (AP) lobe. Whether these represent endocrine cells (e.g., prolactotrophs, corticotrophs) was not determined. (B) High levels of GPER-ir are present in the rat renal pelvis (RP), an extension of the ureter, with projections into the renal inner medulla (IM). (C) In the rat ovary, GPER-ir is found mainly in the granulosa cells (G), with some staining of theca cells (T) of the developing follicle. Scale bars, 400μm in (B); 50μm in (A,C).

3.3.4 Distribution of GPER mRNA

We determined the expression of GPER mRNA in tissues that displayed abundant GPER-ir in tissues from three male and three female rats and mice. In the rat CNS a hybridisation signal for GPER was detected in the PVN and SON particularly in the magnocellular region of the PVN (Figure 3.7A, 3.7C). In the pituitary gland, the intermediate lobe was intensely labelled (Figure 3.7D-F) and scattered cells exhibited a moderate signal in the anterior lobe. The neural lobe was unlabelled. In the adrenal glands, high levels of GPER mRNA were present in the adrenal medulla and cells within the zona glomerulosa of the adrenal cortex (3.8A,B). In the kidney, intense labelling was present in the smooth muscle of the renal pelvis, and to a lesser extent in the medulla, with some sparse labelling in the cortex (Figure 3.8C). A few developing follicles of the rat ovary exhibited a hybridisation signal (data not shown). A similar distribution of GPER transcripts were observed in mouse tissues - the SON, the adrenal medulla and pituitary intermediate lobe expressed the highest amount of GPER mRNA compared with kidney, ovary and PVN based on signal intensities observed for the same film exposures. Figure 3.8E shows GPER mRNA expression in developing follicles of the mouse ovary, with silver grains accumulated mainly in the granulosa and theca cells. No signal was detected in the corpora lutea. Rat and mouse sections hybridised with sense GPER riboprobes as controls showed only background level of labelling (Figures 3.7B, 3.8D, 3.8E).

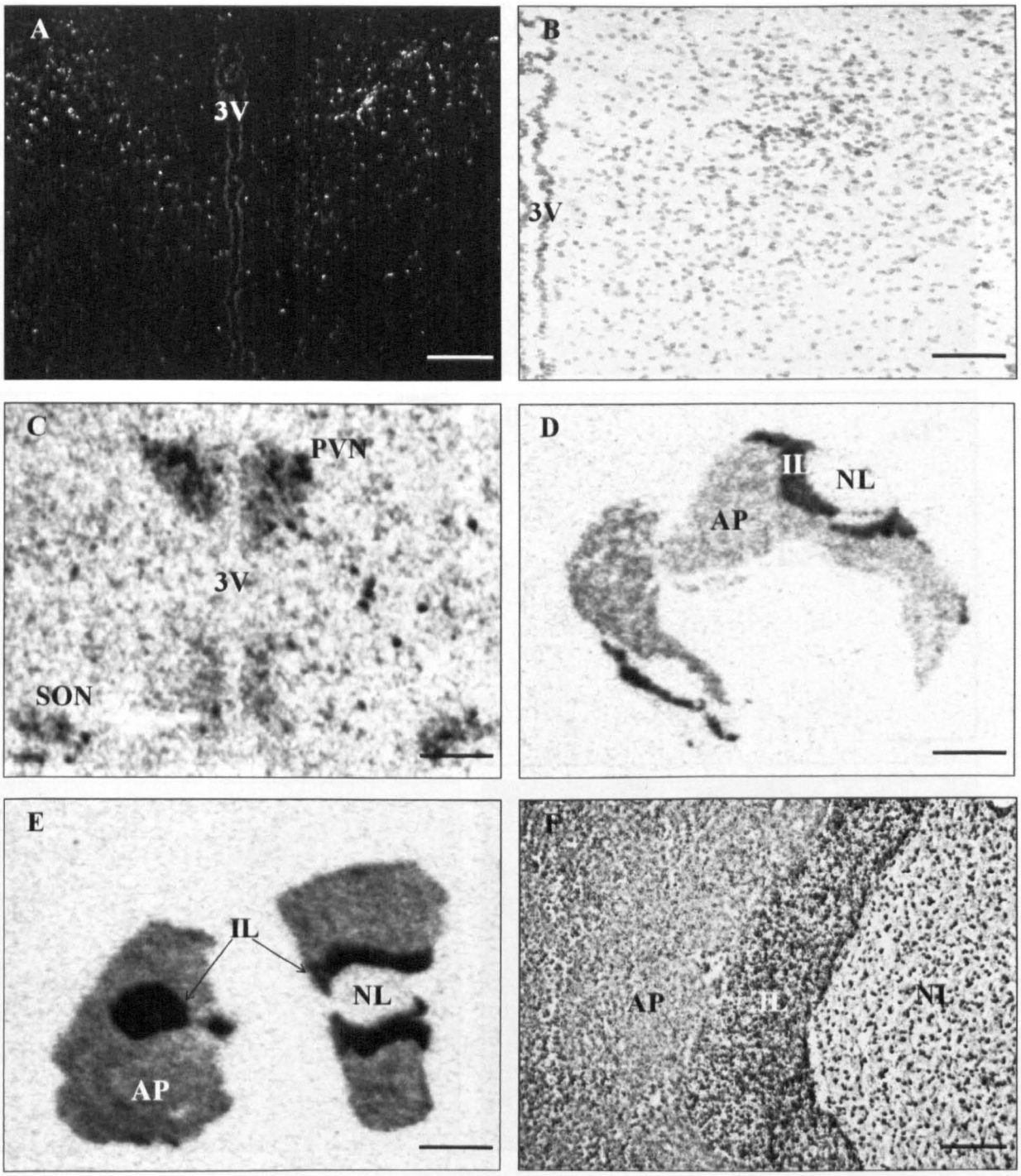

Figure 3.7. *In situ* hybridisation of GPER mRNA in the rodent PVN, SON and pituitary gland:

Reversed image of emulsion dipped section of the rat PVN the GPER hybridisation grains appear white in the picture (A) (but black on the actual slide); the corresponding sense slide is absent of black GPER hybridisation grains (B); low magnification photographs of film autoradiographic images of a slide mounted hypothalamic section hybridised with a GPER probe, with signal in the PVN and SON of the rat brain (C), and pituitary sections hybridised with a GPER probe in rat (D) and mouse (E) with intense signal in both intermediate lobes; emulsion dipped section of the mouse pituitary, hybridisation signal for GPER mRNA appears as black grains (F). 3V, Third ventricle; AP, anterior pituitary; IL, intermediate lobe of the pituitary; NL, neural lobe of the pituitary. Scale bars, 1mm in (C-E); 100μm in (A, F); 50 μm in (B).

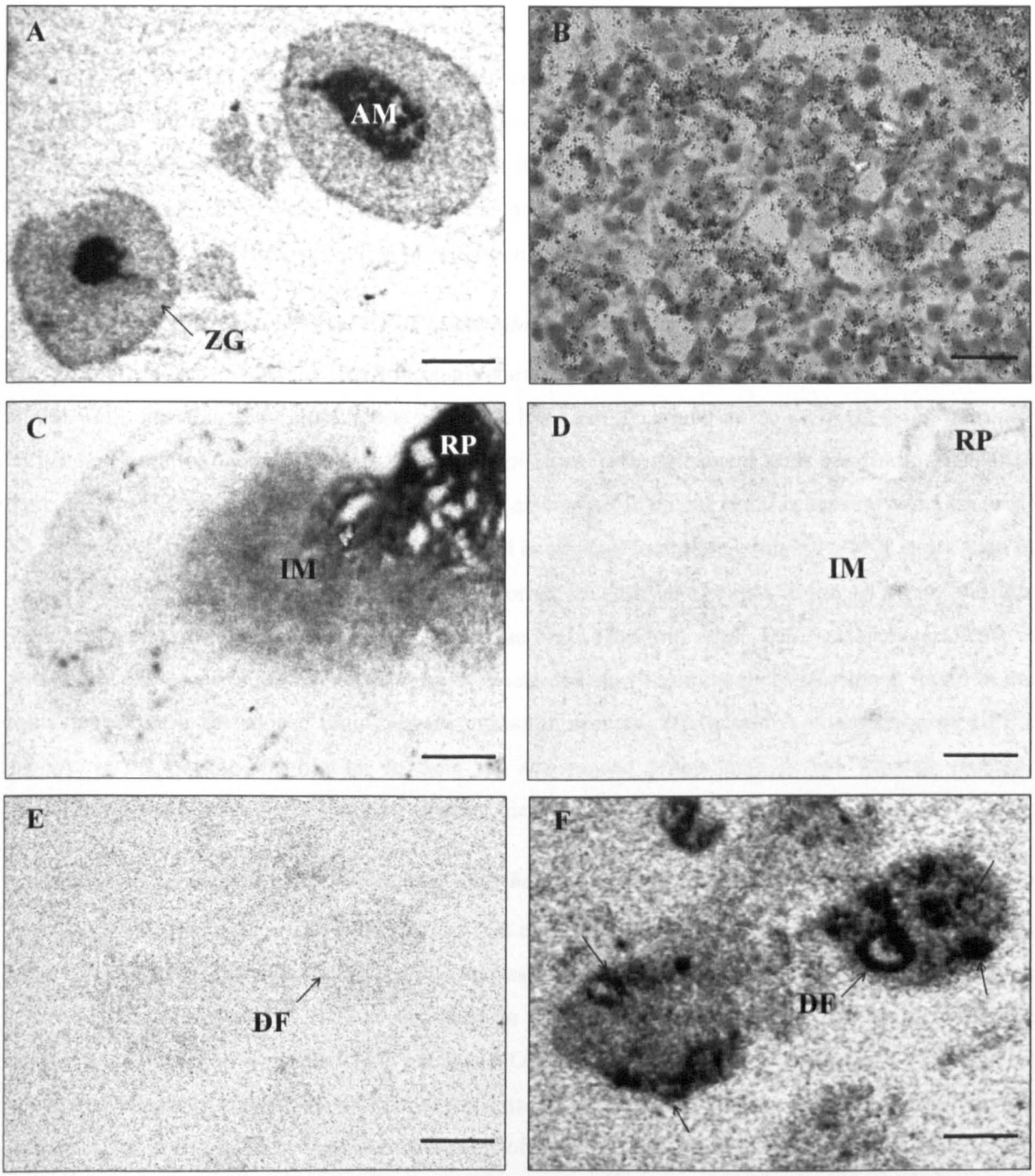

Figure 3.8. *In situ* hybridisation of GPER mRNA in the rodent peripheral tissues:

Low magnification photograph of a film autoradiographic image of a slide mounted, rat adrenal section hybridised with a GPER probe (A); emulsion dipped section of the mouse adrenal medulla - hybridisation signal for GPER mRNA appears as black grains on toluidine blue counterstained cells (B); low magnification photograph of a film autoradiographic image of a slide mounted, rat kidney section hybridised with a GPER probe (C), with an absence of signal in the sense control (D); low magnification photograph of a film autoradiographic image of a slide mounted, mouse ovary section hybridised with a GPER probe, with signal localised predominantly in the developing follicles (F), with an absence of signal in the sense control (E). AM, Adrenal Medulla; ZG, Zona glomerulosa; RP, Renal pelvis; IM, Renal medulla; DF, developing follicle. Scale bars, 1mm in (A, C-F); 25μm in (B).

3.4 Discussion

The GPER gene is widely distributed in human and rat central and peripheral tissues as shown by northern blot, and in rat brain by immunohistochemical analyses (Owman *et al.*, 1996; Bonini *et al.*, 1997; Carmeci *et al.*, 1997; Fung & Gregor, 1997; Kvingedal & Smeland, 1997; Brailoiu *et al.*, 2007). These observations have been extended in the present study using IHC and ISHH to obtain the cellular context of GPER expression in mouse brain and peripheral tissues.

3.4.1 Distribution of GPER-ir in the adult mouse brain

The present study provides the first full comprehensive characterisation of GPER distribution in the mouse CNS. Previously the distribution of GPER has been illustrated in the rat brain using the same GPER antiserum as described here (Brailoiu *et al.*, 2007). In agreement with our findings in mice there are no apparent gender differences in GPER expression in the rat and this appears common to all E2 receptors (Laflamme *et al.*, 1998). Brailoiu and coworkers found predominant GPER expression in the hypothalamic PVN and SON, hippocampal formation, substantia nigra in the rat brain, and this correlates well with our observations in the mouse brain (Brailoiu *et al.*, 2007). However, GPER is also highly expressed in the nucleus ambiguus where only low to moderate expression is found in the equivalent area in the mouse brain, suggesting some species differences. A comparison of GPER mRNA versus protein localisation in both rat and mouse brains may reveal whether receptor transcription and translation coincide or whether there are mismatches.

3.4.2 Comparison of E2 receptor distribution in the adult mouse brain

There appears to be only a few brain regions that express high levels of GPER and high amounts of either ERα or ERβ, and even fewer regions that express all three receptors (see Table 3.3) to a high degree. For example, GPER is most abundant in the hypothalamus of the mouse, particularly the arcuate nucleus, PVN, periventricular nucleus, SON and the dorsomedial, central and ventrolateral regions of the ventromedial hypothalamic nucleus. Of these nuclei ERα is highly expressed in the arcuate nucleus and in the ventrolateral portion of the ventromedial hypothalamic nucleus (VMH), and in rats priming the VMH with E2 over days promotes lordosis, seemingly through ERα (Pfaff & Sakuma, 1978). In the rat and mouse hypothalamus ERβ is the predominant ER isoform found in the PVN (Mitra *et al.*, 2003; Merchenthaler *et al.*, 2004). Interestingly E2 has been shown to activate the ERK1/2 pathway in the PVN and SON of the mouse (Ábrahám *et al.*, 2004). In the PVN this is potentially mediated via either ERβ and/or GPER (as both are highly expressed in the PVN), and presumably GPER in the SON (as GPER appears to be the predominantly expressed receptor in the SON).

In the forebrain GPER is also highly expressed in the cingulate, motor and somatosensory regions of the isocortex, piriform cortex, the hippocampal dentate gyrus hilus, subiculum and entorhinal cortex, and the zona incerta where ERα and ERβ expression is either low or absent. Interestingly E2 has been shown to induce c-Fos protein expression in some brain regions (e.g., cingulate cortex) of double ERα/β KO mice. As GPER is abundant in this region it or another E2-binding protein may mediate the effects of E2 (Dominguez-Salazar *et al.*, 2006). On the other hand, ERα and β are both highly expressed in the bed nucleus of the stria terminalis and the medial nucleus of the amygdala, where only minimal amounts of GPER can be detected.

In the midbrain/pons high expression of GPER is found in the pontine nuclei, anterior tegmental nucleus, the medioventral periolivary nucleus and superior paraolivary nucleus of the superior olive, and the locus coeruleus. Of these only the locus coeruleus contains high levels of the ERs. Interestingly in the mouse, noradrenaline neurones of the locus coeruleus have been shown to be responsive to E2 stimulation with an upregulation in tyrosine hydroxylase transcription in females, and attenuation of transcription in males (Thanky *et al.*, 2002). This gender difference could be indicative of the varying roles of all three E2 receptors which are highly expressed in this brain region.

Brain Region	GPER	ERα	ERβ
Allocortex			
Piriform	+++	+	+
Isocortex			
Cingulate	+++	-	-/+
Motor	+++	-	-/+
Somatosensory	+++	-/+	-/+
Hippocampus			
Dentate gyrus hilus	+++	+	-
Subiculum	+++	-/+	+/++
Entorhinal cortex	+++	-	+
Bed nucleus of the stria terminalis	+	+++	+++
Preoptic area			
Medial Preoptic nucleus	++/+++	+++	++
Amygdala			
Medial nucleus	+	+++	+++
Hypothamalmus			
Arcuate nucleus	+++	+++	+
Paraventricular nucleus	+++	+	+++
Periventricular nucleus	+++	++/+++	-/+
Supraoptic nucleus	+++	-	+
Ventromedial hypothalamic nucleus			
Dorsomedial	+++	-/+	-
Central	+++	++	-
Ventrolateral	+++	+++	+/++
Substantia nigra			
Reticular	+	-	+++
Ventral tegmental area	-	-	++
Periqueductal gray	+/++	++/+++	+
Raphe nuclei			
Dorsal raphe	+	+	+++
Pontine nuclei	+++	-	+
Anterior tegmental nucleus	+++	-	+
Superior Olive			
Medioventral periolivary nucleus	+++	-	+
Superior paraolivary nucleus	+++	-	+
Locus coeruleus	+++	++	++
Spinal trigeminal nucleus	+++	++	-/+
Cerebellum			
Purkinje layer	+++	-	-

Intensity of label: +++ intense; ++ moderate; + low; - absent

Table 3.3. An overall comparison of the distribution of GPER, ERα and ERβ, in the mouse brain.

Results for ERα and ERβ are a summary of the mouse brain atlases from Mitra *et al.*, 2003 and Merchenthaler *et al.*, 2004.

3.4.3 GPER co-localises with OT and VP neurones

The present study also aimed to clarify the inconsistencies in the literature regarding the distribution of GPER in hypothalamic magnocellular neurones. Our findings confirm that in the rat and mouse hypothalamus both OT and VP neurones express GPER. This is in agreement with observations of Brailoiu and co-workers who found co-localisation of GPER with OT and VP in magnocellular neurones of the rat PVN and SON, but contrasts with those of another study that detected GPER only in OT neurones of the PVN and SON of the same species (Brailoiu *et al.*, 2007; Sakamoto *et al.*, 2007). The reasons for these discrepancies are not readily apparent, especially since all three studies used the same antiserum directed against the GPER protein (Revankar *et al.*, 2005). To confirm the specificity of GPER-ir in the current study we substituted normal rabbit IgG serum for primary antibody at the same concentration, and did not observe any staining (Figure 3.1F).

E2 mediates the release of OT and VP *in vivo* and *in vitro*. It rapidly stimulates intrahypothalamic OT and VP release and rapid peripheral OT and possibly VP release (Wang *et al.*, 1995; Burbach *et al.*, 2001). In addition, E2 inhibits the release of both peptides from hypothalamo-neurohypophysial explants stimulated hyperosmotically via a non-genomic action (Swenson and Sladek, 1997), and rapidly alters the electrophysiological properties of OT cells in the SON of lactating, or morphine-dependent rats (Israel & Poulain, 2000; Brown *et al.*, 2008). There is very little or no ERα in the rat and mouse PVN/SON (Merchenthaler *et al.*, 2004; Shughrue *et al.*, 1998b) suggesting that E2 may not directly influence OT/VP release via this receptor. On the other hand the presence of ERα in many central regions that project to the PVN/SON, including the organum vasculosum of the lamina terminalis and subfornical organ (regions implicated in blood volume and plasma osmolality regulation), and the medial preoptic nuclei and ventromedial hypothalamus (essential areas in reproductive behaviour) suggests that E2 may modulate VP/OT secretion indirectly via ERα (Merchenthaler *et al.*, 2004; Voisin *et al.*, 1997). ERβ is expressed in the magnocellular OT neurones of both the rat PVN and SON (Alves *et al.*, 1998; Hrabovszky *et al.*, 2004) and provides a direct route for possible E2 manipulation of VP/OT-expressing neurones.

The relative contribution of GPER in E2 effects on hypothalamo-neurohypophysial activity is not known. However, ERβ-ir is absent from the neural lobe suggesting that E2 does not directly mediate peripheral release of OT and VP at the level of the pituitary via this receptor (Pelletier *et al.*, 2000). Interestingly in the current study we found high levels of GPER-ir in the neural lobe, indicating that E2 could modulate the peripheral release of OT and VP through GPER signalling. As we were unable to detect GPER mRNA in the neural lobe, it can be assumed that the receptor had been transported, presumably from the magnocellular neurones in the PVN and SON, as we also observed co-localisation of GPER with OT and VP fibres in the internal zone of the median eminence. It is possible that GPER regulates OT/VP synthesis in PVN/SON magnocellular cell bodies, and/or modulates OT/VP release from PVN/SON magnocellular neurone dendrites, or from fibres that terminate in the posterior pituitary. Our studies also suggest that GPER could mediate E2 effects on the hypothalamic-pituitary-adrenal axis by modulating the release of OT, VP or perhaps CRF into portal blood from neurones originating from the parvocellular region of the PVN.

3.4.4 Peripheral distribution of GPER

The current study demonstrates high expression of GPER mRNA and protein in the pituitary gland, adrenal medulla, renal pelvis, and ovary of the rat and mouse. There is a strong correlation between the tissue distribution of both GPER mRNA and protein, apart from in the neural lobe of the pituitary.

While GPER protein is expressed in all three lobes of the pituitary, the highest mRNA expression was observed in the intermediate lobe. ERα and ERβ are also expressed in the anterior and intermediate

lobes but are absent from the posterior lobe of the pituitary (Mitchner *et al.*, 1998; Pelletier *et al.*, 2000; González *et al.*, 2008). It is well established that the anterior pituitary is a target tissue for E2, regulating gonadotrophin and prolactin secretion from gonadotrophs and lactrotrophs, and this response can be rapid, with E2 increasing excitability in prolactin-secreting pituitary cells lines within minutes (Dufy *et al.*, 1979). High expression of GPER mRNA and protein in the intermediate lobe and the presence of the traditional E2 receptors, suggests a possible role for E2 in POMC synthesis and α-melanocyte stimulating hormone (αMSH) and ACTH-like peptide release. A previous study has shown that E2 stimulates the release of αMSH from the intermediate lobe which in turn appears to exert a rapid stimulatory effect on prolactin secretion (Ellerkmann *et al.*, 1992).

In agreement with the current study GPER has been reported to be strongly expressed in the zona glomerulosa and the medulla of the human adrenal glands (Baquedano *et al.*, 2007). Fast effects of E2 have previously been described in primary cultures of bovine adrenal medullary cells with an up-regulation in catecholamine synthesis within 20 min of E2 stimulation (Yanagihara *et al.*, 2006). This suggests a role for GPER in E2 signalling either independently or synergisitically with extranuclear ERβ which is also expressed in cells of the rat adrenal cortex and medulla (Saunders *et al.*, 1997).

In the kidney ERα/β are found mainly in the glomeruli and arterioles of the renal cortex where E2 treatment has been shown to upregulate angiotensin type II receptors that regulate sodium and water reabsorption, renal blood flow and glomerular filtration rate (Baiardi *et al.*, 2005; Oestreicher *et al.*, 2006). We found high expression of GPER mRNA and protein in the contracting muscle of the pelvis and to a moderate extent in the medulla. In the renal pelvis the role of E2 is presently unclear but there are suggestions that prolonged E2 administration can encourage renal pelvic tumour growth (Oberley *et al.*, 1991; Adsay *et al.*, 2000). In other carcinomas (e.g., breast, endometrial) GPER expression has been demonstrated (Filardo *et al.*, 2006; Smith *et al.*, 2007). Taken together it is tempting to speculate that GPER is an alternative E2 responsive receptor in the production and maintenance of renal pelvic tumours.

E2 has been shown to promote cell division and survival of granulosa cells in developing follicles of the ovary (Adashi, 1994). E2 also induces rapid (seconds) increases in cytosolic calcium concentration of human granulosa cells *in vitro* (Younglai *et al.*, 2005). While this could be mediated through the ERβ which has been shown to be highly expressed within the granulosa cells of developing follicles and corpora lutea of the rat (Saunders *et al.*, 1997), our results also indicate a role for GPER. GPER mRNA and protein have been found in both granulosa and theca cells of the hamster and expression is sensitive to cyclic changes in FSH and LH (Wang *et al.*, 2007). It has also been suggested that GPER is required for primordial follicle formation (Wang *et al.*, 2008c). These observations appear to contradict a recent report which concluded that GPER did not mediate E2

responses in reproductive organs due to the fertile phenotype of the GPER KO mice (Otto *et al.*, 2008). In GPER KO animals the normal phenotypes in E2 responsive tissues such as the ovary, uterus and mammary gland does not necessarily preclude the possibility that GPER binds E2 *in vivo*. For example, in the KO model ERα and/or ERβ may compensate for the loss of GPER especially in tissues of co-expression where there is potential for receptor cross-talk (Sirianni *et al.*, 2008). In addition it is well known that ERβ KOs remain fertile; it is only the deletion of ERα that appears to create the infertile phenotype (Walker & Korach, 2004).

Whilst this manuscript was in preparation, a few papers relevant to the possible function of GPER in the brain and adrenal have been published. Isensee and co workers analysed the distribution of GPER using GPER-LacZ reporter mice and found predominant expression in subpopulations of cells in the cortex and the dentate gyrus of the brain, in the intermediate and anterior lobe of the pituitary gland, and in the adrenal medulla (Isensee *et al.*, 2008). As shown in Table 3.1 GPER-ir is also highly expressed in regions of the cortex, and in the dentate gyrus of the adult mouse brain. Our results also confirm the presence of GPER mRNA in the anterior and intermediate lobes of the pituitary and the adrenal medulla. However, in contrast to our data that clearly demonstrate both GPER mRNA and protein in the PVN and SON, GPER was only identified in the hypothalamic vasculature and not neurones in the GPER-LacZ reporter mice (Isensee *et al.*, 2008). Recently Xu and co-workers demonstrated an interaction between GPER and the OT system. Ovariectomised female rats were administered a subcutaneous injection of E2, or an icv injection of G-1, a selective GPER agonist (to a region directly above the PVN) for 2 consecutive days, and it was found that E2 and G-1 were unable to alter basal plasma OT levels (Xu *et al.*, 2008). Conversely in rats concomitantly treated with the 5-HT1A receptor agonist ((+)-8-hydroxy-2-dipropylaminotetralin (DPAT)) G-1 (albeit a high dose - 100nM) significantly attenuated a DPAT induced rise in plasma OT. A similar, although less pronounced response was observed with E2 (Xu *et al.*, 2008). Other studies have also implicated that GPER may mediate E2-stimulated GnRH release from primate neurones (Noel *et al.*, 2009) as well as from mouse neurones, which may possibly corroborate the expression of GPER in the VMH and/or the anterior pituitary gland (Sun *et al.*, 2010). Finally the expression of GPER in the adrenal medulla of the rat has been confirmed by Dun *et al.*, with GPER located in tyrosine hydroxylase-positive chromaffin cells, further suggesting a likely role for GPER in E2-mediated noradrenaline release from the adrenal glands (Dun *et al.*, 2009).

3.5 Conclusion

The distribution of GPER in the adult mouse brain appears distinct from ERα and ERβ receptors and offers an additional site for E2 action. The expression of GPER in OT and VP neurones in the PVN, SON, and in the median eminence, and its presence in the pituitary gland provides a likely means by which E2 can modulate fast 'non-genomic' effects on these specific neuropeptide systems. In the

periphery, GPER may be involved in multiple functions including hormone release and development. Whether E2 initiates responses through GPER alone or in concert with the other E2 receptors (e.g., in regions of co-expression) is yet to be fully investigated but the cellular distribution of GPER in the brain and peripheral tissues provides a basis for further studies on E2 mediated signalling.

Chapter 4: *In vitro* characterisation of GPER

4.1 Introduction

4.1.1 The GPER story so far: recognised mechanisms and possible functions

GPER (previously known as GPR30, CMKRL2, LyGPR, GPCR-Br, FEG-1, GPR41) first cloned by Dr Stephen Lolait and colleagues in 1996 from a human B-cell lymphoblast cDNA library, is a member of the class A rhodopsin-like family of GPCRs, and shares closest homology with the angiotensin II and chemokine receptors (Owman *et al.*, 1996; Takada *et al.*, 1997). GPER is the first official steroid binding GPCR, and has been shown to rapidly activate a variety of transduction pathways in response to E2 including the adenylyl cyclase/cAMP, calcium, ERK1/2 and phosphoinositide 3-kinase (PI3K) cascades (Maggiolini and Picard, 2010). GPER is also activated by the anti-E2s tamoxifen and ICI-182,780, and various environmental E2s e.g., Bisphenol A, genistein, nonylphenol, quercetin, and zearalonone (Thomas and Dong, 2006; Maggiolini *et al.*, 2004). It has been shown that GPER may couple to more than one family of G proteins e.g., direct GPER-$G\alpha_s$ binding has been demonstrated in the membranes of HEK293 and SKBR3 cells; and the E2-mediated increase in ERK1/2 phosphorylation in Ishikawa, MCF-7, MDA-MB-231 and SKBR3 cells is sensitive to pertussis toxin which is indicative of $G\alpha_i$ coupling (Filardo *et al.*, 2000, 2007; Vivacqua *et al.*, 2006b; Maggiolini *et al.*, 2004). GPER also transactivates the receptor tyrosine kinase EGFR, which activates the ERK pathway, induces calcium mobilisation and stimulates P13K signalling (Filardo *et al.*, 2000; Revenkar *et al.*, 2005). Figure 4.1 summaries the diverse range of GPER mediated signalling cascades.

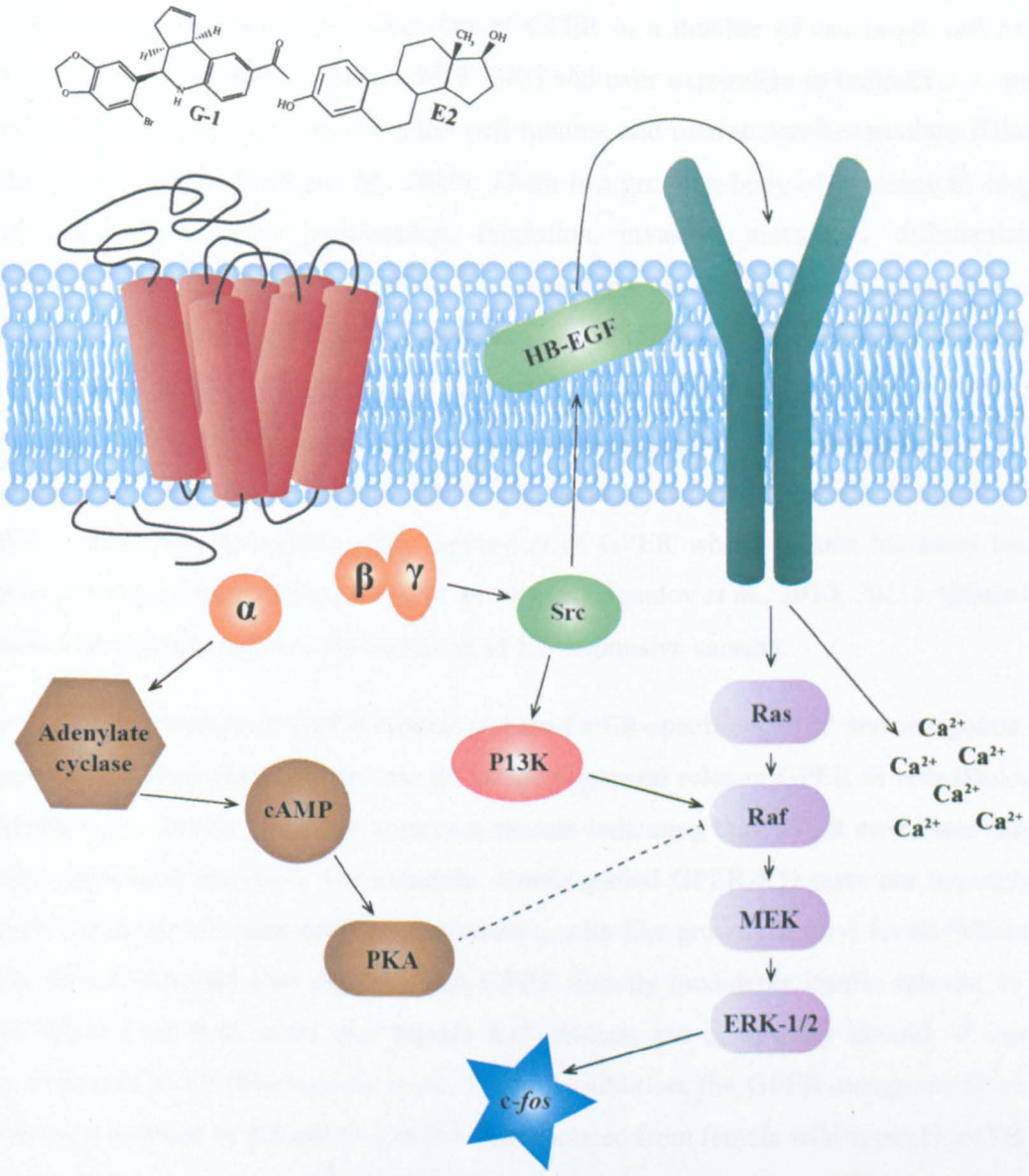

Figure 4.1. Schematic diagram depicting some examples of GPER mediated signalling.

Activation of GPER by E2 (or G-1, anti-E2s tamoxifen and ICI 182780, and various environmental E2s) causes a conformational change in the G protein complex leading to free Gα and Gβγ subunits that can stimulate a number of effectors. GPER appears to couple to at least two different α subunits: $G\alpha_s$ and $G\alpha_i$. Many of the actions of GPER are dependent on the transactivation of the receptor tyrosine kinase EGFR. Transactivation occurs following the dissociation of the Gβγ subunit which stimulates an increase in Src tyrosine kinase (Src) activity and 'membrane impermeable' heparan bound EGF (HB-EGF) – it is HB-EGF that stimulates EGFR to activate a variety of pathways including ERK/calcium/P13K (it is worth noting that Revenkar *et al.*, demonstrated that GPER/EGFR stimulated calcium mobilisation was not inhibited by the PLC inhibitor U73122 - suggesting a PLC independent mechanism of action) (Filardo *et al.*, 2000, 2002; Vivacqua *et al.*, 2006b; Revenkar *et al.*, 2005). In many instances, the βγ subunit that activates EGFR appears to be coupled to the $G\alpha_i$ subunit, as transactivation is inhibited by pertussis toxin, a potent $G\alpha_i$ inhibitor (prevents uncoupling). However, Revenkar *et al.*, found that pertussis toxin only partially inhibits signalling suggesting an alternative mechanism/coupling to a different Gα subunit (Revenkar *et al.*, 2005). Stimulation of GPER when coupled to $G\alpha_s$ activates adenylyl cyclase leading to an increase in cAMP and in turn protein kinase A (PKA). This pathway has negative effects on E2/GPER-mediated increase in ERK1/2 phosphorylation (i.e., E2 via GPER stimulates the accumulation of phosphorylated ERK1/2; concurrently, GPER also stimulates an increase in cAMP. The rise in cAMP has negative effects on ERK1/2 phosphorylation, and an ERK response is inhibited 30 mins after the initial activation) (Filardo *et al.*, 2002). Therefore, E2/GPER can regulate ERK1/2 activation via at least two distinct pathways.

Various studies have reported over-expression of GPER in a number of cancerous cell lines (e.g., ishikawa, MCF-7, MDA-MB-231 and SKBR3 cells) and over expression in tumours e.g., pancreatic adenocarcinoma, post-puberal testicular germ cell tumors, and uterine carcinosarcomas (Glass *et al.*, 2011; Franco *et al.*, 2011; Huang *et al.*, 2010). There is a growing body of evidence to suggest that GPER is involved in cancer proliferation, migration, invasion, metastasis, differentiation and prognosis (reviewed in Wang *et al.*, 2010). The receptor's affinity for anti-E2s has also provoked comments since tamoxifen and ICI-182,780 are often administered to counteract the proliferative actions of ERα and ERβ in E2-responsive cancers. For example, long term use of anti-E2s in E2 positive breast carcinomas can lead endometrial hyperplasia (Cano and Hermenegildo, 2000), and GPER has been shown to be involved in the development of acquired tamoxifen resistance in breast carcinomas - tamoxifen up-regulates the expression of GPER which in turn increases taxoxifen's proliferative activity (contradicting its role as an anti-E2) (Ignatov *et al.*, 2010, 2011). Hence GPER is an alternative therapeutic target in the treatment of E2-responsive cancers.

The development of transgenic GPER models and the GPER-specific agonist and antagonist G-1 and G-15, respectively, have given insight into the possible general roles of GPER *in vivo* (Bologa *et al.*, 2006; Dennis *et al.*, 2009). There are numerous reports indicating that GPER modulates metabolism particularly via insulin secretion. For example, female global GPER KO mice are hyperglycaemic, have impaired glucose tolerance and reduced serum insulin-like growth factor-1 levels (Mårtensson *et al.*, 2009). This KO model also indicates that GPER directly modulates insulin release, as isolated pancreatic islets from both male and female KO animals are completely devoid of insulin and glucagon responses to E2 (Mårtensson *et al.*, 2009). In addition, the GPER antagonist G-15 inhibits insulin secretion induced by E2 and G-1 in the islets isolated from female wild-type mice (Mårtensson *et al.*, 2009; Sharma and Prossnitz, 2011). Meanwhile in humans, E2 and G-1 have anti-diabetic actions in islets taken from healthy and type II diabetic female subjects - E2 and G-1 improve glucose-stimulated insulin release while suppressing glucagon and somatostatin secretion (Kumar *et al.*, 2011). In contrast, there are mixed views on the role of GPER in fat metabolism – some studies report both male and female GPER KO mice have increased body weight and visceral adiposity (Haas *et al.*, 2009; Ford *et al.*, 2011), whereas others describe no alterations e.g., the body weight and fat mass of both male and female GPER-LacZ mice remain unchanged when compared to wildtype controls, even if overfed on a high fat diet (Isensee *et al.*, 2009).

Transgenic animals have also implicated GPERs involvement in other systems including bone development. For example, Ford and colleagues found that male GPER KO mice exhibit increased skeletal growth, bone mineral density and growth plate proliferation, and Windahl and co-workers demonstrated that E2 reduces longitudinal bone growth and growth plate height in ovariectomised wildtype but not GPER KO mice (Ford *et al.*, 2011; Windahl *et al.*, 2009). This suggests that GPER is

required for a normal inhibitory effect of E2 on bone growth and growth plate height in male and female mice. Conversely, Mårtensson and colleagues report that female but not male GPER KO mice have reduced skeletal growth characterised by reduced crown-rump and femur length (Mårtensson *et al.*, 2009). Discrepancies between GPER KO models are perhaps indicative of strain differences, age, diet (e.g., phytoestrogen content), or technology used to create the colony.

As GPER was cloned from a human B-cell lymphoblast cDNA library, it is perhaps unsurprising that GPER has been shown to be involved in immune system regulation. Both male and female GPER-LacZ mice have impaired thymic T cell production with a reduction in CD4+ and CD8+ cells, and a decreased expression of CD62L in the T cell compartment (Isensee *et al.*, 2009). Although, in another transgenic model, E2-induced thymic atrophy is attenuated in female GPER KO when compared with wildtype controls, and chronic treatment of female wildtype animals with G-1 induces significant thymic atrophy and thymocyte apoptosis (Wang *et al.*, 2008a). Together the later points suggest that GPER may have immunosuppressive effects. This is further supported by a study which reports that G-1 inhibits the production of lipopolysaccharide (LPS)-induced cytokines TNF-α, IL-6, and IL-12 in human primary macrophages (Blasko *et al.*, 2009). Moreover, it has been shown that GPER has protective actions in experimental models of the autoimmune disease multiple sclerosis (experimental autoimmune encephalomyelitis (EAE)) (Blasko *et al.*, 2009; Wang *et al.*, 2009b; Yates *et al.*, 2010). For instance, insertion of an E2 pellet (constant release over 40-60 days) into female wildtype mice and GPER KO mice one week prior to the induction of EAE protects against the development of EAE in wildtype but not GPER KO mice (Wang *et al.*, 2009b). Furthermore, insertion of a G-1 pellet into wildtype mice completely protected against EAE, suggesting that the other ERs may oppose the protective (immunosuppressant) actions of GPER (Wang *et al.*, 2009b).

GPER is expressed in rat and mouse arteries, in human arteries and veins, and rat and human myocardial tissue, suggesting a role for GPER in the cardiovascular system (Isensee *et al.*, 2009; Broughton *et al.*, 2010; Haas *et al.*, 2007; Patel *et al.*, 2010). Indeed, when G-1 is infused into normotensive Sprague-Dawley male rats there is an acute reduction in blood pressure, and both pressurised male rat mesenteric resistance arteries, precontracted murine arteries, and human internal mammary arteries dilate in response to G-1 (Haas *et al.*, 2009) suggesting that GPER modulates blood pressure. Furthermore, it has been demonstrated that G-1 elicits a nitric oxide-dependant relaxation of the carotid artery endothelium in male and female Sprague-Dawley rats, and decreases vascular superoxide production in carotid and intracranial arteries (although the latter is most likely by direct inactivation (acting as a scavenger) rather than GPER-mediated enzyme inhibition) (Broughton *et al.*, 2010). Therefore, G-1 acting via GPER acts as vasodilator in both rodent and human tissues and possibly independently acts as an antioxidant - thus G-1 may be a potential therapeutic agent during vascular diseases such as stroke. Interestingly, chronic G-1 treatment reduces infact volume in

response to middle cerebral artery occlusion in ovariectomised mice (Zhang *et al.*, 2010); and acute G-1 administration prior to global ischemia/reperfusion improves functional recovery and decreases myocardial inflammation in hearts from male and female Sprague-Dawley rats (Deschamps and Murphy, 2009; Weil *et al.*, 2010a).

As shown in Chapter 3, GPER has a wide spread distribution in the brain, and this suggests the receptor may have a prominent central role. However, only a few studies have investigated the possible central functions of GPER. For example, G-1 promotes the release of prolactin release in ovariectomised rats (Lebesgue *et al.*, 2009), stimulates an increase in intracellular calcium oscillations in embryonic primate GnRH neurones (Noel *et al.*, 2009), and inhibits $5HT_{1A}$-mediated OT and ACTH release in ovariectomised females rats (Xu *et al.*, 2008; Rossi *et al.*, 2010). In addition, chronic G-1 treatment restores the cognitive performance of ovariectomised rats in the T-maze to that of intact controls, suggesting that GPER also has a role in cognition (Hammond *et al.*, 2009).

4.1.2 GPER and its intracellular localisation

Unlike many peptidergic GPCR ligands, E2 can freely diffuse through the plasma membrane. This has lead to the notion that GPER may be an atypical GPCR and function as an intracellular receptor. However, discrepancies surrounding the cellular localisation of GPER have plagued the field for some time. In 2005, Thomas and co workers suggested that GPER may be a plasma membrane E2 receptor by demonstrating that [^{3}H]E2 binds to the plasma membranes of ERα/β negative SKBR3 cells that endogenously express GPER, and HEK293 cells (ERα-/ERβ-/GPER-) transiently transfected with human GPER (Thomas *et al.*, 2005). The group later confirmed this by visualising the expression of HA-tagged GPER in stably transfected HEK293 cells, and found that HA-GPER mainly colocalised with lectin concanavalin A, a plasma membrane marker. They also confirmed that the HA-tag in the N-terminus of GPER did not compromise receptor functionality – E2 provoked a rapid increase in intracellular calcium in cells transfected with HA-GPER but not in control cells transfected with empty vector (Filardo *et al.*, 2007). It is important to point out that in these studies the GPER-expressing HEK293 cells were selected (by flow activated cell sorting) for high plasma membrane GPER expression.

On the contrary, Prossnitz and colleagues reported that transiently transfected GFP-tagged human GPER is not found at the plasma membrane of COS-7 cells but instead localises to the endoplasmic reticulum and golgi apparatus (Revenkar *et al.*, 2005). The GFP tag was on the C-terminus of GPER, immediately following the stop codon. Stimulation of these cells with E2 yields an intracellular calcium response suggesting that GFP-tagged GPER is functional. The intracellular localisation of the GFP-GPER was verified using primary antibodies generated against the predicted N- and C-terminal peptides of GPER. Furthermore, staining of endogenously expressed GPER with the same primary

antibodies corroborates this intracellular distribution pattern in several cancer cell lines e.g., MCF7, SKBR3, and MDA-MB231 breast cancer cell lines, and a Hec50 uterine carcinoma line (Revenkar *et al.*, 2005). Another study also demonstrated that GFP-tagged rat GPER localised to the endoplasmic reticulum and cytoplasm in transiently transfected HeLa cells (Funakoshi *et al.*, 2006). Although, when the experiment was repeated with a FLAG-tagged rat GPER, the receptor was mainly found on the plasma membrane. This suggests that different types of tagging (GFP vs FLAG) may encourage alternative intracellular trafficking of the receptors (Funakoshi *et al.*, 2006).

Studies comparing the ability of impermeable vs permeable E2 ligands to activate GPER have not helped clarify the cellular localisation of GPER. One group reports that cell-impermeable E2 conjugates (e.g., E2-BSA and E2-horseradish peroxidase) are able to activate GPER, suggesting the presence of the receptor at the cell membrane (Filardo *et al.*, 2007). Conversely another group demonstrated that only permeable E2 derivatives (e.g., 17α-Phenylethynyl-E2 and indium-labelled G-1analogues) are able to stimulate GPER - providing evidence that GPER is capable of initiating signalling from an intracellular localisation (Revenkar *et al.*, 2007; Nayak *et al.*, 2010).

4.1.3 Scepticism surrounds the identification of GPER as a putative fast E2 receptor

A few publications have raised concern about the E2-binding capabilities of GPER. In 2006, Levin and co-workers were unable to demonstrate E2-activation of ERK, P13K or adenylyl cyclase in SKBR3 cells (Pedram *et al.*, 2006). Even though the group was able to show rapid stimulation of these pathways with E2 in MCF-7 cells that express ERα, ERβ and GPER, this activation was significantly prevented with siRNA directed to ERα (but importantly not prevented with siRNA directed to GPER), suggesting a role for ERα but not GPER in the fast E2-signalling in these cells (Pedram *et al.*, 2006). Likewise, Otto and colleagues were unable to show specific E2 binding in COS-7 cells transfected with human GPER, GFP-tagged human GPER or mouse GPER. Furthermore, these investigators failed to demonstrate that E2 or G-1 1) stimulated cAMP in MDA-MB231, MCF-7, or COS-7 cells transiently transfected with human GPER; or 2) increased intracellular calcium levels in MDA-MB231, HEC50, MCF-7 cells, or CHO or COS-7 cells transiently transfected with human GPER (Otto *et al.*, 2008).

One possible explanation for the discrepancies in GPER/E2/G-1 signalling was provided by Kang and colleagues who illustrated that E2 and G-1 induced stimulation of the ERK pathway in SKBR3 cells is not mediated by GPER, but rather ERα-36, an ERα isoform (Kang *et al.*, 2010). This relationship is plausible considering that (1) ERα-36 lacks the intrinsic transcriptional activity of ERα; (2) is localised to the plasma membrane from which it mediates non-genomic E2 signalling; and (3) is up-regulated in cells that do not normally express this ERα isoform or ERα, (e.g., HEK293 cells and COS-7 cells) following a transient transfection with GPER (Kang *et al.*, 2010). However, a recent

study has added further ambiguity by implicating GPER in ALD signalling: ALD appears to stimulate ERK phosphorylation in freshly isolated rat aortic segments via both a MR- and GPER-dependent mechanism (Gros *et al.*, 2011). Collectively, these studies suggest that GPER may have an elusive and possibly promiscuous role in steroid signalling. In stark contrast, another study has shown that the chemokine CCL18 directly interacts with GPER, and inhibits an E2/G-1-mediated increase in intracellular calcium (Catusse *et al.*, 2010). This is an intuitive relationship considering GPER's homology with the chemokine receptors (Owman *et al.*, 1996) – although it still indicates a role for GPER in E2 signalling.

The current study was undertaken to try to clarify the controversies surrounding the cellular localisation and role of GPER *in vitro*. Particular interest was paid to the rodent receptors as few studies have characterised rat and mouse GPER *in vitro*, which is surprising considering the vast majority of *in vivo* functional studies have been conducted in these species. To find out the cellular localisation of GPER we generated a stable HEK293 cell line expressing an N-terminus HA-tagged rat GPER. The HA tag was preferred as it has previously been used in this lab to determine the cellular distribution pattern of HA-tagged versions of the V_{1A}, V_{1B} and OT receptors (constructed using the same PCR protocol), all of which behave similarly to their untagged counterparts (Dr Stephen Lolait, unpublished observations). In addition, the HA tag has been used extensively in the literature to characterise GPCR internalisation and (sub)cellular localisation, e.g., vasopressin V_{1A} and V_2 receptors amongst many others including the GnRH and GPER receptors (Innamorati *et al.*, 1996, 1998; Sedgley *et al.*, 2006; Finch *et al.*, 2008; Filardo *et al.*, 2007). For this reason, one would anticipate a HA-GPER cellular distribution pattern comparable with that described by Filardo and colleagues (Filardo *et al.*, 2007).

Next we endeavoured to determine whether or not E2 activates GPER. As numerous publications have demonstrated that E2 rapidly stimulates the ERK1/2 pathway and mobilises intracellular calcium via GPER, we used an ERK phosphorylation assay and calcium stimulation assay to assess the E2/G-1 responsiveness of HEK293 cells stably transfected with rodent GPER. If successful, we hoped to further characterise E2-GPER signalling *in vitro* and also expand the current known functions of GPER *in vivo* - notably the possible roles of GPER in the HPA and HNS systems.

4.2 Materials and Methods

4.2.1 Chemicals

ALD, adenosine 5'-triphosphate (ATP), Carbachol, E2 (water-soluble and ethanol-soluble), EGF, ionomycin, PDBU were purchased from Sigma, UK. G-1 (Dimethyl sulphoxide (DMSO)-soluble and ethanol-soluble) was purchased from Calbiochem (Merck), UK, VP was purchased from Bachem, UK, and N-(3-chlorophenyl)-6,7-dimethoxy-4-quinazolinamine (AG1478; EGFR inhibitor) was purchased from Cayman Chemical, USA.

4.2.2 Cell culture and transfections

Cell lines were obtained from various sources: CHO-K1 and COS-7 cells were purchased from the American Type Culture Collection, USA; HeLa and Ishikawa cells were a kind gift from Professor Craig McArdle (LINE, DHB); SKBR3 cells were a kind gift from Professor Eric Prossnitz; and HEK293 cells were a kind gift from Professor David Murphy. Cells were cultured as described in section 2.5.2.

The epitope-tagged and untagged rat GPER receptors were generated by PCR using approximately 250ng rat genomic DNA. For the untagged receptor, primers were directed to 5' and 3'-untranslated regions of the receptor (upstream: 5'- AGCTT*AAGCTT*GAAGCCATGGCTGCAACTACT -3'; downstream: 5'- AGAGC*CTCGAG*GTGGTTTGTTAAAGGGCC -3') and corresponded to 15718643-15720408bp of the rat GPER gene (Genbank Accession number NC_005111), generating a 1765bp product. Primers for the tagged receptor were again directed to 5' and 3'-untranslated regions of the receptor, but the 5' primer contained an additional 27bp which coded for the Influenza hemagglutinin (HA) epitope tag (upstream: 5'-AAGCTT*AAGCTT*GAAGCCATG**TATCCATATGATGTTCCAGATTATGCT**GCTGCAACTAC TCCAGC -3' (bold underlined letters highlight the additional HA tag sequence); downstream: 5'-AGAGC*CTCGAG*GTGGTTTGTTAAAGGGCC -3'), and gave rise to a 1793bp product corresponding to 15718642-15718643bp of the rat GPER gene. Primers for both tagged/untagged receptors contained recognition sequences for the restriction endonucleases HindIII and XhoI (represented by underlined italics). The untagged mouse GPER receptor was generated by PCR using 7.5ng mouse GPER cDNA (cloned from a mouse AtT-20 pituitary tumour cDNA library; Dr Stephen Lolait unpublished data) as a template. Primers were directed to 5' and 3'-untranslated regions of the receptor (upstream: 5'- ACTG*GGATCC*GAAGCCATGGATGCGACTACC -3'; downstream: 5'-GCATC*CTCGAG*CAGGAAGGCGTTTTGTTA -3') and corresponded to 595-2323bp of the mouse GPER gene (Genbank Accession number NM_029771), generating a 1728bp product, and contained recognition sequences for the restriction endonucleases BamHI and XhoI (represented by underlined italics). Primer restriction endonuclease sites allowed subcloning into the vector pcDNA3.1(+)

(containing AMP and neomycin resistance genes) for expression in mammalian cells. The human GPER cDNA was a kind gift from Professor Eric Prossnitz; the mouse E2 sulphotransferase cDNA clone was purchased from Geneservice, and subcloned into pcDNA3.1(+)Hygro as described in section 2.4.2; and the rat V_{1B} receptor cDNA was obtained from Dr Stephen Lolait (Lolait *et al.*, 1995).

Rat tagged and untagged GPER, mouse untagged GPER, and mouse E2 sulphotransferase cDNAs were introduced into HEK293 cells by calcium phosphate-mediated transfection, and clonal cell lines expressing the cDNA was obtained as described in section 2.5.4. In some experiments we used either untagged rat or mouse GPER as transcript expression were similar. The stable V_{1B} receptor/CHO-K1 cell line was established by Dr Stephen Lolait as previously described (Lolait *et al.*, 1995). Transient transfection experiments were performed 24 hours after seeding COS-7 or HeLa cells in Costar plain black-wall 96-well plates using Nanofectin as described in section 2.5.3. It was estimated using the X-gal staining assay (previously described in section 2.5.3 and Appendix I) that Nanofectin successfully transfected 30% of COS-7 and HeLa cells with cDNA.

4.2.3 Northern 'dot' blot hybridisation

To determine the endogenous transcript expression of some genes of interest or cDNAs introduced into cells by transfection we performed northern 'dot' blot hybridisation. This is a semi-quantitative method and it can be used to assess the relative levels of mRNA expression. Cells were cultured in clear 96 well plates until 80-90% confluent, and transferred to nitrocellulose membranes using a 96-well vacuum manifold. The blots were UV-cross-linked, baked for 2 hours at 80°C, and pre-hybridised at 37°C in pre-hybridisation buffer (see Appendix II) for at least 4 hours. Two oligonucleotides were designed against individual target mRNAs (sequences are provided in Table 4.1) and purchased from Invitrogen. Oligonucleotides were tailed on the 3' end with Terminal deoxynucleotidyl transferase and α-^{32}P-ATP. Blots were hybridised with α-^{32}P-ATP-labelled probes in hybridisation buffer overnight at 37°C, and washed for 4 x 15 min in 1xSSPE/0.2% SDS at 56°C. Hybridised blots were exposed to Amersham Hyper film MP for 4-10 days at -80°C with intensifying screens.

Gene oligonucleotide is directed towards	Oligonucleotide sequences		Corresponding bp of cDNA sequence (example of one variant given)		Genbank Accession (and acknowledged mRNA variants)	GC content of probe (%)		Estimated Tm (°C)		High stringency wash (°C)
	Probe 1	Probe 2	Probe 1	Probe 2		Probe 1	Probe 2	Probe 1	Probe 2	
rat GPER	5'-GAGGGCCAGAGGGGTG CTGTTGGAAGGGGCTG GCCACACGGGACCTAG-3'	5'-GAAAGACTGCTTGCAG GGAGTGTCCCCTGGCT GCGCCCACTGCAGTAG-3'	91-138 (variant 1)	892-939 (variant 1)	NM_133573 (variant 1)	69	63	70	68	56
mouse E2 sulphotransferase	5'-ATGCTGGAAGGACCT TGGGTGGCAGGTGAGTT TTTACTATTCTGGGAG-3'	5'-GAATGATTCTGTCCA CAAGCTCTGCCGAGGG C TTTCTCTCCAGGAAC-3'	433-480 (variant 1)	758-805 (variant 1)	NM_023135 (variant 1)	50	52	63	64	56
human ERα-36	5'-AGACACGAGGAAACCA CTTGTTTCCAAATATT TTAGGATGCAAGTTC-3'	5'-GCCCATGGTCATGTAA CTGCCTCAAAACAAAA TGTCCCCACGTCCACA-3'	1118-1164 (variant 1)	1217-1264 (variant 1)	BX640939 (variant 1)	38	50	57	63	54
human ERα	5'-CGACAGCTGCGGCGGC GGGTGCAGTAGCATCA GCGGGCTCGGAGACAC-3'	5'-GCGTCGATTATCTGAA TTTGGCCTGTAGAATG CCGGCGGGCCGGCCTC-3'	541-588 (variant 1)	661-708 (variant 1)	NM_000125 (variant 1) NM_001122740 (variant 2) NM_001122741(variant 3) NM_001122742(variant 4)	71	60	71	67	56
human ERβ	5'-CCACAACACATTTGGG CTTGTGGTCTGCCGAC CAGGCCCACCTTCCAA-3'	5'-CCTCTTTGAACCTGGA CCAGTAACAGGGCTGG CGCAACGGTTCCCACT-3'	661-708 (variant 1)	853-900 (variant 1)	NM_001437 (variant 1) NM_001040275 (variant 2) NM_001040276 (variant 3) NM_001214902 (variant 4) NM_001214903 (variant 5)	58	58	66	66	56
human EGFR	5'-AGCCAGCAGCGCCAG GAGCGCTGCCCCGGCC GTCCCGGAGGGTCGCAT-3'	5'-TACGGTTTTCAGAAT ATCCAGTTCCTGTGGAT CCAGAGGAGGAGTATG-3'	246-293 (variant 1)	1393-1499 (variant 1)	NM_005228 (variant1) NM_201282 (variant 2) NM_201283(variant 3) NM_201284 (variant 4)	77	46	74	61	56

Table 4.1. Summary of oligonucleotide sequences and their predicted properties.

Two oligonucleotides 48bp in length were designed against individual target genes. As some genes code for more than one transcript variant (which may be physiologically active, e.g., human ERα has four different mRNA variants all of which code for the same protein) probes were designed against regions of the gene common to all known transcript variants. This also included homologues (and variants) from other species (e.g., human, hamster, and monkey) as expression was investigated in a variety of cells lines (human (HEK293/HeLa), hamster (CHO-K1), or monkey (COS-7) cells)). In instances where the probe was directed to the translated region of the mRNA, maximum effort was made to aim for non-conserved (i.e., limited homology to other proteins within a class, or other distinct proteins) regions of the gene. Oligonucleotides were directed as follows: rat GPER (also recognised human and mouse GPER) probe 1 was directed to a sequence in the translated region shortly following the initiating methionine, and probe 2 was directed to a non-conserved region between TM 6 and 7; mouse E2 sulphotransferase probes 1 and 2 were directed to non-conserved sequences in the translated regions (in non-cofactor binding regions); human ERα-36 probe 1 was directed to the final 48bp in the coding region of the gene (the final 3bp corresponding to the stop codon), and probe 2 was directed a sequence shortly after the stop codon in the 3'-untranslated region; human ERα and ERβ probes 1 and 2 were both directed to a non-conserved portion of the 5'-translated region which occurs shortly after the initiating methionine; and the human EGFR probe 1 began at the initiating methionine and probe 2 was directed to a non-conserved sequence in the N-terminal translated region. Optimum hybridisation temperature for oligonucleotides is between 37-45°C in a hybridisation solution containing 50% formamide, while the high stringency wash temperature is approximately 5-20°C below Tm (Wilkinson, 1999).

4.2.4 Semi-automated Image Acquisition and Analysis

Imaging experiments (sections 4.2.5-4.2.7) were performed using a semiautomated system for image acquisition (IN CELL Analyser 1000), and validated algorithms for image segmentation and quantification (IN CELL Analyser version 1.0 software) as described in sections 2.7-2.9. Digital images were acquired, collecting one to four fields per well (each field capturing 0.602mm^2 area with a 10x objective), in order to obtain images of approximately 50-3000 cells per well.

4.2.5 Cellular localisation of HA-tagged GPER

HA-tagged and untagged GPER HEK293 stables were cultured in poly-L-lysine-coated Costar plain black-wall 96-well plates at 15,000 cells per well. If serum starving/treatment was required, cells were plated at 10,000 and incubated the next day in 90µl phenol-red free DMEM with P/S, Q, 0.44mM calcium chloride dihydrate and 100µg/µl BSA, with or without treatment (100nM E2 or G-1) overnight. For cell surface receptor staining, cells were incubated at 4°C for 1 hour in mouse monoclonal anti-HA.11 (diluted 1:200 in 1% BSA/1x PBS), washed (ice-cold 1x PBS) and fixed for 30 min (with 2% PFA/1x PBS). Cells were permeabilised (0.1% TX-100/1x PBS 10 mins), washed (3 x 1x PBS) and non-specific secondary antibody binding blocked with 1% BSA/0.1% TX-100/1x PBS for one hour. Cells were incubated in Alexa Fluor 488 goat anti-mouse IgG (H+L) secondary antibody (diluted 1:500 in 1% BSA/0.1% TX-100/1x PBS) for 1 hour, washed (3 x), and incubated in 300 nM DAPI for 15 min at room temperature. Cells were washed (1 x) prior to imaging. For whole cell imaging, cells were washed, fixed, permeabilised, and blocked as previously and incubated at 4°C for 1 hour in mouse monoclonal anti-HA.11. Cells were washed (3 x) and incubated in Alexa Fluor 488 goat anti-mouse IgG (H+L) secondary antibody and then DAPI stained. Cells were washed (1 x) prior to imaging. Immunofluorescence was detected with excitation filters 475-nm (HA) and 360-nm (DAPI), and monitored through emission filters 535-nm (detecting Alexa 488, green fluorescence: HA signal) and 460-nm (detecting blue fluorescence: DAPI signal), with a 61002 trichroic mirror (GE Healthcare, UK). Analysis of HA-GPER localisation was performed using the IN Cell 1000 Analysis Software. Within each cell the software used green channel images (535-nm emission filter) to measure HA fluorescence intensity and defined the cytoplasm; while blue channel images (460-nm emission filter) measured DAPI intensity and defined the nucleus. Subtraction of background fluorescence (measured in wells without primary antibody) gave the average fluorescence intensity in AFU per field/well. To calculate the percentage of HA-GPER at the plasma membrane, the average AFU value obtained from cell surface receptor staining was calculated as a percentage relative to the average AFU value from the whole cell receptor staining.

4.2.6 Calcium stimulation assay

Cells were seeded at varying concentrations (10,000 - 20,000 cells per well) into Costar plain black-wall 96-well plates. The following day, cell types that were to be treated with steroids were serum-starved overnight (constituents of serum free media are described in section 2.8.1). Prior to treatment cells were loaded with 2.5-5μM Fluo-4 and 0.5μM Hoechst in either serum free media or physiological salt solution (PSS) (for CHO-K1 cells - see Appendix II for PSS recipe). Cells were stimulated and imaged in an environmental control chamber at 37°C in a 5% CO_2 humidified atmosphere. Fluorescence images of one field per well were acquired every 12000ms ranging from 0 ms to 72000ms, and immunofluorescence was detected with excitation filters 475-nm (fluo-4) and 360-nm (Hoechst), and monitored through emission filters 535-nm (detecting green fluorescence; fluo-4 signal) and 460-nm (detecting blue fluorescence; Hoechst signal). Analysis was performed using the IN Cell 1000 Analysis Software. Within each cell the software used green channel images (535-nm emission filter) to measure fluo-4 fluorescence intensity to define staining in the cytoplasm, while blue channel images (460-nm emission filter) measured Hoechst intensity to define the nucleus. For each field, the average total amount of fluo-4 in the cell cytoplasm was calculated. This value, following the subtraction of background florescence (measured in regions of the field absent of cells), was expressed as AFU. Data was presented as fold change over time point 0ms.

4.2.7 ERK phosphorylation assay

Cells were seeded at varying concentrations (10,000 - 20,000 cells per well) into Costar plain black-wall 96-well plates. The following day (following seeding for CHO, HEK293, Ishikawa or SKBR3 cells or transfection for COS-7 and HeLa cells) cells were serum-starved overnight prior to treatment (constituents of serum free media are described in section 2.9.1). Cells were stimulated (5-30 min), washed (ice-cold 1x PBS for 3-5 min), fixed for 10 min (with 4% PFA/1x PBS), and permeabilised for 5 min at -20°C with absolute methanol. Cells were washed (1x PBS) and non-specific antibody binding blocked with 5% normal goat serum/1x PBS for 2 hours. Cells were washed (1 x) and incubated in mouse anti-ppERK1/2 antibody (1:800-1:12000) and rabbit anti-ERK1/2 (1:400-1:3200) in 1% normal goat serum/1x PBS overnight at 4°C. N.B., the titre of anti-ppERK antibody was greatly reduced to 1:6400 for SKBR3 cells (to 1:12000 in some experiments - depending on the antibody batch) and still the EGF-induced increase in ppERK fluorescence did not exceed (or even reach) 2-fold. The following day, cells were washed (3 x), incubated in Alexa Fluor 488 goat anti-mouse IgG (H+L) secondary antibody for 1 hour at room temperature, and further washed (2 x) prior to 15 min incubation with 300 nM DAPI. Cells were washed (1 x) prior to imaging. Immunofluorescence was detected using excitation filters 535-nm (tERK), 475-nm (ppERK) and 360-nm (DAPI), and emission filters 620-nm (detecting Alexa 546, red fluorescence: total ERK signal), 535-nm (detecting Alexa 488, green fluorescence: ppERK signal) and 460-nm (detecting blue fluorescence: DAPI signal) with

a 61002 trichroic mirror. Analysis of total ERK and ppERK activity was performed using the IN Cell 1000 Analysis Software. Within each cell the software used red channel images (620-nm emission filter) to measure tERK fluorescence intensity and define the cytoplasm perimeter; green channel images (535-nm emission filter) to measure ppERK fluorescence intensity and also define the cytoplasm perimeter; while the blue channel images (460-nm emission filter) measured DAPI intensity and defined the nucleus. For each field the average total amount of tERK and ppERK in the whole cell was calculated. These values, following the subtraction of background florescence (measured in regions of the field where there were no cells; or in the case of cells that sheath (e.g., HEK293) or were confluent (transiently transfected COS-7 and HeLa cells) measured in wells without primary antibody as described in section 2.9.2), was expressed as AFU. Data was normalised to vehicle to allow pooling of independent experiments.

Analysis of ppERK values in transiently transfected cells.

ppERK fluorescence intensity values were obtained as above for transiently transfected cells, and the data collected was subject to further analysis. As the transient transfection used in this assay is approximately 30% efficient (as determined by the X-gal staining assay; for more details see section 2.5.3), a 'ppERK fluorescence threshold' was introduced for the analyses of fields containing cells transiently-transfected with GPCRs, in an attempt to identify transfected cells from unresponsive non-transfected cells. The 'ppERK fluorescence threshold' was based on V_{1B} receptor data that accompanied each assay. As demonstrated in Figure 4.2, nuclear and cytoplasmic ppERK fluorescence values for control vs. VP treated V_{1B} receptor transfected cells were plotted against each other on a scatter diagram using the new linear discriminant filter tool within the IN CELL Analyser version 1.0 software. The cells that had comparatively high levels of ppERK fluorescence in both the nucleus and cytoplasm are shown in the upper right quartile (B) as marked with threshold lines on Figure 4.2. The vast majority of these cells corresponded with VP responsive V_{1B} transfected cells. Cells that had comparatively low levels of ppERK fluorescence in the nucleus and cytoplasm were located in the lower right quartile (C) and were either unresponsive to VP (unsuccessfully transfected) or were treated with vehicle. Cells that possessed high ppERK fluorescence values in the nucleus but not the cytoplasm (A), or vice versa (D), were considered unstimulated. While in some cells types, the rise in ppERK may remain in the cytoplasm or fully translocate to the nucleus, the cells used in this assay/thesis demonstrate a concomitant rise in nuclear and cytoplasmic ppERK in response to stimulation (at the time points investigated) as shown in Figure 4.2. Hence cells in the (A) or (D) quartiles were considered to be either non-specifically activated by agonist or vehicle (i.e., mechanically stimulated) or cells possessed intrinsic/background ERK activity. The threshold lines in Figure 4.2 were positioned so that approximately 30% of VP responsive cells were located in quartile (B) to correspond with the approximate 30% transfection efficiency observed with Nanofectin (the IN

CELL Analyser version 1.0 software re-analysed the data each time the threshold lines were adjusted to establish the percentage of cells in quartile (B) – this was repeated until (B) contained approximately 30% of responsive cells). Therefore, the 'ppERK fluorescence threshold' corresponded to the points at which the threshold lines intersected the x- and y-axis, and the cells that emitted AFU values below these limits were discarded. Once the 'ppERK fluorescence threshold' had been determined it could be applied to ppERK fluorescence data obtained from wells transfected with other GPCRs (on the same assay plate; as AFU values vary between plates, the V_{1B} receptor transfection and subsequent stimulation was performed on each plate). The ppERK fluorescence values for agonist- or vehicle- treated GPCR-transfected cells were reanalysed by the IN CELL Analyser version 1.0 software and the percentage of cells present in quartile (B) was calculated. Thus if a transfected receptor was responsive to agonist stimulation it would be expected that significantly more agonist-treated transfected cells would be found in quartile (B) when compared with vehicle-treated cells.

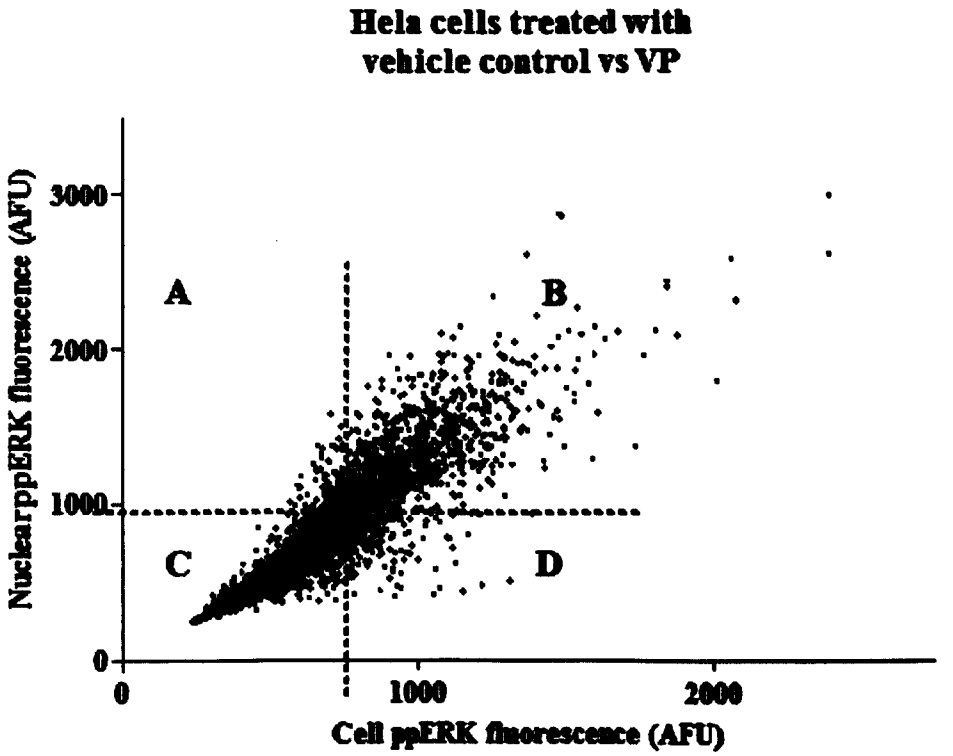

Figure 4.2. Setting the 'ppERK fluorescence threshold' for transiently transfected cells.

The ppERK fluorescence intensity emitted by HeLa cells either treated with vehicle or 100nM VP were plotted on scatter diagram using the 'new linear discriminant filter' function within the IN CELL Analyser version 1.0 software. Two threshold lines were implemented into the scatter diagram to separate the data into four quartiles (A-D). The threshold lines were adjusted until 30% of cells were in quartile B to correspond with the 30% transfection efficiency observed with Nanofectin. The 'ppERK fluorescence threshold' corresponded to the points which the threshold lines intersected the x and y axis.

4.2.8 Statistical analysis

IN CELL Analyser 1000 experiments were performed in 3-6 replicate wells, and experiments were performed at least 2 times. Data is represented in Figures as mean ± standard error of the mean (SEM). Statistical analysis was either a Student's *t*-test, a one-way ANOVA and post hoc test, or two-way ANOVA and post hoc test (as described in Figure legends) accepting $P < 0.05$ as significantly different.

4.3 Results

4.3.1 Detection of endogenous or 'exogenous' transcript expression in cells by Northern blot 'dot' hybridisation

Table 4.2 summaries GPER, mouse E2 sulphotransferase, ERα, ERβ, and EGFR transcript expression in cell lines that are frequently used for stable and transient transfections in our laboratory. GPER transcript expression was not detected in untransfected HEK293 cells, but was expressed in HEK293 cells stably transfected with rat HA-tagged, rat untagged, and mouse untagged GPER (see Figure 4.3). Similarly, mouse E2 sulphotransferase hybridisation signal was undetected in untransfected HEK293 cells but was observed in HEK293 cells stably transfected with mouse E2 sulphotransferase cDNA. Endogenous ERα-36, ERα and ERβ transcript expression was negligible in the four cell types investigated (and ERα-36 mRNA was not expressed following stable transfection with GPER). On the other hand, EGFR hybridisation signal was high in COS-7, HEK293 and HeLa cells, but was low-moderate in CHO-K1 cells.

(A)

Transcript	Level of endogenous transcript expression				
	CHO-K1	COS-7	HEK293	GPER-HEK293	HeLa
GPER	N/A	N/A	-	N/A	N/A
E2 sulphotransferase	N/A	N/A	-	N/A	N/A
ERα-36	-	-	-	-	-
ERα	-	-	-	-	-
ERβ	-	-	-	-	-
EGFR	+/++	+++	+++	+++	+++

(B)

Transcript	Level of 'exogenous' expression in HEK293 cells (introduced by transfection)	
	Single transfection	Double transfection
rat HA-GPER	+++	N/A
rat GPER	++	N/A
mouse GPER	+++	+++
mouse E2 sulphotransferase	+++	+++

Table 4.2. Results from northern 'dot' blot hybridisation.

(A) Represents endogenous transcript expression of GPER, E2 sulphotransferase, ERα-36, ERα, ERβ, EGFR in CHO-K1, COS-7, HEK293, and HeLa cells, and also HEK293 cells transfected with GPER. As some genes code for more than one transcript variant (which may be physiologically active) probes were designed against regions of the gene common to all known transcript variants. This also included homologues (and variants) from other species as expression was investigated in human (HEK293/HeLa), hamster (CHO-K1), or monkey (COS-7) cell lines. **(B)** 'Exogenous' transcript expression of rat HA tagged GPER, rat untagged GPER, mouse GPER, or mouse E2 sulphotransferase, introduced by single or double transfection of cDNAs into HEK293 cells. The transfected cell lines used in this study were those assessed to have the highest mRNA expression. Oligonucleotides were labelled with α-^{32}P-ATP and designed towards all transcript variants of the gene of interest. This also included homologues (and variants) from other species e.g., human, hamster monkey as expression was investigated in a variety of cells lines (human (HEK293/HeLa), hamster (CHO-K1), or monkey (COS-7) cells). +++, high expression; ++, moderate expression; +, low expression; -, negligible expression (signal not above background); N/A, expression in these cell lines were not investigated. Note that the levels of expression are relative – negligible, low or absent mRNA expression by this method does not imply that the cells do not express any mRNA, or that this mRNA is (or isn't) translated into a functional protein.

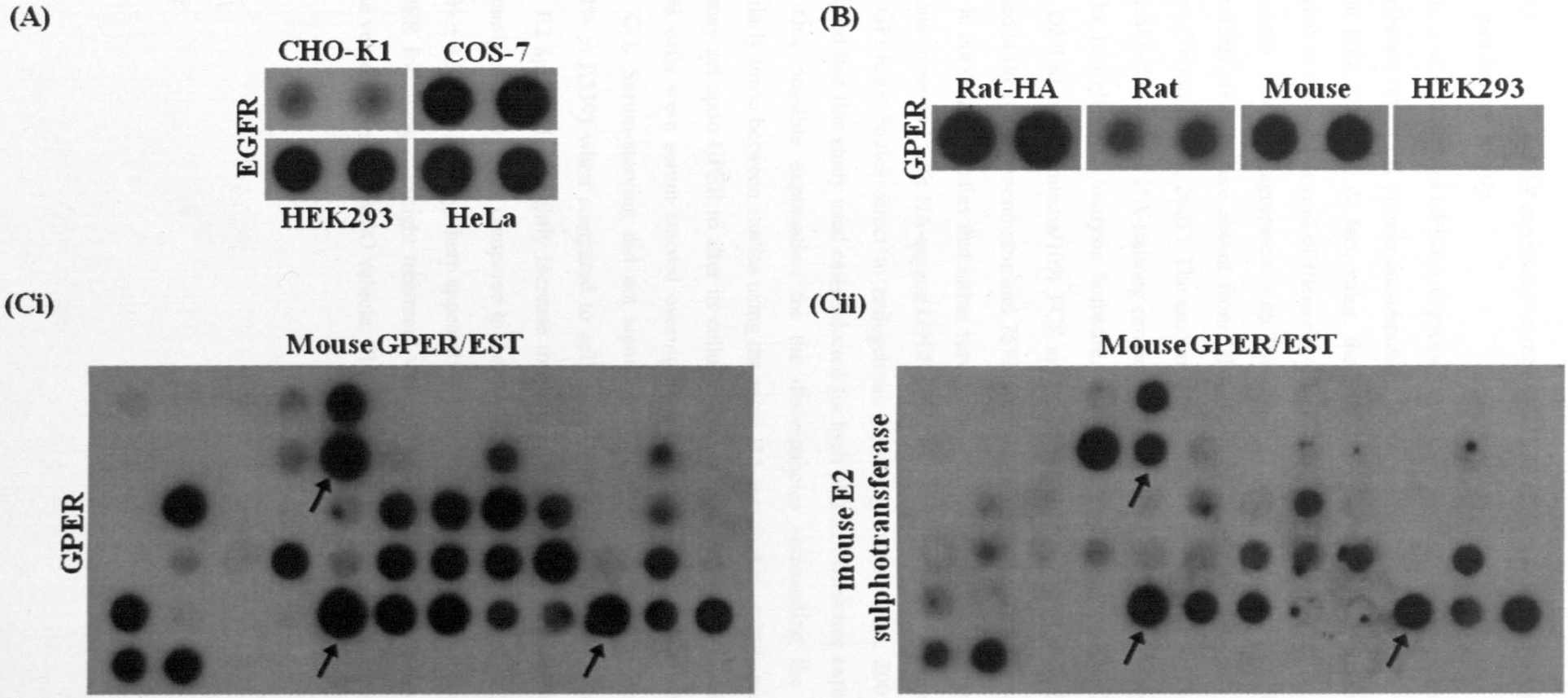

Figure 4.3. Examples of northern 'dot' blot hybridisation film images.

(A) Endogenous EGFR transcript expression in CHO-K1, COS-7, HEK293 and HeLa cells. **(B)** GPER hybridisation signal was observed in HEK293 clonal lines stably transfected with rat HA-tagged GPER (rat-HA), rat untagged GPER (rat), or mouse untagged GPER (mouse), but not in untransfected HEK293 cells (HEK293). **(C)** HEK293 cells were stably transfected with GPER and mouse E2 sulphotransferase and plated into 96 well plates (1 cell/well) to create clonal lines. Clones were grown to confluency and were then trypsinised and split, with some of the cells transferred to sister 96 well plates. The sister plates were hybridised with oligonucleotides directed to GPER mRNA **(Ci)** or mEST mRNA **(Cii)**. Note the extreme variation in GPER/EST mRNA expression even though all the cells express the cDNA i.e., all clones have G418 and Hygro resistance, or some cells were resistant to the antibiotics before transfection. Note that some wells (arrowed) have high GPER and EST gene expression.

4.3.2 *Rat GPER expressed 'stably' in HEK293 cells is located both on the cell surface and intracellularly*

To address whether or not GPER is expressed at the cell surface and/or intracellularly, we engineered a recombinant rat GPER protein encompassing a HA epitope tag on its N-terminus, and expressed it stably in HEK293 cells. At face value, the HEK293 cells are an appropriate model for HA-GPER expression as they are devoid of transcript encoding ERα, ERβ or GPER as determined by northern blot analysis. This is in agreement with Thomas *et al.*, who found that GPER mRNA and protein or ERα or ERβ mRNA were absent from HEK293 cells (as assessed by RT-PCR and Western blot analysis) (Thomas *et al.*, 2005). The amount of GPER expressed at the cell surface vs intracellularly was visualised using the HA-staining protocol, imaged in the IN CELL Analyser 1000, and analysed using the In Cell 1000 Analysis Software. In the total population of HEK293 cells maintained in normal DMEM growth media/10% FCS approximately 24% of HA-GPER (23.898% ± 0.390) was expressed at the plasma membrane and 76% (76.102% ± 0.390) expressed intracellularly (Figure 4.4). This is in contrast to studies that either report that GPER is predominantly expressed on the plasma membrane (observed with HA-tagged GPER), or expressed solely inside the cell (detected with GFP-tagged GPER/antibodies direct to endogenous GPER) (Filardo *et al.*, 2007, although it must be emphasised that this study used cells selected for high plasma membrane expression; Revenkar *et al.*, 2005). One possible explanation for the discrepancies surrounding the localisation of GPER (particularly those between studies using the same HA-tag) is that oestrogenic compounds within the media may act upon GPER to alter its cellular localisation. With this in mind, HA-GPER expressing HEK293 cells were serum starved overnight with or without treatment with either 100nM E2 or 100nM G-1. Serum-starving did not significantly alter the cell surface expression of HA-GPER (22.184% ± 1.339) when compared to cells incubated in normal media. Overnight treatment with 100nM E2 appeared to slightly increase the cell surface expression of HA-GPER but this was not significantly different when compared to the vehicle control (ethanol vehicle: 26.247% ± 2.619 vs E2: 32.816% ± 4.312). Similarly, there appeared to be a slight increase in plasma membrane expression in HA-GPER following overnight treatment with 100nM G-1 yet this was not significantly different from the vehicle control (DMSO vehicle: 23.008% ± 2.170 vs G-1: 27.589% ± 1.127) (Figure 4.4).

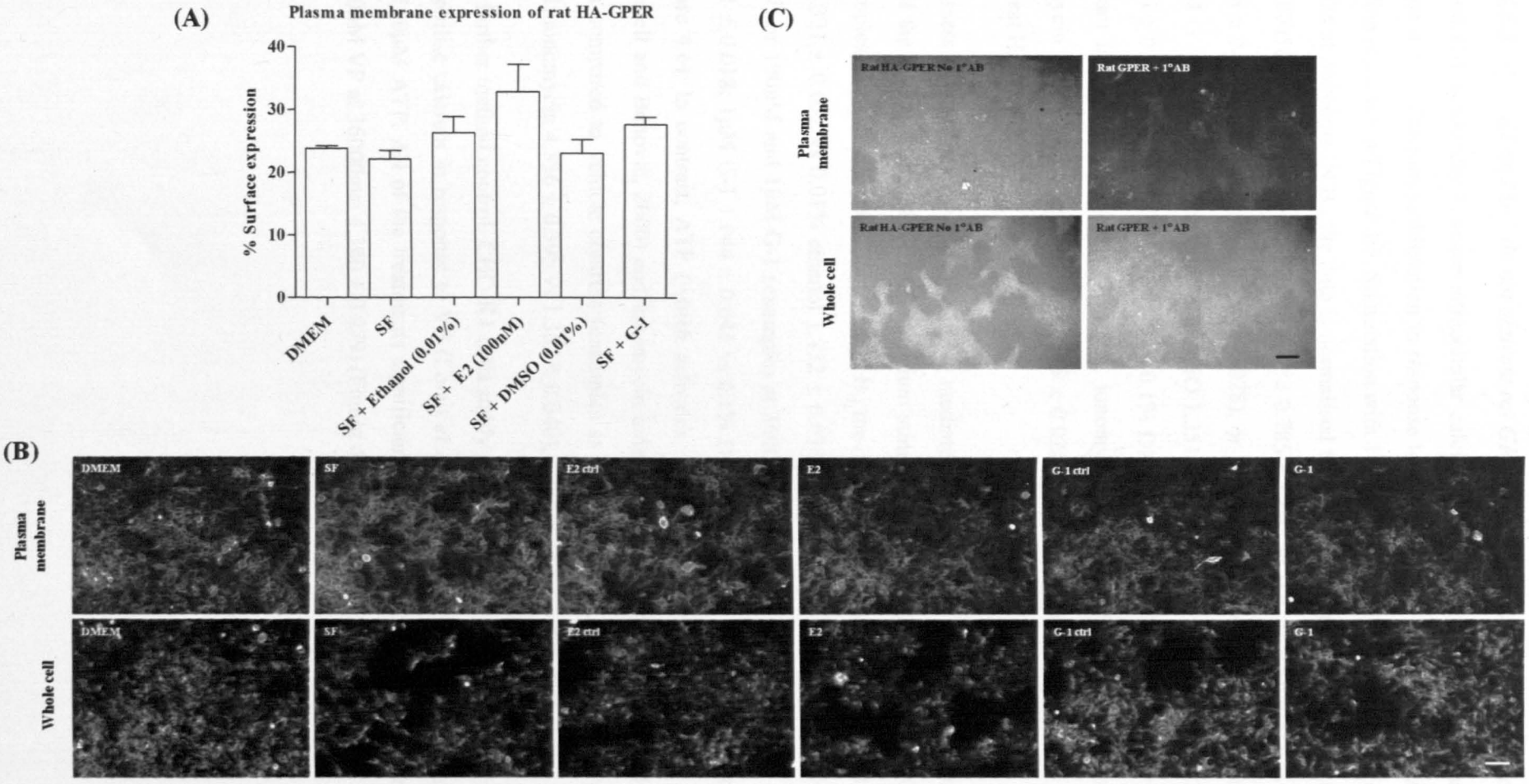

Figure 4.4. Plasma membrane and intracellular expression of HA-GPER in cultured, serum starved, and treated HEK293 cells.

HEK293 cells stably transfected with HA-tagged rat GPER were cultured in normal media or serum- and phenol-free media, plus or minus 100nM E2 or 100nM G-1. Plasma membrane expression of HA-GPER was calculated as a percentage of whole cell expression (thus intracellular expression was 100% (whole cell) minus the plasma membrane expression). **(A)** In HEK293 cells maintained overnight in normal growth media (DMEM) HA-GPER fluorescence was expressed at the plasma membrane and intracellularly. Overnight incubation in serum free media (SF) did not significantly alter the cell surface expression of HA-GPER when compared to cells incubated in normal media. Treatment with E2 did not significantly alter the plasma membrane expression of HA-GPER when compared with the ethanol control, and no significant differences were observed following treatment with G-1 vs the DMSO control. All values are means ± SEM from 1-2 fields, from 3-6 wells and 3 separate experiments. Statistical analysis was performed using a one-way ANOVA and the Bonferroni multiple comparison test. **(B)** Representative images of HA-tagged GPER transfected HEK293 cells stained with anti-HA antibodies. Note that the HA-GPER fluorescence is restricted to the plasma membrane of non-permeabilised HEK293 cells, but was expressed by both the plasma membrane and cytoplasm of the permeabilised HEK293 cells. **(C)** Only background HA staining in wells containing HEK293 cells stably transfected with untagged rat GPER, and in wells containing HA-tagged GPER transfected HEK293 cells but are absent of primary antibody. Ctrl, control. Scale bar, 100μm.

4.3.3 E2 and G-1 do not activate rat GPER to increase intracellular calcium

E2 and G-1 reportedly increase intracellular calcium responses in cell lines expressing GPER (see section 4.1.1). Calcium mobilisation in response to E2 and G-1 in the stable rat HA-GPER/HEK293 cell line is shown in Figure 4.5. Stimulation with 10nM E2, 100nM E2 or 1μM E2 (examples of mean ± SEM at 36000ms (N.B., the data is normalised to the value at time 0ms): 10nM E2 0.935 ± 0.078, vs 0.001% ethanol 0.867 ± 0.03; 100nM E2 0.785 ± 0.043 vs 0.01% ethanol 0.923 ± 0.171; 1μM E2 1.076 ± 0.080 vs 0.1% ethanol 0.954 ± 0.028), or 10nM, 100nM or 1μM G-1 (examples at 36000ms: 10nM G-1 1.147 ± 0.196 vs 0.001% DMSO 1.251 ± 0.19; 100nM G-1 0.895 ± 0.076 vs 0.01 DMSO 1.136 ± 0.177; 1μM G-1 0.852 ± 0.16 vs 0.1% DMSO 0.980 ± 0.038) failed to increase intracellular calcium in the HEK293 cells. However, ionomycin induced a 3-fold rise (example at 36000ms: ionmycin 3.141 ± 0.027 vs vehicle 0.8525 ± 0.025) in fluo-4 in the HEK293 cells stably transfected with rat HA-GPER.

To assess whether absence in an E2/G-1 mediated response was a product of receptor tagging we tested the untagged rat GPER in the calcium stimulation assay. Again, neither 100nM and 1μM E2 (examples of mean ± SEM at 36000ms (N.B., the data is normalised to the value at time 0ms): 100nM E2 1.321 ± 0.032 vs 0.01% ethanol 1.132 ± 0.031; 1μM E2 1.331 ± 0.044 vs 0.1% ethanol 1.317 ± 0.137) or 100nM and 1μM G-1 (examples at 36000ms: 100nM G-1 1.229 ± 0.071 vs 0.01% DMSO 1.131 ± 0.018; 1μM G-1 1.044 ± 0.041 vs 0.1% DMSO 1.41 ± 0.136) increased intracellular calcium (Figure 4.6). In contrast, ATP (which activates endogenous purinergic receptors in HEK293 cells (Mundell and Benovic, 2000) and ionomycin induced 2- and 4-fold increases in fluo-4 fluorescence when compared to vehicle controls (examples at 36000ms: ATP 2.141 ± 0.125 vs vehicle 1.181 ± 0.011; ionomycin 4.336 ± 0.395 vs 1.353 ± 0.040).

As a further method control, CHO-K1 cells stably transfected with the V_{1B} receptor previously shown to mobilise calcium in response to VP (Lolait *et al.*, 1995), were treated with 10nM or 100nM VP, and 100μM ATP. All of the treatments significantly increased intracellular calcium (example given for 10nM VP at 36000ms: 4.380 ± 0.079) (Figure 4.7).

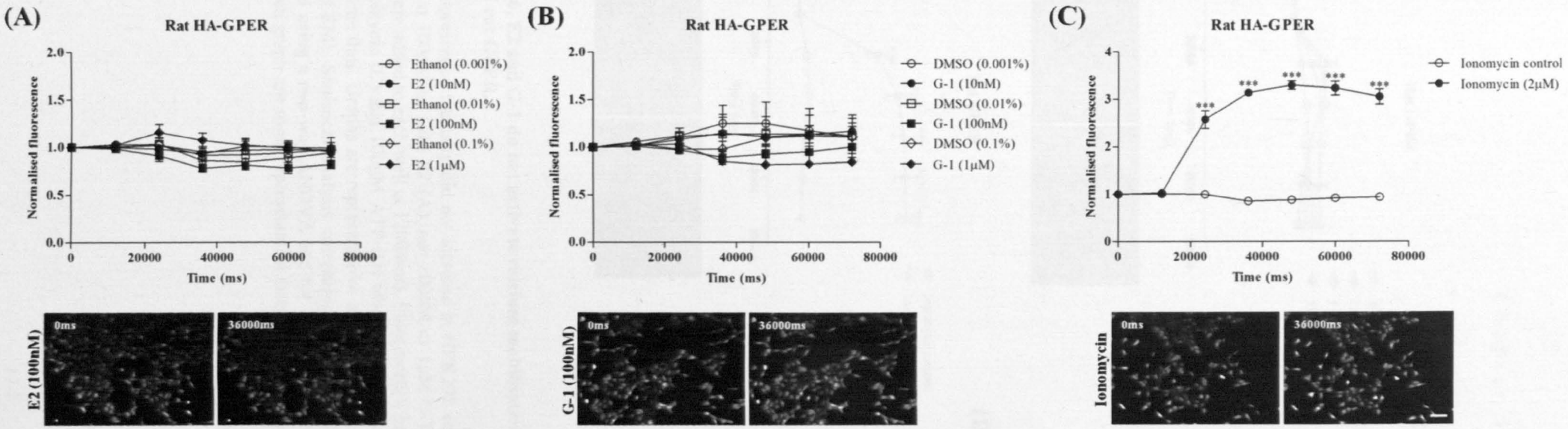

Figure 4.5. E2 and G-1 do not activate calcium mobilisation in HEK293 cells stably transfected with rat HA-GPER.

Fluo-4 fluorescence intensity did not increase in HEK293 cells stably transfected with rat HA-tagged GPER in response to 10nM, 100nM or 1μM E2 (A) or 10nM, 100nM nor 1μM G-1 (B) when compared to vehicle (N.B., vehicle or agonist were added to each well at 12000ms). Fluorescence intensity significantly increased in cells treated with 2μM ionomycin when compared to controls (C). The data shown are normalised to the value at time 0ms. Graphs are representative of one field, from triplicate wells and three separate experiments (mean ± SEM). Statistical analysis comparing vehicle-treated versus agonist-treated at each time point was performed using a two-way ANOVA and the Bonferroni post test. ***, $p < 0.001$. Below each graph are some representative images of cells treated with agonist at 0ms and 36000ms. Scale bar, 100μm.

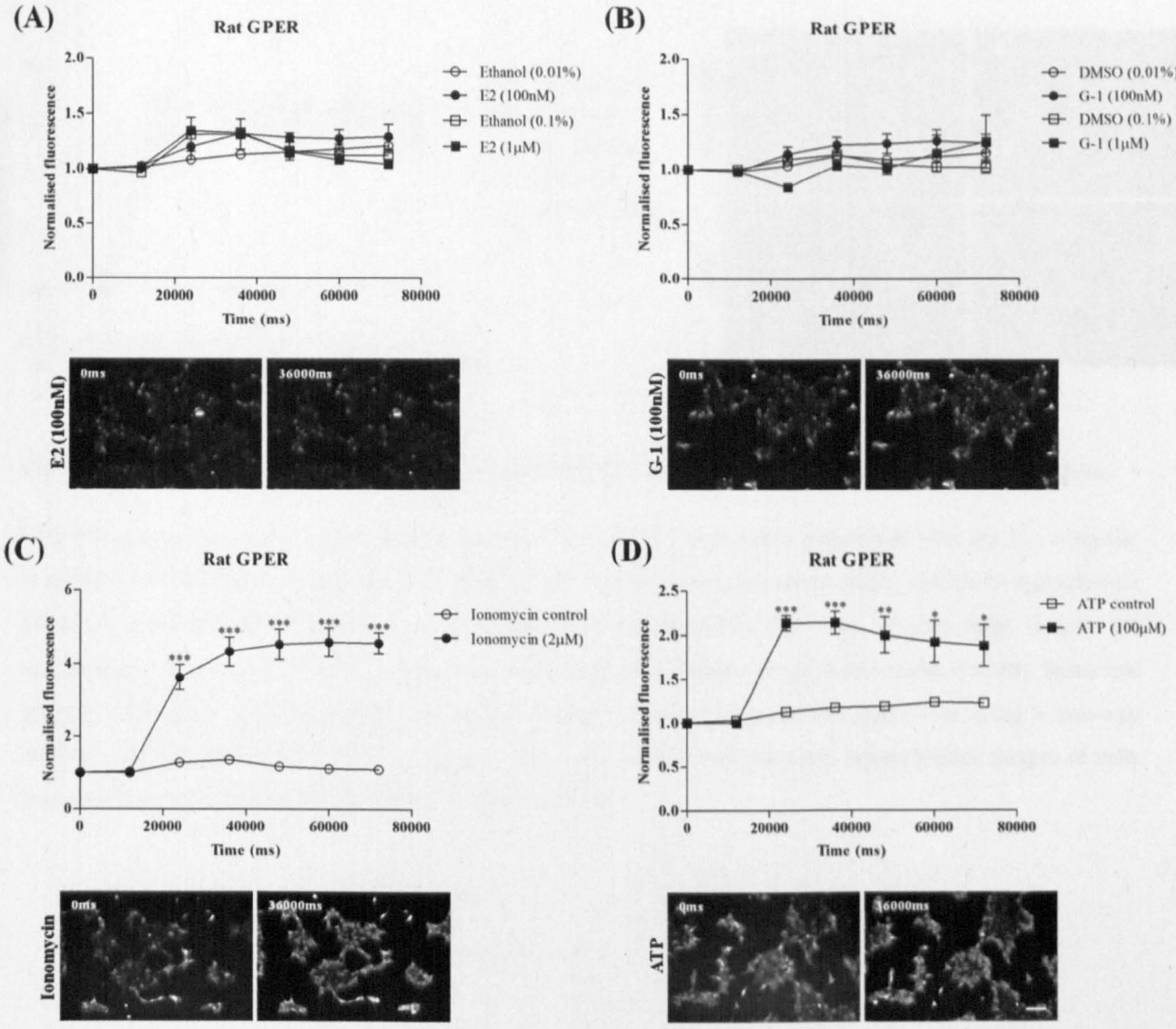

Figure 4.6. E2 and G-1 do not activate calcium mobilisation in HEK293 cells stably transfected with untagged rat GPER.

Fluo-4 fluorescence intensity did not increase in HEK293 cells stably transfected with rat untagged GPER in response to 100nM or 1μM E2 (A), nor 100nM or 1μM G-1 (B) when compared to vehicle (N.B., vehicle or agonist were added to each well at 12000ms). Fluorescence intensity significantly increased in cells treated with 2μM ionomycin (C) and 100μM ATP (D) when compared to controls. The data shown are normalised to the value at time 0ms. Graphs are representative of one field, from triplicate wells and three separate experiments (mean ± SEM). Statistical analysis comparing vehicle-treated versus agonist-treated at each time point was performed using a two-way ANOVA and the Bonferroni post test. *, $p < 0.05$; **, $p < 0.01$; ***, $p < 0.001$. Below each graph are some representative images of cells treated with agonist at 0ms and 36000ms. Scale bar, 100μm.

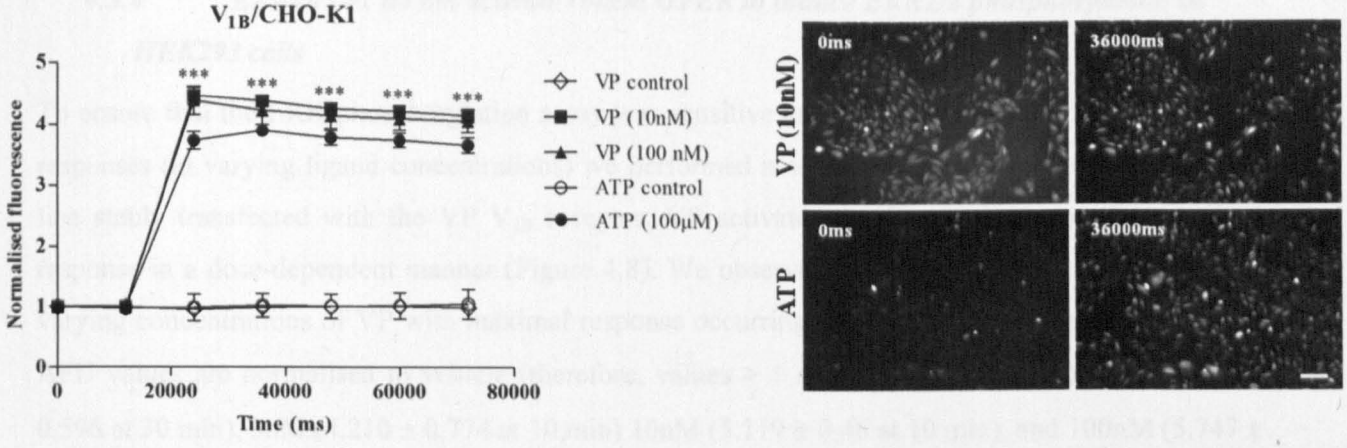

Figure 4.7. VP activates calcium mobilisation in CHO-K1 cells stably transfected with the V_{1B} receptor.

Fluo-4 fluorescence intensity significantly increased in CHO-K1 cells stably transfected with the V_{1B} receptor, in response to 10nM and 100nM VP and 100μM ATP when compared to control (N.B., vehicle or agonist were added to each well at 12000ms). The data shown are normalised to the value at time 0ms. Graphs are representative of one field, from triplicate wells and at least two separate experiments (mean ± SEM). Statistical analysis comparing vehicle-treated versus agonist-treated at each time point was performed using a two-way ANOVA and the Bonferroni post test. ***, $p < 0.001$. Next to the graph are some representative images of cells treated with agonist at 0ms and 36000ms. Scale bar, 100μm.

4.3.4 E2 and G-1 do not activate rodent GPER to induce ERK1/2 phosphorylation in HEK293 cells

To ensure that the ERK phosphorylation assay was sensitive enough to detect GPCR-mediated ERK responses (at varying ligand concentrations) we performed a series of experiments using a CHO-K1 line stably transfected with the VP V_{1B} receptor. VP activates the V_{1B} receptor to elicit an ERK response in a dose-dependent manner (Figure 4.8). We observed a 2-6 fold increase in ppERK with varying concentrations of VP with maximal response occurring between 10 and 15 min: 1nM (N.B., AFU values are normalised to vehicle (therefore, values > 1 are required for an increase): 2.421 ± 0.596 at 30 min), 3nM (4.210 ± 0.774 at 10 min) 10nM (5.119 ± 0.45 at 10 min), and 100nM (5.747 ± 0.165 at 10min). In non-transfected CHO-K1 cells, 1-10nM VP did not increase ppERK fluorescence levels from that of control (example of 10nM: 1.032 ± 0.062) (Figure 4.9).

As some GPCRs including GPER elicit an ERK response via transactivating the EGFR, we tested whether EGFR is involved in V_{1B} receptor mediated ERK responses. Incubation with the EGFR inhibitor, AG1478 (100nM for 30 min) did not inhibit the increase of ppERK in response to 10nM or 100nM VP (10 min) (example of 100nM: VP + AG1478 2.340 ± 0.279 vs VP + AG1478 vehicle 2.573 ± 0.058) (Figure 4.10). Treatment of V_{1B} transfected CHO-K1 cells with 100ng/ml (1.010 ± 0.008) and 500ng/ml (1.052 ± 0.026) EGF for 10 min did not increase ppERK (Figure 4.10). Although northern blot analysis revealed that CHO-K1 cells express moderate levels EGFR mRNA, this tyrosine kinase receptor is presumably not functional, and V_{1B} receptor stimulates ppERK in CHO-K1 cells through an EGFR independent pathway. Therefore, based on the V_{1B}/ERK results, the sensitivity of the assay in our hands, is sufficient to allow observation of E2/G-1/GPER activation of the ERK pathway in HEK293 cells (especially as previous studies show maximal GPER-mediated ERK response at doses of 1nM-1μM E2 and 10nM-1μM G-1 occurs within 5-30 min (Filardo *et al.*, 2000; Vivacqua *et al.*, 2006b; Sirianni *et al.*, 2008; Dennis *et al.*, 2011)).

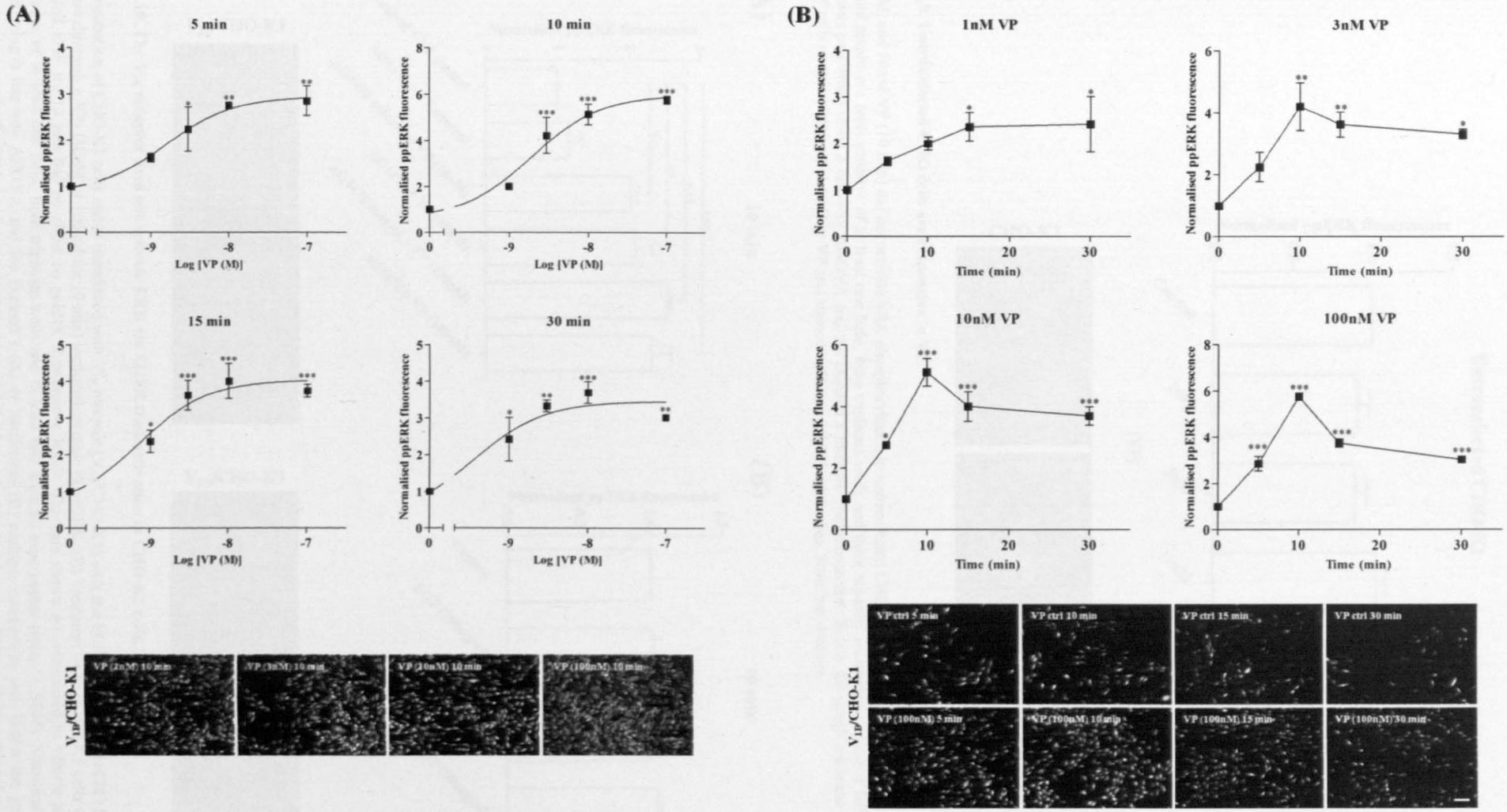

Figure 4.8. VP stimulated ERK phosphorylation in CHO-K1 cells stably transfected with V_{1B} receptor cDNA.

CHO-K1 cells stably transfected with V_{1B} receptor (V_{1B}/CHO-K1) were stimulated with 1nM, 3nM, 10nM or 100nM for 5, 10, 15 or 30 min. All concentrations of VP stimulated a significant increase in ERK phosphorylation in the treated V_{1B}/CHO-K1 cells. The ERK phosphorylation assay produced sufficient dose response (A) and time course (B) graphs. The data shown are normalised to vehicle and graphs are representative of at least two fields, from triplicate wells and at least two separate experiments (mean ± SEM). Statistical analysis was performed using a one-way ANOVA and the Bonferroni multiple comparison test *, $p < 0.05$; **, $p < 0.01$; ***, $p < 0.001$. Below each set of graphs are some representative images of cells treated with control (ctrl) or agonist and stained with anti-ppERK antibodies. Scale bar, 100μm.

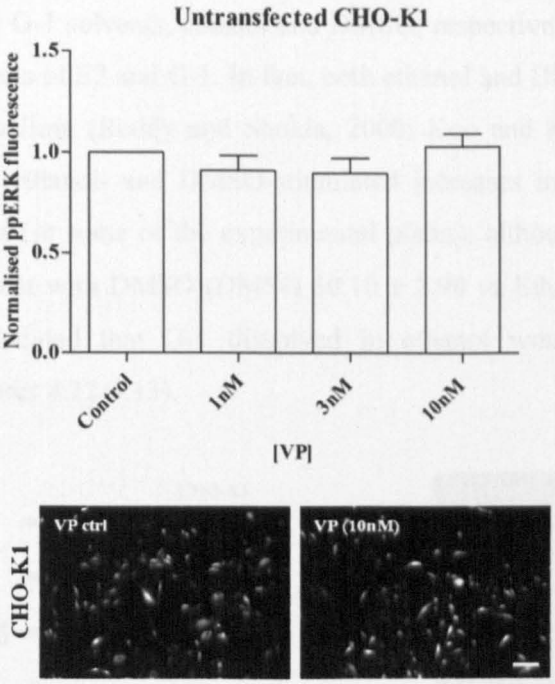

Figure 4.9. Untransfected CHO cells are responsive to VP.

1nM, 3nM, and 10nM VP (10 min) did not activate ERK phosphorylation in untransfected CHO-K1cells. The data shown are normalised to vehicle and graphs are representative of at least one field, from triplicate wells and three separate experiments (mean ± SEM). Statistical analysis was performed using a one-way ANOVA and the Dunnett's multiple comparison test. Below the graph are some representative images of cells treated with control (ctrl) or VP and stained with anti-ppERK antibodies. Scale bar, 100μm.

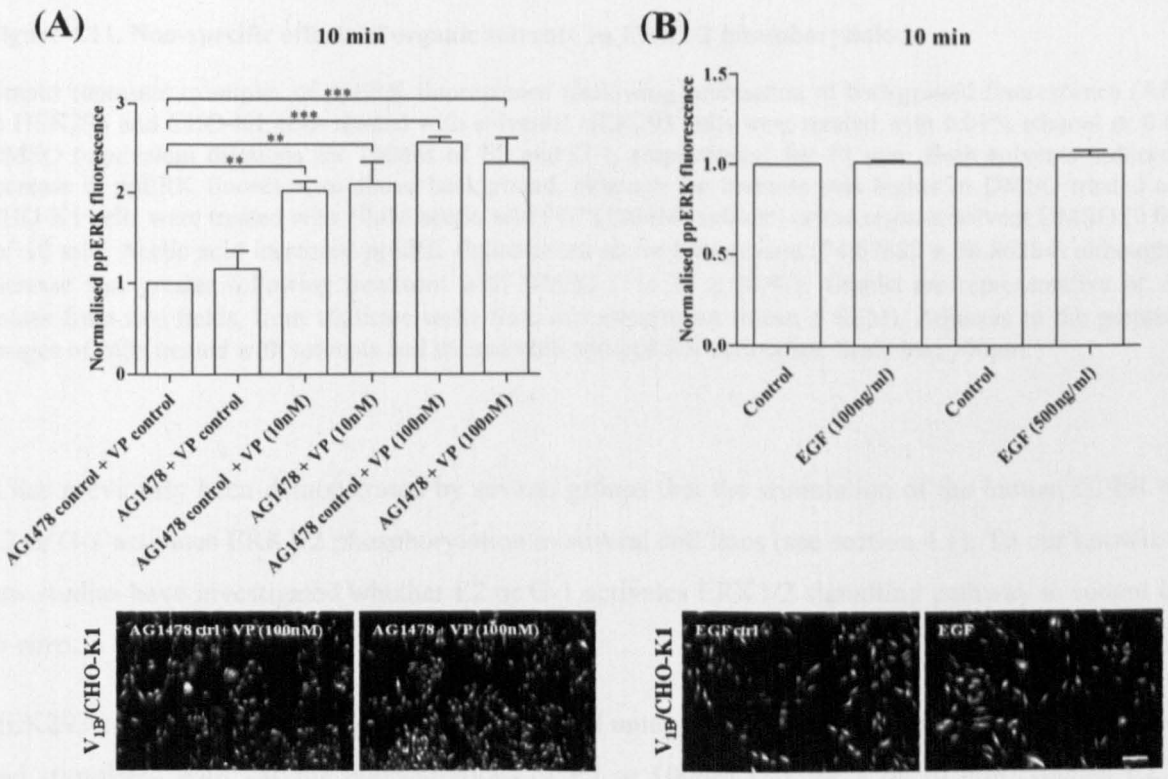

Figure 4.10. The V_{1B} receptor does not activate ERK via EGFR transactivation in CHO-K1 cells.

(A) Pre-incubation of CHO-K1 cells stably transfected with V_{1B} receptor (V_{1B}/CHO-K1) with the EGFR inhibitor AG1478 (100nM) for 30 min did not diminish a VP- (10nM or 100nM for 10 min) mediated increase in ppERK. (B) Treatment of V_{1B}/CHO-K1 cells with 100ng/ml or 500ng/ml EGF for 10 min had no effect on ppERK fluorescence levels. The data shown are normalised to vehicle and graphs are representative of at least one field, from triplicate wells and at least two separate experiments (mean ± SEM). Statistical analysis was performed using a one-way ANOVA and the Dunnett's (A) or Bonferroni (B) multiple comparison test. Below the graph are some representative images of cells treated with control (ctrl) or agonist/inhibitor and stained with anti-ppERK antibodies. Scale bar, 100μm.

It is possible that the E2 and G-1 solvents, ethanol and DMSO, respectively, may also promote ERK activation, and mask the effects of E2 and G-1. In fact, both ethanol and DMSO have previously been shown to activate ERK signalling (Reddy and Shukla, 2000; Koo and Kim, 2009). In the current study, we experienced both ethanol- and DMSO-stimulated increases in ERK fluorescence above background in HEK293 cells (in some of the experimental plates), although the fluorescence signal was higher following treatment with DMSO (DMSO 60.10 ± 3.90 vs Ethanol 42.00 ± 8.45) (Figure 4.11). Therefore, it was decided that G-1 dissolved in ethanol would be used in the ERK phosphorylation assays (Figures 4.12-4.13).

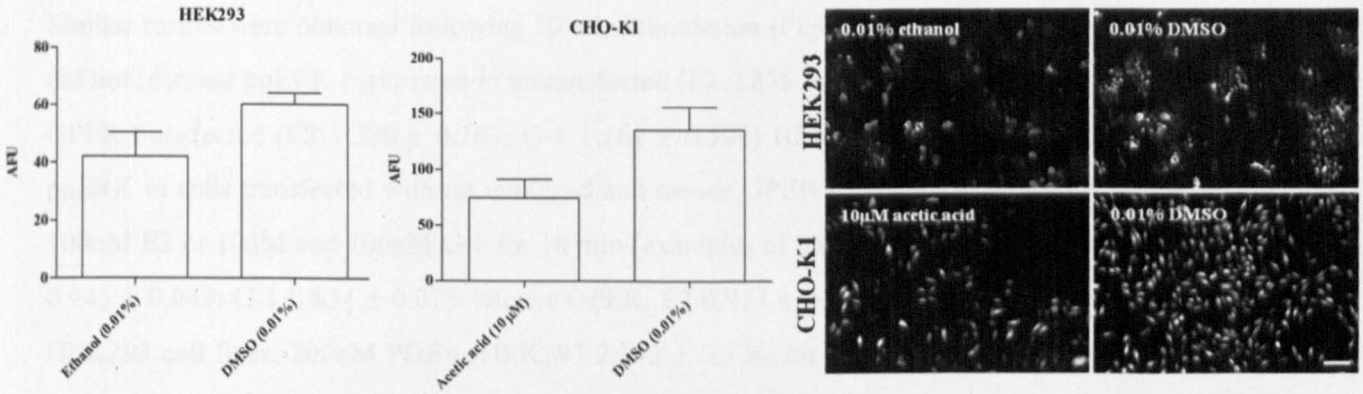

Figure 4.11. Non-specific effects of organic solvents on ERK1/2 phosphorylation.

Graphs represent examples of ppERK fluorescence (following subtraction of background fluorescence (AFU)) in HEK293 and CHO-K1 cells treated with solvents. HEK293 cells were treated with 0.01% ethanol or 0.01% DMSO (equivalent dilutions for 100nM of E2 and G-1, respectively) for 10 min. Both solvents induced an increase in ppERK fluorescence above background, although the increase was higher in DMSO treated cells. CHO-K1 cells were treated with 10μM acetic acid (VP (100nM) vehicle) or the organic solvent DMSO (0.01%) for 10 min. Acetic acid increased ppERK fluorescence above background (74.67683 ± 16.86284) although the increase was greater following treatment with DMSO (135.23 ± 20.97). Graphs are representative of AFU values from two fields, from triplicate wells from one experiment (mean ± SEM). Adjacent to the graphs are images of cells treated with solvents and stained with anti-ppERK antibodies. Scale bar, 100μm.

It has previously been demonstrated by several groups that the stimulation of the human GPER with E2 or G-1 activates ERK1/2 phosphorylation in several cell lines (see section 4.1). To our knowledge, few studies have investigated whether E2 or G-1 activates ERK1/2 signalling pathway in rodent cells *in vitro*.

HEK293 cells stably expressing rat HA-tagged and untagged GPER and mouse untagged GPER were and stimulated with varying concentrations of E2 or 100nM G-1 for 5 or 10 min. 100nM E2 and 100nM G-1 (N.B., AFU values are normalised to vehicle (therefore, values > 1 are required for an increase): 100nM E2 0.977 ± 0.027; G-1 0.922 ± 0.085) did not induce ERK phosphorylation in untransfected HEK293 cells at 5 min (Figure 4.12). Similarly, treatment of 100nM E2 and 100nM G-

1 for 5 min did not increase ppERK fluorescence in HEK293 cells transfected with rat HA-GPER (100nM E2 0.880 ± 0.064; 100nM G-1 1.232 ± 0.271). 10nM and 100nM E2 and G-1 also failed to increase ppERK in rat untagged GPER (examples given for 100nM: E2 0.872 ± 0.034; G-1 1.162 ± 0.035) and mouse GPER (examples of mean ± SEM given for 100nM: E2 1.099 ± 0.029; G-1 0.988 ± 0.028). 200nM PDBu (stimulator of the PKC pathway) (HEK293 1.876 ± 0.370; rat HA-GPER 2.107 ± 0.042; rat GPER 2.546 ± 0.5; mouse GPER 2.493 ± 0.479) and 100ng/ml EGF significantly increased ppERK fluorescence in all four cells lines by 2- to 7-fold (Figure 4.12) (HEK293 4.903 ± 0.301; rat HA-GPER 7.074 ± 0.294; rat GPER 6.0954 ± 0.586; mouse GPER 4.905 ± 0.743).

Similar results were obtained following 10 min stimulation (Figure 4.13). 100nM E2 and 100nM G-1 did not increase ppERK expression in untransfected (E2 0.876 ± 0.113; G-1 1.096 ± 0.079) or rat HA-GPER transfected (E2 1.320 ± 0.263; G-1 1.161 ± 0.194) HEK293 cells. There was no increase in ppERK in cells transfected with rat untagged and mouse GPER following incubation with 10nM and 100nM E2 or 10nM and 100nM G-1 for 10 min (examples of mean ± SEM for 100nM: rat GPER, E2 0.945 ± 0.043; G-1 0.834 ± 0.075. Mouse GPER, E2 0.913 ± 0.036; G-1 0.925 ± 0.075). In all four HEK293 cell lines, 200nM PDBu (HEK293 2.142 ± 0.326; rat HA-GPER 2.279 ± 0.437; rat GPER 2.627 ± 0.565; mouse GPER 2.290 ± 0.426) and 100ng/ml EGF (HEK293 3.085 ± 0.425; rat HA-GPER 7.990 ± 1.329; rat GPER 6.599 ± 0.64; mouse GPER 5.385 ± 0.644) significantly increased ppERK fluorescence by 2- to 8- fold (Figure 4.13).

The levels of total ERK fluorescence (tERK) did not change during this study even after treatment with 100ng/ml EGF for 10 min (N.B., AFU values are normalised to vehicle: 1.1 ± 0.078) (example given in Figure 4.14). As summarised in Figure 4.14, this was consistent with other cell lines used within this thesis - tERK fluorescence did not deviate from control levels, even after treatment with EGF for 10 min that significantly increased ppERK fluorescence, in COS-7 (1.361 ± 0.236), HeLa (0.934 ± 0.039), Ishikawa (1.040 ± 0.011), SKBR3 cells (0.962 ± 0.103), and CHO-K1 cells (expressing the V_{1B} receptor, as CHO-K1) following VP (100nM) treatment for 10 min (1.035 ± 0.024) (as CHO-K1 cells do not respond to EGF, see Figure 4.10).

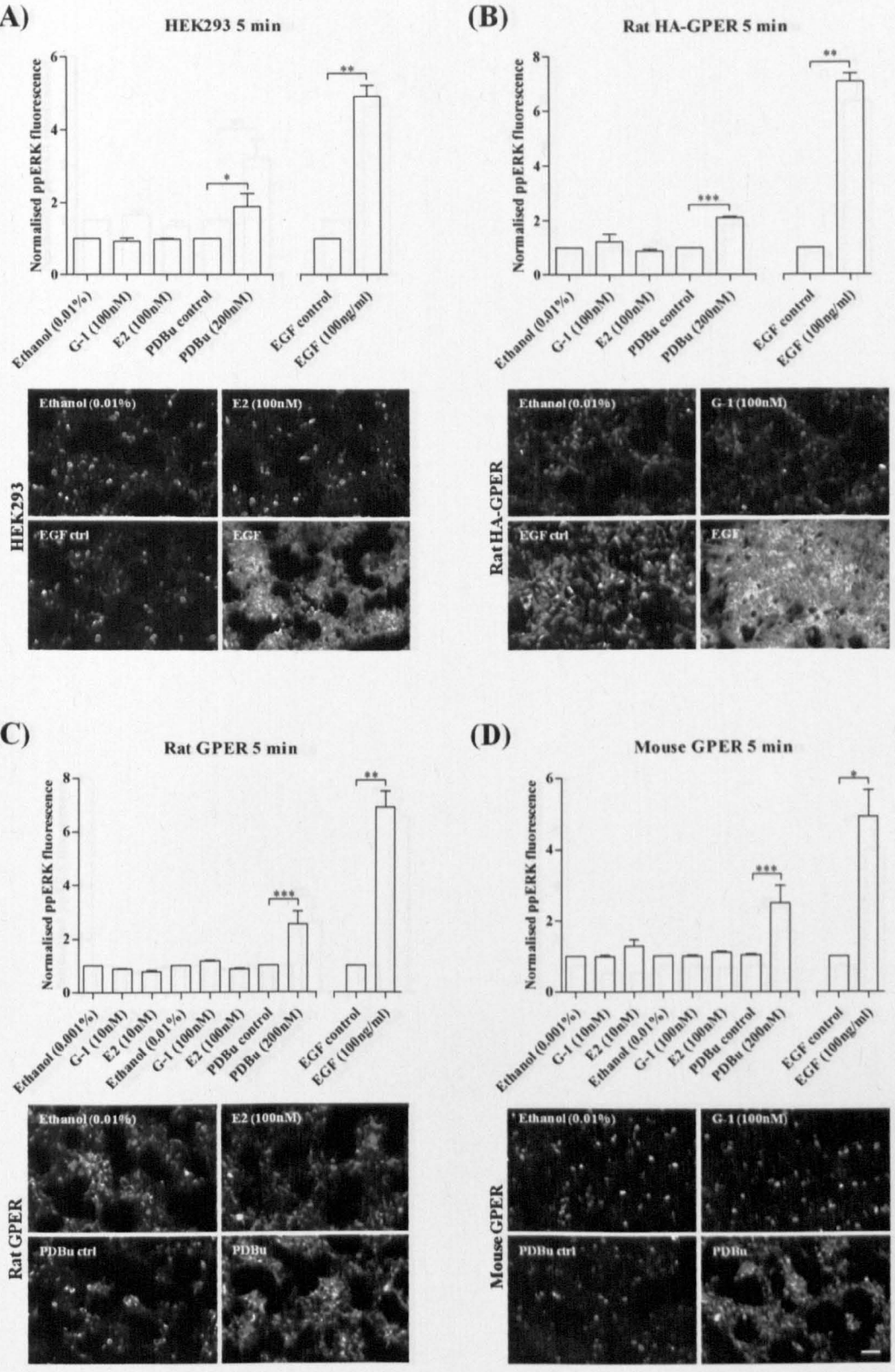

Figure 4.12. 5 min E2 or G-1 treatment (5 min) does not stimulate ERK phosphorylation in HEK293 stably transfected with rodent GPER.

100nM E2 and 100nM G-1 (5 min) did not increase ppERK fluorescence in untransfected HEK293 cells (A), or in HEK293 cells stably transfected with either HA-tagged rat GPER (B), untagged rat GPER (C), and untagged mouse GPER (D). There was a significant increase in ppERK fluorescence in all of the cell lines (A-D) in response to 200nM PDBu and 100ng/ml EGF when compared to controls. The data shown are normalised to vehicle and graphs are representative of at least two fields, from triplicate wells and three separate experiments (mean ± SEM). Statistical analysis comparing vehicle-treated versus agonist-treated (for all treatments apart from EGF and control) was performed using a one-way ANOVA and the Bonferroni multiple comparison test. Vehicle-treated vs EGF-treated data was compared separately using a Student's *t*-test (data sets were split up to avoid a type II false negative statistical error at the lower end of the response e.g., a large EGF-mediated increase in ppERK fluorescence may mask a subtle response induced by the other agonists). *, $p < 0.05$; **, $p < 0.01$; and ***, $p < 0.001$. Below each graph are some representative images of cells treated with control (ctrl) or agonist and stained with anti-ppERK antibodies. Scale bar, 100μm.

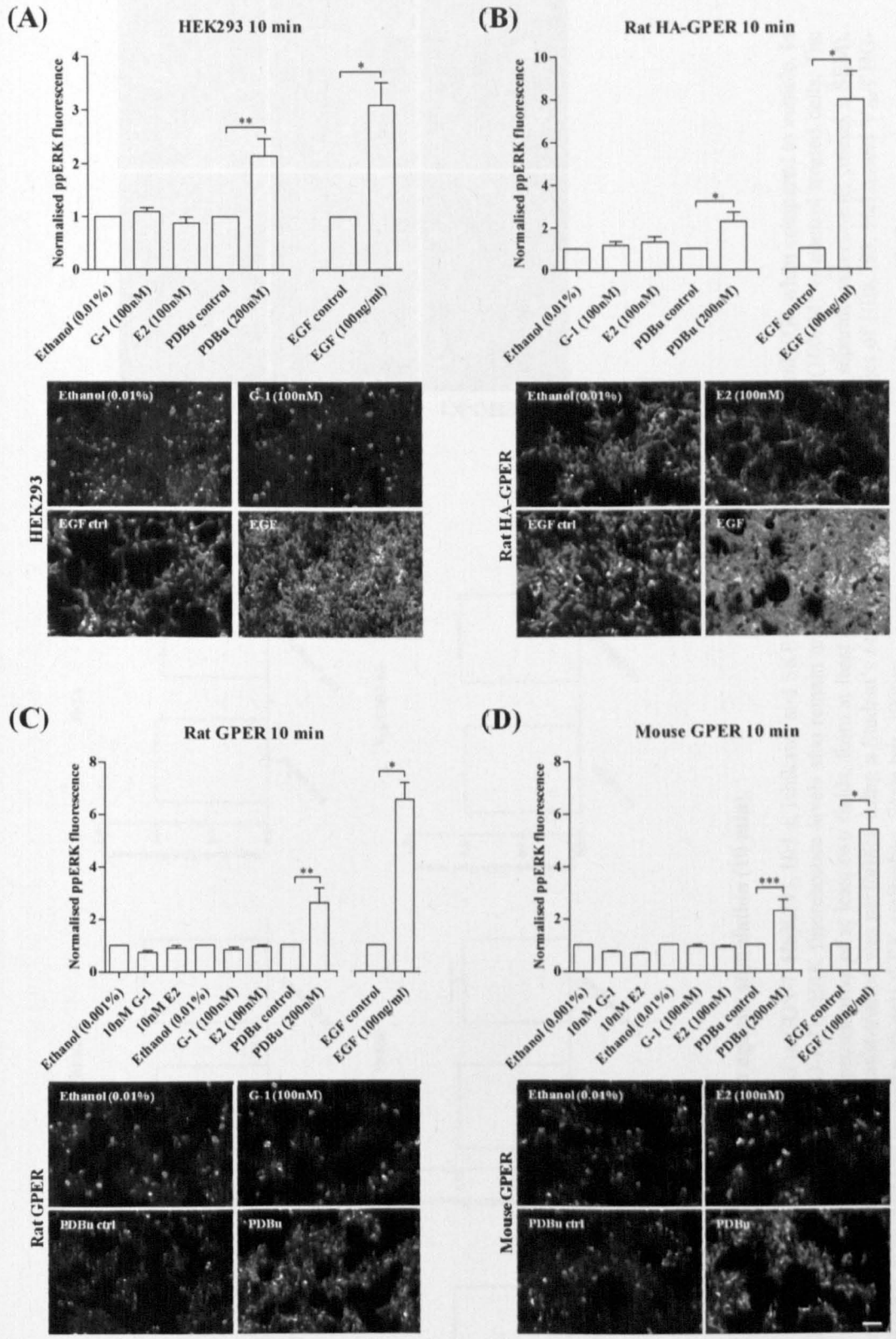

Figure 4.13. 10 min E2 or G-1 (10 min) treatment does not stimulate ERK phosphorylation in HEK293 stably transfected with rodent GPER.

100nM E2 and 100nM G-1 (10 min) did not increase ppERK fluorescence in untransfected HEK293 cells (A), or in HEK293 cells stably transfected with either HA-tagged rat GPER (B), untagged rat GPER (C), and untagged mouse GPER (D). There was a significant increase in ppERK fluorescence in all of the cell lines (A-D) in response to 200nM PDBu and 100ng/ml EGF when compared to controls. The data shown are normalised to vehicle and graphs are representative of at least two fields, from triplicate wells and three separate experiments (mean ± SEM). Statistical analysis comparing vehicle-treated versus agonist-treated (for all treatments apart from EGF and control) was performed using a one-way ANOVA and the Bonferroni multiple comparison test. Vehicle-treated vs EGF-treated data was compared separately using a Student's *t*-test (data sets were split up to avoid a type II false negative statistical error at the lower end of the response e.g., a large EGF-mediated increase in ppERK fluorescence may mask a subtle response induced by the other agonists). *, $p < 0.05$; **, $p < 0.01$; and ***, $p < 0.001$. Below each graph are some representative images of cells treated with control (ctrl) or agonist and stained with anti-ppERK antibodies. Scale bar, 100μm.

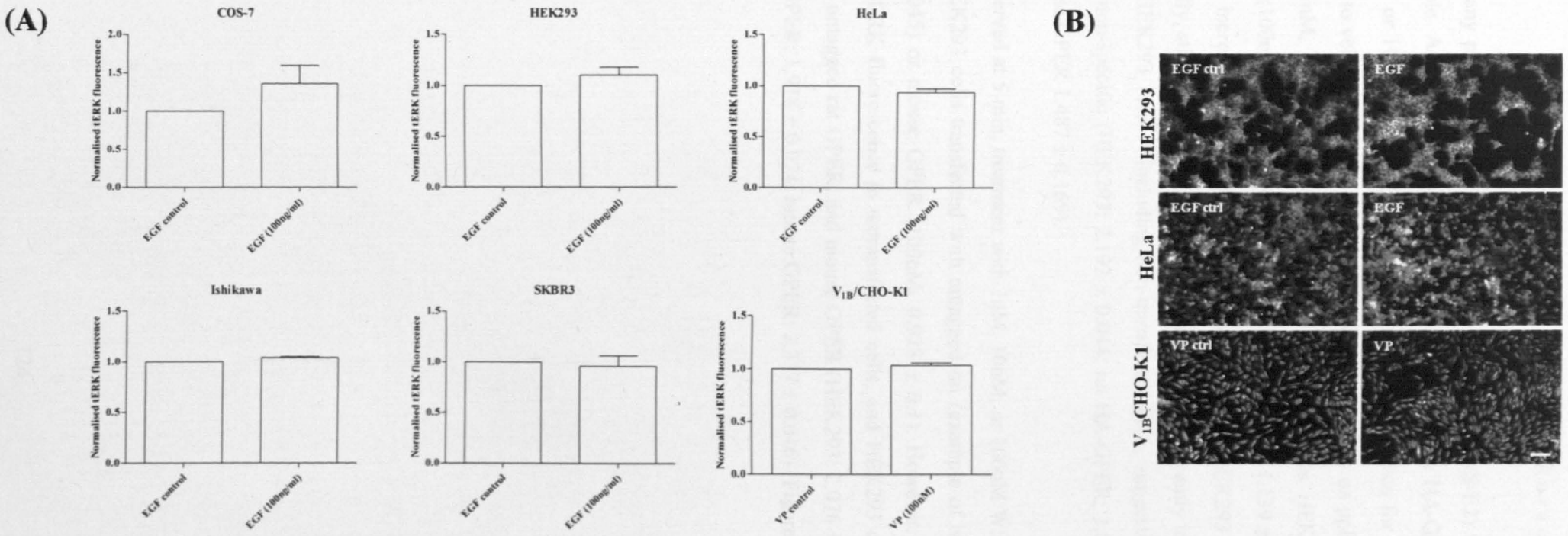

Figure 4.14. tERK levels do not change in response to agonist stimulation (10 min).

(A) tERK fluorescence levels are not significantly altered in COS-7, HEK293, HeLa, Ishikawa and SKBR3 cells treated with 100ng/ml EGF when compared to vehicle. In CHO-K1 cells stably transfected V_{1B} receptor (V_{1B}/CHO-K1), tERK fluorescence levels also remain unchanged in response to VP (100nM) vs control treated cells. The data shown are normalised to vehicle and graphs are representative of at least two fields, from at least three wells and at least two separate experiments (mean ± SEM). Statistical analysis comparing vehicle-treated versus agonist-treated was performed using a Student's *t*-test. (B) Representative images of HEK293, HeLa, and V_{1B}/CHO-K1 cells treated with control (ctrl) or agonist and stained with anti-tERK antibodies. Scale bar, 100μm.

To reduce any possible vehicle effects, water-soluble E2 (WS-E2) was also purchased. G-1 is not water-soluble. As with ethanol-soluble E2, incubation of rat HA-GPER transfected HEK293 cells with 10nM or 100nM WS-E2 (example of mean ± SEM given for 100nM (N.B., AFU values are normalised to vehicle): 1.157 ± 0.075) for 5 min had no effect on ppERK fluorescence (Figure 4.15). Similarly 1nM, 10nM, or 100nM did not activate ERK in HEK293 cells transfected with rat (untagged) (100nM: 1.132 ± 0.040) or mouse GPER (100nM: 1.139 ± 0.062). 10nM and 100nM WS-E2 did not increase ppERK fluorescence in untransfected HEK293 cells (100nM: 0.961 ± 0.051). Unexpectedly, stimulation with 1μM WS-E2 for 5 min significantly increased ppERK fluorescence in all of the HEK293 lines – including non-transfected cells, suggesting the effect was unrelated to GPER and non-specific (HEK293: 2.192 ± 0.044; rat HA-GPER: 3.046 ± 0.252; rat GPER 1.506 ± 0.079; mouse GPER 1.487 ± 0.169).

As was observed at 5 min, treatment with 1nM, 10nM, or 100nM WS-E2 for 10 min did not activate ERK in HEK293 cells transfected with untagged rat (example of mean ± SEM given for 100nM: 0.892 ± 0.045) or mouse GPER (100nM: 0.928 ± 0.1). However, 1μM WS-E2 did significantly increase ppERK fluorescence in untransfected cells, and HEK293 cells stably transfected with rat HA-GPER, untagged rat GPER, and mouse GPER (HEK293: 2.076 ± 0.231; rat HA-GPER: 2.572 ± 0.297; rat GPER: 1.918 ± 0.074; mouse GPER: 2.337 ± 0.016) (Figure 4.16).

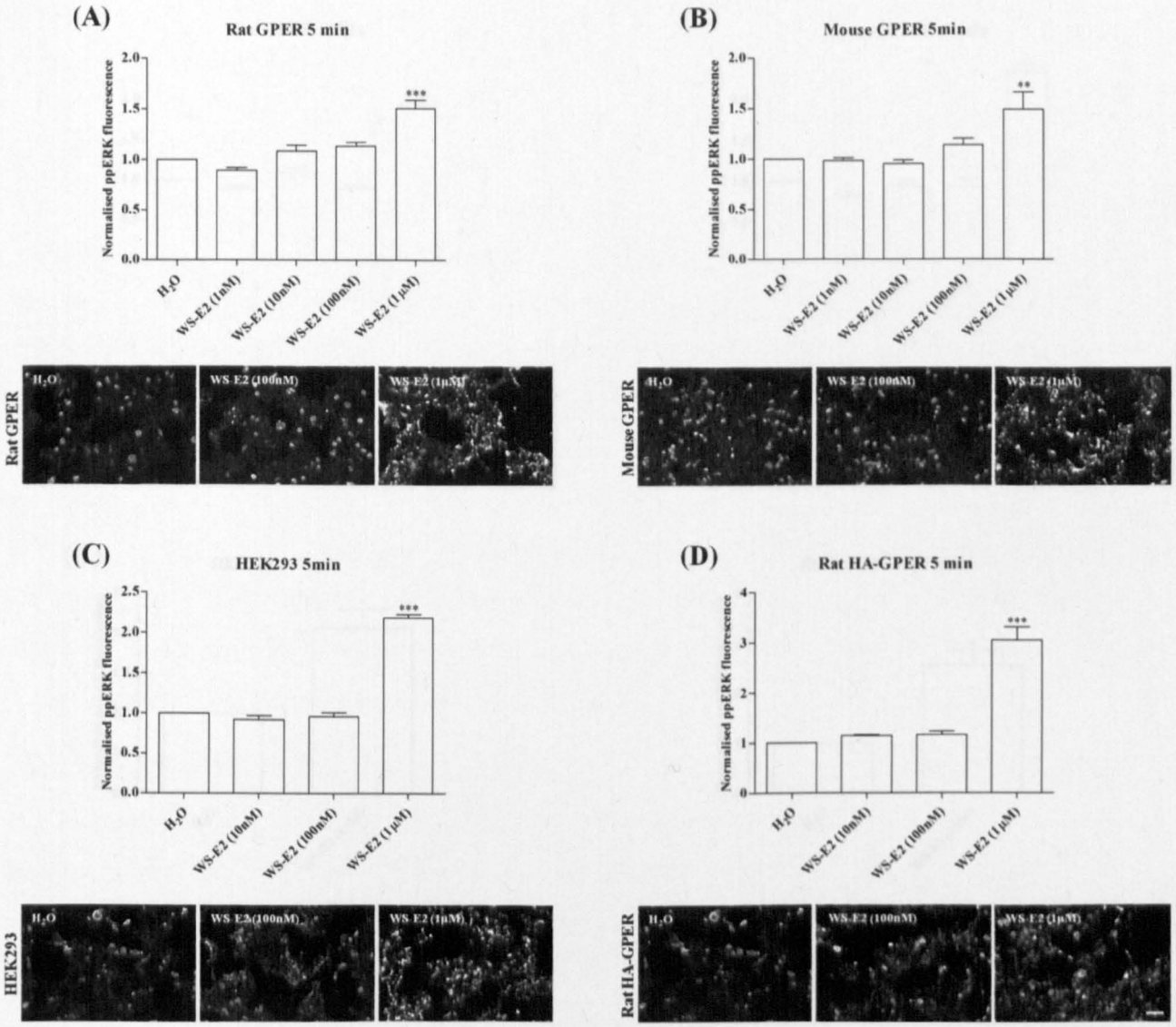

Figure 4.15. Treatment of HEK293 stably transfected with rodent GPER with water soluble E2 for 5 min does not stimulate ERK phosphorylation.

Treatment with either 1nM, 10nM, or 100nM water-soluble E2 for 5 min did not increase ppERK fluorescence in HEK293 cells transfected with untagged rat GPER (A), and untagged mouse GPER (B). Treatment with 10nM or 100nM WS-E2 for 5 min had no effect on ppERK fluorescence in untransfected HEK293 cells (C) or HEK293 cells stably transfected with HA-tagged rat GPER (D). 1μM WS-E2 non-specifically increased ppERK fluorescence in all cell lines investigated. The data shown are normalised to vehicle and graphs are representative of at least two fields, from triplicate wells and at least two separate experiments (mean ± SEM). Statistical analysis was performed using a one-way ANOVA and the Dunnett's multiple comparison test. **, $p < 0.01$; and ***, $p < 0.001$. Below each graph are some representative images of treated cells stained with anti-ppERK antibodies. Scale bar, 100μm.

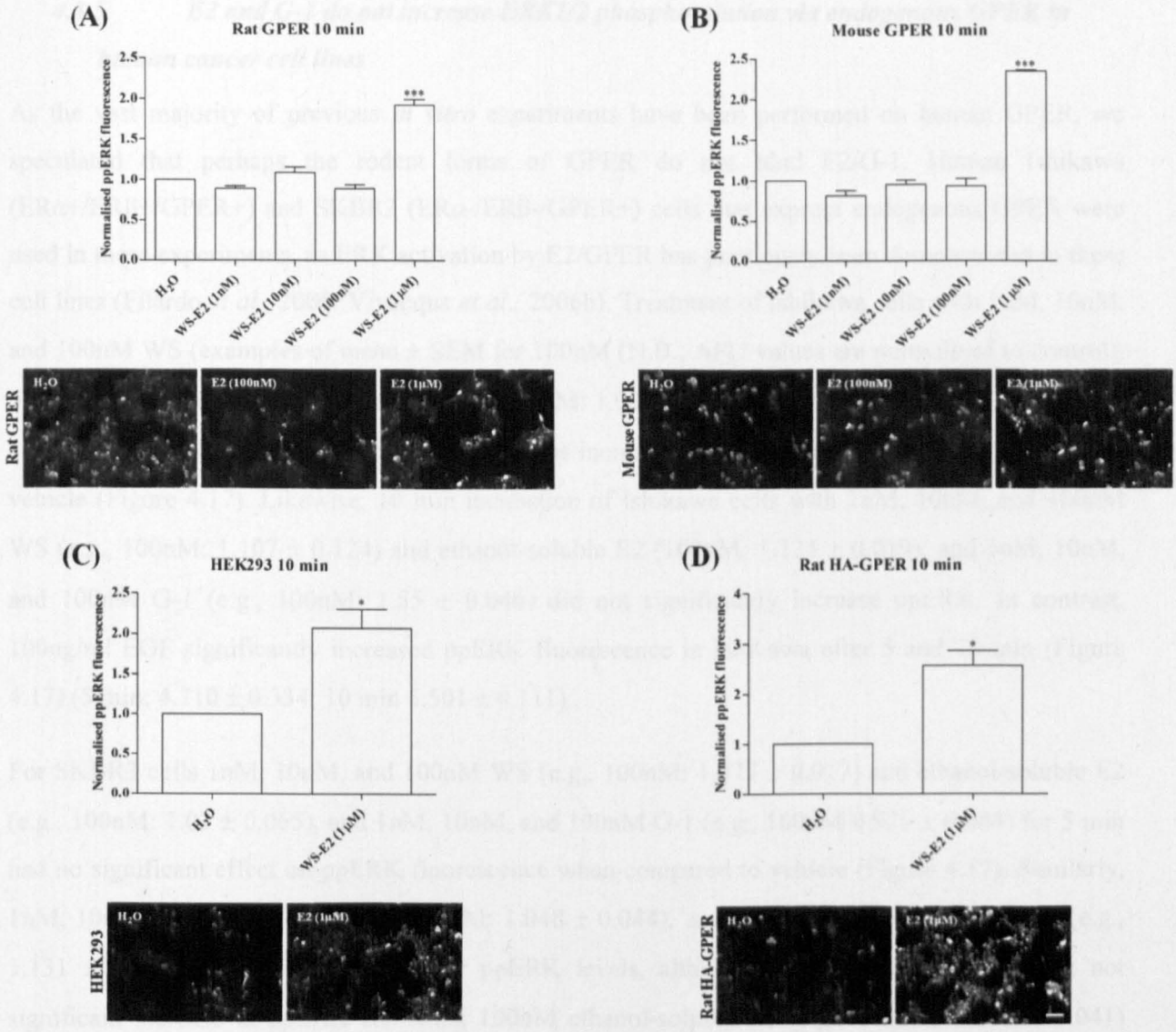

Figure 4.16. Treatment of HEK293 stably transfected with rodent GPER with water soluble E2 for 10 min does not stimulate ERK phosphorylation.

Treatment with either 1nM, 10nM, or 100nM WS-E2 for 10 min did not increase ppERK in HEK293 cells transfected with untagged rat GPER (A), and untagged mouse GPER (B). 1μM WS-E2 non-specifically increased ppERK fluorescence in untransfected HEK293 cells (C), HEK293 cells stably transfected with HA-tagged rat GPER (D), and also in untagged rat GPER (A), and untagged mouse GPER (B). The data shown are normalised to vehicle and graphs are representative of at least two fields, from triplicate wells and at least two separate experiments (mean ± SEM). Statistical analysis was performed using Student's *t*-test in (C and D) and a one-way ANOVA and the Dunnett's multiple comparison test in (A and B). *, $p < 0.05$; and ***, $p < 0.001$. Below each graph are some representative images of treated cells stained with anti-ppERK antibodies. Scale bar, 100μm.

4.3.5 E2 and G-1 do not increase ERK1/2 phosphorylation via endogenous GPER in human cancer cell lines

As the vast majority of previous *in vitro* experiments have been performed on human GPER, we speculated that perhaps the rodent forms of GPER do not bind E2/G-1. Human Ishikawa (ERα+/ERβ+/GPER+) and SKBR3 (ERα-/ERβ-/GPER+) cells that express endogenous GPER were used in these experiments, as ERK activation by E2/GPER has previously been demonstrated in these cell lines (Filardo *et al.*, 2000; Vivacqua *et al.*, 2006b). Treatment of Ishikawa cells with 1nM, 10nM, and 100nM WS (examples of mean ± SEM for 100nM (N.B., AFU values are normalised to control): 0.967 ± 0.048) and ethanol-soluble E2 (e.g., 100nM: 1.003 ± 0.026), and 1nM, 10nM, and 100nM G-1 (e.g., 100nM: 1.087 ± 0.049) for 5 min did not increase ppERK fluorescence when compared to vehicle (Figure 4.17). Likewise, 10 min incubation of Ishikawa cells with 1nM, 10nM, and 100nM WS (e.g., 100nM: 1.107 ± 0.124) and ethanol-soluble E2 (100nM: 1.124 ± 0.019), and 1nM, 10nM, and 100nM G-1 (e.g., 100nM: 1.55 ± 0.046) did not significantly increase ppERK. In contrast, 100ng/ml EGF significantly increased ppERK fluorescence in Ishikawa after 5 and 10 min (Figure 4.17) (5 min: 4.710 ± 0.334; 10 min 5.501 ± 0.111).

For SKBR3 cells 1nM, 10nM, and 100nM WS (e.g., 100nM: 1.077 ± 0.017) and ethanol-soluble E2 (e.g., 100nM: 1.03 ± 0.065), and 1nM, 10nM, and 100nM G-1 (e.g., 100nM 0.925 ± 0.084) for 5 min had no significant effect on ppERK fluorescence when compared to vehicle (Figure 4.17). Similarly, 1nM, 10nM, and 100nM WS (e.g., 100nM: 1.048 ± 0.044), and 1nM, 10nM, and 100nM G-1 (e.g., 1.131 ± 0.09) for 10 min did not alter ppERK levels, although there was a noticeable but not significant increase in ppERK following 100nM ethanol-soluble E2 (e.g., 100nM: 1.257 ± 0.041) (Figure 4.17). 100ng/ml EGF significantly increased ppERK fluorescence at 5 and 10 min (5 min: 1.375 ± 0.108; 10 min: 1.575 ± 0.075), but in contrast to Ishikawa cells, the response was not as robust, with a < 2-fold maximal response observed at 10 min. As the pictures in Figure 4.17 depict, SKBR3 cells have quite high basal levels of ppERK – even after overnight serum starvation in DMEM/F12 media (absent of serum).

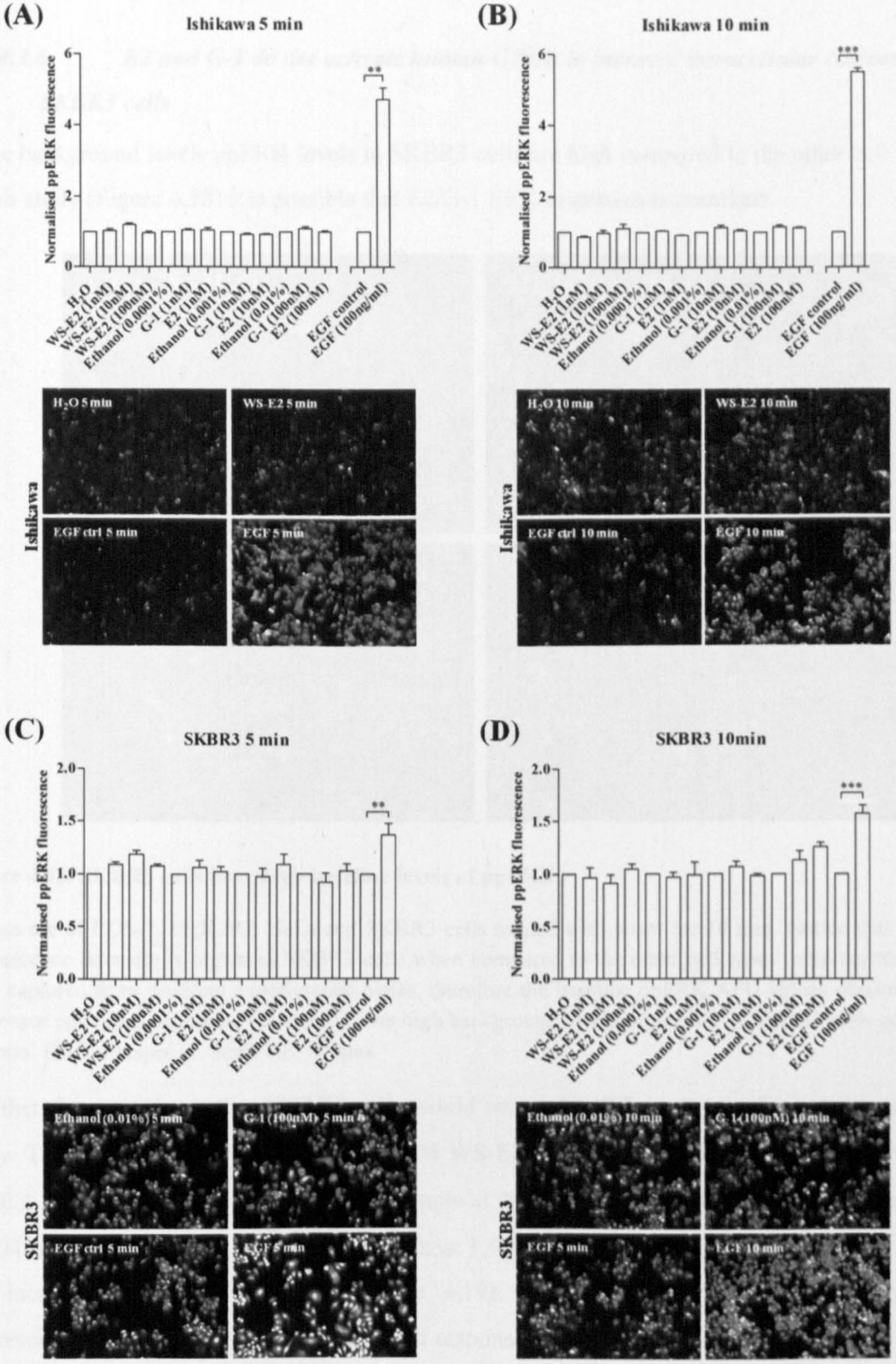

Figure 4.17. Treatment of human cancer cells that endogenously express GPER with E2 and G-1 does not lead to ERK1/2 activation.

Ishikawa and SKBR3 cells were treated with water-soluble E2 (WS-E2; 1nM-100nM), ethanol-soluble E2 (1nM-100nM) and G-1 (1nM-100nM) for 5 (A and C, respectively) and 10 (B and D, respectively) min. None of the treatments significantly increased ppERK fluorescence above control levels. Treatment of both Ishikawa and SKBR3 cells with EGF for 5 and 10 min significantly increased ppERK fluorescence when compared to control. The data shown are normalised to vehicle and graphs are representative of at least two fields, from triplicate wells and three separate experiments (mean ± SEM). Statistical analysis comparing vehicle-treated versus agonist-treated (for all treatments in SKBR3 cells but not EGF and control treated Ishikawa cells) was performed using a one-way ANOVA and the Bonferroni multiple comparison test. Vehicle-treated vs EGF-treated data was compared separately using a Student's *t*-test (data sets were split up to avoid a type II false negative statistical error at the lower end of the response e.g., a large EGF-mediated increase in ppERK fluorescence may mask a subtle response induced by the other agonists). **, $p < 0.01$; and ***, $p < 0.001$. Below each graph are some representative images of cells treated with control (ctrl) or agonist and stained with anti-ppERK antibodies. Scale bar, 100μm.

4.3.6 E2 and G-1 do not activate human GPER to increase intracellular calcium in SKBR3 cells

Since background levels ppERK levels in SKBR3 cells are high compared to the other cell types used in this study (Figure 4.18) it is possible that E2/G-1 ERK responses are masked.

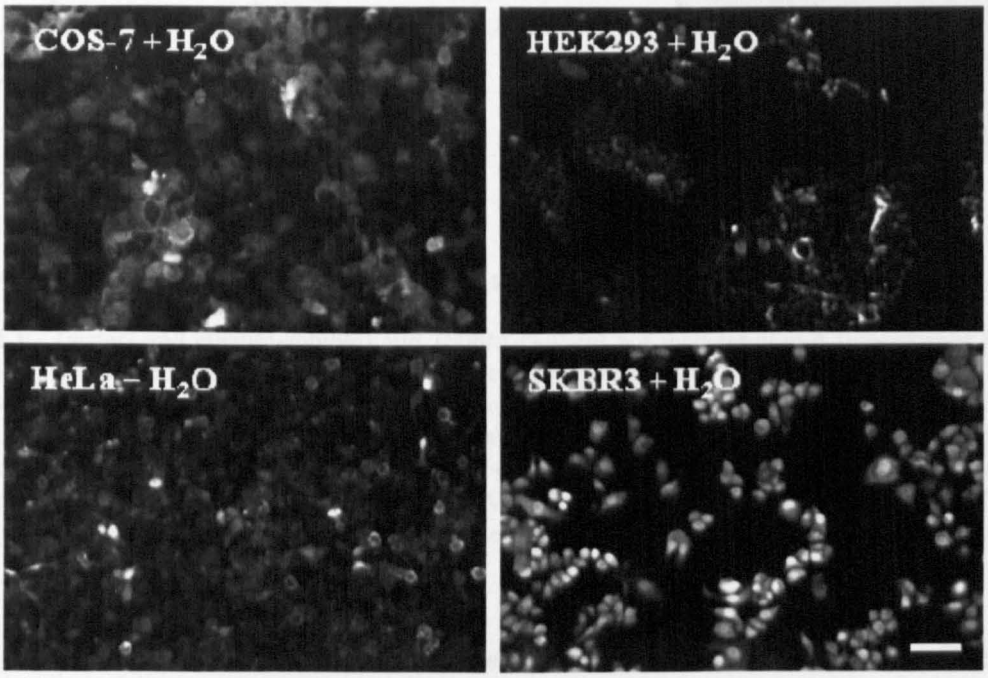

Figure 4.18. SKBR3 cells have high baseline levels of ppERK.

Images are of COS-7, HEK293, HeLa and SKBR3 cells treated with water for 10 min. Notice that the ppERK fluorescence intensity is higher in SKBR3 cells when compared to the other cell types (note that these images were captured from different experimental plates, therefore the baseline ppERK AFU values obtained from the difference cell types cannot be compared). The high background levels of ppERK in SKBR3 cells could mask a potential E2/G-1 response. Scale bar, 100μm.

We therefore tested whether SKBR3 cells would respond to E2 or G-1 in the calcium stimulation assay. Treatment of SKBR3 cells with 100nM WS-E2 (example at 36000ms: 1.009 ± 0.196 vs H_2O 1.020 ± 0.192), 100nM ethanol-soluble (example at 36000ms: 0.979 ± 0.031 vs 0.01% ethanol 1.075 ± 0.045), and 100nM G-1 (example at 36000ms: 1.027 ± 0.026 vs 0.01% ethanol 1.075 ± 0.045) did not increase intracellular calcium (Figure 4.19). 100μM ATP significantly increased fluo-4 fluorescence in SKBR3 cells (maximal 4-fold response at 36000ms: 4.5181 ± 0.400) when compared to vehicle control (H_2O: 1.020 ± 0.192).

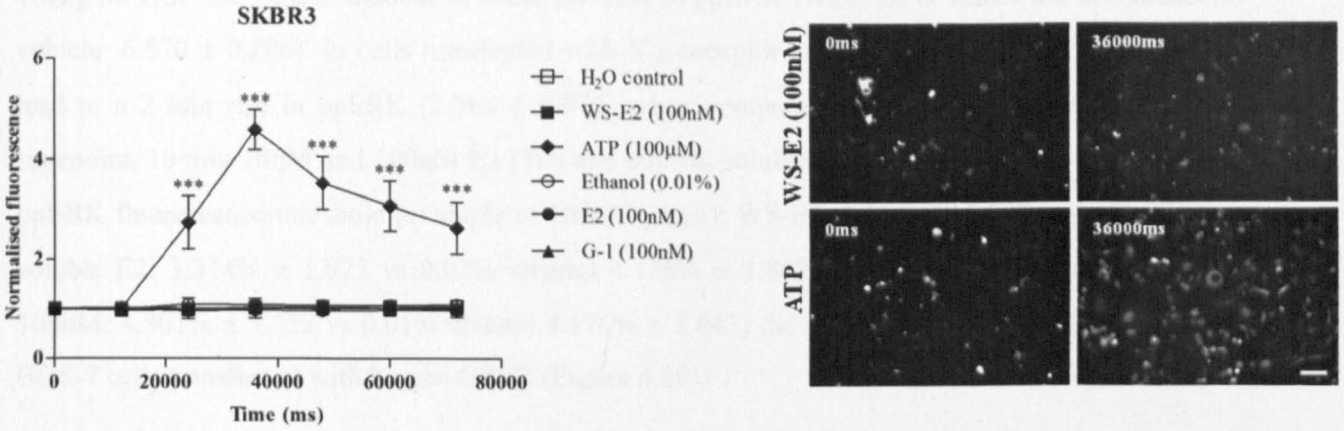

Figure 4.19. GPER does not increase intracellular calcium in response to E2 or G-1 in SKBR3 cells.

(A) 100nM E2 (water- and ethanol-soluble) and 100nM G-1 did not increase fluo-4 fluorescence intensity in SKBR3 cells when compared to vehicle (N.B., vehicle or agonist were added to each well at 12000ms). Fluorescence intensity significantly increased in cells treated with 100μM ATP vs control. The data shown are normalised to the value at time 0ms. Graphs are representative of one field, from triplicate wells and at least two separate experiments (mean ± SEM). Statistical analysis comparing vehicle-treated versus agonist-treated at each time point was performed using a two-way ANOVA and the Bonferroni post test. ***, $p < 0.001$. Below each graph are some representative images of cells treated with agonist at 0ms and 36000ms. Scale bar, 100μm.

4.3.7 E2 and G-1 do not activate transiently transfected human and rodent GPER to stimulate ERK1/2 phosphorylation

To further corroborate our results in cells stably transfected with, or presumably expressing endogenous GPER, we transiently transfected COS-7 and HeLa cells with human, rat or mouse GPER, and stimulated the cells with E2 and G-1 for 5 or 10 min in the ERK phosphorylation assay. In parallel, non-transfected cell were treated with 100ng/ml EGF, and V_{1B} receptor transiently-transfected cells were treated with 100nM VP to ensure that 1) the cells had a functional ERK response; and 2) the assay was robust enough to detect a GPCR response in the 30% of transfected cells, and to set the 'ppERK fluorescence threshold' (see section 4.2.7).

In non-transfected COS-7 cells, 100ng/ml EGF treatment for 5 min stimulated a 4-fold increase in ppERK fluorescence (N.B., AFU values are normalised to vehicle: 3.914 ± 0.191). In COS-7 cells transfected with V_{1B} receptor cDNA, 100nM VP treatment for 5 min increased ppERK by 2-fold (1.968 ± 0.088), when compared with vehicle controls. In contrast, 10nM and 100nM E2 (WS and ethanol soluble) (N.B., values are % of cells above ppERK fluorescence threshold (example of 100nM given): WS-E2, 2.982% ± 1.697 vs H_2O 4.112% ± 1.212; ethanol-soluble E2: 3.375% ± 0.976 vs 0.01% ethanol 2.408% ± 0.097) and 10nM and 100nM G-1 (e.g., 100nM: 2.368% ± 0.544 vs 0.01% ethanol 2.408% ± 0.097) failed to significantly increase ppERK fluorescence in COS-7 cells transfected with human GPER (Figure 4.20). Treatment of non-transfected COS-7 cells with

100ng/ml EGF for 10 min induced a 6-fold increase in ppERK (N.B., AFU values are normalised to vehicle: 6.570 ± 0.206). In cells transfected with V_{1B} receptor cDNA, 10 min 100nM VP treatment lead to a 2-fold rise in ppERK (2.364 ± 0.076) when compared with vehicle. As with the 5 min timepoint, 10 min 10nM and 100nM E2 (WS and ethanol-soluble) (N.B., values are % of cells above ppERK fluorescence threshold (example of 100nM given): WS-E2, 2.410% ± 0.357 vs H_2O; ethanol-soluble E2: 3.314% ± 1.073 vs 0.01% ethanol 4.176% ± 1.842) and 10nM and 100nM G-1 (e.g., 100nM: 4.301% ± 1.752 vs 0.01% ethanol 4.176% ± 1.842) did not significantly increase ppERK in COS-7 cells transfected with human GPER (Figure 4.20).

In non-transfected HeLa cells, EGF treatment (100ng/ml) for 5 min activated a robust ERK response leading to a 20-fold increase in ppERK (N.B., AFU values are normalised to vehicle: 20.674 ± 0.173). In V_{1B} receptor transfected HeLa cells, VP treatment (100nM for 5 min) increased ppERK by 7-fold (7.749 ± 0.081). As was observed in COS-7 cells, 5 min treatment of 10nM and 100nM E2 (water- and ethanol-soluble) (N.B., values are % of cells above ppERK fluorescence threshold (example of 100nM given): WS-E2 0.970% ± 0.083 vs H_2O 0.424% ± 0.048; ethanol-soluble E2 0.624% ± 0.202 vs 0.01% ethanol 0.483% ± 0.105) and 10nM and 100nM G-1 (e.g., 100nM: 0.4% ± 0.043 vs 0.01 % ethanol 0.483% ± 0.105) did not increase ppERK in HeLa cells transfected with human GPER (Figure 4.21).

Stimulation of non-transfected HeLa cells with 100ng/ml EGF for 10 min increased ppERK by 16-fold (N.B., AFU values are normalised to vehicle: 15.760 ± 0.523). In V_{1B} receptor-transfected HeLa cells, 100nM VP treatment for 10 min increased ppERK by 5-fold (5.675 ± 0.145). Concomitant with the COS-7 cell data, 10nM and 100nM E2 (water- and ethanol-soluble) (N.B., values are % of cells above ppERK fluorescence threshold (example of 100nM given): WS-E2 0.147% ± 0.119 vs H_2O 0.363% ± 0.175; ethanol-soluble E2 0.354% ± 0.136 vs 0.01% ethanol 0.256% ± 0.042) and 10nM and 100nM G-1 (for 10 min) (e.g., 100nM: 0.126% ± 0.032 vs 0.01 % ethanol 0.256% ± 0.042) did not significantly induce an ERK response in HeLa cells transfected with human GPER (Figure 4.21).

In COS-7 cells transfected with untagged rat GPER, 10 min treatment with 100nM E2 (e.g., 100nM: WS-E2 3.577% ± 1.075 vs H_2O 4.524% ± 4.366; ethanol-soluble E2 0.747% ± 0.369 vs 0.01% ethanol 0.857% ± 0.237) or 100nM G-1 (G-1 3.452% ± 0.393 vs 0.01% ethanol 0.857% ± 0.237) did not lead to an increase in ppERK (Figure 4.22). As with the rat GPER clone, COS-7 cells transfected with mouse GPER did not respond to 100nM E2 (WS-E2 3.312% ± 1772 vs H_2O 2.574% ± 1.674; ethanol soluble E2 0.686% ± 0.217 vs 0.01% ethanol 1.818% ± 0.899) or 100nM G-1 (1.73771 ± 1.47 vs 0.01% ethanol 1.818% ± 0.899) to increase ppERK levels (Figure 4.22).

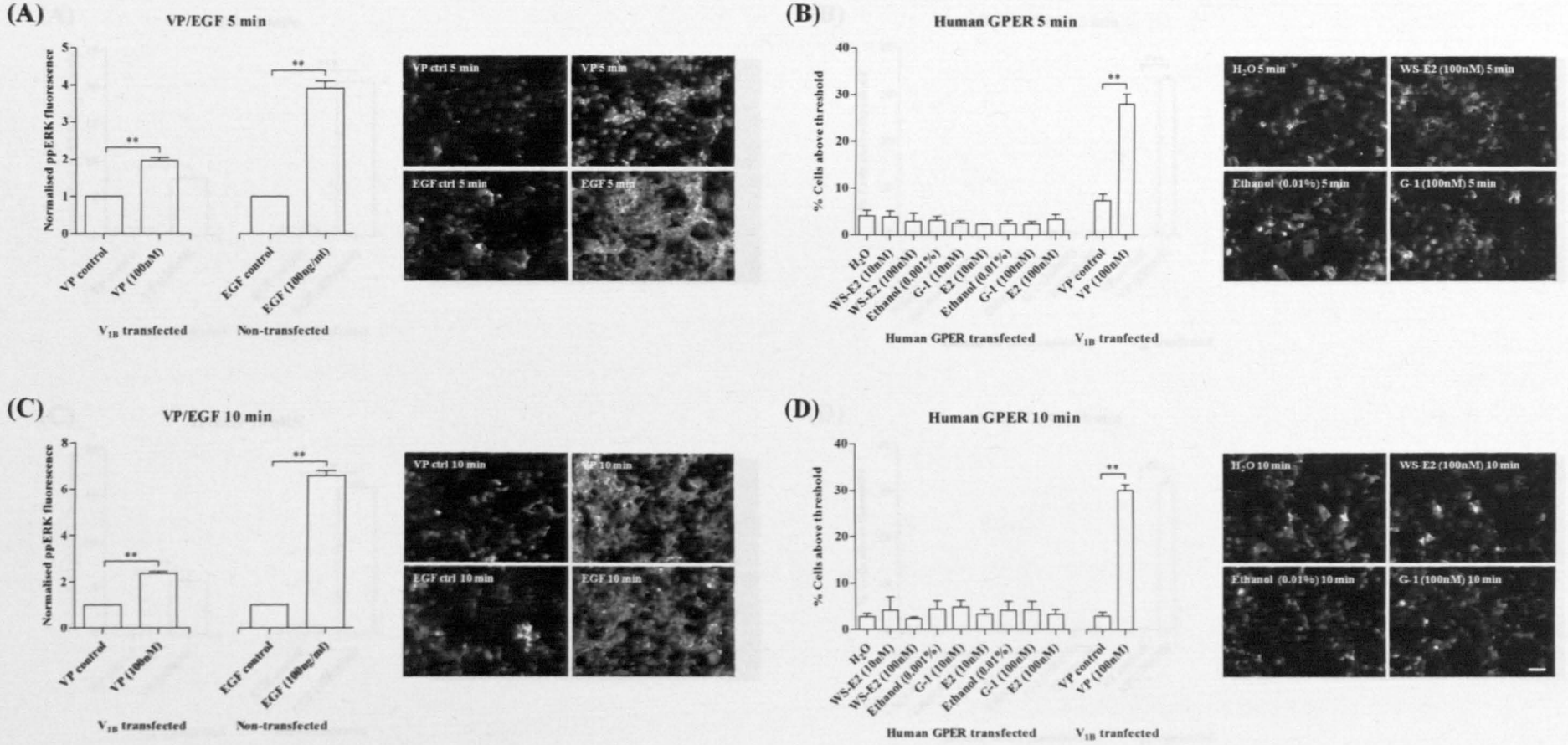

Figure 4.20. Transiently transfected human GPER does not stimulate ERK phosphorylation in COS-7 cells following 5 or 10 min of E2 or G-1 treatment.

In non-transfected cells, 100ng/ml EGF stimulated a significant increase in ppERK fluorescence at 5 and 10 min, as represented by an increase in normalised ppERK fluorescence (A and C, respectively). In COS-7 cells transiently transfected with V_{1B} cDNA, 100nM VP treatment for 5 and 10 min also stimulated a significant increase in ppERK fluorescence when compared with vehicle controls (A and C, respectively). The ppERK fluorescence data obtained with the V_{1B} receptor transfected COS-7 cells was used to set a threshold as described in section 4.2.7. The proportion of cells displaying an ERK response (emit ppERK fluorescence above threshold) at 5 (B) or 10 min (D) following 10nM or 100nM E2 (water- and ethanol-soluble) or 10nM or 100nM G-1 treatment was not significantly different from vehicle in COS-7 cells transfected with human GPER. Graphs are representative of at least two fields, from triplicate wells and three separate experiments (mean ± SEM). Statistical analysis comparing vehicle-treated versus either EGF- or VP-treated (in A-D) was performed with a Student's *t*-test. Statistical analysis comparing vehicle-treated versus either E2-or G-1-treated (in B and D) was performed using one-way ANOVA and the Bonferroni multiple comparison test. **, $p < 0.01$. Adjacent to each graph are some representative images of cells stained with anti-ppERK antibodies treated with control (ctrl) or agonist. Scale bar, 100μm.

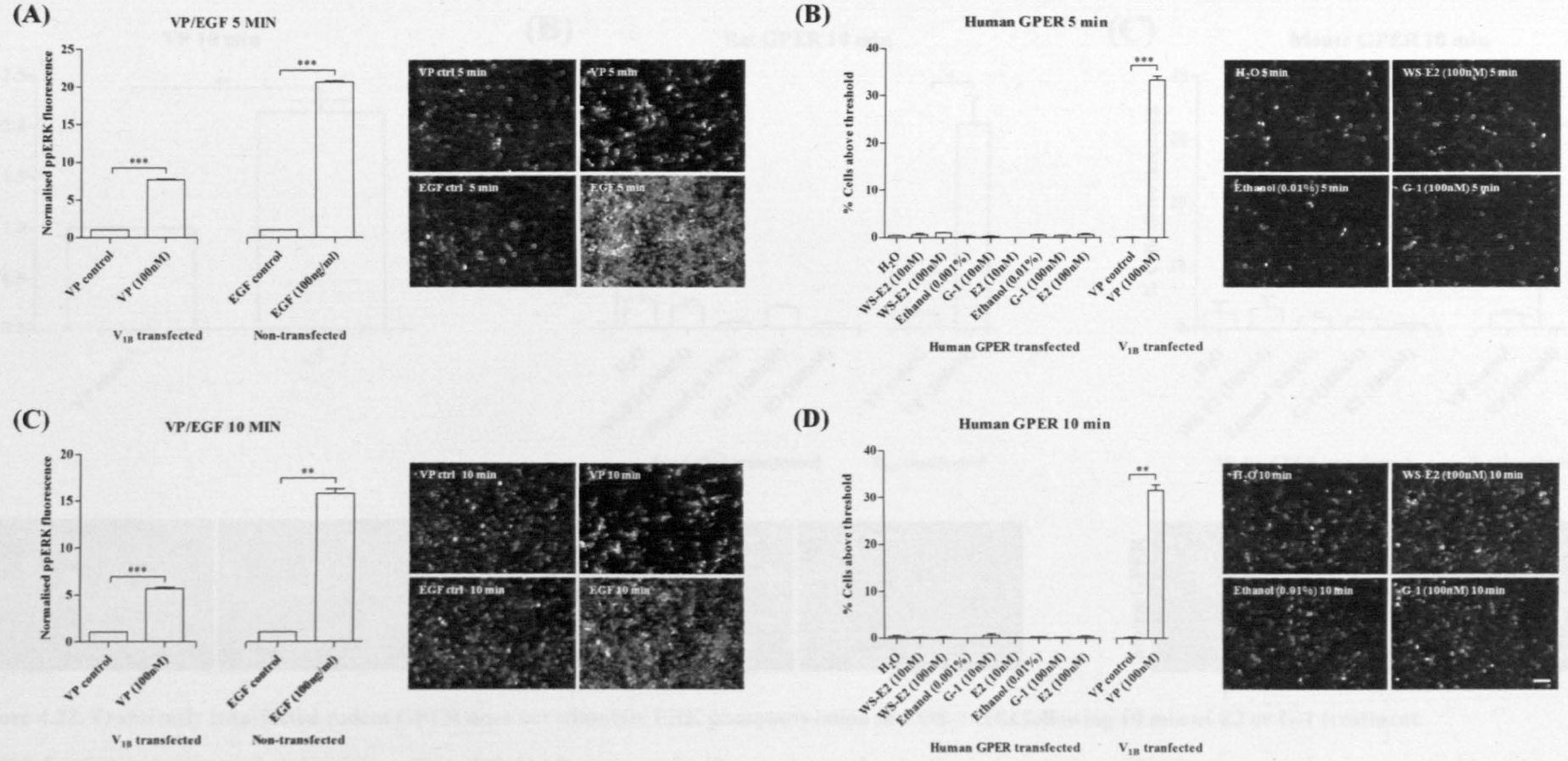

Figure 4.21. Transiently transfected human GPER does not stimulate ERK phosphorylation in HeLa cells following 5 or 10 min of E2 or G-1 treatment.

In non-transfected cells, 100ng/ml EGF stimulated a significant increase in ppERK fluorescence at 5 and 10 min, as represented by an increase in normalised ppERK fluorescence (A and C, respectively). In HeLa cells transiently transfected with V_{1B} cDNA, 100nM VP treatment for 5 and 10 min also stimulated a significant increase in ppERK fluorescence when compared with vehicle controls (A and C, respectively). The ppERK fluorescence data obtained with the V_{1B} receptor transfected HeLa cells was used to set a threshold as described in section 4.2.7. The proportion of cells displaying an ERK response (emit ppERK fluorescence above threshold) at 5 (B) or 10 min (D) following 10nM or 100nM E2 (water- and ethanol-soluble) or 10nM or 100nM G-1 treatment was not significantly different from vehicle in HeLa cells transfected with human GPER. Graphs are representative of at least two fields, from triplicate wells and two separate experiments (mean ± SEM). Statistical analysis comparing vehicle-treated versus either EGF- or VP-treated (A-D) was performed with a Student's *t*-test. Statistical analysis comparing vehicle-treated versus either E2-or G-1-treated (in C and D) was performed using one-way ANOVA and the Bonferroni multiple comparison test. **, $p < 0.01$; ***, $p<0.005$. Adjacent to each graph are some representative images of cells stained with anti-ppERK antibodies treated with control (ctrl) or agonist. Scale bar, 100μm.

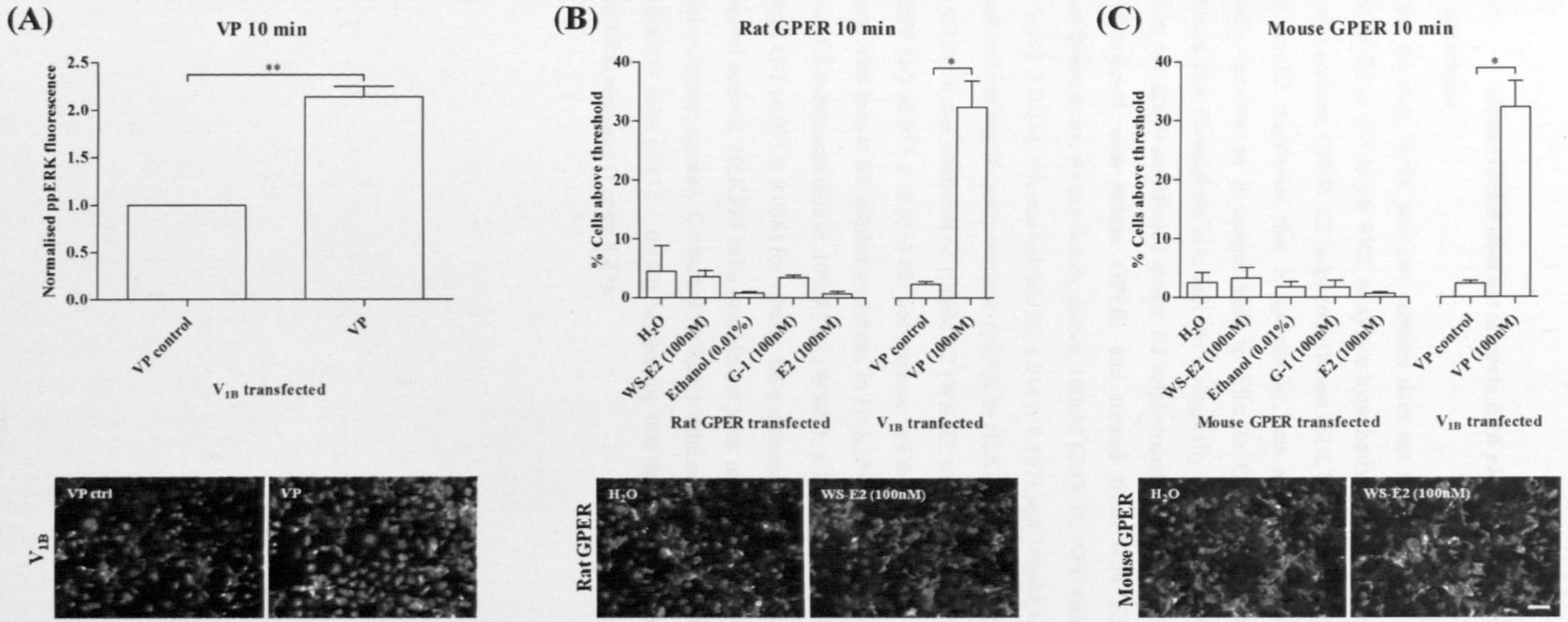

Figure 4.22. Transiently transfected rodent GPER does not stimulate ERK phosphorylation in COS-7 cells following 10 min of E2 or G-1 treatment.

In COS-7 cells transiently transfected with V_{1B} cDNA, 100nM VP treatment for 10 min stimulated a significant increase in ppERK fluorescence when compared with vehicle controls (A). The ppERK fluorescence data obtained with the V_{1B} receptor transfected COS-7 cells was used to set a threshold as described in section 4.2.7. The proportion of cells displaying an ERK response (emit ppERK fluorescence above threshold) 10 min following 100nM E2 (water- and ethanol-soluble) or 100nM G-1 treatment was not significantly different from vehicle in COS-7 cells transfected with rat (B) or mouse (C) GPER. Graphs are representative of at least two fields, from triplicate wells and three separate experiments (mean ± SEM). Statistical analysis comparing vehicle-treated versus either E2-or G-1-treated (in B and C) was performed using one-way ANOVA and the Bonferroni multiple comparison test. Statistical analysis comparing vehicle-treated versus VP-treated (in A-C) was performed with a Student's *t*-test. *, $p < 0.05$; **, $p < 0.01$. Adjacent to each graph are some representative images of cells stained with anti-ppERK antibodies treated with control (ctrl) or agonist. Scale bar, 100μm.

4.3.8 Mouse GPER does not increase ERK phosphorylation via an E2 sulphotransferase metabolite

Given that the data in the previous sections does not reveal that rat, mouse or human GPER are activated by E2 or G-1 in our ERK assay, we hypothesised that an E2 metabolite rather than E2 may bind to and activate GPER. E2 sulphotransferase (SULT1E1) is an enzyme that converts E2 to E2-sulphate, an E2 metabolite that is hydrophilic, has a longer half-life than E2, and is deemed biologically inactive as it cannot bind to ERα or ERβ (Song, 2006; Pasqualini, 2009). We hypothesised that E2-sulphate is in fact the biologically active endogenous ligand for GPER. To test this theory, we stably transfected mouse E2 sulphotransferase into HEK293 cells and HEK293 cells stably transfected with mouse GPER, and treated them with E2 and/or G-1 in the ERK phosphorylation assay. As previously shown, 100nM E2 (N.B., AFU values are normalised to vehicle: WS-E2 1.012 ± 0.224; ethanol-soluble E2 1.014 ± 0.107) and 100nM G-1 (0.904 ± 0.123) treatment for 10 min did not significantly increase ppERK in HEK293 cell stably transfected with mouse GPER (Figure 4.23). 10 min treatment of 100nM E2 (WS-E2: 0.974 ± 0.115; ethanol-soluble: 0.967 ± 0.049) and 100nM G-1 (0.955 ± 0.036) did not increase ppERK fluorescence levels in HEK293 cell stably transfected with mouse E2 sulphotransferase. In HEK293 cells stably co-transfected with both mouse GPER and E2 sulphotransferase, 100nM E2 (WS-E2: 1.116 ± 0.076; ethanol-soluble: 0.964 ± 0.046) and 100nM G-1 (0.955 ± 0.036) for 10min, did not increase ppERK levels (Figure 4.23). As a further experimental control, HEK293 cells (transfected with mouse GPER) were treated with carbachol, a muscarinic receptor agonist. Carbachol (500μM) induced a significant increase ppERK fluorescence in the HEK293 cells (1.831 ± 0.190), suggesting that these cells are capable of mediating a GPCR-mediated ERK response (Figure 4.23).

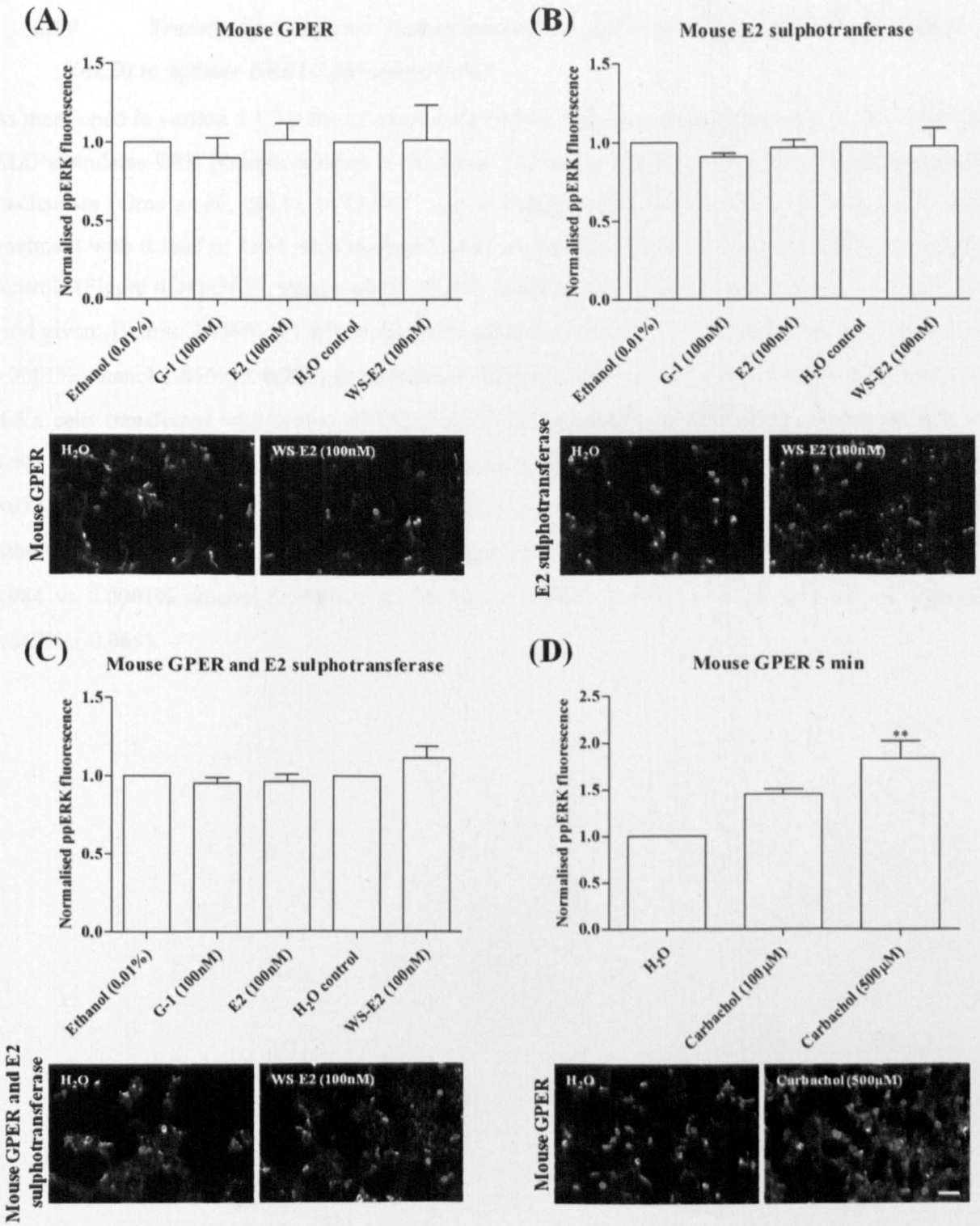

Figure 4.23. 10 min E2 or G-1 treatment does not stimulate ERK phosphorylation in HEK293 cells stably co-transfected with mouse GPER and mouse E2 sulphotransferase.

Treatment with 100nM E2 (water- and ethanol-soluble) or 100nM G-1 for 10 min did not increase ppERK fluorescence in HEK293 cells transfected with mouse GPER (A), mouse E2 sulphotransferase (B), or cells co-transfected with both mouse GPER and mouse E2 sulphotransferase (C). 500μM carbachol significantly increased ppERK fluorescence in HEK293 cells transfected with mouse GPER (D). The data shown are normalised to vehicle and graphs are representative of at least two fields, from triplicate wells and at least two separate experiments (mean ± SEM). Statistical analysis was performed using a one-way ANOVA and the bonforroni (A-C) or Dunnett's multiple comparison test in (D). **, $p < 0.01$. Below each graph are some representative images of treated cells stained with anti-ppERK antibodies. Scale bar, 100μm.

4.3.9 Transiently transfected human and rodent GPER are not activated by aldosterone (ALD) to activate ERK1/2 phosphorylation

As mentioned in section 4.1.3 it has been recently reported that low concentrations (e.g., 0.1-1nM) of ALD stimulates ERK phosphorylation in rat aortic vascular endothelial cells via a GPER-dependant mechanism (Gros *et al.*, 2011). In COS-7 cells transfected with human GPER, 10 min or 15 min treatment with 0.1nM or 1nM ALD did not lead to an increase in ppERK when compared to vehicle controls (Figure 4.24) (N.B., values are % of cells above ppERK fluorescence threshold. Example of 1nM given: 10 min, 3.499% ± 1.856 vs 0.0001% ethanol 4.176% ± 0.651; 15 min, 1.819% ± 0.615 vs 0.0001% ethanol 1.866% ± 0.752). In addition, 0.1nM or 1nM ALD did not increase ppERK levels in HeLa cells transfected with human GPER (Figure 4.25) (example of 1nM given: 10min, 0.152% ± 0.091 vs 0.0001% ethanol 0.019% ± 0.019; 15 min, 0.765% ± 0.328 vs 0.0001% ethanol 0.371% ± 0.077). Furthermore, 100nM ALD did not increase ppERK levels in COS-7 cells transfected with either rat or mouse GPER (for 10 min) when compared to vehicle (Figure 4.26) (rat GPER: 5.947% ± 0.984 vs 0.0001% ethanol 5.598% ± 0.124; mouse GPER: 3.718% ± 1.128 vs 0.0001% ethanol 3.647% ± 0.965).

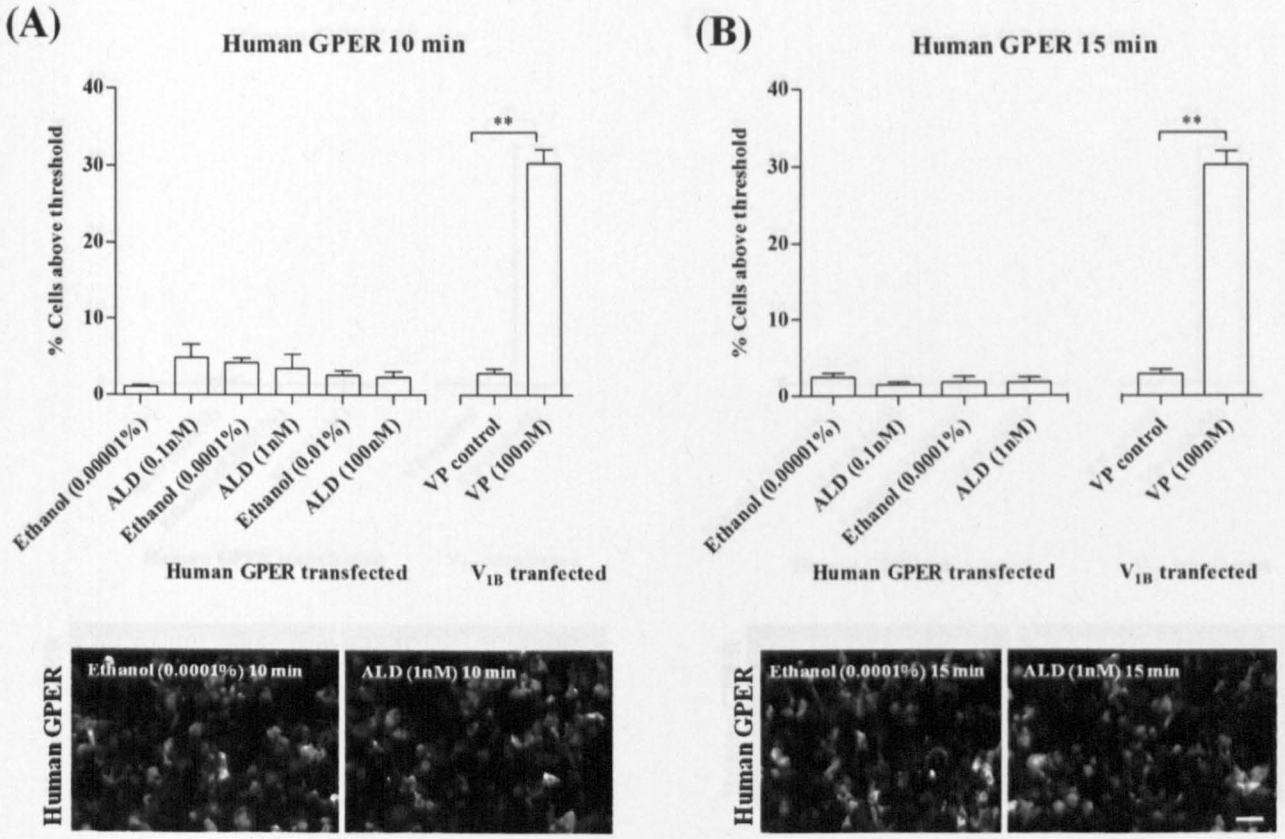

Figure 4.24. Transiently transfected human GPER does not stimulate ERK phosphorylation in COS-7 cells following 10 or 15 min of ALD treatment.

As shown in previous figures (Figures 4.20, 4.22), 100nM VP for 10 min stimulates a significant increase in ppERK fluorescence when compared with vehicle controls in COS-7 cells transiently transfected with V_{1B} cDNA. The ppERK fluorescence data obtained with the V_{1B} receptor transfected COS-7 cells was used to set a threshold as described in section 4.2.7. The proportion of cells displaying an ERK response (emit ppERK fluorescence above threshold) following 0.1nM, 1nM or 100nM ALD treatment for 10 min (A), or 0.1nM or 1nM ALD for 15 min (B) was not significantly different from vehicle COS-7 cells transfected with human GPER. Graphs are representative of at least two fields, from triplicate wells and two separate experiments (mean ± SEM). Statistical analysis comparing vehicle-treated versus ALD-treated was performed using a one-way ANOVA and the Bonferroni multiple comparison test. Statistical analysis comparing vehicle-treated versus VP-treated (in A and B) was performed with a Student's *t*-test. **, $p < 0.01$. Adjacent to each graph are some representative images of cells stained with anti-ppERK antibodies treated with control (ctrl) or agonist. Scale bar, 100μm.

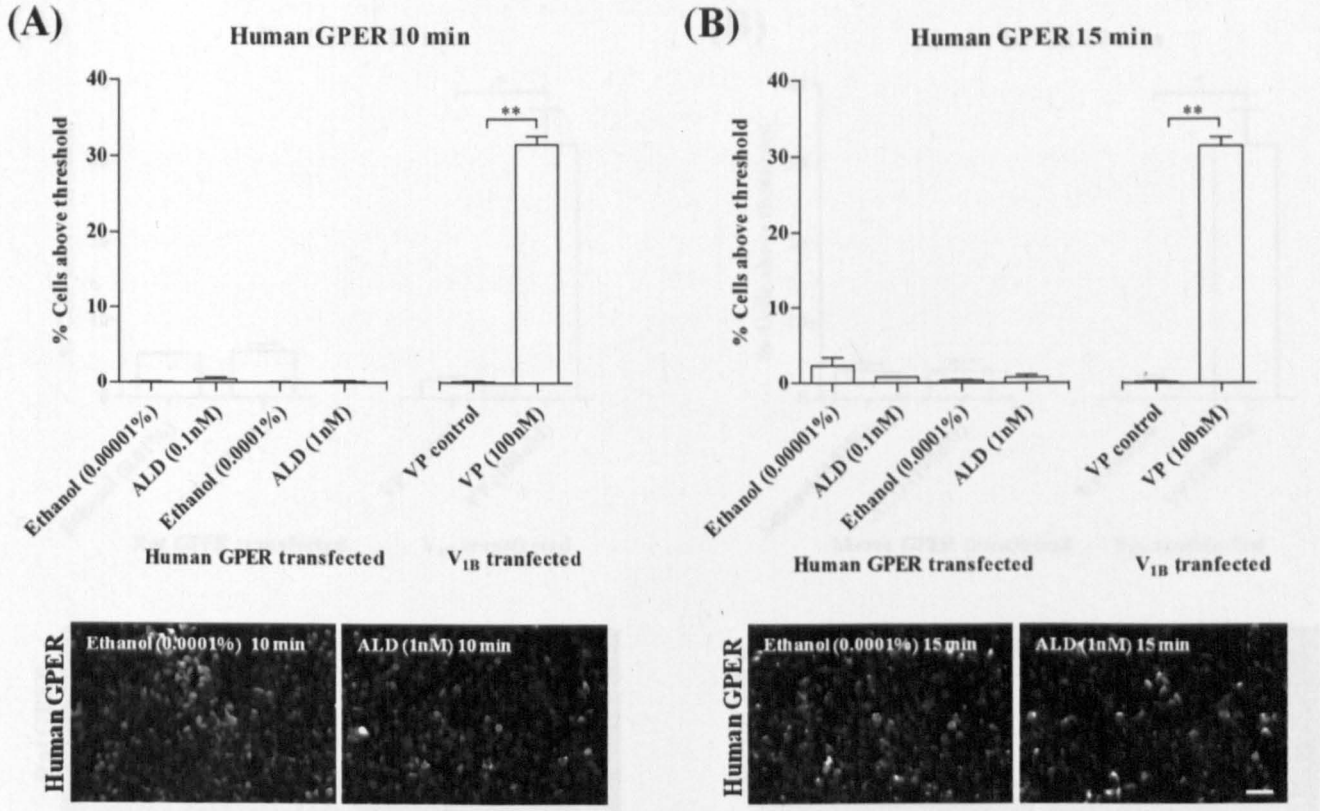

Figure 4.25. Transiently transfected human GPER does not stimulate ERK phosphorylation in HeLa cells following 10 or 15 min of ALD treatment.

As shown in previous figure (Figure 4.21) in HeLa cells transiently transfected with V_{1B} cDNA, 100nM VP for 10 min stimulates a significant increase in ppERK fluorescence when compared with vehicle controls. The ppERK fluorescence data obtained with the V_{1B} receptor transfected HeLa cells was used to set a threshold as described in section 4.2.7. The proportion of cells displaying an ERK response (emit ppERK fluorescence above threshold) following 0.1nM, 1nM or 100nM ALD treatment for 10 min (A), or 0.1nM or 1nM ALD for 15 min (B) was not significantly different from vehicle in COS-7 cells transfected with human GPER. Graphs are representative of at least two fields, from triplicate wells and two separate experiments (mean ± SEM). Statistical analysis comparing vehicle-treated versus ALD-treated was performed using a one-way ANOVA and the Bonferroni multiple comparison test. Statistical analysis comparing vehicle-treated versus VP-treated (in A and B) was performed with a Student's *t*-test. **, $p < 0.01$. Adjacent to each graph are some representative images of cells stained with anti-ppERK antibodies treated with control (ctrl) or agonist. Scale bar, 100μm.

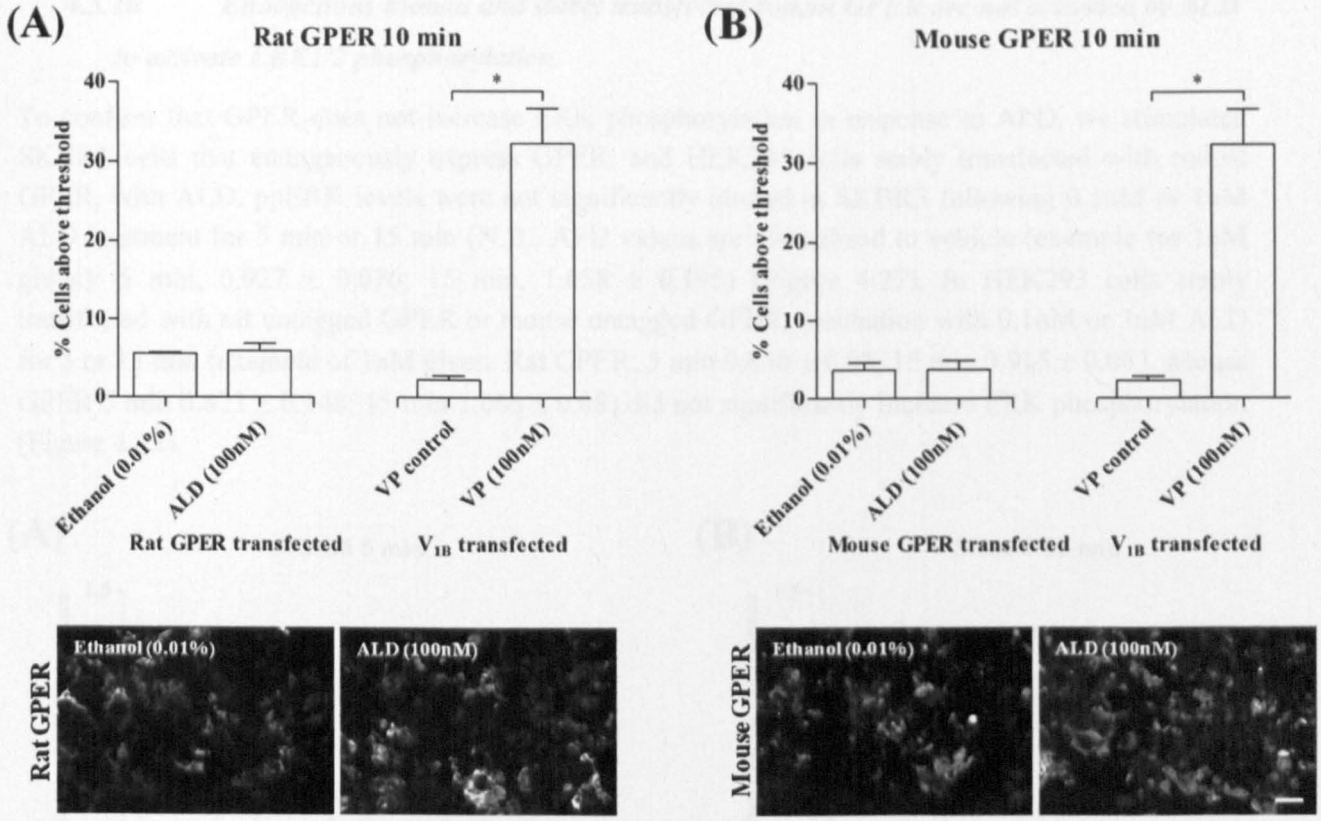

Figure 4.26. Transiently transfected rodent GPER does not stimulate ERK phosphorylation in COS-7 cells following 10 min ALD treatment.

As shown in previous figures (Figures 4.20, 4.22) in COS-7 cells transiently transfected with V_{1B} cDNA, 100nM VP treatment for 10 min stimulates a significant increase in ppERK fluorescence when compared with vehicle controls. The ppERK fluorescence data obtained with the V_{1B} receptor transfected COS-7 cells was used to set a threshold as described in section 4.2.7. The proportion of cells displaying an ERK response (emit ppERK fluorescence above threshold) following 100nM ALD treatment for 10 min was not significantly different from vehicle in COS-7 cells transiently expressing rat GPER (A) or mouse GPER (B). Graphs are representative of at least two fields, from triplicate wells and two separate experiments (mean ± SEM). Statistical analysis comparing vehicle-treated versus ALD-treated was performed using a one-way ANOVA and the Bonferroni multiple comparison test. Statistical analysis comparing vehicle-treated versus VP-treated (in A and B) was performed with a Student's *t*-test. *, $p < 0.05$; **, $p < 0.01$. Adjacent to each graph are some representative images of cells stained with anti-ppERK antibodies treated with control (ctrl) or agonist. Scale bar, 100μm.

4.3.10 Endogenous human and stably transfected rodent GPER are not activated by ALD to activate ERK1/2 phosphorylation

To confirm that GPER does not increase ERK phosphorylation in response to ALD, we stimulated SKBR3 cells that endogenously express GPER, and HEK293 cells stably transfected with rodent GPER, with ALD. ppERK levels were not significantly altered in SKBR3 following 0.1nM or 1nM ALD treatment for 5 min or 15 min (N.B., AFU values are normalised to vehicle (example for 1nM given): 5 min, 0.927 ± 0.076; 15 min, 1.058 ± 0.195) (Figure 4.27). In HEK293 cells stably transfected with rat untagged GPER or mouse untagged GPER, incubation with 0.1nM or 1nM ALD for 5 or 15 min (example of 1nM given. Rat GPER: 5 min 0.830 ± 0.08; 15 min 0.915 ± 0.063. Mouse GPER 5 min 0.823 ± 0.148; 15 min 1.066 ± 0.08) did not significantly increase ERK phosphorylation (Figure 4.28).

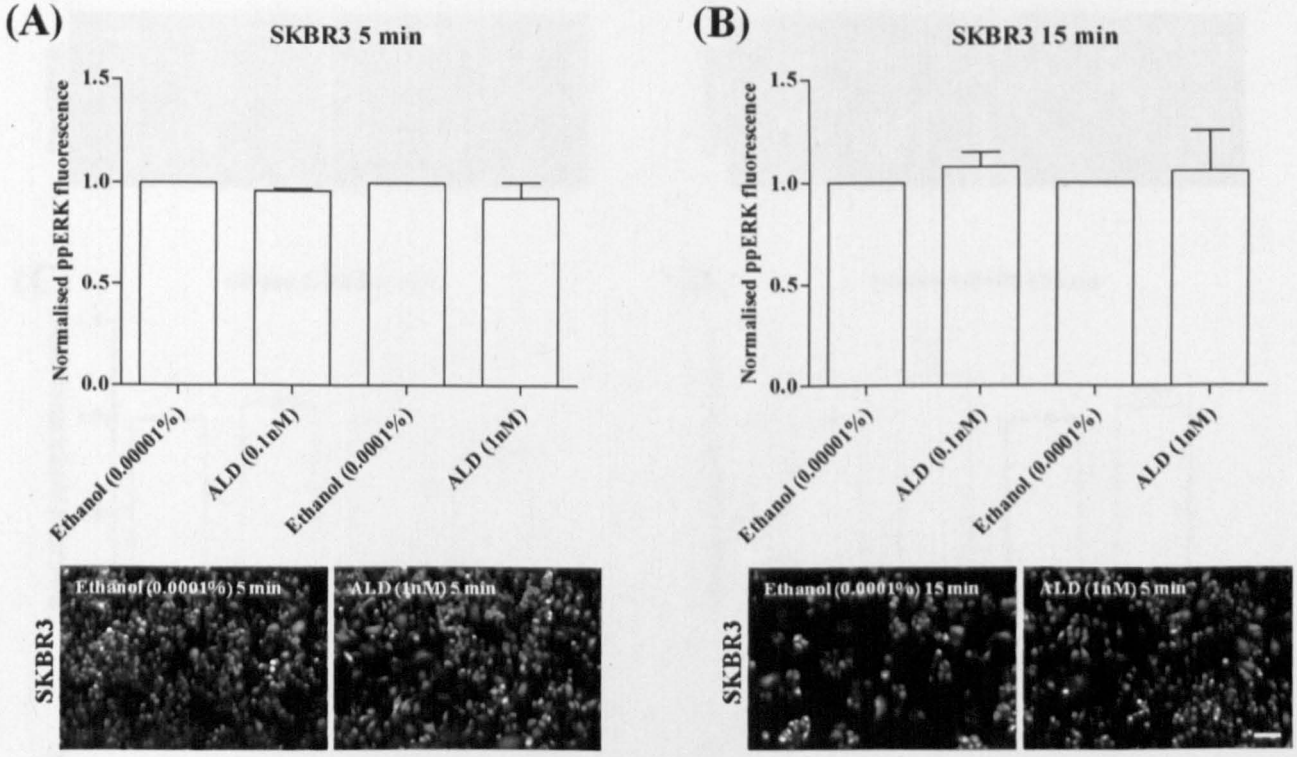

Figure 4.27. ALD does not stimulate ERK activation in SKBR3 cells.

0.1nM and 1nM ALD treatment for 5 (A) or 15 min (B) did not activate ERK phosphorylation in SKBR3 cells. The data shown are normalised to vehicle and graphs are representative of at least one field, from triplicate wells and two separate experiments (mean ± SEM). Statistical analysis was performed using a one-way ANOVA and the Bonferroni multiple comparison test. Below each graph are some representative images of cells treated with ethanol control or ALD and stained with anti-ppERK antibodies. Scale bar, 100μm.

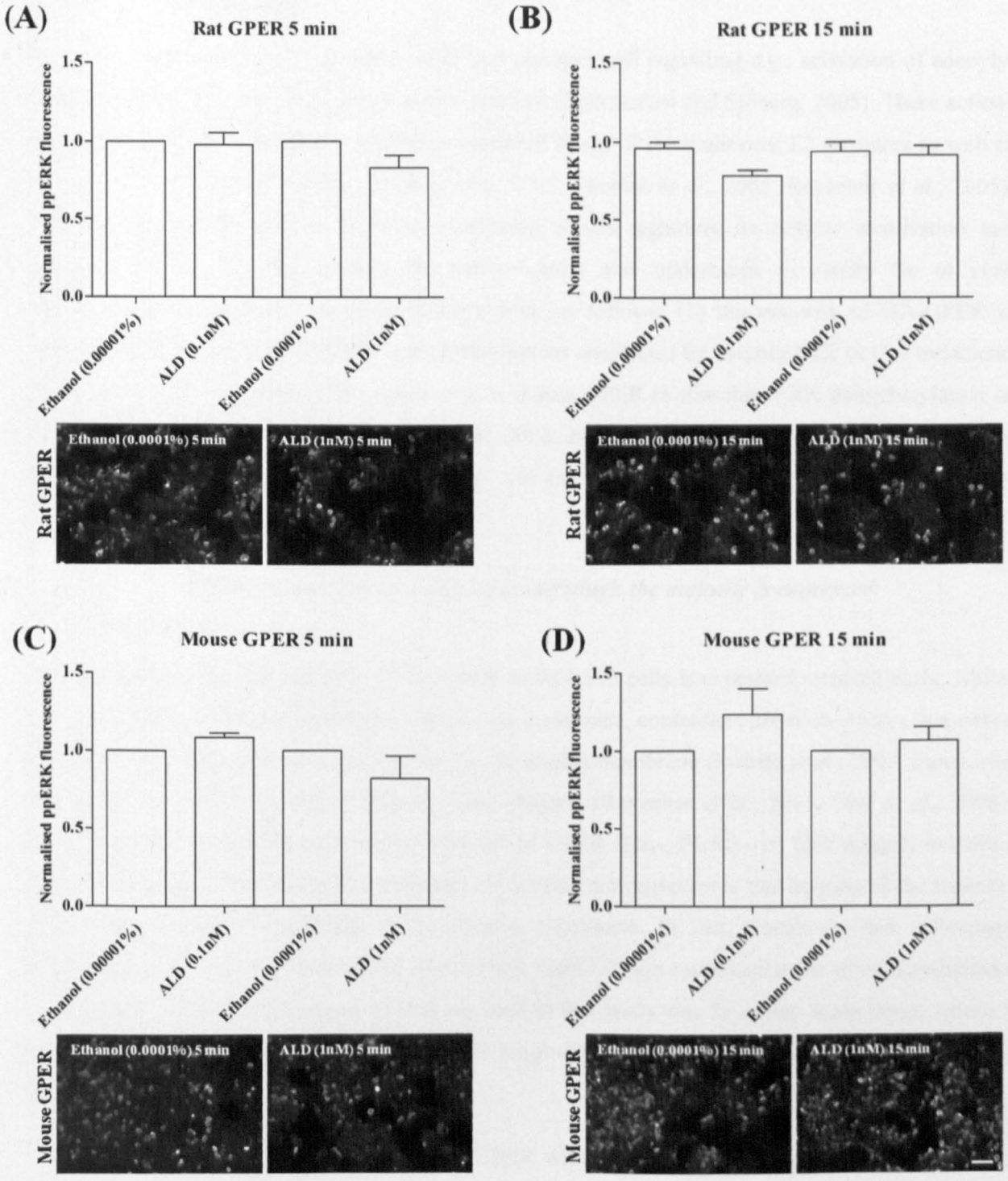

Figure 4.28. ALD does not stimulate ERK phosphorylation in HEK293 cells stably transfected with rodent GPER.

ppERK fluorescence did not alter in HEK293 cells stably transfected with rat or mouse GPER following treatment with 100nM ALD for 5 (A and C, respectively) or 15 min (B and D, respectively). The data shown are normalised to vehicle and graphs are representative of at least one field, from triplicate wells and two separate experiments (mean ± SEM). Statistical analysis was performed using a one-way ANOVA and the Bonferroni multiple comparison test. Below each graph are some representative images of cells treated with ethanol control or ALD and stained with anti-ppERK antibodies. Scale bar, 100μm.

4.4 Discussion

It is well established that E2 provokes rapid non-genomic cell signalling e.g., activation of adenylyl cyclase/cAMP, ERK, and P13K transduction cascades (Björnström and Sjöberg, 2005). These actions are thought to be attributable to membrane associated forms of the traditional E2 receptors as well as the recently identified E2-GPCR, GPER (Levin, 2005; Thomas *et al.*, 2005; Revankar *et al.*, 2005). However, the GPER field is rife with conflicting results regarding its cellular localisation and activation by E2. For this reason, the current study was undertaken to clarify the *in vitro* characterisation of GPER. Our main findings were as follows: (1) the majority of HA-GPER is expressed intracellularly in HEK293 cells, a distribution unaffected by overnight E2 or G-1 treatment; (2) E2 and G-1 do not activate the human, rat, or mouse GPER to stimulate ERK phosphorylation or mobilise intracellular calcium; (3) the mouse GPER is not activated by an E2 sulphotransferase metabolite to stimulate ERK phosphorylation; and (4) the human, rat and mouse GPER are not activated by ALD.

4.4.1 GPER is located at the cell surface although the majority is expressed intracellularly

Our observations that the majority of HA-GPER in HEK293 cells is expressed intracellularly, whilst only approximately 24% is localised to the plasma membrane, contradicts previous studies that either report that the majority of GPER is localised to the plasma membrane (Filardo *et al.*, 2007; Funakoshi *et al.*, 2006) or GPER is solely expressed intracellularly (Revenkar *et al.*, 2005; Otto *et al.*, 2008). Many of the earlier studies used a tagged variant of GPER (HA-, FLAG-, or GFP-tagged) to define cellular localisation. Therefore, one explanation for these discrepancies is that tagging of the receptor could restrict receptor trafficking to the plasma membrane. In fact, Funakoshi and colleagues demonstrated that the rat GPER and another GPCR, GPR175, are expressed at the plasma membrane of HeLa cells when FLAG-tagged (FLAG tag used in this study was 24 amino acids long), whereas their GFP-tagged (GFP tag is 238 amino acids long) counterparts are restricted to the endoplasmic reticulum (Funakoshi *et al.*, 2006).

In the current study, we decided to combine GPER with a small HA-tag (9 amino acids in length) immediately following the initiating methionine that has been shown to have no influence on receptor functionality (Innamorati *et al.*, 1996, 1998; Sedgley *et al.*, 2006; Finch *et al.*, 2008). Filardo and colleagues also stably transfected a HA-GPER construct into HEK293 cells and found predominant HA-GPER expression at the plasma membrane, in contrast to the distribution pattern to that of the current study (Filardo *et al.*, 2007). These investigators employed a biased selection method to select their stable HEK293 lines - they used fluorescence-activated cell sorting (with anti-HA fluorescence staining) to isolate cells that highly express HA-GPER at the cell surface, and only used these cells in

subsequent experiments (Filardo *et al.*, 2007). Our clone selection procedure was based on antibiotic resistance and GPER transcript expression, and perhaps provides a more accurate reflection of the endogenous localisation of HA-GPER in HEK293 cells. The stable cell lines used in this study were those assessed to have the highest transcript expression (see section 4.3.1), and this was stable over the number of passages used in this study. It is worth noting there was extreme variation in GPER or E2 sulphotransferase mRNA expression between separate colonies (in the 96 well plates see section 2.5.4) even though all the cells were resistant to G418 and/or Hygro. This variable expression may be due to the random integration of the GPER or E2 sulphotransferase constructs into different sites in the host genome.

We have not endeavoured to identify the intracellular structures in which GPER is found (e.g., using subcellular markers), but a previous study demonstrated that non-tagged GPER localises to the endoplasmic reticulum in transiently transfected HEK293 cells using anti-GPER antibodies (Otto *et al.*, 2008). Similarly, Revenkar *et al.*, investigated GPER cellular localisation with N- or C-terminal directed antibodies and detected intracellular expression of endogenous GPER in the endoplasmic reticulum and Golgi apparatus of SKBR3, MCF-7 and MDA-MB231 cells, and transiently expressed GPER in COS-7 cells - with no evidence of GPER at the plasma membrane (Revankar *et al.*, 2005). The proportion of GPER at the plasma membranes verses intracellular structures may highlight that GPER cellular localisation is cell type-dependant and equally it could reflect differences in techniques used. Filardo and colleagues investigated the localisation of endogenous GPER in SKBR3 cells by western blot analysis which revealed GPER in preparations enriched in either the plasma membrane or endoplasmic reticulum compartments, while a tritiated E2 binding assay only unmasked E2 binding sites at the plasma membrane (Filardo *et al.*, 2007). In addition, the plasma membrane form of GPER may differ from that found at the endoplasmic reticulum or golgi apparatus. It is well known that the degree of post-translational modification e.g., glycosylation, palmitoylation, or formation of oligomeric complexes can influence GPCR destination (Tan *et al.*, 2004; Chini and Parenti, 2009; Wheatley and Hawtin, 1999).

Cellular GPER localisation may also be influenced by media-borne oestrogenic compounds that could affect the trafficking of the receptor. Therefore, we investigated whether or not overnight incubation in serum- and phenol-free media with or without E2 or G-1 had any effect on GPER surface expression. Neither E2 nor G-1 had any significant effect on HA-GPER distribution at the time point (24 hour) examined. This is unexpected considering the cellular localisation of a GPCR is often significantly altered following agonist treatment, generally leading to receptor desensitisation and/or degradation (Gainetdinov *et al.*, 2004), but additional time-course and dose-response studies in a variety of cell types are necessary understand GPER turnover following exposure to agonist(s).

In this chapter, we did not attempt to determine whether GPER signals from the plasma membrane or from inside the cell (since we were unable to identify a viable ligand). As mentioned in the introduction, Filardo and colleagues report that cell impermeable E2-conjugates (e.g., E2-BSA and E2-horseradish peroxidase) are able to activate GPER (Filardo *et al.*, 2007); while Prossnitz and co-workers demonstrated that only membrane permeable fluorescent E2 or radioactive G-1 derivatives (e.g., 17α-Phenylethynyl-E2 and indium-labelled G-1 analogues) are able to stimulate GPER (Revenkar *et al.*, 2007; Nayak *et al.*, 2010). It is possible that GPER can signal from a number of cellular compartments, as shown for other GPCRs (Boivin *et al.*, 2008; Calebiro *et al.*, 2010; Re *et al.*, 2010). However, it should be noted that the use of E2-conjugates such as E2-BSA to prove cell surface E2-activation has been queried. Stevis and colleagues demonstrated not only that free E2 can leach from E2-BSA compounds which may infuse inside the cell, but E2-BSA also has biological activity that is not mimicked by E2 (Stevis *et al.*, 1999). Equally, studying whole cell receptor binding with labelled-lipophillic compounds such as steroids can be misleading. Labelled-lipophillic compounds can rapidly infuse into intracellular organelles and may not be removed with washing (as the compound is trapped within the organelle) or not be displaced with excess non-labelled ligand (Thomas *et al.*, 2010).

4.4.2 E2 and G-1 do not simulate ERK phosphorylation or calcium mobilisation via the human or rodent GPER

In agreement with several other studies, we were unable to demonstrate E2/G-1 mediated-ERK activation or calcium mobilisation in cells stably transfected with rodent GPER, or transiently transfected with rodent GPER (Pedram *et al.*, 2006; Otto *et al.*, 2008). We speculated that there may be species differences in the ability of E2 to activate GPER (section 4.3.4) and that rodent GPERs may not bind E2/G-1. Sequence alignment of human, rat and mouse GPER (in Figure 4.29) reveals that the human GPER and the rodent GPER are highly homologous from the first transmembrane domain onwards (amino acids 63-375), but differ substantially in the first extracellular domain (amino acids 1-62). This may provide one explanation as to why E2 and G-1 do not activate the rodent receptor, as the first extracellular domain corresponds to the amino-terminus which may be involved in ligand binding (Kristiansen, 2004). Therefore, E2 and G-1 may bind to the human, but not the rodent GPER, as a result of a different ligand binding domain.

```
MDVTSQARGVGLEMYPGTAQPAAPNTTSPELNLSHPLLGTALANGTGELSEHQQYVIGLF 60 GPER_HUMAN
MAATTPAQDVGVEIYLGPVWPAPSNSTPLALNLSLALREDAPGNLTGDLSEHQQYVIALF 60 GPER_RAT
MDATTPAQTVGVEIYLGPVWPAPSNSTPLALNLSLALREDAPGNLTGDLSEHQQYVIALF 60 GPER_MOUSE
* .*: *: **:*:* *.. **..*:*.  **** .*   * .* **:*********.**
LSCLYTIFLFPIGFVGNILILVVNISFREKMTIPDLYFINLAVADLILVADSLIEVFNLH 120 GPER_HUMAN
LSCLYTIFLFPIGFVGNILILVVNISFREKMTIPDLYFINLAAADLILVADSLIEVFNLD 120 GPER_RAT
LSCLYTIFLFPIGFVGNILILVVNISFREKMTIPDLYFINLAAADLILVADSLIEVFNLD 120 GPER_MOUSE
****************************************.***************.
ERYYDIAVLCTFMSLFLQVNMYSSVFFLTWMSFDRYIALARAMRCSLFRTKHHARLSCGL 180 GPER_HUMAN
EQYYDIAVLCTFMSLFLQINMYSSVFFLTWMSFDRYLALAKAMRCGLFRTKHHARLSCGL 180 GPER_RAT
EQYYDIAVLCTFMSLFLQINMYSSVFFLTWMSFDRYLALAKAMRCGLFRTKHHARLSCGL 180 GPER_MOUSE
*:****************:****************:***:****.**************
IWMASVSATLVPFTAVHLQHTDEACFCFADVREVQWLEVTLGFIVPFAIIGLCYSLIVRV 240 GPER_HUMAN
IWMASVSATLVPFTAVHLRHTEEACFCFADVREVQWLEVTLGFIVPFAIIGLCYSLIVRA 240 GPER_RAT
IWMASVSATLVPFTAVHLRHTEEACFCFADVREVQWLEVTLGFIMPFAIIGLCYSLIVRA 240 GPER_MOUSE
******************:**:**********************:**************.
LVRAHRHRGLRPRRQKALRMILAVVLVFFVCWLPENVFISVHLLQRTQPGAAPCKQSFRH 300 GPER_HUMAN
LIRAHRHRGLRPRRQKALRMIFAVVLVFFICWLPENVFISVHLLQWAQPGDTPCKQSFRH 300 GPER_RAT
LIRAHRHRGLRPRRQKALRMIFAVVLVFFICWLPENVFISVHLLQWTQPGDTPCKQSFRH 300 GPER_MOUSE
*:******************:*******:*************** :*** :********
AHPLTGHIVNLAAFSNSCLNPLIYSFLGETFRDKLRLYIEQKTNLPALNRFCHAALKAVI 360 GPER_HUMAN
AYPLTGHIVNLAAFSNSCLSPLIYSFLGETFRDKLRLYVAQKTSLPALNRFCHATLKAVI 360 GPER_RAT
AYPLTGHIVNLAAISNSCLNPLIYSFLGETFRDKLRLYVEQKTSLPALNRFCHATLKAVI 360 GPER_MOUSE
*:***********:*****.******************: ***.**********:*****
PDSTEQSDVRFSSAV 375 GPER_HUMAN
PDSTEQSDVKFSSAV 375 GPER_RAT
PDSTEQSEVRFSSAV 375 GPER_MOUSE
*******:*:*****
```

Figure 4.29. Sequence alignment of human, rat and mouse GPER

Alignment of the human GPER (top line), rat GPER (middle line) and mouse GPER (bottom line) receptor sequences, generated with the aid of the web-based uniprot sequence alignment tool (http://www.uniprot.org/uniprot/). To signify exact residue matches across all three receptors, amino acids are highlighted in dark green and are represented by an asterisk on line 4 (*). Light green denotes amino acid alignment between the rat and mouse GPER only, although amino acids within the human GPER sequence that are akin to rat/mouse are indicated on the fourth line with a semi colon (conserved substitution) or a full stop (semi-conserved substitution). All three receptors have similar amino acid sequences (particular the rat and mouse receptors), apart from the 1st extracellular domain (amino acids 1-62), where the human sequence noticeably differs from that of the rodent. In addition, the last 18 amino acids of the human receptor are underlined as the GPER antibody (used in Chapter 3) was directed towards those residues (Revankar *et al.*, 2005). There is reasonably high sequence homology between human and rodent in these last 18 amino acids, apart from two conserved substitutions in the rat and mouse sequences at residues 368 and 370.

However we could not demonstrate activation of human GPER, whether endogenously expressed or introduced by transfection, in our signal transduction assays. Our results for both rodent and human GPER is in disagreement with a large body of evidence that suggests that E2/G-1 activation of GPER stimulates ERK and calcium signalling as well as many other pathways *in vitro* e.g., the PI3K, cAMP, and RhoA/Rho-kinase signalling cascades (Maggiolini *et al.*, 2004; Revankar *et al.*, 2005; Thomas *et al.*, 2005; Filardo *et al.*, 2007; Chavalmane *et al.*, 2010). It is difficult to reconcile all of the studies surrounding GPER's role as an E2/G-1 receptor.

The unresponsiveness of SKBR3 cells to E2/G-1 is even more baffling considering they were obtained from the Prossnitz group – one of the first laboratories to report E2/GPER signalling in

SKBR3 cells, and those responsible for the identification/synthesis of G-1 and G-15 (Revenkar *et al.*, 2005; Bologa *et al.*, 2006; Dennis *et al.*, 2009). Indeed it is possible (however unlikely) that the E2 responsiveness of the cells may have been reduced during transit (from New Mexico → UK), that we were sent an unresponsive subclone, or even subtle differences in culturing (although every care was taken to ensure that the SKBR3 cells were appropriately maintained – they were cultured in DMEM and DMEM/F12 as recommended). One caveat pertaining to our studies on SKBR3 cells is that we did not measure endogenous GPER expression. However, transfection of human GPER cDNA (also obtained from the Prossnitz group) into COS-7 and HeLa cells did not facilitate E2/G-1 mediated signalling, which has previously been demonstrated in these cells (Revenkar *et al.*, 2005). Together this suggests that in our hands the human GPER is not activated by E2 and G-1.

One possible explanation for the discrepancies surrounding E2/G-1 activation of GPER may be that studies investigating the effects of GPER on cell signalling do not always employ appropriate vehicle controls. For example, Vivacqua and coworkers used 1μM E2 dissolved in ethanol to stimulate GPER in ERK and c-Fos assays, but only used untreated cells as their controls (Vivacqua *et al.*, 2006b). There are other examples of studies that are devoid of vehicle controls and instead use untreated cells or cells transfected with empty vector as controls, or do not mention controls at all (Filardo *et al.*, 2000; Maggiolini *et al.*, 2004; Revenkar *et al.*, 2005; Brailoiu *et al.*, 2007). While in some instances untreated cells and cells transfected with empty vector can be valid controls, in cell stimulation assays vehicle controls must be used - even if it means applying water (e.g., for comparison with WS-E2) to account for possible mechanical/osmotic stimulation (this is of particular importance when applying a ligand for a short time period). As highlighted in the results section 4.3.4, vehicle controls are essential when dealing with organic solvents such as ethanol and DMSO that are known to have effects on ERK signalling (Reddy and Shukla, 2000; Koo and Kim, 2009). For example, Otto and colleagues observed the same time-dependant induction of ERK phosphorylation in transiently transfected COS-7 cells after vehicle (e.g., 0.0001% DMSO) and E2 application - independent of the presence or absence of GPER (Otto *et al.*, 2008).

As indicated above, some studies have used 1μM E2 to stimulate GPER (e.g., Vivacqua *et al.*, 2006b; Maggiolini *et al.*, 2004). This is disconcerting considering that in the current study we observed non-specific E2-mediated ERK phosphorylation in untransfected HEK293 cells, following treatment with 1μM E2. It is proposed that high concentrations of steroids may have physicochemical interactions with phospholipid membranes e.g., high doses of E2 and tamoxifen (μM) reduce membrane fluidity in MCF7 and MDA-MB-4306 cells, while high levels of progesterone (μM) decreases the fluidity of human and hamster spermatozoa membranes, and also induces aggregation and/or fusion of membrane vesicles (Clarke *et al.*, 1990; Shivaji and Jagannadham, 1992). Likewise, high doses of glucocorticoids can inhibit calcium and sodium cycling across the plasma membrane and reduce ATP

availability in lymphocyte cells (by inhibiting the reactions of substrate oxidation and by increasing the leakage of protons across the mitochondrial inner membrane) (Buttgereit and Scheffold, 2002). Thus, high concentrations of steroids can non-specifically interact with phospholipid membranes which may impact on down-stream signalling cascade such as the ERK pathway.

In the majority of our cell assays we used E2 and G-1 at concentrations between 1nM-100nM in an attempt to elicit a GPER response. While these are a high concentrations with respect to circulating levels of E2 (in women [E2] ranges from 146.8–215.1pM in the follicular phase to 734–1570.8pM in the pre-ovulatory peak; in men [E2] ranges from 0.9–157.1 pM), it can be assumed that at the tissue level the concentration of E2 may be much higher, particularly as E2 can be synthesised locally by aromatase activity (Cornil *et al.*, 2006). However, the purpose of this study was not to mimic physiological E2 concentrations, but to verify that GPER is indeed an E2 receptor - therefore we used ligands at concentrations that are pharmacologically relevant. Prossnitz and colleagues have previously described that E2 stimulation of GPER activates calcium mobilisation with a half-maximal effector concentration (EC50) of approximately 0.5nM, with maximal stimulation observed at 100nM (Revenkar *et al.*, 2005). Similarly, the same group report that G-1 also activates calcium mobilisation with an EC50 of approximately 2nM, with a maximal response between 100-500nM (Bologa *et al.*, 2006). Hence 100nM of E2 and G-1 are not only pharmacologically relevant concentrations, but have the potential to illicit maximal GPER mediated-responses.

Another reason for the lack of an E2/G-1/GPER stimulated ERK response in these cells may be that the time points were insufficient to observe response. However, many studies have observed a human GPER-mediated increase in ppERK in response within a 5-15 min course of E2 treatment (Filardo *et al.*, 2000, 2002; Maggiolini *et al.*, 2004). The experimental controls used within this study also confirm that the HEK293 cells are able to elicit an ERK response - EGF and PDBu stimulated ERK phosphorylation in all of the HEK293 cell lines. Indeed, activation by EGF suggests that these HEK293 cells endogenously express the EGFR, which is 1) in agreement with the northern 'dot blot' analysis which illustrates high levels of EGFR mRNA is expressed by HEK293 cells; and 2) implies that E2/G-1 via GPER could transactive this receptor to stimulate the ERK pathway. In addition, PDBu stimulation of ERK suggests that the ERK pathway is functional downstream of the EGFR receptor (Figure 6.1 illustrates how PKC feeds into the ERK pathway). Together, this indicates that ERK signalling is not compromised in these HEK293 cells.

It has been reported that treatment with serum/phenol-free media downregulates GPER transcript expression in HeLa cells, and human endometrial HEC-1-A, KLE and RL-95-2 cells (Leblanc *et al.*, 2007). In the current study, cells were serum starved over night prior to ERK phosphorylation and calcium stimulation assays, to remove the influence from media borne-oestrogenic compounds, and

also reduce baseline ppERK in the ERK stimulation assay (the latter is a standard procedure and is performed for all cell types in this assay) (Caunt *et al.*, 2008). As previously described, the absence of serum overnight had no significant influence on HA-GPER expression in HEK293 cells when compared with media treated controls. This indicates that the receptor was available for activation by E2/G-1 during the ERK and calcium assays. Moreover, many other studies have demonstrated E2/G-1 mediated GPER signalling following overnight/48 hour serum starving (e.g., Filardo *et al.*, 2002; Revenkar *et al.*, 2005; Bologa *et al.*, 2006).

4.4.3 Alternative roles for GPER in steroid signalling

There may be a number of technical/experimental differences that could be attributed to the variation in GPER signalling. However, one assumes that if GPER is activated by E2/G-1 to give ERK and/or calcium responses, we would have observed it in this study, especially since we were able to demonstrate robust VP activation of the V_{1B} receptor, and other endogenous GPCRs, in both signalling assays. It is possible that there is something pivotal to GPER signalling missing from our cells lines. For example, Otto and co-workers report a lack of E2/G-1/GPER activation of ERK phosphorylation in CHO cells. As GPER appears to stimulate the ERK pathway via EGFR transactivation, the lack of signalling may be explained by the fact that EGFR is non-responsive in our CHO-K1 cells. A 'missing' component could be particularly difficult to identify in the other cell types (e.g., HEK293, COS-7, and HeLa) used in our studies, especially since the EGFR- and GPCR-mediated ERK- and calcium-responses appear generally to be intact. If a signal transduction component essential to GPCR signalling was absent it may be something extremely subtle such as some link between GPER receptor agonist binding and EGFR transactivation.

Convergence of ERα and GPER signalling?

In the last few years, a link between ERα and GPER mediated signalling has been reported. In human ovarian cancer and mouse spermatogonial cells, both ERα and GPER are required for an E2 and G-1-induced increase in ERK signalling and c-Fos accumulation (Albanito *et al.*, 2007; Sirianni *et al.*, 2008). As highlighted in Figure 4.30, it has been proposed that GPER collaborates with ERα, transforming early signals from membrane forms of ERα into downstream signalling cascades (Levin, 2009). Therefore, it could be possible that the lack of ERα mRNA (as determined with northern 'dot' blot hybridisation see section 4.3.1) from our HEK293 and COS-7 cells may hinder E2/GPER signalling. However, we observed no E2/G-1 response in Ishikawa cells that are reported to express ERα. It is known that after long-term culture Ishikawa cells can transform into undifferentiated cells, and lose their E2 responsiveness – suggesting that our cell line may no longer express ERα (Nishida *et al.*, 2002). Nonetheless, E2- and/or G-1-mediated GPER activation has been demonstrated in

several lines that are reported to lack the traditional receptors including HEK293, COS-7 and SKBR3 cells (Filardo *et al.*, 2000; Revenkar *et al.*, 2005; Bologa *et al.*, 2006).

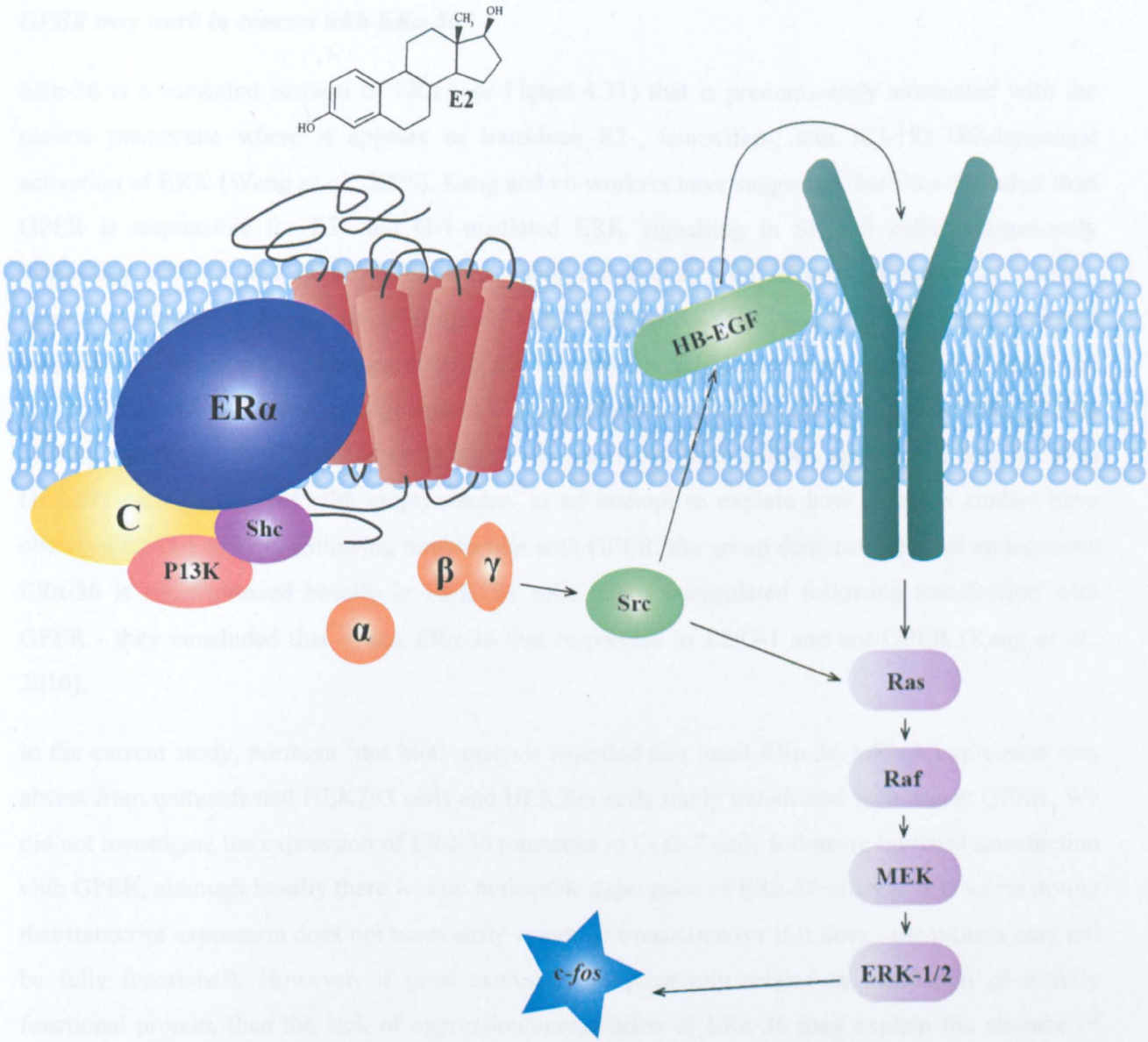

Figure 4.30. GPER may act as an ERα collaborator.

Both ERα and GPER are required for E2- and G-1 stimulation of ERK phosphorylation and c-Fos activation in ovarian cancer and mouse spermatogonial cells (Albanito *et al.*, 2007; Sirianni *et al.*, 2008). Membrane bound ERα is associated with large protein complexes (signalsome) often consisting of scaffold proteins (e.g., caveolin-1 (C)), linker proteins (e.g., Shc), G protein subunits, receptor and non-receptor tyrosine kinases (e.g. EGFR and Src, respectively), and serine/threonine kinases (e.g., p85 subunit of P13K) (Levin *et al.*, 2009). In some cell types it is possible that GPER may also be part of the large signalsome, enabling crosstalk between the two E2 receptors (Levin *et al.*, 2009).

GPER may work in concert with ERα-36?

ERα-36 is a truncated isoform of ERα (see Figure 4.31) that is predominately associated with the plasma membrane where it appears to transduce E2-, tamoxifen-, and ICI-182,780-dependant activation of ERK (Wang *et al.*, 2006). Kang and co-workers have suggested that ERα-36 rather than GPER is responsible for E2- and G-1-mediated ERK signalling in SKBR3 cells endogenously expressing ERα-36 and in HEK293 cells stably transfected with ERα-36 (Kang *et al.*, 2010). Saturation analysis and Scatchard plotting of [^{3}H]E2 binding to SKBR3 and HEK293 cells transfected with ERα-36 showed the presence of high affinity specific E2-binding sites in both cell lines, and competitive binding assays showed that G-1 is an effective competitor of E2. Furthermore, [^{3}H]E2 binding was dramatically reduced in SKBR3 cells transfected with shRNA specific for ERα36, or in HEK293 cells transfected with empty vector. In an attempt to explain how previous studies have observed E2/G-1 activity following transfection with GPER, the group demonstrated that endogenous ERα-36 is not expressed basally in HEK293 cells but is upregulated following transfection with GPER - they concluded that it was ERα-36 that responded to E2/G-1 and not GPER (Kang *et al.*, 2010).

In the current study, northern 'dot blot' analysis revealed that basal ERα-36 mRNA expression was absent from untransfected HEK293 cells and HEK293 cells stably transfected with rodent GPER. We did not investigate the expression of ERα-36 transcript in COS-7 cells following transient transfection with GPER, although basally there was no noticeable expression of ERα-36 mRNA. It is worth noting that transcript expression does not necessarily equate to translation (or if it does - the protein may not be fully functional). However, if gene expression is positively related to translation of a fully functional protein, then the lack of expression/upregulation of ERα-36 may explain the absence of E2/G-1-mediated signalling in the cell lines investigated in our studies. It is unclear why ERα-36 mRNA was not detected in HEK293 cells stably expressing GPER. One possibility is that our HEK293 cell subclone does not express ERα-36 under any circumstances. Kang and colleagues reported that transient transfection of HEK293 cells with GPER resulted in a 3-fold induction of ERα36 promoter activity via a Src/ERK1/2/AP-1 pathway (Kang *et al.*, 2010). The mechanism of the GPER-mediated upregulation in ERα36 promoter activity was not investigated. It is possible that the upregulation of ERα36 is a result of constitutive GPER activity. Alternatively, a media-borne agonist (such as E2 or another unidentified compound) may activate the GPER-mediated upregulation in ERα36. Therefore, if the media used in this study lacks a media-borne agonist, it may explain why, in our hands, ERα is not upregulated by HEK293 cells stably expressing GPER.

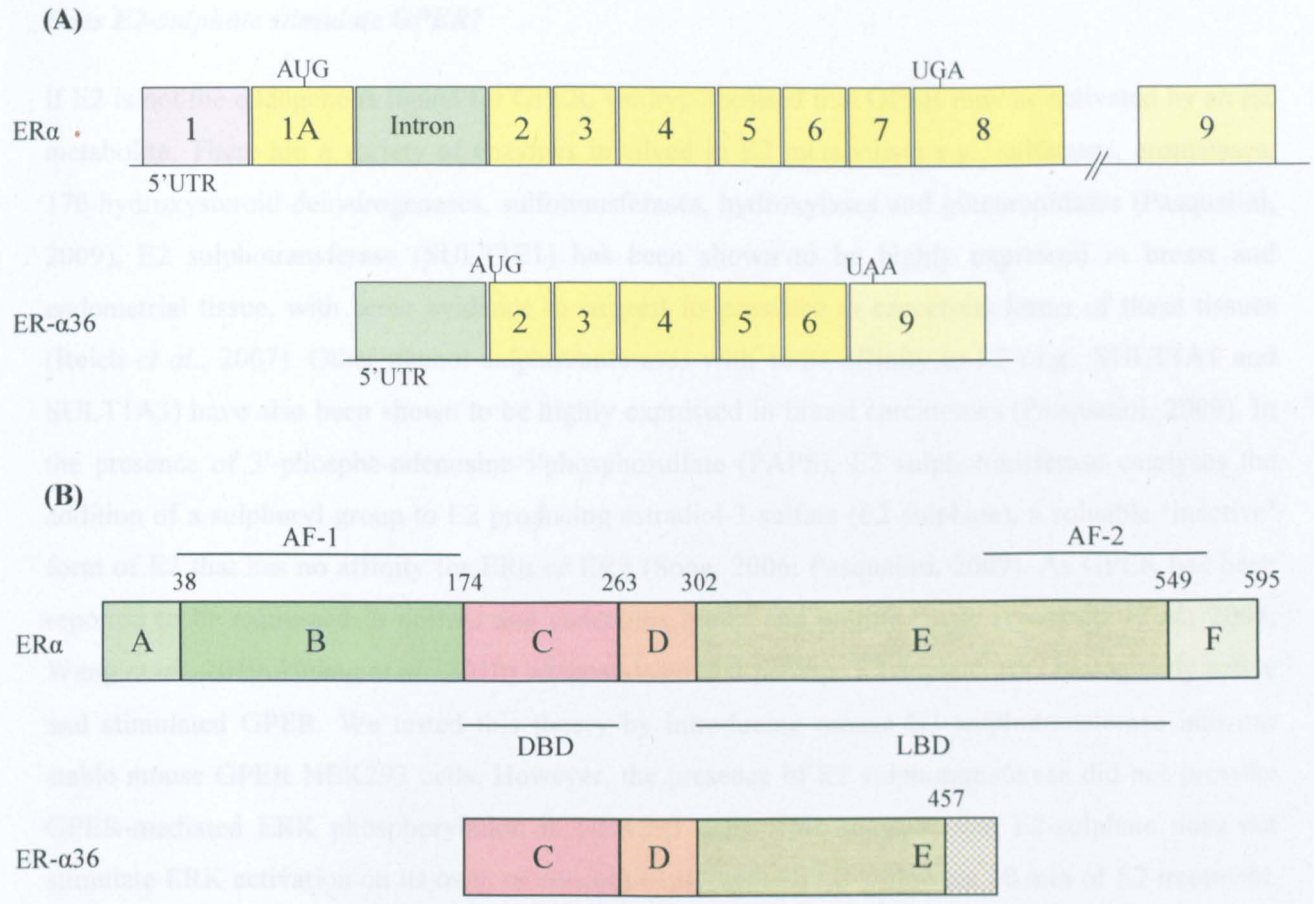

Figure 4.31. Schematic diagrams representing the structural organisation of ERα and ERα-36 mRNA and protein.

(A) Transcriptional organisation of human ERα and its splice variant ERα-36. ERα mRNA is coded by 8 exons, while ERα-36 transcript is coded by 1 intron and 5 exons from the ERα gene and one exon downstream of the ERα coding sequence. Start (AUG) and stop codons (UGA or UAA) are indicated. The 5'-untranslated region of ERα-36 is identical with the first intron (green box) of the ERα gene, and the initiation codon for the predicted ERα-36 protein is located in the second exon of the ERα genomic sequence. ERα and ERα-36 transcript share 100% homology between exons 2-6 (yellow boxes) of the ERα DNA sequence, but the remaining ERα-36 mRNA sequence is transcribed from an exon located 4374bp downstream of the ERα gene (here termed exon 9 (light yellow box)), and is distinct from the latter part of the ERα gene sequence. For this reason, the ERα-36 oligonucleotides used in the northern blot hybridisation in section 4.2.3 were directed to the mRNA sequence from exon 9.

(B) Domain structures of ERα and ERα-36. ERα is assembled from 595 amino acids (amino acid sequence numbers are shown) and has a molecular mass of 66kDa while the ER-α36 variant is 310 amino acids long and is 36 kDa in mass. ERα and ERα-36 share the same predicted protein sequence in domain C (contains the DNA binding domain (DBD)), domain D (hinge region) and a portion of domain E (contains the ligand binding domain (LBD)), although ERα-36 lacks the ERα domains A, B, F and part of E which also contain the activation function domains (AF-1 (ligand-independent activation function) and AF-2 (ligand-dependent transactivation function)). ERα-36 has a unique 27 amino acid domain (represented with a chequered box) instead of the last 138 amino acids of ERα (corresponding to domain E (part of) and F (encoded by exon 7 and 8 of the ERα gene)). Transcript and protein structure of ERα-36 is based on the description by Wang and colleagues (Wang *et al.*, 2005).

Does E2-sulphate stimulate GPER?

If E2 is not the endogenous ligand for GPER, we hypothesised that GPER may be activated by an E2 metabolite. There are a variety of enzymes involved in E2 metabolism e.g., sulfatases, aromatases, 17ß-hydroxysteroid dehydrogenases, sulfotransferases, hydroxylases and glucuronidases (Pasqualini, 2009). E2 sulphotransferase (SULT1E1) has been shown to be highly expressed in breast and endometrial tissue, with some evidence to suggest its presence in cancerous forms of these tissues (Reich *et al.*, 2007). Other phenol sulphotranferases with some affinity to E2 (e.g., SULT1A1 and SULT1A3) have also been shown to be highly expressed in breast carcinomas (Pasqualini, 2009). In the presence of 3'-phospho-adenosine-5'phosphosulfate (PAPS), E2 sulphotransferase catalyses the addition of a sulphuryl group to E2 producing estradiol-3-sulfate (E2-sulphate), a soluable 'inactive' form of E2 that has no affinity for ERα or ERβ (Song, 2006; Pasqualini, 2009). As GPER has been reported to be expressed in normal and cancerous breast and uterine tissue (Prossnitz *et al.*, 2008; Wang *et al.*, 2010; Huang *et al.*, 2010) we postulated that perhaps E2-suphate was biologically active and stimulated GPER. We tested this theory by introducing mouse E2 sulphotransferase into our stable mouse GPER HEK293 cells. However, the presence of E2 sulphotransferase did not provoke GPER-mediated ERK phosphorylation in HEK293 cells. This suggests that E2-sulphate does not stimulate ERK activation on its own, or concomitantly with GPER following 10 min of E2 treatment. It must be emphasised that we do not know whether our E2 sulphotransferase DNA construct directed expression of a functional protein.

Does ALD signal via GPER?

Finally, we investigated the role of GPER in ALD signalling. Gros and colleagues recently reported that ALD exploits both MR and GPER to activate ERK phosphorylation in freshly isolated rat aortic segments (Gros *et al.*, 2011). They also reported that ALD acts solely through GPER to stimulate ERK phosphorylation (blocked with the GPER antagonist, G-15) in rat aortic vascular endothelial cells that lack MR, but endogenously express GPER (and ERα) (Gros *et al.*, 2011). However, we observed no increase in ppERK in response to ALD in COS-7 or HeLa cells transiently transfected with human or rodent GPER. Northern 'dot blot' analysis illustrated that COS-7 and HeLa cells express very little or no endogenous MR, ERα, and ERβ mRNA (see Chapter 6 (section 6.3.1) for details of MR northern 'dot blot' results). Thus, if GPER requires an additional ALD/E2 steroid receptor to facilitate ALD-stimulated ERK phosphorylation in COS-7 cells, the lack in these receptors may explain an absence of signalling.

4.4.4 Conclusion

In summary, our *in vitro* experiments reveal that GPER is both a cell surface and intracellular protein and is not activated by E2 or G-1. One cannot rule out the possibility that E2 and G-1 bind and

activate GPER in other laboratories (e.g., other cell lines may be more responsive to E2/G-1/GPER mediated signalling) particularly when there is such a large body of published evidence (mainly on human cells), suggesting this ligand-receptor interaction takes place. However, the reasons for these inconstancies are not apparent at this time, and thus we would be reluctant to pursue the GPER story any further, especially *in vivo*.

Chapter 5: Distribution of orphan G protein-coupled receptors

5.1 Introduction

5.1.1 Glucocorticoids

As for E2 responses, 'fast', apparently cell surface mediated effects of adrenal steroids have been documented. Glucocorticoids (cortisol and corticosterone (CORT) in human and rats, respectively) are mainly secreted from the zona fasiculata of the adrenal cortex in pulsatile bursts, that under basal conditions are subject to ultradian and circadian rhythms (Lightman and Conway-Campbell, 2010). In response to psychological and physical stressors the pulses increase in amplitude (and/or frequency over a 24 hour period) (Sarabdjitsingh *et al.*, 2010; Windle *et al.*, 2001; Lightman and Conway-Campbell, 2010). Glucocorticoids are crucial for homeostasis and the adaptation to acute (e.g., 'flight and fight' response) and chronic stress (e.g., infection, fasting or cancer), and as a consequence have an array of effects on central and peripheral systems. For example, in response to acute stress, glucocorticoids mobilise energy and protein stores (by elevating blood glucose and increasing muscle catabolism), increase blood pressure and cardiac output, reduce inflammation and dampen the (potentially over-active) immune system (Rose *et al.*, 2010; Vegiopoulos and Herzig, 2007; Sapolsky *et al.*, 2000). In addition, acute and chronic exposure to glucocorticoids modulates appetite, memory consolidation and retrieval, and reproduction (Adam and Epsel, 1997; Roozendaal, 2002; Maeda and Tsukamura, 2006).

Much of the effects of glucocorticoids are attributable to the activation of two conventional nuclear steroid receptors, the glucocorticoid receptor (GR) and the mineralocorticoid receptor (MR). As with all steroid receptors, activation of GR and MR leads to direct regulation of gene transcription and subsequent effects are usually observed after 30 min (although transcription and translation of a target gene can occur within 15 min) (Haller *et al.*, 2008). Furthermore, fast non-genomic effects (generally less than 15 min) of glucocorticoids have been documented in a variety of tissues. Centrally, glucocorticoids have been shown to have immediate effects on behaviour, aggression, HPA axis activity and the hypothalamo-neurohypophyseal system; and in the periphery, fast effects have been observed in an assortment of respiratory, cardiovascular, metabolic, immune, endocrine, and urinary tissues (examples are given in Table 5.1).

Tissue	Fast glucocorticoid effects	Reference
Brain	CORT rapidly increases locomotor activity displayed by rats in response to a novel environment.	Sandi *et al.*, 1996
	CORT quickly promotes aggression during the resident–intruder test.	Mikics *et al.*, 2004
	CORT enhances glutamate transmission in the hippocampal CA1 region (CA1 is implicated in negative regulation of the HPA axis).	Karst *et al.*, 2005
	CORT causes extreme prolongation of NMDA receptor-mediated elevation in intracellular calcium in cultured rat hippocampal neurones, via a non-genomic mechanism.	Takahashi *et al.*, 2002
	CORT rapidly inhibits voltage-activated calcium channel currents in adult guinea pig hippocampal CA1 neurones.	ffrench-Mullen, 1995
	CORT rapidly facilitates synaptic potentiation in the mouse hippocampal CA1 area.	Wiegert *et al.*, 2006
	An intra-PVN infusion of dexamethasone (DEX) a synthetic glucocorticoid receptor agonist rapidly inhibits restraint-induced ACTH and corticosterone release, by means of cannabinoid CB1 receptor-mediated signalling.	Evanson *et al.*, 2010
	Glucocorticoids suppress excitatory glutamatergic synaptic inputs to rat parvocellular PVN and magnocellular PVN/SON neurons via retrograde endocannabinoid release, while facilitating GABAergic input into the SON by stimulating nitric oxide synthesis.	Di *et al.*, 2003, 2005,2009
	CORT rapidly inhibits AVP release from rat hypothalamic slices (containing PVN and SON).	Liu *et al.*, 1995
Pituitary gland	Glucocorticoids rapidly inhibit CRF-induced ACTH release.	Widmaier and Dallman, 1984; Hinz and Hirschelmann, 2000
	DEX suppresses forskolin-induced increase in cAMP, ACTH and POMC transcript in AtT-20 cells.	Iwasaki *et al.*, 1997
Trachea	Glucocorticoids rapidly suppress histamine-induced smooth muscle contractions in guinea pig trachea.	Sun *et al.*, 2006
Thymus	DEX quickly activates internucleosomal cleavage of rat lymphocyte DNA - instigating lymphocytolysis.	Compton and Cidlowski, 1986
	DEX induces the phosphorylation of the Src kinase, Lck, and the activation of other downstream mediators, including Rac1, as well as augments in resting signalling in resting human T cells.	Ghosh *et al.*, 2009
Heart/blood vessels	CORT increases the amplitude of L-type calcium currents of isolated guinea pig ventricular myocytes.	Yano *et al.*, 1994
	Glucocorticoids increase nitric oxide synthase activity in human endothelial cells.	Hafezi-Moghadam *et al.*, 2002
	CORT rapidly increases Na^+/H^+ exchange activity in primary rat aortic vascular smooth muscle.	Muto *et al.*, 2000
Adrenal gland	CORT suppresses nicotine-induced calcium influx in rat PC-12 (adrenal chromaffin tumour) cells.	Qiu *et al.*, 1998
	CORT activates ERK via a PKC dependent pathway in PC-12 cells.	Qiu *et al.*, 2001
Kidney	Glucocorticoids rapidly increase major proximal tubular Na^+/H^+ exchanger activity in the opossum kidney.	Bobulescu *et al.*, 2005
Liver	Rapidly reduces glycogen content of primary cultured rat hepatocytes.	Zhang *et al.*, 2009
Spleen	DEX quickly activates internucleosomal cleavage of rat lymphocyte DNA - instigating lymphocytolysis.	Compton and Cidlowski, 1986
Pancreas	Glucocorticoids rapidly decreases glucose stimulated β-cell insulin release (as opposed to chronic glucocorticoid exposure which has been reported to have stimulatory actions on insulin release).	Sutter-Dub, 2002
Adipose tissue	Acute glucocorticoid administration decreases glucose uptake by rat adipocytes.	Livingston and Lockwood, 1975
Testis	CORT reduces mouse leydig cell cAMP content and testosterone production.	Dong *et al.*, 2004

Table 5.1. Examples of fast glucocorticoid responses in a variety of brain regions and peripheral tissues.

5.1.2 Possible mechanisms of non-genomic action

The mechanisms that underlie the fast effects of glucocorticoids are not yet clear. Some evidence suggests that these fast effects may be mediated by membrane pools of GR and/or MR: GR has been shown to be localised to isolated caveolae rafts in the plasma membrane, from which GR could interact with signalling proteins e.g., GPCRs, growth factor receptors, non-growth factor tyrosine kinases (Jain *et al.*, 2005; Evanson *et al.*, 2010; Hammes and Levin, 2007). Indeed some studies have highlighted the indispensable nature of the traditional receptors in non-genomic glucocorticoid signalling e.g., CORT rapidly increases Na^+/H^+ exchange activity in primary rat aortic vascular smooth muscle via a non-genomic, protein kinase C dependant-mechanism, which is inhibited in the presence of a GR antagonist (Muto *et al.*, 2000). In addition, the fast effects of CORT on glutamate transmission in mouse hippocampus CA1 region is lost in MR KO mice; and intravenous administration of canrenoate (a MR antagonist) rapidly increases plasma ACTH and CORT (Karst *et al.*, 2005; Atkinson *et al.*, 2008). However, in other studies the fast effects are not disrupted by treatment with GR and MR specific antagonists, suggesting an alternative mechanism of action (Sandi *et al.*, 1996; Di *et al.*, 2005; Sun *et al.*, 2006; Wiegert *et al.*, 2006).

It has also been postulated that upon ligand binding, and the dissociation of GR/MR from the multimeric complex of scaffold and signalling proteins, some cellular components themselves (e.g., heat shock proteins, tyrosine kinases, immunophilins etc) rather than the transcription factors, interact with cytoplasmic proteins to illicit non-genomic effects (Haller *et al.*, 2008). As discussed in Chapter 4, high concentrations of steroids can also have non-specific effects on membrane fluidity e.g., disrupting ion cycling and ATP use. Alternatively, the fast effects of glucocorticoids could be mediated by membrane receptors such as ligand gated ion channel or unidentified GPCRs (Falkenstein *et al.*, 2000). Many studies have also shown specific binding of [^{3}H]-CORT and/or [^{3}H]-DEX to plasma membranes of a variety of cells and tissues e.g., rat brain and pituitary, AtT-20 mouse pituitary tumour cells, rat and mouse liver, human placenta, and rabbit skeletal muscle (Towle and Sze, 1983; Koch *et al.*, 1978; Harrison *et al.*, 1979; Suyemitsu and Terayama, 1975; Trueba *et al.*, 1989; Fant *et al.*, 1979; Savart and Cabillic, 1985).

In 2005, Maier and colleagues described high affinity binding of DEX to membranes of AtT-20 cells using fluorescence correlation spectroscopy. They demonstrated that the binding was sensitive to pertussis toxin – a potent inhibitor of $G\alpha_i$ alpha family of G protein subunits, thus suggesting the coupling of G proteins to the membrane-bound glucocorticoid receptors (Maier *et al.*, 2005). Other labs have also reported sensitivity of fast glucocorticoid effects to pertussis toxin. For example, the suppression of a forskolin-induced increase in cAMP, ACTH and POMC transcripts in AtT-20 cells by DEX is inhibited by pertussis toxin (Iwasaki *et al.*, 1997). Furthermore, CORT-mediated rapid inhibition of voltage-activated calcium channel currents in adult guinea pig hippocampal CA1

neurones, and its suppression of nicotine-induced calcium influx in PC-12 adrenal chromaffin tumour cells, is not only prevented by pertussis toxin, but also diminished by PKC inhibitors (ffrench-Mullen, 1995; Qiu *et al.*, 1998). In addition, glucocorticoid-induced endocannabinoid-mediated suppression of postsynaptic glutamate release in the SON is dependent on activation of $G\alpha_s$, cAMP, and PKA (Di *et al.*, 2009) – suggesting that the fast effects of glucocorticoids appear to be mediated by other families of Gα proteins. Therefore, the clear involvement of G proteins indicates that the rapid effects of glucocorticoids are potentially mediated by a GPCR(s).

Glucocorticoids are routinely administered as therapeutics in conditions such as asthma, chronic obstructive pulmonary disease, hypersensitivity reactions, autoimmune disorders (e.g., rheumatoid arthritis and systemic lupus erythematosus), and in organ transplantation (Ng and Celermajer, 2005). Most glucocorticoid treatments target the genomic action of GR and MR to promote the beneficial anti-inflammatory and immunosuppressant effects, but genomic actions have also been associated with a variety of adverse effects e.g., hyperglycaemia, hypertension, central obesity, diabetes mellitus, skin atrophy, osteoporosis, and depression (Ng and Celermajer, 2005; Haller *et al.*, 2008). Therefore, the possible existence of a membrane-bound glucocorticoid receptor distinct from GR and MR, but encompassing some of the beneficial actions of these receptors, has huge therapeutic potential. Its discovery may help eliminate some of the adverse effects associated with the current long-term glucocorticoid use (that targets the nuclear receptors), as drugs targeting a fast glucocorticoid receptor could be administered for shorter periods of time (and perhaps have fewer detrimental effects).

5.1.3 A G protein-coupled glucocorticoid receptor?

In this chapter, we attempted to identify a putative glucocorticoid receptor from the non-chemosensory orphan GPCRs in the mammalian genome. We endeavoured to identify candidate GPCRs by firstly comparing their tissue distribution with tissues which exhibit fast glucocorticoid effects such as: brain (SON, PVN and hippocampus), pituitary gland, trachea, thymus gland, heart, adrenal gland, kidney, liver, spleen, pancreas, adipose tissue, and testis. As the distribution of many orphan GPCRs has yet to be published, we began by searching the expression sequence tag (EST) profiles of orphan GPCRs commonly expressed in both human and rodent tissues (EST profiles: http://www.ncbi.nlm.nih.gov/unigene). ESTs are short sequences of DNA (approximately 200-600bp) usually produced from a single sequencing read from one or both ends of a cDNA clone, that has been selected at random from a tissue specific cDNA library (Pontius *et al.*, 2003; EST sequence data base: http://www.ncbi.nlm.nih.gov/dbEST/). An EST sequence can be compared with known sequences in BLAST to identify the corresponding full-length cDNA clone. The frequency at which an identified cDNA clone is picked from each tissue specific library is recorded and summarised in EST profiles. This gives a rudimentary indication to the density of gene expression within each tissue.

However, it must be noted that EST profiles are not without limitations. For example, sequencing of ESTs is relatively inaccurate with approximately 2 % error; and the random selection of cDNAs from the library favours common transcripts masking those of lower abundance (normalisation and subtraction techniques can be introduced to reduce/remove frequently expressed cDNAs to accommodate rarer transcripts – but NCBI EST profiles do not include counts from any biased libraries) (Schuler, 1997). Detection sensitivity is a particular issue when attempting to document GPCR gene expression (particularly in the brain) because GPCR mRNA is not as abundant compared to other receptor (such as ionotropic receptors) mRNA e.g., according to the V_{1B} receptor NCBI EST profile the mouse V_{1B} receptor gene is not expressed in the brain (zero EST transcripts out of 459991 cDNA clones) when V_{1B} receptor mRNA and protein have been detected in the mouse brain by ISHH and RT-PCR (Young *et al.*, 2006), ARG (Dr. James Roper and Dr. Stephen Lolait, personal communication), and VP is known to have a central role mediated by the V_{1B} receptor (Wersinger *et al.*, 2002). On the other hand, the cannabinoid CB_1 receptor which is abundantly expressed in rat brain (as shown by ISHH, IHC, and ARG (Matsuda *et al.*, 1993; Pettit *et al.*, 1993; Herkenham *et al.*, 1991)) has an EST expression profile of 3/61377. To give some perspective, we can compare the gene expression of these receptors with some of the most abundant glutamate ionotrophic receptor subunits in the rat brain (ionotropic receptors tend to be more abundant than GPCRs): expression patterns of the AMPA receptor subunit GluA2 and the NMDA receptor subunit GluN1 are 31/61377 and 18/61377, respectively. The most abundant kainate receptor subunit GluK2 has a brain expression pattern of 4/61377 (according to NCBI EST profiles), a value similar to that of CB_1. It is important to point out that EST profiles are not yet available for all genes and/or species e.g., V_{1B} receptor and GPER profiles are not available for rat tissues.

Notwithstanding the limitations of EST profiles, they still remain an excellent and dynamic directory with which to examine gene expression in tissues from various species (ranging from zebrafish to human). We searched the EST profiles of approximately 125 orphan GPCRs common to humans (number based on lists in the on-line IUPHAR Database of Receptors and Ion Channels (Harmar *et al.*, 2009) and rodents and located 9 orphans with gene expression (according to EST profiles) in some or all of the tissues known to exhibit fast glucocorticoid effects: GPRC5B, GPR48, GPR56, GPR65, GPR108, GPR125, GPR146, GPR153, TMEM87B (Tables 5.2 and 5.3 summaries the human and rat EST profiles of these orphans). To verify gene expression distributions, riboprobes were designed against the 3'UTR of each candidate transcript and a series of ISHH experiments were performed to determine the anatomical expression of the orphan GPCRs in target brain regions and peripheral tissues.

		GPER	GPRC5B	GPR48	GPR56	GPR65	GPR108	GPR125	GPR146	GPR153	TMEM87B	
	Uni gene ref no.	*20961*	*148685*	*502176*	*513633*	*443243*	*167641*	*99195*	*718624*	*531581*	*656298*	
		No. of receptor clones picked from tissue specific cDNA library										Total no. of inserts sequenced from library
Tissue	Brain	21	465	32	669	0	14	50	9	15	6	1,100,989
	Pituitary	0	0	1	1	0	1	2	0	1	0	16,585
	Trachea	0	1	3	55	0	0	3	0	0	1	52,413
	Thymus	1	1	1	41	1	1	0	0	0	1	81,131
	Heart	1	4	4	1	0	1	6	0	7	0	89,626
	Adrenal	2	1	0	0	0	0	2	0	0	1	33,197
	Kidney	2	29	32	42	3	17	8	5	1	7	211,777
	Liver	2	1	18	6	0	1	11	2	0	6	207,743
	Spleen	0	2	1	1	3	0	0	0	0	0	53,952
	Pancreas	0	2	6	37	1	6	5	1	2	4	214,812
	Adipose tissue	0	0	0	0	1	1	0	1	2	0	13,106
	Testis	0	47	24	294	1	11	21	2	0	16	330,442

Table 5.2. Human orphan GPCR EST profiles.

N.B., NCBI EST profiles are continually updated. These values are correct as of May 2011. GPER is included as the GPER probe acted as a positive method control for the orphan GPCR probes.

		GPER	GPRC5B	GPR48	GPR56	GPR65	GPR108	GPR125	GPR146	GPR153	TMEM87B	
	Uni gene ref no.	*389706*	*47330*	*162671*	*1677*	*198752*	*203125*	*217999*	*224807*	*138305*	*28728*	
		No. of receptor clones picked from tissue specific cDNA library										Total no. of inserts sequenced from library
Tissue	Brain	12/459991	18	0	21	0	6	0	0	0	3	61,377
	Pituitary	4/16965	1	1	0	1	4	0	0	0	0	17,007
	Thymus	6/116168	0	0	3	1	2	0	0	0	0	8,186
	Heart	0/52131	1	1	2	0	0	1	3	2	0	30,798
	Adrenal	0/2044	0	0	0	0	1	0	0	0	0	6,921
	Kidney	1/122453	1	3	10	0	2	0	0	0	0	22,578
	Liver	0/108957	0	2	1	0	1	0	0	0	0	77,670
	Spleen	0/94430	0	0	0	1	3	0	2	1	2	16,370
	Pancreas	0/105756	7	0	4	0	0	0	0	0	4	34,468
	Adipose tissue	0/1564	1	0	0	0	2	0	0	0	1	6,038
	Testis	3/113759	0	0	2	0	4	0	0	1	0	12,189

Table 5.3. Rat orphan GPCR receptor EST profiles.

As the rat GPER EST profile is unavailable on the NCBI database, the mouse profile is shown instead. Trachea profiles are not available for either rat or mouse. Values are correct as of May 2011.

5.2 Materials and methods

5.2.1 Animals

Three adult male Sprague-Dawley rats, weighing 200-250g (Harlan) were used in this study. Animals were sacrificed by decapitation and tissues frozen on dry ice as described in section 2.1.2.

5.2.2 ISHH

Coronal cryostat sections (12μm) were cut, thaw mounted onto polylysine-coated slides, and stored at -80°C until use. Each orphan probe was generated by PCR using approximately 125ng rat genomic DNA extracted from rat testis. The GPER probe was generated from 150ng rat genomic DNA purchased from Promega#G313A, UK. The primers, the primer restriction endonuclease sites, and the size of each riboprobe are described in Table 5.4. Primer restriction endonuclease sites allowed subcloning into the RNA generating vector pGEM4Z, and sense and antisense probes were generated using T7 and SP6 polymerases with ^{35}S-UTP and the MAXIscript *in vitro* transcription kit (summarised in Table 5.5). The integrity of each probe was verified by DNA sequencing. All ISHH experiments were performed as outlined in section 2.2, although the hybridisation and the high stringency wash temperatures were modified depending on the G+C content of each probe, as summarised in Table 5.6. Hybridised sections were exposed to film (Amersham HyperfilmTM MP) for 6 weeks, or emulsion dipped (Ilford K5) for 18 weeks and counterstained with toluidine blue.

Riboprobe	Primer sequence		Corresponding bp of gene/cDNA sequence	Genbank Accession number	Primer restriction endonuclease sites	Riboprobe size (bp)
	Upstream	Downstream				
GPRC5B	5'-GGGACGAATTCCATGGCACCTGTTTAAGT-3'	5'-TTGGCGGATCCAAAAGACAACTCTTCCCC-3'	1274-1773	NM_001106304	EcoRI-HindIII	430
GPER	5'-GAGAGGATCCTCCTAGAGGAAAACGGA-3'	5'-AAACAAGCTTTGTGAGAGGAGCATC-3'	15718722-15718072	NM_133573/ NC_005111	BamHI- HindIII	637
GPR48	5'-TAATAGAATTCCACAGTTGTCCTGTATTG-3'	5'-TTTTCAAGCTTCATTTATTTAGAATAGAG-3'	2667-3160	NM_173328	EcoRI-HindIII	477
GPR56	5'-CCTCTGAATTCGGGGTGCACATGCATGGC-3'	5'-CAGACAAGCTTGGAAGATGCTCAGCTCCTA-3'	2376-2834	NM_152242	EcoRI-HindIII	454
GPR65	5'-TGACGGAATTCGGGAGATCCGATATGTGG-3'	5'-ACCATAAGCTTGAATGGCCCCCGATGTAC-3'	878-1310	XM_001063813	EcoRI-HindIII	417
GPR108	5'-ACTTCCCCGAGTTCAGAGATCCGCCTTC-3'	5'-AATCAAAGCTTTATGAAGCCCAGGCTCT-3'	1752-3005	NM_199399	AvaI-HindIII	329
GPR125	5'-CCAAGGAATTCAGCTGCAGCTGA CCTTGA-3'	5'- TTTTTAAGCTTTGGGGAAGGGCAATTTAG -3'	4198-4549	XM_223485	EcoRI-HindIII	326
GPR146	5'-GGGCCGAATTCCAAGGAGAGGGCCTGACCA-3'	5'-TCCTCAAGCTTTAACACTGGTATTTGCGA-3'	1202-1719	XM_573364	EcoRI-HindIII	501
GPR153	5'-CCCCAGAATTCATGCAGACGGAAGAGGC-3'	5'-AAGGAGGACTTGCTCAATAGAACTTGTT-3'	2059-2521	NM_001034855	EcoRI-HindIII	447
TMEM87B	5'-CCAGTGAATTCAGTGTGCATGGGAGCGCG-3'	5'-TTTCTAAGCTTTGAGGCAGGGTCTCACTA-3'	1998-2452	XM_342515	EcoRI-HindIII	439

Table 5.4. Summary of riboprobe primers.

The riboprobe DNA templates were generated by PCR using 125ng rat genomic DNA (see section 2.2.2 for PCR protocol and Appendix I for the varying PCR conditions). Primers contained restriction endonuclease linkers to allow subcloning into a pGEM4z vector

Riboprobe	Restriction enzyme used to linearise vector		RNA polymerase used to generate probe	
	Antisense	Sense	Antisense	Sense
GPRC5B	EcoRI	HindIII	T7	SP6
GPER	BamHI	HindIII	T7	SP6
GPR48	EcoRI	HindIII	T7	SP6
GPR56	EcoRI	HindIII	T7	SP6
GPR65	EcoRI	HindIII	T7	SP6
GPR108	AvaI	HindIII	T7	SP6
GPR125	EcoRI	HindIII	T7	SP6
GPR146	EcoRI	HindIII	T7	SP6
GPR153	EcoRI	HindIII	T7	SP6
TMEM87B	EcoRI	HindIII	T7	SP6

Table 5.5. Generation of the orphan riboprobes.

Each vector was linearised using a restriction endonuclease site (incorporated in the primers used to PCR the probes) prior to probe synthesis using RNA polymerase and ^{35}S-UTP.

Riboprobe	GC content of probe (%)	Size of probe	Estimated Tm°C	Hybridisation Temp (°C)	High stringency wash (°C)
GPRC5B	50	430	78	55	65
GPER	53.06	637	80	55	65
GPR48	46.75	477	76	55	65
GPR56	56.83	454	83	55	65
GPR65	38.37	417	70	52.5	60
GPR108	54.1	329	80	55	65
GPR125	44.04	327	73	52.5	60
GPR146	43.9	501	74	52.5	60
GPR153	55.48	447	82	55	65
TMEM87B	48.75	439	77	55	65

Table 5.6. Calculating the hybridisation temperature and high stringency wash temperature for the orphan ISHH experiments.

The hybridisation temperature and high stringency wash temperature were based on the Tm for each probe calculated using the formula. Optimum hybridisation temperature is approximately 15-25°C below Tm, while the high stringency wash temperature is approximately 5-15°C below Tm (Wilkinson, 1999).

5.3 Results

5.3.1 Distribution of orphan GPCR mRNA in a collection of brain regions and peripheral tissues

The mRNA distributions of nine orphan GPCRs were mapped in brain regions and peripheral tissues that have been reported to exhibit putative fast glucocorticoid receptors: the brain (at the levels of the PVN, SON and hippocampus), pituitary gland, thymus, trachea, heart, liver, spleen, pancreas, kidney, adrenal, adipose tissue and testis. The mRNA distributions for each probe (based on results from both film and emulsion dipped sections) are summarised in Table 5.7 and film images of hybridised sections are shown in Figure 5.1. As the localisation of the rat GPER mRNA (and protein) has been characterised in Chapter 3, and the GPER gene is expressed at low-moderate levels in the PVN and SON, the GPER probe acted as a positive method control for the orphan GPCR probes. Unless otherwise stated, sections hybridised with control sense riboprobes (directed against antisense sequences of all of the GPCR mRNAs) showed only background/or were absent of hybridisation signal (examples given in Figure 5.6Cii, 5.7Cii and 5.8C).

	GPER	GPRC5B	GPR48	GPR56	GPR65	GPR108	GPR125	GPR146	GPR153	TMEM87B
SON	++	++/+++	-/+	++/+++	-/+	+++	+	+	+++	+++
PVN	++ (mPVN, pPVN)	+/++ (mPVN, pPVN)	-	++ (mPVN, pPVN)	-	++/+++ (mPVN, pPVN)	-/+ (mPVN, pPVN)	+ (mPVN, pPVN)	+/++ (mPVN, pPVN)	+++ (mPVN, pPVN)
Hippocampus	-/+ (CA1-3, DG)	++ (mainly in DG)	-/+ (CA1-3, DG)	++ (DG>CA1-3)	-	+++ (CA1-3, DG)	+/++ (CA3, DG)	+ (CA1-2, DG)	+	+++ (CA1-3, DG)
Pituitary	- NL ++ IL +/++ AL	+++ NL - IL +/++ AL	+++ NL + IL ++ AL	+++ NL +++ IL +/++ AL	-	++ NL +++ IL +++ AL	+/++ NL +/++ IL ++/+++ AL	+/++ NL ++/+++IL ++/+++ AL	-/+ NL -/+ IL + AL	+ NL +++ IL +++ AL
Trachea	-/+ (connective tissue, hyaline cartilage)	+/++ (connective tissue, hyaline cartilage)	+ (connective tissue)	+/++ (connective tissue, hyaline cartilage)	-	++ (connective tissue, hyaline cartilage)	++ (connective tissue)	++ (connective tissue, hyaline cartilage)	+/++ (connective tissue, hyaline cartilage)	++ (connective tissue, hyaline cartilage)
Thymus	+ (cortex, medulla)	-/+ (capsule)	+++ (cortex, medulla)	+++ (cortex, medulla)	++/+++ (cortex, medulla)	+++ (cortex, medulla)	+ (cortex, medulla)	+/++ (medulla)	+ (medulla)	+++ (cortex, medulla)
Heart	-/+ (myocytes)	++ (myocytes)	-/+ (myocytes)	+ (myocytes)	-	+/++ (myocytes)	+ (myocytes)	++ (myocytes, particularly in atria)	+/++ (myocytes)	+/++ (myocytes)
Adrenal	++ (ZG, medulla)	+/++ (mainly in ZG)	+ (cortex)	+ (ZG, medulla)	-/+ (ZG)	+++ (cortex, medulla)	+++ (cortex)	++ (cortex, medulla)	+/++ (ZG, medulla)	+++ (cortex, medulla)
Kidney	+/++ (RM,RP)	++/+++ (RP, thick ascending limb of IM and OM)	+++ (OM,IM,RP)	+++ (OM,IM,RP)	-/+ (ISOM)	++/+++ (RP, IM, ISOM)	++/+++ (RP, proximal tubules of IM and OM)	++ (labelling of all layers)	+/++ (IM,OM)	++/+++ (labelling of all layers)
Liver	-	-	++ (hepatocytes)	-/+ (hepatocytes)	-	+ (hepatocytes)	+/++ (hepatocytes)	++ (hepatocytes)	-	-/+ (hepatocytes)
Spleen	+ (red pulp)	+ (red pulp, PALS)	+/++ (MZ, PALS)	++/+++ (red and white pulp)	+++ (MZ, PALS)	+++ (white pulp > red pulp)	-/+ (red and white pulp)	+++ (red and white pulp)	++ (red and white pulp)	+++ (white pulp)
Pancreas	-	-	+ (acini and islets)	-	-	-	-/+ (acini and islets)	-/+ (acini and islets)	-	-/+ (acini and islets)
Adipose tissue	+ (stroma)	++ (stroma)	++ (stroma, vasculature, adipocytes)	+++ (stroma, vasculature)	+ (stroma)	++/+++ (stroma, vasculature)	++ (stroma, vasculature, adipocytes)	++/+++ (stroma)	-/+ (stroma, vasculature, adipocytes)	++ (stroma, vasculature)
Testis	+ (sertoli cells, spermatogonia)	-	+/++ (sertoli cells, spermatogonia, leydig cells)	+++ (sertoli cells, spermatogonia)	++ (developing spermatocytes)	+++ (spermatogonia and spermatocytes)	++/+++ (all layers of the seminiferous tubules)	++ (sertoli cells, spermatogonia)	+++ (sertoli cells, spermatogonia, developing spermatocytes)	++ (sertoli cells, spermatogonia, developing spermatids and leydig cells)

Table 5.7. Summary of ISHH results from emulsion/film.

The cell type/region where the majority of receptor transcript is expressed is indicated for each tissue. N.B., pancreas signal is based primarily on emulsion dipped sections due to low signal on film. -, Negligible signal; +, low signal; ++ moderate signal; +++, high signal. AL, anterior lobe; CA1-3, hippocampal regions 1-3; DG, dentate gyrus of the hippocampus; IL, intermediate lobe; IM, renal inner medulla; ISOM, renal inner stripe of the outer medulla; MZ, splenic marginal zone; mPVN, magnocellular PVN; NL, neural lobe; OM, renal outer medulla; PALS, splenic periarteriolar lymphoid sheath; pPVN, parvocellular PVN; RM, renal medulla; RP, renal pelvis; ZG, adrenal zona glomerulosa.

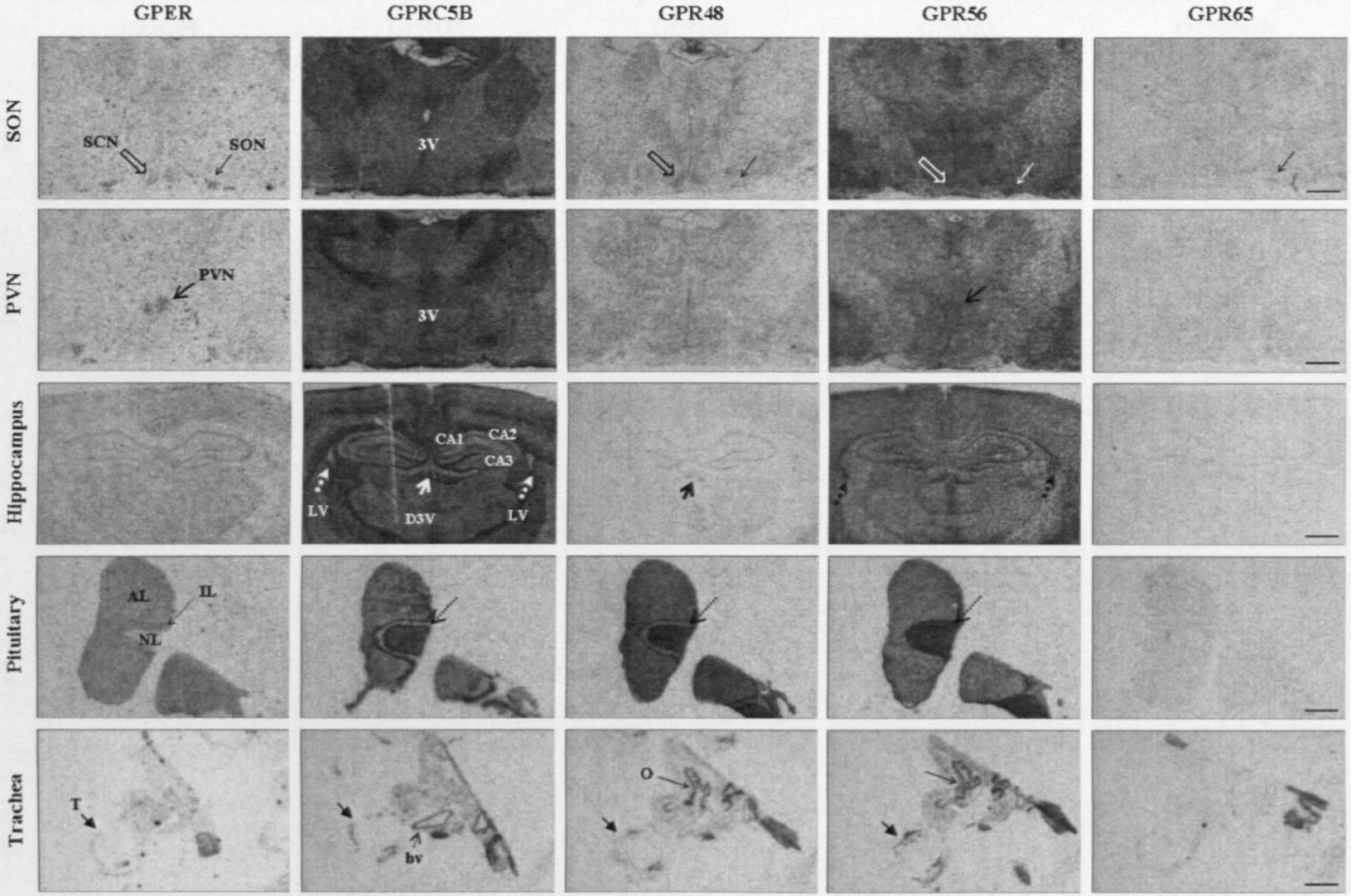

Figure 5.1. Orphan GPCR gene expression in brain and peripheral tissues.

Low magnification photographs of film autoradiographical images of brain (at the level of the SON, PVN and dorsal hippocampus (CA1-CA3), pituitary gland and trachea (T) hybridised with either GPER, GPRC5B, GPR48, GPR56, or GPR65 riboprobes. For some orphans, transcript expression was also observed in other regions of the brain (e.g., suprachiasmatic nucleus (SCN), membranes lining the lateral and dorsal ventricles (LV/D3V)), and/or peripheral tissues (e.g., oesophagus (O) and blood vessels (bv)). The GPER probe acted as a positive method control for the orphan GPCR probes in all studies. 3V, third ventricle; AL, anterior lobe; IL, intermediate lobe; NL, neural lobe. Scale bars, 1 mm.

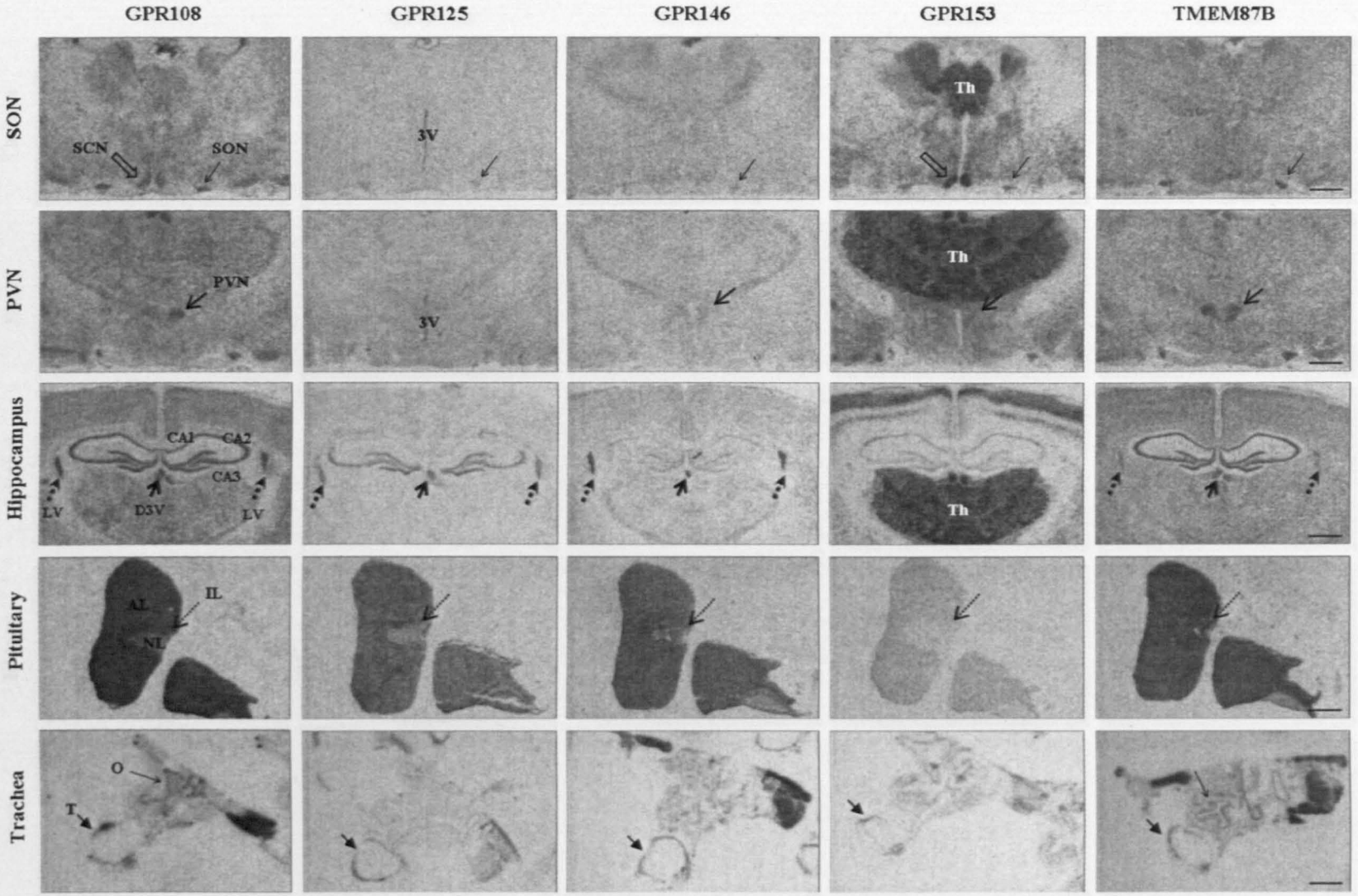

Figure 5.1. Continued. Orphan GPCR gene expression in brain and peripheral tissues.

Low magnification photographs of film autoradiographical images of brain (at the level of the SON, PVN and dorsal hippocampus (CA1-CA3), pituitary gland and trachea (T) hybridised with either GPR108, GPR125, GPR146, GPR153, or TMEM87B riboprobes. For some orphans, transcript expression was also observed in other regions of the brain (e.g., SCN (open arrows), membranes lining the lateral and dorsal ventricles (LV/D3V), and thalamus (Th)), and/or peripheral tissues (e.g., oesophagus (O)). 3V, third ventricle; AL, anterior lobe; IL, intermediate lobe; NL, neural lobe. Scale bars, 1 mm.

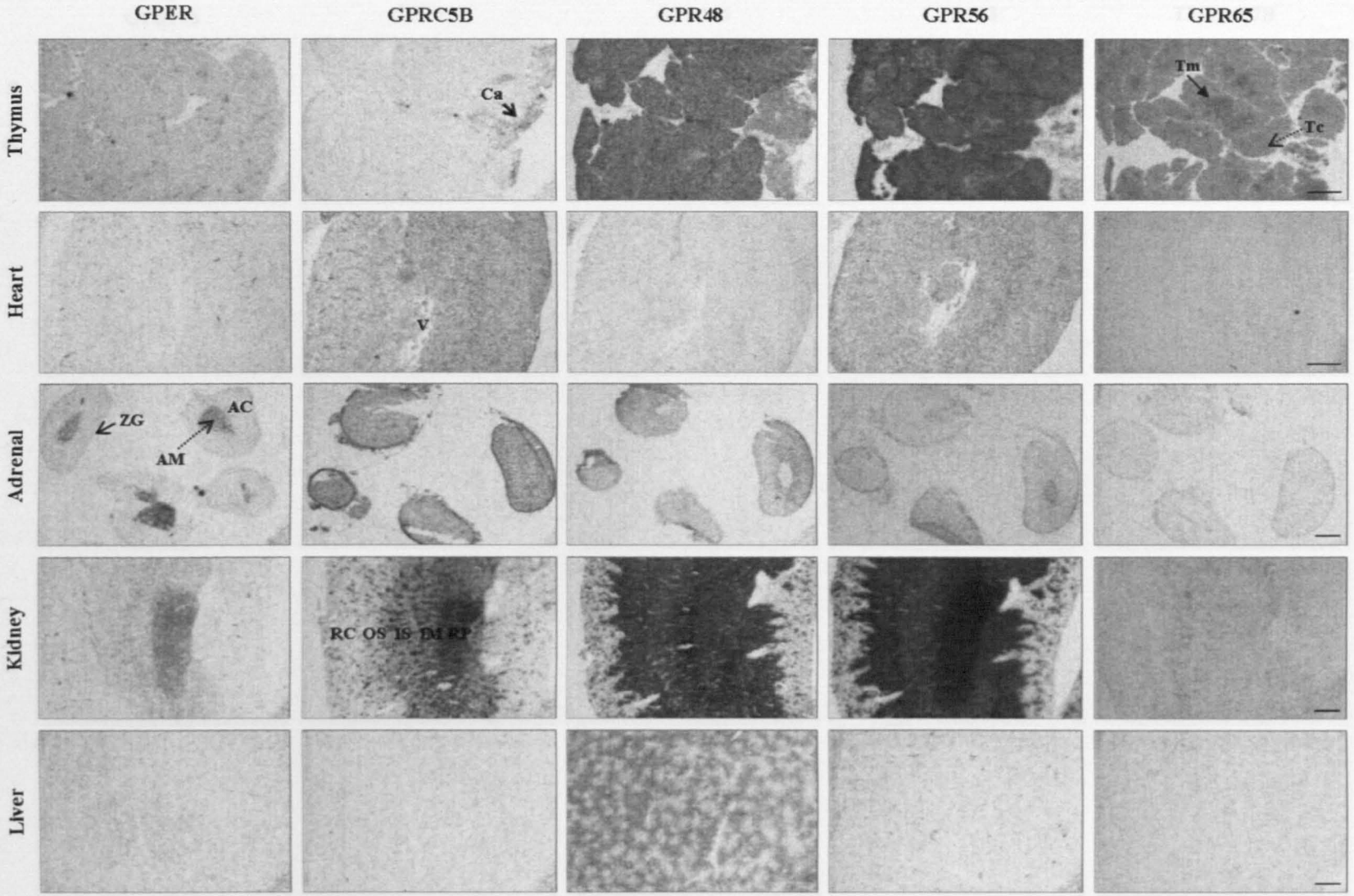

Figure 5.1. Continued. Orphan GPCR gene expression in peripheral tissues.

Low magnification photographs of film autoradiographical images of thymus, heart, adrenal gland, kidney and liver hybridised with either GPER, GPRC5B, GPR48, GPR56, or GPR65 riboprobes. Ca, Capsule; Tc, Thymic cortex; Tm, Thymic medulla; V, heart ventricle; ZG, zona glomerulosa; AC, adrenal cortex; AM, adrenal medulla; RC, renal cortex; OS, outer stripe of the renal outer medulla; IS, inner stripe of the renal outer medulla; IM, renal inner medulla; RP, Renal pelvis. Scale bars, 1 mm.

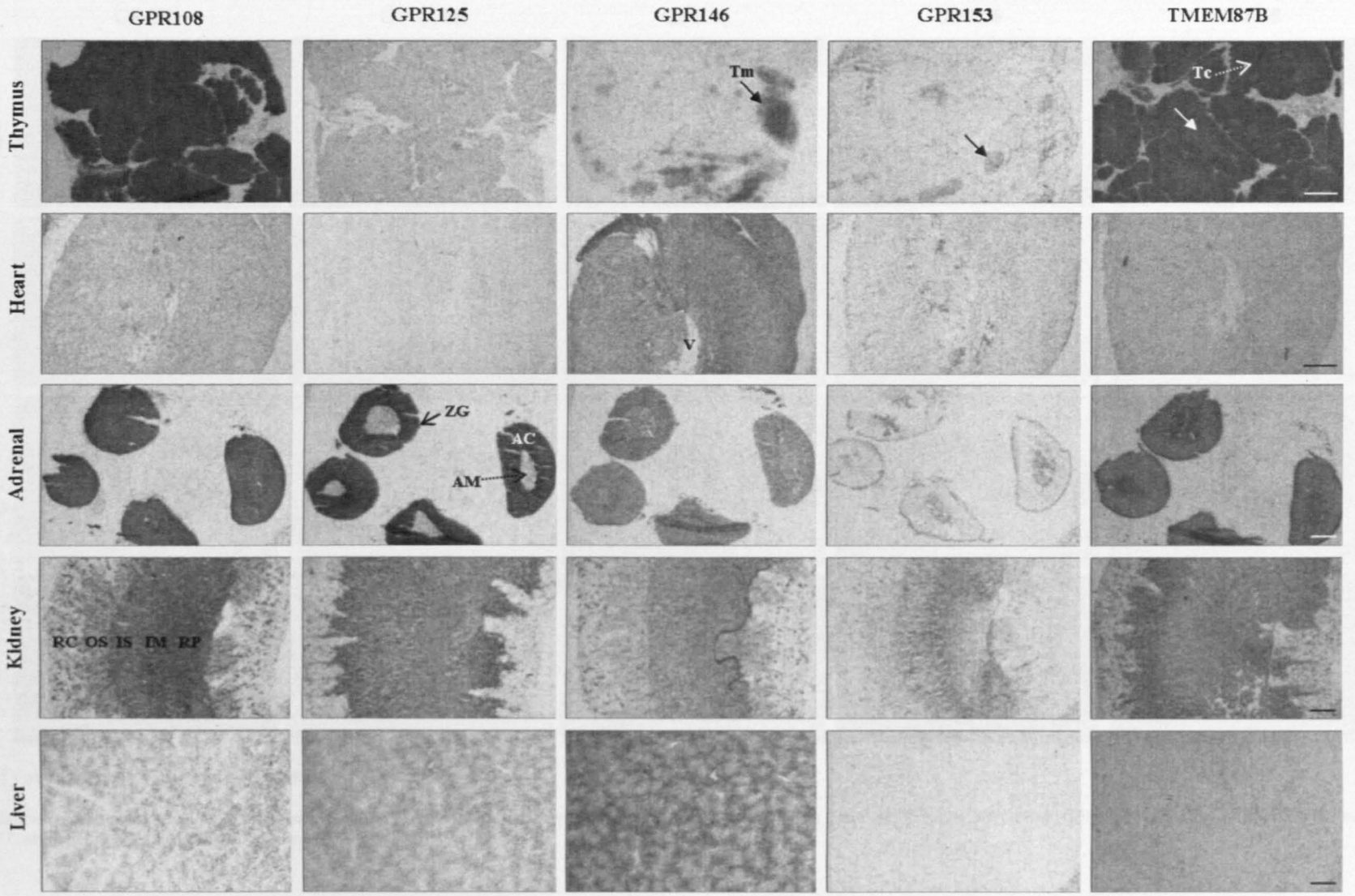

Figure 5.1. Continued. Orphan GPCR gene expression in peripheral tissues.

Low magnification photographs of film autoradiographical images of thymus, heart, adrenal gland, kidney and liver hybridised with either GPR108, GPR125, GPR146, GPR153, or TMEM87B riboprobes. Tc, Thymic cortex; Tm, Thymic medulla; V, heart ventricle; ZG, zona glomerulosa; AC, adrenal cortex; AM, adrenal medulla; RC, renal cortex; OS, outer stripe of the renal outer medulla; IS, inner stripe of the renal outer medulla; IM, renal inner medulla; RP, Renal pelvis. Scale bars, 1 mm.

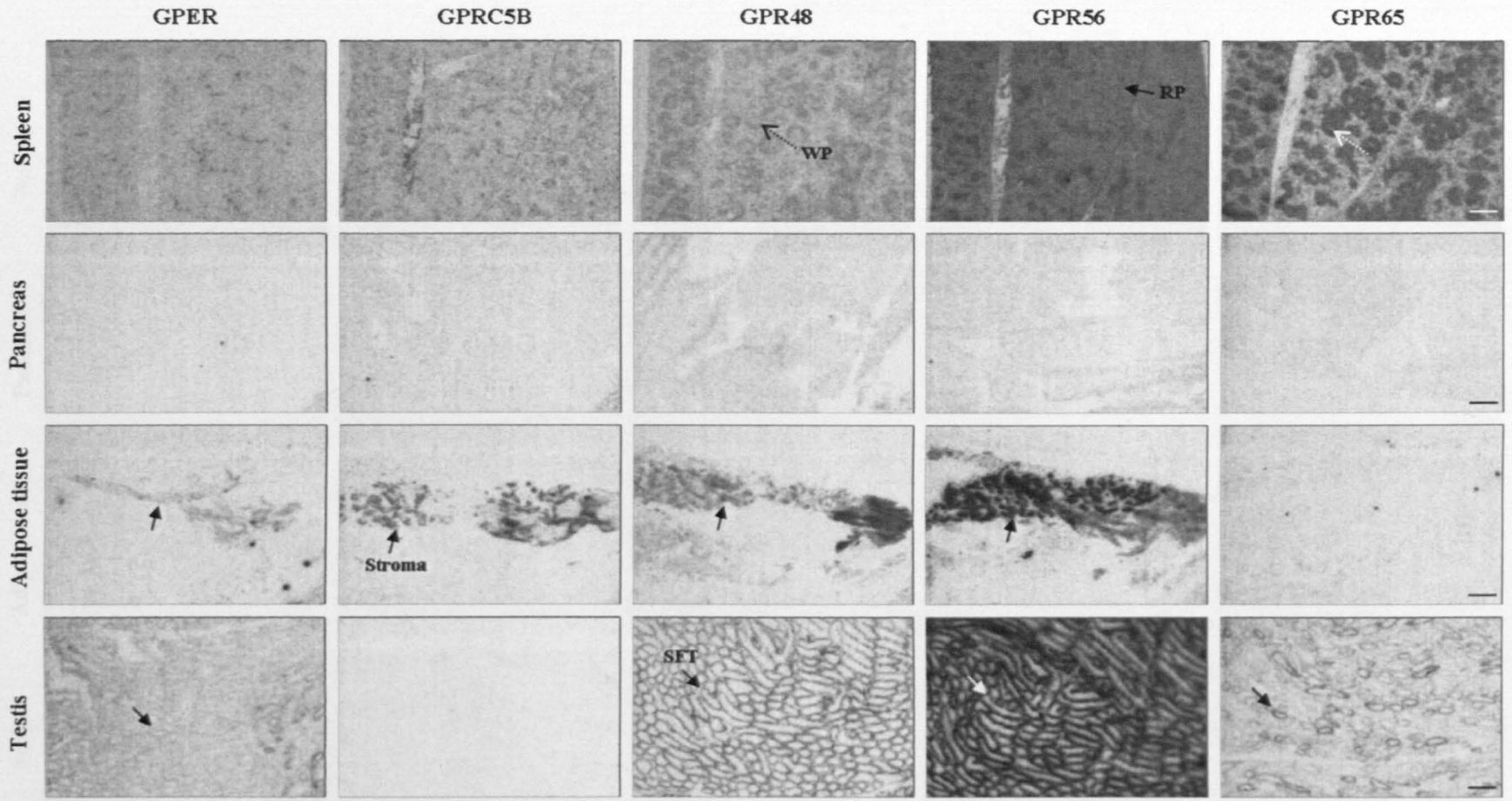

Figure 5.1. Continued. Orphan GPCR gene expression in peripheral tissues.

Low magnification photographs of film autoradiographical images of spleen, pancreas, adipose tissue and testis hybridised with either GPER, GPRC5B, GPR48, GPR56, or GPR65 riboprobes. WP, white pulp; RP, red pulp; SFT, seminiferous tubules. Scale bars, 1 mm.

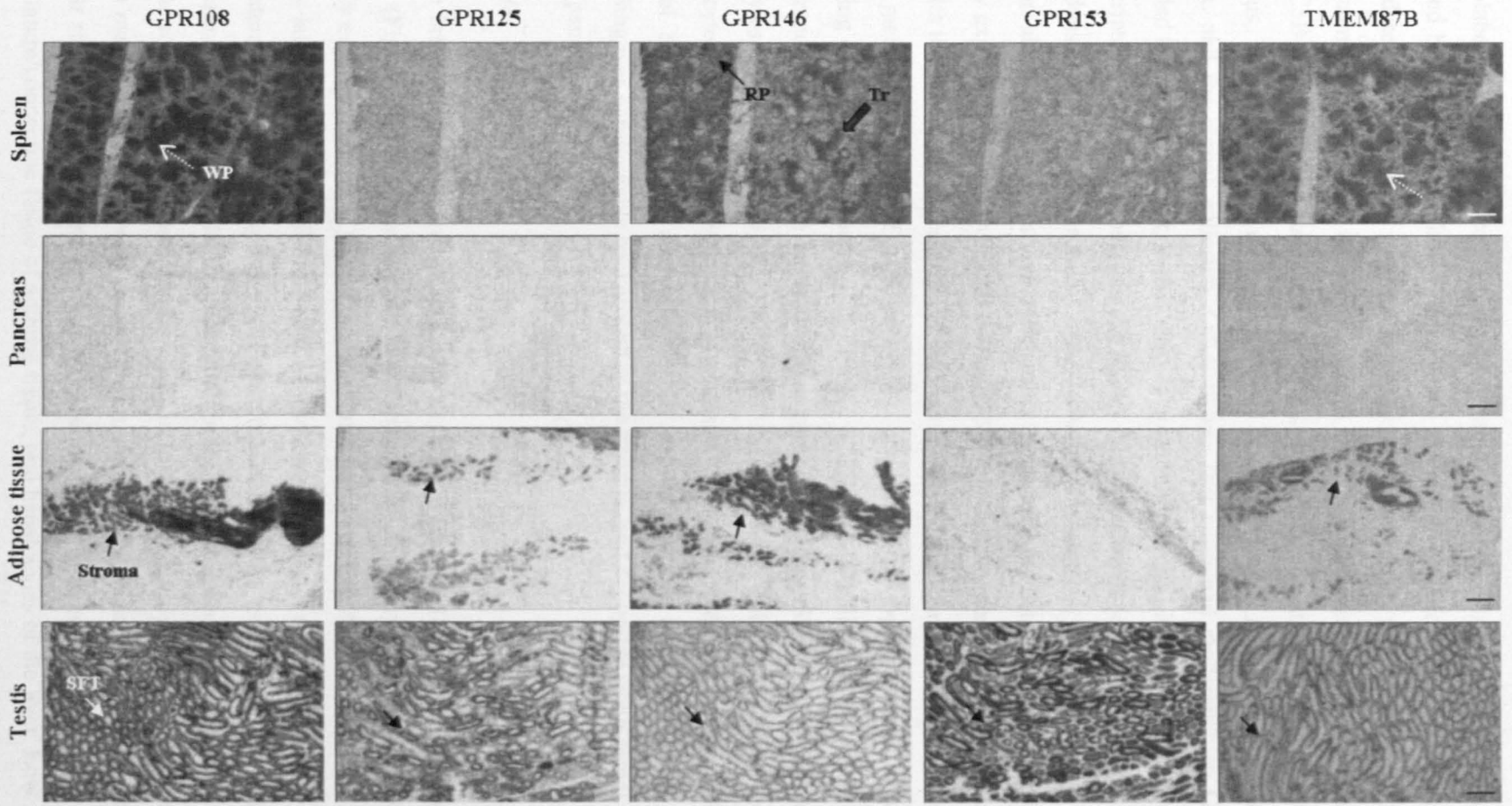

Figure 5.1. Continued. Orphan GPCR gene expression in peripheral tissues.

Low magnification photographs of film autoradiographical images of spleen, pancreas, adipose tissue and testis hybridised with either GPR108, GPR125, GPR146, GPR153, or TMEM87B riboprobes. WP, white pulp; RP, red pulp; Tr, trabeculae ; SFT, seminiferous tubules. Scale bars, 1 mm.

GPRC5B

Radiolabelled GPRC5B receptor transcript appeared to be ubiquitously expressed throughout the selected brain regions as shown in the x-ray film images Figure 5.1. Closer inspection of emulsion dipped sections confirmed high GPRC5B gene expression in the SON and optic chiasm/tract, the hippocampus (in particular the dentate gyrus), and to lesser extent the PVN. Brains regions of intense GPRC5B transcript expression (at the levels of bregma investigated) included the external globus pallidus, anterodorsal and reticular thalamic nuclei (Figure 5.2.1A), layer 3 and 5 of the cerebral cortex, and the corpus callosum. Other tissues that contained moderate/high GPRC5B expression included the pituitary, heart, kidney, and adipose tissue. In the pituitary gland, high levels of GPRC5B transcripts were found throughout the neural lobe, and low-moderate expression in the anterior lobe with dense patches of silver grains concentrated in an unknown cell type (Figure 5.2.2 Ci/Cii). There was an absence of signal above background in the intermediate lobe. In the kidney, GPRC5B was highly expressed in the pelvis, and the medulla, with cells expressing mRNA radiating from the inner medulla through to the inner stripe of the outer medulla, and to a lesser extent to the outer stripe of the outer medulla (Figure 5.5Di). Signal in the outer stripe of the outer medulla was consistent with labelling of the thick ascending limb (Figure 5.5Dii). The labelling in the cortex had a speckled-like appearance associated with an unidentified tubular structure. Signal was moderately diffuse among myocytes of the heart (Figure 5.4C), and stroma of the adipose tissue (with light labelling of adipocytes). There was low transcript expression throughout the adrenal medulla and most of the adrenal cortex, although moderate mRNA expression was observed in the zona glomerulosa. Labelling was barely above background in the thymus, and negligible or no signal was observed in the liver, pancreas or testis.

GPR48

In the brain, there was a noticeably high expression of GPR48 receptor mRNA in the subfornical organ (Figure 5.2.1B) and to a lesser extent in the SCN. In the hypothalamus, GPR48 transcripts were weakly expressed in the SON, and appeared not to be expressed in the PVN. The pituitary gland was highly labelled with the GPR48 probe with intense, moderate, and low signal in the neural, anterior and intermediate lobes, respectively (Figure 5.2.2D). GPR48 gene expression was found throughout the cortex and medulla of the thymus gland. In the kidney, intense labelling was dispersed throughout tubular structures in the inner medulla and in tubules of both stripes of the outer medulla some of which may be proximal tubules (Figure 5.5C), with some light labelling of glomeruli and unidentified tubular structures in the cortex. There was also moderate of expression of GPR48 mRNA in cells and vasculature/connective tissue of adipose tissue, and hepatocytes of the liver. Low hybridisation signal was observed in the exocrine (acini) and endocrine (islets of langerhans) pancreas (Figure 5.6Ci)

which was negligible in sections treated with sense probe (Figure 5.6Cii). Low transcript expression was found in the trachea, pancreas and adrenal cortex. There was a low-negligible GPR48 signal in the cardiac muscle, and an absence of detectable expression in the adrenal medulla.

GPR56

As with GPRC5B mRNA, GPR56 receptor transcripts were highly expressed in brain regions such as the SON, lateral ventricles, paraventricular nucleus and intermediodorsal thalamic nucleus of the thalamus, and the medial habenular. Moderate expression was observed in the CA1-3 of the hippocampus, SCN and PVN (Figure 5.2.1C). The intermediate and neural lobes of the pituitary were also intensely labelled, while the anterior pituitary was moderately labelled (Figure 5.2.2E). GPR56 mRNA is distributed throughout the cortex and medulla of the thymus (cortex > medulla) with distinct labelling of an unknown cell type/structure in the medulla (Figure 5.3C). GPR56 labelling was throughout the red and white pulp of the spleen, although it appeared to be a higher in the germinal centres of the white pulp. Intense labelling was evident in the blood vessels and stroma within the adipose tissue, with some labelling of adipocytes. A high level of GPR56 mRNA was also dispersed throughout the cortex, medulla and pelvis of the kidney. GPR56 gene expression appeared to be in the proximal tubules in the outer strip of the outer medulla (Figure 5.5B), while signal accumulated over both the collecting tubules and the thick ascending limbs in the inner stripe of the outer medulla, and possibly in the thin (descending and ascending) limbs of the inner medulla. In the testis, GPR56 transcripts were present in both the seminiferous tubules and leydig cells. Highest expression was found mainly around the outer layer of the seminiferous tubules (containing sertoli cells and spermatogonia), as well as in the developing spermatocytes. High levels of GPR56 transcripts were also identified in the oesophagus (Figure 5.1.1) (where it appeared to be localised within the lamina propria). A moderate-low level of GPR56 mRNA expression was found in the trachea, and low expression in the heart and adrenal. A low-negligible GPR56 signal was observed in the liver.

GPR65

Apart from an extremely faint signal in the SON, the brain sections were virtually absent of GPR65 receptor mRNA. In the periphery, the white pulp of the spleen was intensely labelled with the GPR65 probe, particularly in the marginal zone and periarteriolar lymphoid sheath (PALS) of the white pulp (5.6D). Moderate-high signal was found in the thymus gland with slightly more labelling in the medulla when compared with the cortex. In the testis, moderate expression of GPR65 mRNA was also in the developing spermatocytes (Figure 5.7E). Low labelling was observed in adipose tissue, and low-negligible labelling was in the adrenal and kidney. GPR65 hybridisation signal was not above background in liver, heart, pituitary gland, and pancreas.

GPR108

GPR108 receptor transcripts were highly expressed in the SCN, SON, PVN, CA1-3 (and dentate gyrus (Figure 5.2.1D)) of the hippocampus, dorsal third and lateral ventricles, and all three lobes (anterior and intermediate lobe > neural lobe) of the pituitary gland. GPR108 mRNA was equally as prevalent in the periphery. Intense expression of GPR108 mRNA was observed in the both the cortex and medulla of the thymus gland, although expression was highest within an unidentified cell type/region within the medulla (Figure 5.3D). Dense labelling was found in the spleen (particularly the white pulp), all layers of the adrenal gland, while moderate labelling was observed in the connective tissue and vasculature of the adipose tissue (Figure 5.7B). In the testis, GPR108 mRNA expression was localised to the outer perimeter (containing sertoli cells and spermatogonia) and developing spermatocytes of the seminiferous tubules, with some labelling of leydig cells. Moderate to high levels of transcripts were found in the kidney, with diffuse labelling of possible tubular structures extending from the inner medulla to the inner stripe of the outer medulla, and moderate labelling of tubular structures in the outer stripe of the outer medulla and cortex. Interestingly, the GPR108 sense probe also hybridised to the kidney with a distinct pattern compared to that of the antisense (Figure 5.8A). High sense probe labelling was found in the outer stripe of the outer medulla consistent with proximal tubules which radiated into the cortex (Figure 5.5E), while the inner medulla and pelvis appeared conspicuously devoid of any signal. Moderate GPR108 expression was observed in the connective tissue and hyaline cartilage of the trachea, low-moderate expression was found in heart myocytes, and low expression in the liver. There was no discernible GPR108 probe labelling in the pancreas.

GPR125

GPR125 receptor mRNA expression was observed in the dentate gyrus and CA3 of the hippocampus, and the dorsal third and lateral ventricles, with faint expression in the PVN and SON. The anterior lobe of the pituitary was strongly labelled with GPR125 probe with a faint, diffuse signal in the intermediate and neural lobes. High levels of transcript were found in the adrenal cortex but not medulla (Figure 5.3E). In the testis, moderate-high expression was observed in the seminiferous tubules with light labelling of leydig cells (Figure 5.7Di/Dii). However, the seminiferous tubules had varying patterns of expression – in some instances spermatids were strongly labelled, in others labelling was not prevalent in the developing spermatocytes, and/or the outer perimeter of the tubules (Figure 5.7 Dii). In the kidney, signal was diffuse throughout the pelvis, and inner and outer medulla. Labelling appears to concentrate to a tubular structure that radiated from the medulla into the cortex such as the proximal tubules. Moderate GPR125 mRNA expression was observed in the trachea, particularly in the mucosa and submucosa but also the hyaline cartilage with faint expression in the

fibroelastic tissue (Figure 5.3A) (N.B., hyaline cartilage is the most abundant cartilage in the body, which acts to support tissues such as the trachea, and also cover the articular surfaces of bones in synovial joints). Moderate-low GPR125 transcript expression was found in the hepatocytes of the liver. Low hybridisation signal was observed in the heart and thymus, and low-negligible signal was found in the pancreas and spleen.

GPR146

GPR146 mRNA was present in the PVN, SON and hippocampus, and highly expressed in the dorsal third and lateral ventricles (Figure 5.2.2B) and anterior lobes of the pituitary, with moderate/faint expression found in intermediate and neural lobes. In the spleen, transcript expression was particularly high in the red pulp trabeculae. In the white pulp, signal appeared to be concentrated around the perimeter of the germinal centres, presumably in the marginal sinus, although the germinal centres themselves were absent of labelling (Figure 5.6E). In some splenic areas there was slightly denser labelling of the PALS compared with the rest of the white pulp. Transcript was predominantly expressed by stroma of the adipose tissue, with some expression in vessels and adipocytes. In the heart, GPR146 signal was generally well distributed over the myocytes of the ventricular walls, but GPR146 gene expression was higher in myocytes of the atrial muscle (Figure 5.4A). Moderate labelling was seen throughout the liver (Figure 5.6B), over hyaline cartilage (Figure 5.3B), submucosa, and fibroelastic tissue of the trachea, in the outer layer of cells in the seminiferous tubules of the testis, and all layers of the adrenal glands. Labelling of the inner medulla and pelvis of the kidney was uniform, although labelling appeared to branch out from the inner medulla through to the inner and outer stripes of the outer medulla. Punctuate labelling in the renal cortex appeared to label the glomeruli. Low-negligible GPR146 transcript expression was observed in the pancreas.

GPR153

GPR153 labelling was striking throughout the thalamus, in the medial habenular nucleus (Figure 5.1.2 and 5.2.1E), SCN (Figure 5.2.2A), and cortical layers 2, 3 and 5. Moderate signal was observed in the PVN and SON, with weak expression in CA1-3 of the hippocampus and anterior pituitary. In the periphery, GPR153 transcript was highly expressed in the testis. Expression varied between seminiferous tubules, with transcript confined to the developing spermatocytes in some but also the outer layer of the seminiferous tubules in others (Figure 5.7F). Low levels of mRNA were also found in the leydig cells. In the kidney, faint to moderate labelling in the inner medulla radiated out into the inner stripe of the outer medulla and also dispersed into the outer medulla. Faint labelling was observed in the renal cortex whereas there was no absence of labelling in the pelvis. In the spleen, moderate transcript expression was mainly found in the red pulp, although there was some labelling in

the PALS surrounding central arterioles of the white pulp. Moderate-low hybridisation signal was observed in the heart and trachea, and there was an absence of signal in the liver and pancreas.

TMEM87B

TMEM87B receptor transcripts were highly expressed in all the brain regions of interest: PVN, SON (Figure 5.2.1F) and CA1-3 and dentate gyrus of the hippocampus. Intense signal was also found in the medial habenular and dorsal third and lateral ventricles. In the pituitary, TMEM87B mRNA was highly expressed in the anterior and intermediate lobes, and weakly expressed in the neural lobe. Intense labelling was ubiquitous throughout the lobes of the thymus and all layers of the adrenal gland (Figure 5.3F). In the spleen, there was a high level of transcript in the white pulp, and to a lesser extent in the red pulp. TMEM87B transcripts were highly expressed in the renal pelvis and medulla. The labelling in the pelvis, and inner medulla and inner stripe of the outer stripe was diffuse, while the signal in the outer stripe of the outer medulla appeared to radiate out to the cortex, labelling tubular structures such as the proximal tubules. Signal was found over the glomeruli and tubules in the renal cortex (Figure 5.5A). There was labelling dispersed throughout the adipose tissue stroma and lightly scattered over the adipocytes (Figure 5.7Ci) – an example of section labelled with sense probe is shown in Figure 5.7Cii. A moderate level of transcripts were found throughout the heart muscle, and was also in the testis - in the latter tissue labelling was mainly in the perimeter of the seminiferous tubules and in occasional spermatids and supporting leydig cells.

GPER

The hybridised GPER probe is usually exposed to film for at least 2 months (particularly in the brain) (see Chapter 3) nevertheless it clearly labels the SON, PVN, and anterior and intermediate lobes of the pituitary gland, but not the neural lobe after a 6 week exposure. An extremely faint signal is also observed in the SCN, and CA1/CA2 and CA3 hippocampal regions. In agreement with Chapter 3, moderate expression of GPER was also found in the adrenal medulla (with faint expression in the zona glomerulosa) and renal medulla and pelvis (pelvis > medulla). In addition to the data reported in Chapter 3, faint labelling was also observed in the spleen (mainly in the red pulp). Interestingly, the GPER sense probe labelled the spleen, with a pattern distinct from that of the antisense probe labelling. Sense signal was confined to the white pulp, largely is labelling germinal centres and PALS (5.8B).

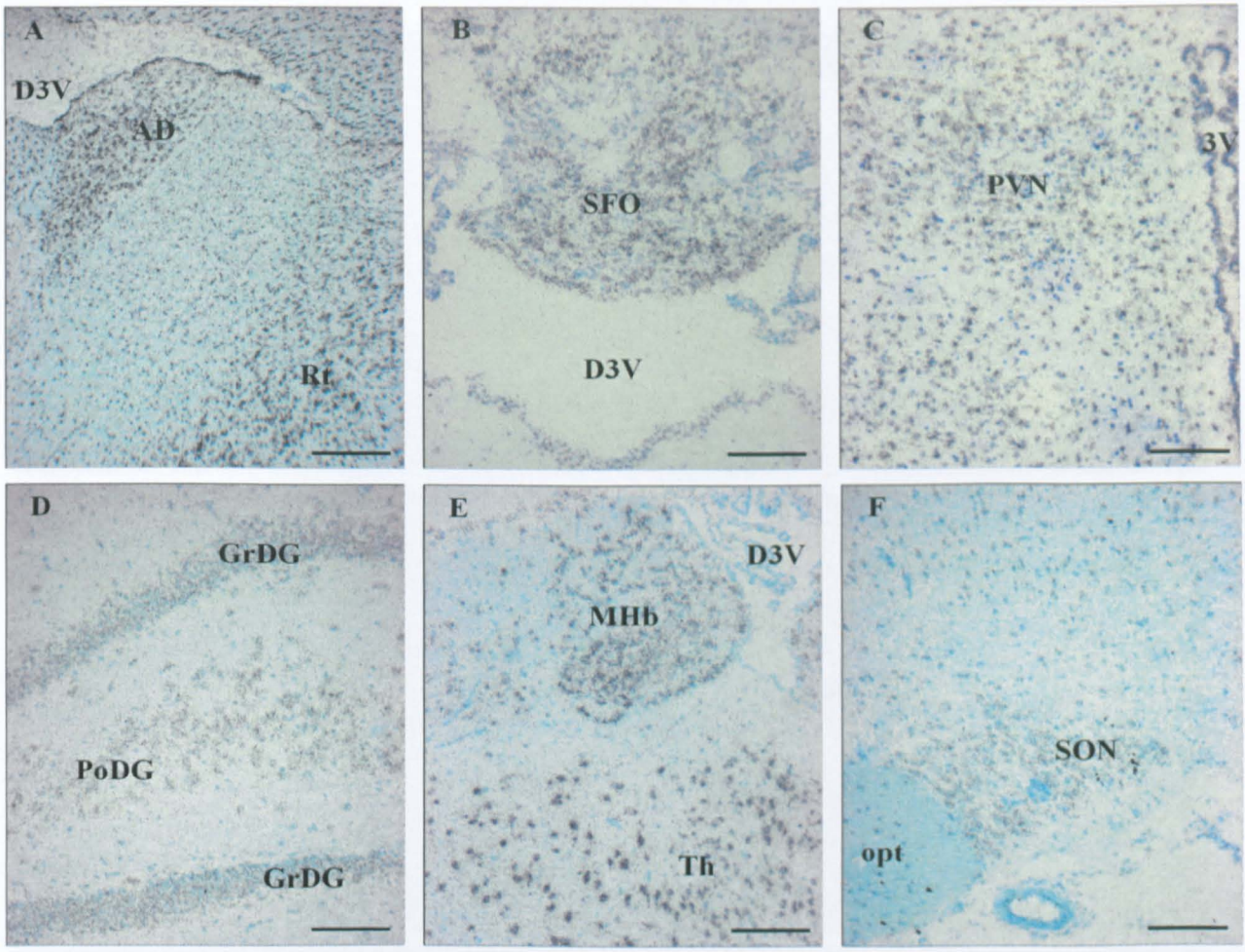

Figure 5.2. Examples of orphan gene expression in the brain - images from emulsion-dipped sections.

(A) GPRC5B mRNA is ubiquitously expressed throughout the brain sections investigated, although it is particularly evident in anterodorsal and reticular thalamic nuclei (AD and Rt, respectively). (B) Labelling of the subfornical organ (SFO) with GPR48 probe. (C) As with GPRC5B, GPR56 transcript is highly expressed throughout the brain levels investigated, including the PVN. (D) GPR108 hybridisation signal in the dentate gyrus of hippocampus. (E) Intense GPR153 probe labelling in the medial habenular nucleus (MHb) and thalamus (Th). (F) TMEM87B mRNA in the SON. D3V, dorsal third ventricle; 3V, third ventricle; GrDG, granular dentate gyrus; PoDG, polymorph layer of the dentate gyrus; opt, optic tract. Scale bars, 400μm in (A); 100μm in (B-F).

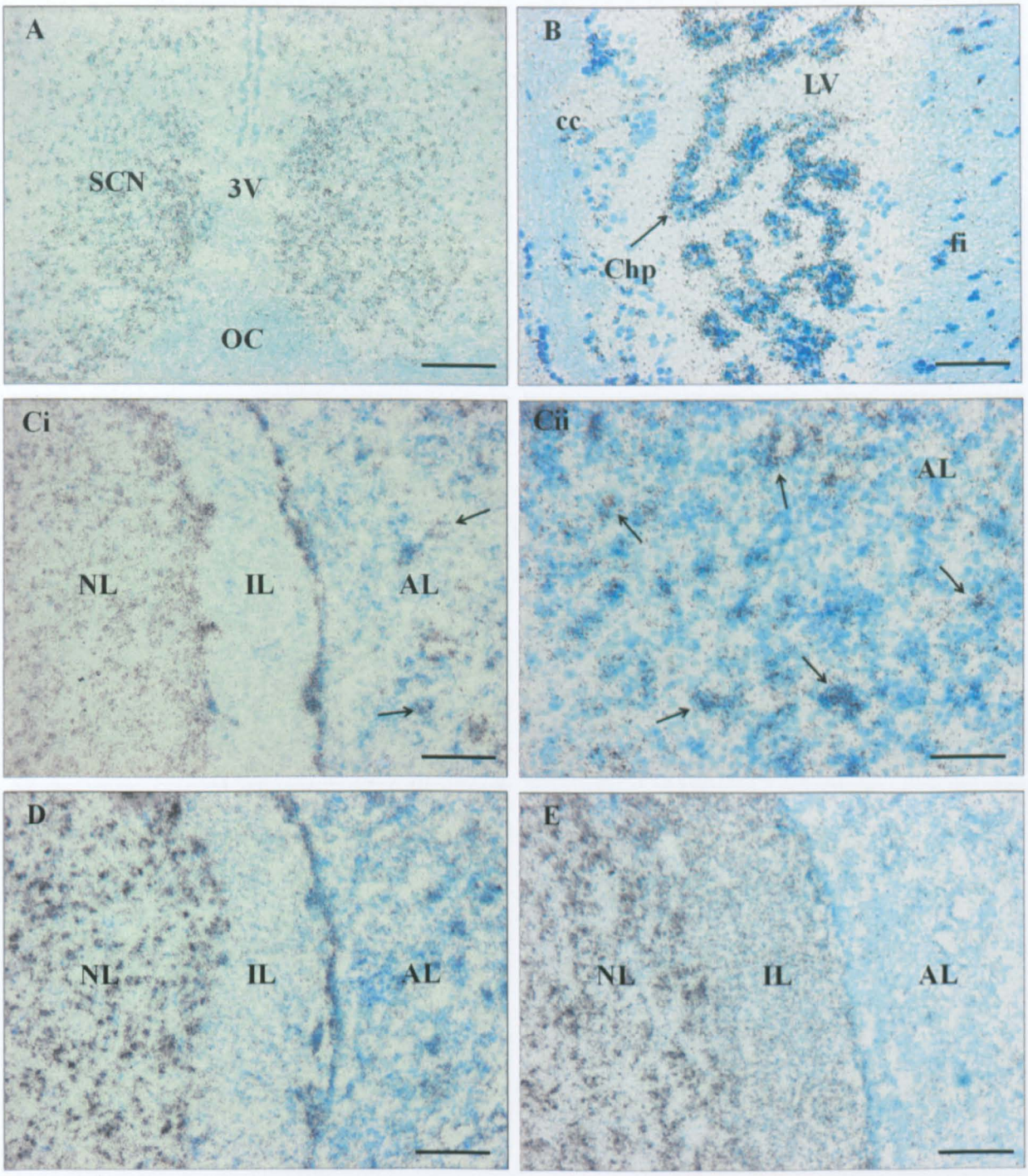

Figure 5.2. Continued. Examples of orphan gene expression in the brain and pituitary gland - images from emulsion-dipped sections.

(A) GPR153 hybridisation signal in the SCN. (B) GPR146 transcript expression in the choroid plexus (Chp) of the lateral ventricle (LV). (C-E) Different expression patterns of orphan mRNA in the pituitary gland: (Ci) high levels of GPRC5B mRNA in the neural lobe (NL), low-moderate expression in an unidentified cell type in the anterior pituitary (AP) (arrows), and an absence of expression in the intermediate lobe (IL); (Cii) higher magnification of GPRC5B labelling of an unknown cell type in the anterior pituitary (arrows); (D) intense GPR48 probe signal in the neural lobe, moderate signal in the anterior lobe, and low signal in the intermediate lobe; (E) High levels of GPR56 transcript in the neural and intermediate lobes, with moderate expression in anterior lobe. 3V, third ventricle; OC, optic chiasm; cc, corpus callosum; fi, fimbria of the hippocampus. Scale bars, 100μm in (A, Ci, D and E); 50μm in (B and Cii).

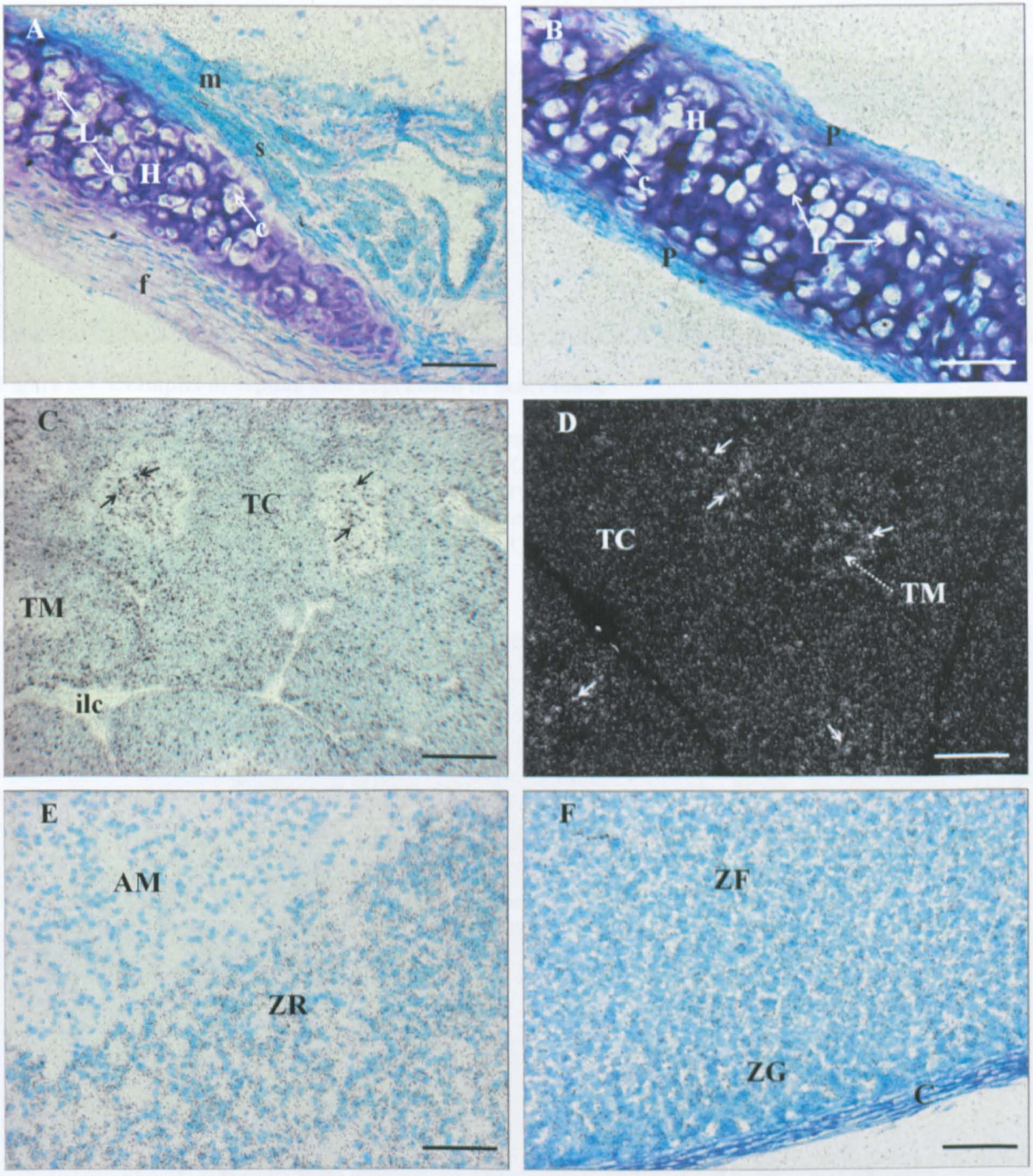

Figure 5.3. Examples of orphan gene expression in trachea, thymus and adrenal gland - images from emulsion-dipped sections.

Trachea: (A) GPR125 hybridisation signal in the mucosa (m) and submucosa (s), with some labelling of the hyaline cartilage (H) and faint labelling in the fibroelastic tissue (f). (B) GPR146 transcript in the perichondrium and in hyaline cartilage chondrocytes (c), although some chondrocytes have been lost during processing leaving empty lacuna (L). The probe has also bound non-specifically around the tissue. *Thymus:* labelling of the cortex (TC) and medulla (TM) by GPR56 (C) and GPR108 (D) probes, with signal concentrating around an unidentified cell type(s) in the medulla (arrows). Picture (D) is a reversed image of the thymus section (reversing highlighted the labelling of the unidentified cell types(s) in the medulla) - GPR108 probe hybridisation grains appear white in the picture (but black on the actual slide). *Adrenal gland:* (E) GPR125 transcript was highly expressed in the adrenal cortex (zona reticularis (ZR) layer shown here) but not in the adrenal medulla (AM). (F) TMEM87B mRNA was highly expressed throughout the entire adrenal gland – only examples of labelling in the capsule (c) and the zona glomerulosa (ZG) and zona fasiculata (ZF) of the cortex are shown here. ilc, intralobular connective tissue. Scale bar, 200μm in (C); 100μm in (D); 50μm in (A, B, E and F).

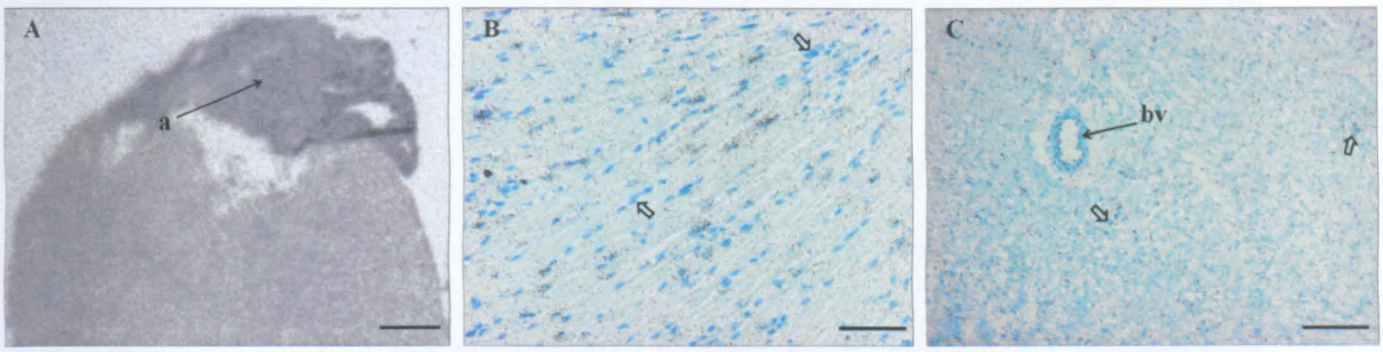

Figure 5.4. Examples of orphan gene expression in heart tissue.

(A) low-magnification photograph of a film autoradiographic image of a heart section hybridised with GPR146 probe. Labelling was quite prevalent in the atrial wall (a). (B) Emulsion dipped heart section hybridised again with GPR146 probe. GPR146 labelling was also observed in myocytes (open arrows point towards myocyte nuclei) in the ventricular walls. (C) Emulsion-dipped heart section demonstrating GPRC5B mRNA expression in myocytes and a blood vessel (bv). Scale bars, 1mm (A); 50μm in (B and C).

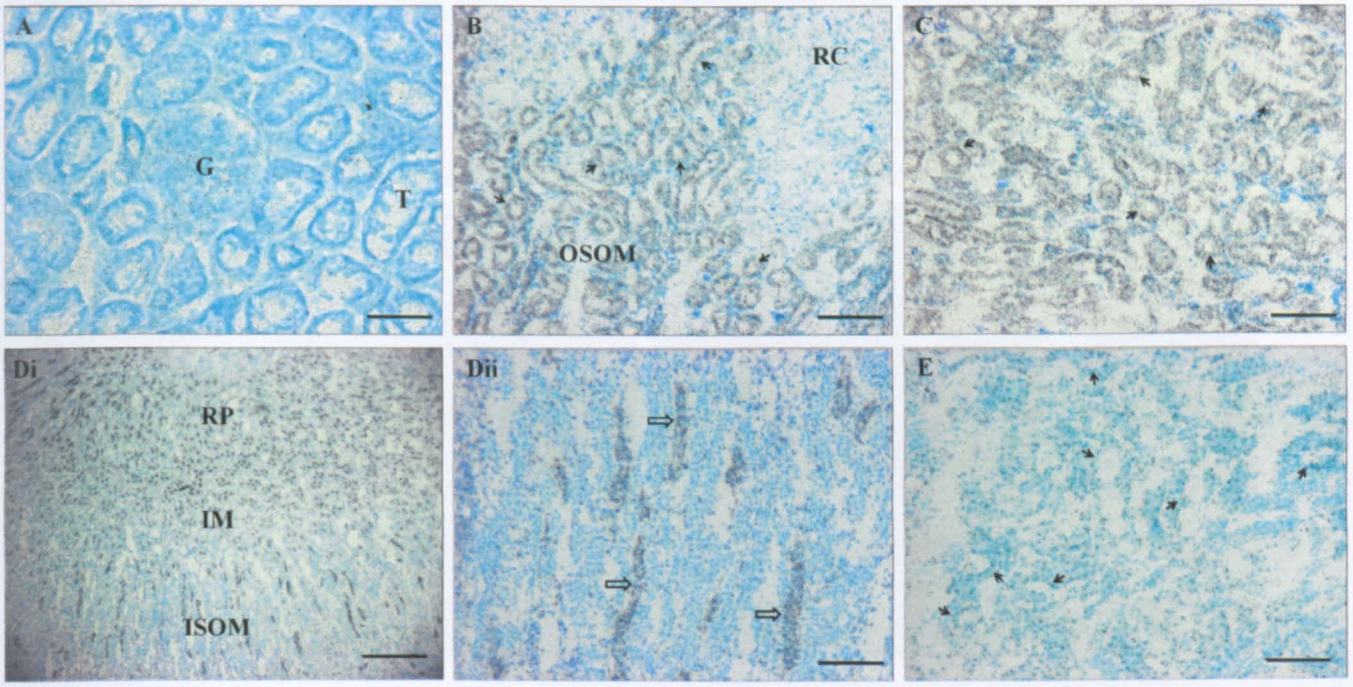

Figure 5.5. Orphan gene expression in the kidney - images from emulsion-dipped sections.

(A) TMEM87B mRNA expression in glomeruli (G) and tubules (T) of the cortex. (B) GPR56 hybridisation signal in proximal tubules (small arrows) of a medullary ray. (C) Labelling by GPR48 probe in tubules of the outer stripe of the outer medulla (OSOM), some of which appear to be proximal tubules. (Di). GPRC5B transcript expression in the inner stripe of the outer medulla (ISOM), inner medulla (IM), and pelvis (RP). (Dii) Higher magnification image of GPRCRB mRNA in the ISOM, and possibly the thick ascending limb (open arrows). (E) GPR108 sense probe binding in the OSOM – perhaps localised in the proximal tubules. RC, renal cortex. Scale bars, 400μm in (Di); 100μm in (B, C, Dii, E); 50μm in (A).

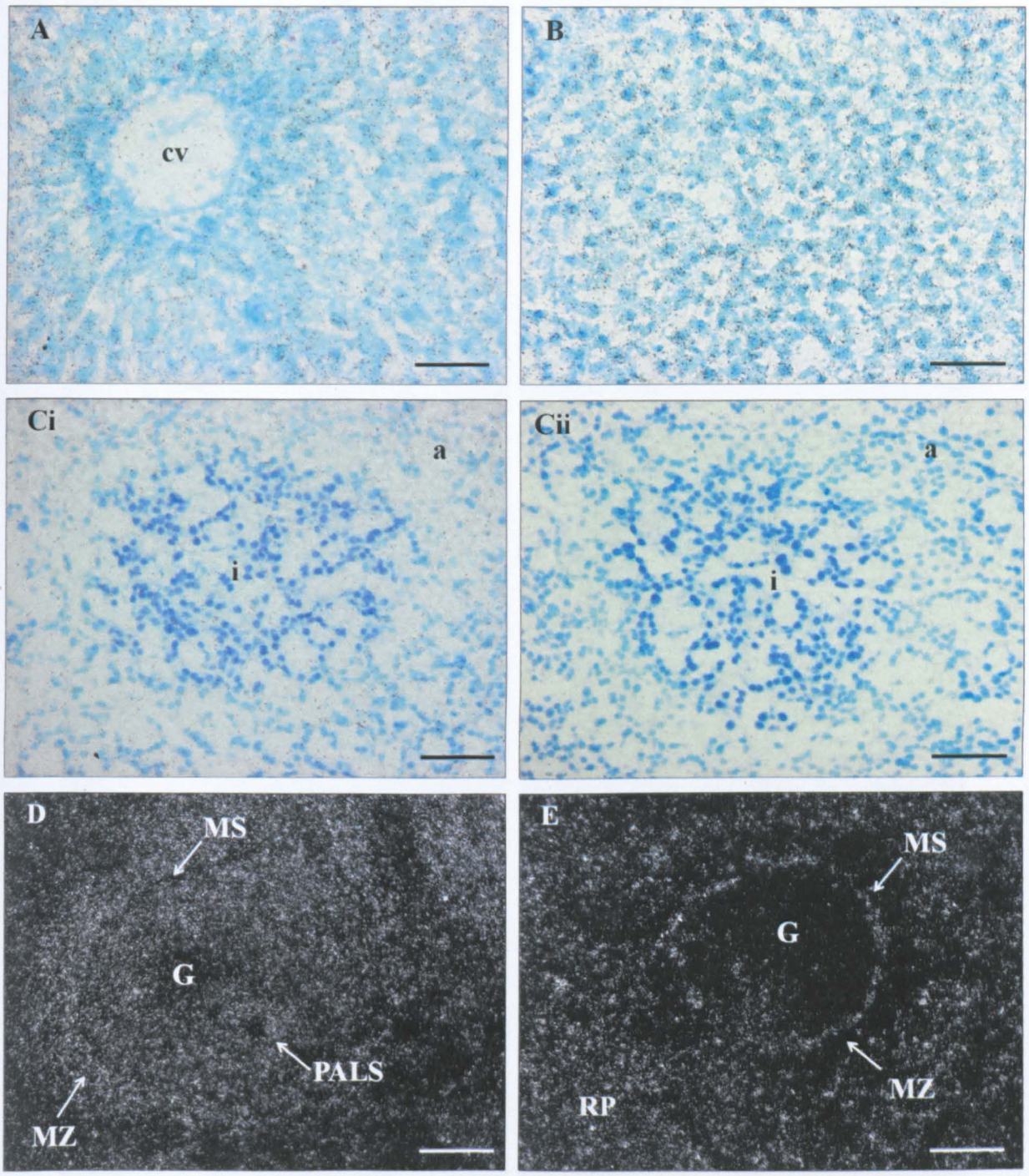

Figure 5.6. Examples of orphan gene expression in liver, pancreas and spleen – images from emulsion-dipped sections.

Liver: labelling of hepatocytes by GPR48 (A) and GPR146 (B) probes. *Pancreas:* (Ci) Low GPR48 transcript expression in cells of the islets of langerhans (i) and acinar cells (a). (Cii) GPR48 sense probe binding in islets of langerhans and acinar cells - only a few grains are visible when compared to the antisense probe sense labelling. *Spleen*: reverse images of emulsion-dipped spleen sections hybridised with GPR65 (D) and GPR146 (E) probes – silver grains appear white. In (D), note that GPR65 mRNA is expressed in the germinal centre (abbreviated to G), periarteriolar lymphoid sheath (PALS) and marginal zone (MZ), but is absent from the marginal sinus (MS). (E) GPR146 transcript expression in the red pulp (RP) and marginal sinus, and is absent from the germinal centre and marginal zone. cv, central vein. Scale bars, 100μm in (A, D, and E); 50μm in (B, Ci and Cii).

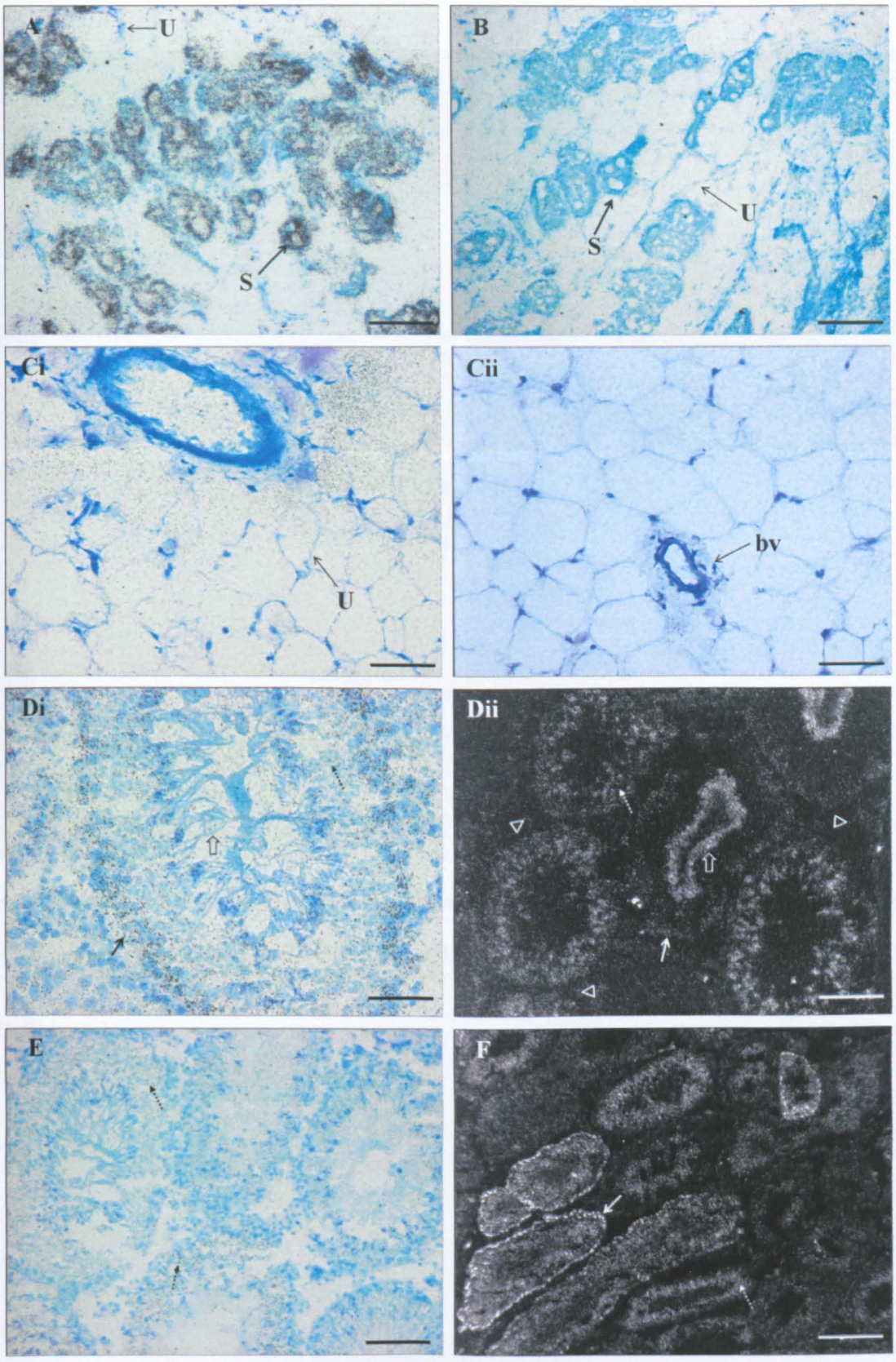

Figure 5.7. Examples of orphan gene expression in adipose tissue and testis – images from emulsion-dipped sections.

Adipose tissue: (A) Intense GPRC5B mRNA expression observed in stroma (S), with some mRNA found on the perimeter of unilocular adipocytes (U). (B) Labelling of stroma with GPR108 probe, and low labelling of unilocular adipocytes. (Ci) Grains of hybridised TMEM87B probe on adipocytes, which are absent in a section hybridised with sense probe (Cii). *Testis:* (Di) High GPR125 transcript expression in the perimeter of the seminiferous tubules (containing sertoli cells and spermatogonia) (arrows), low-moderate levels of transcript also found in developing spermatocytes (dashed arrows) and spermatids (open arrows). (Dii) Inverted lower magnification image of GPR125 mRNA expression in the testis (black grains appear white). Note that the location of transcript varies in each seminiferous tubule (although the functional significance of this is currently unknown). Faint hybridisation is also observed in leydig cells (arrow heads). (E) Labelling of developing spermatocytes with GPR65 probe. (F) Inverted image of GPR153 probe binding (appears white) in the perimeter of seminiferous tubules and developing spermatocytes. Scale bars, 200μm in (F); 100μm in (A, B, Dii, and E); 50μm in (Ci, Cii, and Di).

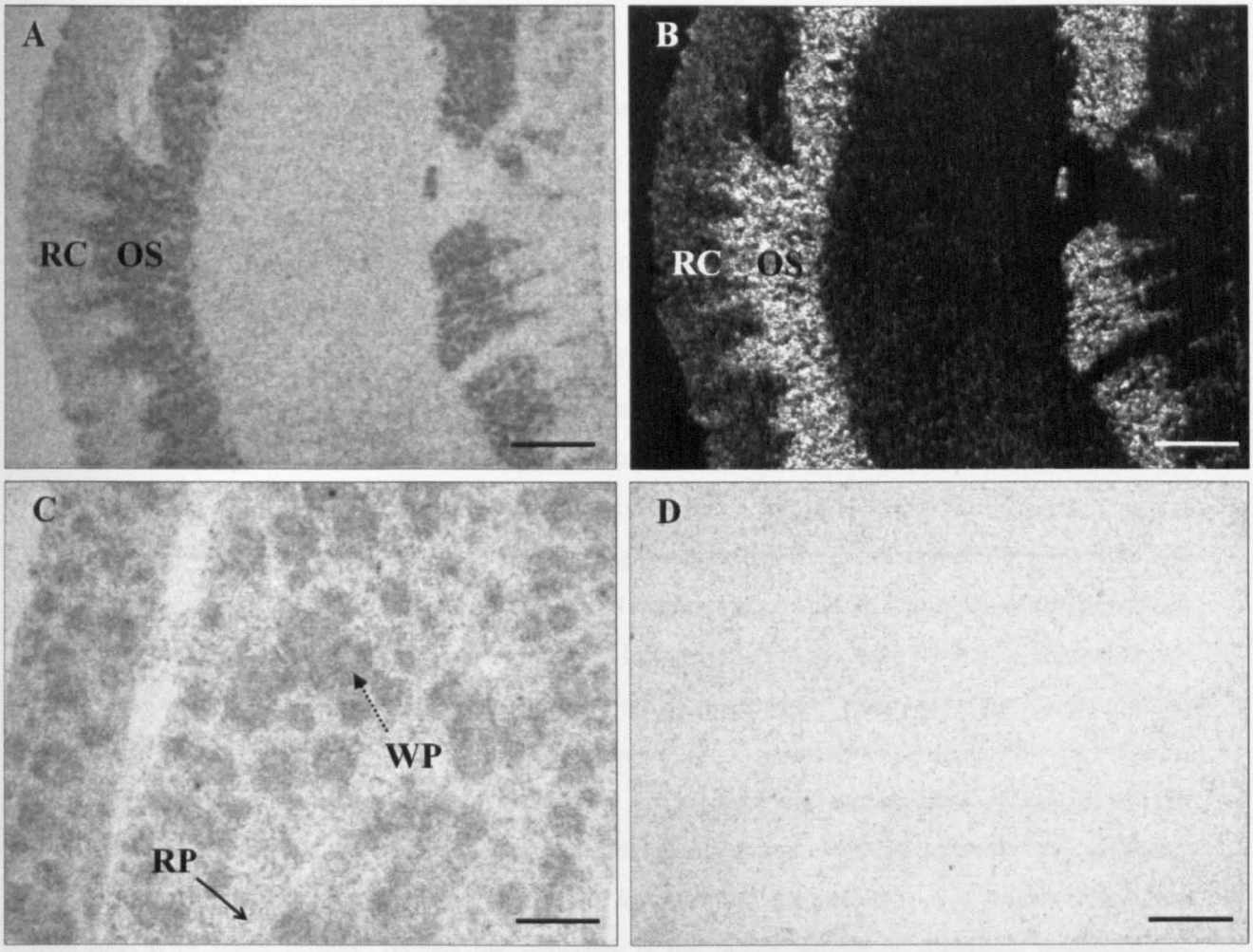

Figure 5.8. Examples of sense binding - low magnification photographs of film autoradiographic images.

(A) GPR108 sense probe binding in the renal cortex (RC) and outer stripe of the outer medulla (OS). Inverted image of GPR108 mRNA expression in the renal cortex (hybridisation signal appears white). (C) GPER sense probe binding in the white pulp (WP) of the spleen. (D) Absence of GPR65 sense binding in the spleen. RP, red pulp. Scale bars, 1mm.

Discussion

5.4.1 Narrowing the search for a fast glucocorticoid receptor to four orphan GPCRs

The aim of the present study was to find a candidate orphan GPCR for 'fast' glucocorticoid responses. To accomplish this, we screened a number of orphan GPCRs to determine their expression in brain regions/peripheral tissues that exhibit fast glucocorticoid responses; namely brain (SON, PVN and hippocampus), pituitary gland, trachea, thymus gland, heart, adrenal gland, kidney, liver, spleen, pancreas, adipose tissue, and testis. The validity of such an approach is not without precedent. For example, the cannabinoid CB_1 receptor was deorphanised principally on the basis of its expression in cells and brain regions known to show responses to tetra-hydrocannabis and cannabinoid derivatives (Matsuda *et al.*, 1990). As summarised in schematic Figure 5.9, out of the 9 orphan GPCRs, at least 4 (GPR108, GPR146, GPR56, TMEM87B) have a gene expression profile that closely maps to the regions/tissues of interest. However, the ISHH gene expression profiles in this study are by no means definitive; for example negligible gene expression in the some tissues may be due to low transcript expression - the 6 week film exposure (18 week emulsion exposure) used here may not be enough time to develop sufficient signal i.e., GPER hybridised probe is normally exposed to film for 8 weeks. The pancreas exhibited low-negligible expression for most of the orphan transcripts – of all the orphans GPR48 had the highest gene expression in the pancreas and even this was very low. This may imply that pancreatic orphan gene expression is low, or that the pancreas is a difficult target to hybridise with these probes. Indeed the pancreas is the major source of digestive ribonucleases (RNases) and thus it is possible that some endogenous RNA was degraded by pancreatic RNases after tissue removal (the pancreas was frozen about 10-15 min following animal sacrifice) (Bernard, 1969). In future studies it may be prudent to prioritise freezing the pancreas following sacrifice. Alternatively, immediately submerging the pancreas in 4% PFA would fix and in turn inactivate RNAses. It is assumed that the orphan transcripts in this study translate into fully functional and active proteins. There are examples of mRNA and protein mismatches in the literature e.g., GLP-1 mRNA is highly expressed in the PVN, but only weak autoradiographic binding is observed (Tauchi *et al.*, 2008) and in Chapter 3, GPER protein but not transcript is located in the posterior pituitary. The questions of technique sensitivity and gene verses protein expression has been addressed in Chapter 1.

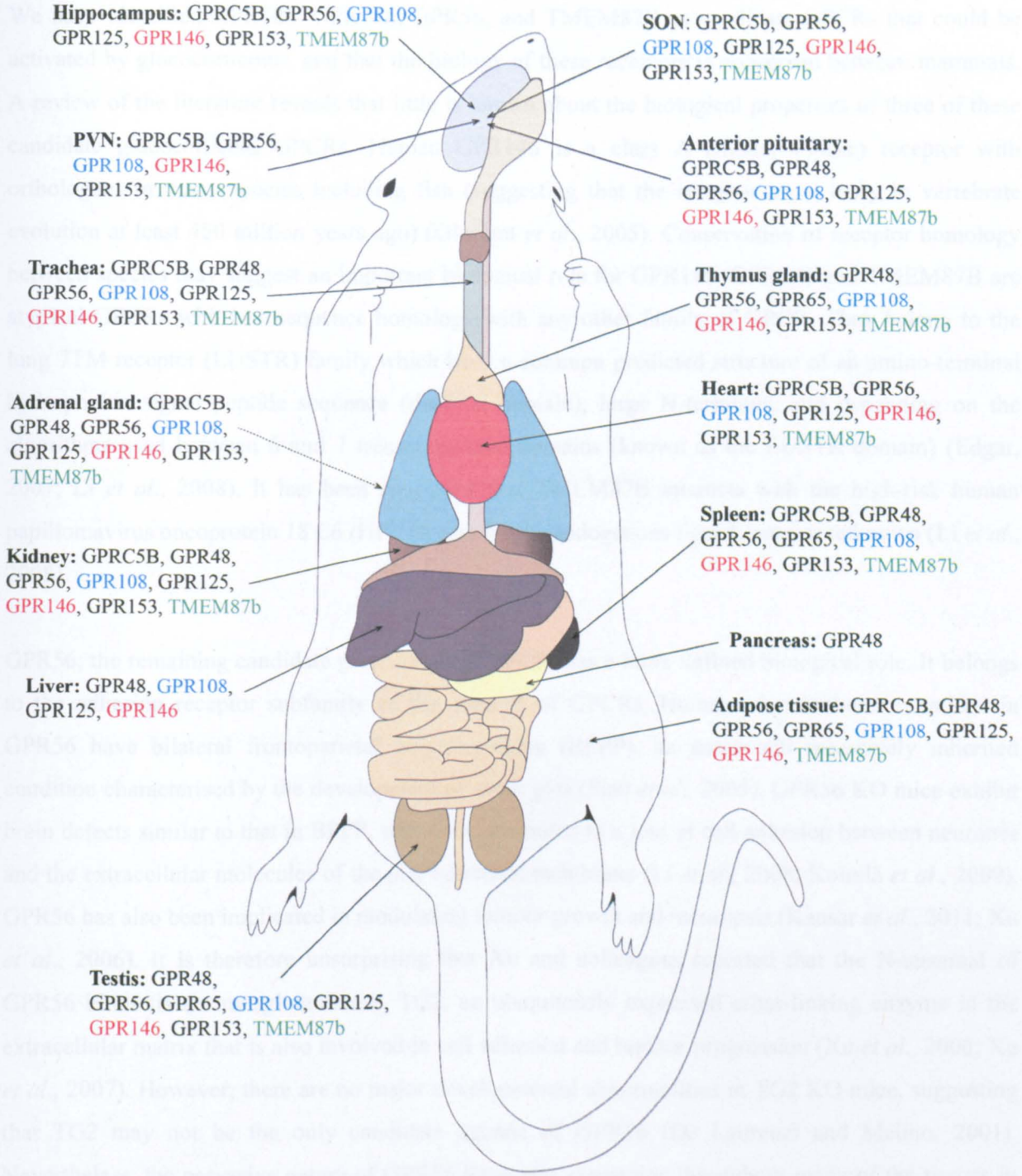

Figure 5.9. Schematic illustration demonstrating orphan GPCR gene expression in some rat tissues known to exhibit fast glucocorticoids responses.

N.B., only high-low transcript-expressing tissues are shown. Of the fourteen brain regions/peripheral tissues investigated low-high levels of GPR108 and GPR146 mRNA were expressed in all brain regions/peripheral tissues investigated, except the pancreas (although GPR146 was expressed at low-negligible levels). GPR56 and TMEM87B gene expression was also found in all brain regions and tissues, but not in liver and pancreas (TMEM87B mRNA was expressed at low-negligible levels in the liver); GPR125 in all areas/tissues apart from PVN, spleen and pancreas; GPR153 in all areas/tissues except liver, pancreas and adipose tissue; GPRC5B in all areas but not thymus, liver, pancreas, and testis; GPR48 transcripts were not observed in any of the brain regions of interest but were found in all peripheral tissues apart from the heart; and finally GPR65 transcripts were only expressed by the thymus, spleen, adipose tissue and testis.
Even though the gene expression pattern shown here is not definitive (e.g., longer exposure of hybridised sections to film/emulsion may further reveal low expression of some of the orphan GPCRs currently considered low-negligible/negligible; ISHH needs to be optimised for pancreas), it indicates that many of the orphan GPCRs are in the tissues of interest. As summarised in the text (5.4.1), GPR108 GPR146 and TMEM87B have been chosen as preferred candidates based on the high correlation between their transcript expression in tissues that exhibit rapid glucocorticoid responses (even though GPR56 transcript has a wide distribution profile like TMEM87B – it's possible role in cell adhesion (and reports it binds tissue transglutaminase, TG2 (Xu *et al.*, 2006) makes it an unlikely candidate). Rat diagram adapted from an illustration by Chris McKee (http://ratguide.com/health/basics/rat_anatomy.php).

We have identified GPR108, GPR146, GPR56, and TMEM87B as candidate GPCRs that could be activated by glucocorticoids, and that the biology of these receptors is conserved between mammals. A review of the literature reveals that little is known about the biological properties of three of these candidate glucocorticoid GPCRs. Human GPR146 is a class A (rhodopsin-like) receptor with orthologues in many species including fish (suggesting that the receptor arose early in vertebrate evolution at least 450 million years ago) (Gloriam *et al.*, 2005). Conservation of receptor homology between species may suggest an important biological role for GPR146. GPR108 and TMEM87B are atypical GPCRs with low sequence homology with any other family of GPCR. They belong to the lung 7TM receptor (LUSTR) family which have a common predicted structure of an amino-terminal hydrophobic signal peptide sequence (docking domain), large N-terminus, and depending on the algorithms used between 6 and 7 transmembrane domains (known as the LUSTR domain) (Edgar, 2007; Li *et al.*, 2008). It has been suggested that TMEM87B interacts with the high-risk human papillomavirus oncoprotein 18 E6 (HPV18 E6), but its endogenous ligand remains unknown (Li *et al.*, 2008).

GPR56, the remaining candidate glucocorticoid GPCR, has a more defined biological role. It belongs to the adhesion receptor subfamily of the class B of GPCRs. Humans that harbour mutations in GPR56 have bilateral frontoparietal polymicrogyria (BFPP), an autosomal recessively inherited condition characterised by the development of small gyri (Piao *et al.*, 2005). GPR56 KO mice exhibit brain defects similar to that in BFPP, which are attributed to a loss in cell adhesion between neurones and the extracellular molecules of the pial basement membrane (Li *et al.*, 2008; Koirala *et al.*, 2009). GPR56 has also been implicated in modulating tumour growth and metastasis (Kausar *et al.*, 2011; Xu *et al.*, 2006). It is therefore unsurprising that Xu and colleagues reported that the N-terminal of GPR56 binds tissue transglutaminase, TG2, an ubiquitously expressed cross-linking enzyme in the extracellular matrix that is also involved in cell adhesion and tumour progression (Xu *et al.*, 2006; Xu *et al.*, 2007). However, there are no major developmental abnormalities in TG2 KO mice, suggesting that TG2 may not be the only candidate agonist of GPR56 (De Laurenzi and Melino, 2001). Nevertheless, the pervasive nature of GPR56 transcript expression throughout many of the tissues in this study, particularly the brain (at the levels of the SON/PVN/ and dorsal hippocampus), together with its clear involvement in cell adhesion (as its family name suggests) and its close interaction with TG2, suggests that it is an unlikely candidate for a fast glucocorticoid receptor.

5.4.2 *The other five orphan GPRCRs - could they still be candidates for a fast glucocorticoid receptor?*

GPR125

Like GPR56, GPR125 is also a member of the adhesion family (Bjarnadóttir *et al.*, 2004). GPR125 was found in all of the tissues in the study (but at almost negligible levels in the PVN, spleen and pancreas), and as such may be a good candidate for a fast glucocorticoid receptor. Centrally, high GPR125 mRNA was observed in the choroid plexus of the dorsal and lateral ventricles, and the dentate gyrus and CA3 region of the hippocampus, which is consistent with reports that suggest mouse GPR125 gene expression increases two fold (as shown by qPCR) in the choroid plexus and hippocampus in response to traumatic brain injury (Pickering *et al.*, 2008). In addition, an association study has identified GPR125 as a possible gene involved in bipolar disorder and schizophrenia, diseases that are linked to dysfunction in limbic-related regions such as the hippocampus (Christoforou *et al.*, 2007). However, much of the literature surrounding GPR125 concerns its role as a marker for human and mouse spermatogonial stem cells (He *et al.*, 2010; Seandel *et al.*, 2007). In the current study, we located GPR125 transcript in all stages of rat sperm development and not simply restricted to spermatogonia – this may indicate possible species differences between rats, mice and humans. On the other hand, as described in Table 5.1 fast glucocorticoid responses have been observed in mouse leydig cells - but according to Seandel *et al.*, (2007) GPR125 is confined to mouse spermatogonia (Seandel *et al.*, 2007). Fast glucocorticoid responses have been reported in the hippocampal CA1 region which is devoid of GPR125 mRNA (Wigert *et al.*, 2006). Taken together this suggests that perhaps GPR125 may not be a high-priority candidate as a fast glucocorticoid receptor.

GPR153

GPR153 mRNA was also found in many of the tissues in this study, excluding the liver and pancreas. Of all the orphans investigated GPR153 has the most striking transcript distribution in the brain at the levels investigated, with intense expression in the cortex and thalamus. It is somewhat surprising that little, if anything is known about the receptor's role in the brain. Intriguingly, the pattern of GPR153 gene expression in the cortex and thalamus is similar to that of the α_{1B}-adrenoceptor (see Figure 5.10) (Day *et al.*, 1999). Interestingly, as a class A (rhodopsin-like) receptor, GPR153 has closest sequence homology to the biogenic amine subfamily of receptors (Gloriam *et al.*, 2005). Given this, one would speculate that GPR153 would more likely bind a biogenic amine rather than a glucocorticoid. This

could be tested by expressing this receptor in heterologous cells and examining signal transduction parameters in response to amines such as noradrenaline, adrenaline, serotonin, and dopamine.

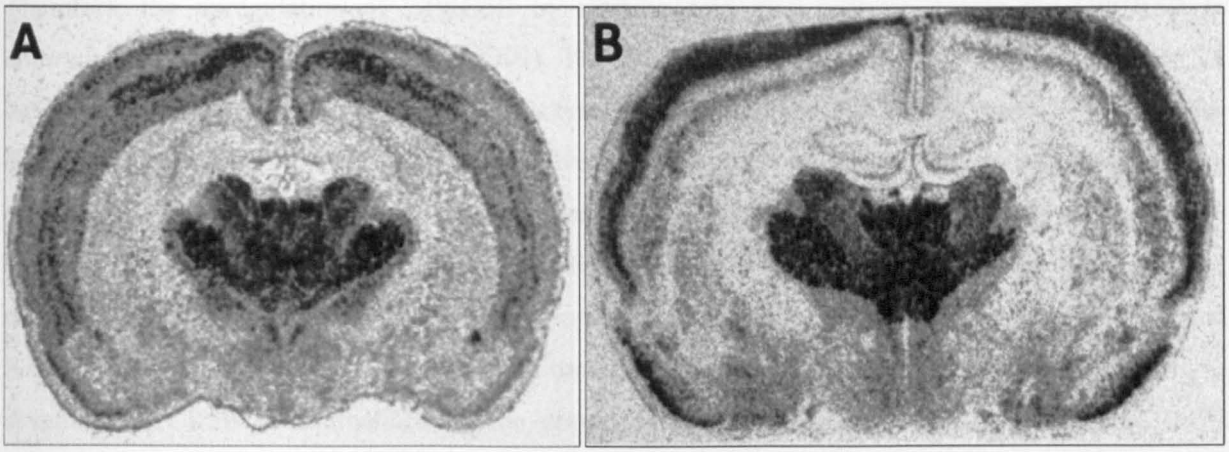

Figure 5.10. Similarities between α_{1B}-adrenoceptor and GPR153 transcript distributions in the rat brain.

A) Autographical film image of α_{1B}-adrenoceptor riboprobe binding in the brain (at the level of the PVN) – picture taken from Day *et al.*, (1999). B) Central expression of GPR153 (at the level of the PVN, but slightly caudal when compared with (A)).

GPRC5B

GPRC5B (previously known as retinoic acid-induced gene 2 (RAIG 2) or bride of sevenless) is a member of the class C (metabotropic glutamate-like) family of receptors (Bräuner-Osborne and Krogsgaard-Larsen, 2000). Unlike most of the orphans in this study the distribution of GPRC5B has previously been investigated in human and rat tissue. For example, northern blot analysis of human tissues revealed that GPCR5B mRNA is highly expressed in brain (e.g., corpus callosum, striatum, substantia nigra, thalamus, hippocampus, and spinal cord), and low relatively weakly expressed in the heart, kidney, lung, pancreas, testis and stomach (Robbins *et al.*, 2000). A northern blot analysis of rat tissues revealed that GPRC5B gene expression was also high in brain (e.g., neocortex, striatum, substantia nigra, thalamus, amygdala and cerebellum) and pituitary, and low in heart, adipose tissue, kidney, lung, mammary gland, testis and ovary (Robbins *et al.*, 2002). These reports are broadly in agreement with the current study, where we found ubiquitous distribution of GPRC5B transcript throughout the brain levels investigated (notably the SON, external globus pallidus, anterodorsal and reticular thalamic nuclei, cerebral cortex, and the corpus callosum), the pituitary gland, kidney, heart and adipose tissue (but not testis, pancreas and liver). Therefore, based solely on its distribution across three different species GPRC5B may contender for a fast glucocorticoid receptor. However, functional studies indicate that GPCR5B may have a different role.

As its previous name RAIG2 suggests, GPRC5B is upregulated in a variety of cell lines following treatment with all-trans-retinoic acid, a synthetic form of retinoic acid (Robbins *et al.*, 2000). Retinoic acid is a metabolite of vitamin A and plays a key role in embryonic cell and tissue differentiation. Therefore, the upregulation of GPRC5B by retinoic acid may indicate a role for GPCR5B in embryonic development (Mark *et al.*, 2009). This has been demonstrated in Drosophila - GPRC5B has been identified as the ligand for sevenless tyrosine kinase (sevenless; hence GPRC5B's alternative name 'bride of sevenless'), a receptor involved in photoreceptor neuron R7 development in the embryonic eye (Hart *et al.*, 1990; Cagan *et al.*, 1992). GPRC5B and sevenless are expressed by Drosophila photoreceptor neurones R8 and R7, respectively, and GPCRC5b expression by R8 neurones is required for normal R7 cell development. Surprisingly, communication between R8 and R7 neurones occurs via a receptor-mediated transfer of GPRC5B from cell to cell. Upon binding to sevenless GPCR5B is internalised by the opposite R7 neurone (Cagan *et al.*, 1992). Kohyama-Koganeya and co-workers have subsequently identified the endogenous ligand for GPRC5B in Drosophila as glucose, and shown that it is required for homeostatic metabolism of glucose and lipids (Kohyama-Koganeya *et al.*, 2008). Whether glucose is the endogenous ligand of the mammalian GPRC5B has not been substantiated. However, a recent association study further indicates a role for human GPCR5B in metabolism by suggesting the receptor is involved in body weight regulation (Speliotes *et al.*, 2010).

GPR48

GPR48 (also known as LGR4) is a class A receptor in the leucine-rich, G protein–coupled receptor (LGR) subfamily (otherwise known as glycoprotein hormone receptor subfamily) (Loh *et al.*, 2001). As with GPRC5B, the distribution of GPR48 has been investigated using northern blot analysis and GPR48-LacZ reporter mice, but differences exists between species and techniques. In human tissue, GPR48 transcript was highly expressed in pancreas, while only moderate expressed in placenta, kidney, brain, heart and muscle (Loh *et al.*, 2001). Northern blot analysis of mouse tissue revealed a species difference in GPR48 mRNA distribution between human and mouse with high transcript expression in liver and kidney, moderate expression in muscle, and low expression in brain, heart and testis (Loh *et al.*, 2001). This is in contrast to GPR48-LacZ reporter mice which showed highest GPR48 transcript expression in kidney, adrenal gland, and testis, medium expression in eye, trachea, cartilage, and cerebellum, and weak expression in brain, with no expression in spleen and pancreas (Van Schoore *et al.*, 2005). Overall, our rat GPR48 ISHH revealed transcript expression similar to that of the mouse but with some species differences. We observed highest mRNA expression in pituitary, thymus and kidney, moderate expression in liver and adipose tissue, low-moderate expression in spleen and testis, and low expression in pancreas and adrenal. Since GPR48 is widely expressed it

may still be a valid candidate to be a fast glucocorticoid receptor. GPR48 transgenic animals have given some insight into the receptor's role *in vivo*. In the uterus, GPR48 KO embryos display eye lid and bone growth retardation characterised by delayed bone formation and decreased osteoblast differentiation and mineralisation, while foetuses display transient anaemia and abnormal definitive erythropoiesis (Jin *et al.*, 2008; Luo *et al.*, 2009; Song *et al.*, 2008). Post gestation, only 40 % of GPR48 KOs survive (with some reports that none reach weaning age), and those that do are born with anterior segment dysgenesis (symptoms include small eyes and cataracts), severely compromised kidney function, and males have a deformed reproductive tract (Luo *et al.*, 2009; Van Schoore *et al.*, 2005; Weng *et al.*, 2008; Kato *et al.*, 2006; Mendive *et al.*, 2006). In addition, ERα is down regulated in male reproductive tissues lacking GPR48 (Li *et al.*, 2010).

Glucocorticoids produced by the foetal adrenals or from the mother via the placenta act as potent differentiation factors close to term. Glucocorticoids promote the maturation of foetal lungs, heart, kidney, gastrointestinal tract and CNS (Ng *et al.*, 2000). Therefore, one would expect that if GPR48 was a fast glucocorticoid receptor, a GPR48 mutant phenotype may possibly have some form of dysfunctional/undeveloped lungs, heart, or gastrointestinal tract, or even be functionally intact due to the presence of GR/MR. This is in contrast to the devastating effects the absence of GPR48 has on embryonic and foetal eye, bone, red blood cells, and male reproductive organ development. GPR48 clearly has an indispensible role in development, and we consider it unlikely to be a prominent candidate for a glucocorticoid receptor. Since the completion of this study, the apparent deorphanisation of the mouse GPR48 has been reported. Carmon and colleagues demonstrated that mouse GPR48 binds the novel extracellular molecules R-spondins 1-4 with high affinity, and mediates R-spondin/Wnt/β-catenin signalling in HEK293 cells (Carmon *et al.*, 2011).

GPR65

The final orphan, GPR65, is a class A receptor previously known as T-cell death-associated gene 8 (TDAG8) (Kyaw *et al.*, 1998). We find GPR65 gene expression predominately in rat thymus, spleen and testis. This is in agreement with a previous northern blot analysis of human tissue which located GPR48 mRNA mainly in lymphoid tissues, including peripheral blood leukocytes, spleen, lymph nodes, and thymus (Kyaw *et al.*, 1998). The prominent expression of GPR65 in lymphoid tissues suggests a role for GPR65 in the immune system. In fact, GPR65 is upregulated in thymocytes during T cell receptor or glucocorticoid-induced apoptosis (Choi *et al.*, 1996). In addition, it has also been suggested that GPR65 binds psychosine (D-galactosyl-β-1,1'sphingosine), a glycosphingolipid that accumulates in the condition Globoid cell leukodystrophy (GLD, also known as Krabbe's disease) (Im *et al.*, 2001). It is proposed that psychosine acts via a GPR65-dependant mechanism to increase

the formation of multinuclear globoid cells from macrophages in the brain (Im *et al.*, 2001). GPR65 has also been identified as a proton-sensing GPCR – extracellular acidic pH stimulates GPR65 to activate cAMP formation in CHO-S cells, inhibits proinflammatory cytokine production via a cAMP/PKA signalling pathway in mouse macrophages, and enhances the tumour development by Lewis lung carcinoma (LLC) cells (Ishii *et al.*, 2005; Mogi *et al.*, 2009; Ihara *et al.*, 2010). Therefore it appears more likely that GPR65 is a photon and/or psychosine receptor rather than a glucocorticoid receptor.

5.4.3 Is this targeted approach the best way to identify a candidate 'fast' glucocorticoid receptor?

After assessing the EST distribution profiles of all known orphan GPCRs (common to human and rodent), determining the tissue expression of nine orphan GPCRs, and reviewing the literature surrounding their potential biological roles, we have deemed three orphans as suitable candidates for a fast glucocorticoid receptor: GPR108, GPR146 and TMEM87B. It should be noted that in some cases where orphan GPCRs have been assigned ligands in the literature, IUPHAR may still acknowledge them as orphans. This is due to 1) prospective ligands have not been confirmed in more than one study; 2) deorphanising has yet to be confirmed in humans; and 3) the lack of evidence that ligand stimulation results in the activation of signalling pathways. Therefore, it is possible that some of the other orphan GPCRs in this study remain glucocorticoid receptor candidates, even if a different candidate ligand has already been proposed.

It is also feasible that a fast glucocorticoid receptor is actually a GPCR with a known validated ligand e.g., CORT may bind the same or a different binding pocket to another ligand. As such, the alternative ligand may have a similar or dissimilar structure to CORT. For example, some reports indicate that progesterone at high concentrations binds the OT receptor, and inhibits OT-induced signalling (Burger *et al.*, 1999). In addition, the CB_1 cannabinoid receptor binds 'endocannabinoids' (e.g., derivatives of arachidonic acid), tetrahydrocannabis derivatives as well as a protein called hemopressin (Heinmann *et al.*, 2007). In this study, we have also made an assumption that a glucocorticoid-binding GPCR is not a chemosensory receptor, yet these receptors are not restricted to sensory tissues and hence may have non-chemosensory ligands (Feldmesser *et al.*, 2006). Moreover, Neuhaus *et al.*, reported that an odorant GPCR, prostate-specific G protein-coupled receptor (PSGR), is activated not only by the odorant β-ionone but also by testosterone metabolites (although specific binding has yet to be shown) (Neuhaus *et al.*, 2009). Similarly, we have assumed that a single GPCR will evoke the fast glucocorticoid response rather than working in concert with, for example, additional proteins (e.g., the pharmacological specificity of the family of calcitonin receptors and calcitonin receptor-like receptors are dictated by additional proteins known as receptor activity-

modifying proteins (RAMPs) (Sexton *et al.*, 2006), or forming a heterodimer with another GPCR (e.g., $GABA_{B1}$ and $GABA_{B2}$ heterodimerise to form the functional $GABA_B$ receptor (Marshall *et al.*, 2010)), or a different family of receptor such as ion channel subunit (e.g., dimerisation between dopamine D_5 and $GABA_A$ γ2 ligand-gated ion channel subunit reduces D_5 mediated cAMP signalling (Liu *et al.*, 2000)). In addition, by initially searching ESTs profiles for candidate GPCRs based on their gene expression in the tissues of interest, we may have possibly discarded some good candidates because of their relatively low abundance. For example, if we were looking for a mouse vasopressin receptor in the same way, we would have missed the V_{1B} receptor due to its general low gene expression (e.g., in the mouse pituitary there was 0 EST transcript out of 16965 cDNA clones), according to the EST profile.

An alternative to the targeted approach of this study would be to test all chemosensory/non-chemosensory orphan GPCRs in unbiased, high-throughput screening assays that could detect glucocorticoid-mediated second messenger responses. This would involve screening approximately 125 mammalian non-chemosensory orphans (common to human and rat) and approximately 418 human chemosensory orphans (which there are approximately 1,474 in rodents) (Gloriam *et al.*, 2007; Harmar et al., 2009). Expression- or functional-based screens may miss unidentified splice variants which may also have a biological role – a GPCR splice variant could behave as a fast glucocorticoid receptor alone or in concert with another receptor (GPCR/steroid receptor/ion channel). Sequencing RNA from all tissues that exhibit fast glucocorticoid responses would likely detect most, if not all GPCRs and their splice variants, and deep (transcriptome) sequencing can achieve this quickly and efficiently (e.g., Roche 454 GS FLX instrument can sequence 500 megabases in 10 hours (Voelkerding *et al.*, 2009). However, these approches are expensive and high throughput assays demand cloning of all receptors for screening. In an attempt to deorphanise our three candidate receptors (see Chapter 6) we used the only high through-put assay available in the laboratory, the IN CELL Analyser 1000. The 96 well plate format of the IN CELL is on a much smaller scale than that of some high throughput assays (with plate formats ranging from 384 to 3456 wells), but is adequate considering we are only testing three orphans in the first instance.

5.4.4 Sense transcript expression?

An interesting observation from the current study was specific GPER and GPR108 sense probe binding in the spleen and kidney, respectively. Although the sense probe is normally used to control the specificity of antisense probe binding, on occasions it highlights the presence of antisense transcript (Foletta *et al.*, 2002). However, according to NCBI/Gene the sequence on the opposing strand to the GPER gene does not code for an obvious protein (i.e., NCBI have termed the sequence

hypothetical protein LOC498154). Intriguingly, the next identified gene upstream of human, rat and mouse GPER encodes GPR146 – whether this has any functional relevance remains to be seen.

GPR108 sense probe binding in the kidney was quite distinct, with binding restricted to the cortex and outer stripe of the outer medulla, possibly labelling the proximal tubules. Referring to NCBI database (e.g., Gene) it appears that the sequence on the opposite strand to GPR108 does not code for a recognised protein, although the gene downstream of this sequence codes for thyroid hormone receptor interactor 10 (Trip10), a protein that has been shown to localise to proximal tubules (Tsuji *et al.*, 1998). It is possible that the sense probe is in fact binding a transcript variant of Trip10 – a variant which shares part of the coding region of Trip10 with a sequence that lays adjacent to the 3'untranslated region of GPR108 (where the riboprobes were directed). This hypothesis could be tested by screening a rat kidney cDNA library with the radiolabelled sense probe and sequencing any cDNA clones obtained. These clones may correspond to a variation of Trip10, or may express a cDNA that has high homology to GPR108. It is highly unlikely that the probe is cross-reacting with another mRNA from a known gene as all of our probes are subject to a BLAST search. The BLAST search with the GPR108 probe obtained sequence matches with a maximum of 20 contiguous bp, which is extremely low considering the GPR108 probe is 329bp long. In any case, hybridisation between 20bp and a target gene is unlikely to remain following the stringent washes within the ISHH protocol (2 x 30 min wash in 0.1 x SSPE at 65°C).

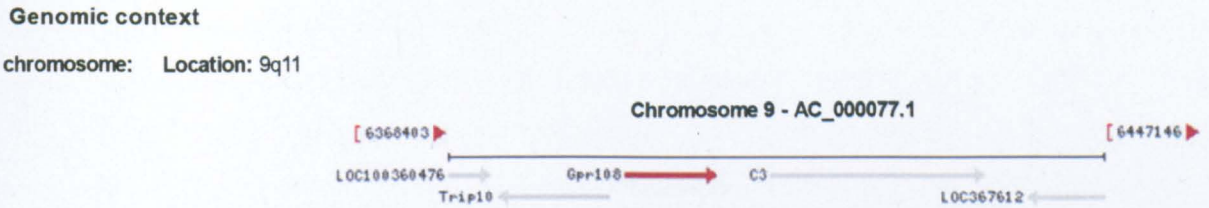

Figure 5.11. Genomic context of the rat GPR108 gene.

Schematic diagram taken from the NCBI database (http://www.ncbi.nlm.nih.gov/gene/316136) depicting the genomic context of the rat GPR108 gene. The sequence on the opposite strand to GPR108 does not code for a recognised protein, while the gene downstream of this sequence codes for Trip10 a protein that has been shown to localise to proximal tubules (Tsuji *et al.*, 1998). It is possible that the sense GPR108 probe binding observed in the kidney is in fact binding a transcript variant of Trip10 – a variant which shares part of the coding region of Trip10 with a sequence that lays adjacent to the 3'untranslated region of GPR108 (where the riboprobes were directed).

5.4.5 Conclusion

Deorphanising receptors based on their distribution profile is not a novel approch - for example, as mentioned previously Matsuda and colleagues deorphanised the CB_1 receptor based partly on similarities between its central transcript distribution and that of a previous binding study with [^{3}H]CP 55,940, a radiolabelled synthetic cannabinoid (Matsuda *et al.*, 1990; Herkenham *et al.*, 1990). Using this same principle we have narrowed down our search for a fast glucocorticoid receptor to three candidates: GPR108, GPR146, and TMEM87B. In the next chapter, we attempt to determine whether the three orphans respond to glucocorticoids via activating the ERK signalling pathway.

Chapter 6: A fast G protein-coupled glucocorticoid receptor?

6.1 Introduction

6.1.1 History of orphan GPCR receptors: discovery and methods of deorphanisation.

In 1986, after exhaustive efforts to biochemically purify adrenergic receptors, Dixon and colleagues cloned the mammalian β2-adrenergic receptor from a hamster genomic library (Dixon *et al.*, 1986). This was a fortunate find, facilitated by the fact that the β2-adrenergic receptor was intronless. It was also a significant discovery - the group not only recognised that the receptor shared sequence homology with bovine opsin but also shared similarities in function: both receptors were involved in G protein-mediated signal transduction (Lefkowitz, 2007). This invigorated research into, and commenced the cloning era of, the GPCRs.

In an attempt to clone related GPCRs, the cDNA for the coding region of the β2-adrenergic receptor gene was radioactively labelled and used to screen genomic libraries under low-stringency hybridisation conditions. In this manner, the rat D_2 receptor (Bunzow *et al.*, 1988), rat 5-HT_{1A} (Albert *et al.*, 1990) and the rat β_1-adrenoceptor were cloned (Machida *et al.*, 1990). Development of increasingly complex cDNA libraries (i.e., libraries containing larger and more cDNA inserts) and the PCR fuelled further GPCR discovery. For example, degenerate primers corresponding to conserved TM regions of known GPCRs were used to amplify fragments from cDNA and genomic templates. Clone fragments were sequenced to check for homology to existing GPCRs, and if novel, used to screen cDNA libraries. Libert and coworkers were one of the first to publish this technique, and identified four orphan GPCRs, RDC1, RDC4, RDC7, and RDC8 from a dog thyroid cDNA library (Libert *et al.*, 1989). The orphans have subsequently been identified as the chemokine CXCR7, serotonin 5-HT_{1D}, adenosine A_1 and A_{2A} receptors, respectively. Numerous other receptors were cloned using this approach including the rat cannabinoid CB_1 (Matsuda *et al.*, 1990), rat vasopressin V_2 (Lolait *et al.*, 1992), rat somatostatin sst_5 (O'Carroll *et al.*, 1992), and human GPER receptors (although GPER remained an orphan until 2005) (Owman *et al.*, 1996). Sequencing of the genome in the late 90's (finally completed in 2003) paved the way for bioinformatic homology screening which predicted the existence of many more orphan (particularly chemosensory) GPCRs, and thus increased the number of known human GPCRs to about 800 (Chung *et al.*, 2008).

In the absence of GPCR sequence homology that may assist in predicting ligand classes – e.g., usually greater than 30% amino acid homology can place a GPCR in a particular subclass – reverse pharmacological techniques have been employed by many laboratories in an effort to deorphanise newly described GPCRs. Often mammalian cells are transfected with orphan GPCRs and screened with a plethora of ligands in the hope of obtaining a functional response. However, the bank of known

potential GPCR ligands is not vast enough to accommodate the growing number of GPCRs. As many of the orphan GPCRs are expressed in the CNS, it seemed intuitively obvious that brain tissue may be the source of novel GPCR ligands. For example, peptidergic brain extracts have been purified and fractionated, and the fractions tested for their ability to stimulate cells expressing orphan GPCRs (Chung *et al.*, 2008). This lead to the discovery of the novel peptides nociceptin, orexins-A and -B, prolactin-releasing peptide, and apelin, the endogenous ligands for the orphan receptors NOP, OX1 and OX2, PRRP, and APJ, respectively (Meunier *et al.*, 1995; Sakurai *et al.*, 1998; Hinuma *et al.*, 1998; Tatemoto *et al.*, 1998). The prospect of deorphanising a receptor at the same time as discovering a new ligand, and in turn unveiling a new biological system, has been an attractive proposition to the pharmaceutical industry. High throughput assays were developed, and a multitude of candidate ligands were screened against orphan receptors expressed in mammalian cells, yeast, or xenopus melanophores. The compiled sets of ligands included known GPCR ligands, possible lipid, peptide, and protein ligands, candidate ligands from other organisms, those predicted from the structure of known GPCR ligands using bioinformatics, and synthetic ligands (Wise *et al.*, 2004). Within a few years 40 receptors were deorphanised (Chung *et al.*, 2008). Unfortunately, in the last 10 years interest has dwindled, and the rate of receptor deorphanisation has declined (Chung *et al.*, 2008). Consequently, the endogenous ligands for about one hundred mammalian orphan GPCRs common to human and rat remain to be identified, although ligands (usually small-molecule, non-peptidergic) from pharmaceutical platforms have been identified in some cases (e.g., Omeros Corporation, press release, 2011).

6.1.2 Are GPR108, GPR146 or TMEM87B fast glucocorticoid receptors?

Numerous lines of evidence suggest the existence of a glucocorticoid binding GPCR (e.g., the binding of [^{3}H]-CORT to amphibian neuronal membranes is inhibited by nonhydrolysable guanyl nucleotides (Orchinik *et al.*, 1992)). In Chapter 5, we hypothesised that one of the remaining mammalian orphan GPCRs may be a fast glucocorticoid receptor, and narrowed the search down to three candidates: GPR108, GPR146, TMEM87B. In this Chapter, we tested this hypothesis by transiently transfecting mammalian cells with each orphan GPCR and determining whether any of the receptors provoked a cellular signalling cascade in response to glucocorticoid treatment. As it is difficult to predict the likely G protein-coupling of each receptor it was imperative that we use a cell signalling assay that would best reflect the stimulation of all of the main G protein-coupling systems. A growing body of evidence has revealed that most GPCR signalling can feed into the ERK1/2 cascade (summarised in Figure 6.1) (Osmond *et al.*, 2005; Gutkind, 2000; Werry *et al.*, 2005; Rozengurt, 2007; Marinissen and Gutkind, 2001; New and Wong, 2007). In addition, glucocorticoids have been shown to activate ERK e.g., DEX augments ERK phosphorylation in the mouse amygdala in response to fear

conditioning, via a non-genomic mechanism (Lee *et al.*, 2011). For these reasons we used the IN CELL Analyser/ERK phosphorylation assay as previously described in chapter 4.

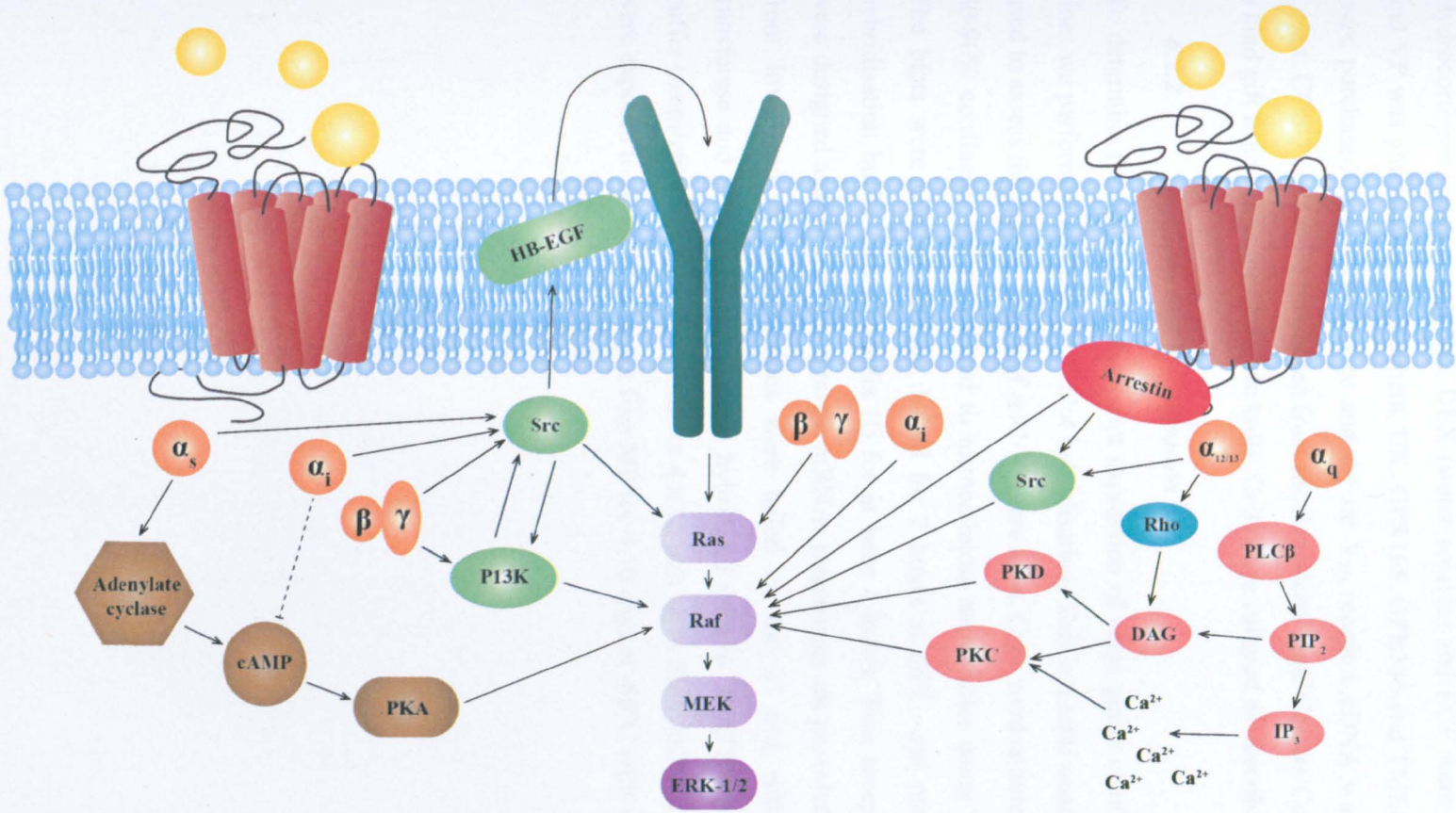

Figure 6.1 Many G protein-coupled signalling pathways converge to stimulate ERK activation.

ERK1/2 is a member of the mitogen-activated protein kinase (MAPK) family of proteins, and has a prominent role in cell differentiation and proliferation (Johnson and Lapadat, 2002). Classically, ERK is activated following the sequential activation of Ras G proteins (Ras), Raf kinases (Raf) and MAPK/ERK kinase 1 and 2 (MEK) (Roux and Blenis, 2004). GPCRs can feed into this pathway via a variety of different G protein-mediated signalling cascades (reviewed in Gutkind, 2000; Werry *et al.*, 2005; Rozengurt, 2007; Marinissen and Gutkind, 2001; New and Wong, 2007) which can be cell context-dependent. The diagram highlights a few examples: **(1)** the $G\alpha_s$ subfamily of G proteins activate adenylyl cyclases to increase adenosine 3',5'-monophosphate (cAMP). Increasing cellular concentrations of cAMP stimulates protein kinase A (PKA), and this can directly activate (and in some instances inhibit) Raf. $G\alpha_s$ may also form a complex with Src tyrosine kinase (Src) leading to receptor tyrosine kinase transactivation (e.g., EGFR). **(2)** $G\alpha_i$ is well known for its inhibition of cAMP production, but it can also interact with Src. Src can directly influence the ERK pathway by activating Ras and also via the stimulation of phosphoinositide 3-kinases (P13K) and/or receptor tyrosine kinases. $G\alpha_i$ can also directly stimulate MEK1-2 via Raf kinases. **(3)** $G\alpha_{q/11}$ activates the phospholipase C isoform β (PLCβ) which catalyses the hydrolyses of phosphatidylinositol 4,5-bisphosphate (PIP_2) into diacylglycerol (DAG) and IP_3. IP_3 subsequently stimulates the release of calcium from intracellular stores. DAG and calcium synergistically act to stimulate protein kinase C (PKC). PKC activates the ERK pathway by direct phosphorylation of Raf (and can also activate Ras). DAG can also stimulate protein kinase D (PKD) and this leads to further activation of Raf. **(4)** Gβγ subunits (often associated with $G\alpha_i$) have been shown to interact with the ERK cascade in many ways. Gβγ can directly stimulate Ras, activate Src, and interact with P13K isoforms which can in turn stimulate Src as well as directly enhance Raf activity. **(5)** $G\alpha_{12/13}$ can also activate the ERK pathway. $G\alpha_{12/13}$ stimulates Rho which infiltrates the PLC/calcium pathway by stimulating DAG – this in turn activates ERK as per point (3). $G\alpha_{12/13}$ can also stimulate Src. **(6)** It is worth noting that GPCRs can activate ERK phosphorylation independently of G proteins (Sun *et al.*, 2007; Luttrell and Gesty-Palmer, 2010). For example, the binding of arrestins to activated receptors can either directly stimulate ERK signalling or via the recruitment of Src. GPCRs can also directly couple to Src – activation of which induces ERK signalling.

6.2 Materials and Methods

6.2.1 Chemicals, cDNA, and cell culture

Hydrocortisone (ethanol soluble), DEX (water soluble) and EGF were purchased from Sigma, UK, and VP was purchased from Bachem, UK. GPR108, GPR146 and TMEM87B receptor cDNA clones were purchased from Geneservice and the rat V_{1B} receptor cDNA was obtained from Dr Stephen Lolait. COS-7 cells were purchased from the American Type Culture Collection and HeLa cells were a kind gift from Professor Craig McArdle. Cells were cultured as described in section 2.5.2.

6.2.2 Northern blot hybridisation

To determine the endogenous transcript expression of some genes of interest in commonly used cell lines we performed northern 'dot' blot hybridisation. This is a semi-quantitative method and it can be used to assess the relative levels of mRNA expression. Cells were cultured in clear 96 well plates until 80-90% confluent, and transferred to nitrocellulose membranes using a 96-well vacuum manifold. The blots were UV-cross-linked, baked for 2 hours at 80°C, and pre-hybridised at 37°C in pre-hybridisation buffer (see Appendix II) for at least 4 hours. Two receptor specific oligonucleotides were designed against individual target mRNAs (sequences are provided in Table 6.1) and purchased from Invitrogen. Oligonucleotides were tailed on the 3' end with terminal deoxynucleotidyl transferase and α-^{32}P-ATP. Blots were hybridised with α-^{32}P-ATP-labelled probes in hybridisation buffer overnight at 37°C, and washed for 4 x 15 min in 1x SSPE/0.2% SDS at 54°C. Hybridised blots were exposed to Amersham Hyper film MP for 4-10 days at -80°C with intensifying screens.

Gene oligonucleotide is directed towards	Oligonucleotide sequences		Corresponding bp of cDNA sequence (example of one variant given)		Genbank Accession number of mRNA variants	GC content of probe (%)		Estimated Tm (°C)		High stringency wash (°C)
	Probe 1	Probe 2	Probe 1	Probe 2		Probe 1	Probe 2	Probe 1	Probe 2	
human GR	5'-CACACTGCTGGGGTTT TCTTCTCTACCAGGAG TTAATGATTCTTTGGA-3'	5'CAGTCCCATTGAGAGT GAAACTGCTTTGGACA GATCTGGCTGCTGCGC-3'	1001-1048 (variant 1)	1211-1258 (variant 1)	NM_001018077 (variant 1) NM_001018074 (variant 2) NM_001018075 (variant 3) NM_001018076 (variant 4) NM_000176 (variant 5) NM_001020825 (variant 6) NM_001024094 (variant 7)	44	54	60	64	54
human MR	5'-CTGATAAATCTTAGCT GGACTCATGCTTCCT TGTTGGTTCTGCTGCTC-3'	5'-CTTCTCTTCATTAAG ACTAGGTCTGGTGCAA AATAGAGAAATTGGCT-3'	721-768 (variant 1)	2833-2880 (variant 1)	NM_000901 (variant 1) NM_001166104 (variant 2)	46	38	61	58	54
human GPR108	5'-ATTACTTGCTCCATCT GAACATCCTCCTCGTCC TCCTGGGGCAGCTGC-3'	5'-TCATAACAGTTCCCGC CCGCTGGCTGTTTTGT TGACTTTGGAGAGGCC-3'	1561-1608 (variant 1)	1631-1678 (variant 1)	NM_001080452 (variant 1) NM_020171 (variant 2)	56	54	65	64	54
human GPR146	5'-CAGGGCAGCTTTTTCA TCAGCCGTTGGAGCTTGC TGGGGAAGCTCTGG-3'	5'-CTACGCCAGCACCTGC TGCACCCCCATGTGGT CCGGGGAGCAGTGCCG-3'	911-958	966-1013	NM_138445	58	71	66	71	54
human TMEM87B	5'-ATCCACTAACACTGGA AGAGCTACATCTGTGA ATGAAGAGGGAATATT-3'	5'-CTGAAGAGAACATTTT TTCAGCCATTTCAGAT CTGGTCATGATTTCCT-3'	1921-1968	1976-2023	NM_032824	40	38	59	58	54

Table 6.1. Summary of oligonucleotide sequences and their predicted properties.

Two oligonucleotides approximately 48bp in length were designed against individual target genes. As some genes code for more than one transcript variant (which may be physiologically active) e.g., human GR has seven different mRNA variants: 1-5 codes for the same protein isoform GRα; 6 codes the protein isoform GRβ; and 7 codes for the protein isoform GRγ, probes were designed against regions of the gene common to all known transcript variants. This also included homologues (and variants) from other species (e.g., human, hamster, and monkey) as expression was investigated in a variety of cells lines (human (HEK293/HeLa), hamster (CHO-K1), or monkey (COS-7) cells)). In instances where the probe was directed to the translated region of the mRNA, maximum effort was made to aim for non-conserved regions of the gene. Oligonucleotides were directed as follows: human GR probes 1 and 2 were both directed to non-conserved portions of the translated region which occurred shortly after the initiating methionine; human MR probe 1 was directed to a sequence in the translated region shortly following the initiating methionine, and probe 2 was directed to a non-conserved translated sequence in the steroid binding region; GPR108, GPR146, and TMEM87B probes 1 and 2 were directed to non-conserved sequences in the translated region just prior to the stop codon. Optimum hybridisation temperature for oligonucleotides is between 37-45°C in a hybridisation solution containing 50% formamide, while the high stringency wash temperature is approximately 5-20°C below Tm (Wilkinson, 1999). As the (% G+C) of the second human MR and TMEM87B probes were low, we reduced the high stringency wash temperature to 54°C (as opposed to 56°C in Chapter 4), even for probes (e.g., GPR146) that could potentially withstand higher washing temperatures.

6.2.3 *Transient transfections and ERK phosphorylation assay*

Cells were seeded (COS-7 cells at 10,000 cells and HeLa cells 15,000 cells per well) into Costar plain black-wall 96-well plates so that the cells were 50% confluent the following day. Transient transfection experiments were performed 24 h after seeding COS-7 or HeLa cells in Costar plain black-wall 96-well plates using Nanofectin as described in section 2.5.3. It was estimated using the X-gal staining assay (previously described in section 2.5.3 and Appendix I) that Nanofectin successfully transfected approximately 30% of COS-7 and HeLa cells with cDNA. The following day cells were serum-starved overnight prior to treatment (constituents of serum-free media are described in section 2.9.1). Cells were stimulated (5-10 min), and processed for the IN CELL ERK assay as previously described in Chapter 4, section 4.2.7.

For wells treated with VP and control or EGF and control, the total amount of ppERK in the whole cell was calculated for each field. These values, following the subtraction of background florescence measured in wells absent of primary antibody (the background was difficult to detect in individual wells due to the high density of cells required for transient transfection), was expressed as AFU. The data obtained from VP and vehicle treated wells was used to calculate a 'ppERK fluorescence threshold' previously described in detail in section 4.2.7. The 'ppERK fluorescence threshold' was applied to ppERK fluorescence data from the glucocorticoid treated or vehicle treated cells transfected with orphan GPCRs. Cells which emitted ppERK fluorescence above that threshold were deemed responsive to agonist stimulation.

6.2.4 *Statistical analysis*

IN CELL Analyser 1000 experiments were performed in 3-6 replicate wells, and experiments were performed at least 2 times. Data is represented in Figures as mean ± standard error of the mean (SEM). Statistical analysis was a one- way ANOVA and Bonferroni multiple comparison test accepting $P < 0.05$ as significantly different.

6.3 Results

6.3.1. Expression of endogenous transcript expression in cells by Northern blot 'dot' hybridisation.

The endogenous transcript expression levels of the orphan GPCRs and glucocorticoid receptors (GR and MR) were investigated in cell lines that are frequently used for stable and transient transfections in our laboratory, and is summarised in Table 6.2. Notably, low-moderate GR transcript expression was observed in HeLa cells, and low-negligible GR expression was found in CHO-K1, COS-7 and HEK293 cells. Low-negligible MR mRNA expression was observed in all of the four cell types. The CHO-K1 and COS-7 cells exhibited moderate GPR108 hybridisation signal, while low-negligible signal was detected in HEK293 and HeLa cells. Low-negligible levels of GPR146 transcript was observed in HeLa cells, but no GPR146 mRNA was detected in CHO-K1, COS-7 and HEK293 cells. Low-negligible TEMEM87B hybridisation signal was found in CHO-K1, COS-7 and HeLa cells, and no TMEM87B was detected in HEK293 cells.

Transcript	Level of expression			
	CHO-K1	COS-7	HEK293	HeLa
GR	-/+	-/+	-/+	+/++
MR	-/+	-/+	-/+	-/+
GPR108	++	++	-/+	-/+
GPR146	-	-	-	-/+
TMEM87B	-/+	-/+	-	-/+

Table 6.2. Results from northern 'dot' blot hybridisation.

The table is a summary of the endogenous transcript expression levels of human GR, MR, GPR108, GPR146, TMEM87B receptors in CHO-K1, COS-7, HEK293 and HeLa cells. Oligonucleotides were labelled with α-^{32}P-ATP and designed towards all transcript variants of the gene of interest. This also included homologues (and variants) from other species e.g., human, hamster monkey as expression was investigated in a variety of cells lines (human (HEK293/HeLa), hamster (CHO-K1), or monkey (COS-7) cells)). +++, high expression; ++, moderate expression; +, low expression; -, negligible expression (signal not above background); N/A, expression in these cell lines were not investigated. Note that the levels of expression are relative – negligible, low or absent mRNA expression by this method does not imply that the cells do not express any mRNA, or that this mRNA is (or isn't) translated into a functional protein.

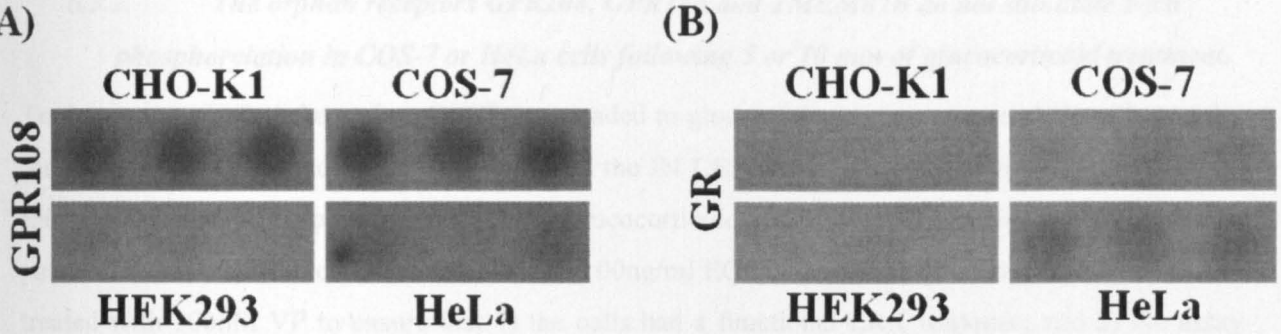

Figure 6.2. Examples of northern 'dot' blot hybridisation film images.

Endogenous GPR108 and GR transcript expression in CHO-K1, COS-7, HEK293 and HeLa cells. **(A)** Moderate GPR108 hybridisation signal was observed in CHO-K1 and COS-7 cells while low-negligible signal was detected in HEK293 and HeLa cells. **(B)** Low-moderate levels of GR mRNA was expressed in HeLa cells, whereas low-negligible GR transcript expression was found in the other cell types.

With the exception of GPR108, the endogenous GPCR orphan transcript expression are low or absent in the cell types investigated. Assuming that GPR108 mRNA translated to protein, CHO-K1 or COS-7 cells would appear suitable for use in the ERK assay without transfection of the GPR108 cDNA i.e., endogenous GPR108 expression in these cell lines may be sufficient to express the orphan receptor. The transfection of additional GPR108 receptor into CHO-K1 or COS-7 cells could even amplify a glucocorticoid response beyond that attributable to endogenous GPR108. The cell types tested are commonly used in deorphanising assays (Irelan and Morgon, 2010; Lecca and Abbacchio, 2008). However, if the orphan GPCRs require the transactivation of EGFR to mediate the glucocorticoid response, then the CHO-K1 line would likely be inappropriate. As described in section 4.3.4 EGF does not stimulate an ERK response in CHO-K1 cells in our hands. The HEK293 cell line used in this thesis is also not the best cell type for transient transfections, since no more than 5% of HEK293 cells were transfected with control vector in the X-gal assay as described in Chapter 2 (see Figure 2.1 in section 2.5.3). On the other hand, at least 30% of COS-7 and HeLa cells were consistently transfected using Nanofectin (see Figure 2.1). Hence COS-7 and HeLa cells were considered the preferable cell types for the deorphanising assay in this Chapter. It is possible that the low-moderate expression of GR in HeLa cells may influence the glucocorticoid signalling in these cells.

6.3.2. *The orphan receptors GPR108, GPR146 and TMEM87B do not stimulate ERK phosphorylation in COS-7 or HeLa cells following 5 or 10 min of glucocorticoid treatment.*

To determine whether the orphan GPCRs responded to glucocorticoids, we transiently transfected the receptors into COS-7 and HeLa cells and used the IN CELL Analyser/ERK phosphorylation assay. Each transfected cell type was treated with glucocorticoids (CORT or DEX) for 5 or 10 mins. In parallel, non-transfected cell were treated with 100ng/ml EGF, and V_{1B} receptor transfected cells were treated with 100nM VP to ensure that 1) the cells had a functional ERK response; and 2) the assay was robust enough to detect a GPCR response in the 30% of transfected cells, and to set the 'ppERK fluorescence threshold' (see section 4.2.7).

In non-transfected COS-7 cells, 100ng/ml EGF treatment for 5 min stimulated almost a 4-fold increase in ppERK fluorescence (N.B., AFU values are normalised to vehicle (therefore, values > 1 are required for an increase): 3.871 ± 0.168). In COS-7 cells transfected with V_{1B} receptor cDNA, 100nM VP treatment for 5 min increased ppERK by approximately 2-fold when compared with vehicle controls (1.837 ± 0.039). However, none of the glucocorticoid treatments (10nM CORT, 100nM CORT, or 100nM DEX) significantly increased ppERK fluorescence in COS-7 cells transfected with GPR108, GPR146, or TMEM87B (Figure 6.3) (N.B., values are % of cells above ppERK fluorescence threshold (example of 100nM given): GPR108, CORT 3.771 ± 0.6074 vs 0.001% ethanol 4.722 ± 1.358, DEX 3.027 ± 0.218 vs vehicle (H_2O) 4.298 ± 0.207; GPR146, CORT 9.910 ± 1.773 vs 0.001% ethanol 10.155 ± 1.669, DEX 7.571 ± 0.045 vehicle 8.144 ± 0.374; TMEM87B, CORT 5.354 ± 0.715 vs 0.001% ethanol 7.312 ± 0.057, DEX 4.573 ± 0.441 vs vehicle 3.958 ± 0.301).

Treatment of non-transfected COS-7 cells with 100ng/ml EGF for 10 min induced a 6-fold increase in ppERK (N.B., AFU values are normalised to vehicle: 6.525 ± 0.328). In cells transfected with V_{1B} receptor cDNA, 10 min 100nM VP treatment lead to a 2-fold rise in ppERK when compared with vehicle (2.398 ± 0.033). As with 5 min, 10 min glucocorticoid treatment (10nM CORT, 100nM CORT, or 100nM DEX) did not significantly increase ppERK in COS-7 cells transfected with GPR108, GPR146 or TMEM87B (Figure 6.4) (N.B., values are % of cells above ppERK fluorescence threshold (example of 100nM given): GPR108, CORT 4.963 ± 0.607 vs 0.001% ethanol 1.561 ± 0.163, DEX 1.389 ± 0.161 vs vehicle 1.558 ± 0.336; GPR146, CORT 4.440 ± 0.547 vs 0.001% ethanol 1.327 ± 0.081, DEX 2.121 ± 1.057 vs vehicle 0.910 ± 0.036; TMEM87B, CORT 1.838 ± 0.626 vs 0.001% ethanol 0.906 ± 0.418, DEX 0.665 ± 0.129 vs vehicle 1.407 ± 0.466).

It is worth noting that background levels of ppERK were elevated in COS-7 cells following 5 min agonist- or vehicle-treatment when compared with respective 10 min treatments. Thus there was a

higher percentage of vehicle- or agonist-treated cells emitting ppERK fluorescence above threshold at 5 min when compared with 10 min. Mechanical stimulation during agonist loading may have lead to a the increase in baseline ppERK which was apparent at 5 min, but not at 10 min – 10 min was perhaps long enough to diminish the non-specific loading effects on ERK activation in this case.

In non-transfected HeLa cells, EGF treatment (100ng/ml for 5 min) activated a robust ERK response leading to a 16-fold increase in ppERK (N.B., AFU values are normalised to vehicle: 16.690 ± 0.474). In V_{1B} receptor transfected HeLa cells, VP treatment (100nM for 5 min) increased ppERK by almost 5-fold (4.919 ± 0.251). As was observed in COS-7 cells, glucocorticoid treatment (10nM CORT, 100nM CORT, or 100nM DEX for 5 min) did not increase ppERK in HeLa cells transfected with GPR108, GPR146, or TMEM87B (Figure 6.5) (N.B., values are % of cells above ppERK fluorescence threshold (example of 100nM given): GPR108, CORT 0.176 ± 0.09 vs 0.001% ethanol 0.105 ± 0.038, DEX 0.057 ± 0.057 vs vehicle 0.019 ± 0.019; GPR146, CORT 0.064 ± 0.064 vs 0.001% ethanol 0.138 ± 0.083, DEX 0.135 ± 0.083 vs vehicle 0.022 ± 0.022; TMEM87B, CORT 0.021 ± 0.021 vs 0.001% ethanol 0.141 ± 0.071, DEX 0.039 ± 0.039 vs vehicle 0.0 ± 0.0).

Stimulation of non-transfected HeLa cells with 100ng/ml EGF for 10 min increased ppERK by 14-fold (N.B., AFU values are normalised to vehicle: 14.343 ± 0.704) . In V_{1B} receptor-transfected HeLa cells, 100nM VP treatment for 10 min increased ppERK by 3-fold (3.339 ± 0.083). Concomitant with the COS-7 cell data, glucocorticoid treatment (10nM CORT, 100nM CORT, or 100nM DEX for 10 min) did not significantly induce an ERK response in HeLa cells transfected with GPR108, GPR146, TMEM87B (Figure 6.6) (N.B., values are % of cells above ppERK fluorescence threshold (example of 100nM given): GPR108, CORT 0.040 ± 0.020 vs 0.001% ethanol 0.097 ± 0.052, DEX 0.764 ± 0.418 vs vehicle 0.252 ± 0.087; GPR146, CORT 0 ± 0 vs 0.001% ethanol 0.17 ± 0.17, DEX 1.653 ± 0.393 vs vehicle 1.673 ± 0.402; TMEM87B, CORT 0.188 ± 0.053 vs 0.001% ethanol 0.142 ± 0.057, DEX 1.962 ± 0.642 vs vehicle 1.718 ± 0.191).

While the mechanical element of agonist loading appeared to have non-specific effects on ppERK levels in COS-7 cells, it showed little effect on HeLa cells. The background ppERK levels were noticeably lower in HeLa cells when compared with COS-7 cells (as depicted by the % of cells expressing ppERK above threshold in the graphs of Figures 6.3-6.6), which meant that there were far less vehicle or glucocorticoid treated HeLa cells with ppERK fluorescence above the 'ppERK fluorescence threshold'.

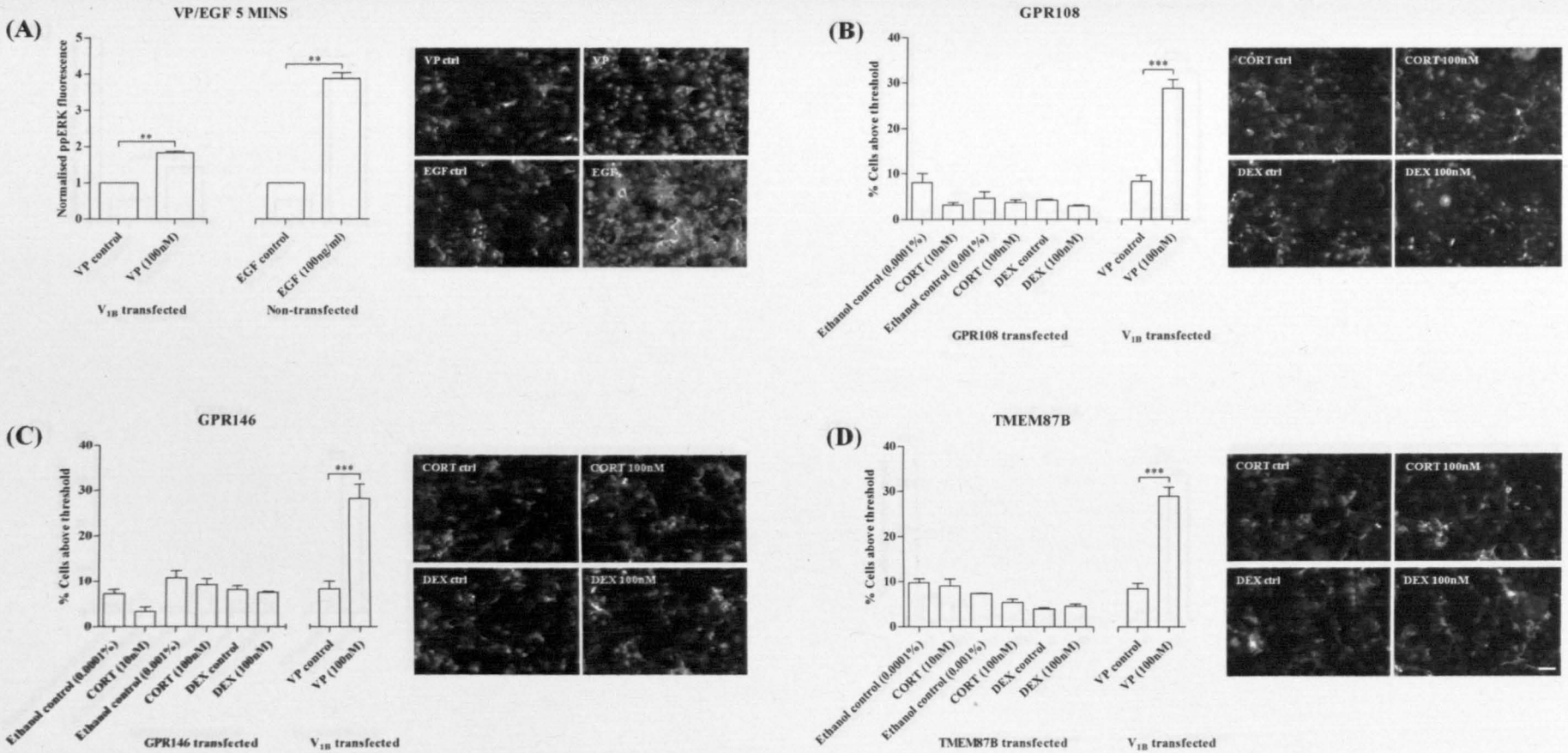

Figure 6.3. The orphan receptors GPR108, GPR146 and TMEM87B do not stimulate ERK phosphorylation in COS-7 cells following 5 min of glucocorticoid treatment.

(A) In non-transfected cells, 100ng/ml EGF stimulated a highly significant increase in ppERK fluorescence, as represented by an increase in ppERK fluorescence. In COS-7 cells transiently transfected with V_{1B} cDNA, 100nM VP treatment for 5 min also stimulated a significant increase in ppERK fluorescence when compared with vehicle controls. The AFU data obtained with the V_{1B} receptor transfected COS-7 cells was used to set a threshold as described in section 4.2.7. The proportion of cells displaying an ERK response (emit ppERK fluorescence above threshold) following glucocorticoid treatment (10nM or 100nM CORT, or 100nM DEX for 5 min) was not significantly different from vehicle in GPR108 transfected (B), GPR146 transfected (C), or TMEM87B transfected (D) COS-7 cells. Graphs are representative of at least two fields, from triplicate wells and two separate experiments (mean ± SEM, n=2). Statistical analysis comparing vehicle-treated vs either EGF- or VP-treated (A-D) was performed using a students *t*-test. Statistical analysis comparing vehicle-treated versus glucocorticoid-treated was performed using one-way ANOVA and the Bonferroni multiple comparison test. **, $p < 0.01$; ***, $p < 0.001$. Adjacent to each graph are some representative images of cells stained with anti-ppERK antibodies treated with control (ctrl) or agonist. Scale bar, 100µm.

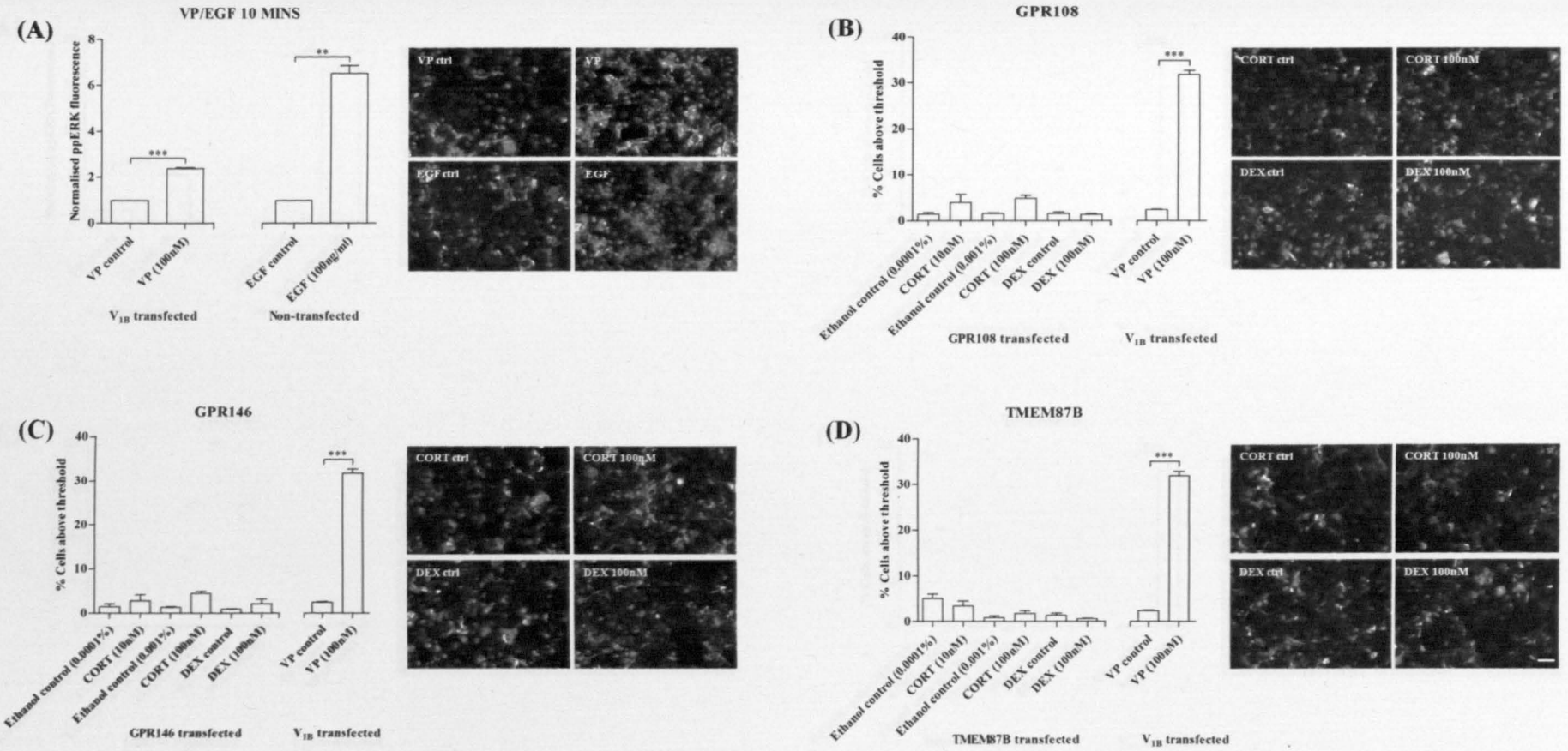

Figure 6.4. The orphan receptors GPR108, GPR146 and TMEM87B do not stimulate ERK phosphorylation in COS-7 cells following 10 min of glucocorticoid treatment.

In non-transfected cells, 100ng/ml EGF stimulated a highly significant increase in ppERK fluorescence, as represented by an increase in ppERK fluorescence. In COS-7 cells transiently transfected with V_{1B} cDNA, 100nM VP treatment for 10 min also stimulated a highly significant increase in ppERK fluorescence when compared with vehicle controls. The AFU data obtained with the V_{1B} receptor transfected COS-7 cells was used to set a threshold as described in section 4.2.7. The proportion of cells displaying an ERK response (emit ppERK fluorescence above threshold) following glucocorticoid treatment (10nM or 100nM CORT, or 100nM DEX for 10 min) was not significantly different from vehicle in GPR108 transfected (B), GPR146 transfected (C), or TMEM87B transfected (D) COS-7 cells. Graphs are representative of at least two fields, from triplicate wells and two separate experiments (mean ± SEM, n=2). Statistical analysis comparing vehicle-treated vs either EGF- or VP-treated (A-D) was performed using a students *t*-test. Statistical analysis comparing vehicle-treated versus glucocorticoid-treated was performed using one-way ANOVA and the Bonferroni multiple comparison test. **, $p < 0.01$; ***, $p < 0.001$. Adjacent to each graph are some representative images of cells stained with anti-ppERK antibodies treated with control (ctrl) or agonist. Scale bar, 100μm.

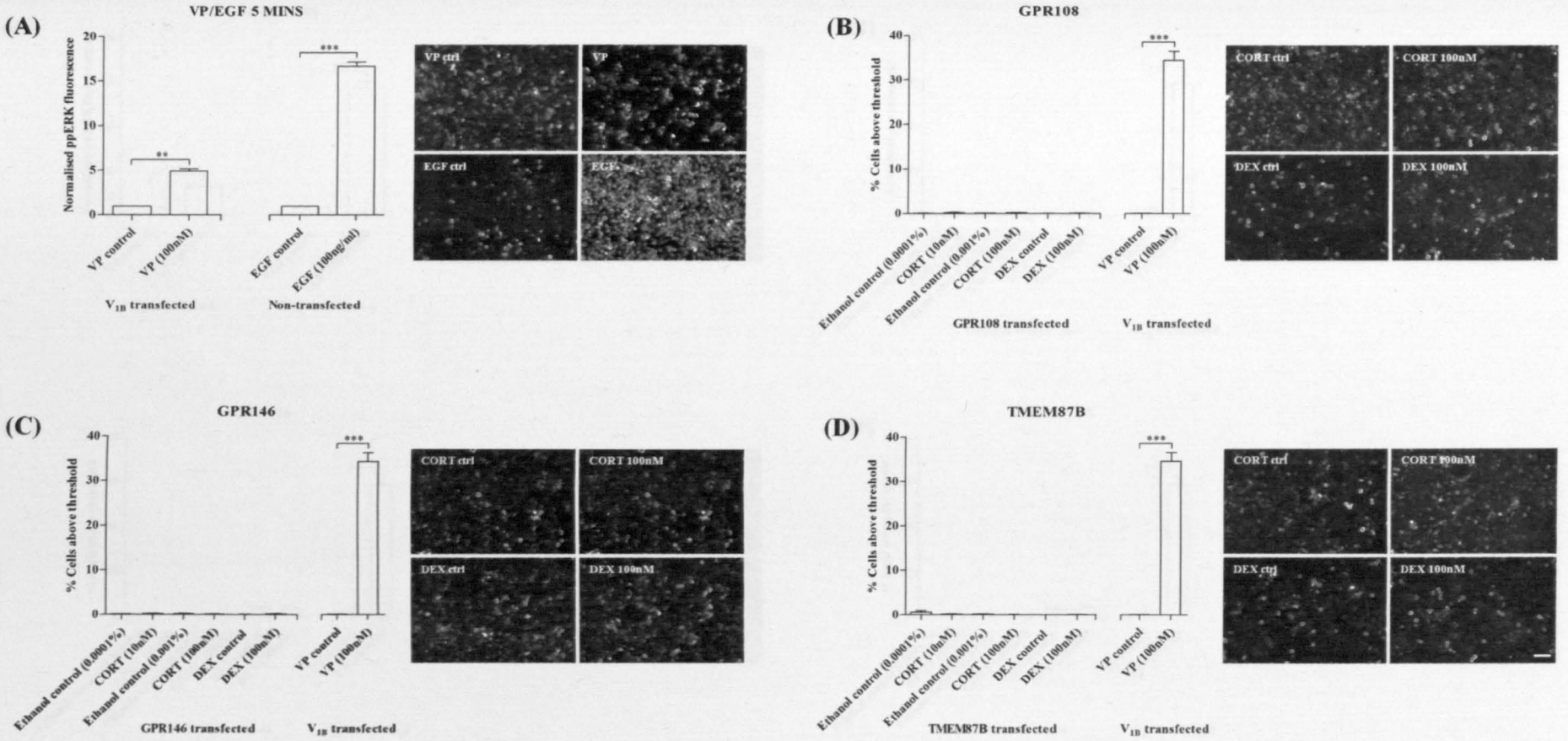

Figure 6.5. The orphan receptors GPR108, GPR146 and TMEM87B do not stimulate ERK phosphorylation in HeLa cells following 5 min of glucocorticoid treatment.

(A) In non-transfected cells, 100ng/ml EGF stimulated a highly significant increase in ppERK fluorescence, as represented by an increase in ppERK fluorescence. In HeLa cells transiently transfected with V_{1B} cDNA, 100nM VP treatment for 5 min also stimulated a highly significant increase in ppERK fluorescence when compared with vehicle controls. The AFU data obtained with the V_{1B} receptor transfected HeLa cells was used to set a threshold as described in section 4.2.7. The proportion of cells displaying an ERK response (emit ppERK fluorescence above threshold) following glucocorticoid treatment (10nM or 100nM CORT, or 100nM DEX for 5 min) was not significantly different from vehicle in GPR108 transfected (B), GPR146 transfected (C), or TMEM87B transfected (D) HeLa cells. Graphs are representative of at least two fields, from triplicate wells and two separate experiments (mean ± SEM, n=2). Statistical analysis comparing vehicle-treated vs either EGF- or VP-treated (A-D) was performed using a students *t*-test. Statistical analysis comparing vehicle-treated versus glucocorticoid-treated was performed using one-way ANOVA and the Bonferroni multiple comparison test. **, $p < 0.01$; ***, $p < 0.001$. Adjacent to each graph are some representative images of cells stained with anti-ppERK antibodies treated with control (ctrl) or agonist. Scale bar, 100μm.

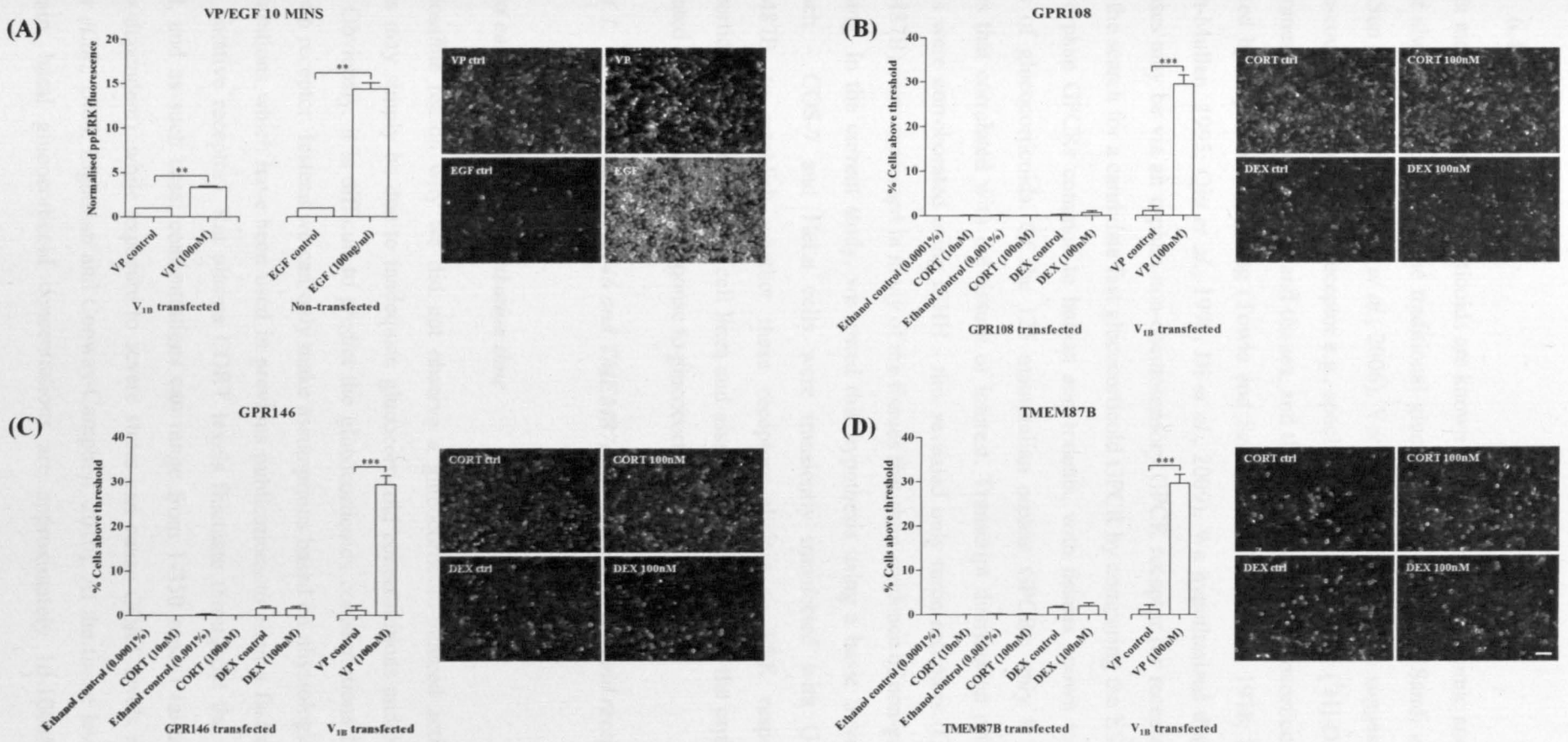

Figure 6.6 The orphan receptors GPR108, GPR146 and TMEM87B do not stimulate ERK phosphorylation in HeLa cells following 10 min of glucocorticoid treatment.

(A) In non-transfected cells, 100ng/ml EGF stimulated a highly significant increase in ppERK fluorescence, as represented by an increase in ppERK fluorescence. In HeLa cells transiently transfected with V_{1B} cDNA, 100nM VP treatment for 10 min also stimulated a highly significant increase in ppERK fluorescence when compared with vehicle controls. The AFU data obtained with the V_{1B} receptor transfected HeLa cells was used to set a threshold as described in section 4.2.7. The proportion of cells displaying an ERK response (emit ppERK fluorescence above threshold) following glucocorticoid treatment (10nM or 100nM CORT, or 100nM DEX for 10 min) was not significantly different from vehicle in GPR108 transfected (B), GPR146 transfected (C), or TMEM87B transfected (D) HeLa cells. Graphs are representative of at least two fields, from triplicate wells and two separate experiments (mean ± SEM, n=2). Statistical analysis comparing vehicle-treated vs either EGF- or VP-treated (A-D) was performed using a students *t*-test. Statistical analysis comparing vehicle-treated versus glucocorticoid-treated was performed using one-way ANOVA and the Bonferroni multiple comparison test. **, $p < 0.01$; ***, $p < 0.001$. Adjacent to each graph are some representative images of cells stained with anti-ppERK antibodies treated with control (ctrl) or agonist. Scale bar, 100μm.

6.4 Discussion

As with many steroids, glucocorticoids are known to elicit fast non-genomic and genomic effects that are not always attributable to the traditional glucocorticoid receptors (Sandi *et al.*, 1996; Di *et al.*, 2005; Sun *et al.*, 2006; Wiegert *et al.*, 2006). Various lines of evidence suggest the existence of a G protein-coupled glucocorticoid receptor e.g., specific [^{3}H]-CORT and/or [^{3}H]-DEX binding to plasma membranes of a variety of cells and tissues, and the fast effects of glucocorticoids often appear to be mediated by G protein signalling (Towle and Sze, 1983; Koch *et al.*, 1978; Harrison *et al.*, 1979, ffrench-Mullen, 1995; Qiu *et al.*, 1998, Di *et al.*, 2009). We hypothesised that 'fast' glucocorticoid responses may be via an orphan non-chemosensory GPCR receptor (or receptors). In Chapter 5, we began the search for a candidate fast glucocorticoid GPCR by comparing the EST distribution profiles of all orphan GPCRs common to human and rodents, with tissues known to exhibit non-genomic effects of glucocorticoids. Of the 125 mammalian orphan GPCRs, only 9 had EST distribution profiles that correlated with the tissues of interest. Transcript distribution profiles of the 9 orphan GPCRs were corroborated using ISHH - this revealed only three receptors (GPR108, GPR146 and TMEM87B) were expressed in many of the tissues that show evidence of non-genomic glucocorticoid signalling. In the current study, we tested this hypothesis using a basic 'reverse pharmacological' approach – COS-7 and HeLa cells were transiently transfected with GPR108, GPR146, or TMEM87B, to establish whether these receptors elicited an ERK response in response to glucocorticoid treatment. In the cell lines and assay we chose, none of the orphan GPCR candidates stimulated ERK signalling in response to glucocorticoids.

6.4.1. GPR108, GPR146 and TMEM87B are not glucocorticoid receptors?

Agonist concentrations and incubation time

One possible reason why we did not observe a glucocorticoid-induced activation of the orphan GPCRs may simply be due to inadequate glucocorticoid concentrations and/or (agonist) incubation times. Obviously, it is difficult to predict the glucocorticoids concentrations that would activate an unknown receptor. Instead we can only make assumptions based on physiological levels and also the concentrations which have been used in previous publications to elicit a fast non-genomic response (via a putative receptor). Rat plasma CORT levels fluctuate throughout the day in the unstressed animal, and as such basal concentrations can range from 1-350 nmol/l (although this is sex- and species-dependent), while exposure to severe stress can cause CORT levels to rise to 1500 nmol/l (Haller *et al.*, 2008; Lightman and Conway-Campbell, 2010). At the tissue level, for example in the rat brain, basal glucocorticoid concentrations are approximately 10-100nM, and can increase

anywhere from 1μM to 10μM during stressful periods (Haller *et al.*, 2008). Studies which have observed non-genomic effects of glucocorticoids in the brain have done so with locally delivered concentrations ranging from 10pM to 500μM (ffrench-Mullen, 1995; Evanson *et al.*, 2010; Di *et al.*, 2005; Liu *et al.*, 1995; Takahashi *et al.*, 2002; Wiegert *et al.*, 2006). For example, CORT concentrations from 10pM to 1μM rapidly inhibits voltage-activated calcium channel currents in adult guinea pig hippocampal CA1 neurones, and CORT concentrations between 100nM and 500μM prolong NMDA receptor-mediated elevations in intracellular calcium in cultured rat hippocampal neurones (ffrench-Mullen, 1995; Takahashi *et al.*, 2002).

ERK 1/2 are activated in minutes to a large range of stimuli e.g., for many GPCRs (e.g., acetylcholine M_1 and M_3, neurotensin NTS_1, cholecystokinin CCK_2, and gherlin receptors) the maximal ERK1/2 response occurs somewhere between 5 and 10 minutes after agonist activation (Ebisuya *et al.*, 2005; Osmond *et al.*, 2005; Mousseaux *et al.*, 2006). The duration and magnitude of an ERK response is controlled by many other regulators in the cell, including scaffold proteins, GTPases, and other signalling pathways (Ebisuya *et al.*, 2005). For this reason, it cannot be assumed that the putative glucocorticoid receptor will have an ERK response comparable to other GPCRs - although previous studies have indicated that an ERK response to glucocorticoids occurs rapidly and is maintained for periods well within the scope of this study. For example, DEX (100nM) rapidly induces ERK 1/2 phosphorylation in rat preovulatory granulosa GSP53-10 cells (within 1 min), with a maximal ERK response appearing between 10 and 20 min (Sasson *et al.*, 2003).

Therefore, the CORT/DEX concentrations and ligand incubation times used within this Chapter are comparable with other studies that have observed fast effects of glucocorticoids. This suggests that GPR108, GPR146 or TMEM87B are not glucocorticoid receptors. Nevertheless, we cannot rule out the possibility that the orphan receptors may well be activated by glucocorticoids in a different experimental paradigm e.g., in an alternative cell type or using another cell signalling assay.

COS-7 and HeLa Cells

It is possible that COS-7 and HeLa cells lack a component vital for GPCR/glucocorticoid signalling. However, this is unlikely considering that 1) COS-7 and HeLa cells are very common cell types used in GPCR mediated-cell signalling assays involving many types of GPCR subfamilies that couple to similar and different G-proteins; 2) COS-7 cells in particular are often used in deorphanisation assays; and 3) the activation of ERK 1/2 in COS-7 cells has been shown to be possible from a variety of GPCR signalling inputs (Irelan and Morgon, 2010; Lecca and Abbacchio, 2008; Osmond *et al.*, 2005). Besides, the VP/V_{1B} receptor activation of ERK provides evidence that these cell lines in our hands are not devoid of GPCR- and G protein-mediated signalling.

As mentioned in Chapter 5, the orphans may also require the expression of an additional protein to conduct glucocorticoid-mediated signalling. For example, the receptor may rely on a modifying protein (e.g., RAMPS), or is only functionally active on forming a heterodimer (or oligomer/ signalsome) with another receptor (or a multitude of receptors and/or proteins) - possibly another GPCR (e.g., dopamine receptor D_2 and the somatostatin receptor SSTR5 heterodimer has greater affinity for both dopamine and SST agonists and enhanced G protein and effector coupling to adenylyl cyclase (Rocheville *et al.*, 2000)), a non-related receptor such as an ion channel (e.g., direct interaction between dopamine D_1 receptors and NMDA glutamate receptor subunits GluN1 and GluN2A inhibits NMDA receptor-gated currents (Lee *et al.*, 2002)), or even a steroid receptor such as GR and/or MR. As stated in Chapter 4, it is suspected that in some instances GPER may work in concert with ERα (Levin, 2009). Transfection of orphan GPCRs into cell lines that endogenously express other receptor(s) or interacting protein(s) has the potential to affect receptor trafficking and signalling as well as ligand binding (Prinster *et al.*, 2005). For instance, α_{1D}-adrenoceptor requires heterodimerisation with α_{1B}- or β_2-adrenoceptors to enhance cell surface expression and functional activity (Uberti *et al.*, 2003, 2005). Thus if activation of the putative glucocorticoid-binding GPCR is dependent on oligomer formation then perhaps GPCR/glucocorticoid signalling is limited to cell types which express the correct proteins - which may or may not be present in COS-7 or HeLa cells.

If the putative receptor requires the expression of GR or MR to elicit a response, the low expression or possible absence of these receptors from COS-7 and HeLa (as indicated with Northern 'blot' hybridisation) may explain why there was an absence of glucocorticoid activation. On the other hand, there are studies that indicate that the traditional receptors are not always involved in fast glucocorticoid signalling suggesting they do not always need to be present. For instance, high doses of CORT (2.5 or 5mg/kg that mimic plasma concentrations produced by substantial stress) rapidly increase the locomotor response displayed by rats in a novel environment, which is not prevented with administration of GR and MR antagonists (Sandi *et al.*, 1996); BSA-CORT (presumptive cell membrane-impermeable CORT) increases ERK1/2 phosphorylation in rat embryonic hippocampal neurones independently of GR and MR (Xiao *et al.*, 2005); and DEX (via PKA and ERK1/2 signalling pathways) accelerates intracellular pH recovery after acid load in human bronchial epithelial (16HBE14o$^-$) cells which is unaffected by treatment with classical GR or MR antagonists (Verrière *et al.*, 2005).

Alternative deorphanisation assays

It is difficult to predict which G proteins the orphan GPCRs are likely to couple to, particularly as GPCRs often have promiscuous relationships with these proteins. For instance, the coupling of GPCRs to G proteins can change depending the nature of the ligands, e.g., the recently deorphanised

GPCR, LPAR6, is stimulated by the endogenous ligands lysophosphatidic acid (LPA) and farnesyl pyrophosphate (FPP), and following activation by LPA, LPAR6 can couple to both $G\alpha_i$ and/or $G\alpha_{12/13}$ family of proteins to initiate the ERK and Rho signalling pathways, respectively, whereas FPP activates $G\alpha_{12/13}$ but not $G\alpha_i$ (Pasternack *et al.*, 2008; Lee *et al.*, 2009). For this reason, we used an ERK signalling assay, since many GPCR/G protein-mediated signalling cascades converge into this pathway (see Figure 6.1) and of all the GPCR-mediated signalling pathways it is considered one of the most 'universal'. On the other hand, if activation of the orphan GPCRs by glucocorticoids stimulated an alternative (or even 'unknown') signalling pathway in COS-7 and HeLa cells types which does not stimulate ERK phosphorylation, then deorphanisation would likely be impossible using our IN CELL assay. Other deorphanising protocols have also addressed this issue, by using for example, [^{35}S]GTPγS binding assays and cell lines engineered to express promiscuous G proteins.

The [^{35}S]GTPγS binding assay relies solely on the stimulation of G proteins to determine receptor activation. As described in Chapter 1, GPCR-ligand interaction results in guanine nucleotide exchange (the replacement of GDP for GTP) on the α-subunit, leading to the dissociation of the α-subunit from the βγ complex. Hence, ligand induced-GPCR stimulation can be monitored by measuring the binding of [^{35}S]GTPγS. While this assay appears attractive at face value, it is often restricted to $G\alpha_i$ family of proteins (unless the assay is combined with immuno-capture techniques e.g., immunoprecipitation of Gα-subunits, and/or over expression of GPCR-Gα fusion proteins), as they have substantially higher rates of guanine nucleotide exchange compared to other G proteins (Milligan, 2003; Seifert *et al.*, 1999).

Murine $G\alpha_{15}$, and its human counterpart $G\alpha_{16}$, are members of the $G\alpha_q$ family of G proteins and are only expressed in a subset of haematopoietic cells. Their promiscuous nature was first identified by Offermanns and Simon, who noticed that $G\alpha_{15}$ and $G\alpha_{16}$ are able to couple to a wide variety of GPCRs that would otherwise associate with a different family of Gα protein (i.e., $G\alpha_s$, $G\alpha_i$, $G\alpha_{12/13}$) - upon ligand mediated-stimulation these GPCRs (via $G\alpha_{15}$ or $G\alpha_{16}$) activate calcium mobilisation (Offermanns and Simon, 1995). Therefore, in terms of deorphanisation, cDNAs encoding orphan GPCRs and $G\alpha_{15/16}$ can be co-transfected into cell lines (e.g., COS-7) and stimulated with an array of putative ligands in the hope of eliciting a calcium response (Offermanns and Simon, 1995). However, $G\alpha_{15}$ and $G\alpha_{16}$ do not recognise all GPCRs e.g., several $G\alpha_i$-linked receptors are incapable of activating phospholipase C via $G\alpha_{16}$. Attempts to construct 'universal' G protein adapters have uncovered two highly promiscuous chimeras: $16z_{25}$ or $16z_{44}$ - hybrids between the G proteins $G\alpha_{16}$ and $G\alpha_z$ (member of the Gαi family). $16z_{25}$ and $16z_{44}$ have the back bone $G\alpha_{16}$ protein and also 25 or 44 amino acids from the C-terminal domain of of $G\alpha_z$, respectively (Mody *et al.*, 2000). They are said to be superior in sensitivity and efficiency when mediating ligand-induced PLCβ activity for $G\alpha_i$-

linked receptors when compared with the parental $G\alpha_{16}$, but their interactions with $G\alpha_s$-linked receptors are slightly impaired (Mody *et al.*, 2000; Liu *et al.*, 2003).

The above techniques are examples of deorphanising strategies that are not reliant on prior knowledge of GPCR signalling. However, both techniques appear to show a certain level of bias towards different GPCRs i.e., receptors that would normally couple to G_i (binding assay) and/or $G\alpha_q$ (promiscuous G proteins) (Lecca and Abbracchio, 2008; Mody *et al.*, 2000). The ERK phosphorylation assay used in this Chapter has the potential to incorporate signalling from all of the major G protein families ($G\alpha_s$, $G\alpha_i$, $G\alpha_q$ and $G\alpha_{12/13}$), as well as G protein-independent pathways i.e., GPCRs are also involved in G protein-independent (possibly arrestin and/or Tyrosine kinase Src dependent) activation of ERK1/2 (see Figure 6.1) (Sun *et al.*, 2007; Luttrell and Gesty-Palmer, 2010). Therefore, even if GPR108, GPR146 and TMEM87B signal in the absence of G proteins, they may still activate the ERK pathway. Moreover, glucocorticoids have been reported to activate ERK in a variety of cell types e.g., rat PC-12 (adrenal chromaffin tumour) (Liu *et al.*, 2001), rat preovulatory granulosa (Sasson *et al.*, 2003), rat embryonic hippocampal neurones (Xiao *et al.*, 2005), human bronchial epithelial (Verrière *et al.*, 2005), and bovine lens epithelial cells (Samadi and Cenedella, 2003) suggesting that responsiveness may be less rather than more 'tissue-specific.'

It is conceivable that GPR108, GPR146 and TMEM87B do not have endogenous ligands, or even biological roles. Some calculations suggest that approximately 17% of non-olfactory GPCRs have become redundant during evolution (Schöneberg *et al.*, 2004) – although this is based on identified pseudogenes, of which non-functionality is disputable (Pink *et al.*, 2011). In the absence of known ligands it is difficult to demonstrate that GPR108, GPR146 and TMEM87B are functionally active. To address this issue, one could induce constitutive receptor activity with the view to activate second messenger signalling. Constitutive activity can be induced by a number of means including receptor overexpression, site-directed mutagenesis (e.g., alteration of the ionic lock between TM3 and TM6, by charge-neutralisation mutation of D/E residue in TM6 or mutation of D/E in TM3 to either A or N) or even by G protein overexpression (i.e., overexpression of Gαq in HEK293 cells upregulates constitutive activity of angiotensin II AT_1 receptors) (Scragg *et al.*, 2005; Smit *et al.*, 2007). Inducing constitutive activity in functional receptors may give insight into possible G protein-coupling, and providing the GPCR couples to the same G proteins during ligand-dependant and -constitutive signalling, indicate the most appropriate cell signalling assay for deorphanisation. Drug discovery programmes have benefited from screening approaches that use constitutively active GPCRs, for example constitutively activating receptor technology (CART) screens constitutive active non-orphan and orphan GPCRs to identify reagents that regulate ligand-independent receptor activity, such as allosteric modulators and inverse agonists (Chalmers and Behan, 2002). This is of particular importance in diseases where the eitology relates to gain or loss in GPCR constitutively activity e.g.,

constitutively active mutants in the thyroid-stimulating hormone TSH receptor gene causes autonomous secretion of thyroid hormones, and constitutively active mutations of the calcium sensing CaS receptor results in hypoparathyroidism; while that loss of constitutive activity in mutant melanocortin MC_4 receptors is one cause of obesity (reviewed in Smit *et al.*, 2007 and Tao, 2008). Thus, CART can identify potential antagonists and inverse agonists of GPCRs that lack known endogenous/exogenous ligands, which are subsequently used *in vitro*/*in vivo* to elucidate biological roles of the orphan receptors (reducing the need for transgenic animals) (Chalmers and Behan, 2002).

6.4.2. Other potential candidates?

Since the orphan candidates within this Chapter are unlikely glucocorticoid receptors, the identity of the putative fast glucocorticoid receptor still remains to be discovered. As emphasised in Chapter 5, we restricted out pursuit for a fast glucocorticoid receptor to orphan non-olfactory GPCRs. Of course it is possible that the initial EST distribution profile search of the 125 orphan GPCRs overlooked some potential candidates i.e., EST profiles did not accurately reflect orphan receptor expression in the tissues of interest, and thus some orphans would inevitably be disregarded. Equally, it is possible that other non-orphan or even olfactory GPCRs may remain candidates. Furthermore, one cannot rule out the possibility that the fast-glucocorticoid receptor is in fact a membrane-bound nuclear receptor, distinct from GR and MR.

A different orphan GPCR?

With approximately 360 human non-chemosensory GPCRs of which approximately 125 are orphans (Chung *et al.*, 2008; Harmar *et al.*, 2009), it seemed intuitive to begin the search for a fast glucocorticoid receptor with receptors yet to be assigned a ligand. Our initial search of human and rodent EST distribution profiles of the 125 orphan GPCRs gave rise to 9 potential candidates – but the fast glucocorticoid receptor could conceivably be any of the other 91. Whether any of the other orphans are activated by glucocorticoids could be investigated in the deorphanising assay used in this study - although all 91 receptors would have to be cloned and expressed in cells which would be quite daunting given the time it would take, materials consumed, and the possibility of 'failure'.

As highlighted in Chapter 1 and in Supplementary Table 8, there are instances in the literature of agonist-mediated regulation in GPCR transcript expression. For example, noradrenaline treatment (6 hours) increases α_{1B} adrenoceptor transcripts (6-fold) in cultured pineal glands via a cAMP-dependent mechanism (Coon *et al.*, 1997), while noradrenaline (4 hours) greatly reduces (75%) α_{1B} adrenoceptor mRNA in rabbit aorta vascular smooth muscle cells (Izzo *et al.*, 1990). In the PVN, chronic (4 week) subcutaneous infusions of angiotensin II increases AT_1 receptor mRNA expression (1.5-2 fold), while an acute 0.1μg CRF intra-PVN microinjection increases CRF_1 transcript (~3 fold) (Wei *et al.*, 2009; Konishi *et al.*, 2003). Therefore, it may be possible to determine which of the orphan GPCRs are most

likely to be a fast glucocorticoid receptor by observing changes in transcript expression (possibly up- or down-regulation) following treatment with CORT or DEX or in response to an acute stressor (although this would likely activate non-glucocorticoid pathways as well). This global approach may be achieved by employing DNA microarray-based transcriptional analysis: rats would be exposed to acute or chronic glucocorticoids, sacrificed, and then RNA extracted from tissues known to exert fast glucocorticoid effects (listed in Chapter 5). The RNA extractions from control vs treated tissue would be exposed to rat genome cDNA arrays, in the hope of identifying regulated orphan GPCR transcripts. The existence of a GPCR-specific and correctly annotated array (currently not commercially available) covering all GPCRs would obviously be highly beneficial to such an enterprise. As highlighted in Chapter 1, there are limitations to DNA microarrays – not all GPCRs (including orphans) are included on the chips, some lowly expressed transcripts may escape detection, and some RNAs may cross-hybridise with a cDNA probe designed against a different gene. Obviously, results from an array would have to be verified with another technique such as ISHH and qPCR (and also verify protein expression in a western/IHC if an antibody is available).

Hindmarch and colleagues used microarrays to investigate transcript expression in the PVN and SON, the data from which is presented in-part in Chapter 1 and the Supplementary data (Hindmarch *et al.*, 2006). Indeed, the array data in Chapter 1 demonstrates gene expression of many GPCRs in the rat PVN and SON, some of which are orphans. Of the 9 candidate orphan GPCRs in Chapter 5, the transcripts of GPRC5b, GPR48, GPR56, GPR108, GPR146 and GPR153 were detected in both the PVN and SON with Affymetrix 230 2.0 rat genome chips, while GPR125 mRNA was only detected in the PVN (see Supplementary Tables 5 and 6). This is in general agreement with our ISHH results from Chapter 5, although we observed high expression of TMEM87B mRNA in the PVN and SON (absent from arrays), low-negligible levels of GPR65 transcript in the SON (absent from arrays), low expression GPR125 mRNA in the SON (absent from arrays), and found no expression of GPR48 transcript in the PVN (detected by arrays), following the exposure of ^{35}S-UTP orphan GPCR-specific riboprobes to 6 week film/18 week emulsion exposure. Therefore, microarrays as with many other global techniques have sensitivity issues (Murphy, 2002a). But arrays are undoubtedly a refined alternative to EST distribution profiles, and can potentially detect changes in gene expression – which may allude towards a fast glucocorticoid receptor. A downside of this semi-targeted DNA array approach would be that we would also detect changes in glucocorticoid-regulated genes (dependent on e.g., the transcriptional activity of GR) which may also include the up- or down-regulation of orphan GPCR transcript – an effect that may be unrelated to direct orphan receptor occupancy by glucocorticoids.

Other orphan GPCRs detected in the PVN and SON by arrays include GPR19, GPR34, GPR37, GPR37L1, GPR61, GPR68, GPR83, GPR85, GPR88, GPR98, GPR107, GPR116, GPR123, GPR149,

GPR158, GPR162, and GPR176. Anyone of these receptors could possibly be a fast glucocorticoid receptor (particularly as they are expressed in two of the target tissues). Interestingly, of the listed orphans, the gene expression of GPR83 is upregulated in murine thymoma WEHI-7TG cells following treatment with glucocorticoids and forskolin (hence its unofficial name glucocorticoid-induced receptor); while acute DEX administration has been reported to down regulate GPR83 transcript in various mouse brain regions (Harrigan *et al.*, 1991; Adams *et al.*, 2003). However, in disagreement with the array data, Sah and collegues found no expression of GPR83 transcript in the rat PVN or SON using ISHH – although others have observed GPR83 mRNA expressed in the human PVN and SON (by ISHH) (Sah *et al.*, 2005; Brézillon *et al.*, 2001). As GPR83 has highest sequence homology with the NPY family of receptors, much emphasis has been placed on GPR83 belonging to the NPY receptor subfamily (Parker *et al.*, 2000). A recently study has shown that the rat GPR83 binds NPY compounds with high affinity, but has low affinity for NPY (13nM) when compared with the other NPY receptors (sub-nanomolar). The authors concluded that central levels of NPY were sufficient to activate GPR83, but that there may be an alternative endogenous ligand that binds GPR83 with higher affinity (Sah *et al.*, 2007). To our knowledge, whether GPR83 has any affinity for glucocorticoids has yet to be determined.

Of course, while glucocorticoid treatment may regulate the expression of many genes, some of which may be orphan GPCRs (such as GPR83), it is not certain that receptor occupancy will result in transcriptional or translational changes in a putative fast glucocorticoid receptor.

A non-orphan GPCR?

The idea that fast glucocorticoid receptor may be a GPCR with a known endogenous ligand is not inconceivable. There are examples of GPCRs that bind related peptides i.e., the chemokine CCR1 receptor is activated by the chemokines CCL3, CCL5, CCL7, CCL8, CCL13-16 and CCL23 (Murphy *et al.*, 2002b), and the associated peptides cholecystokinin and gastrin are the physiological agonists of the cholecystokinin CCK_2 receptor (Rehfeld *et al.*, 2007). Non-related endogenous compounds, such as steroids and proteins, would seem less likely to bind the same GPCR. However, Berger and colleagues demonstrated that high concentrations of progesterone (μM range) directly inhibits agonist-stimulated signalling of the OT receptor (Berger *et al.*, 1999), suggesting that GPCRs can bind both peptides and steroids. Yet, it is worth noting that while the same group also describe the same progesterone mediated-inhibition of agonist-stimulated signalling for several other GPCRs e.g., bradykinin B_2 and histamine H_1 receptors they do not show specific binding of progesterone to any receptors other than the OT receptor (Berger *et al.*, 1999). This along with the μM concentrations of steroid used in the study may suggest the effects of progesterone were non-specific. Therefore, the competitive nature of progesterone on [^{3}H]OT/OT receptor binding affinity could be attributed to the

fact that high μM levels of steroids can affect membrane fluidity and as such cause conformational changes within the GPCR that could alter ligand binding (Clarke *et al.*, 1990).

Olfactory receptors?

Olfactory receptors are the largest group of chemosensory GPCRs, and there are at least 388 human, 1234 rat and 1081 mouse olfactory receptors (Gloriam *et al.*, 2007). Mammalian olfactory receptors share the structural features common to all GPCRs (particularly those of the rhodopsin subgroup) including 7TMs, a potential disulfide bond between highly conserved cysteines in the first and second extracellular loops (EL), a conserved (NXS/T consensus) glycosylation site in the N-terminus, several potential phosphorylation sites in intracellular regions, and numerous conserved short sequences (Gaillard *et al.*, 2004). Characteristics that are unique to olfactory receptors include an extremely long second EL which contains two cysteines, and five conserved amino acid motifs –sequence homology to which is enough to classify a GPCR as an olfactory receptor (LHTPMY in the first intracellular loop1, MAYDRYVAIC at the end of TM3 and the beginning of the second intracellular loop 2, SY at the end of TM5, and FSTCSSH at the beginning of TM6 and PMLNPF in TM7) (Mombaerts, 1999; Gaillard *et al.*, 2004). These receptors are classed as olfactory receptors based on a general: 1) high prevalence of receptors in olfactory tissue; 2) evolution divergence - high number of receptors in mammals with renowned sense of smell; 3) some evidence of activation by known odorants (Foord, 2002). We precluded olfactory GPCRs as candidate fast glucocorticoid receptors since the vast majority of the fast effects of glucocorticoids have been observed in non-olfactory tissues (reviewed in Chapter 5). However, it is now coming to light that olfactory GPCRs are not restricted to tissues associated with olfaction, for example the olfactory receptor HT2 (NCBI gene name OR7E24) transcript is expressed in human embryonic primordial germ cells (Goto *et al.*, 2001). In addition, the odorant receptor PSGR (NCBI gene name OR51E2) abundantly expressed in the prostate, has been reported to be activated by testosterone metabolites as well as its conventional ligand the odorant β-ionone (Neuhaus *et al.*, 2009). The premise that an olfactory receptor may bind a steroid is feasible considering that many olfactory receptors bind other organic compounds (made up of various alcohols, aldehydes, ketones and esters; and chemicals with aromatic, non-aromatic, or polycyclic ring structures) (Gaillard *et al.*, 2004).

Another steroid receptor?

The fast effects of glucocorticoids may also be associated with an unknown splice variant of GR and/or MR. As addressed in Chapter 4, it has been suggested that a membrane-bound splice variant of ERα, ERα-36, mediates some of the fast effects of E2; and is also activated by the anti-E2s tamoxifen and ICI-182,780. This suggests that if there is are alternative forms of GR and MR they may have a distinct pharmacological profile i.e., the GR and MR antagonists, mifepristone and spironolactone,

respectively, do not inhibit the rapid glucocorticoid-mediated suppression of glutamate synaptic inputs to OT and VP magnocellular neurones of the PVN and SON (Di *et al.*, 2005).

Alternatively, the fast effects may be attributable to an orphan steroid receptor. There are currently 23 orphan nuclear receptors (out of 49 known nuclear receptors; numbers from the IUPHAR database) with unidentified endogenous ligands. Since their initial discovery, it has become evident that the orphan receptors themselves form a highly diverse group (Benoit *et al.*, 2006). They are not linked functionally or evolutionarily, have varied structures (e.g., receptor domains range in size, and receptors may only contain one of the two distinguishing domains (DBD or LBD) of the NR superfamily), and bind to DNA in a manner of ways (e.g., most bind DNA as homodimers, while others form DNA-binding heterodimers (e.g., with retinoid X receptors) or even oligomers) (Benoit *et al.*, 2006). Of the orphan receptors that have been shown to interact with ligands (e.g., pregnane X receptor (PXR; NR1I2)) it is understood that their ligand-binding pockets are larger than classical NRs and can bind to a large diversity of molecules with lower affinity (Mukherjee and Mani, 2010). Therefore, orphan nuclear receptors are functionally and structurally different from the classical steroid receptors – and thus could be the potential mediators of fast steroid effects. For example, the once orphan (now termed 'adopted' orphans) liver X receptors LXRα (NR1H3) and LXRβ (NR1H2) are activated by a subgroup of steroids, the oxysterols (Lu *et al.*, 2001; Germain *et al.*, 2006).

6.4.3. Conclusion

The ERK phosphorylation assay offers a universal receptor signalling platform for deorphanising GPCRs. Therefore, the lack of ERK phosphorylation in response to CORT/DEX strongly suggests that the orphan GPCRs, GPR108, GPR146 and TMEM87B are not fast glucocorticoid receptors. Whether or not the fast glucocorticoid receptor is another orphan GPCR remains to be seen. There is technology available to extend the search for possible candidates to non-orphan and chemosensory GPCRs, as well as steroid receptor splice-variants and orphans which may (directly or indirectly) couple to G proteins.

Chapter 7: General Discussion

The PVN and SON are important mediators in homeostatic control, and influence an array of processes including appetite, labour and lactation, reproductive behaviour, the cardiovascular system, and the stress response. Thus the receptors within these nuclei interpret and translate a plethora of incoming signals (e.g., from higher brain regions/brain stem/humoral signals) and ultimately regulate the output of various hormones and/or neurotransmitters (e.g., the release of CRF, VP and OT into the peripheral blood or other brain regions). As GPCRs are the largest family of transmembrane receptors in the genome, it is unsurprising that GPCRs are known to interpret many of the inputs arriving at the PVN/SON. The rat genome codes for at least 224 non-chemosensory GPCRs (with known endogenous ligands) and another 132 orphan GPCRs. Approximately 134 GPCRs have been located in the rat PVN, 26 of which are orphans, and 110 GPCRs have been found in the SON, of which 30 that are orphans (values from Table 1.1). However, only a few studies have investigated the distribution of orphan receptors in the PVN and SON (numbers are mainly based on array data), and so the true value is likely even higher. The presence of orphan GPCRs in the PVN/SON raises questions with regards to their role in these nuclei. Are these receptors artefacts of evolution, inherited from ancestral creatures, and the functions of which have become functionally redundant? Do they lack an endogenous ligand, and are instead constitutively active, and serve to regulate the expression and function of other GPCRs and/or other proteins? Are the ligands for these orphans co-expressed in the PVN and SON e.g., peptides yet to be assigned receptors such as NERPS-1/2 or neuronostatin (Toshinai and Nakazato, 2009; Samson *et al.*, 2008). Or alternatively, their ligands may be derived from other regions of the brain and/or are blood-borne factors that can cross the blood-brain barrier such as steroids. With relation to the latter point, the concept of GPCRs as steroid receptors has been deliberated for some time. Fast effects of steroids have been observed in numerous tissues including the PVN and SON. In 2005, the 'apparent' discovery of a G protein-coupled E2 receptor, the once orphan GPER, implied there may be other steroid-binding GPCRs. GPER proved to be of particular interest (especially in our laboratory) as it was shown to be expressed in the PVN and SON, suggesting that it may mediate the fast effects of E2 in neuroendocrine systems.

The studies within this thesis were undertaken to further explore the concept of GPCRs as steroid receptors. The first experimental Chapter (Chapter 3) investigated the rodent distribution of the putative E2 receptor, to gain insight into its possible physiological roles. We found high expression of GPER in tissues associated with neuroendocrine and endocrine systems such as the PVN/SON, the pituitary and adrenal glands, and the ovary. Chapter 4 attempted to clarify the discrepancies surrounding the activation of GPER by E2. In agreement with various other published studies we were unable to demonstrate that GPER was indeed a bona fide E2 receptor, and as a consequence

GPER (at least in our hands) may still remain an orphan. Given there is a large amount of evidence to suggest the existence of other fast steroid receptors that act via G protein-dependent pathways, and are different from the traditional nuclear receptors, we postulated there may be other steroid binding GPCRs. Undeterred by the GPER story, in Chapter 5 we began to search for a fast glucocorticoid receptor. With distribution profiling, we narrowed the search to just three orphan GPCR candidates: GPR108, GPR146 and TMEM87B. A universal ERK deorphanising assay in Chapter 6 revealed that none of the orphans were a G protein-coupled glucocorticoid receptor.

7.1.1. GPER - an E2 receptor? Inherent problems associated with steroid assays.

It is unclear why some laboratories are able to obtain an E2-/G-1-mediated GPER response whilst others cannot. One explanation is that not all studies have employed satisfactory vehicle controls. Steroids are often dissolved in lipophillic vehicles (e.g., ethanol or DMSO) that can have non-specific effects on cellular activity (Otto *et al.*, 2008). In our own experiments we experienced an above baseline increase in phosphorylated ERK in HEK293 cells in response to organic vehicles (particularly DMSO). In a very recent study, Prossnitz and colleagues performed an ERK phosphorylation assay on SKBR3 cells and demonstrated that E2 (10nM) and G-1 (10nM) treatment (for an unspecified period of time) activated ERK. A close inspection of the representative Western blot (Figure 8 of Dennis *et al.*, 2011), reveals that DMSO (0.1%) also induced a slight ERK response (Dennis *et al.*, 2011). This indicates that if adequate controls are not in place then a vehicle response may be misinterpreted as an E2/G-1 response. Nonetheless, in the same study, the E2/G-1 induced activation of ERK was 5 times that of the DMSO control, which was comparable with the EGF-mediated ERK response, indicating that in the current thesis, the magnitude of an E2 and G-1 stimulated ERK response should have been sufficient to be observed above any non-specific vehicle effects. In Chapter 4 (section 4.3.6), we investigated the E2/G-1 activation of ERK1/2 in the same SKBR3 cells (kindly provided by Professor Eric Prossnitz). Not only were we unable to demonstrate E2/G-1 induction of ERK phosphorylation, but we were only able to show relatively modest increases in ppERK following EGF treatment (< 2-fold at 10 min). Admittedly, it is difficult to compare the two experiments directly, as Dennis and co-workers failed to specify the stimulation times (Dennis *et al.*, 2011).

The same study also showed that E2 (200nM) and G-1 (200nM) rapidly increased calcium mobilisation in SKBR3 cells (Dennis *et al.*, 2011). However, it is difficult to understand why 200nM of E2 and G-1 was used in the calcium mobilisation assay considering this group have observed maximal calcium responses with concentrations of E2/G-1 between 1nM and 100nM, in previous publications (Revenkar *et al.*, 2005; Bologa *et al.*, 2006). Equally, the group have changed the SKBR3 culture media from that used previously (DMEM or DMEM/F12) to RPMI 1640. The reasons for the change in media are not explained, but it may be indicative of the fickle nature of GPER signalling

i.e., GPER signalling may be reliant on the presence of certain media-borne chemicals, the concentration of which may be enhanced in RPMI 1640 media – for example, the media-borne factors may upregulate other GPCRs that form a functional heterodimer with GPER.

The inconstancies between laboratories associated with E2/GPER binding and/or signalling emulate the situation previously observed with the putative membrane bound progesterone receptors. In 2003, Zhu and colleagues cloned and characterised a new family of G protein-coupled, membrane bound progesterone receptors (mPR) consisting of the three isoforms mPRα, mPRβ, or mPRγ (Zhu *et al.*, 2003a). Binding assays revealed that the mouse mPRβ and human mPRα and mPRγ receptors bound progesterone with high affinity, and progesterone rapidly reduced cAMP production and activated ERK1/2 in MDA-MB-231 breast cancer cells transfected with fish mPRα (Zhu *et al.*, 2003a; Zhu *et al.*, 2003b). Conversely, Krietsch and co-workers found that the human mPRα, mPRβ and mPRγ localised to the endoplasmic reticulum and did not bind progesterone. They also observed no evidence that the fish mPRα or the three human mPR isoforms regulate cAMP or ERK signalling following progesterone administration (Krietsch *et al.*, 2006). Like that observed with GPER, these two groups had two opposing results with regards to the binding and activation of the G protein-coupled steroid receptors.

There are clear inherent problems with regard to GPCR/steroid assays - the reasons for which remain unidentified. Inconsistencies may be attributable to the varying non-specific effects that steroids or their vehicles can have on cell membranes. Similarly, cellular binding with labelled-steroids can be misleading: these compounds can infuse into internal compartments, become entrapped, and in turn are not displaced with non-labelled ligand – thus conveying a false impression of specific steroid binding (Thomas *et al.*, 2010). However, some studies in the GPER field have shown robust activation of the receptor by E2 or G-1 with various dose-response curves, appropriate controls, and inhibition with antagonists, which would usually be indicative of an authentic receptor.

However, the recent 'discovery' of another steroid-binding GPCR is an encouraging sign in the search for other possible fast steroid receptors. $GPRC_6$ is an amino acid, calcium and osteocalcin-sensing GPCR that has also been implicated in testosterone signalling. A recent study has demonstrated that transfection of the orphan $GPRC_6$ into HEK293 cells renders the cells responsive to testosterone (and also certain concentrations of the testosterone metabolites dihydrotestosterone (200nM-400nM) and E2 (60-80nM), but is inhibited with progesterone (concentrations $\leq$ 80nM), and increases specific [^{3}H]-testosterone binding sites on the plasma membrane (Pi *et al.*, 2010). In addition, the fast effects of testosterone on ERK phosphorylation are abolished in bone marrow stromal cells derived from $GPRC_6$ KO mice (Pi *et al.*, 2010). The same study also used computational modelling to provide a preliminary hypothesis regarding which residues on $GPRC_6$ would be responsible for testosterone

binding. The modelling predicted that testosterone would dock under EL2 (see Figure 7.1 for $GPRC_6$ sequence). While more studies are required to determine the credibility of this androgen (and potentially E2) binding GPCR, the possible discovery of another fast steroid receptor provides encouragements for attempts to find the fast glucocorticoid receptor.

7.1.2. The search for the fast glucocorticoid receptor continues.

As addressed in Chapter 6, there is an abundance of orphan GPCRs that are potential candidates for the fast glucocorticoid receptor (not forgetting the numerous other non-orphan or olfactory GPCRs and orphan steroid receptors). Therefore, a high-throughput universal assay is essential to provide quick and efficient screening of many receptors. Whilst it is generic, the ERK phosphorylation assay within this thesis is long-winded - the immunocytochemistry requires two days to process (which follows 3 days of cell culture). A potential alternative is Surface Plasmon Resonance (SPR) – a 'label-free' analysis method that detects molecular interactions. SPR-based instruments use polarized laser light to measure the change in the refractive index of a solvent that occurs near a sensor chip surface during complex formation or dissociation. In brief, sensor chips are coated with a 'ligand', while its binding partner (the analyte) is dissolved in a running buffer which is continuously infused over the sensor surface. A ligand-analyte interaction is indicated by an increase in the refractive index – a 'SPR response' (van der Merwe, 2000). Many attempts have been made to adapt SPR into a new GPCR-deorphanising screening strategy. Protocols have been developed that immobilise ligands to sensor chips which are then treated with a detergent-solubilised GPCR perfusate (Harding *et al.*, 2000; Navratilova *et al.*, 2011). This technique is an excellent way to screen large ligand catalogues with one GPCR - and if testing steroid ligands it would hopefully bi-pass the non-specific actions of steroids or their organic buffers. However, to perform this method for numerous GPCRs would prove awkward and time consuming as GPCRs are notoriously difficult to dissolve in detergents due to their inherent hydrophobicity.

Reversing the technique (fusing the GPCR to the chip and infusing the ligand) is equally as difficult as SPR is unsuitable for investigating small analytes (molecular weight <1000 Da), or analytes that are extremely small when compared with the molecules attached to the chip (such as GPCRs and their respective ligands) (van der Merwe, 2000). Furthermore, removing GPCRs from a cellular context will remove native proteins that may be imperative for receptor activation. Recently, Chen and colleagues adapted the SPR protocol in the hope of eventually developing a SPR GPCR deorphanising screening method (Chen *et al.*, 2010). CHO-K1 cells stably expressing (non-orphan) GPCRs are cultured directly onto SPR sensor chips and stimulated with respective ligands. In this instance a SPR response is not based on direct molecular interactions but instead represents a GPCR-mediated alteration in cell shape (which is indicative of overall cytoskeletal actin rearrangements). Although, the authors concluded that although the sensitivity of SPR was comparable to calcium or

cAMP assays, the activation of actin rearrangement is restricted to $G\alpha_i$ and $G\alpha_{12/13}$ coupled-receptors (Chen *et al.*, 2010). Moreover, the cells require stable transfection of the receptors of interest, which is a laborious procedure in itself (especially for lots of receptors!).

It is clear that deorphanising GPCRs is a long and arduous process – it requires cloning of many receptors and the selection of an assay that is efficient, inexpensive, non-bias towards certain receptor Gα protein-coupling, and is not sensitive to non-specific effects of vehicle solvents. Even then, it is difficult to predict the necessary conditions for ligand-receptor activation. Mapping the central and peripheral distribution of an orphan gene or protein expression (as demonstrated within Chapter 5 of this thesis) will undoubtedly give insight into 1) the identity of a possible endogenous ligand(s); 2) the function of the receptor; and/or 3) the possible interacting proteins or receptors that may accentuate ligand binding. As for uncovering a fast steroid receptor, it is perhaps reasonable to continue, but refine, the strategies of the current thesis. One could continue to use distribution profiling such as array and ISHH (and deep transcriptome sequencing – see section 5.4.3) to narrow down possible candidates (whether it be orphan, non-orphans, or chemosensory GPCRs, or even orphan steroid receptors). This could be used in conjunction with bioinformatics – potential targets could be screened for homology with known steroid binding GPCRs e.g., search for hydrophobicity in EL2 (see Figure 7.1).

As it is one of the only assays to provide an excellent universal platform with which to deorphanise receptors, it may be advisable to continue to test the potential candidates in the ERK phosphorylation assay. However, the assay may be improved by utilising a fast acting ppERK directed primary antibody that requires only a short incubation period (e.g., 1 hour - as opposed to overnight, this would likely require an antibody with higher affinity than ones currently used, so that signal-noise ratios are maximised at shorter incubation times). Also the steroids used for stimulation should be dissolved in a variety of different solvents (e.g., water and ethanol) to counteract non-specific, vehicle effects. In addition, other steroids should be tested alongside the steroid of interest, to check that increases in ppERK are steroid-specific e.g., if many steroid hormones activate the same receptor then it is indicative of non-specific activity (such as non-specific interactions with the membrane/hydrophobic regions on the receptor). Finally it would be advantageous for any orphan responses to be validated in animal models in which the GPCR has either been knocked out or suppressed (e.g., by RNA-interference).

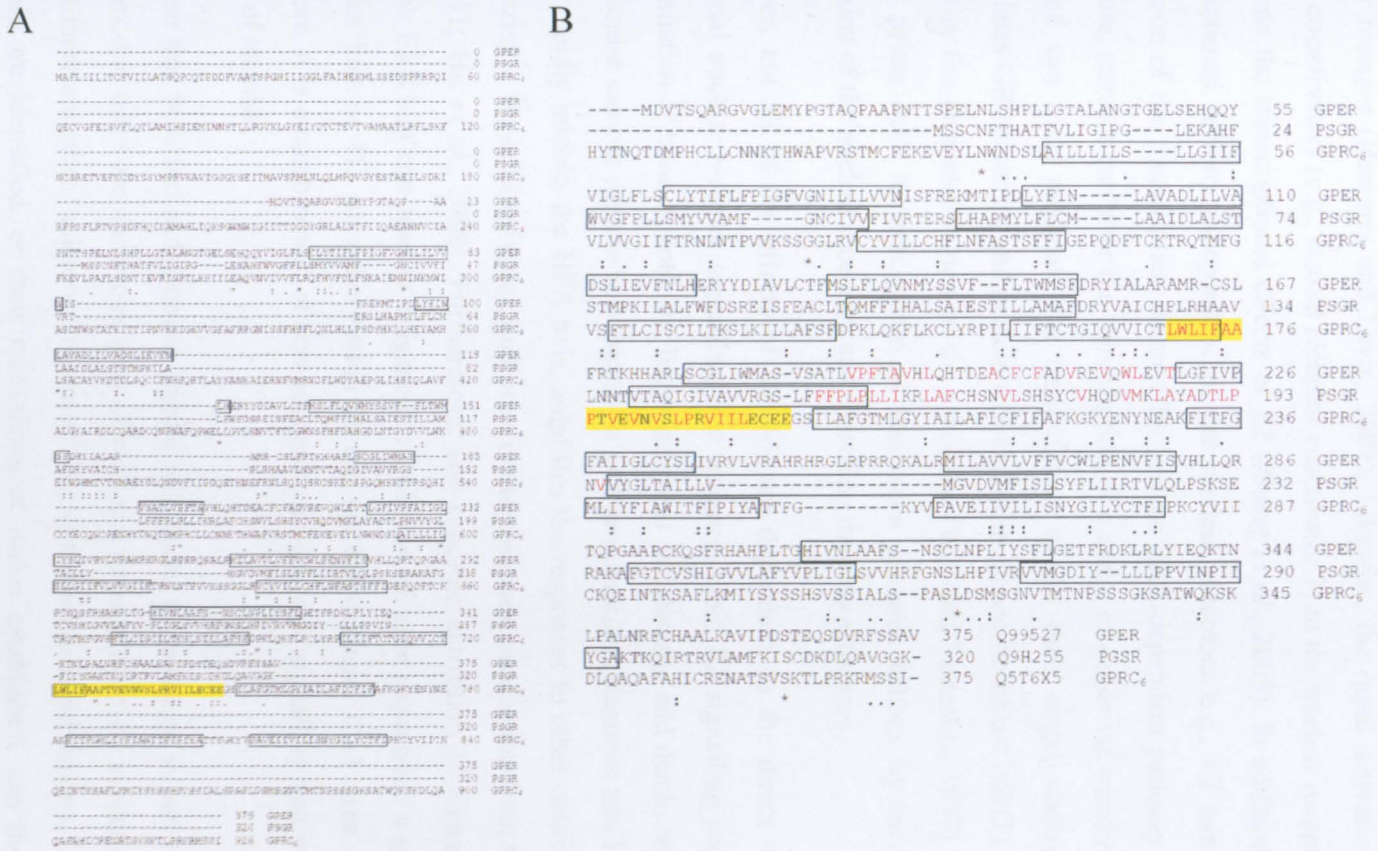

Figure 7.1. Sequence alignment of human GPER, PSGR, and $GPRC_6$.

(A) Sequence alignment of the human GPER (top line), human odorant receptor PSGR (middle line), and human $GPRC_6$ (bottom line) receptors, generated with the aid of the web-based uniprot sequence alignment tool (http://www.uniprot.org/uniprot/). Exact residue matches across all three receptors are represented by an asterisk on line 4 (*). Amino acids that have similar properties are indicated on the fourth line with a semi colon (conserved substitution) or a full stop (semi-conserved substitution). Residues that form the predicted transmembrane domains (TMs; as designated by uniprot) are boxed. All three of the GPCRs thought to be activated by steroids (GPER, putative E2 receptor (Revenkar *et al.*, 2005); PSGR, reported to be activated by testosterone metabolites (Neuhaus *et al.*, 2009); $GPRC_6$, though to bind testosterone (Pi *et al.*, 2010)). Studying the sequences of the GPCRs may reveal certain sequence motifs that are indicative of steroid binding, and thus may be used to find other such receptors using a bioinformatic search engine. For example, Pi and colleagues used computational modelling to indicate which residues on $GPRC_6$ would be responsible for testosterone binding. The modelling predicted that testosterone would dock under EL2 surrounded by common hydrophobic residues (the amino acids that Pi *et al.*, deemed as EL2 are highlighted in yellow). Note that $GPRC_6$ has a longer N-terminal than the other receptors - as such $GPRC_6$'s TMs do not line up with the TMs of the other receptors. (B) Re-alignment of the last 375 amino acids of $GPRC_6$ with PSGR and GPER to enable a sequence comparison between the extracellular domains, particularly EL2. For each receptor, the hydrophobic residues within the EL2 are highlighted in red (these amino acids may interact with the steroid ligand). The EL2s of PSGR and GPER are much longer than $GPRC_6$, and share no obvious sequence motifs with the putative testosterone receptor. It remains to be seen whether hydrophobicity within the EL2 holds the key to steroid binding.

7.1.3. Why are fast steroid receptors required?

One wanders, if steroids mainly exhibit prolonged genomic effects, why is there a biological need for rapid steroid signalling? One theory is that non-genomic signalling primes the cell ready for steroid-mediated alterations in transcription. For example, E2 can stimulate ERK, PI3K, or PKA activation which in turn can phosphorylate key residues on ERα, and augment the transcriptional activity of the nuclear receptor (Hammes and Levin, 2007). Likewise, the rapid activation of kinases by E2 can recruit co-activators (e.g., steroid receptor coactivator 3) to the nuclear receptor complex and thereby accelerate the transcriptional effects of E2 (Zheng *et al.*, 2005). In addition, steroids can modulate transcriptional activity independent of the nuclear receptors e.g., E2 can rapidly upregulate the expression of the transcription factor c-Fos via an ERK-dependent pathway (Albanito *et al.*, 2007). Therefore, steroids can alter the transcription of a range of genes via transcription factors such as c-Fos, and can even modulate the transcription of the their target nuclear receptors e.g., c-Fos upregulates GR transcript and protein expression in mouse fibroblast NIH3T3 cells, via an AP-1 site present in the promoter region of the GR gene (Wei and Vedeckis, 1997). Therefore, steroids can rapidly prime cells in anticipation of their own genomic actions by increasing the activity and expression of the nuclear receptors and recruiting their co-activators.

However, not all of the effects of steroids are dependent on the direct or indirect activation of traditional nuclear receptor signalling. For instance, rapid E2 signalling promotes the survival and differentiation of bone osteoblasts, limits neuronal cell damage and death, and modulates endothelial and vascular smooth muscle cell migration and proliferation (Hammes and Levin, 2007). Similarly, CORT rapidly inhibits the HPA axis, amplifies the responses to other neurotransmitters in the CNS (i.e., during a stressful episode), and prevents testosterone production from the testis (Groeneweg *et al.*, 2011; Hu *et al.*, 2008). Furthermore, non-genomic activation of signal-transduction pathways (such as ERK1/2) can lead to epigenetic regulation of gene expression e.g., activation of ERK1/2 increases histone H3 phosphorylation in the rat hippocampal CA1 area (Chwang *et al.*, 2006). Therefore, it is a combination of non-genomic and genomic signalling that mediates the fundamental effects of steroids.

It is clear that both fast and genomic steroid effects can be mediated in part by the traditional nuclear receptors, but there are numerous lines of evidence (examples given in sections 1.6.2 and 5.1.2) that suggest there are other 'unknown' receptors that also mediate rapid actions. Only when these putative receptors are identified, or their mechanism of action established, can the true nature of steroid signalling be understood.

References

N. Aaltonen, V.A. Palomäki, A. Lecklin, J.T. Laitinen, Neuroanatomical mapping of juvenile rat brain regions with prominent basal signal in [(35)S]GTPgammaS autoradiography, J. Chem. Neuroanat. 35 (2008) 233-241.

I. Ábrahám, M.G. Todman, K.S. Korach, A.E. Herbison, Critical in vivo roles for classical estrogen receptors in rapid estrogen actions on intracellular signalling in mouse brain, Endocrinology 145 (2004) 3055-3061.

T.C. Adam, E.S. Epel, Stress, eating and the reward system, Physiol. Behav. 91 (2007) 449-458.

F. Adams, M. Grassie, M. Shahid, D.R. Hill, B. Henry, Acute oral dexamethasone administration reduces levels of orphan GPCR glucocorticoid-induced receptor (GIR) mRNA in rodent brain: potential role in HPA-axis function, Brain Res. Mol. Brain Res. 117 (2003) 39-46.

E.Y. Adashi, Endocrinology of the ovary, Hum. Reprod. 9 (1994) 815-827.

N.V. Adsay, J.N. Eble, J.R. Srigley, E.C. Jones, D.J. Grignon, Mixed epithelial and stromal tumor of the kidney, Am. J. Surg. Pathol. 24 (2000) 958-970.

G. Aguilera, S. Subburaju, S. Young, J. Chen, The parvocellular vasopressinergic system and responsiveness of the hypothalamic pituitary adrenal axis during chronic stress, Prog. Brain Res. 170 (2008) 29-39.

L. Albanito, A. Madeo, R. Lappano, A. Vivacqua, V. Rago, A. Carpino, T.I. Oprea, E.R. Prossnitz, A.M. Musti, S. Andò, M. Maggiolini, G protein-coupled receptor 30 (GPR30) mediates gene expression changes and growth response to 17beta-estradiol and selective GPR30 ligand G-1 in ovarian cancer cells, Cancer Res. 67 (2007) 1859-1866.

K.A. Al-Barazanji, S. Wislon, J. Baker, D.S. Jessop, M.S. Harbuz, Central orexin-A activates hypothalamic-pituitary-adrenal axis and stimulates hypothalamic corticotropin releasing factor and arginine vasopressin neurones in conscious rats, J. Neuroendocrinol. 13 (2001) 421-424.

P.R. Albert, Q.Y. Zhou, H.H. Van Tol, J.R. Bunzow, O. Civelli, Cloning, functional expression, and mRNA tissue distribution of the rat 5-hydroxytryptamine1A receptor gene, J. Biol. Chem. 265 (1990) 5825-5832.

L. Albizu, M. Cottet, M. Kralikova, S. Stoev, R. Seyer, I. Brabet, T. Roux, H. Bazin, E. Bourrier, L. Lamarque, C. Breton, M.L. Rives, A. Newman, J. Javitch, E. Trinquet, M. Manning, J.P. Pin, B. Mouillac, T. Durroux, Time-resolved FRET between GPCR ligands reveals oligomers in native tissues, Nat. Chem. Biol. 6 (2010) 587-594.

G. Alonso, E. Gallibert, C. Lafont, G. Guillon, Intrahypothalamic angiogenesis induced by osmotic stimuli correlates with local hypoxia: a potential role of confined vasoconstriction induced by dendritic secretion of vasopressin, Endocrinology. 149 (2008) 4279-4288.

H.C. Atkinson, S.A. Wood, E.S. Castrique, Y.M. Kershaw, C.C. Wiles, S.L. Lightman, Corticosteroids mediate fast feedback of the rat hypothalamic-pituitary-adrenal axis via the mineralocorticoid receptor, Am. J. Physiol. Endocrinol. Metab. 294 (2008) 1011-1022.

M. Altstein, H. Gainer, Differential biosynthesis and posttranslational processing of vasopressin and oxytocin in rat brain during embryonic and postnatal development, J. Neurosci. 8 (1988) 3967-3977.

F.A. Antoni, Vasopressinergic control of pituitary adrenocorticotropin secretion comes of age, Front. Neuroendocrinol. 14 (1993) 76-122.

M.A. Ariano, F.J. Monsma, A.C. Barton, H.C. Kang, R.P. Haugland, D.R. Sibley DR, Direct visualization and cellular localization of D1 and D2 dopamine receptors in rat forebrain by use of fluorescent ligands, Proc. Natl. Acad. Sci. USA 86 (1989) 8570-5874.

H. Arima, S.B. House, H. Gainer, G. Aguilera, Direct stimulation of arginine vasopressin gene transcription by cAMP in parvocellular neurons of the paraventricular nucleus in organotypic cultures, Endocrinology 142 (2001) 5027-5030.

H. Arima, T. Murase, K. Kondo, Y. Iwasaki, Y. Oiso, Centrally administered neuropeptide FF inhibits arginine vasopressin release in conscious rats, Endocrinology 137 (1996) 1523-1529.

S.P. Armstrong, C.J. Caunt, R.C. Fowkes, K. Tsaneva-Atanasova, C.A. McArdle, Pulsatile and sustained gonadotropin-releasing hormone (GnRH) receptor signaling: does the Ca2+/NFAT signaling pathway decode GnRH pulse frequency? J. Biol. Chem. 284 (2009) 35746-35757.

W.E. Armstrong, B.N. Smith, M. Tian, Electrophysiological characteristics of immunochemically identified rat oxytocin and vasopressin neurones in vitro, J. Physiol. 475 (1994) 115-128.

N. Aznavour, C. Benkelfat, P. Gravel, A. Aliaga, P. Rosa-Neto, B. Bedell, L. Zimmer, L. Descarries, MicroPET imaging of 5-HT 1A receptors in rat brain: a test-retest [18F]MPPF study, Eur. J. Nucl. Med. Mol. Imaging. 36 (2009) 53-62.

G. Baiardi, M. Macova, I. Armando, H. Ando, D. Tyurmin, J.M. Saavedra, Estrogen upregulates renal angiotensin II AT1 and AT2 receptors in the rat, Regul. Pept. 15 (2005) 7-17.

J.S. Bains, A. Potyok, A.V. Ferguson, Angiotensin II actions in paraventricular nucleus: functional evidence for neurotransmitter role in efferents originating in subfornical organ, Brain Res. 599 (1992) 223-229.

R.A. Bakker, P. Casarosa, H. Timmerman, M.J. Smit, R. Leurs, Constitutively active Gq/11-coupled receptors enable signaling by co-expressed G(i/o)-coupled receptors, J. Biol. Chem. 279 (2004) 5152-5161.

N. Balthasar, L.T. Dalgaard, C.E. Lee, J. Yu, H. Funahashi, T. Williams, M. Ferreira, V. Tang, R.A. McGovern, C.D. Kenny, L.M. Christiansen, E. Edelstein, B. Choi, O. Boss, C. Aschkenasi, C.Y. Zhang, K. Mountjoy, T. Kishi, J.K. Elmquist, B.B. Lowell, Divergence of melanocortin pathways in the control of food intake and energy expenditure, Cell 123 (2005) 493-505.

M.S. Baquedano, N. Saraco, E. Berensztein, C. Pepe, M. Bianchini, E. Levy, J. Goñi, M.A. Rivarola, A. Belgorosky, Identification and developmental changes of aromatase and estrogen receptor expression in prepubertal and pubertal human adrenal tissues, J Cli.n Endocrinol. Metab. 92 (2007) 2215-2222.

T.Z. Baram, S.P. Lerner, Ontogeny of corticotropin releasing hormone gene expression in rat hypothalamus--comparison with somatostatin, Int. J. Dev. Neurosci. 9 (1991) 473-478.

E.A. Barnard, Biological function of pancreatic ribonucleases, Nature 221 (1969) 340-344.

S.L. Bealer, W.E. Armstrong, W.R. Crowley, Oxytocin release in magnocellular nuclei: neurochemical mediators and functional significance during gestation, Am. J. Physiol. Regul. Integr. Comp. Physiol. 299 (2010) 452-458.

S.L. Bealer, W.R. Crowley, Stimulation of central and systemic oxytocin release by histamine in the paraventricular nucleus: evidence for an interaction with norepinephrine, Endocrinology 140 (1999) 1158-1164.

M. Beato, J. Klug, Steroid hormone receptors: an update. Hum. Reprod. Update. 6 (2000) 225-236.

J.A. Becker, K. Befort, C. Blad, D. Filliol, A. Ghate, D. Dembele, C. Thibault, M. Koch, J. Muller, A. Lardenois, O. Poch, B.L. Kieffer, Transcriptome analysis identifies genes with enriched expression in the mouse central extended amygdala, Neuroscience 156 (2008) 950-965.

E.E. Benarroch, Paraventricular nucleus, stress response, and cardiovascular disease, Clin. Auton. Res. 15 (2005) 254-263.

G. Benoit, A. Cooney, V. Giguere, H. Ingraham, M. Lazar, G. Muscat, T. Perlmann, J.P. Renaud, J. Schwabe, F. Sladek, M.J. Tsai, V. Laudet, International Union of Pharmacology. LXVI. Orphan nuclear receptors, Pharmacol. Rev. 58 (2006) 798-836.

L. Birnbaumer, J. Abramowitz, A.M. Brown, Receptor-effector coupling by G proteins, Biochim. Biophys. Acta. 1031 (1990) 163-224.

S. Bischoff, S. Leonhard, N. Reymann, V. Schuler, R. Shigemoto, K. Kaupmann, B. Bettler, Spatial distribution of GABA(B)R1 receptor mRNA and binding sites in the rat brain, J. Comp. Neurol. 412 (1999) 1-16.

R.S. Bitner, A.L. Nikkel, S. Otte, B. Martino, E.H. Barlow, P. Bhatia, A.O. Stewart, J.D. Brioni, M.W. Decker, R.B. Moreland, Dopamine D4 receptor signaling in the rat paraventricular hypothalamic nucleus: Evidence of natural coupling involving immediate early gene induction and mitogen activated protein kinase phosphorylation, Neuropharmacology 50 (2006) 521-531.

T.K. Bjarnadóttir, R. Fredriksson, P.J. Höglund, D.E. Gloriam, M.C. Lagerström, H.B. Schiöth, The human and mouse repertoire of the adhesion family of G-protein-coupled receptors, Genomics 84 (2004) 23-33.

L. Björnström, M. Sjöberg, Mechanisms of estrogen receptor signaling: convergence of genomic and nongenomic actions on target genes, Mol. Endocrinol. 19 (2005) 833-842.

E. Blasko, C.A. Haskell, S. Leung, G. Gualtieri, M. Halks-Miller, M. Mahmoudi, M.K. Dennis, E.R. Prossnitz, W.J. Karpus, R. Horuk, Beneficial role of the GPR30 agonist G-1 in an animal model of multiple sclerosis, J. Neuroimmunol. 214 (2009) 67-77.

A. Blume, O.J. Bosch, S. Miklos, L. Torner, L. Wales, M. Waldherr, I.D. Neumann, Oxytocin reduces anxiety via ERK1/2 activation: local effect within the rat hypothalamic paraventricular nucleus, Eur. J. Neurosci. 27 (2008) 1947-1956.

M.N. Bobrow, T.D. Harris, K.J. Shaughnessy, G.J. Litt, Catalyzed reporter deposition, a novel method of signal amplification. Application to immunoassays, J. Immunol. Methods. 125 (1989) 279-285.

I.A. Bobulescu, V. Dwarakanath, L. Zou, J. Zhang, M. Baum, O.W. Moe, Glucocorticoids acutely increase cell surface Na+/H+ exchanger-3 (NHE3) by activation of NHE3 exocytosis, Am. J. Physiol. Renal Physiol. 289 (2005) 685-691.

B. Boivin, G. Vaniotis, B.G. Allen, T.E. Hébert, G protein-coupled receptors in and on the cell nucleus: a new signaling paradigm? J. Recept. Signal Transduct. Res. 28 (2008) 15-28.

C.G. Bologa, C.M. Revankar, S.M. Young, B.S. Edwards, J.B. Arterburn, A.S. Kiselyov, M.A. Parker, S.E. Tkachenko, N.P. Savchuck, L.A. Sklar, T.I. Oprea, E.R. Prossnitz, Virtual and biomolecular screening converge on a selective agonist for GPR30, Nat. Chem. Biol. 2 (2006) 207-212.

J.A. Bonini, S.M. Anderson, D.F. Steiner, Molecular cloning and tissue expression of a novel orphan G protein-coupled receptor from rat lung, Biochem. Biophys. Res. Commun. 8 (1997) 190-193.

A. Bora, S.P. Annangudi, L.J. Millet, S.S. Rubakhin, A.J. Forbes, N.L. Kelleher, M.U. Gillette, J.V. Sweedler, Neuropeptidomics of the supraoptic rat nucleus, J. Proteome Res. 7 (2008) 4992-5003.

T. Bossmar, M. Forsling, M. Akerlund, Circulating oxytocin and vasopressin is influenced by ovarian steroid replacement in women, Acta. Obstet. Gynecol. Scand. 74 (1995) 544-548.

C. Boudaba, S. Di, J.G. Tasker, Presynaptic noradrenergic regulation of glutamate inputs to hypothalamic magnocellular neurons, J. Neuroendocrinol. 15 (2003) 803-810.

C. Boudaba, D.M. Linn, K.C. Halmos, J.G. Tasker, Increased tonic activation of presynaptic metabotropic glutamate receptors in the rat supraoptic nucleus following chronic dehydration, J. Physiol. 551 (2003) 815-823.

G.C. Brailoiu, S.J. Dun, E. Brailoiu, S. Inan, J. Yang, J.K. Chang, N.J. Dun, Nesfatin-1: distribution and interaction with a G protein-coupled receptor in the rat brain, Endocrinology. 148 (2007) 5088-5094.

E. Brailoiu, S.L. Dun, G.C. Brailoiu, K. Mizuo, L.A. Sklar, T.I. Oprea, E.R. Prossnitz, N.J. Dun, Distribution and characterization of estrogen receptor G protein-coupled receptor 30 in the rat central nervous system, J. Endocrinol. 193 (2007) 311-321.

S.J. Brandt, J.E. Niedel, R.M. Bell, W.S. Young, Distinct patterns of expression of different protein kinase C mRNAs in rat tissues, Cell 49 (1987) 57-63.

H. Bräuner-Osborne, P. Krogsgaard-Larsen, Sequence and expression pattern of a novel human orphan G-protein-coupled receptor, GPRC5B, a family C receptor with a short amino-terminal domain, Genomics, 65 (2000) 121-128.

S. Brézillon, M. Detheux, M. Parmentier, T. Hökfelt, Y.L. Hurd, Distribution of an orphan G-protein coupled receptor (JP05) mRNA in the human brain, Brain Res. 921 (2001) 21-30.

I. Brouns, L. Van Nassauw, J. Van Genechten, M. Majewski, D.W. Scheuermann, J.P. Timmermans, D. Adriaensen, Triple immunofluorescence staining with antibodies raised in the same species to study the complex innervation pattern of intrapulmonary chemoreceptors, J. Histochem. Cytochem. 50 (2002) 575-582.

B.R. Broughton, A.A. Miller, C.G. Sobey, Endothelium-dependent relaxation by G protein-coupled receptor 30 agonists in rat carotid arteries, Am. J. Physiol. Heart Circ. Physiol. 298 (2010) 1055-1061.

C.H. Brown, C.W. Bourque, Autocrine feedback inhibition of plateau potentials terminates phasic bursts in magnocellular neurosecretory cells of the rat supraoptic nucleus, J. Physiol. 557 (2004) 949-960.

C.H. Brown, P.J. Brunton, J.A. Russell, Rapid estradiol-17β modulation of opioid actions on the electrical and secretory activity of rat oxytocin neurons in vivo, Neurochemistry Research 33 (2008) 614-623.

C.H. Brown, M. Ludwig, G. Leng, Temporal dissociation of the feedback effects of dendritically co-released peptides on rhythmogenesis in vasopressin cells, Neuroscience 124 (2004) 105-111.

C.H. Brown, V. Scott, M. Ludwig, G. Leng, C.W. Bourque, Somatodendritic dynorphin release: orchestrating activity patterns of vasopressin release, Biochem. Soc. Trans. 35 (2007) 1236-1242.

P.J. Brunton, S. Arunachalam, J.A. Russel, Control of neurohypophysial hormone secretion, blood osmolality and volume in pregnancy, J. Physiol. Pharmacol. 59 (2008) 27-45.

P.J. Brunton, J.A. Russell, A.J. Douglas, Adaptive responses of the maternal hypothalamic-pituitary-adrenal axis during pregnancy and lactation, J. Neuroendocrinol. 20 (2008) 764-776.

J. Bundzikova, Z. Pirnik, D. Zelena, J.D. Mikkelsen, A. Kiss, Response of substances co-expressed in hypothalamic magnocellular neurons to osmotic challenges in normal and Brattleboro rats, Cell Mol. Neurobiol. 28 (2008) 1033-1047.

J.R. Bunzow, H.H. Van Tol, D.K. Grandy, P. Albert, J. Salon, M. Christie, C.A. Machida, K.A. Neve, O. Civelli, Nature 336 (1988) 783-787.

M. Buongiorno-Nardelli, F. Amaldi, Autoradiographic detection of molecular hybrids between RNA and DNA in tissue sections, Nature 225 (1970) 946-948.

T.C.D. Burazin, J.A. Larm, A.L. Gundlach, Regulation by osmotic stimuli of galanin-R1 receptor expression in magnocellular neurones of the paraventricular and supraoptic nuclei of the rat, J. Neuroendocrinol. 13 (2001) 358-370.

J.P. Burbach, S.M. Luckman, D. Murphy, H. Gainer, Gene regulation in the magnocellular hypothalamo-neurohypophysial system, Physiol. Rev. 81 (2001) 1197-1267.

K. Burger, F. Fahrenholz, G. Gimpl, Non-genomic effects of progesterone on the signaling function of G protein-coupled receptors, FEBS Lett. 464 (1999) 25-29.

F. Buttgereit, A. Scheffold, Rapid glucocorticoid effects on immune cells, Steroids 67 (2002) 529-534.

R.L. Cagan, H. Krämer, A.C. Hart, S.L. Zipursky, The bride of sevenless and sevenless interaction: internalization of a transmembrane ligand, Cell 69 (1992) 393-399.

D. Calebiro, V.O. Nikolaev, L. Persani, M.J. Lohse, Signaling by internalized G-protein-coupled receptors, Trends Pharmacol. Sci. 31 (2010) 221-228.

C. Callewaere, G. Banisadr, M.G. Desarménien, P. Mechighel, P. Kitabgi, W.H. Rostène, S. Mélik Parsadaniantz, The chemokine SDF-1/CXCL12 modulates the firing pattern of vasopressin neurons and counteracts induced vasopressin release through CXCR4, Proc. Natl. Acad. Sci. USA 103 (2006) 8221-8226.

A. Cano, C. Hermenegildo, The endometrial effects of SERMs, Hum. Reprod. Update 6 (2000) 244–254.

C. Carmeci, D.A. Thompson, H.Z. Ring, U. Francke, R.J. Weigel, Identification of a gene (GPR30) with homology to the G-protein-coupled receptor superfamily associated with estrogen receptor expression in breast cancer, Genomics 1 (1997) 607-617.

K.S. Carmon, X. Gong, Q. Lin, A. Thomas, Q. Liu, R-spondins function as ligands of the orphan receptors LGR4 and LGR5 to regulate Wnt/beta-catenin signalling, Proc Natl Acad Sci USA, 108 (2011) 11452-11457.

M.P. Castelli, A.P. Piras, T. Melis, S. Succu, F. Sanna, M.R. Melis, S. Collu, M.G. Ennas, G. Diaz, K. Mackie, A. Argiolas, Cannabinoid CB1 receptors in the paraventricular nucleus and central control of penile erection: immunocytochemistry, autoradiography and behavioural studies, Neuroscience 147 (2007) 197-206.

J. Catusse, S. Wollner, M. Leick, P. Schröttner, I. Schraufstätter, M. Burger, Attenuation of CXCR4 responses by CCL18 in acute lymphocytic leukemia B cells, J. Cell. Physiol. 225 (2010) 792-800.

C.J. Caunt, C.A. Rivers, B.L. Conway-Campbell, M.R. Norman, C.A. McArdle, Epidermal growth factor receptor and protein kinase C signaling to ERK2: spatiotemporal regulation of ERK2 by dual specificity phosphatises, J. Biol. Chem. 283 (2008) 6241-6252.

A. Cavanaugh, J. McKenna, A. Stepanchick, G.E. Breitwieser, Calcium-sensing receptor biosynthesis includes a cotranslational conformational checkpoint and endoplasmic reticulum retention, J. Biol. Chem. 285 (2010) 19854-19864.

S. Ceccatelli, M. Eriksson, T. Hökfelt, Distribution and coexistence of corticotropin-releasing factor-, neurotensin-, enkephalin-, cholecystokinin-, galanin- and vasoactive intestinal polypeptide/peptide histidine isoleucine-like peptides in the parvocellular part of the paraventricular nucleus, Neuroendocrinology 49 (1989) 309-323.

D.T. Chalmers, D.P. Behan, The use of constitutively active GPCRs in drug discovery and functional genomics, Nat. Rev. Drug Discov. 1 (2002) 599-608.

E. Charmandari, C. Tsigos, G. Chrousos, Endocrinology of the stress response, Annu. Rev. Physiol. 67 (2005) 259-284.

A.K. Chavalmane, P. Comeglio, A. Morelli, S. Filippi, B. Fibbi, L. Vignozzi, E. Sarchielli, M. Marchetta, P. Failli, P. Sandner, F. Saad, M. Gacci, G.B. Vannelli, M. Maggi, Sex Steroid Receptors in Male Human Bladder: Expression and Biological Function, J. Sex. Med. 7 (2010) 2698-713 doi: 10.1111/j.1743-6109.2010.01811.x

W.B. Chwang, K.J. O'Riordan, J.M. Levenson, J.D. Sweatt, ERK/MAPK regulates hippocampal histone phosphorylation following contextual fear conditioning, Learn Mem. 13 (2006) 322-328.

Q. Chen, D.P. Li, H.L. Pan, Presynaptic α1 adrenergic receptors differentially regulate synaptic glutamate and GABA release to hypothalamic presympathetic neurons, J. Pharmacol. Exp. Therap. 316 (2006) 733-742.

C.A. Chen, H. Okayama, Calcium phosphate-mediated gene transfer: a highly efficient transfection system for stably transforming cells with plasmid DNA, Biotechniques 6 (1988) 632-638.

X.Q. Chen, J.Z. Du, Y.S. Wang, Regulation of hypoxia-induced release of corticotropin-releasing factor in the rat hypothalamus by norepinephrine, Regul. Pept. 119 (2004) 221-228.

S.B. Cheng, C.T. Graeber, J.A. Quinn, E.J. Filardo, Retrograde transport of the transmembrane estrogen receptor, G-protein-coupled-receptor-30 (GPR30/GPER) from the plasma membrane towards the nucleus, Steroids (2011) In press.

V. Cherezov, D.M. Rosenbaum, M.A. Hanson, S.G. Rasmussen, F.S. Thian, T.S. Kobilka, H.J. Choi, P. Kuhn, W.I. Weis, B.K. Kobilka, R.C. Stevens, High-resolution crystal structure of an engineered human beta2-adrenergic G protein-coupled receptor, Science 318 (2007) 1258-1265.

B. Chini, M. Parenti, G-protein-coupled receptors, cholesterol and palmitoylation: facts about fats, J. Mol. Endocrinol. 42 (2009) 371-379.

J.W. Choi, S.Y. Lee, Y. Choi, Identification of a putative G protein-coupled receptor induced during activation-induced apoptosis of T cells, Cell. Immunol. 168 (1996) 78-84.

M. Christ, C. Eisen, J. Aktas, K. Theisen, M. Wehling, The inositol-1,4,5-trisphosphate system is involved in rapid effects of aldosterone in human mononuclear leukocytes, J. Clin. Endocrinol. Metab. 77 (1993) 1452-1457.

A. Christoforou, S. Le Hellard, P.A. Thomson, S.W. Morris, A. Tenesa, B.S. Pickard, N.R. Wray, W.J. Muir, D.H. Blackwood, D.J. Porteous, K.L. Evans, Association analysis of the chromosome 4p15-p16 candidate region for bipolar disorder and schizophrenia, Mol. Psychiatry 12 (2007) 1011-1025.

S. Chung, T. Funakoshi, O. Civelli, Orphan GPCR research, Br. J. Pharmacol. 153 (2008) 339-346.

K.Y. Chung, J. Shia, N.E. Kemeny, M. Shah, G.K. Schwartz, A. Tse, A. Hamilton, D. Pan, D. Schrag, L. Schwartz, D.S. Klimstra, D. Fridman, D.P. Kelsen, L.B. Saltz, Cetuximab shows activity in colorectal cancer patients with tumors that do not express the epidermal growth factor receptor by immunohistochemistry, J. Clin. Oncol. 23 (2005) 1803-1810.

F. Ciruela, V. Casadó, R.J. Rodrigues, R. Luján, J. Burgueño, M. Canals, J. Borycz, N. Rebola, S.R. Goldberg, J. Mallol, A. Cortés, E.I. Canela, J.F. López-Giménez, G. Milligan, C. Lluis, R.A. Cunha, S. Ferré, R. Franco, Presynaptic control of striatal glutamatergic neurotransmission by adenosine A1-A2A receptor heteromers, J. Neurosci. 26 (2006) 2080-2087.

R. Clarke, H.W. van den Berg, R.F. Murphy, Reduction of the membrane fluidity of human breast cancer cells by tamoxifen and 17 beta-estradiol, J. Natl. Cancer Inst. 82 (1990) 1702-1705.

M.M. Compton, J.A. Cidlowski, Rapid in vivo effects of glucocorticoids on the integrity of rat lymphocyte genomic deoxyribonucleic acid, Endocrinology 118 (1986) 38-45.

J.V. Conaglen, R.A. Donald, E.A. Espiner, J.H. Livesey, M.G. Nicholls, Effect of naloxone on the hormone response to CRF in normal man, Endocr. Res. 11 (1985) 39-44.

S.L. Coon, S.K. McCune, D. Sugden, D.C. Klein, Regulation of pineal alpha1B-adrenergic receptor mRNA: day/night rhythm and beta-adrenergic receptor/cyclic AMP control, Mol. Pharmacol. 51 (1997) 551-557.

J.D. Coppola, B.A. Horwitz, J. Hamilton, R.B. McDonald, Expression of NPY Y1 and Y5 receptors in the hypothalamic paraventricular nucleus of aged Fischer 344 rats, Am. J. Physiol. Regul. Integr. Comp. Physiol. 287 (2004) 69-75.

C.A. Cornil, G.F. Ball, J. Balthazart, Functional significance of the rapid regulation of brain estrogen action: where do the estrogens come from? Brain Res. 1126 (2006) 2-26.

S. Costanzi, J. Siegel, I.G. Tikhonova, K.A. Jacobson, Rhodopsin and the others: a historical perspective on structural studies of G protein-coupled receptors, Curr. Pharm. Des. 15 (2009) 3994-4002.

S. Cotecchia, The α1-adrenergic receptors: diversity of signaling networks and regulation, J. Recept. Signal Transduct. Res. 30 (2010) 410-419.

J.W. Crane, K. Shimizu, G.A. Carrasco, F. Garcia, C. Jia, N.R. Sullivan, D.N. D'Souza, Y. Zhang, L.D. Van de Kar, N.A. Muma, G. Battaglia, 5-HT1A receptors mediate (+)8-OH-DPAT-stimulation of extracellular signal-regulated kinase (MAP kinase) in vivo in rat hypothalamus: time dependence and regional differences, Brain Res. 1183 (2007) 51-59.

L. Cristino, L. de Petrocellis, G. Pryce, D. Baker, V. Guglielmotti, V. Di Marzo, Immunohistochemical localization of cannabinoid type 1 and vanilloid transient receptor potential vanilloid type 1 receptors in the mouse brain, Neuroscience 139 (2006) 1405-1415.

P. Cuatrecasas, M.D. Hollenberg, Binding of insulin and other hormones to non-receptor materials: saturability, specificity and apparent "negative cooperativity," Biochem. Biophys. Res. Commun. 62 (1975) 31-41.

E.T. Cunningham, P.E. Sawchenko, Reflex control of magnocellular vasopressin and oxytocin secretion, Trends Neurosci. 14 (1991) 406-411.

C.J. Daly, J.C. McGrath, Fluorescent ligands, antibodies, and proteins for the study of receptors, Pharmacol. Ther. 100 (2003) 101-118.

H.E. Day, S. Campeau, S.J. Watson, H. Akil, Expression of alpha(1b) adrenoceptor mRNA in corticotropin-releasing hormone-containing cells of the rat hypothalamus and its regulation by corticosterone. J. Neurosci. 19 (1999) 10098-10106.

G. Dayanithi, N. Sabatier, H. Widmer, Intracellular calcium signalling in magnocellular neurones of the rat supraoptic nucleus: understanding the autoregulatory mechanisms, Exp. Physiol. 85 (2000) 75-84.

M.K. Dennis, R. Burai, C. Ramesh, W.K. Petrie, S.N. Alcon, T.K. Nayak, C.G. Bologa, A. Leitao, E. Brailoiu, E. Deliu, N.J. Dun, L.A. Sklar, H.J. Hathaway, J.B. Arterburn, T.I. Oprea, E.R. Prossnitz, In vivo effects of a GPR30 antagonist, Nat. Chem. Biol. 5 (2009) 421-427.

M.K. Dennis, A.S. Field, R. Burai, C. Ramesh, W.K. Petrie, C.G. Bologa, T.I. Oprea, Y. Yamaguchi, S.I. Hayashi, L.A. Sklar, H.J. Hathaway, J.B. Arterburn, E.R. Prossnitz, Identification of a GPER/GPR30 antagonist with improved estrogen receptor counterselectivity, J. Steroid Biochem. Mol. Biol. (2011) doi:10.1016/j.jsbmb.2011.07.002.

M.C. Defagot, E.L. Malchiodi, M.J. Villar, M.C. Antonelli, Distribution of D4 dopamine receptor in rat brain with sequence-specific antibodies, Brain Res. Mol. Brain Res. 45 (1997) 1-12.

V. De Laurenzi, G. Melino, Gene disruption of tissue transglutaminase, Mol. Cell. Biol. 21 (2001) 148-155.

W. de Ronde, H.A. Pols, J.P. van Leeuwen, F.H. de Jong, The importance of oestrogens in males, Clinical Endocrinology 58 (2003) 529–542.

A.M. Deschamps, E. Murphy, Activation of a novel estrogen receptor, GPER, is cardioprotective in male and female rats, Am. J. Physiol. Heart Circ. Physiol. 297 (2009) 1806-1813.

S. Di, C. Boudaba, I.R. Popescu, F.J. Weng, C. Harris, V.L. Marcheselli, N.G. Bazan, J.G. Tasker, Activity-dependent release and actions of endocannabinoids in the rat hypothalamic supraoptic nucleus. J. Physiol 569 (2005) 751-760.

S. Di, R. Malcher-Lopes, K.C. Halmos, J.G. Tasker, Nongenomic glucocorticoid inhibition via endocannabinoid release in the hypothalamus: a fast feedback mechanism, J. Neurosci. 23 (2003) 4850-4857.

S. Di, R. Malcher-Lopes, V.L. Marcheselli, N.G. Bazan, J.G. Tasker, Rapid glucocorticoid-mediated endocannabinoid release and opposing regulation of glutamate and gamma-aminobutyric acid inputs to hypothalamic magnocellular neurons, Endocrinology 146 (2005) 4292-4301.

S. Di, M.M. Maxson, A. Franco, J.G. Tasker, Glucocorticoids regulate glutamate and GABA synapse-specific retrograde transmission via divergent nongenomic signaling pathways, J. Neurosci. 29 (2009) 393-401.

R.A. Dixon, B.K. Kobilka, D.J. Strader, J.L. Benovic, H.G. Dohlman, T. Frielle, M.A. Bolanowski, C.D. Bennett, E. Rands, R.E. Diehl, R.A. Mumford, E.E. Slater, I.S. Sigal, M.G. Caron, R.J. Lefkowitz, C.D. Strader, Cloning of the gene and cDNA for mammalian beta-adrenergic receptor and homology with rhodopsin, Nature. 321 (1986) 75-79.

E. Dominguez-Salazar, S. Shetty, E.F. Rissman, Rapid neural Fos responses to oestradiol in oestrogen receptor αβ double knockout mice, J. Neuroendocrinol. 18 (2006) 195-202.

Q. Dong, A. Salva, C.M. Sottas, E. Niu, M. Holmes, M.P. Hardy, Rapid glucocorticoid mediation of suppressed testosterone biosynthesis in male mice subjected to immobilization stress, J. Androl. 25 (2004) 973-981.

G.B. Downes, N. Gautam, The G protein subunit gene families, Genomics 62 (1999) 544-552.

M.T. Drake, S.K. Shenoy, R.J. Lefkowitz, Trafficking of G protein-coupled receptors, Circ. Res. 99 (2006) 570-582.

B. Dufy, J.D. Vincent, H. Fleury, P. Du Pasquier, D. Gourdji, A. Tixier-Vidal, Membrane effects of thyrotropin-releasing hormone and estrogen shown by intracellular recording from pituitary cells, Science 4 (1979) 509-511.

Dun SL, Brailoiu GC, Gao X, Brailoiu E, Arterburn JB, Prossnitz ER, Oprea TI & Dun NJ 2009 Expression of estrogen receptor GPR30 in the rat spinal cord and in autonomic and sensory ganglia, J. Neurosci. Res. 87 (2009) 1610-1619.

A.J, Dunn, A.H. Swiergiel, V. Palamarchouk, Brain circuits involved in corticotropin-releasing factor-norepinephrine interactions during stress, Ann. NY Acad. Sci. 1018 (2004) 25-34.

J. Eberwine, T. Bartfai, Single cell transcriptomics of hypothalamic warm sensitive neurons that control core body temperature and fever response Signaling asymmetry and an extension of chemical neuroanatomy, Pharmacol. Ther. 129 (2011) 241-259.

M. Ebisuya, K. Kondoh, E. Nishida, The duration, magnitude and compartmentalization of ERK MAP kinase activity: mechanisms for providing signaling specificity, J. Cell Sci. 118 (2005) 2997-3002.

A.J. Edgar, Human GPR107 and murine Gpr108 are members of the LUSTR family of proteins found in both plants and animals, having similar topology to G-protein coupled receptors, DNA Seq. 18 (2007) 235-241.

E. Ellerkmann, G.M. Nagy, L.S. Frawley, α-Melanocyte-Stimulating Hormone is a mammotrophic factor released by neurointermediate lobe cells after estrogen treatment, Endocrinology 130 (1992) 133-138.

E. Elliott, G. Ezra-Nevo, L. Regev, A. Neufeld-Cohen, A. Chen, Resilience to social stress coincides with functional DNA methylation of the Crf gene in adult mice, Nat. Neurosci. 13 (2010) 1351-1353.

M. Engelmann, R. Landgraf, C.T. Wotjak, The hypothalamic-neurohypophysial system regulates the hypothalamic-pituitary-adrenal axis under stress: an old concept revisited, Front. Neuroendocrinol. 25 (2004) 132-149.

M. Engelmann, M. Ludwig, The activity of the hypothalamo-neurohypophysial system in response to acute stressor exposure: neuroendocrine and electrophysiological observations, Stress 7 (2004) 91-96.

M. Estrada, A. Espinosa, M. Müller, E. Jaimovich, Testosterone stimulates intracellular calcium release and mitogen-activated protein kinases via a G protein-coupled receptor in skeletal muscle cells, Endocrinology 144 (2003) 3586-3597.

N.K. Evanson, J.G. Tasker, M.N. Hill, C.J. Hillard, J.P. Herman, Fast feedback inhibition of the HPA axis by glucocorticoids is mediated by endocannabinoid signalling, Endocrinology, 151 (2010) 4811-4819.

E. Falkenstein, H.C. Tillmann, M. Christ, M. Feuring, M. Wehling, Multiple actions of steroid hormones--a focus on rapid, nongenomic effects, Pharmacol. Rev. 52 (2000) 513-556.

J. Fan, X. Yang, W. Wang, W.H. Wood, K.G. Becker, M. Gorospe, Global analysis of stress-regulated mRNA turnover by using cDNA arrays, Proc. Natl. Acad. Sci. USA 99 (2002) 10611-10616.

M.E. Fant, R.D. Harbison, R.W. Harrison, Glucocorticoid uptake into human placental membrane vesicles, J. Biol. Chem. 254 (1979) 6218-6221.

A. Fedelli, S Braconi, D. Economidou, N. Cannella, M. Kallupi, R. Guerrini, C. Calo, M. Massi, R. Ciccocioppo, The paraventricular nucleus of the hypothalamus is a neuroanatomical substrate for the inhibition of palatable food intake by neuropeptide S, Eur. J. Neurosci. 30 (2009) 1594-1602.

H.H. Feder, J.A. Resko, R.W. Goy, Progesterone levels in the arterial plasma of pre-ovulatory and ovariectomized rats, J. Endocrinol. 41 (1968) 563-569.

E. Feldmesser, T. Olender, M. Khen, I. Yanai, R. Ophir, D. Lancet, Widespread ectopic expression of olfactory receptor genes, BMC Genomics 7 (2006) 121-139.

C. Fekete, J. Kelly, E. Mihaly, S. Sarkar, W.M. Rand, G. Legradi, C.H. Emerson, R.M. Lechan, Neuropeptide Y has a central inhibitory action on the hypothalamic-pituitary-thyroid axis, Endocrinology 142 (2001) 2602-2613.

C. Fekete, S. Sarkar, W.M. Rand, J.W. Harney, C.H. Emerson, A.C. Bianco, A. Beck-Sickinger, R.M. Lechan, Neuropeptide Y1 and Y5 receptors mediate the effects of neuropeptide Y on the hypothalamic-pituitary-thyroid axis, Endocrinology 143 (2002) 4513-4519.

Y.H. Feng, Y. Ding, S. Ren, L. Zhou, C. Xu, S.S. Karnik, Unconventional homologous internalization of the angiotensin II type-1 receptor induced by G-protein-independent signals, Hypertension 46 (2005) 419-425.

Y. Feng, P. Gregor P, Cloning of a novel member of the G protein-coupled receptor family related to peptide receptors. Biochem. Biophys. Res. Commun. 24 (1997) 651-654.

A.V. Ferguson, Angiotensinergic regulation of autonomic and neuroendocrine outputs: critical roles for the subfornical organ and paraventricular nucleus, Neuroendocrinology 89 (2009) 370-376.

J.M. ffrench-Mullen, Cortisol inhibition of calcium currents in guinea pig hippocampal CA1 neurons via G-protein-coupled activation of protein kinase C, J. Neurosci. 15 (1995) 903-911.

E.J. Filardo, C.T. Graeber, J.A. Quinn, M.B. Resnick, D. Giri, R.A. DeLellis, M.M. Steinhoff, E. Sabo, Distribution of GPR30, a seven membrane-spanning estrogen receptor, in primary breast cancer and its association with clinicopathologic determinants of tumor progression, Clin. Cancer Res. 1 (2006) 6359-6366.

E.J. Filardo, J.A. Quinn, K.I. Bland, A.R. Frackelton, Estrogen-induced activation of Erk-1 and Erk-2 requires the G protein-coupled receptor homolog, GPR30, and occurs via trans-activation of the epidermal growth factor receptor through release of HB-EGF. Mol. Endocrinol. 14 (2000) 1649-1660.

E.J. Filardo, J.A. Quinn, A.R. Frackelton, K.I. Bland, Estrogen action via the G protein-coupled receptor, GPR30: stimulation of adenylyl cyclase and cAMP-mediated attenuation of the epidermal growth factor receptor-to-MAPK signaling axis. Mol. Endocrinol. 16 (2002) 70-84.

E. Filardo, J. Quinn, Y. Pang, C. Graeber, S. Shaw, J. Dong, P. Thomas, Activation of the novel estrogen receptor G protein-coupled receptor 30 (GPR30) at the plasma membrane, Endocrinology 148 (2007) 3236-3245.

A.R. Finch, K.R. Sedgley, C.J. Caunt, C.A. McArdle, Plasma membrane expression of GnRH receptors: regulation by antagonists in breast, prostate, and gonadotrope cell lines, J. Endocrinol. 196 (2008) 353-367.

J.N. Flak, M.M. Ostrander, J.G. Tasker, J.P. Herman, Chronic stress-induced neurotransmitter plasticity in the PVN, J. Comp. Neurol. 517 (2009) 156-165.

V.C. Foletta, F.D. Brown, W.S. Young, Cloning of rat ARHGAP4/C1, a RhoGAP family member expressed in the nervous system that colocalizes with the Golgi complex and microtubules, Brain Res. Mol. Brain Res. 107 (2002) 65-79.

J. Ford, A. Hajibeigi, M. Long, L. Hahner, C. Gore, J.T. Hsieh, D. Clegg, J. Zerwekh, O.K. Oz, GPR30 deficiency causes increased bone mass, mineralization, and growth plate proliferative activity in male mice, J. Bone. Miner. Res. 26 (2011) 298-307.

M.L. Forsling, A.J. Williams, The effect of exogenous melatonin on stimulated neurohypophysial hormone release in man, Clin. Endocrinol. 57 (2002) 615-620.

C.A. Fox, A. Mansour, R.C. Thompson, J.R. Bunzow, O. Civelli, S.J. Watson, The distribution of dopamine D2 receptor heteronuclear RNA (hnRNA) in the rat brain, J. Chem. Neuroanat. 6 (1993) 363-373.

R. Franco R, G-protein-coupled receptor heteromers or how neurons can display differently flavoured patterns in response to the same neurotransmitter, Br. J. Pharmacol. 158 (2009) 23-31.

R. Franco, F. Boscia, V. Gigantino, L. Marra, F. Esposito, D. Ferrara, P. Pariante, G. Botti, M. Caraglia, S. Minucci, P. Chieffi, GPR30 is overexpressed in post-puberal testicular germ cell tumors, Cancer Biol. Ther. 11 (2011) 609-613.

J.M. Fritschy, V. Meskenaite, O. Weinmann, M. Honer, D. Benke, H. Mohler, GABAB-receptor splice variants GB1a and GB1b in rat brain: developmental regulation, cellular distribution and extrasynaptic localization, Eur. J. Neurosci. 11 (1999) 761-768.

T. Funakoshi, A. Yanai, K. Shinoda, M.M. Kawano, Y. Mizukami, G protein-coupled receptor 30 is an estrogen receptor in the plasma membrane, Biochem. Biophys. Res. Commun. 346 (2006) 904-910.

I. Gaillard, S. Rouquier, D. Giorgi, Olfactory receptors, Cell Mol. Life Sci. 61 (2004) 456-469.

R.R. Gainetdinov, R.T. Premont, L.M. Bohn, R.J. Lefkowitz, M.G. Caron, Desensitization of G protein-coupled receptors and neuronal functions, Annu. Rev. Neurosci. 27 (2004) 107-144.

J.G. Gall, M.L. Pardue, Formation and detection of RNA-DNA hybrid molecules in cytological preparations, Proc. Natl. Acad. Sci. USA. 63 (1969) 378-383.

R.R. Gainetdinov, R.T. Premont, L.M. Bohn, R.J. Lefkowitz, M.G. Caron, Desensitization of G protein-coupled receptors and neuronal functions, Annu. Rev. Neurosci. 27 (2004) 107-144.

W.F. Ganong, Circumventricular organs: definition and role in the regulation of endocrine and autonomic function, Clin Exp Pharmacol Physiol. 27 (2000) 422-427.

D. García-Galiano, V.M. Navarro, F. Gaytan, M. Tena-Sempere, Expanding roles of NUCB2/nesfatin-1 in neuroendocrine regulation, J. Mol. Endocrinol. 45 (2010):281-90.

J.C. Garza, C.S. Kim, J. Liu, W. Zhang, X.Y. Lu, Adeno-associated virus-mediated knockdown of melanocortin-4 receptor in the paraventricular nucleus of the hypothalamus promotes high-fat diet-induced hyperphagia and obesity, J. Endocrinol. 197 (2008) 471-482.

K.L. Gearing, A. Barnes, J. Barnett, A. Brown, D. Cousens, S. Dowell, A. Green, K. Patel, P. Thomas, F. Volpe, F. Marshall, Complex chimeras to map ligand binding sites of GPCRs, Protein Eng. 16 (2003):365-372.

P. Germain, B. Staels, C. Dacquet, M. Spedding, V. Laudet, Overview of nomenclature of nuclear receptors, Pharmacol. Rev. 58 (2006) 685-704.

M. Ghamari-Langroudi, D. Srisai, R.D. Cone, Multinodal regulation of the arcuate/paraventricular nucleus circuit by leptin, Proc. Natl. Acad. Sci USA. 108 (2011) 355-360.

A. Ghate, K. Befort, J.A. Becker, D. Filliol, C. Bole-Feysot, D. Demebele, B. Jost, M. Koch, B.L. Kieffer, Identification of novel striatal genes by expression profiling in adult mouse brain, Neuroscience 146 (2007) 1182-1192.

M.C. Ghosh, D. Baatar, G. Collins, A. Carter, F. Indig, A. Biragyn, D.D. Taub, Dexamethasone augments CXCR4-mediated signaling in resting human T cells via the activation of the Src kinase Lck, Blood, 113 (2009) 575-584.

G. Gimpl, F. Fahrenholz, The oxytocin receptor system: structure, function, and regulation. Physiol. Rev. 81 (2001) 629-683.

J.P. Glass, G. Parasher, H. Arias-Pulido, R. Donohue, L.A. Cerilli, Mesothelin and GPR30 Staining Among a Spectrum of Pancreatic Epithelial Neoplasms, Int. J. Surg. Pathol. (2011) DOI: 10.1177/1066896911409575.

D.E. Gloriam, R. Fredriksson, H.B. Schiöth, The G protein-coupled receptor subset of the rat genome, BMC Genomics. 8 (2007) 338.

D.E. Gloriam, H.B. Schiöth, R. Fredriksson, Nine new human Rhodopsin family G-protein coupled receptors: identification, sequence characterisation and evolutionary relationship, Biochim. Biophys. Acta. 1722 (2005) 235-246.

R. Goke, P.J. Larsen, J.D. Mikkelsen, S.P. Sheikh, Distribution of GLP-1 binding sites in the rat brain: evidence that exendin-4 is a ligand of brain GLP-1 binding sites, Eur. J. Neurosci. 7 (1995) 2294-2300.

S.J. Gold, Y.G. Ni, H.G. Dohlman, E.J. Nestler, Regulators of G-protein signaling (RGS) proteins: region-specific expression of nine subtypes in rat brain, J. Neurosci. 17 (1997) 8024-8037.

V. Goncharuk, Z. Zeng, R. Wang, D. MacTavish, J.H. Jhamandas, Distribution of the neuropeptide FF1 receptor (hFF1) in the human hypothalamus and surrounding basal forebrain structures: immunohistochemical study, J. Comp. Neurol. 474 (2004) 487-503.

M. González, R. Reyes, C. Damas, R. Alonso, A.R. Bello, Oestrogen receptor α and β in female rat pituitary cells: An immunochemical study, Gen. Comp. Endocrinol. 1 (2008) 857-868.

T. Goto, A. Salpekar, M. Monk, Expression of a testis-specific member of the olfactory receptor gene family in human primordial germ cells, Mol. Hum. Reprod. 7 (2001) 553-558.

C. Gouarderes, I. Quelven, C. Mollereau, H. Mazarguil, S.Q. Rice, J.M. Zajac, Quantitative autoradiographic distribution of NPFF1 neuropeptide FF receptor in the rat brain and comparison with NPFF2 receptor by using [125I]YVP and [125I]EYF as selective radioligands, Neuroscience 115 (2002) 349-361.

L. Gouzénes, N. Sabatier, P. Richard, F.C. Moos, G. Dayanithi, V1a- and V2-type vasopressin receptors mediate vasopressin-induced Ca2+ responses in isolated rat supraoptic neurones, J. Physiol. 517 (1999) 771-779.

N.L. Grimsey, C.E. Goodfellow, E.L. Scotter, M.J. Dowie, M. Glass, E.S. Graham, Specific detection of CB1 receptors; cannabinoid CB1 receptor antibodies are not all created equal! J. Neurosci. Methods 171 (2008) 78-86.

F.L. Groeneweg, H. Karst, E.R. de Kloet, M. Joëls, Rapid non-genomic effects of corticosteroids and their role in the central stress response, J. Endocrinol. 209 (2011) 153-167.

R. Gros, Q. Ding, L.A. Sklar, E.E. Prossnitz, J.B. Arterburn, J. Chorazyczewski, R.D. Feldman, GPR30 expression is required for the mineralocorticoid receptor-independent rapid vascular effects of aldosterone, Hypertension 57 (2011) 442-451.

K.L. Grove, S. Allen, B.E. Grayson, M.S. Smith, Postnatal development of the hypothalamic neuropeptide Y system, Neuroscience. 116 (2003) 393-406.

A.J. Guastella, A.R. Kenyon, G.A. Alvares, D.S. Carson, I.B. Hickie IB, Intranasal Arginine Vasopressin Enhances the Encoding of Happy and Angry Faces in Humans, Biol. Psychiatry 67 (2010) 1220-1222.

E.V. Gurevich, J.N. Joyce, Distribution of dopamine D3 receptor expressing neurons in the human forebrain: comparison with D2 receptor expressing neurons, Neuropsychopharmacology 20 (1999) 60-80.

J.S. Gutkind, Regulation of mitogen-activated protein kinase signaling networks by G protein-coupled receptors, Sci. STKE. 2000 (40) 1-13.

E. Haas, I. Bhattacharya, E. Brailoiu, M. Damjanović, G.C. Brailoiu, X. Gao, L. Mueller-Guerre, N.A. Marjon, A. Gut, R. Minotti, M.R. Meyer, K. Amann, E. Ammann, A. Perez-Dominguez, M. Genoni, D.J. Clegg, N.J. Dun, T.C. Resta, E.R. Prossnitz, M. Barton, Regulatory role of G protein-coupled estrogen receptor for vascular function and obesity, Circ. Res. 104 (2009) 288-291.

E. Haas, M.R. Meyer, U. Schurr, I. Bhattacharya, R. Minotti, H.H. Nguyen, A. Heigl, M. Lachat, M. Genoni, M. Barton, Differential effects of 17beta-estradiol on function and expression of estrogen receptor alpha, estrogen receptor beta, and GPR30 in arteries and veins of patients with atherosclerosis, Hypertension 49 (2007) 1358-1363.

J.R. Hadcock, H.Y. Wang, C.C. Malbon, Agonist-induced destabilization of beta-adrenergic receptor mRNA. Attenuation of glucocorticoid-induced up-regulation of beta-adrenergic receptors, J. Biol. Chem. 264 (1989) 19928-19933.

A. Hafezi-Moghadam, T. Simoncini, Z. Yang, F.P. Limbourg, J.C. Plumier, M.C. Rebsamen, C.M. Hsieh, D.S. Chui, K.L. Thomas, A.J. Prorock, V.E. Laubach, M.A. Moskowitz, B.A. French, K. Ley, J.K. Liao, Acute cardiovascular protective effects of corticosteroids are mediated by non-transcriptional activation of endothelial nitric oxide synthase, Nat. Med. 8 (2002) 473-479.

G.E. Haley, F.W. Flynn, Agonist and hypertonic saline-induced trafficking of the NK3-receptors on vasopressin neurons within the paraventricular nucleus of the hypothalamus, Am. J. Physiol. Integr. Comp. Physiol. 290 (2006) 1242-1250.

J. Haller, E. Mikics, G.B. Makara, The effects of non-genomic glucocorticoid mechanisms on bodily functions and the central neural system. A critical evaluation of findings, Front. Neuroendocrinol. 29 (2008) 273-291.

S.R. Hammes, E.R. Levin ER, Extranuclear steroid receptors: nature and actions, Endocr. Rev 28 (2007) 726-741.

R. Hammond, R. Mauk, D. Ninaci, D. Nelson, R.B. Gibbs, Chronic treatment with estrogen receptor agonists restores acquisition of a spatial learning task in young ovariectomized rats, Horm. Behav. 56 (2009) 309-314.

P.J. Harding, H. Attrill, S. Ross, J.R. Koeppe, A.N. Kapanidis, A. Watts, Neurotensin receptor type 1: Escherichia coli expression, purification, characterization and biophysical study, Biochem. Soc. Trans. 35 (2007) 760-763.

A.J. Harmar, R.A. Hills, E.M. Rosser, M. Jones, O.P. Buneman, D.R. Dunbar, S.D. Greenhill, V.A. Hale, J.L. Sharman, T.I. Bonner, W.A. Catterall, A.P. Davenport, P. Delagrange, C.T. Dollery, S.M. Foord, G.A. Gutman, V. Laudet, R.R. Neubig, E.H. Ohlstein, R.W. Olsen, J. Peters, J.P. Pin, R.R. Ruffolo, D.B. Searls, M.W. Wright, M. Spedding, IUPHAR-DB: the IUPHAR database of G protein-coupled receptors and ion channels, Nucl. Acids Res. 37 (2009) 680-685.

M.T. Harrigan, N.F. Campbell, S. Bourgeois, Identification of a gene induced by glucocorticoids in murine T-cells: a potential G protein-coupled receptor, Mol. Endocrinol. 5 (1991) 1331-1338.

R.W. Harrison, K. Balasubramanian, J. Yeakley, M. Fant, F. Svec, S. Fairfield, Heterogeneity of AtT-20 cell glucocorticoid binding sites: evidence for a membrane receptor, Adv. Exp. Med. Biol. 117 (1979) 423-440.

C. Harrison, J.R. Traynor, The [35S]GTPαS binding assay: approaches and applications in pharmacology, Life Sci. 74 (2003) 489-508.

A.C. Hart, H. Krämer, D.L. Van Vactor, M. Paidhungat, S.L. Zipursky, Induction of cell fate in the Drosophila retina: the bride of sevenless protein is predicted to contain a large extracellular domain and seven transmembrane segments, Genes Dev. 4 (1990) 1835-1847.

N. Hatae, N. Aksentijevich, H.W. Zemkova, K. Kretschmannova, M. Tomic, S.S. Stojilkovic, Cloning and functional identification of novel endothelin receptor type A isoforms in pituitary, Mol. Endocrinol. 21 (2007) 1192-1204.

G.I. Hatton, Emerging concepts of structure-function dynamics in adult brain: the hypothalamo-neurohypophysial system, Prog. Neurobiol. 34 (1990) 437-504.

G.I. Hatton, Glial-neuronal interactions in the mammalian brain, Adv. Physiol. Educ. 26 (2002) 225-237.

Z. He, M. Kokkinaki, J. Jiang, I. Dobrinski, M. Dym, Isolation, characterization, and culture of human spermatogonia, Biol. Reprod. 82 (2010) 363-372.

A.S. Heimann, I. Gomes, C.S. Dale, R.L. Pagano, A. Gupta, L.L. de Souza, A.D. Luchessi, L.M. Castro, R. Giorgi, V. Rioli, E.S. Ferro, L.A. Devi, Hemopressin is an inverse agonist of CB1 cannabinoid receptors, Proc Natl. Acad. Sci. USA 104 (2007) 20588-20593.

S.C. Heinrichs, F. Menzaghi, E.M. Pich, R.L. Hauger, G.F. Koob, Corticotropin-releasing factor in the paraventricular nucleus modulates feeding induced by neuropeptide Y, Brain Res. 611 (1993) 18-24.

L.K. Heisler, N. Pronchuk, K. Nonogaki, L. Zhou, J. Raber, L. Tung, G.S. Yeo, S. O'Rahilly, W.F. Colmers, J.K. Elmquist, L.H. Tecott, Serotonin activates the hypothalamic-pituitary-adrenal axis via serotonin 2C receptor stimulation, J. Neurosci. 27 (2007) 6956-6964.

M. Herkenham, Mismatches between neurotransmitter and receptor localizations in brain: observations and implications, Neuroscience. 23 (1987) 1-38.

M. Herkenham, A.B. Lynn, M.D. Little, M.R. Johnson, L.S. Melvin, B.R. de Costa, K.C. Rice, Cannabinoid receptor localization in brain, Proc. Natl. Acad. Sci. USA 87 (1990) 1932-1936.

J.P. Herman, M.K. Schäfer, S.J. Watson, T.G. Sherman, In situ hybridization analysis of arginine vasopressin gene transcription using intron-specific probes, Mol. Endocrinol. 5 (1991) 1447-1456.

S.A. Hesketh, A.K. Brennan, D.S. Jessop, D.P. Finn, Effects of chronic treatment with citalopram on cannabinoid and opioid receptor-mediated G-protein coupling in discrete rat brain regions, Psychopharmacology 198 (2008) 29-36.

C. Hindmarch, Fry, P.M. Smith, S.T. Yao, G.G. Hazell, S.J. Lolait, J.F. Paton, A.V. Ferguson, D. Murphy, The transcriptome of the medullary area postrema: The thirsty rat, the hungry rat and the hypertensive rat, Exp. Physiol. (2011) In Press.

C. Hindmarch, M. Fry, S.T. Yao, P.M. Smith, D. Murphy, A.V. Ferguson, Microarray analysis of the transcriptome of the subfornical organ in the rat: regulation by fluid and food deprivation, Am. J. Physiol. Regul. Integr. Comp. Physiol. 295 (2008) 1914-1920.

C. Hindmarch, S. Yao, G. Beighton, J. Paton, D. Murphy, A comprehensive description of the transcriptome of the hypothalamoneurohypophyseal system in euhydrated and dehydrated rats, Proc. Natl. Acad. Sci. USA 103 (2006) 1609-1614.

G.L. Hinks, J.A. Poat, J. Hughes, Changes in hypothalamic cholecystokinin A and cholecysotkinin B receptor subtypes and associated neuropeptide expression in response to salt-stress in the rat and mouse, Neuroscience 68 (1995) 765-781.

S. Hinuma, Y. Habata, R. Fujii, Y. Kawamata, M. Hosoya, S. Fukusumi, C. Kitada, Y. Masuo, T. Asano, H. Matsumoto, M. Sekiguchi, T. Kurokawa, O. Nishimura, H. Onda, M. Fujino, A prolactin-releasing peptide in the brain, Nature 393 (1998) 272-276.

B. Hinz, R.Hirschelmann, Rapid non-genomic feedback effects of glucocorticoids on CRF-induced ACTH secretion in rats, Pharm. Res. 17 (2000) 1273-1277.

M.K. Ho, Y. Su, W.W. Yeung, Y.H. Wong, Regulation of transcription factors by heterotrimeric G proteins, Curr. Mol. Pharmacol. 2 (2009) 19-31.

G.E. Hoffman, M.S. Smith, J.G. Verbalis, c-Fos and related immediate early gene products as markers of activity in neuroendocrine systems, Front. Neuroendocrinol. 14 (1993) 173-213.

K.P. Hofmann, P. Scheerer, P.W. Hildebrand, H.W. Choe, J.H. Park, M. Heck, O.P. Ernst OP, A G protein-coupled receptor at work: the rhodopsin model, Trends Biochem. Sci. 34 (2009) 540-552.

B. Holst, N.D. Holliday, A. Bach, C.E. Elling, H.M. Cox, T.W. Schwartz, Common structural basis for constitutive activity of the ghrelin receptor family, J. Biol. Chem. 279 (2004) 53806-53817.

A.L. Hopkins, C.R. Groom, The druggable genome, Nat. Rev. Drug Discov. 1 (2002) 727-730.

H.E. Howe, S.J. Somponpon, C.D. Sladek, Role of neurokinin 3 receptors in supraoptic vasopressin and oxytocin neurons, J. Neurosci. 24 (2004) 10103-10110.

E. Hrabovszky, I. Kalló, A. Steinhauser, I. Merchenthaler, C.W. Coen, S.L. Petersen, Z. Liposits, Estrogen Receptor-β in oxytocin and vasopressin neurons of the rat and human hypothalamus: immunocytochemical and in situ hybridization Studies, J. Comp. Neurol. 31 (2004) 315-333.

L. Hu, R.L. Gustofson, H. Feng, P.K. Leung, N. Mores, L.Z. Krsmanovic, K.J. Catt, Converse regulatory functions of estrogen receptor-alpha and -beta subtypes expressed in hypothalamic gonadotropin-releasing hormone neurons, Mol. Endocrinol. 22 (2008) 2250-2259.

G.X. Hu, Q.Q. Lian, H. Lin, S.A. Latif, D.J. Morris, M.P. Hardy, R.S. Ge, Rapid mechanisms of glucocorticoid signaling in the Leydig cell, Steroids 73 (2008) 1018-1024.

P. Huang, V. Chandra, F. Rastinejad, Structural overview of the nuclear receptor superfamily: insights into physiology and therapeutics, Annu. Rev. Physiol. 72 (2010) 247-272.

G.S. Huang, M.J. Gunter, R.C. Arend, M. Li, H. Arias-Pulido, E.R. Prossnitz, G.L. Goldberg, H.O. Smith, Co-expression of GPR30 and ERbeta and their association with disease progression in uterine carcinosarcoma, Am. J. Obstet. Gynecol. 203 (2010) 242-247.

M.H. Huang, E.C. So, Y.C. Liu, S.N. Wu, Glucocorticoids stimulate the activity of large-conductance Ca2+ -activated K+ channels in pituitary GH3 and AtT-20 cells via a non-genomic mechanism, Steroids 71 (2006) 129-140.

A. Hurbin, L. Boissin-Agasse, H. Orcel, A. Rabié, N. Joux, MG. Desarménien, P. Richard, F.C. Moos, The V1a and V1b, but not V2, vasopressin receptor genes are expressed in the supraoptic nucleus of the rat hypothalamus, and the transcripts are essentially colocalized in the vasopressinergic magnocellular neurons, Endocrinology 139 (1998) 4701-4707.

A. Hurbin, H. Orcel, G. Alonso, F. Moos, A. Rabié, The vasopressin receptors colocalize with vasopressin in the magnocellular neurons of the rat supraoptic nucleus and are modulated by water balance, Endocrinology 143 (2002) 456-466.

J. Huynh, W.G. Thomas, M.I. Aguilar, L.K. Pattenden, Role of helix 8 in G protein-coupled receptors based on structure-function studies on the type 1 angiotensin receptor, Mol. Cell. Endocrinol. 302 (2009) 118-127.

C.K. Hwang, K.Y. Song, C.S. Kim, H.S. Choi, X.H. Guo, P.Y. Law, L.N. Wei, H.H. Loh, Evidence of endogenous mu opioid receptor regulation by epigenetic control of the promoters, Mol. Cell. Biol. 27 (2007) 4720-4736.

A. Ignatov, T. Ignatov, A. Roessner, S.D. Costa, T. Kalinski, Role of GPR30 in the mechanisms of tamoxifen resistance in breast cancer MCF-7 cells, Breast Cancer Res. Treat. 123 (2010) 87-96.

A. Ignatov, T. Ignatov, C. Weissenborn, H. Eggemann, J. Bischoff, A. Semczuk, A. Roessner, S.D. Costa, T. Kalinski, G-protein-coupled estrogen receptor GPR30 and tamoxifen resistance in breast cancer, Breast Cancer Res. Treat. 128 (2011) 457-466.

Y. Ihara, Y. Kihara, F. Hamano, K. Yanagida, Y. Morishita, A. Kunita, T. Yamori, M. Fukayama, H. Aburatani, T. Shimizu, S. Ishii, The G protein-coupled receptor T-cell death-associated gene 8 (TDAG8) facilitates tumor development by serving as an extracellular pH sensor, Proc. Natl. Acad. Sci. USA 107 (2010) 17309-17314.

D.S. Im, C.E. Heise, T. Nguyen, B.F. O'Dowd, K.R. Lynch, Identification of a molecular target of psychosine and its role in globoid cell formation, J. Cell. Biol. 153 (2001) 429-434.

T. Imaki, H. Katsumata, M. Miyata, M. Naruse, J. Imaki, S. Minami, Expression of corticotropin-releasing hormone type 1 receptor in paraventricular nucleus after acute stress, Neuroendocrinology 73 (2001) 293-301.

G. Innamorati, H. Sadeghi, M. Birnbaumer, Transient phosphorylation of the V1a vasopressin receptor, J. Biol. Chem. 273 (1998) 7155-7161.

G. Innamorati, H. Sadeghi, M. Birnbaumer, A fully active nonglycosylated V2 vasopressin receptor, Mol Pharmacol. 50 (1996) 467-473.

P.A. Insel, C.M. Tang, I. Hahntow, M.C. Michel, Impact of GPCRs in clinical medicine: monogenic diseases, genetic variants and drug targets, Biochim. Biophys. Acta. 1768 (2007) 994-1005.

B.G. Irani, J. Donato, D.P. Olson, B.B. Lowell, T.C. Sacktor, M.E. Reyland, K.P. Tolson, A.R. Zinn, Y. Ueta, I. Sakata, J.M. Zigman, C.F. Elias, D.J. Clegg, Distribution and neurochemical characterization of protein kinase C-theta and -delta in the rodent hypothalamus, Neuroscience. 170 (2010) 1065-1079.

J. Irelan, J. Morgon, Featured Study: Functional Cell Profiling of Endogenous GPCRs using the xCELLigence System, Roche Diagnostics GmbH, Germany (2010).

J. Isensee, L. Meoli, V. Zazzu, C. Nabzdyk, H. Witt, D. Soewarto, K. Effertz, H. Fuchs, V, Gailus-Durner, D. Busch, T. Adler, M.H. de Angelis, M. Irgang, C. Otto, P.R. Noppinger, Expression pattern of G protein-coupled receptor 30 in LacZ reporter mice, Endocrinology 150 (2009) 1722-1730.

S. Ishii, Y. Kihara, T. Shimizu, Identification of T cell death-associated gene 8 (TDAG8) as a novel acid sensing G-protein-coupled receptor, J. Biol. Chem. 280 (2005) 9083-9087.

J.M. Israel, D.A. Poulain, 17β-oestradiol modulates in vitro electrical properties and responses to kainate of oxytocin neurones in lactating rats, J. Physiol. 524 (2000) 457-470.

K. Itoi, N. Horiba, F. Tozawa, Y. Sakai, K. Sakai, K. Abe, H. Demura, T. Suda, Major role of 3',5'-cyclic adenosine monophosphate-dependent protein kinase A pathway in corticotropin-releasing factor gene expression in the rat hypothalamus in vivo, Endocrinology 137 (1996) 2389-2396.

K. Itoi, Y.Q. Jiang, Y. Iwasaki, S.J. Watson, Regulatory mechanisms of corticotropin-releasing hormone and vasopressin gene expression in the hypothalamus, J. Neuroendocrinol. 16 (2004) 348-355.

Y. Iwasaki, Y. Aoki, M. Katahira, Y. Oiso, H. Saito, Non-genomic mechanisms of glucocorticoid inhibition of adrenocorticotropin secretion: possible involvement of GTP-binding protein, Biochem. Biophys. Res. Commun. 235 (1997) 295-299.

N.J. Izzo, C.E. Seidman, S. Collins, W.S. Colucci, Alpha 1-adrenergic receptor mRNA level is regulated by norepinephrine in rabbit aortic smooth muscle cells, Proc. Natl. Acad. Sci. USA. 87 (1990) 6268-6271.

V.P. Jaakola, M.T. Griffith, M.A. Hanson, V. Cherezov, E.Y. Chien, J.R. Lane, A.P. Ijzerman, R.C. Stevens, The 2.6 angstrom crystal structure of a human A2A adenosine receptor bound to an antagonist, Science. 322 (2008) 1211-1217.

S. Jain, Y. Li, A. Kumar, P.B. Sehgal, Transcriptional signaling from membrane raft-associated glucocorticoid receptor, Biochem. Biophys. Res. Commun. 336 (2005) 3-8.

J.H. Jhamandas, W. Raby, J. Rogers, R.M. Buijs, L.P. Renaud, Diagonal band projection towards the hypothalamic supraoptic nucleus: light and electron microscopic observations in the rat, J. Comp. Neurol. 282 (1989) 15-23.

M. Jhanwar-Uniyal, C.R. Roland, S.F. Leibowitz SF, Diurnal rhythm of alpha 2-noradrenergic receptors in the paraventricular nucleus and other brain areas: relation to circulating corticosterone and feeding behavior, Life Sci. 38 (1986) 473-482.

C. Jin, F. Yin, M. Lin, H. Li, Z. Wang, J. Weng, M. Liu, X. Da Dong, J. Qu, L. Tu, GPR48 regulates epithelial cell proliferation and migration by activating EGFR during eyelid development, Invest. Ophthalmol. Vis. Sci. 49 (2008) 4245-4253.

J.H. Jjamandas, D. MacTavish, Central administration of neuropeptide FF causes activation of oxytocin paraventricular hypothalamic neurones that project to the brainstem, J. Neuroendocrinol. 15 (2003) 24-32.

M. Joëls, T.Z. Baram, The neuro-symphony of stress, Nat. Rev. Neurosci. 10 (2009) 459-466.

H.A. John, M.L. Birnstiel, K.W. Jones, RNA-DNA hybrids at the cytological level, Nature 223 (1969) 582-587.

G.L. Johnson, R. Lapadat, Mitogen-activated protein kinase pathways mediated by ERK, JNK, and p38 protein kinases, Science 298 (2002) 1911-1912.

P.G. Jones, S.P. Nawoschik, K. Sreekumar, A.J. Uveges, E. Tseng, L. Zhang, J. Johnson, L. He, J.E. Paulsen, B. Bates, M.H. Pausch, Tissue distribution and functional analyses of the constitutively active orphan G protein coupled receptors, GPR26 and GPR78, Biochim. Biophys. Acta. 1170 (2007) 890-901.

G. Jositsch, T. Papadakis, R.V. Haberberger, M. Wolff, J. Wess, W. Kummer, Suitability of muscarinic acetylcholine receptor antibodies for immunohistochemistry evaluated on tissue sections of receptor gene-deficient mice. Naunyn Schmiedebergs Arch. Pharmacol. 379 (2009) 389-395.

H. Joun, B. Lanske, M. Karperien, F. Qian, L. Defize, A. Abou-Samra, Tissue-specific transcription start sites and alternative splicing of the parathyroid hormone (PTH)/PTH-related peptide (PTHrP) receptor gene: a new PTH/PTHrP receptor splice variant that lacks the signal peptide, Endocrinology 138 (1997) 1742-1749.

S.P. Kalra, P.S. Kalra, NPY and cohorts in regulating appetite, obesity and metabolic syndrome: beneficial effects of gene therapy, Neuropeptides 38 (2004) 201-211.

L. Kang, X. Zhang, Y. Xie, Y. Tu, D. Wang, Z. Liu, Z.Y. Wang, Involvement of estrogen receptor variant ER-alpha36, not GPR30, in nongenomic estrogen signalling, Mol. Endocrinol. 24 (2010) 709-721.

H. Karst, S. Berger, M. Turiault, F. Tronche, G. Schütz, M. Joëls, Mineralocorticoid receptors are indispensable for nongenomic modulation of hippocampal glutamate transmission by corticosterone, Proc. Natl. Acad. Sc.i USA 102 (2005) 19204-19207.

R.S. Kasai, K.G. Suzuki, E.R. Prossnitz, I. Koyama-Honda, C. Nakada, T.K. Fujiwara, A. Kusumi, Full characterization of GPCR monomer-dimer dynamic equilibrium by single molecule imaging, J. Cell. Biol. 192 (2011) 463-480.

A.J. Kastin, V. Akerstrom, Nonsaturable entry of neuropeptide Y into brain, Am J Physiol. 276 (1999) 479-482.

A.J. Kastin, V. Akerstrom, Orexin A but not orexin B rapidly enters brain from blood by simple diffusion, J Pharmacol Exp Ther 289 (1999) 219–223.

S. Katayama, Y. Tomaru, T. Kasukawa, K. Waki, M. Nakanishi, M. Nakamura, H. Nishida, C.C. Yap, M. Suzuki, J. Kawai, H. Suzuki, P. Carninci, Y. Hayashizaki, C. Wells, M. Frith, T. Ravasi, K.C. Pang, J. Hallinan, J. Mattick, D.A. Hume, L. Lipovich, S. Batalov, P.G.

Engström, Y. Mizuno, M.A. Faghihi, A. Sandelin, A.M. Chalk, S. Mottagui-Tabar, Z. Liang, B. Lenhard, C. Wahlestedt, Antisense transcription in the mammalian transcriptome, Science. 309 (2005) 1564-1566.

S. Kato, M. Matsubara, T. Matsuo, Y. Mohri, I. Kazama, R. Hatano, A. Umezawa, K. Nishimori, Leucine-rich repeat-containing G protein-coupled receptor-4 (LGR4, Gpr48) is essential for renal development in mice, Nephron Exp. Nephrol. 104 (2006) 63-75.

S.D. Katugampola, J.J. Maguire, S.R. Matthewson, A.P. Davenport, [(125)I]-(Pyr(1))Apelin-13 is a novel radioligand for localizing the APJ orphan receptor in human and rat tissues with evidence for a vasoconstrictor role in man, Br. J. Pharmacol. 132 (2001) 1255-1260.

T. Kausar, R. Sharma, M.R. Hasan, S.C. Tripathi, A. Saraya, T.K. Chattopadhyay, S.D. Gupta, R. Ralhan, Clinical significance of GPR56, transglutaminase 2, and NF-κB in esophageal squamous cell carcinoma, Cancer Invest. 29 (2011) 42-48.

M. Kawasaki, T.A. Ponzio, C. Yue, R.L. Fields, H. Gainer, Neurotransmitter regulation of c-fos and vasopressin gene expression in the rat supraoptic nucleus, Exp. Neurol. 219 (2009): 212-222.

T. Kenakin, L.J. Miller, Seven transmembrane receptors as shapeshifting proteins: the impact of allosteric modulation and functional selectivity on new drug discovery, Pharmacol. Rev. 62 (2010) 265-304.

S. Khositseth, T. Pisitkun, D.H. Slentz, G. Wang, J.D. Hoffert, M.A. Knepper, M.J. Yu, Quantitative protein and mRNA profiling shows selective post-transcriptional control of protein expression by vasopressin in kidney cells, Mol. Cell. Proteomics. 10 (2011) M110.004036.

T. Kishi, C.J. Aschkenasi, B.J. Choi, M.E. Lopez, C.E. Lee, H. Liu, A.N. Hollenberg, J.M. Friedman, J.K. Elmquist, Neuropeptide Y Y1 receptor mRNA in rodent brain: distribution and colocalization with melanocortin-4 receptor, J. Comp. Neurol. 482 (2005) 217-243.

J. Kiss, T.J. Görcs, R. Kuhn, T. Knöpfel, A. Csáky, B. Halász, Distribution of metabotropic glutamate receptor 1a in the rat hypothalamus: an immunocytochemical study using monoclonal and polyclonal antibody, Acta. Biol. Hung. 47 (1996) 221-237.

V. Kistler-Heer, M.E. Lauber, W. Lichtensteiger, Different developmental patterns of melanocortin MC3 and MC4 receptor mRNA: predominance of MC4 in fetal rat nervous system, J. Neuroendocrinol. 10 (1998) 133-146.

I. Kita, Y. Yoshida, S. Nishino, An activation of parvocellular oxytocinergic neurons in the paraventricular nucleus in oxytocin-induced yawning and penile erection. Neurosci. Res. 54 (2006) 269-275.

E.C. Klaasse, A.P. Ijzerman, W.J. de Grip, M.W. Beukers, Internalization and desensitization of adenosine receptors, Purinergic Signal. 4 (2008) 21-37.

B. Koch, B. Lutz-Bucher, B. Briaud, C. Mialhe, Specific interaction of corticosteroids with binding sites in the plasma membranes of the rat anterior pituitary gland, J. Endocrinol. 79 (1978) 215-222.

K. Kocsis, J. Kiss, T. Görcs, B. Halász, Metabotropic glutamate receptor in vasopressin, CRF and VIP hypothalamic neurones, NeuroReport 9 (1998) 4029–4033.

T.A. Kohout, R.J. Lefkowitz, Regulation of G protein-coupled receptor kinases and arrestins during receptor desensitization, Mol. Pharmacol. 63 (2003) 9-18.

A. Kohyama-Koganeya, Y.J. Kim, M. Miura, Y. Hirabayashi, A Drosophila orphan G protein-coupled receptor BOSS functions as a glucose-responding receptor: loss of boss causes abnormal energy metabolism, Proc. Natl. Acad. Sci. USA 105 (2008) 15328-15333.

S. Koirala, Z. Jin, X. Piao, G. Corfas, GPR56-regulated granule cell adhesion is essential for rostral cerebellar development, J. Neurosci. 29 (2009) 7439-7449.

S Konishi, Y. Kasagi, H. Katsumata, S. Minami, T. Imaki, Regulation of corticotropin-releasing factor (CRF) type 1 receptor gene expression by CRF in the hypothalamus, Endocr. J. 50 (2003) 21-36.

N. Koo, K.M. Kim, Distinct effects on M2-type pyruvate kinase are involved in the dimethylsulfoxide-induced modulation of cellular proliferation and degranulation of mast cells, Arch. Pharm. Res. 32 (2009) 1637-1642.

Y. Koutcherov, K.W. Ashwell, G. Paxinos, The distribution of the neurokinin B receptor in the human and rat hypothalamus, Neuroreport. 11 (2000) 3127-3131.

K.J Kovács, P.E. Sawchenko, Regulation of stress-induced transcriptional changes in the hypothalamic neurosecretory neurons, J. Mol. Neurosci. 7 (1996) 125-133.

T. Krietsch, M.S. Fernandes, J. Kero, R. Lösel, M. Heyens, E.W. Lam, I. Huhtaniemi, J.J. Brosens, B. Gellersen, Human homologs of the putative G protein-coupled membrane progestin receptors (mPRalpha, beta, and gamma) localize to the endoplasmic reticulum and are not activated by progesterone, Mol. Endocrinol. 20 (2006) 3146-3164.

K. Kristiansen, Molecular mechanisms of ligand binding, signaling, and regulation within the superfamily of G-protein-coupled receptors: molecular modeling and mutagenesis approaches to receptor structure and function, Pharmacol. Ther. 103 (2004) 21-80.

T. Kubo, K. Fukuda, A. Mikami, A. Maeda, H. Takahashi, M. Mishina, T. Haga, K. Haga, A. Ichiyama, K. Kangawa, et al., Cloning, sequencing and expression of complementary DNA encoding the muscarinic acetylcholine receptor, Nature 323 (1986) 411-416.

R. Kumar, A. Balhuizen, S. Amisten, I. Lundquist, A. Salehi, Insulinotropic and antidiabetic effects of 17β-estradiol and the GPR30 agonist G-1 on human pancreatic islets, Endocrinology 152 (2011) 2568-2579.

A.M. Kvingedal, E.B. Smeland, A novel putative G-protein-coupled receptor expressed in lung, heart and lymphoid tissue, FEBS Letters 407 (1997) 59-62.

H. Kyaw, Z. Zeng, K. Su, P. Fan, B.K. Shell, K.C. Carter, Y. Li, Cloning, characterization, and mapping of human homolog of mouse T-cell death-associated gene, DNA Cell. Biol. 17 (1998) 493-500.

S.E. Kyrkouli, B.G. Stanley, R.D. Seirafi, S.F. Leibowitz, Stimulation of feeding by galanin: anatomical localization and behavioral specificity of this peptide's effects in the brain, Peptides 11 (1990) 995-1001.

N. Laflamme, R.E. Nappi, G. Drolet, C. Labrie, S Rivest, Expression and neuropeptidergic characterization of estrogen receptors (ERalpha and ERbeta) throughout the rat brain: anatomical evidence of distinct roles of each subtype. Journal of Neurobiology 5 (1998) 357-378.

R.C. Lambert, G. Dayanithi, F.C. Moos, P. Richard, A rise in the intracellular Ca2+ concentration of isolated rat supraoptic cells in response to oxytocin, J. Physiol. 478 (1994) 275-287.

R. Landgraf, I.D. Neumann, Vasopressin and oxytocin release within the brain: a dynamic concept of multiple and variable modes of neuropeptide communication, Front. Neuroendocrinol. 25 (2004) 150-176.

K.M. Lang, R.A. Spritz, In vitro splicing pathways of pre-mRNAs containing multiple intervening sequences? Mol. Cell. Biol. 7 (1987) 3428-3437.

P.J. Larsen, M. Tang-Christensen, D.S. Jessop, Central administration of glucagon-like peptide-1 activates hypothalamic neuroendocrine neurons in the rat, Endocrinology 138 (1997) 4445-4455.

K.J. Latchford, A.V. Ferguson, ANG II-induced excitation of paraventricular nucleus magnocellular neurons: a role for glutamate interneurons, Am. J. Physiol. Regul. Integr. Comp. Physiol. 286 (2004) 894-902.

D. Lebesgue, A. Reyna-Neyra, X. Huang, A.M. Etgen, GPR30 differentially regulates short latency responses of luteinising hormone and prolactin secretion to oestradiol, J. Neuroendocrinol. 21 (2009) 743-752.

K. Leblanc, E. Sexton, S. Parent, G. Bélanger, M.C. Déry, V. Boucher, E. Asselin, Effects of 4-hydroxytamoxifen, raloxifene and ICI 182 780 on survival of uterine cancer cell lines in the presence and absence of exogenous estrogens, Int. J. Oncol. 30 (2007) 477-487.

D. Lecca, M.P. Abbracchio, Deorphanisation of G protein-coupled receptors: A tool to provide new insights in nervous system pathophysiology and new targets for psycho-active drugs, Neurochem. Int. 52 (2008) 339-351.

M. Lee, S. Choi, G. Halldén, S.J. Yo, D. Schichnes, G.W. Aponte, P2Y5 is a G(alpha)i, G(alpha)12/13 G protein-coupled receptor activated by lysophosphatidic acid that reduces intestinal cell adhesion, Am. J. Physiol. Gastrointest. Liver Physiol. 297 (2009) 641-654.

N.H. Lee, J. Earle-Hughes, C.M. Fraser, Agonist-mediated destabilization of m1 muscarinic acetylcholine receptor mRNA. Elements involved in mRNA stability are localized in the 3'-untranslated region, J. Biol. Chem. 269 (1994) 4291-4298.

S.Y. Lee, J.S. Kang, G.Y. Song, C.S. Myung, Stress induces the expression of heterotrimeric G protein beta subunits and the phosphorylation of PKB/Akt and ERK1/2 in rat brain, Neurosci. Res. 56 (2006) 180-192.

T.T. Lee, V.A. Redila, M.N. Hill, B.B. Gorzalka, 5-HT(2A) receptor mediated neuronal activation within the paraventricular nucleus of the hypothalamus is desensitized following prolonged glucocorticoid treatment, Eur. J. Pharmacol. 602 (2009) 54–57.

S.P. Lee, C.H. So, A.J. Rashid, G. Varghese, R. Cheng, A.J. Lança, B.F. O'Dowd, S.R. George, J. Biol. Chem. 279 (2004) 35671-35678.

E.J Lee, G.H. Son, S. Chung, S. Lee, J. Kim, S. Choi, K. Kim, Impairment of fear memory consolidation in maternally stressed male mouse offspring: evidence for nongenomic glucocorticoid action on the amygdala, J. Neurosci. 31 (2011) 7131-7140.

F.J. Lee, S. Xue, L. Pei, B. Vukusic, N. Chéry, Y. Wang, Y.T. Wang, H.B. Niznik, X.M. Yu, F. Liu, Dual regulation of NMDA receptor functions by direct protein-protein interactions with the dopamine D1 receptor, Cell 111 (2002) 219-230.

R.J. Lefkowitz, Seven transmembrane receptors: something old, something new, Acta. Physiol. (Oxf). 190 (2007) 9-19.

R.J. Lefkowitz, S.K. Shenoy, Transduction of receptor signals by beta-arrestins, Science. 308 (2005) 512-517.

E.S. Lein, M.J. Hawrylycz, N. Ao, M. Ayres, A. Bensinger, A. Bernard, A.F. Boe, M.S. Boguski, K.S. Brockway, E.J. Byrnes et al., Genome-wide atlas of gene expression in the adult mouse brain, Nature 445 (2007) 168-176.

E.S. Lein, X. Zhao, F.H. Gage, Defining a molecular atlas of the hippocampus using DNA microarrays and high-throughput in situ hybridization, J Neurosci. 24 (2004) 3879-3889.

M.D. Lemonick, D. Cray, A. Park, C.B. Thomas, D. Thompson, Brave New Pharmacy, Time magazine, U.S. 157 (Jan 15, 2001).

G. Leng, C. Brown, N. Sabatier, V. Scott, Population dynamics in vasopressin cells, Neuroendocrinology. 88 (2008) 160-172.

Z. Lenkei, M. Palkovits, P. Corvol, C. Llorens-Cortes, Distribution of angiotensin type-1 receptor messenger RNA expression in the adult rat brain, Neuroscience. 82 (1998) 827-841.

E.R. Levin, Plasma membrane estrogen receptors, Trends Endocrinol. Metab. 20 (2009) 477-482.

E.R. Levin, Integration of the extranuclear and nuclear actions of estrogen, Mol. Endocrinol. 19 (2005) 1951–1959.

A. Levoye, J. Dam, M.A. Ayoub, J.L. Guillaume, R. Jockers, Do orphan G-protein-coupled receptors have ligand-independent functions? New insights from receptor heterodimers, EMBO Rep. 7 (2006) 1094-1098.

D.P. Li, L.M. Atnip, S.R. Chen, H.L. Pan, Regulation of synaptic inputs to paraventricular-spinal output neurons by α2 adrenergic receptors, J. Neurophysiol. 93 (2005) 393-402.

X. Li, M. Fan, L. Shen, Y. Cao, D. Zhu, Z. Hong, Excitatory responses of cardiovascular activities to urocortin3 administration into the PVN of the rat, Auton Neurosci. 154 (2010) 108-111.

S. Li, Z. Jin, S. Koirala, L. Bu, L. Xu, R.O. Hynes, C.A. Walsh, G. Corfas, X. Piao, GPR56 regulates pial basement membrane integrity and cortical lamination, J. Neurosci. 28 (2008) 5817-5826.

S. Li, P. Liu, L. Xi, X. Jiang, M. Wu, D. Deng, J. Wei, T. Zhu, L. Zhou, S. Wang, G. Xu, L. Meng, J. Zhou, D. Ma, Expression of TMEM87B interacting with the human papillomavirus type 18 E6 oncogene in the Hela cDNA library by a yeast two-hybrid system, Oncol. Rep. 20 (2008) 421-427.

X.Y. Li, Y. Lu, H.Y. Sun, J.Q. Wang, J. Yang, H.J. Zhang, N.G. Fan, J. Xu, J.J. Jiang, R.Y. Liu, D.L. Li, M.Y. Liu, G. Ning, G protein-coupled receptor 48 upregulates estrogen receptor alpha expression via cAMP/PKA signaling in the male reproductive tract, Development 137 (2010) 151-157.

D.P. Li, H.L. Pan, Increased group I metabotropic glutamate receptor activity in paraventricular nucleus supports elevated sympathetic vasomotor tone in hypertension, Am. J. Physiol. Regul. Integr. Comp. Physiol. 299 (2010) 552-561.

J.J. Liang, M. Cockett, X.Z. Khawaja, Immunohistochemical localization of G protein beta1, beta2, beta3, beta4, beta5, and gamma3 subunits in the adult rat brain, J. Neurochem. 71 (1998) 345-355.

F. Libert, M. Parmentier, A. Lefort, C. Dinsart, J. Van Sande, C. Maenhaut, M.J. Simons, J.E. Dumont, G. Vassart, Selective amplification and cloning of four new members of the G protein-coupled receptor family, Science 244 (1989) 569-572.

D.D. Licatalosi, R.B. Darnell, RNA processing and its regulation: global insights into biological networks, Nat. Rev. Genet. 11 (2010) 75-87.

W. Lichtensteiger, B. Hanimann, W. Siegrist, A.N. Eberle, Region- and stage-specific patterns of melanocortin receptor ontogeny in rat central nervous system, cranial nerve ganglia and sympathetic ganglia, Brain Res. Dev. Brain Res. 91 (1996) 93-110.

S.L. Lightman, The neuroendocrine paraventricular hypothalamus: receptors, signal transduction, mRNA and neurosecretion, J. Exp. Biol. 139 (1988) 31-49.

S.L. Lightman, B.L. Conway-Campbell, The crucial role of pulsatile activity of the HPA axis for continuous dynamic equilibration, Nat. Rev. Neurosci. 11 (2010) 710-718.

S.H. Lin, F.M. Leslie, O. Civelli, Neurochemical properties of the prolactin releasing peptide (PrRP) receptor expressing neurons: evidence for a role of PrRP as a regulator of stress and nociception, Brain Res. 952 (2002) 15-30.

D.W. Lincoln, J.B. Wakerley, Electrophysiological evidence for the activation of supraoptic neurones during the release of oxytocin, J. Physiol. 242 (1974) 533-554.

K.Y. Little, G.E. Duncan, G.R. Breese, W.E. Stumpf, Beta-adrenergic receptor binding in human and rat hypothalamus, Biol. Psychiatry 32 (1992) 512-522.

A.M. Liu, M.K. Ho, C.S. Wong, J.H. Chan, A.H. Pau, Y.H. Wong, Galpha(16/z) chimeras efficiently link a wide range of G protein-coupled receptors to calcium mobilization, J. Biomol. Screen 8 (2003) 39-49.

F. Liu, Q. Wan, Z.B. Pristupa, X.M. Yu, Y.T. Wang, H.B. Niznik, Direct protein-protein coupling enables cross-talk between dopamine D5 and gamma-aminobutyric acid A receptors, Nature 403 (2000) 274-280.

X. Liu, C.A. Wang, A.L. Ye, P. Jiang, Y.Z. Chen, Effect of glucocorticoids and other steroids on arginine vasopressin release from rat hypothalamic slices, Sheng Li Xue Bao 47 (1995) 201-206.

J.N. Livingston, D.H. Lockwood, Effect of glucocorticoids on the glucose transport system of isolated fat cells, J. Biol. Chem. 250 (1975) 8353-8360.

E.D. Loh, S.R. Broussard, L.F. Kolakowski, Molecular characterization of a novel glycoprotein hormone G-protein-coupled receptor, Biochem. Biophys. Res. Commun. 282 (2001) 757-764.

S.J. Lolait, A.M. O'Carroll, L.C. Mahan, C.C. Felder, D.C. Button, W.S. Young, E. Mezey, M.J. Brownstein MJ, Extrapituitary expression of the rat V1b vasopressin receptor gene. Proc. Natl. Acad. Sci. USA 92 (1995) 6783-6787.

S.J. Lolait, A.M. O'Carroll, O.W. McBride, M. Konig, A. Morel, M.J. Brownstein, Cloning and characterization of a vasopressin V2 receptor and possible link to nephrogenic diabetes insipidus, Nature 357 (1992) 336-339.

R.M. Losel, E. Falkenstein, M. Feuring, A. Schultz, H.C. Tillmann, K. Rossol-Haseroth, M. Wehling, Nongenomic steroid action: controversies, questions, and answers, Physiol. Rev. 83 (2003) 965-1016.

X.Y. Lu, G.S. Barsh, H. Akil, S.J. Watson, Interaction between α-melanocyte-stimulating hormone and corticotropin-releasing hormone in the regulation of feeding and hypothalamo-pituitary-adrenal responses, J. Neurosci 23 (2003) 7863-7872.

T.T. Lu, J.J. Repa, D.J. Mangelsdorf, Orphan nuclear receptors as eLiXiRs and FiXeRs of sterol metabolism, J. Biol. Chem. 276 (2001) 37735-37738.

B. Lu, X.J. Yang, K. Chen, D.J. Yang, J.Q. Yan, Dietary sodium deprivation evokes activation of brain regional neurons and down-regulation of angiotensin II type 1 receptor and angiotensin-convertion enzyme mRNA expression, Neuroscience 164 (2009) 1303-1311.

J. Luo, W. Zhou, X. Zhou, D. Li, J. Weng, Z. Yi, S.G. Cho, C. Li, T. Yi, X. Wu, X.Y. Li, B. de Crombrugghe, M. Höök, M. Liu, Regulation of bone formation and remodeling by G-protein-coupled receptor 48, Development 136 (2009) 2747-2756.

M. Ludwig, Dendritic release of vasopressin and oxytocin, J. Neuroendocrinol. 10 (1998) 881-895.

M. Ludwig, G. Leng, Autoinhibition of supraoptic nucleus vasopressin neurons in vivo: a combined retrodialysis/electrophysiological study in rats, Eur. J. Neurosci. 9 (1997) 2532-2540.

M. Ludwig, G. Leng, Dendritic peptide release and peptide-dependent behaviours, Nat. Rev. Neurosci. 7 (2006) 126-136.

K. Lundstrom, Latest development in drug discovery on G protein-coupled receptors, Curr. Protein Pept. Sci. 7 (2006) 465-470.

X. Luo, A. Kiss, G. Makara, S.J. Lolait, G. Aguilera, Stress-specific regulation of corticotropin releasing hormone receptor expression in the paraventricular and supraoptic nuclei of the hypothalamus in the rat, J. Neuroendocrinol. 6 (1994) 689-696.

J.A. Luther, S.S. Daftary, C. Boudaba, G.C. Gould, K.C. Halmos, J.G. Tasker, Neurosecretory and non-neurosecretory parvocellular neurones of the hypothalamic paraventricular nucleus express distinct electrophysiological properties, J. Neuroendocrinol. 14 (2002) 929-932.

L.M. Luttrell, D. Gesty-Palmer, Beyond desensitization: physiological relevance of arrestin-dependent signalling, Pharmacol. Rev. 62 (2010) 305-330.

B. Lutz-Bucher, D. Monnier, B. Koch, Evidence for the presence of receptors for pituitary adenylate cyclase-activating polypeptide in the neurohypophysis that are positively coupled to cyclic AMP formation and neurohypophyseal hormone secretion, Neuroendocrinology 64 (1996) 153-161.

D. Ma, B. Tao, S. Warashina, S. Kotani, L. Lu, D.B. Kaplamadzhiev, Y. Mori, A.B. Tonchev, T. Yamashima, Expression of free fatty acid receptor GPR40 in the central nervous system of adult monkeys, Neurosci. Res. 58 (2007) 394-401.

C.A. Machida, J.R. Bunzow, R.P. Searles, H. Van Tol, B. Tester, K.A. Neve, P. Teal, V. Nipper, O. Civelli, Molecular cloning and expression of the rat beta 1-adrenergic receptor gene, J. Biol. Chem. 265 (1990) 12960-12965.

M. Macova, J. Pavel, J.M. Saavedra, A peripherally administered, centrally acting angiotensin II AT2 antagonist selectively increases brain AT1 receptors and decreases brain tyrosine hydroxylase transcription, pituitary vasopressin and ACTH, Brain Res. 1250 (2009) 130-140.

K. Maeda, H. Tsukamura, The impact of stress on reproduction: are glucocorticoids inhibitory or protective to gonadotropin secretion? Endocrinology 147 (2006) 1085-1086.

Y. Maejima, U. Sedbazar, S. Suyama, D. Kohno, T. Onaka, E. Takano, N. Yoshida, M. Koike, Y. Uchiyama, K. Fujiwara, T. Yashiro, T.L. Horvath, M.O. Dietrich, S. Tanaka, K. Dezaki, S. Oh-I, K. Hashimoto, H. Shimizu, M. Nakata, M. Mori, T. Yada, Nesfatin-1-regulated oxytocinergic signaling in the paraventricular nucleus causes anorexia through a leptin-independent melanocortin pathway, Cell Metab. 10 (2009) 355-365.

M. Maggiolini, D. Picard, The unfolding stories of GPR30, a new membrane-bound estrogen receptor, J. Endocrinol. 204 (2010) 105-114.

M. Maggiolini, A. Vivacqua, G. Fasanella, A.G. Recchia, D. Sisci, V. Pezzi, D. Montanaro, A.M. Musti, D. Picard, S. Andò, The G protein-coupled receptor GPR30 mediates c-fos up-regulation by 17beta-estradiol and phytoestrogens in breast cancer cells, J. Biol. Chem. 279 (2004) 27008-27016.

L.C. Mahan, P.A. Insel, Expression of beta-adrenergic receptors in synchronous and asynchronous S49 lymphoma cells. I. Receptor metabolism after irreversible blockade of receptors and in cells traversing the cell division cycle, Mol. Pharmacol. 29 (1986) 7-15.

C. Maier, D. Rünzler, J. Schindelar, G. Grabner, W. Waldhäusl, G. Köhler, A. Luger, G-protein-coupled glucocorticoid receptors on the pituitary cell membrane, J. Cell Sci. 118 (2005) 3353-3361.

M.J. Marinissen, J.S. Gutkind, G-protein-coupled receptors and signaling networks: emerging paradigms, Trends Pharmacol. Sci. 22 (2001) 368-376.

S. Marion, D.M. Weiner, M.G. Caron, RNA editing induces variation in desensitization and trafficking of 5-hydroxytryptamine 2c receptor isoforms, J. Biol. Chem. 279 (2004) 2945-2954.

M. Mark, N.B. Ghyselinck, P. Chambon, Function of retinoic acid receptors during embryonic development, Nucl. Recept. Signal. 7 (2009) 2-17.

D. Markovic, R.A Challiss, Alternative splicing of G protein-coupled receptors: physiology and pathophysiology, Cell. Mol. Life Sci. 66 (2009) 3337-3352.

S.S. Marroni, F.N. Nakano, C.D.C. Gati, J.A.C. Oliveira, J. Antunes-Rodrigues, N. Garcia-Cairasco, Neuroanatomical and cellular substrates of hypergrooming induced by microinjection of oxytocin in central nucleus of amygdala, an experimental model of compulsive behaviour, Mol. Psychiatry. 12 (2007) 1103-1117.

F.H. Marshall, S.M. Foord, Heterodimerization of the GABAB receptor-implications for GPCR signaling and drug discovery, Adv. Pharmacol. 58 (2010) 63-91.

U.E. Mårtensson, S.A. Salehi, S. Windahl, M.F. Gomez, K. Swärd, J. Daszkiewicz-Nilsson, A. Wendt, N. Andersson, P. Hellstrand, P.O. Grände, C. Owman, C.J. Rosen, M.L. Adamo, I. Lundquist, P. Rorsman, B.O. Nilsson, C. Ohlsson, B. Olde, L.M. Leeb-Lundberg, Deletion of the G protein-coupled receptor GPR30 impairs glucose tolerance, reduces bone growth, increases blood Pressure, and eliminates estradiol-stimulated insulin release in female mice, Endocrinology 150 (2009) 687-698.

L.A. Matsuda, T.I. Bonner, S.J. Lolait, Localization of cannabinoid receptor mRNA in rat brain, J. Comp. Neurol. 327 (1993) 535-550.

L.A. Matsuda, S.J. Lolait, M.J. Brownstein, A.C. Young, T.I. Bonner, Structure of a cannabinoid receptor and functional expression of the cloned cDNA, Nature 346 (1990) 561-564.

M. Matsumoto, M. Maruyama, J. Noguchi, Y. Horikoshi, K. Fujiwara, C. Kitada, S. Hinuma, H. Onda, O. Nishimura, K. Inoue, M. Fujino, Stimulation of corticotropin-releasing hormone-mediated adrenocorticotropin secretion by central administration of prolactin-releasing peptide in rats, Neurosci. Lett. 285 (2000) 234-238.

S. Maudsley, B. Martin, L.M. Luttrell, The origins of diversity and specificity in g protein-coupled receptor signalling, J. Pharmacol. Exp. Ther. 314 (2005) 485-494.

B. McEwan, Estrogen actions throughout the brain. Recent Progress in Hormone Research 57 (2002) 357-384.

H.H. McIntosh, C. Song, A.C. Howlett, CB1 cannabinoid receptor: cellular regulation and distribution in N18TG2 neuroblastoma cells, Brain Res. Mol. Brain Res. 53 (1998) 163-173.

D.N. McKenzie, G. Leng, R.E. Dyball, Electrophysiological evidence for mutual excitation of oxytocin cells in the supraoptic nucleus of the rat hypothalamus, J. Physiol. 485 (1995) 485-492.

B. Meister, C. Broberger, M.J. Villar, T. Hökfelt, Cholecystokinin B receptor gene expression in hypothalamic neurosecretory neurons after experimental manipulations, Neuroendocrinology 60 (1994) 458-469.

F. Mendive, P. Laurent, G. Van Schoore, W. Skarnes, R. Pochet, G. Vassart, Defective postnatal development of the male reproductive tract in LGR4 knockout mice, Dev. Biol. 290 (2006) 421-434.

I. Merchenthaler, M.V. Lane, S. Numan, T.L. Dellovade, Distribution of estrogen receptor alpha and beta in the mouse central nervous system: in vivo autoradiographic and immunocytochemical analyses, J. Comp. Neurol. 24 (2004) 270-291.

J.C. Meunier, C. Mollereau, L. Toll, C. Suaudeau, C. Moisand, P. Alvinerie, J.L. Butour, J.C. Guillemot, P. Ferrara, B. Monsarrat, et al., Isolation and structure of the endogenous agonist of opioid receptor-like ORL1 receptor, Nature 377 (1995) 532-535.

R.P. Michael, Oestrogens in the central nervous system, Br. Med. Bull. 21 (1965) 87-90.

M.C. Michel, T. Wieland, G. Tsujimoto, How reliable are G-protein-coupled receptor antibodies? Naunyn Schmiedebergs Arch. Pharmacol. 379 (2009) 385-388.

E. Mikics, M.R. Kruk, J. Haller, Genomic and non-genomic effects of glucocorticoids on aggressive behavior in male rats, Psychoneuroendocrinology 29 (2004) 618-635.

G. Milligan, G protein-coupled receptor hetero-dimerization: contribution to pharmacology and function, Br. J. Pharmacol. 158 (2009) 5-14.

G. Milligan, Principles: extending the utility of [35S]GTP gamma S binding assays, Trends Pharmacol. Sci. 24 (2003) 87-90.

G.L. Ming, H.J. Song, B. Berninge, C.E. Holt, M. Tessier-Lavigne, M.M. Poo, cAMP-dependent growth cone guidance by netrin-1, Neuron 19 (1997) 1225-1235.

N.A. Mitchner, C. Garlick, N. Ben-Jonathan, Cellular distribution and gene regulation of estrogen receptors alpha and beta in the rat pituitary gland, Endocrinology 139 (1998) 3976-3983.

S.W. Mitra, E. Hoskin, J. Yudkovitz, L. Pear, H.A. Wilkinson, S. Hayashi, D.W. Pfaff, S. Ogawa, S.P. Rohrer, J.M. Schaeffer, B.S. McEwen, S.E. Alves, Immunolocalization of estrogen receptor beta in the mouse brain: comparison with estrogen receptor alpha, Endocrinology 144 (2003) 2055-2067.

S.M. Mody, M.K. Ho, S.A. Joshi, Y.H. Wong, Incorporation of Galpha(z)-specific sequence at the carboxyl terminus increases the promiscuity of galpha(16) toward G(i)-coupled receptors, Mol. Pharmacol. 57 (2000) 13-23.

C. Mogi, M. Tobo, H. Tomura, N. Murata, X.D. He, K. Sato, T. Kimura, T. Ishizuka, T. Sasaki, T. Sato, Y. Kihara, S. Ishii, A. Harada, F. Okajima, Involvement of proton-sensing TDAG8 in extracellular acidification-induced inhibition of proinflammatory cytokine production in peritoneal macrophages, J. Immunol. 182 (2009) 3243-3251.

P. Mombaerts, Seven-transmembrane proteins as odorant and chemosensory receptors, Science 286 (1999) 707-711.

N. Mons, D.M. Cooper, Adenylyl cyclase mRNA expression does not reflect the predominant Ca2+/calmodulin-stimulated activity in the hypothalamus, J. Neuroendocrinol. 6 (1994) 665-671.

T. Moore-Morris, A. Varrault, M.E. Mangoni, A. Le Digarcher, V. Negre, C. Dantec, L. Journot, J. Nargeot, B. Couette, Identification of potential pharmacological targets by analysis of the comprehensive G protein-coupled receptor repertoire in the four cardiac chambers, Mol. Pharmacol. 75 (2009) 1108-1116.

M. Mori, H. Eguchi, Screening method of nesfatin-1-action regulating substance or nesfatin-1-like action substance with the use of receptor protein selected from the group consisting of gpr3, gpr6 and gpr12. Patent USPTO#20090155833 (2009).

S. Morisset, A. Rouleau, X. Ligneau, F. Gbahou, J. Tardivel-Lacombe, H. Stark, W. Schunack, C.R. Ganellin, J.C. Schwartz, J.M. Arrang, High constitutive activity of native H3 receptors regulates histamine neurons in brain, Nature. 408 (2000) 860-864.

J.F. Morris, H. Christian, D. Ma, H. Wang, Dendritic secretion of peptides from hypothalamic magnocellular neurosecretory neurones: a local dynamic control system and its functions, Exp. Physiol. 85 (2000) 131-138.

A.J. Morris, C.C. Malbon, Physiological regulation of G protein-linked signalling, Physiol. Rev. 79 (1999) 1373-1430.

D. Mousseaux, L. Le Gallic, J. Ryan, C. Oiry, D. Gagne, J.A. Fehrentz, J.C. Galleyrand, J. Martinez, Regulation of ERK1/2 activity by ghrelin-activated growth hormone secretagogue receptor 1A involves a PLC/PKCvarepsilon pathway, Br. J. Pharmacol. 148 (2006) 350-365.

S. Mukherjee, S. Mani, Orphan nuclear receptors as targets for drug development, Pharm. Res. 27 (2010) 1439-1468.

S.J. Mundell, J.L. Benovic, Selective regulation of endogenous G protein-coupled receptors by arrestins in HEK293 cells, J. Biol. Chem. 275 (2000) 12900-12908.

C. Murgatroyd, A.V. Patchev, Y. Wu, V. Micale, Y. Bockmühl, D. Fischer, F. Holsboer, C.T. Wotjak, O.F. Almeida, D. Spengler, Dynamic DNA methylation programs persistent adverse effects of early-life stress, Nat. Neurosci. 12 (2009) 1559-1566.

D. Murphy, Gene expression studies using microarrays: principles, problems, and prospects, Adv. Physiol. Educ. 26 (2002a) 256-270.

P.M. Murphy, International Union of Pharmacology. XXX. Update on chemokine receptor nomenclature, Pharmacol. Rev. 54 (2002b) 227-229.

S. Muto, S. Ebata, K. Okada, T. Saito, Y. Asano, Glucocorticoid modulates Na+/H+ exchange activity in vascular smooth muscle cells by nongenomic and genomic mechanisms, Kidney Int. 57 (2000) 2319-2333.

J. Nabekura, Y. Oomura, T. Minami, Y. Mizuno, A. Fukuda, Mechanism of the rapid effect of 17 beta-estradiol on medial amygdala neurons, Science 233 (1986) 226-228.

K. Nakamura, T. Kaneko, Y. Yamashita, H. Hasegawa, H. Katoh, M. Negishi, Immunohistochemical localization of prostaglandin EP3 receptor in the rat nervous system, J. Comp. Neurol. 421 (2000) 543-569.

I. Navratilova, J. Besnard, A.L. Hopkins, Screening for GPCR Ligands Using Surface Plasmon Resonance, ACS Med. Chem. Lett. 2 (2011) 549-554.

T.K. Nayak, M.K. Dennis, C. Ramesh, R. Burai, R.W. Atcher, L.A. Sklar, J.P. Norenberg, H.J. Hathaway, J.B. Arterburn, E.R. Prossnitz, Influence of charge on cell permeability and tumor imaging of GPR30-targeted 111in-labeled nonsteroidal imaging agents, ACS Chem. Biol. 5 (2010) 681-690.

A. Negoescu, F. Labat-Moleur, P. Lorimier, L. Lamarcq, C. Guillermet, E. Chambaz, E. Brambilla, F(ab) secondary antibodies: a general method for double immunolabeling with primary antisera from the same species. Efficiency control by chemiluminescence, J. Histochem. Cytochem. 42 (1994) 433-437.

E.M. Neuhaus, W. Zhang, L. Gelis, Y. Deng, J. Noldus, H. Hatt, Activation of an olfactory receptor inhibits proliferation of prostate cancer cells, J. Biol. Chem. 284 (2009) 16218-16225.

D.C. New, Y.H. Wong, Molecular mechanisms mediating the G protein-coupled receptor regulation of cell cycle progression, J. Mol. Signal. 26 (2007) 2:12.

P.C. Ng, The fetal and neonatal hypothalamic-pituitary-adrenal axis. Arch. Dis. Child Fetal Neonatal Ed. 82 (2000) 250-254.

M.K. Ng, D.S. Celermajer, Glucocorticoid treatment and cardiovascular disease, Heart 90 (2004) 829-830.

Y.G. Ni, S.J. Gold, P.A. Iredale, R.Z. Terwilliger, R.S. Duman, E.J. Nestler, Region-specific regulation of RGS4 (Regulator of G-protein-signaling protein type 4) in brain by stress and glucocorticoids: in vivo and in vitro studies, J. Neurosci. 19 (1999) 3674-3680.

K.A. Nichol, A. Morey, M.H. Couzens, J. Shine, H. Herzog, A.M. Cunningham, Conservation of expression of neuropeptide Y5 receptor between human and rat hypothalamus and limbic regions suggests an integral role in central neuroendocrine control, J. Neurosci. 19 (1999) 10295-10304.

W.A. Nijenhuis, J. Oosterom, R.A. Adan, AgRP(83-132) acts as an inverse agonist on the human-melanocortin-4 receptor, Mol. Endocrinol. 15 (2001) 164-171.

M. Nishida, The Ishikawa cells from birth to the present, Hum. Cell. 15 (2002) 104-117.

C.M. Niswender, P.J. Conn, Metabotropic glutamate receptors: physiology, pharmacology, and disease, Annu. Rev. Pharmacol. Toxicol. 50 (2010) 295-322.

S.D. Noel, K.L. Keen, D.I. Baumann, E.J. Filardo, E. Terasawa, Involvement of G protein-coupled receptor 30 (GPR30) in rapid action of estrogen in primate LHRH neurons, Mol. Endocrinol. 23 (2009) 349-359

Nuclear Receptor Nomenclature Committee, A unified nomenclature system for the nuclear receptor superfamily, Cell 97 (1999) 161–163.

A.M. Nuyt, Z. Lenkei, P. Corvol, M. Palkovits, C. Llorens-Cortés, Ontogeny of angiotensin II type 1 receptor mRNAs in fetal and neonatal rat brain, J. Comp. Neurol. 440 (2001) 192-203.

T.D. Oberley, A. Gonzalez, L.J. Lauchner, L.W. Oberley, J.J. Li, Characterization of early kidney lesions in estrogen-induced tumors in the Syrian hamster, Cancer Res. 1 (1991) 1922-1929.

A-M O'Carroll, S.J. Lolait, Regulation of rat APJ receptor messenger ribonucleic acid expression in magnocellular neurones of the paraventricular and supraopric nuclei by osmotic stimuli, J. Neuroendocrinol. 15 (2003) 661-666.

A.M. O'Carroll, S.J. Lolait, M. König, L.C. Mahan, Molecular cloning and expression of a pituitary somatostatin receptor with preferential affinity for somatostatin-28, Mol. Pharmacol. 42 (1992) 939-946.

A-M. O'Carroll, T.L. Selby, M. Palkovits, S.J. Lolait, Distribution of mRNA encoding B78/apj, the rat homologue of the human APJ receptor, and its endogenous ligand apelin in brain and peripheral tissues, Biochim. Biophys. Acta. 1492 (2000) 72-80.

E.M. Oestreicher, C. Guo, E.W. Seely, T. Kikuchi, D. Martinez-Vasquez, L. Jonasson, T. Yao, D. Burr, S. Mayoral, W. Roubsanthisuk, V. Ricchiuti, G.K. Adler, Estradiol increases proteinuria and angiotensin II type 1 receptor in kidneys of rats receiving L-NAME and angiotensin II, Kidney Int. 70 (2006) 1759-68.

S. Offermanns, M.I. Simon, G alpha 15 and G alpha 16 couple a wide variety of receptors to phospholipase C, J. Biol. Chem. 270 (1995) 15175-15180.

T. Oka, K. Oka, T.E. Scammell, C. Lee, J.F. Kelly, F. Nantel, J.K. Elmquist, C.B. Saper. Relationship of EP1-4 prostaglandin receptors with rat hypothalamic cell groups involved in lipopolysaccharide fever responses. J. Comp. Neurol. 428 (2000) 20-32.

B.J. Oldfield, P.J. Davern, M.E. Giles, A.M. Allen, E. Badoer, M.J. McKinley, Efferent neural projections of angiotensin receptor (AT1) expressing neurones in the hypothalamic paraventricular nucleus of the rat, J. Neuroendocrinol. 13 (2001) 139-146.

W.M. Oldham, H.E. Hamm, Heterotrimeric G protein activation by G-protein-coupled receptors, Nat. Rev. Mol. Cell. Biol. 9 (2008) 60-71.

Omeros Corporation press release, Omeros Unlocks Four Additional Orphan GPCRs (Orphans Linked to Cancer, Metabolism, Eye, Immune and CNS Disorders), Seattle, Sept. 13, (2011).

M. Orchinik, T.F. Murray, P.H. Franklin, F.L. Moore, Guanyl nucleotides modulate binding to steroid receptors in neuronal membranes, Proc. Natl. Acad. Sci. USA 89 (1992) 3830-3834.

R.I. Osmond, A. Sheehan, R. Borowicz, E. Barnett, G. Harvey, C. Turner, A. Brown, M.F. Crouch, A.R. Dyer, GPCR screening via ERK 1/2: a novel platform for screening G protein-coupled receptors, J. Biomol. Screen 10 (2005) 730-737.

N.L. Ostrowski, W.S. Young WS, M.A. Knepper, S.J. Lolait, Expression of vasopressin V1a and V2 receptor messenger ribonucleic acid in the liver and kidney of embryonic, developing, and adult rats, Endocrinology (1993) 1849-1859.

C. Otto, I. Fuchs, G. Kauselmann, H. Kern, B. Zevnik, P. Andreasen, G. Schwarz, H. Altmann, M. Klewer, M. Schoor, R. Vonk, K.H. Fritzemeier, GPR30 does not mediate estrogenic responses in reproductive organs in mice, Biol. Reprod. 80 (2009) 34-41.

C. Otto, B. Rohde-Schulz, G. Schwarz, I. Fuchs, M. Klewer, D. Brittain, G. Langer, B. Bader, K. Prelle, R. Nubbemeyer, K.H. Fritzemeier, G protein-coupled receptor 30 localizes to the endoplasmic reticulum and is not activated by estradiol, Endocrinology 149 (2008) 4846-4856.

C. Owman, P. Blay, C. Nilsson, S.J. Lolait, Cloning of human cDNA encoding a novel heptahelix receptor expressed in Burkitt's lymphoma and widely distributed in brain and peripheral tissues, Biochem. Biophys. Res. Commun. 228 (1996) 285-229

K. Palczewski, T. Kumasaka, T. Hori, C.A. Behnke, H. Motoshima, B.A. Fox, I. Le Trong, D.C. Teller, T. Okada, R.E. Stenkamp, M. Yamamoto, M. Miyano, Crystal structure of rhodopsin: A G protein-coupled receptor, Science 289 (2000) 739-745.

J.H. Park, P. Scheerer, K.P. Hofmann, H.W. Choe, O.P. Ernst, Crystal structure of the ligand-free G-protein-coupled receptor opsin, Nature 454 (2008) 183-187.

K.J. Parker, C.L. Buckmaster, A.F. Schatzberg, D.M. Lyons, Intranasal oxytocin administration attenuates the ACTH stress response in monkeys, Psychoneuroendocrinology 30 (2005) 924-929.

R. Parker, M. Liu, H.J. Eyre, N.G. Copeland, D.J. Gilbert, J. Crawford, G.R. Sutherland, N.A. Jenkins, H, Herzog, Y-receptor-like genes GPR72 and GPR73: molecular cloning, genomic organisation and assignment to human chromosome 11q21.1 and 2p14 and mouse chromosome 9 and 6, Biochim. Biophys. Acta. 1491 (2000) 369-375.

D. Parkes, S. Rivest, S. Lee, C. Rivier, W. Vale W, Corticotropin-releasing factor activates c-fos, NGFI-B, and corticotropin-releasing factor gene expression within the paraventricular nucleus of the rat hypothalamus, Mol. Endo. 7 (1993) 1357-1367.

J.R. Pasqualini, Estrogen sulfotransferases in breast and endometrial cancers, Ann. N.Y. Acad. Sci. 1155 (2009) 88-98.

S.M. Pasternack, I. von Kügelgen, K.A. Aboud, Y.A. Lee, F. Rüschendorf, K. Voss, A.M. Hillmer, G.J. Molderings, T. Franz, A. Ramirez, P. Nürnberg, M.M. Nöthen, R.C. Betz, G protein-coupled receptor P2Y5 and its ligand LPA are involved in maintenance of human hair growth, Nat. Genet. 40 (2008) 329-334.

V.H. Patel, J. Chen, M. Ramanjaneya, E. Karteris, E. Zachariades, P. Thomas, M. Been, H.S. Randeva, G-protein coupled estrogen receptor 1 expression in rat and human heart: Protective role during ischaemic stress, Int. J. Mol. Med. 26 (2010) 193-199.

H.H. Patel, R.S. Ostrom, An orphan GPCR finds a home in the heart, Am. J. Physiol. Heart Circ. Physiol. 295 (2008) 479-481.

A. Pazos, A. Probst, J.M. Palacios, Serotonin receptors in the human brain--III. Autoradiographic mapping of serotonin-1 receptors, Neuroscience 21 (1987) 97-122.

G. Pelletier, C. Labrie, F. Labrie, Localization of oestrogen receptor α, oestrogen receptor β and androgen receptors in the rat reproductive organs, J. Endocrinol. 165 (2000) 359–370.

R.G. Pertwee, A.C. Howlett, M.E. Abood, S.P. Alexander, V. Di Marzo, M.R. Elphick, P.J. Greasley, H.S. Hansen, G. Kunos, K. Mackie, R. Mechoulam, R.A. Ross, International Union of Basic and Clinical Pharmacology. LXXIX. Cannabinoid receptors and their ligands: beyond CB_1 and CB_2, Pharmacol. Rev. 62 (2010) 588-631.

D.A. Pettit, M.P. Harrison, J.M. Olson, R.F. Spencer, G.A. Cabral, Immunohistochemical localization of the neural cannabinoid receptor in rat brain, J. Neurosci. Res. 51 (1998) 391-402.

D.W. Pfaff, Y. Sakuma, Facilitation of the lordosis reflex of female rats from the ventromedial nucleus of the hypothalamus, J. Physiol. 288 (1978) 189-202.

M. Pi, A.L. Parrill, L.D. Quarles, GPRC6A mediates the non-genomic effects of steroids, J. Biol. Chem. 285 (2010) 39953-39964.

X. Piao, B.S. Chang, A. Bodell, K. Woods, B. Benzeev, M. Topcu, R. Guerrini, H. Goldberg-Stern, L. Sztriha, W.B. Dobyns, A.J. Barkovich, C.A. Walsh, Genotype-phenotype analysis of human frontoparietal polymicrogyria syndromes, Ann. Neurol. 58 (2005) 680-687.

C. Pickering, M. Hägglund, J. Szmydynger-Chodobska, F. Marques, J.A. Palha, L. Waller, A. Chodobski, R. Fredriksson, M.C. Lagerström, H.B. Schiöth, The Adhesion GPCR GPR125 is specifically expressed in the choroid plexus and is upregulated following brain injury, BMC Neurosci. 9 (2008) 97-111.

K.L. Pierce, R.T. Premont, R.J. Lefkowitz, Seven-transmembrane receptors, Nat. Rev. Mol. Cell. Biol. 3 (2002) 639-650.

R.J. Pietras, C.M. Szego, Partial purification and characterization of oestrogen receptors in subfractions of hepatocyte plasma membranes, Biochem. J. 191 (1980) 743-760.

R.C. Pink, K. Wicks, D.P. Caley, E.K. Punch, L. Jacobs, D.R. Carter, Pseudogenes: pseudo-functional or key regulators in health and disease? RNA 17 (2011) 792-798.

J.U. Pontius, L. Wagner, G.D. Schuler, UniGene: a unified view of the transcriptome. In: The NCBI Handbook, Bethesda (MD): National Center for Biotechnology Information (2003).

D.A. Poulain, J.B. Wakerley, Electrophysiology of hypothalamic magnocellular neurones secreting oxytocin and vasopressin, Neuroscience 7 (1982) 773-808.

W. Pradidarcheep, W.T. Labruyère, N.F. Dabhoiwala, W.H. Lamers, Lack of specificity of commercially available antisera: better specifications needed, J. Histochem. Cytochem. 56 (2008) 1099-1111.

W.B. Pratt, D.O. Toft, Steroid receptor interactions with heat shock protein and immunophilin chaperones, Endocr. Rev. 18 (1997) 306-360.

C.J. Price, T.D. Hoyda, W.K. Samson, A.V. Ferguson, Nesfatin-1 influences the excitability of paraventricular nucleus neurones, J. Neuroendocrinol. 20 (2008) 245-250.

C.J. Price, R. Scott, D.A. Rusakov, M. Capogna, GABA(B) receptor modulation of feedforward inhibition through hippocampal neurogliaform cells, J. Neurosci. 28 (2008) 6974-6982.

S.C. Prinster, C. Hague, R.A. Hall, Heterodimerization of g protein-coupled receptors: specificity and functional significance, Pharmacol. Rev. 57 (2005) 289-298.

E.R. Prossnitz, J.B. Arterburn, H.O. Smith, T.I. Oprea, L.A. Sklar, H.J. Hathaway, Estrogen signalling through the transmembrane G protein-coupled receptor GPR30, Annu. Rev. Physiol. 70 (2008) 165-190.

S. Pyner, Neurochemistry of the paraventricular nucleus of the hypothalamus: implications for cardiovascular regulation, J. Chem. Neuroanat. 38 (2009) 197-208.

D.L. Qiu, C.P. Chu, H. Tsukino, T. Shirasaka, H. Nakao, K. Kato, T. Kunitake, T. Katoh, H. Kannan, Neuromedin U receptor subtype -2 mRNA and HCN channels mRNA expression NMU-sensitive neurons in rat hypothalamic paraventricular nucleus, Neurosci. Lett. 374 (2005) 69-72.

J. Qiu, L.G. Lou, X.Y. Huang, S.J. Lou, G. Pei, Y.Z. Chen, Nongenomic mechanisms of glucocorticoid inhibition of nicotine-induced calcium influx in PC12 cells: involvement of protein kinase C, Endocrinology 139 (1998) 5103-5108.

J. Qiu, P. Wang, Q. Jing, W. Zhang, X. Li, Y. Zhong, G. Sun, G. Pei, Y. Chen, Rapid activation of ERK1/2 mitogen-activated protein kinase by corticosterone in PC12 cells, Biochem. Biophys. Res. Commun. 287 (2001) 1017-1024.

U. Quitterer, S. AbdAlla, K. Jarnagin, W. Müller-Esterl, Na+ ions binding to the bradykinin B2 receptor suppress agonist-independent receptor activation, Biochemistry 35 (1996) 13368-13377.

C.L. Raison, A.H. Miller, When not enough is too much: the role of insufficient glucocorticoid signaling in the pathophysiology of stress-related disorders, Am. J. Psychiatry. 160 (2003) 1554-1565.

S.G. Rasmussen, H.J. Choi, D.M. Rosenbaum, T.S. Kobilka, F.S. Thian, P.C. Edwards, M. Burghammer, V.R. Ratnala, R. Sanishvili, R.F. Fischetti, G.F. Schertler, W.I. Weis, B.K. Kobilka, Crystal structure of the human beta2 adrenergic G-protein-coupled receptor, Nature 450 (2007) 383-387.

M. Razandi, A. Pedram, I. Merchenthaler, G.L. Greene, E.R. Levin, Plasma membrane estrogen receptors exist and functions as dimmers, Mol. Endocrinol. 18 (2004) 2854-2865.

Razandi M, Pedram A, Park ST & Levin ER 2003 Proximal events in signaling by plasma membrane estrogen receptors. Journal of Biology Chemistry 278 2701-2712.

M. Re, M. Pampillo, M. Savard, C. Dubuc, C.A. McArdle, R.P. Millar, P.M. Conn, F. Gobeil, M. Bhattacharya, A.V. Babwah, The human gonadotropin releasing hormone type I receptor is a functional intracellular GPCR expressed on the nuclear membrane, PLoS One 5 (2010) 11489.

M.A. Reddy, S.D. Shukla, Nuclear activation and translocation of mitogen-activated protein kinases modulated by ethanol in embryonic liver cells, Biochim. Biophys. Acta. 1497 (2000) 271-278.

J.F. Rehfeld, L. Friis-Hansen, J.P. Goetze, T.V. Hansen, The biology of cholecystokinin and gastrin peptides, Curr. Top. Med. Chem. 7 (2007) 1154-1165.

O. Reich, C. Singer, G. Hudelist, S. Regauer, Estrogen sulfotransferase expression in endometrial stromal sarcomas: an immunohistochemical study, Pathol. Res. Pract. 203 (2007) 85-87.

L.P. Renaud, C.W. Bourque, Neurophysiology and neuropharmacology of hypothalamic magnocellular neurons secreting vasopressin and oxytocin, Prog. Neurobiol. 36 (1991) 131-169.

C.M. Revankar, D.F. Cimino, L.A. Sklar, J.B. Arterburn, E.R. Prossnitz, A transmembrane intracellular estrogen receptor mediates rapid cell signalling, Science 307 (2005) 1625-1630.

C.M. Revankar, H.D. Mitchell, A.S. Field, R. Burai, C. Corona, C. Ramesh, L.A. Sklar, J.B. Arterburn, E.R. Prossnitz, Synthetic estrogen derivatives demonstrate the functionality of intracellular GPR30, ACS Chem. Biol. 17 (2007) 536-544.

C.H. Rhodes, J.I. Morrell, D.W. Pfaff, Immunohistochemical analysis of magnocellular elements in rat hypothalamus: distribution and numbers of cells containing neurophysin, oxytocin, and vasopressin, J Comp Neurol. 198 (1981) 45-64.

D.S. Richards, R.M. Villalba, F.J Alvarez, J.E. Stern, Expression of GABAB receptors in magnocellular neurosecretory cells of male, virgin female and lactating rats, J. Neuroendocrinol. 17 (2005) 413-423.

S.L. Ritter, R.A. Hall, Fine-tuning of GPCR activity by receptor-interacting proteins, Nat. Rev. Mol. Cell. Biol. 10 (2009) 819-830.

S.A. Rivkees, J.E. Lachowicz, Functional D1 and D5 dopamine receptors are expressed in the suprachiasmatic, supraoptic, and paraventricular nuclei of primates, Synapse 26 (1997) 1-10.

M.J. Robbins, K.J. Charles, D.C. Harrison, M.N. Pangalos, Localisation of the GPRC5B receptor in the rat brain and spinal cord, Brain Res, Mol, Brain Res. 106 (2002) 136-144.

M.J. Robbins, D. Michalovich, J. Hill, A.R. Calver, A.D. Medhurst, I. Gloger, M. Sims, D.N. Middlemiss, M.N. Pangalos, Molecular cloning and characterization of two novel retinoic acid-inducible orphan G-protein-coupled receptors (GPRC5B and GPRC5C), Genomics 67 (2000) 8-18.

A. Robertson, A.M. Gonzalez, E. Stopa, W. Leadbeater, R. Coimbra, C. Johanson, B. Eliceiri, A. Baird, Immunohistochemical evidence that Argillin, the product of the ECRG4 gene, encodes a novel neuroendocrine peptide, Society for Endocrinology; Endocrine Abstracts 19 (2009) OC16.

M. Rocheville, D.C. Lange, U. Kumar, S.C. Patel, R.C. Patel, Y.C. Patel, Receptors for dopamine and somatostatin: formation of hetero-oligomers with enhanced functional activity, Science 288 (2000) 154-157.

K.V. Rogers, C.K. Dunn, S.C. Hebert, E.M. Brown, Localization of calcium receptor mRNA in the adult rat central nervous system by in situ hybridization, Brain Res. 744 (1997) 47-56.

B. Roozendaal, Stress and memory: opposing effects of glucocorticoids on memory consolidation and memory retrieval, Neurobiol. Learn Mem. 78 (2002) 578-595.

J. Roper, A.M. O'Carroll, W. Young, S. Lolait, The vasopressin Avpr1b receptor: molecular and pharmacological studies, Stress 14 (2011) 98-115.

D.M. Rosenbaum, S.G. Rasmussen, B.K. Kobilka, The structure and function of G-protein-coupled receptors, Nature 459 (2009) 356-363.

D.L. Rosin, A. Robeva, R.L. Woodward, P.G. Guyenet, J. Linden, Immunohistochemical localization of adenosine A2A receptors in the rat central nervous system, J. Comp. Neurol. 401 (1998) 163-186.

D.V. Rossi, Y. Dai, P. Thomas, G.A. Carrasco, L.L. DonCarlos, N.A. Muma, Q. Li, Estradiol-induced desensitization of 5-HT1A receptor signaling in the paraventricular nucleus of the hypothalamus is independent of estrogen receptor-beta, Psychoneuroendocrinology 35 (2010) 1023-1033.

P.P. Roux, J. Blenis, ERK and p38 MAPK-activated protein kinases: a family of protein kinases with diverse biological functions, Microbiol. Mol. Biol. Rev. 68 (2004) 320-344.

E. Rozengurt, Mitogenic signaling pathways induced by G protein-coupled receptors, J. Cell. Physiol. 213 (2007) 589-602.

N. Sabatier, C. Caquineau, G. Dayanithi, P. Bull, A.J. Douglas, X.M. Guan, M. Jiang, L. Van der Ploeg, G. Leng, α-Melanocyte-stimulating hormone stimulates oxytocin release from the dendrites of hypothalamic neurons while inhibiting oxytocin release from their terminals in the neurohypophysis, J. Neurosci. 23 (2003) 10351-10358.

N. Sabatier, G. Leng, Presynaptic action of endocannabinoids mediate α-MSH-induced inhibition of oxytocin cells, Am. J. Physio. Integr. Comp. Physiol. 290 (2006) 577-584.

R. Sah, S.L. Parker, S. Sheriff, K. Eaton, A. Balasubramaniam, F.R. Sallee, Interaction of NPY compounds with the rat glucocorticoid-induced receptor (GIR) reveals similarity to the NPY-Y2 receptor, Peptides 28 (2007) 302-309.

R. Sah, L.M. Pritchard, N.M. Richtand, R. Ahlbrand, K. Eaton, F.R. Sallee, J.P. Herman, Expression of the glucocorticoid-induced receptor mRNA in rat brain, Neuroscience 133 (2005) 281-292.

H. Sakamoto, K. Matsuda, K. Hosokawa, M. Nishi, J. Morris, E.R. Prossnitz, M. Kawata, Expression of G protein-coupled receptor-30, a G protein-coupled membrane estrogen receptor, in oxytocin neurons of the rat paraventricular and supraoptic nuclei, Endocrinology 148 (2007) 5842-5850.

M. Sakaue, B.B. Hoffman, Glucocorticoids induce transcription and expression of the alpha 1B adrenergic receptor gene in DTT1 MF-2 smooth muscle cells, J. Clin. Invest. 88 (1991) 385-389.

T. Sakurai, A. Amemiya, M. Ishii, I. Matsuzaki, R.M. Chemelli, H. Tanaka, S.C. Williams, J.A. Richardson, G.P. Kozlowski, S. Wilson, J.R. Arch, R.E. Buckingham, A.C. Haynes, S.A. Carr, R.S. Annan, D.E. McNulty, W.S. Liu, J.A. Terrett, N.A. Elshourbagy, D.J. Bergsma, M. Yanagisawa, Orexins and orexin receptors: a family of hypothalamic neuropeptides and G protein-coupled receptors that regulate feeding behaviour, Cell 92 (1998) 573-585.

A.K. Samadi, R.J. Cenedella, Rapid Activation of ERK1/2 Mitogen-Activated Protein Kinase by Corticosterone in Bovine Lens Epithelial Cells, Invest Ophthalmol Vis Sci 44 (2003) E-Abstract 3505.

W.K. Samson, J.V. Zhang, O. Avsian-Kretchmer, K. Cui, G.L. Yosten, C. Klein, R.M. Lyu, Y.X. Wang, X.Q. Chen, J. Yang, C.J Price, T.D. Hoyda, A.V. Ferguson, X.B. Yuan, J.K. Chang, A.J. Hsueh, Neuronostatin encoded by the somatostatin gene regulates neuronal, cardiovascular, and metabolic functions, J. Biol. Chem. 283 (2008) 31949-31959.

C. Sandi, C. Venero, C. Guaza, Novelty-related rapid locomotor effects of corticosterone in rats, Eur. J. Neurosci. 8 (1996) 794-800.

S.A. Sands, D.A. Morilak, Expression of alpha1D adrenergic receptor messenger RNA in oxytocin- and corticotropin-releasing hormone-synthesizing neurons in the rat paraventricular nucleus, Neuroscience 91 (1999) 639–649.

R.M. Sapolsky, L.M. Romero, A.U. Munck, How do glucocorticoids influence stress responses? Integrating permissive, suppressive, stimulatory, and preparative actions, Endocr. Rev. 21 (2000) 55-89.

R.A. Sarabdjitsingh, S. Isenia, A. Polman, J. Mijalkovic, S. Lachize, N. Datson, E.R. de Kloet, O.C. Meijer, Disrupted corticosterone pulsatile patterns attenuate responsiveness to glucocorticoid signaling in rat brain, Endocrinology 151 (2010) 1177-1186.

R. Sasson, V. Shinder, A. Dantes, A. Land, A. Amsterdam, Activation of multiple signal transduction pathways by glucocorticoids: protection of ovarian follicular cells against apoptosis, Biochem. Biophys. Res. Commun. 311 (2003) 1047-1056.

K. Sato, T. Numata, T. Saito, Y. Ueta, Y. Okada, V_2 receptor-mediated autocrine role of somatodendritic release of AVP in rat vasopressin neurons under hypo-osmotic conditions, Sci. Signal. 4 (2011) ra5.

C. Saunders, L.E. Limbird, Disruption of microtubules reveals two independent apical targeting mechanisms for G-protein-coupled receptors in polarized renal epithelial cells, J. Biol. Chem. 272 (1997) 19035-19045.

P.T. Saunders, S.M. Maguire, J. Gaughan, M.R. Millar, Expression of oestrogen receptor beta (ER beta) in multiple rat tissues visualised by immunohistochemistry, J. Endocrinol. 154 (1997) 13-16.

M. Savart, Y. Cabillic, Specific binding of dexamethasone to plasma membranes from skeletal muscle, Biochim. Biophys. Acta. 813 (1985) 87-95.

P.E. Sawchenko, Toward a new neurobiology of energy balance, appetite, and obesity: the anatomists weigh in, J. Comp. Neurol. 402 (1998) 435-441.

T. Schöneberg, A. Schulz, H. Biebermann, T. Hermsdorf, H. Römpler, K. Sangkuhl, Mutant G-protein-coupled receptors as a cause of human diseases, Pharmacol. Ther. 104 (2004) 173-206.

L.A. Schrader, J.G. Tasker, Presynaptic modulation by metabotropic glutamate receptors of excitatory and inhibitory synaptic inputs to hypothalamic magnocellular neurons, J. Neurophysiol. 77 (1997) 527-536.

G.D. Schuler, Pieces of the puzzle: expressed sequence tags and the catalog of human genes, J. Mol. Med. 75 (1997) 694-698.

M.W. Schwartz, S.C. Woods, D. Porte, R.J. Seeley, D.G. Baskin, Central nervous system control of food intake, Nature 404 (2000) 661-671.

J.L. Scragg, P. Warburton, S.G. Ball, A.J. Balmforth, Constitutive activity of human angiotensin II type-1 receptors by Gq overexpression, Biochem. Biophys. Res. Commun. 334 (2005) 134-139.

M. Seandel, D. James, S.V. Shmelkov, I. Falciatori, J. Kim, S. Chavala, D.S. Scherr, F. Zhang, R. Torres, N.W. Gale, G.D. Yancopoulos, A. Murphy, D.M. Valenzuela, R.M. Hobbs, P.P Pandolfi, S. Rafii, Generation of functional multipotent adult stem cells from GPR125+ germline progenitors, Nature 449 (2007) 346-350.

K.R. Sedgley, A.R. Finch, C.J. Caunt, C.A. McArdle, Intracellular gonadotropin-releasing hormone receptors in breast cancer and gonadotrope lineage cells, J. Endocrinol. 191 (2006) 625-636.

R. Seifert, K. Wenzel-Seifert, B.K. Kobilka, GPCR-Galpha fusion proteins: molecular analysis of receptor-G-protein coupling, Trends Pharmacol. Sci. 20 (1999) 383-389.

P.M. Sexton, M. Morfis, N. Tilakaratne, D.L. Hay, M. Udawela, G. Christopoulos, A. Christopoulos, Complexing receptor pharmacology: modulation of family B G protein-coupled receptor function by RAMPs, Ann. NY Acad. Sci. 1070 (2006) 90-104.

G. Sharma, E.R. Prossnitz, Mechanisms of estradiol-induced insulin secretion by the G protein-coupled estrogen receptor GPR30/GPER in pancreatic beta-cells, Endocrinology 152 (2011) 3030-3039.

J.L. Shaw, S.L. Gackenheimer, D.R. Gehlert, Functional autoradiography of neuropeptide Y Y1 and Y2 receptor subtypes in rat brain using agonist stimulated [35S]GTPgammaS binding, J. Chem. Neuroanat. 26 (2003) 179-193.

E.A. Sheader, E.T. Wargent, N. Ashton, R.J. Balment, Rapid stimulation of cyclic AMP production by aldosterone in rat inner medullary collecting ducts, J. Endocrinol. 175 (2002) 343-347.

B. Shen, L.M. Harrison-Bernard, A.J. Fuller, V. Vanderpool, Z. Saifudeen, S.S. El-Dahr, The Bradykinin B2 receptor gene is a target of angiotensin II type 1 receptor signaling, J. Am. Soc. Nephrol. 18 (2007) 1140-1149.

B. Shi, G. Bhat, V.B. Mahesh, M. Brotto, T.M. Nosek, D.W. Brann, Bradykinin receptor localization and cell signaling pathways used by bradykinin in the regulation of gonadotropin-releasing hormone secretion, Endocrinology. 140 (1999) 4669-4676.

I. Shibuya, J. Noguchi, K. Tanaka, N. Harayama, U. Inoue, N. Kabashima, Y. Ueta, Y. Hattori, H. Yamashita, PACAP increases the cytosolic Ca2+ concentration and stimulates somatodendritic vasopressin release in rat supraoptic neurons, J. Neuroendocrinol. 10 (1998) 31-42.

I. Shibuya, S.V. Setiadji, N. Ibrahim, N. Harayama, T. Maruyama, Y. Ueta, H. Yamashita, Involvement of postsynaptic EP4 and presynaptic EP3 receptors in actions of prostaglandin E2 in rat supraoptic nucleus, J. Neuroendocrinol. 14 (2002) 64-72.

S. Shivaji, M.V. Jagannadham, Steroid-induced perturbations of membranes and its relevance to sperm acrosome reaction, Biochim. Biophys. Acta. 1108 (1992) 99-109.

Y.B. Shrestha, K. Wickwire, S. Giraudo, Effect of reducing ghrelin receptor gene expression on energy balance, Peptides 30 (2009) 1336-1341.

D.J. Shuey, M. Betty, P.G. Jones, X.Z. Khawaja, M.I. Cockett, RGS7 attenuates signal transduction through the G(alpha q) family of heterotrimeric G proteins in mammalian cells, J. Neurochem. 70 (1998) 1964-1972.

P.J. Shughrue, M.V. Lane, I, Merchenthaler, Comparative distribution of estrogen receptor-α and -β mRNA in the rat central nervous system, Journal of Comparative Neurology 388 (1997) 507-525.

P.J. Shughrue, M.V. Lane, I. Merchenthaler, Glucagon-like peptide-1 receptor (GLP1-R) mRNA in the rat hypothalamus, Endocrinology. 137 (1996) 5159-5162.

R.E. Siegel, W.S. Young, Detection of preprocholecystokinin and preproenkephalin A mRNAs in rat brain by hybridization histochemistry using complementary RNA probes, Neuropeptides 6 (1985) 573-580.

D.M. Simmons, L.W. Swanson, Comparison of the spatial distribution of seven types of neuroendocrine neurons in the rat paraventricular nucleus: toward a global 3D model, J. Comp. Neurol. 516 (2009) 423-441.

G. Simonnet, F. Rodriguez, F. Fumoux, P. Czernichow, J.D. Vincent, Vasopressin release and drinking induced by intracranial injection of angiotensin II in monkey, Am. J. Physiol. 237 (1979) 20-25.

R. Sirianni, A. Chimento, C. Ruggiero, A. De Luca, R. Lappano, S. Andò, M. Maggiolini, V. Pezzi, The novel estrogen receptor, G protein-coupled receptor 30, mediates the proliferative effects induced by 17beta-estradiol on mouse spermatogonial GC-1 cell line, Endocrinology 149 (2008) 5043-5051.

L.A. Sklar, P.A. Hyslop, Z.G. Oades, G.M. Omann, A.J. Jesaitis, R.G. Painter, C.G. Cochrane, Signal transduction and ligand-receptor dynamics in the human neutrophil. Transient responses and occupancy-response relations at the formyl peptide receptor, J. Biol. Chem. 260 (1985) 11461-11467.

C.D. Sladek, Antidiuretic hormone: synthesis and release. Handbook of Physiology, The Endocrine System, Endocrine Regulation of Water and Electrolyte Balance, American Physiological Society, 2000.

C.D. Sladek, S.J. Somponpun, Oestrogen receptor β: role in neurohyphyseal neurones. Journal of Neuroendocrinology 16 (2004) 365-371.

H.O. Smith, K.K. Leslie, M. Singh, C.R. Qualls, C.M. Revankar, N.E. Joste, E.R. Prossnitz, GPR30: a novel indicator of poor survival for endometrial carcinoma, Am. J. Obstet. Gynecol. 196 (2007) 386.e1-9; discussion 386.e9-11.

M.J. Smit, H.F. Vischer, R.A. Bakker, A. Jongejan, H. Timmerman, L. Pardo, R. Leurs, Pharmacogenomic and structural analysis of constitutive g protein-coupled receptor activity, Annu. Rev. Pharmacol Toxicol. 47 (2007) 53-87.

M.J. Smith, P.M. Wise, Localization of kappa opioid receptors in oxytocin magnocellular neurons in the paraventricular and supraoptic nuclei, Brain Res. 898 (2001) 162-165.

M.V. Sofroniew, Projections from vasopressin, oxytocin, and neurophysin neurons to neural targets in the rat and human. J. Histochem. Cytochem. 28 (1980) 475-478.

W.C. Song, Biochemistry and reproductive endocrinology of estrogen sulphotransferase, Ann. NY Acad. Sci. 948 (2001) 43-50.

Z. Song, D.A. Gomes, W. Stevens, C.D. Sladek, Multiple α1 adrenergic receptor subtypes support synergistic stimulation of vasopressin and oxytocin release by ATP and phenylephrine, Am. J. Physiol. Regul. Integr. Comp. Physiol. 299 (2010) 1529-1537.

H. Song, J. Luo, W. Luo, J. Weng, Z. Wang, B. Li, D. Li, M. Liu, Inactivation of G-protein-coupled receptor 48 (Gpr48/Lgr4) impairs definitive erythropoiesis at midgestation through down-regulation of the ATF4 signaling pathway, J. Biol. Chem. 283 (2008) 36687-36697.

Z. Song, S. Vijayaraghavan, C.D. Sladek, ATP increases intracellular calcium in supraoptic neurons by activation of both P2X and P2Y purinergic receptors, Am. J. Physiol. Regul. Integr. Comp. Physiol. 292 (2007) 423-431.

J. Sóvágó, D.S. Dupuis, B. Gulyás, H. Hall, An overview on functional receptor autoradiography using [35S]GTPgammaS, Brain Res. Brain Res. Rev. 38 (2001) 149-164.

E.K. Speliotes, C.J. Willer, S.I. Berndt, K.L. Monda, G. Thorleifsson, A.U. Jackson, H.L. Allen, C.M. Lindgren, J. Luan, R. Mägi, J.C. Randall, Association analyses of 249,796 individuals reveal 18 new loci associated with body mass index, Nat. Genet. 42 (2010) 937-948.

J.Y. Springael, E. Urizar, S. Costagliola, G. Vassart, M. Parmentier, Allosteric properties of G protein-coupled receptor oligomers, Pharmacol. Ther. 115 (2007) 410-418.

J. Stankova, S. Turcotte, J. Harris, M. Rola-Pleszczynski, Modulation of leukotriene B4 receptor-1 expression by dexamethasone: potential mechanism for enhanced neutrophil survival, J. Immunol. 168 (2002) 3570-3576.

J.E. Stern, Nitric oxide and homeostatic control: an intercellular signalling molecule contributing to autonomic and neuroendocrine integration? Prog. Biophys. Mol. Biol. 84 (2004) 197-215.

J.E. Stern, W. Zhang, Cellular sources, targets and actions of constitutive nitric oxide in the magnocellular neurosecretory system of the rat, J. Physiol. 562 (2005) 725-744.

P.E. Stevis, D.C. Deecher, L. Suhadolnik, L.M. Mallis, D.E. Frail, Differential effects of estradiol and estradiol-BSA conjugates, Endocrinology 140 (1999) 5455-5458.

L. Stewart, C.C. Hindmarch, J. Qiu, Y.C. Tung, G.S. Yeo, D. Murphy, Hypothalamic transcriptome plasticity in two rodent species reveals divergent differential gene expression but conserved pathways, J. Neuroendocrinol. 23 (2011) 177-185.

E.E. Storm, L.H. Tecott, Social circuits: peptidergic regulation of mammalian social behaviour, Neuron. 47 (2005) 483-486.

A. Stofkova, M. Skurlova, A. Kiss, B. Zelezna, S. Zorad, J. Jurcovicova, Activation of hypothalamic NPY, AgRP, MC4R, AND IL-6 mRNA levels in young Lewis rats with early-life diet-induced obesity, Endocr. Regul. 43 (2009) 99-106.

E.M. Stricker, A.F. Sved, Controls of vasopressin secretion and thirst: similarities and dissimilarities in signals, Physiol. Behav. 77 (2002) 731-736.

S. Succu, F. Sanna, T. Melis, A. Boi, A. Argiolas, M.R. Melis, Stimulation of dopamine receptors in the paraventricular nucleus of the hypothalamus of male rats induces penile erection and increases extra-cellular dopamine in the nucleus accumbens: involvement of central oxytocin, Neuropharmacology 52 (2007) 1034-1043.

J. Sun, Z. Chu, S.M. Moenter, Diurnal in vivo and rapid in vitro effects of estradiol on voltage-gated calcium channels in gonadotropin-releasing hormone neurons, J. Neurosci. 30 (2010) 3912-3923.

Y. Sun, J. Huang, Y. Xiang, M. Bastepe, H. Jüppner, B.K. Kobilka, J.J. Zhang, X.Y. Huang, Dosage-dependent switch from G protein-coupled to G protein-independent signaling by a GPCR, EMBO J. 26 (2007) 53-64.

Y. Sun, D. McGarrigle, X.Y. Huang, When a G protein-coupled receptor does not couple to a G protein, Mol. Biosyst. 3 (2007) 849-854.

H.W. Sun, C.Y. Miao, L. Liu, J. Zhou, D.F. Su, Y.X. Wang, C.L. Jiang, Rapid inhibitory effect of glucocorticoids on airway smooth muscle contractions in guinea pigs, Steroids 71 (2006) 154-159.

M.T. Sutter-Dub, Rapid non-genomic and genomic responses to progestogens, estrogens, and glucocorticoids in the endocrine pancreatic B cell, the adipocyte and other cell types, Steroids 67 (2002) 77-93.

T. Suyemitsu, H. Terayama, Specific binding sites for natural glucocorticoids in plasma membranes of rat liver, Endocrinology 96 (1975) 1499-1508.

D.F. Swaab, The human hypothalamo-neurohypophysial system in health and disease, Prog. Brain Res. 119 (1998) 577-618.

D.F. Swaab, C.W. Pool, F.W. Van Leeuwen, Can specificity ever be proved in immunocytochemical staining, J. Histochem. Cytochem. 25 (1977) 388-391.

L.W. Swanson, P.E. Sawchenko, Hypothalamic integration: organization of the paraventricular and supraoptic nuclei, Annu. Rev. Neurosci. 6 (1983) 269-324.

K.L. Swenson, C.D. Sladek, Gonadal steroid modulation of vasopressin secretion in response to osmotic stimulation, Endocrinology 138 (1997) 2089-2097.

E. Szarek, P.S. Cheah, J. Schwartz, P. Thomas, Molecular genetics of the developing neuroendocrine hypothalamus, Mol. Cell. Endocrinol. 323 (2010) 115-123.

J.A. Tadross, M. Patterson, K. Suzuki, K.E. Beale, C.K. Boughton, K.L. Smith, S. Moore, M.A. Ghatei, S.R. Bloom, Augurin stimulates the hypothalamo-pituitary-adrenal axis via the release of corticotrophin-releasing factor in rats, Br. J. Pharmacol. 159 (2010) 1663-1671.

Y. Takada, C. Kato, S. Kondo, R. Korenaga, J. Ando, Cloning of cDNAs encoding G protein-coupled receptor expressed in human endothelial cells exposed to fluid shear stress, Biochem. Biophys. Res. Commun. 240 (1997) 737-741.

A. Takahashi, H. Ishimaru, Y. Ikarashi, E. Kishi, Y. Maruyama, Opposite regulation of body temperature by cholinergic input to the paraventricular nucleus and supraoptic nucleus in rats, Brain Res. 909 (2001) 102-111.

T. Takahashi, T. Kimoto, N. Tanabe, T.A. Hattori, N. Yasumatsu, S. Kawato, Corticosterone acutely prolonged N-methyl-d-aspartate receptor-mediated Ca2+ elevation in cultured rat hippocampal neurons, J. Neurochem. 83 (2002) 1441-1451.

Y. Takano, Y. Nakayama, T. Matsumoto, R. Saito, H.O. Kamiya, The mechanism of central pressor actions of tachykinin NK-3 receptor in the paraventricular nucleus of the hypothalamus in rats, Regul. Peptides. 46 (1993) 360-363.

C.M. Tan, A.E. Brady, H.H. Nickols, Q. Wang, L.E. Limbird, Membrane trafficking of G protein-coupled receptors, Annu. Rev. Pharmacol. Toxicol. 44 (2004) 559-609.

S. Tanaka, K. Ishii, K. Kasai, S.O. Yoon, Y. Saeki, Neural expression of G protein-coupled receptors GPR3, GPR6, and GPR12 up-regulates cyclic AMP levels and promotes neurite outgrowth, J. Biol. Chem. 282 (2007) 10506-10515.

Y.X. Tao, Constitutive activation of G protein-coupled receptors and diseases: insights into mechanisms of activation and therapeutics, Pharmacol. Ther. 120 (2008) 129-148.

J.G. Tasker, S. Di, C. Boudaba, Functional synaptic plasticity in hypothalamic magnocellular neurons, Prog. Brain Res. 139 (2002) 113-119.

J.G. Tasker, S. Di, R. Malcher-Lopes, Minireview: rapid glucocorticoid signaling via membrane-associated receptors, Endocrinology 147 (2006) 5549-5556.

J.G. Tasker, F.E. Dudek, Electrophysiological properties of neurones in the region of the paraventricular nucleus in slices of rat hypothalamus, J. Physiol. 434 (1991) 271-293.

K. Tatemoto, M. Hosoya, Y. Habata, R. Fujii, T. Kakegawa, M.X. Zou, Y. Kawamata, S. Fukusumi, S. Hinuma, C. Kitada, T. Kurokawa, H. Onda, M. Fujino, Isolation and characterization of a novel endogenous peptide ligand for the human APJ receptor, Biochem. Biophys. Res. Commun. 251 (1998) 471-476.

M. Tauchi, R. Zhang, D.A. D'Alessio, J.E. Stern, J.P. Herman, Distribution of glucagon-like peptide-1 immunoreactivity in the hypothalamic paraventricular and supraoptic nuclei, J. Chem. Neuroanat. 36 (2008) 144-149.

N.R. Thanky, J.H. Son, A.E. Herbison, Sex differences in the regulation of tyrosine hydroxylase gene transcription by estrogen in the locus coeruleus of TH9-LacZ transgenic mice, Brain Res. Mol. Brain, 15 (2002) 220-226.

P. Thomas, R. Alyea, Y. Pang, C. Peyton, J. Dong, A.H. Berg, Conserved estrogen binding and signaling functions of the G protein-coupled estrogen receptor 1 (GPER) in mammals and fish, Steroids 75 (2010) 595-602.

P. Thomas, J. Dong, Binding and activation of the seven-transmembrane estrogen receptor GPR30 by environmental estrogens: a potential novel mechanism of endocrine disruption, J. Steroid Biochem. Mol. Biol. 102 (2006) 175-179.

P. Thomas, Y. Pang, E.J. Filardo, J. Dong, Identity of an estrogen membrane receptor coupled to a G protein in human breast cancer cells. Endocrinolology 146 (2005) 624–632.

J.Y. Tiao, A. Bradaia, B. Biermann, K. Kaupmann, M. Metz, C. Haller, A.G. Rolink, E. Pless, P.N. Barlow, M. Gassmann, B. Bettler, The sushi domains of secreted GABA(B1) isoforms selectively impair GABA(B) heteroreceptor function, J. Biol. Chem. 283 (2008) 31005-31011.

A.B. Tobin, A.J. Butcher, K.C. Kong, Location, location, location...site-specific GPCR phosphorylation offers a mechanism for cell-type-specific signalling, Trends Pharmacol. Sci. 29 (2008) 413-420.

V.A. Tobin, P.M. Bull, S. Arunachalam, A-M. O'Carroll, Y. Ueta, M. Ludwig, The Effects of Apelin on the Electrical Activity of Hypothalamic Magnocellular Vasopressin and Oxytocin Neurons and Somatodendritic Peptide Release, Endocrinology 149 (2008) 6136–6145.

K. Toshinai, M. Nakazato, Neuroendocrine regulatory peptide-1 and -2: novel bioactive peptides processed from VGF, Cell. Mol. Life Sci. 66 (2009) 1939-1945.

A.C. Towle, P.Y. Sze, Steroid binding to synaptic plasma membrane: differential binding of glucocorticoids and gonadal steroids, J. Steroid Biochem. 18 (1983) 135-143.

M. Toyooka, T. Tujii, S. Takeda, The N-terminal domain of GPR61, an orphan G-protein-coupled receptor, is essential for its constitutive activity, J. Neurosci. Res. 87 (2009) 1329-1333.

T.M. Tran, J. Friedman, E. Qunaibi, F. Baameur, R.H. Moore, R.B. Clark, Characterization of agonist stimulation of cAMP-dependent protein kinase and G protein-coupled receptor kinase phosphorylation of the beta2-adrenergic receptor using phosphoserine-specific antibodies, Mol. Pharmacol. 65 (2004) 196-206.

M. Trueba, I. Ibarrola, A.I. Vallejo, M.J. Sancho, A. Marino, J.M. Macarulla, Characterization of specific binding sites for corticosterone in mouse liver plasma membrane, Membr. Biochem. 8 (1989) 229-239.

E. Tsuji, Y. Tsuji, M. Sasaguri, K. Arakawa, Function and expression of a novel rat salt-tolerant protein: evidence of a role in cellular sodium metabolism, J. Am. Soc. Nephrol. 9 (1998) 1574-1580.

M.A. Uberti, C. Hague, H. Oller, K.P. Minneman, R.A. Hall, Heterodimerization with beta2-adrenergic receptors promotes surface expression and functional activity of alpha1D-adrenergic receptors, J. Pharmacol. Exp. Ther. 313 (2005) 16-23.

M.A. Uberti, R.A. Hall, K.P. Minneman, Subtype-specific dimerization of alpha 1-adrenoceptors: effects on receptor expression and pharmacological properties, Mol. Pharmacol. 64 (2003) 1379-1390.

Y.M. Ulrich-Lai, J.P. Herman, Neural regulation of endocrine and autonomic stress responses, Nat. Rev. Neurosci. 10 (2009) 397-409.

R.J. Valentino, M. Page, E. Van Bockstaele, G. Aston-Jones, Corticotropin-releasing factor innervation of the locus coeruleus region: distribution of fibers and sources of input, Neuroscience 48 (1992) 689-705.

M.A. Valverde, P. Rojas, J. Amigo, D. Cosmelli, P. Orio, M.I. Bahamonde, G.E. Mann, C. Vergara, R. Latorre, Acute activation of Maxi-K channels (hSlo) by estradiol binding to the beta subunit. Science 17 (1999) 1929-1931.

E.H. van den Burg, I.D. Neumann, Bridging the Gap between GPCR activation and behaviour: oxytocin and prolactin signalling in the hypothalamus, J. Mol. Neurosci. 43 (2011) 200-208.

P.A. van der Merwe, Surface Plasmon Resonance in Protein-Ligand interactions: hydrodynamics and calorimetry, edited by S. Harding, P.Z. Chowdhry, Practical Approach series, Oxford University Press (2001) 137-170.

G. Van Schoore, F. Mendive, R. Pochet, G. Vassart, Expression pattern of the orphan receptor LGR4/GPR48 gene in the mouse, Histochem. Cell Biol. 124 (2005) 35-50.

D.K. Vassilatis, J.G. Hohmann, H. Zeng, F. Li, J.E. Ranchalis, M.T. Mortrud, A. Brown, S.S. Rodriguez, J.R. Weller, A.C. Wright, J.E. Bergmann, G.A. Gaitanaris, The G protein-coupled receptor repertoires of human and mouse, Proc. Natl. Acad. Sci. USA. 100 (2003) 4903-4908.

J.G. Veening, H.P. Barendregt, The regulation of brain states by neuroactive substances distributed via the cerebrospinal fluid; a review, Cerebrospinal Fluid Res. 6 (2010) 7:1.

A. Vegiopoulos, S. Herzig, Glucocorticoids, metabolism and metabolic diseases, Mol. Cell Endocrinol. 275 (2007) 43-61.

V.A. Verrière, D. Hynes, S. Faherty, J. Devaney, J. Bousquet, B.J. Harvey, V. Urbach, Rapid effects of dexamethasone on intracellular pH and Na+/H+ exchanger activity in human bronchial epithelial cells, J. Biol. Chem. 280 (2005) 35807-35814.

A. Vivacqua, D. Bonofiglio, L. Albanito, A. Madeo, V. Rago, A. Carpino, A.M. Musti, D. Picard, S. Andò, M. Maggiolini, 17beta-estradiol, genistein, and 4-hydroxytamoxifen induce the proliferation of thyroid cancer cells through the g protein-coupled receptor GPR30, Mol. Pharmacol. 70 (2006a) 1414-1423.

A. Vivacqua, D. Bonofiglio, A.G. Recchia, A.M. Musti, D. Picard, S. Andò, M. Maggiolini, The G protein-coupled receptor GPR30 mediates the proliferative effects induced by 17beta-estradiol and hydroxytamoxifen in endometrial cancer cells, Mol. Endocrinol. 20 (2006b) 631-646.

K.V. Voelkerding, S.A. Dames, J.D. Durtschi, Next-generation sequencing: from basic research to diagnostics, Clin. Chem. 55 (2009):641-658.

R.D. Wainford, D.R. Kapusta, Hypothalamic paraventricular nucleus G alpha q subunit protein pathways mediate vasopressin dysregulation and fluid retention in salt-sensitive rats, Endocrinology 151 (2010) 5403-5414.

J.B. Wakerley, D.A. Poulain, D. Brown, Comparison of firing patterns in oxytocin- and vasopressin-releasing neurones during progressive dehydration, Brain Res. 148 (1978) 425-440.

J.B. Wakerley, D.A. Poulain, R.E. Dyball, B.A. Cross, Activity of phasic neurosecretory cells during haemorrhage, Nature 258 (1975) 82-84.

V.R. Walker, K.S. Korach, Estrogen receptor knockout mice as a model for endocrine research, ILAR Journal 45 (2004) 455-461.

Z. Wang, M. Gerstein, M. Snyder, RNA-Seq: a revolutionary tool for transcriptomics, Nat. Rev. Genet. 10 (2009a) 57-63.

D. Wang, L. Hu, G. Zhang, L. Zhang, C. Chen, G protein-coupled receptor 30 in tumor development, Endocrine. 38 (2010) 29-37.

C. Wang, B. Dehghani, Y. Li, L.J. Kaler, T. Proctor, A.A. Vandenbark, H. Offner, Membrane estrogen receptor regulates experimental autoimmune encephalomyelitis through up-regulation of programmed death 1, J. Immunol. 182 (2000b) 3294-3303.

C. Wang, B. Dehghani, I.J. Magrisso, E.A. Rick, E. Bonhomme, D.B. Cody, L.A. Elenich, S. Subramanian, S.J. Murphy, M.J. Kelly, J.S. Rosenbaum, A.A. Vandenbark, H. Offner, GPR30 contributes to estrogen-induced thymic atrophy, Mol. Endocrinol. 22 (2008a) 636-648.

S.S. Wang, W. Kamphuis, I. Huitinga, J.N. Zhou, D.F. Swaab, Gene expression analysis in the human hypothalamus in depression by laser microdissection and real-time PCR: the presence of multiple receptor imbalances, Mol. Psychiatry. 13 (2008b) 786-799.

T. Wang, M. Palkovits, M. Rusnak, E. Mezey, T.B. Usdin, Distribution of parathyroid hormone 2 receptor-like immunoreactivity and messenger mRNA in the rat nervous system, Neuroscience 100 (2000) 629-649.

C. Wang, E.R. Prossnitz, S.K. Roy, G protein-coupled receptor 30 expression is required for estrogen stimulation of primordial follicle formation in the hamster ovary, Endocrinology 149 (2008c) 4452-4461.

C. Wang, E.R. Prossnitz, S.K. Roy, Expression of G protein-coupled receptor 30 in the hamster ovary: differential regulation by gonadotropins and steroid hormones, Endocrinology 148 (2007) 4853-4864.

H. Wang, A.R. Ward, J.F. Morris, Oestradiol acutely stimulates exocytosis of oxytocin and vasopressin from dendrites and somata of hypothalamic magnocellular neurons, Neuroscience 68 (1995) 1179-1188.

Z. Wang, X. Zhang, P. Shen, B.W. Loggie, Y. Chang, T.F. Deuel, A variant of estrogen receptor-{alpha}, hER-{alpha}36: transduction of estrogen- and antiestrogen-dependent membrane-initiated mitogenic signalling, Proc. Natl. Acad. Sci. USA 103 (2006) 9063-9068.

Z. Wang, X. Zhang, P. Shen, B.W. Loggie, Y. Chang, T.F. Deuel, Identification, cloning, and expression of human estrogen receptor-alpha36, a novel variant of human estrogen receptor-alpha66, Biochem. Biophys. Res. Commun. 336 (2005) 1023-1027.

W.J. Wasserman, L.H. Pinto, C.M. O'Connor, L.D. Smith, Progesterone induces a rapid increase in [Ca2+] in of Xenopus laevis oocytes, Proc. Natl. Acad. Sci. USA 77 (1980) 1534-1536.

C.S. Watson, B. Gametchu, Membrane estrogen and glucocorticoid receptors-implications for hormonal control of immune function and autoimmunity. Int. Immunopharmacol. 1 (2001) 1049–1063.

A.M. Watson, M.J. McKinley, C.N. May, Effect of central urotensin II on the heart rate, blood pressure and brain fos immunoreactivity in conscious rats, Neuroscience 155 (2008) 241-249.

J. Wayte, J.C. Buckingham, A.M. Cowell, The role of phospholipase C in arginine vasopressin secretion by rat hypothalami in vitro, Neuroreport. 8 (1997) 1277-1282.

M.P. Weekes, R. Antrobus, J.R. Lill, L.M. Duncan, S. Hör, P.J. Lehner, Comparative analysis of techniques to purify plasma membrane proteins, J. Biomol. Tech. 21 (2010) 108-115.

K. Wei, J.H. Eubanks, J. Francis, Z. Jia, O.C. Snead, Cloning and tissue distribution of a novel isoform of the rat GABA(B)R1 receptor subunit, Neuroreport 12 (2001) 833-837.

P. Wei, W.V. Vedeckis, Regulation of the glucocorticoid receptor gene by the AP-1 transcription factor, Endocrine 7(1997) 303-310.

S.G. Wei, Y. Yu, Z.H. Zhang, R.B. Felder, Angiotensin II upregulates hypothalamic AT1 receptor expression in rats via the mitogen-activated protein kinase pathway, Am. J. Physiol. Heart Circ. Physiol. 296 (2009) 1425-1433.

B.R. Weil, M.C. Manukyan, J.L. Herrmann, Y. Wang, A.M. Abarbanell, J.A. Poynter, D.R. Meldrum, Signaling via GPR30 protects the myocardium from ischemia/reperfusion injury, Surgery 148 (2010a) 436-443.

T.T. Weil, R.M. Parton, I. Davis, Making the message clear: visualizing mRNA localization, Trends Cell. Biol. 20 (2010b) 380-390.

H.G. Wendelboe, K. Bisgaard, Education guide: Immunohistochemical (IHC) staining methods, 5th edition, Dako North America, California, 2009.

J. Weng, J. Luo, X. Cheng, C. Jin, X. Zhou, J. Qu, L. Tu, D. Ai, D. Li, J. Wang, J.F. Martin, B.A. Amendt, M. Liu, Deletion of G protein-coupled receptor 48 leads to ocular anterior segment dysgenesis (ASD) through down-regulation of Pitx2, Proc. Natl. Acad. Sci. USA 105 (2008) 6081-6086.

T.D. Werry, P.M. Sexton, A. Christopoulos, "Ins and outs" of seven-transmembrane receptor signalling to ERK, Trends Endocrinol. Metab. 16 (2005) 26-33.

S.R. Wersinger, E.L. Ginns, A.M. O'Carroll, S.J. Lolait, W.S. Young, Vasopressin V1b receptor knockout reduces aggressive behavior in male mice, Mol. Psychiatry. 7 (2002) 975-984.

J. Wess, Mutational analysis of muscarinic acetylcholine receptors: structural basis of ligand/receptor/G protein interactions, Life Sci. 53 (1993) 1447-1463.

M. Wheatley, S.R. Hawtin, Glycosylation of G-protein-coupled receptors for hormones central to normal reproductive functioning: its occurrence and role, Hum. Reprod. Update 4 (1999) 356-364.

M. Wheatley, S.R. Hawtin, V.J. Wesley, H.C. Howard, J. Simms, A. Miles, K. McEwan, R.A. Parslow, Agonist binding to peptide hormone receptors, Biochem. Soc. Trans. 31 (2003) 35-39.

M.H. Whitnall, Regulation of the hypothalamic corticotropin-releasing hormone neurosecretory system, Prog. Neurobiol. 40 (1993) 573-629.

E.P. Widmaier, M.F. Dallman, The effects of corticotropin-releasing factor on adrenocorticotropin secretion from perifused pituitaries in vitro: rapid inhibition by glucocorticoids, Endocrinology 115 (1984) 2368-2374.

O. Wiegert, M. Joëls, H. Krugers, Timing is essential for rapid effects of corticosterone on synaptic potentiation in the mouse hippocampus, Learn Mem. 13 (2006) 110-113.

M.E. Wierman, Sex steroid effects at target tissues: mechanisms of action, Adv. Physiol. Educ. 31 (2007) 26-33.

D.G. Wilkinson, In situ hybridization: a practical approach, Second edition, Oxford University Press (1999).

M.H. Wilson, L.E. Limbird, Mechanisms regulating the cell surface residence time of the alpha 2A-adrenergic receptor, Biochemistry 39 (2000) 693-700.

S.H. Windahl, N. Andersson, A.S. Chagin, U.E. Mårtensson, H. Carlsten, B. Olde, C. Swanson, S. Movérare-Skrtic, L. Sävendahl, M.K. Lagerquist, L.M. Leeb-Lundberg, C. Ohlsson, The role of the G protein-coupled receptor GPR30 in the effects of estrogen in ovariectomized mice, Am. J. Physiol. Endocrinol. Metab. 296 (2009) 490-496.

R.J. Windle, L.E. Gamble, Y.M. Kershaw, S.A. Wood, S.L. Lightman, C.D. Ingram, Gonadal steroid modulation of stress-induced hypothalamo-pituitary-adrenal activity and anxiety behavior: role of central oxytocin, Endocrinology 147 (2006) 2423-2431.

R.J. Windle, S.A. Wood, Y.M. Kershaw, S.L. Lightman, C.D. Ingram, M.S. Harbuz, Increased corticosterone pulse frequency during adjuvant-induced arthritis and its relationship to alterations in stress responsiveness, J. Neuroendocrinol. 13 (2001) 905-911.

A. Wise, S.C. Jupe, S. Rees, The identification of ligands at orphan G-protein coupled receptors, Annu. Rev. Pharmaco.l Toxicol. 44 (2004) 43-66.

A. Woehler, E.G. Ponimaskin, G protein--mediated signaling: same receptor, multiple effectors, Curr. Mol. Pharmacol. 2 (2009) 237-248.

L.F. Wong, T. Harding, J. Uney, D. Murphy, cAMP-dependent protein kinase A mediation of vasopressin gene expression in the hypothalamus of the osmotically challenged rat, Mol. Cell. Neurosci. 24 (2003) 82-90.

A.M. Wren, C.J. Small, C.R. Abbott, P.H. Jethwa, A.R. Kennedy, K.G. Murphy, S.A. Stanley, A.N. Zollner, M.A. Ghatei and S.R. Bloom, Hypothalamic Actions of Neuromedin U, Endocrinology 143 (2002) 4227-4234.

Q. Wu, P.Y. Law, L.N. Wei, H.H. Loh, Post-transcriptional regulation of mouse mu opioid receptor (MOR1) via its 3' untranslated region: a role for microRNA23b, FASEB J. 22 (2008) 4085-4095.

M. Wu, M. Tang, D. Adriaensen, I. Depoortere, T.L. Peeters, J.P. Timmermans, Central, but not peripheral application of motilin increases c-Fos expression in hypothalamic nuclei in the rat brain, Histochem. Cell Biol. 123 (2005) 139-145.

Y.H. Wu, J.N. Zhou, R. Balesar, U. Unmehopa, A. Bao, R. Jockers, J. Van Heerikhuize, D.F. Swaab, Distribution of MT1 melatonin receptor immunoreactivity in the human hypothalamus and pituitary gland: colocalization of MT1 with vasopressin, oxytocin, and corticotropin-releasing hormone, J. Comp. Neurol. 499 (2006) 897-910.

L. Xiao, A. Qi, Y. Chen, Cultured embryonic hippocampal neurons deficient in glucocorticoid (GC) receptor: a novel model for studying nongenomic effects of GC in the neural system, Endocrinology. 146 (2005) 4036-4041.

G.X. Xie, T. Meuser, C. Pietruck, M. Sharma, P.P Palmer, Presence of opioid receptor-like (ORL1) receptor mRNA splice variants in peripheral sensory and sympathetic neuronal ganglia, Life Sci. 64 (1999) 2029-2037.

L. Xu, S. Begum, J.D. Hearn, R.O. Hynes, GPR56, an atypical G protein-coupled receptor, binds tissue transglutaminase, TG2, and inhibits melanoma tumor growth and metastasis. Proc. Natl. Acad. Sci. USA 103 (2006) 9023-9028.

L. Xu, R.O. Hynes, GPR56 and TG2: possible roles in suppression of tumor growth by the microenvironment, Cell Cycle 6 (2007) 160-165.

H. Xu, S. Qin, G.A. Carrasco, Y. Dai, E.J. Filardo, E.R. Prossnitz, G. Battaglia, L.L. Doncarlos, N.A. Muma, Extra-nuclear estrogen receptor GPR30 regulates serotonin function in rat hypothalamus, Neuroscience 158 (2008) 1599-1607.

T. Yamada, A. Mochiduki, Y. Sugimoto, Y. Suzuki, K. Itoi, K. Inoue, Prolactin-releasing peptide regulates the cardiovascular system via corticotrophin-releasing hormone, J. Neuroendocrinol. 21 (2009) 586-593.

H. Yamaguchi, K. Sasaki, Y. Satomi, T. Shimbara, H. Kageyama, M.S. Mondal, K. Toshinai, Y. Date, L.J. González, S. Shioda, T. Takao, M. Nakazato, N. Minamino, Peptidomic identification and biological validation of neuroendocrine regulatory peptide-1 and -2, J. Biol. Chem. 282 (2007) 26354-26360.

N. Yanagihara, M. Liu, Y. Toyohira, M. Tsutsui, S. Ueno, Y. Shinohara, K. Takahashi, K. Tanaka K, Stimulation of catecholamine synthesis through unique estrogen receptors in the bovine adrenomedullary plasma membrane by 17beta-estradiol, Biochem Biophys Res Commun. 13 (2006) 548-553.

K. Yano, Y. Tsuda, Y. Kaji, S. Kanaya, T. Fujino, Y. Niho, Effects of hydrocortisone on transmembrane currents in guinea pig ventricular myocytes-possible evidence for positive inotropism, Jpn. Circ. J. 58 (1994) 836-843.

S.T.Yao, J.A. Barden, D.I. Finkelstein, M.R. Bennett, A.J. Lawrence, Comparative study on the distribution patterns of P2X1-P2X6 receptor immunoreactivity in the brainstem of the rat and the common marmoset (Callithrix jacchus): association with catecholamine cell groups, J. Comp. Neurol. 427 (2000) 485-507.

S.T. Yao, J.A. Barden, A.J. Lawrence, On the immunohistochemical distribution of ionotropic P2X receptors in the nucleus tractus solitarius of the rat, Neuroscience 108 (2001) 673-685.

M.A. Yates, Y. Li, P.J. Chlebeck, H. Offner, GPR30, but not estrogen receptor-alpha, is crucial in the treatment of experimental autoimmune encephalomyelitis by oral ethinyl estradiol, BMC Immunol. 19 (2010) 11-20.

H. Yokoi, H. Arima, K. Kondo, T. Murase, Y. Iwasaki, H.Y. Yang, Y. Oiso, Antiserum against neuropeptide FF augments vasopressin release in conscious rats, Peptides 19 (1998) 393-395.

W.S. Young, M.J. Kuhar, A new method for receptor autoradiography: [3H]opioid receptors in rat brain, Brain Res. 179 (1979) 255-270.

W.S. Young, J. Li, S.R. Wersinger, M. Palkovits, The vasopressin 1b receptor is prominent in the hippocampal area CA2 where it is unaffected by restraint stress or adrenalectomy, Neuroscience 143 (2006) 1031-1039.

L.J. Young, R. Nilsen, K.G. Waymire, G.R. MacGregor, T.R. Insel, Increased affiliative response to vasopressin in mice expressing the V1a receptor from a monogamous vole, Nature 400 (1999) 766-768.

W.S. Young, E.A. Shepard, R.M. Burch, Plasma hyperosmolality increases G protein and 3',5'-cyclic adenosine monophosphate synthesis in the paraventricular and supraoptic nuclei, Mol Endocrinol. 1 (1987) 884-888.

E.V. Younglai, Y.J. Wu, T.K. Kwan, C.Y. Kwan, Non-genomic action of estradiol and progesterone on cytosolic calcium concentrations in primary cultures of human granulosa-lutein cells, Hum. Reprod. 20 (2005) 2383-2390.

C. Yue, N. Mutsuga, Y. Sugimura, J. Verbalis, H. Gainer, Differential kinetics of oxytocin and vasopressin heteronuclear RNA expression in the rat supraoptic nucleus in response to chronic salt loading in vivo, J. Neuroendocrinol. 20 (2008) 227-232.

Y. Zhang, T.S. Gray, D.N. D'Souza, G.A. Carrasco, K.J. Damjanosk, B. Dudas, F. Garcia, G.M. Zainelli, N.R. Sullivan Hanley, G. Battaglia, N.A. Muma, L.D.Van de Kar, Desensitization of 5-HT1A receptors by 5-HT2A receptors in neuroendocrine neurons in vivo, J. Pharmacol. Exp. Ther. 310 (2004) 59-66.

B. Zhang, S. Subramanian, S. Dziennis, J. Jia, M. Uchida, K. Akiyoshi, E. Migliati, A.D. Lewis, A.A. Vandenbark, H. Offner, P.D. Hurn, Estradiol and G1 reduce infarct size and improve immunosuppression after experimental stroke, J. Immunol. 184 (2010) 4087-4094.

X.F. Zheng, L. Liu, J. Zhou, M.Y. Miao, J.R. Zhou, D. Zhu, Z.F. Xia, C.L. Jiang, Biphasic effects of dexamethasone on glycogen metabolism in primary cultured rat hepatocytes, J. Endocrinol. Invest. 32 (2009) 756-758.

H. Zheng, H.H. Loh, P.Y. Law, Agonist-selective signaling of G protein-coupled receptor: mechanisms and implications, IUBMB Life 62 (2010) 112-119.

F.F. Zheng, R.C. Wu, C.L. Smith, B.W. O'Malley, Rapid estrogen-induced phosphorylation of the SRC-3 coactivator occurs in an extranuclear complex containing estrogen receptor, Mol. Cell. Biol. 25 (2005) 8273-8284.

H. Zheng, Y. Zeng, X. Zhang, J. Chu, H.H. Loh, P.Y. Law, mu-Opioid receptor agonists differentially regulate the expression of miR-190 and NeuroD, Mol. Pharmacol. 77 (2010) 102-109.

M.K. Zhong, Z. Shi, L.M. Zhou, J. Gao, Z.H. Liao, W. Wang, X.Y. Gao, G.Q. Zhu, Regulation of cardiac sympathetic afferent reflex by GABA(A) and GABA(B) receptors in paraventricular nucleus in rats, Eur. J. Neurosci. 27 (2008) 3226-3232.

X.J. Zhou, J. Yang, F.L. Yan, D.X. Wang, X.Y. Li, X.Q. Fan, F. Hao, X.Q. Yan, X.P. Li, H. Li, W.Y. Liu, B.C. Lin, Norepinephrine plays an important role in antinociceptive modulation of hypothalamic paraventricular nucleus in the rat, Int. J. Neurosci. 120 (2010) 428-438.

Y. Zhu, J. Bond, P. Thomas, Identification, classification, and partial characterization of genes in humans and other vertebrates homologous to a fish membrane progestin receptor, Proc. Natl. Acad. Sci. USA 100 (2003a) 2237-2242.

Y. Zhu, C.D. Rice, Y. Pang, M. Pace, P. Thomas, Cloning, expression, and characterization of a membrane progestin receptor and evidence it is an intermediary in meiotic maturation of fish oocytes, Proc. Natl. Acad. Sci. USA. 100 (2003b) 2231-2236.

Appendix I: Extra Protocols

Molecular biology techniques

PCR conditions for riboprobes

Probe	PCR reaction mix	PCR conditions
rat GPRC5B	5µl 10 x HotStar buffer ; 8µl dNTPs; 0.5µl 2.5U amplitaq polymerase; 2µl 10µM primers; distilled H_2O to 50µl	95°C 1 min; 94°C 45s, 52.5°C 1 min, 72°C 30s for 40 cycles; 72°C 10 min; 4°C soak
rat GPER	5µl 10 x HotStar buffer ; 8µl dNTPs; 0.5µl 2.5U amplitaq polymerase; 2µl 10µM primers; distilled H_2O to 50µl	95°C 1 min; 94°C 1 min, 55°C 1 min, 72°C 1 min for 40 cycles; 72°C 10 min; 4°C soak
rat GPR48	5µl 10 x HotStar buffer ; 8µl dNTPs; 0.5µl 2.5U amplitaq polymerase; 2µl 10µM primers; distilled H_2O to 50µl	95°C 1 min; 94°C 45s, 45°C 1 min, 72°C 30s for 40 cycles; 72°C 10 min; 4°C soak
rat GPR56	5µl 10 x HotStar buffer ; 8µl dNTPs; 0.5µl 2.5U amplitaq polymerase; 2µl 10µM primers; distilled H_2O to 50µl	95°C 1 min; 94°C 45s, 50°C 1 min, 72°C 30s for 40 cycles; 72°C 10 min; 4°C soak
rat GPR65	5µl 10 x HotStar buffer ; 8µl dNTPs; 0.5µl 2.5U amplitaq polymerase; 2µl 10µM primers; distilled H_2O to 50µl	95°C 1 min; 94°C 45s, 52.5°C 1 min, 72°C 30s for 40 cycles; 72°C 10 min; 4°C soak
rat GPR108	5µl 10 x HotStar buffer ; 8µl dNTPs; 0.5µl 2.5U amplitaq polymerase; 2µl 10µM primers; distilled H_2O to 50µl	95°C 1 min; 94°C 45s, 47.5°C 1 min, 72°C 30s for 40 cycles; 72°C 10 min; 4°C soak
rat GPR125	5µl 10 x HotStar buffer ; 8µl dNTPs; 0.5µl 2.5U amplitaq polymerase; 2µl 10µM primers; distilled H_2O to 50µl	95°C 1 min; 94°C 45s, 50°C 1 min, 72°C 30s for 40 cycles; 72°C 10 min; 4°C soak
rat GPR146	5µl 10 x HotStar buffer ; 8µl dNTPs; 0.5µl 2.5U amplitaq polymerase; 2µl 10µM primers; distilled H_2O to 50µl	95°C 1 min; 94°C 45s, 50°C 1 min, 72°C 30s for 40 cycles; 72°C 10 min; 4°C soak
rat GPR153	5µl 10 x HotStar buffer ; 8µl dNTPs; 0.5µl 2.5U amplitaq polymerase; 2µl 10µM primers; distilled H_2O to 50µl	95°C 1 min; 94°C 45s, 50°C 1 min, 72°C 30s for 40 cycles; 72°C 10 min; 4°C soak
rat TMEM87B	5µl 10 x HotStar buffer ; 8µl dNTPs; 0.5µl 2.5U amplitaq polymerase; 2µl 10µM primers; distilled H_2O to 50µl	95°C 1 min; 94°C 45s, 50°C 1 min, 72°C 30s for 40 cycles; 72°C 10 min; 4°C soak
mouse GPER	5µl 10 x HotStar buffer ; 8µl dNTPs; 0.5µl 2.5U amplitaq polymerase; 2µl 10µM primers; distilled H_2O to 50µl	95°C 1 min; 94°C 1 min, 55°C 1 min, 72°C 1 min for 40 cycles; 72°C 10 min; 4°C soak

Filling-in DNA.

The process of filling in uses T4 DNA Polymerase to catalyze the synthesis of DNA in the 5′→ 3′ direction to create blunt ends. This is used to ensure there is complete extension of PCR products, particularly if subsequent steps require unmitigated restriction enzyme recognition sites.

1) PCR product is made up to 300µl with TE or H_2O and DNA precipitated overnight at -20°C with 24µl 5N NaCl and 990µl absolute ethanol.

2) Solution was centrifuged (16,000xg) and pellet washed with 70% ethanol and resuspended in 21µl H_2O.

3) Added to the 21µl DNA were 25µl dNTPs, 6µl BSA, 6µl T4 polymerase buffer (New England BioLabs, UK) and 2µl T4 polymerase (3U/µl; New England BioLabs, UK).

4) The reaction mix was incubated at 12°C for 45 min and then at room temperature for 15 min.

5) 140µl TE was added to the product and phenol/chloroform/isoamyl alcohol (P/C/I) extracted (with 200µl P/C/I; see Appendix II) and then chloroform/isoamyl alcohol (C/I) extracted (with 200µl C/I; see Appendix II).

6) DNA was precipitated with 80µl 7.5N ammonium acetate, 600µl ethanol and 2µl tRNA on dry ice for 15 min, and centrifuged (16,000xg) for 10 min. DNA was resuspended in TE.

Gel electrophoresis

Gel electrophoresis was used to separate, and identify, different sized strands of DNA. To perform electrophoresis an ethidium bromide agarose gel (see Appendix II on how to make a gel) was placed into a gel tank (VWR, UK) filled with 1x TAE buffer/100µl and 5µl 10mg/ml ethidium bromide (see Appendix II). DNA premixed with 10% stop buffer (Appendix II) was loaded into the gel lanes, leaving one lane for a DNA marker (Appendix II). An electric current (between 50-80V) was run through the tank for approximately 2 hours.

Gel extraction

Agarose gel is extracted from DNA using the Qiaex II gel extraction kit and protocol (Qiagen, UK).

1) Bands of interest were cut out of agarose gel and weighed.

2) QX1 buffer was added to agarose (DNA fragments < 100bp add 6 volumes QX1; DNA fragments 100bp-4kb add 3 volumes of buffer QX1; DNA fragments > 4kb add 3 volumes of buffer QX1 and 2 volumes distilled H_2O; agarose gels > 2% add 6 volumes of buffer QX1), followed by Qiaex II beads (≤ 2µg DNA add 10µl; 2-10µg DNA add 30µl).

3) Bands were incubated at 50°C for 10 min, vortexing every 2 min.

4) Solution was centrifuged at (16,000xg) for 30s and supernatant removed leaving DNA pellet.

5) DNA pellet washed with 500 µl QX1 buffer.

6) 2x wash with buffer PE.

7) DNA was left to air dry for 5-15 min, and resuspended in 20 µl TE, ph 8 and incubated for 5-10 min (DNA fragments < 4kb for 5 min at room temperature; DNA fragments 4-10 kb at 50°C for 5 min; DNA fragments > 10 kb at 50°C for 10 min).

8) Solution was centrifuged (16,000xg) for 30s and supernatant collected.

Vector-Insert ligations

Vectors were digested with the same restriction endonucleases used to digest the insert, and run on a 0.8% ethidium bromide gel. Linearised vectors were removed from the ethidium bromide agarose gel (over a UV light box) and the DNA extracted using the Qiaex II gel extraction kit and protocol. To ligate insert into a vector, 4µl Vector (50-100ng), was added to 10µl insert DNA (approximately 3x vector concentration), plus 4µl 5x DNA ligase buffer (Invitrogen, UK), 1µl 100mM ATP (Sigma, UK) and 1µl T4 DNA ligase (Invitrogen, UK) and incubated at 14°C overnight.

Transforming recombinant plasmids into E.coli cells

The recombinant vectors were introduced into DH5α *E.coli* via a heat shock protocol:

1) Vector added to 50-100µl DH5α and placed on ice for 30 min.

2) *E.coli* heat shocked with 20s at 37°C and 2 min on ice.

3) Bacteria were rocked (225rpm) for 1 hour at 37°C in 950µl SOC medium (Sigma, UK), centrifuged (16,000xg) for 10 s, and resuspended in 100µl SOC medium.

4) Using an aseptic technique, the bacteria were spread on to an LB-agar plate (containing antibiotics that corresponds to the antibiotics resistance gene within the vector), and left to grow overnight at 37 °C.

DNA miniprep

1) Single colonies were picked from the LB-agar plate and put into 5ml LB (plus antibiotic) and grown overnight (placed at 37°C and rocked (225rpm)).

2) 500µl of bacteria culture was centrifuged (16,000xg) for 5 min and supernatant discarded. The bacterial pellet was resuspended in 100µl of lysosome solution (see Appendix II) and incubated on ice for 30 min.

3) 0.2N sodium hydroxide/1% SDS was added and incubated on ice for 5 min to continue lysis, followed by the addition of 150µl 3M sodium acetate and incubated on ice for a further 30 min to precipitate the bacterial DNA.

4) The lysis was centrifuged (16,000xg) for 10 min, supernatant collected. 900µl of absolute ethanol was added to the supernatant and DNA precipitated out for 10 min on dry ice. This was followed by a 10 min centrifuge (16,000xg), and supernatant removed.

5) Pellet was washed with 70% ethanol for 3-5 min, allowed to air dry for 3-5 min, and dissolved in 40µl TE.

6) 10µl DNA was digested with appropriate restriction endonucleases and ran on a low percentage agarose gel to check the vector contained the correct insert.

Qiagen plasmid maxiprep protocol

Plasmid DNA was retrieved from E.coli using the Qiagen plasmid maxiprep kit (Qiagen, UK). The kit contained Qiagen tips that purified the DNA.

1) Colonies that contained the correct insert were cultured overnight in 100ml LB (and antibiotics).

2) Bacteria were centrifuged (~2,500xg) for 10 min and LB removed. Pellet was resuspended in 10ml of the supplied Qiagen resuspension buffer P1, then 10ml of lysis buffer P2, and incubated at room temp for 5 min.

3) 10ml neutralization buffer 3 was added and solution incubated on ice for 20 min and then at -20°C for 20 min, inverting every 5 min. The suspension was then centrifuged (20,000xg) at 4°C for 30 min.

4) Supernatant was removed and applied to a Qiagen tip.

5) Qiagen tip was washed with wash buffer QC x 2.

6) DNA was eluted from tip with elution buffer QF, precipitated with 10.5ml isopropanol, and centrifuged (15,000xg) for 30 min at 4°C.

7) Supernatant was removed and pellet washed with 70% ethanol, and centrifuged (15,000xg) for 10 min at 4°C.

8) Ethanol was removed and pellet was air-dried for 5-10 min, and dissolved in 200µl TE, pH 8.0.

Further to the Qiagen protocol, the vector was precipitated and cleaned up by P/C/I extraction as follows:

1) DNA precipitated with 4µl 5 N NaCl and 400µl absolute ethanol at -20°C overnight.

2) Centrifuged (16,000xg) for 5-10 min and DNA pellet washed with 1ml 70% ethanol.

3) Pellet resuspended in 500µl (10mM Tris-HCl, pH 7.5, 1mM ethylenediaminetetraacetic acid (EDTA), 0.4M NaCl, 0.5% SDS). If pellet did not dissolve straight away the solution was incubated at 60°C for 10 min.

4) DNA was cleaned by P/C/I extraction (500µl P/C/I; see Appendix II) and upper phase collected.

5) DNA was precipitated overnight at -20°C with 10µl 5N NaCl and 1ml absolute ethanol.

6) Solution was centrifuged (16,000xg) and DNA pellet washed in 70% ethanol, and dissolved in 100-200µl TE.

ISHH techniques

Linearising vectors that generate riboprobes

To 10-20µg vector DNA, 10µl 10x CORE (see Appendix II for CORE recipe), 5µl 1 N NaCl, 5µl restriction endonucleases, was added and made up to 100µl with distilled H_2O, and placed at 37°C for 2 hours. Another 2µl of enzyme was added and incubated for another 2 hours at 37 °C.

5-10µl digested vector was run on a 0.8-1% ethidium bromide agarose gel to check the DNA had linearised. Remaining DNA was cleaned-up by P/C/I (200µl P/C/I; see Appendix II) and C/I (200µl; see Appendix II) extraction. DNA was reprecipitated overnight with 80µl 7.5N sodium acetate and 560µl absolute ethanol at -20°C. Following a 10-15 min spin the DNA pellet was washed in 70% ethanol, and resuspended in 21µl TE. 1µl was taken and DNA concentration calculated using an spectrophotometer (at a 260nm wavelength).

Ambion MAXIscript® transcription protocol.

Added to each 500ng of DNA starting template:

1) 1µl 10 x reaction buffer (from Ambion kit), 1.5µl 10mM ATP/CTP/GTP (0.5µl of each nucleotide; from Ambion kit), 2.5µl ^{35}S-UTP (PerkinElmer®, UK), 0.5µl SP6 or T7 (from Ambion kit), and incubated at 37°C for 30 min.

2) An additional 0.5µl SP6 or T7 and further incubated at 37°C for 30 min.

3) 0.5µl DNase (Ambion, UK) and 0.5µl RNasin (Promega, UK) and incubated at 37°C for 15 min.

4) Finally 190µl TE, pH 8, 2µl tRNA (Invitrogen, UK), 80µl 7.5N ammonium acetate and 700µl ethanol.

Emulsion dipping

Performed in a dark room:

1) A solution containing 30µl glycerol and 6ml distilled H_2O, was make up to 10ml with emulsion (Ilford K5, UK), and heated to 43-45°C to melt emulsion for 15-20 min. This was inverted and left for another 15-20 min.

2) Slides were dipped in emulsion, and left to dry for approximately 2 hours.

3) Once dry, slides were put into a slide holder with 1-2 sachets of silica gel, and sealed to prevent light penetration.

4) Slides were stored at 4°C until developing (slides stay in emulsion for 3 x the duration of film exposure).

5) To develop dipped slides were placed in a slide rack (still in dark room), and immersed in D19 developer (Sigma, UK) for 3.5 min, indicator stop (Sigma, UK) for 0.5 min, fixer (Sigma, UK) for 3.5 min and washed in H_2O for 5-30 min.

6) Slides were counterstained in 0.1-0.5% toluidine blue (dissolved in 70% ethanol/distilled H_2O) 20-30s, and rinsed in running H_2O and leave to air dry.

7) Slides were coverslipped with Cytoseal (Richard Allen Scientific, UK).

Cell culture techniques

Media Change

Media was removed by aspiration and cells washed with 1x PBS (approximately 5ml was used for a small petri dish, 1ml for each well of a 6 well plate, and 100µl for each well of a 96 well plate) for up to 5 mins, with occasional agitation of the plate. 1x PBS was discarded and fresh media replaced (approximately 10ml for a small petri dish, 2ml for each well of a 6 well plate, and 100-200µl for each well of a 96 well plate).

Passaging cells

For a small petri dish, media was removed by aspiration and washed with 5ml 1 x PBS. The PBS was aspirated and 2.5ml trypsin was applied and the plate incubated at 37°C/5% CO_2 until the cells no longer adhered to the plate (the cells looked rounded up under the microscope). 2.5ml of media was added to the plate to deactivate the trypsin. The cells were then split into a new plate or frozen down.

Freezing down cells

Following trypsinisation and the addition of media, cells were moved to a 15ml falcon tube and centrifuged (~2,500xg) for 5 min. The supernatant was aspirated and cells resuspended in 2-3ml freezing down media (Appendix II) and transferred to 2-3 Cryotube vials. Cryotube vials were immediately placed on ice and moved to -20°C freezer. After a couple of hours the vials were placed over night at -80°C and then transferred to liquid nitrogen stores for long-term storage.

Thawing cells from liquid nitrogen stocks

Cells were removed from liquid nitrogen stores and placed on dried ice for transportation. Cells were defrosted very quickly in 37°C water with constant agitation. Once thawed, cells were placed in a small petri dish with 10ml media and left O/N at 37°C/5% CO_2. Media was changed the following day to remove any residual DMSO.

Poly-l-lysine coating coverslips and plates

Poly-l-lysine coating greatly increases cell adherence and thereby reduces the amount of cells lost during processing. This is of particular use when dealing with cells that adhere less well to cell culture apparatus or during a procedure with multiple wash steps.

A working solution of 0.1mg/ml poly-l-lysine was made by dissolving 5mg of poly-l-lysine (Sigma, UK) into 50ml distilled H_2O or 1x PBS and stored at -20°C. The poly-l-lysine was defrosted in a 37°C water bath when required.

To poly-l-lysine coat coverslips: 2-3 coverslips were placed in a well of a 6 well plate. Enough poly-l-lysine solution was applied to each well until the cover slips were completely submerged and left for 30 min. The poly-l-lysine was removed and washed 5 x with 100µl 1x PBS for 10 min. For a 96 well plate 100µl of poly-l-lysine was applied to each well for 30 min. Again the poly-l-lysine was removed and washed 5 x with 100µl 1x PBS for 10 min. The poly-l-lysine can be re-frozen and thawed up to 6 times.

X-Gal staining for expression of LacZ in cultured cells

Control cells were transfected with a pSV mammalian vector (pSV-β-Galactosidase control vector; Promega, UK) containing the LacZ gene. LacZ encodes for the β-galactosidase (β-Gal) enzyme that catalyses the hydrolysis of β-galactosides. This assay relies on the cleavage of 5-bromo-4-chloro-3-indolyl-β-D-galactopyranoside (X-Gal) by β-Gal into galactose and 5-bromo-4-chloro-3-hydroxyindole. The latter is oxidised into 5,5'-di-bromo-4,4'-dichloro-indigo (the reaction is facilitated by ferric and ferrous ions), an insoluble dark blue product.

$$\text{Transfection efficiency} = \frac{\text{Amount of cells that express the dark blue product}}{\text{Total number of cells}} \times 100$$

The protocol below was used to test for β-gal activity (the volumes stated are for a 6 well plate, but when performed on a 96 well plate, the volumes were reduced approximately 1:10 e.g., 1ml → 100µl)

1) 24-48 hours after transfection media was removed from cells and washed with 1 x PBS for 5 min at room temperature.
2) Cells were fixed in 1ml 4% PFA in 1 x PFA for 15 min on ice.
3) 3 x washes with 2ml 1x PBS for 5 min at room temperature.
4) Cells were permeabilised in 1ml 0.1% TX-100 in 1 x PBS for 10 min at room temperature.
5) 3 x washes with 2ml 1x PBS for 5 min at room temperature.
6) Cells were incubated for 3-20 hours in the dark at 37°C in 1ml X-gal staining solution (see Appendix II) containing 1mg/ml X-gal.
7) Once the dark blue colour had sufficiently developed, cells were washed 3 times with 2ml 1 x PBS for 5 min at room temperature. Cells were left in 1ml 1 x PBS and viewed under a light microscope.

Northern Blot hybridization techniques

Roche Terminal Transferase tailing protocol.

The addition of nucleotides to the 3' terminus of DNA is catalysed by the DNA polymerase terminal deoxynucleotidyl transferase (TdT) - in this instance TdT catalyses the addition of α-^{32}P-ATP to the 3' end of an oligonucleotide.

Oligonucleotides were reconstituted with 100µl TE ph8.0 and diluted to form a 35µM solution. Added to each 3.5µM oligonucleotide (on ice) was 1µl 5x reaction buffer (Invitrogen, UK), 0.5µl α-^{32}P-ATP (PerkinElmer®, UK), 0.625µl TdT (Roche, UK) and made up to 2.375µl dH_2O (not DEPC treated), and incubated at 37°C for 15 mins.

Appendix II: Buffers and Solutions

Microbiological media

1 litre LB

10g Tryptone (Appleton Woods Ltd., UK), 5g Yeast extract (Appleton Woods Ltd., UK), 10g NaCl, made up to 1 litre with distilled H_2O, autoclaved and stored at 4°C. The correct antibiotics (50μg/ml AMP; or 30μg/ml kanamycin sulphate; or 34μg/ml chloraphenicol) are added prior to use.

1 litre LB/agar

10g Tryptone, 5g Yeast extract, 10g NaCl, 15g agar, made up to 1 litre with distilled H_2O and autoclaved. LB-agar was cooled following autoclaving and the correct antibody added (50μg/ml AMP; or 30μg/ml kanamycin sulphate; or 34μg/ml chloraphenicol). 50ml of LB-agar was added to a large Petri dish and left to set prior to storing at 4°C until use.

Antibiotics.

AMP was dissolved in distilled H_2O (concentration of 50mg/ml), divided into aliquots and kept at -80°C. When required, AMP was thawed on ice and added 1:1000 to LB or LB/agar.

Kanamycin sulphate was dissolved in distilled H_2O (concentration of 30mg/ml) divided into aliquots and kept at -80°C. When required, kanamycin sulphate was thawed on ice and added 1:1000 to LB or LB/agar.

Choloramphenicol was dissolved in ethanol at a concentration of 34mg/ml. When required, chloramphenicol was and dissolved 1:1000 in LB or LB/agar.

Molecular biology buffers and solutions

Tris- ethylenediaminetetraaceticacid (Tris-EDTA/TE)

500μl Tris-EDTA (100x pH 8, Sigma, UK) in 49.5ml distilled H_2O.

10x Core

500mM Tris, pH 7.6, 100mM $MgCl_2$, 500mM NaCl, 100μg/ml BSA (New England Biolabs, UK), 10mM DTT in distilled H_2O.

Phenol/chloroform/isoamyl alcohol (P/C/I)

25ml tris-saturated phenol, 23ml chloroform and 2ml isoamyl alcohol. 1x volume P/C/I was added to solution, vortexed and centrifuged (16,000xg) for 5 min. Upper phase containing DNA was collected.

Chloroform/isoamyl alcohol (C/I)

23ml chloroform and 2ml isoamyl alcohol. 1x volume C/I was added to solution, vortexed and centrifuged (16,000xg) for 5 min. Upper phase containing DNA was collected.

Lysozyme solution

5mg/ml lysozyme (Sigma, UK) in 25mM Tris-HCL, pH7.9, 10mM sodium-EDTA (pH adjusted to pH 7) and 9mg/ml glucose added.

Agarose gel

E.g., to make a 1% gel 1.2g of agarose was dissolved in 1x TAE (see below) to a total volume of 120µl. To dissolve the agarose, the solution was heated in a microwave on full power for 1-5 min with frequent agitation. Once cool 5µl 10mg/ml ethidium bromide was added to the gel, and the gel poured into a mould containing a 15 tooth comb, and allowed to set.

Ultra Pure™ agarose (Invitrogen, UK) was used to make an agarose gel, whereas low gel agarose (Severn Biotech Ltd, UK) was used to make a microsieve gel.

50x TAE buffer solution

484g Tris, 272g sodium acetate • $3H_2O$, 37g disodium EDTA, ~ 200ml glacial acetic acid (pH adjusted to 7.5-8.0), and made up to 2 litres with distilled H_2O.

Ethidium bromide

1g ethidium bromide (Sigma, UK) was dissolved in 100ml distilled H_2O (final concentration 10mg/ml). Stored at room temperature in a foil-covered bottle.

DNA markers

40µg HaeIII-ϕX digest (NEB, UK), 40µg λ-HindIII digest (NEB, UK), 100µl STOP-dye (lacking RNase A, see below), 780µl TE, pH7.6, heated at 60°C for 10-15 mins.

Restriction stop buffer

0.4% Bromophenol blue, 10% Ficoll 400, 0.2M EDTA (pH8.0), 100µl 10mg/ml RNase A, made up to 1ml with distilled H_2O.

ISHH buffers and solutions

DEPC-H_2O

4ml of DEPC (Sigma, UK) to 4 litres distilled H_2O. Incubated overnight at 37°C with occasional shaking. Autoclaved.

10x PBS

90g NaCl, 1.22 g potassium dihydrogen phosphate, 8.15g disodium hydrogen phosphate, made up to 1 litre with DEPC-H_2O. Diluted in DEPC H_2O 1:10 to acquire 1x PBS.

Ribonucleic acid solution

100µg/ml Sperm DNA (Sigma, UK); 250µg/ml Yeast total RNA (Sigma, UK); 250µg/ml Yeast tRNA (Invitrogen, UK) made up in DEPC-H_2O.

50ml Hybridisation buffer

23.8ml formamide *(50%)*; 0.95ml 1M Tris-HCL *(25mM)*, ph 7.5; 0.19ml 250mM EDTA *(1mM)*, pH 8.0; 3.75ml 4M NaCl *(100mM)*; 9.52ml dextran sulphate *(10%)* (Sigma, UK); 0.95ml 50x denhardts

solution[ψ] *(1x)*; 0.84ml DEPC-H_2O *(1.7%). Brackets indicate the percentage or concentration of reagent when made up to total volume of hybridisation solution.*

[ψ]50x Denhardt's solution

1g ficoll 400 (Sigma, UK), 1g polyvinylpyrrolidone-360 (Sigma, UK), 1g BSA (Sigma, UK), DEPC-H_2O up to 100ml.

RNase solution

50ml NaCl, 5ml Tris-HCl, pH 8.0, 0.25ml 500ml EDTA, pH 8.0 and 444.75ml DEPC-H_2O.

IHC/ immunocytochemistry buffers and solutions

10x PBS

Same recipe as 10x PBS in the ISHH buffers and solutions section, although made up with distilled H_2O (not DEPC treated).

4% PFA in 1x PBS

To make 100ml 4g PFA (Sigma, UK) was dissolved in 10ml 10x PBS and 80ml distilled H_2O (preheated to 58°C) by incubating at 58°C for about 30min. To ensure all of the PFA dissolved, the solution was placed on a stirrer and 1N sodium hydroxide was added dropwise until all PFA had dissolved. It was then made up to a total volume of 100ml with distilled H_2O and then pH was adjusted to approximately 7.4. It was then cooled to room temperature, filtered (to remove any polymers formed during heating) and stored at 4°C. 2% PFA in 1x PBS was make up with 2g PFA rather than 4g and made up to 100ml with 1x PBS (or dilute 4% PFA/1x PBS 1:2). If the PFA was intended for use during perfusion fixation, the PFA was made up fresh (could be used the next day providing it had been stored overnight at 4°C). For immunocytochemistry 10ml aliquots of 2%/4% PFA in 1x PBS were placed at -20°C and defrosted when required.

Cell culture media and solutions

Trypsin

10x Trypsin (Trypsin-EDTA solution; Sigma, UK) was stored at -20°C in 5ml aliquots. Aliquots were defrosted in a 37°C when required and diluted 1:10 in 1x PBS (5ml 10 x trypsin into 45ml 1x PBS).

Freezing down media

All cells apart from CHO-K1: 10% DMSO in DMEM, supplemented with 20% FCS, 500 units/ml Penicillin, 0.5mg/ml Streptomycin, and 2mM L-glutamate.

CHO-K1: 10% DMSO in αMEM, supplemented with 20% FCS, 500 units/ml Penicillin and 0.5mg/ml Streptomycin.

X-gal staining solution

5mM potassium ferrocyanide (Sigma, UK), 5mM potassium ferrocyanide (Sigma, UK), 2mM magnesium chloride hexahydrate (Sigma, UK), and 1mg/ml X-gal made up in 1x PBS.

0.25M calcium chloride dihydrate

2.5M $CaCl_2 \cdot 2H_2O$ stock and filtered through a 0.2μm filter. 2.5M $CaCl_2 \cdot 2H_2O$ stock was split into 5ml aliquots and stored at -20°C. Aliquots were defrosted at 37°C when required, and diluted 1:10 with sterile H_2O for 0.25M $CaCl_2 \cdot 2H_2O$ solution.

2x BES

2x BES: 50mM N,N-Bis(2-hydroxyethyl)-2-aminoethanesulfonic acid, N,N-Bis(2 hydroxyethyl) taurine (BES; Sigma, UK), 280mM NaCl, 1.5mM Na_2HPO_4.

1.07 g BES, 1.6g NaCl and 0.0213g Na_2HPO_4 was dissolved in a total volume of 90ml H_2O. pH was adjusted to 6.96 with HCl and volume made up to 100ml with distilled H_2O. Solution was sterilised through a 0.2μm filter and stored in 5ml aliquots at -20°C.

Physiological salt solution (PSS) for calcium imaging

For 1 litre of PSS: 127nM NaCl, 0.5mM $NaH_2PO_4 \cdot H_2O$, 1.8mM $CaCl_2 \cdot 2H_2O$, 2mM $MgCl_2$, 5mM KCl_2, 5mM $NaHCO_3$, 10mM Hepes in dH_2O (not quite 1 litre-allow for displacement by BSA and glucose) and pH adjusted to 7.4. An additional 0.1% BSA and 10mM glucose was added (and more dH_2O to 1 litre if needed). PSS was sterile-filtered with a 0.45μm filter in a cell culture hood. 50ml aliquots were frozen immediately at -20°C. On day of use PSS was defrosted at 37°C.

Northern blot buffers and solutions

50ml Pre/hybridisation buffer

10ml 20x SSPE, 5ml 50x Denhardt's, 2.5ml ssDNA (10mg/ml), 500μl yeast tRNA (25mg/ml), 500μl 10% SDS, 25ml formamide, and 6.5ml DEPC-H_2O.

Appendix III: Supplementary data

Expression level	Signal transduction components in the PVN	Expression level	Signal transduction components in the PVN
2806	Calmodulin 2	226.7	Protein kinase C, zeta
2731	Calmodulin 1	221.8	Guanine nucleotide binding protein 12
2265	Dynamin 1	203.6	Mitogen activated protein kinase 3 (Mapk3)
1745	Clathrin, heavy polypeptide	197.5	Adenylate cyclase 5
1447	Guanine nucleotide binding protein, beta 2-like 1 (Gnb2l1)	188.2	Adenylate cyclase 6
1277	Protein kinase, cAMP dependant regulatory, type 1, alpha	162.6	Guanine nucleotide binding protein, alpha z (Gnaz)
1235	Clathrin, light polypeptide	161.2	Mitogen activated protein kinase kinase 5 (Map2k5)
1071	Calmodulin 3	150.1	Regulator of G protein signalling 19
1045	Guanine nucleotide binding protein, beta 1 (Gnb1)	141	Dynamin 3
794	Mitogen activated protein kinase kinase 1 (Map2k1)	134.7	G protein-coupled receptor kinase 6
794	Guanine nucleotide binding protein, gamma 10 (Gng10)	127.5	Phospholipase C, delta 4
734.2	Protein kinase C, beta 1	118	Regulator of G protein signalling 2
679.1	Guanine nucleotide binding protein, alpha 12 (Gna12)	116	MAP kinase-activated protein kinase 2 (Mapkapk2)
616.4	Regulator of G protein signalling 4	111.9	Protein kinase, cAMP-dependent, regulatory, type 2, alpha
613.2	Guanine nucleotide binding protein, beta 5 (Gnb5)	105.5	Arrestin, beta 2
530.4	Calcium/calmodulin-dependent protein kinase II, delta	103.3	Protein kinase C, gamma
494.5	Calcium/calmodulin-dependent protein kinase II, beta	102.2	Guanine nucleotide binding protein, alpha 11 (Gna11)
471.8	Regulator of G protein signalling 2	102.2	Regulator of G protein signalling 9
454	Phospholipase A2, gamma	90.1	Phospholipase D2
430.3	Adenylate cyclase 2	81.02	Guanine nucleotide binding protein, beta 4 (Gnb4)
406.6	Guanine nucleotide binding protein, beta 2 (Gnb2)	79.78	Regulator of G protein signalling 5
400.8	Calcium/calmodulin-dependent protein kinase II, gamma	77.96	Mitogen activated protein kinase 12 (Mapk12)
396.7	Protein kinase C, lambda	75.9	Regulator of G protein signalling 12
387	Protein kinase C, epsilon	70.46	Guanine nucleotide binding protein, gamma 11 (Gng11)
386.1	Mitogen activated protein kinase kinase 2 (Map2k2)	67.14	Phospholipase C, delta 1
382.4	Phospholipase C, gamma 1	65.22	Protein kinase C, delta
381.3	Regulator of G protein signalling 7	63.5	Calcium/calmodulin-dependent serine protein kinase
367.8	Guanine nucleotide binding protein, alpha o (Gnao)	62.06	Phospholipase D1
367.6	Phospholipase C, beta 4	60.54	Guanine nucleotide binding protein, gamma 12 (Gng12)
350.1	Mitogen activated protein kinase kinase kinase 12 (Map3k12)	50.62	Guanine nucleotide binding protein, beta 3 (Gnb3)
330.4	Regulator of G protein signalling 17	41.7	Phospholipase A2, group IVA (cytosolic, calcium-dependent)
307.8	Mitogen activated protein kinase 10 (Mapk10)	41.4	Calcium/calmodulin-dependent protein kinase kinase 2,beta
282.5	G protein-coupled receptor kinase 5	40.6	Phospholipase A2, group VI
264.3	Regulator of G protein signalling 10	38.24*	* Regulator of G protein signalling 14
261.7	Mitogen activated protein kinase 6 (Mapk6)	34.06	Regulator of G protein signalling 8
257.7	Calcium/calmodulin-dependent protein kinase II, alpha	32.08	Protein kinase C, eta
251.6	Mitogen activated protein kinase 14 (Mapk14)	27.2	Protein kinase C, alpha
235.3	Adenylate cyclase 3	23.24	Phospholipase C, epsilon 1
230.2	Mitogen activated protein kinase 1 (Mapk1)	21.38	Regulator of G protein signalling 3

Supplementary Table 1. GPCR signal transduction components detected in the PVN by DNA microarrays Comparative levels (arbitary units) of genes listed as present in the PVN on Affymetrix 230 2.0 rat genome chips as in [115]. The chips contain 31,099 individual probe sets covering about 30,000 transcripts encoded by 28,000 genes. Selected intracellular signalling component transcripts on the DNA microarray were isolated using specific wildcard operator terms such as 'calmodulin', 'protein kinase', 'guanine nucleotide', 'phospholipase', 'G protein' and 'adenylate cyclase'. The list is not a comprehensive coverage of all signalling molecule transcripts in the PVN - many kinases and potential splice variants, for example, have not been included. Apart from differences in relative gene expression levels, all genes in the PVN are present in the SON except RGS14 (asterisk). Signalling molecule data sets such as those presented here can be searched in general gene/protein databases such as the National Center for Biotechnology Information (NCBI - http://www.ncbi.nlm.nih.gov/) and the European Bioinformatics Institute (http://www.ebi.ac.uk/), and/or some specific online databases (e.g., http://www.afcs.org/; http://www.signaling-gateway.org/; http://dip.doe-mbi.ucla.edu/dip/Main.cgi) that provide resources for the analysis of core signalling components and signalling clusters, including the importance of individual components such as calcium and cAMP. There are also a number of useful Web resources that deal with various aspects of cell signalling listed at http://www.cellsignal.com/reference/webResources.html.

Expression level	Signal transduction components in the SON	Expression level	Signal transduction components in the SON
2652	Calmodulin 2	196.9	Adenylate cyclase 6
2545	Calmodulin 1	188.4	Adenylate cyclase 3
1879	Clathrin, heavy polypeptide	187.6	Protein kinase C, zeta
1779	Dynamin 1	186.5	Mitogen activated protein kinase 3 (Mapk3)
1759	Guanine nucleotide binding protein, beta 2-like 1 (Gnb2l1)	183.5	Regulator of G protein signalling 17
1427	Protein kinase C, beta 1	163.3	Dynamin 3
1220	Clathrin, light polypeptide	145.4	MAP kinase-activated protein kinase 2 (Mapkap2)
1164	Protein kinase, cAMP dependent regulatory, type I, alpha	138.1	Protein kinase C, delta
922.6	Guanine nucleotide binding protein, beta 1 (Gnb1)	137.7	Mitogen activated protein kinase kinase 5 (Map2k5)
832.3	Calmodulin 3	132.2	Phospholipase C, delta 4
807.9	Guanine nucleotide binding protein, gamma 10 (Gng10)	105.1	Regulator of G protein signalling 2
771.1	Calcium/calmodulin-dependent protein kinase II, gamma	104.1	G protein- coupled receptor kinase 6
767.3	Guanine nucleotide binding protein, alpha 12 (Gna12)	101.3	Regulator of G protein signalling 5
691.6	Mitogen activated protein kinase kinase 1 (Map2k1)	100.9	Guanine nucleotide binding protein, alpha 11 (Gna11)
588.5	Regulator of G protein signalling 4	98.74	Guanine nucleotide binding protein, alpha z (Gnaz)
523.5	Guanine nucleotide binding protein, gamma 11 (Gng11)	97.54	Regulator of G protein signalling 9
499.8	Guanine nucleotide binding protein, beta 5 (Gnb5)	97.28	Phospholipase D2
488.4	Calcium/calmodulin-dependent protein kinase II, delta	94.14	Guanine nucleotide binding protein, beta 4 (Gnb4)
423.6	Adenylate cyclase 2	93.24	Calcium/calmodulin-dependent protein kinase II, alpha
410.4	Phospholipase A2, gamma	91.5	Phospholipase D1
386.1	Phospholipase C, gamma 1	83.12	Arrestin, beta 2
382.7	Phospholipase C, beta 4	82.4	Regulator of G protein signalling 12
380.6	Protein kinase C, lambda	82.36	Guanine nucleotide binding protein, gamma 12 (Gng12)
379.3	Guanine nucleotide binding protein, beta 2 (Gnb2)	82.18	Regulator of G protein signalling 4
364.9	Mitogen activated protein kinase kinase 2 (Map2k2)	79.5	Phospholipase C, delta 1
332.9	Regulator of G protein signalling 2	74.12	Mitogen activated protein kinase 12 (Mapk12)
299.8	Calcium/calmodulin-dependent protein kinase II, beta	72.18	Phospholipase A2, group IVA (cytosolic, calcium-dependent)
293.8	Mitogen activated protein kinase kinase kinase 12 (Map3k12)	64.34	Regulator of G protein signalling 19
290.5	Regulator of G protein signalling 7	61.42	Protein kinase C, gamma
281.5	Guanine nucleotide binding protein, alpha o (Gnao)	60.08	Calcium/calmodulin-dependent serine protein kinase
271	Regulator of G protein signalling 10	58.16	Phospholipase C, delta 4
267.5	Protein kinase C, epsilon	54.46	Guanine nucleotide binding protein, beta 3 (Gnb3)
245.1	Mitogen activated protein kinase 10 (Mapk10)	46.92	Protein kinase C, eta
238	Guanine nucleotide binding protein, beta 12 (Gnb12)	44.9	Phospholipase A2, group VI
224.3	G protein-coupled receptor kinase 5	40.36	Calcium/calmodulin-dependent protein kinase kinase 2, beta
209.2	Mitogen activated protein kinase 1 (Mapk1)	34.64	Protein kinase C, alpha
208.4	Mitogen activated protein kinase 14 (Mapk14)	30.72*	* Adenylate cyclase 4
202.8	Adenylate cyclase 5	29.6	Protein kinase, cAMP-dependent, regulatory, type 2, alpha
199.3	Mitogen activated protein kinase 6 (Mapk6)	25.68	Regulator of G protein signalling 3

Supplementary Table 2. GPCR signal transduction components detected in the SON by DNA microarrays

Comparative levels (arbitary units) of genes listed as present in the SON on Affymetrix 230 2.0 rat genome chips as in [115]. The intracellular signalling component transcripts were isolated as in Table 1. All gene transcripts in the SON are present in the PVN except Adenylate cyclase 4 (asterisk).

GPCR Family	GPCR receptor	Region	Reference
5-Hydroxytryptamine	5-HT_{1A} and 5-HT_2 (subtype unknown)	PVN	[281,8,181]
"	5-HT_7	PVN*	[101]
Acetylcholine muscarinic	subtype unknown	PVN and SON	[153]
Adrenoceptor	$\alpha_{1/2}$ (subtype unknown)	pPVN	[56]
"	α_2 (subtype unknown)	PVN and SON	[133]
"	β_2	SON	[164]
Angiotensin	AT_1	PVN and SON	[279]
Apelin	APJ	PVN and SON	G. Pope and A-M. O'Carroll unpublished data
Bombesin	BB_2	PVN and SON	[163]
Calcitonin	CT	PVN	[114]
Cannabinoid	CB_1	PVN and SON	[111]
Cholecystokinin	CCK_1 and CCK_2	PVN and SON**	[116]
Corticotropin-releasing factor	subtype unknown	PVN	[63]
Endothelin	subtype unknown	PVN and SON	[155]
$GABA_B$	$GABA_{B1}$ or subtype unknown	PVN and SON	[24]
Galanin	subtype unknown	PVN and SON	[35]
Ghrelin	Ghrelin	PVN	[104]
Glucagon	GLP-1	PVN	[94]
Histamine	H_1	PVN and SON	[184]
"	H_3	PVN and SON	[249]
Melanocortin	subtype unknown	PVN and SON	[300,183]
Neuropeptide FF/AF	NPFF1	PVN	[96]
Neuropeptide Y	Y_1 or unknown subtype	PVN and SON	[70,194]
"	Y_2	PVN and SON	[81]
"	Y_4	pPVN	[81]
Neurotensin	subtype unknown	PVN	[226]
Opioid	κ	PVN and SON	[201]
"	NOP	PVN and SON	[223]
Relaxin	RXFP3	PVN and SON	[296]
Somatostatin	subtype unknown	pPVN and SON	[176]
Tachykinin	NK_1	PVN and SON	[258]
"	NK_3	PVN and SON	[258,72]
VIP and PACAP	$VPAC_1$	PVN and SON	[311,205]
"	subtype unknown	SON	[208]

Supplementary Table 3. GPCRs detected in the rat PVN and SON by receptor ARG

For receptor ARG, typically 8-30μm sections from frozen adult male rat brain are incubated with [^{3}H]- or [^{125}I]-labelled GPCR ligands (with/without enzyme inhibitors to reduce protelolytic degradation of radiolabeled peptides), washed in cold buffer, and exposed to X-ray film for weeks-months depending on factors such as GPCR abundance, ligand specific activity and signal-noise ratios. pPVN, parvocellular region of the paraventricular nucleus; * receptor subtype discriminated by presence after displacement with other 5-HT ligands; ** receptors discriminated by displacement with CCK_1 or CCK_2 ligands.

GPCR	PVN				SON			
	IHC	ISHH	Arrays	Reference	IHC	ISHH	Arrays	Reference
5-Hydroxytryptamine								
5-HT_{1A}[iii]	✓	✓	-	[339,327]	-	✓	-	[327]
5-HT_{1B}[iii]	✓	-	-	[198,262]	✓	-	-	[198]
5-HT_{1D}	-	-	-		-	-	-	
5-HT_{1e}	-	-	-		-	-	-	
5-HT_{1F}	-	-	-		-	-	-	
5-HT_{2A}[i]	✓	-	-	[339,337]	-	-	-	
5-HT_{2B}	-	-	-		-	-	-	
5-HT_{2C}[i]	-	✓	-	[110]	-	✓	-	[221]
5-HT_4	-	-	-		-	-	-	
5-HT_{5a}	-	-	-		-	-	-	
5-HT_{5b}								
5-HT_6	-	-	-		-	-	-	
5-HT_7[ii]	-	-	✓	[115]	-	-	✓	[115]
Acetylcholine (muscarinic)								
M_1[i]	-	-	-		-	-	-	
M_2[iii]	-	-	-		-	-	-	
M_3[i]	-	-	✓	[115]	-	-	-	
M_4	-	-	-		-	-	-	
M_5	-	-	-		-	-	-	
Adenosine								
A_1[iii]	✓	-	✓	[179,115]	✓	-	✓	[259,115]
A_{2A}[ii]	✓	-	-	[263]	✓	-	-	[263]
A_{2B}[ii]	-	-	✓	[115]	-	-	✓	[115]
A_3[iii]	-	-	✓	[115]	-	-	-	
Adrenoceptors								
α_{1A}-adrenoceptor[i]	-	✓	-	[68]	-	✓	-	[68]
α_{1B}-adrenoceptor[i]	✓	✓	✓	[321,59,115]	-	-	✓	[115]
α_{1D}-adrenoceptor[i]	-	✓	-	[275]	-	-	-	
α_{2A}-adrenoceptor[iii]	✓	-	-	[7]	✓	-	-	[7]
α_{2B}-adrenoceptor	-	-	-		-	-	-	
α_{2C}-adrenoceptor	-	-	-		-	-	-	
β_1-adrenoceptor	-	-	-		-	-	-	
β_2-adrenoceptor[ii]	-	-	-		-	-	✓	[115]
β_3-adrenoceptor	-	-	-		-	-	-	
Anaphylatoxin								
C3a	-	-	-		-	-	-	
C5a[iii]	-	-	-		-	-	-	
C5L2	-	-	-		-	-	-	
Angiotensin								
AT_{1A}[i,iii]	✓	✓	✓	[248,319,279,115]	✓	-	-	[248]
AT_{1B}	-	-	-		-	-	-	
AT_2[iii]	✓	-	-	[10]	✓	-	-	[10]
Apelin								
APJ[iii]	✓	✓	-	[216,233]	✓	✓	-	[302,233]
Bile Acid								
GPBA	-	-	-		-	-	-	
Bombesin								
BB_1	-	-	-		-	-	-	
BB_2[i]	-	✓	-	[313]	-	✓	-	[313]
BB_3[i]	✓	-	-	[130]	✓	-	-	[130]
Bradykinin								
B_1	-	-	-		-	-	-	
B_2[i,ii,iii]	✓	-	-	[253]	✓	-	-	[253]
Calcitonin								
CT[i]	✓	✓	✓	[22,280,115]	✓	-	✓	[22,115]
AMY_1	-	-	-		-	-	-	
AMY_2	-	-	-		-	-	-	
AMY_3	-	-	-		-	-	-	
Calcitonin receptor-like	-	-	✓	[115]	-	-	✓	[115]
CGRP	-	-	-		-	-	-	
AM_1	-	-	-		-	-	-	
AM_2	-	-	-		-	-	-	
Calcium-sensing								
CaS[i]	✓	✓	-	[220,260]	-	✓	-	[220,260]
$GPRC_6$	-	-	-		-	-	-	
Cannabinoid								
CB_1[iii]	✓	✓	✓	[39,209,115]	-	-	✓	[115]
CB_2	-	-	-		-	-	-	

Supplementary Table 4. GPCRs in the paraventricular nucleus (PVN) and supraoptic nucleus (SON) of the rat hypothalamus: a summary of the literature (page 1 of 5).

GPCR	PVN				SON			
	IHC	ISHH	Arrays	Reference	IHC	ISHH	Arrays	Reference
Chemokine								
CCR1	-	-	-		-	-	-	
CCR2[iii]	✓	-	-	[15]	✓	-	-	[15]
CCR3	-	-	-		-	-	-	
CCR4	-	-	-		-	-	-	
CCR5	-	-	-		-	-	-	
CCR6	-	-	-		-	-	-	
CCR7	-	-	-		-	-	-	
CCR8	-	-	-		-	-	-	
CCR9	-	-	-		-	-	-	
CCR10	-	-	-		-	-	-	
CXCR1	-	-	-		-	-	-	
CXCR2	-	-	-		-	-	-	
CXCR3[iii]	-	-	✓	[115]	-	-	✓	[115]
CXCR4[iii]	✓	-	✓	[36,115]	✓	-	✓	[36,115]
CXCR5	-	-	-		-	-	-	
CXCR6	-	-	-		-	-	-	
CXCR7	-	-	✓		-	-	✓	
CX_3CR1[iii]	✓	-	-	S.T. Yao *et al.*, unpublished data	-	-	-	
XCR1	-	-	-		-	-	-	
Cholecystokinin								
CCK_1[i]	-	✓	✓	[117,115]	-	✓	-	[116]
CCK_2[i]	-	✓	-	[117,217]	-	✓	-	[116,217]
Corticotropin-releasing factor								
CRF_1[ii]	✓	✓	-	[127,310]	-	✓	-	[310]
CRF_2[ii]	-	✓	-	[310]	-	✓	-	[310]
Dopamine								
D_1[ii]	✓	✓	-	[57,320,83]	-	✓	-	[83]
D_2[iii]	-	✓	-	[320]	-	-	-	
D_3	-	✓	-	[30]	-	-	-	
D_4[iii]	✓	-	-	[61]	✓	-	-	[61]
D_5	-	-	-		✓	-	-	[147]
Endothelin								
ET_A[i]	✓	-	✓	[161,115]	✓	-	✓	[161,115]
ET_B[i,ii,iii]	-	-	✓	[115]	-	-	✓	[115]
E2								
GPER[i,ii]	✓	✓	-	[31,108]	✓	✓	-	[31,108]
Formylpeptide								
FPR1	-	-	-		-	-	-	
FPR2/ALX	-	-	-		-	-	-	
FPR3	-	-	-		-	-	-	
Free fatty acid								
FFA1 (GPR40)	-	-	-		-	-	-	
FFA2	-	-	-		-	-	-	
FFA3	-	-	-		-	-	-	
Frizzled								
FZD_1[i,iii]	-	-	✓	[115]	-	-	✓	[115]
FZD_2[iii]	-	-	✓	[115]	-	-	-	
FZD_3	-	-	-		-	-	-	
FZD_4	-	-	-		-	-	-	
FZD_5	-	-	-		-	-	-	
FZD_6	-	-	-		-	-	-	
FZD_8	-	-	-		-	-	-	
FZD_9	-	-	-		-	-	-	
SMO	-	-	-		-	-	-	
$GABA_B$								
$GABA_{B1}$	✓	✓	✓	[203,257,24,115]	✓	✓	✓	[203,257,24,115]
$GABA_{B2}$	✓	✓	-	[257,71]	✓	✓	✓	[257,71]
GABAB[iii]	-	-	-		-	-	-	
Galanin								
GAL_1[iii]	-	✓	-	[100]	-	✓	-	[100]
GAL_2[i,iii]	-	✓	✓	[100,62,115]	-	✓	✓	[62,115]
GAL_3[iii]	-	✓	-	[218]	-	-	-	
Ghrelin								
ghrelin[i]	-	✓	-	[345]	-	✓	-	[99]
Glucagon								
GHRH	-	-	-		-	-	-	
GIP	-	-	-		-	-	-	
GLP-1[ii]	-	✓	-	[219]	-	✓	-	[219]
GLP-2	-	-	-		-	-	-	
glucagon	-	-	-		-	-	-	
secretin[ii]	✓	✓	-	[47]	✓	✓	-	[47]
Glycoprotein hormone								

GPCR	PVN				SON			
	IHC	ISHH	Arrays	Reference	IHC	ISHH	Arrays	Reference
FSH	-	-	-		-	-	-	
LH	-	-	-		-	-	-	
TSH	-	-	-		-	-	-	
Gonadotrophin-releasing hormone								
GnRH	-	-	-		-	-	-	
Histamine								
H_1[i]	-	✓	-	[184]	-	✓	-	[184]
H_2[i]	-	-	-		-	-	-	
H_3[iii]	-	✓	✓	[249,115]	-	✓	-	[249]
H_4	-	-	-		-	-	-	
Hydroxycarboxylic acid								
HCA_1	-	-	-		-	-	-	
HCA_2	-	-	-		-	-	-	
Kisspeptin								
kisspeptin	-	-	-		-	-	-	
Leukotriene								
BLT_1	-	-	-		-	-	-	
BLT_2	-	-	-		-	-	-	
$CysLT_1$	-	-	-		-	-	-	
$CysLT_2$	-	-	-		-	-	-	
FPR2/ALX	-	-	-		-	-	-	
Lysophospholipid								
LPA_1[i,iii]	-	-	✓	[115]	-	-	✓	[115]
LPA_2	-	-	-		-	-	-	
LPA_3	-	-	-		-	-	-	
LPA_4								
LPA_5								
S_1P_1[i,iii]	-	-	✓	[115]	-	-	✓	[115]
S_1P_2	-	-	-		-	-	-	
S_1P_3	-	-	-		-	-	-	
S_1P_4	-	-	-		-	-	-	
S_1P_5	-	-	-		-	-	-	
Melanin-concentrating hormone								
MCH_1[i,ii,iii]	✓	✓	-	[112]	✓	✓	-	[112]
Melanocortin								
MC_1	-	-	-		-	-	-	
MC_2	-	-	-		-	-	-	
MC_3	-	-	-		-	-	-	
MC_4[ii]	-	✓	-	[151]	-	✓	-	[151]
MC_5	-	-	-		-	-	-	
Melatonin								
MT_1[iii]	-	-	-		-	-	-	
MT_2	-	-	-		-	-	-	
Metabotropic glutamate								
$mGlu_1$[i]	✓	✓	✓	[154,284,115]	✓	✓	✓	[154,284,6,115]
$mGlu_2$	-	-	-		-	-	-	
$mGlu_3$[iii]	-	✓	✓	[235,115]	-	✓	✓	[6,235,115]
$mGlu_4$[iii]	-	-	✓	[115]	-	-	✓	[115]
$mGlu_5$[i]	✓	✓	-	[74]	-	-	-	
$mGlu_6$	-	-	-		-	-	-	
$mGlu_7$[iii]	✓	✓	✓	[149,150,115]	✓	✓	✓	[149,150,115]
$mGlu_8$[iii]	-	-	✓	[115]	-	-	-	
Motilin								
motilin[i]	-	-	-		-	-	-	
Neuromedin U								
NMU1	-	-	-		-	-	-	
NMU2[i]	-	✓	-	[98]	-	✓	-	[98]
Neuropeptide FF/Neuropeptide AF								
NPFF1[iii]	-	✓	-	[185]	-	-	-	
NPFF2	-	-	-		-	-	-	
Neuropeptide S								
NPS[i,ii]	✓	✓	-	[175,329]	✓	-	-	[329]
Neuropeptide W/neuropeptide B								
NPBW1[iii]	-	✓	-	[171]	-	✓	-	[171]
Neuropeptide Y								
Y_1[iii]	✓	✓	-	[307,323,245]	✓	✓	-	[307,323,245]
Y_2[iii]	-	✓	-	[323]	-	✓	-	[323]
Y_4[iii]	-	✓	-	[323]	-	✓	-	[245]
Y_5[iii]	✓	✓	✓	[323,245,81,115]	✓	✓	✓	[245,81,115]

GPCR	PVN				SON			
	IHC	ISHH	Arrays	Reference	IHC	ISHH	Arrays	Reference
Neurotensin								
NTS_1[i]	-	✓	-	[3]	✓	✓	-	[3,75]
NTS_2[i]	-	-	✓	[115]	-	-	✓	[115]
Opioid								
δ[iii]	-	✓	-	[200]	-	✓	-	[200]
κ[iii]	✓	✓	✓	[11,88,115]	✓	✓	✓	[11,88,115]
μ[iii]	✓	✓	-	[200,199]	✓	✓	-	[88,199]
NOP[iii]	-	✓	✓	[223,115]	-	✓	✓	[223,115]
Orexin								
OX_1[i,iii]	✓	-	-	[113]	✓	✓	-	[113,202]
OX_2[i]	✓	✓	✓	[113,50,303,115]	✓	✓	-	[50,202]
P2Y								
$P2Y_1$[i]	✓	-	-	[289]	✓	-	-	[289]
$P2Y_2$	-	-	-		-	-	-	
$P2Y_4$	-	-	-		-	-	-	
$P2Y_6$	-	-	-		-	-	-	
$P2Y_{12}$[iii]	-	-	-		-	-	✓	[115]
$P2Y_{13}$[iii]	-	-	✓	[115]	-	-	✓	[115]
$P2Y_{14}$	-	-	-		-	-	-	
Parathyroid hormone								
PTH1[ii]	-	✓	✓	[318,115]	-	✓	✓	[318,115]
PTH2[ii]	✓	✓	-	[314]	✓	-	-	[314]
Peptide P518								
QRFP1[i,iii]	-	✓	-	[84]	-	-	-	
QRFP2[i]	-	✓	-	[141]	-	-	-	
Platelet-activating factor								
PAF[i]	-	-	-		-	-	-	
Prokineticin								
PKR_1	-	-	-		-	-	-	
PKR_2[i,iii]	-	✓	-	[45,224]	-	-	-	
Prolactin-releasing peptide								
PRRP[i]	-	✓	-	[261]	-	-	-	
Prostanoid								
DP_1	-	-	-		-	-	-	
DP_2	-	-	-		-	-	-	
EP_1[i]	✓	✓	-	[212,236]	-	-	-	
EP_2	-	-	-		-	-	-	
EP_3[iii]	✓	-	-	[222]	-	-	-	
EP_4[ii]	-	✓	-	[236,340]	-	✓	-	[340]
FP	-	-	-		-	-	-	
IP_1	-	-	-		-	-	-	
TP	-	-	-		-	-	-	
Protease-activated								
PAR1[i,iii]	-	-	✓	[115]	-	-	✓	[115]
PAR2	-	-	-		-	-	-	
PAR3	-	-	-		-	-	-	
PAR4	-	-	-		-	-	-	
Relaxin family peptide								
RXFP1[ii,iii]	-	✓	-	[195]	-	✓	-	[195]
RXFP2	-	-	-		-	-	-	
RXFP3[iii]	-	✓	-	[296]	-	✓	-	[296]
Somatostatin								
sst_1[iii]	✓	✓	-	[160,21]	-	-	✓	[115]
sst_2[iii]	✓	✓	✓	[160,21,115]	-	-	-	
sst_3[iii]	✓	-	✓	[160,115]	-	-	✓	[115]
sst_4[iii]	✓	-	-	[160]	-	-	-	
sst_5	-	-	-		-	-	-	
Tachykinin								
NK_1[i]	-	✓	✓	[197,115]	-	-	✓	[115]
NK_2	-	-	-		-	-	-	
NK_3[i]	✓	✓	-	[67,102,72]	✓	✓	✓	[67,102,72,115]
Thyrotropin-releasing hormone								
TRH_1[i]	-	✓	✓	[234,115]	-	-	✓	[115]
TRH_2[i]	-	✓	-	[234]	-	-	-	
Trace amine								
TA_1[ii]	-	-	-		-	-	-	
Urotensin								
UT[i]	-	✓	-	[129]	-	✓	-	[129]
VIP and PACAP								
PAC_1[ii]	✓	✓	-	[136,229]	✓	✓	-	[136,229]
$VPAC_1$[ii]	✓	-	-	[136]	✓	-	-	[136]
$VPAC_2$[ii]	✓	✓	-	[136,192]	✓	✓	-	[136,192]

GPCR	PVN				SON			
	IHC	ISHH	Arrays	Reference	IHC	ISHH	Arrays	Reference
Vasopressin and oxytocin								
V_{1A}^{i}	✓	✓	-	[122,121]	✓	✓	-	[122,121]
V_{1B}^{i}	✓	✓	-	[122,121]	✓	✓	-	[122,121]
V_2	-	-	-		-	-	-	
OT^{i}	✓	✓	-	[204,214]	✓	✓	-	[204,214]

Supplementary Table 4. GPCRs in the paraventricular nucleus (PVN) and supraoptic nucleus (SON) of the rat hypothalamus: a summary of the literature

Detection of GPCR expression by immunohistochemistry (IHC), *in situ* hybridisation histochemistry (ISHH) and DNA microarrays (arrays). Receptor nomenclature is based on the official family receptor names given in the on-line IUPHAR Database of Receptors and Ion Channels (www.iuphar-db.org/) excluding chemosensory GPCRs (e.g., olfactory, vomeronasal and taste receptors), and only includes receptors known to be in the rat genome. For some GPCR sub-families, e.g., calcitonin, pharmacological responses are dictated by additional proteins (e.g., RAMPS: receptor activity-modifying proteins), whereas in others e.g., $GABA_B$, heterodimerization of two GPCR subunits is required for a functional response. In some instances only functional GPCRs have been documented (see Supplementary Table 9) – examples of these include responses to anaphylatoxins (C5a), formyl peptides, kisspetin, leukotrienes, platelet-activating factor and trace amines in the PVN, and responses to melatonin and motilin in both the PVN and SON. For the GPCRs expressed (or where functional responses of known or unknown subtypes are indicated), the major Gα protein involved in signal transduction (as per www.iuphar-db.org/) is provided: i, coupled to the $G_{q/11}$: downstream signal increases intracellular Ca^{2+} and stimulates phosphatidyl inositol phosphorylation (also activates phospholipase C, and sometimes phospholipase A_2 and D); ii, coupled to G_s: downstream signal increases cAMP; iii, coupled to $G_{i/o}$: downstream signal decreases cAMP. (✓) indicates the presence of either receptor mRNA or protein in the PVN or SON, and (-) denotes either an absence of mRNA or protein in the PVN or SON, or a localisation study for that GPCR has not been undertaken or reported to our knowledge. Known or possible splice variants for the rat GPCRs have not been indicated but for some GPCRs (e.g., metabotropic glutamate $mGlu_1$ receptors [228]) splice variants have been detected in the PVN and SON.

Expression level	PVN GPCRs	Expression Level	PVN GPCRs
1,270	$GABA_{B1}$* (1f)^{SON}	79.74	***GPR83***^{SON}
1,197	NTS_2 neurotensin^{SON}	79.05	***GPR123***^{SON}
1,046	$GABA_{B1}$* (1j)^{SON}	77.38	FZD_2 frizzled
900	ET_B endothelin ^{SON}	76.42	CXCR7^{SON}
853	S_1P_1 lysophospholipid^{SON}	75.98	NK_1 tachykinin^{SON}
830.6	$GABA_{B2}$^{SON}	71.42	$GABA_{B1}$* (1a)
703.1	***GPR37-like1***^{SON}	69.52	OX_2 orexin
596.2	***GPRC5b****^{SON}	68.82	CCK_1 cholecystokinin
504.3	***GPRC5b****^{SON}	62.44	***GPR149***^{SON}
428.2	***GPR56***^{SON}	61.88	***GPR34***^{SON}
390.9	CB_1 cannabinoid^{SON}	60.14	M_3 muscarinic
378.8	$mGlu_1$ metabotropic glutamate^{SON}	60.08	SST_2 somatostatin
375.5	***GPR37***^{SON}	59.86	5-HT_7 serotonin^{SON}
362.8	***GPR158***^{SON}	58.26	FZD_1 frizzled^{SON}
355.8	***GPR162***^{SON}	58.06	AT_1 angiotensin II
351.3	PAR1 protease-activated^{SON}	53.94	SST_3 somatostatin^{SON}
286.2	CT calcitonin^{SON}	50.62	GAL_2 galanin*
228.7	LPA_1 lysophospholipid^{SON}	49.44	$mGlu_4$ metabotropic glutamate^{SON}
190.6	***GPR48***^{SON}	49.38	Y_5 neuropeptide Y^{SON}
179.3	H_3 histamine	42.74	CXCR4 chemokine*^{SON}
156.5	***GPR123***^{SON}	40.7	***GPR116****^{SON}
152.3	***GPR98***^{SON}	40.62	$mGlu_8$ metabotropic glutamate*
148.8	TRH_1 thyrotrophin releasing factor^{SON}	39.96	***P2Y5***^{SON}
136.9	***GPR85***^{SON}	36.94	***GPR125***
129.6	Calcitonin receptor-like^{SON}	34.58	GAL_2 galanin*
128.8	κ opioid*^{SON}	33.78	***GPR88***^{SON}
121.7	mGlu3 metabotropic glutamate^{SON}	33.08	***GPR61***^{SON}
120.6	***GPR116****^{SON}	31.38	$P2Y_{13}$ purinergic^{SON}
114.2	***GPR108***^{SON}	31.02	CXCR4 chemokine*^{SON}
113.5	***GPR176***^{SON}	30.7	PTH_1 parathyroid hormone*^{SON}
111.8	***GPR68***^{SON}	29.34	κ opioid*^{SON}
109.1	NOP nociceptin*^{SON}	28.36	ET_A endothelin*^{SON}
104.5	SST_1 somatostatin^{SON}	27.42	***GPR153***^{SON}
104.3	***GPR146***^{SON}	26.66	ET_A endothelin*^{SON}
102.9	***GPR19***^{SON}	25.66	$mGlu_7$ metabotropic glutamate^{SON}
102.8	***GPR107***^{SON}	23.82	PTH_1 parathyroid hormone*^{SON}
85.54	$mGlu_8$ metabotropic glutamate*	20.36	NOP nociceptin*^{SON}
85.24	A_{2B} adenosine	17.82	A_3 adenosine
83.78	A_1 adenosine^{SON}	15.96	CXCR3 chemokine^{SON}
82.24	α_{1B} adrenoceptor^{SON}		

Supplementary Table 5. GPCRs noted as present in rat PVN arrays

Comparative levels (arbitary units) of GPCR genes listed as present in the PVN on Affymetrix 230 2.0 rat genome chips as in [115]. Lists of genes that are represented on the Affymetrix array were isolated using the wildcard operator terms 'receptor', 'GPCR', 'GPR' and 'G protein-coupled receptor' and hand-finished. The Tas1r2 (taste R, type I) and Vom2r44 vomeronasal 2 receptors were also detected in the PVN (expression levels of 175 and 18.72, respectively). The pharmacological specificity of the family of calcitonin (CT) receptors and calcitonin receptor-like receptors are dictated by additional proteins known as receptor activity-modifying proteins (RAMPs). These are integral parts of the receptor complex and were detected in the PVN (expression levels of 333.2 and 324 for Ramp1 and Ramp2, respectively). GPCRs also found in the SON (superscript) are indicated. GPR107 and GPR108 appear to have a 7TM structure but show little homology to other GPCRs. Orphan GPCRs are in ***bold italics***. For comparison, OT, VP, β-actin, TRH and CRF were detected at expression levels of 4,090, 3,531, 2801, 614.7 and 282, respectively. * denotes GPCRs with possible spliced transcripts.

Expression level	SON GPCRs	Expression Level	SON GPCRs
1,312	NTS_2 neurotensin	70.88	A_1 adenosine
1,096	ET_B endothelin	70.24	CXCR4 chemokine*
1,006	$GABA_{B1}$* (1f)	68.3	***P2Y5***
857.5	$GABA_{B1}$* (1j)	67.94	α_{1B} adrenoceptor
750.1	S_1P_1 lysophospholipid	61.3	***GPR149***
734.9	***GPR37-like 1***	60.96	FZD_1 frizzled
574.5	***GPRC5b***	59.86	NK_3 tachykinin
521.3	LPA_1 lysophospholipid*	59.24	ET_A endothelin*
499.2	$GABA_{B2}$	56.22	***GPR34***
351	$mGlu_1$ metabotropic glutamate	56.1	SST_1 somatostatin
337.8	PAR1 protease-activated	55.26	***GPR116****
331.4	***GPR37***	54.58	SST_3 somatostatin
308.5	***GPR158***	53.72	CXCR4 chemokine*
285.6	CB_1 cannabinoid	51.7	***GPR88***
249.4	***GPR56***	51.14	PTH_1 parathyroid hormone
246.2	***GPR162***	47.82	***GPR83***
191.3	***GPR116****	42.92	***GPR84***
168	***GPR48***	41.26	***GPR126***
165.3	Calcitonin receptor-like	40.52	$P2Y_{12}$ purinergic
159.2	$mGlu_3$ metabotropic glutamate	37.54	$5\text{-}HT_7$ serotonin
147.9	***GPR107***	34.72	***GPR182***
145.8	***GPR123****	33.4	***GPR61***
136.3	CXCR7	30.62	$GABA_{B1}$* (1g)
129.3	***GPR85***	30.22	CXCR4 chemokine*
126	***GPR108***	29.92	$mGlu_4$ metabotropic glutamate
122.7	***GPR123****	29.68	***GPR116****
118.4	***GPR176***	28.82	ET_A endothelin*
117.1	***GPR19***	27.34	PTH_1 parathyroid hormone*
114.7	***GPR98***	26.64	$P2Y_{13}$ purinergic
113.8	***GPR146***	25.76	κ opioid*
104.3	A_{2B} adenosine	21.76	Y_5 neuropeptide Y
97.52	κ opioid*	20.18	***GPR153***
94.66	CT calcitonin	19.78	$mGlu_7$ metabotropic glutamate
94.36	***GPR68***	19.22	LPA_1 lysophospholipid*
89.88	TRH_1 thyrotrophin releasing factor	19.22	***GPR26***
74.46	NK_1 tachykinin	18.32	CXCR3 chemokine
72.92	NOP nociceptin	15.88	β_2 adrenoceptor

Supplementary Table 6. GPCRs noted as present in rat SON arrays

Comparative levels (arbitary units) of GPCR genes listed as present in the SON on Affymetrix 230 2.0 rat genome chips as in [115]. The GPCR transcripts were isolated as in Supplementary Table 5. Tas1r2 (taste R, type 1) and olfactory receptor Olr414 were also detected at expression levels of 188.2 and 29.4, respectively. Ramps 1 and 2 were detected at expression levels of 358.7 and 388.5, respectively. GPR107 and GPR108 appear to have a 7TM structure but show little homology to other GPCRs. Orphan GPCRs are in ***bold italics***. For comparison, VP, OT and β-actin were detected at expression levels of 4,996, 4,588 and 3014, respectively. * denotes GPCRs with possible spliced transcripts.

Common to PVN and SON	Receptor mRNA by ISHH	Reference
GPR19	-	-
GPR34	-	-
GPR37	-	-
GPR37-like 1	-	-
GPR48	-	-
GPR56	✓*(PVN/SON)	[186] (PVN only); see figure 1 (PVN and SON)
GPR61	✓ (PVN/SON)	[169]
GPR68	-	-
GPR83	x	[272]
GPR85	✓ (PVN/SON)	[210]
GPR88	-	-
GPR98	-	-
GPR101Ψ	✓ (PVN/SON)	[227]
GPR107	-	-
GPR108	✓*(PVN/SON)	see figure 1
GPR116	-	-
GPR123	✓ (PVN/SON)	[165]
GPR125	✓*(PVN+/-SON)	see figure 1
GPR146	✓*(PVN/SON)	see figure 1
GPR149	-	-
GPR153	✓*(PVN/SON)	see figure 1
GPR158	-	-
GPR162	-	-
GPR176	-	-
GPRC5b	-	-
P2Y5	-	-
SON only	-	-
GPR26	-	-
GPR84	-	-
GPR126	-	-
GPR182	-	-

Supplementary Table 7. Orphan GPCRs in the rat PVN & SON

There are 30 orphan GPCR genes expressed in the PVN and/or SON with 26 common to each nuclei. Expression was detected by DNA microarray profiling [115] with the exception of GPR101 (Ψ). Orphan GPCR expression has been confirmed by ISHH in this study (*) or previously published work. x = present in periventricular PVN, and not detected in pPVN, mPVN or SON by ISHH. (-) denotes that orphan GPCR mRNA has not been reported present in the PVN/SON as assayed by ISHH to our knowledge. There are some interesting features of a number of these orphans, e.g., GPR84 is proposed to be a free fatty acid receptor in one study [124] and GPR126 appears to be preferentially expressed in glia [156,276]. GPR107 and GPR108 appear to have a 7TM structure but show little homology to other GPCRs. Orphan GPCR mRNA is clearly expressed in the mouse PVN and/or SON in some instances, e.g., GPR88, 98, 116, 123, 162, 165 and 176 - see Allen Brain Atlas; http://www.brain-map.org/. GPR101 and GPR165 are not represented by probe sets on the Affymetix 230 2.0 rat genome chip used to derive this list [115]. Potential orphan GPCR splice variants are not included in the table.

GPCR	Experimental Conditions	Change in GPCR expression*	Reference
5-HT_{1A}	Daily ip injections of paroxetine, a 5-HT uptake inhibitor (1-14 days).	No effect on 5-HT_{1A} expression (ARG in PVN)	[181]
5-HT_{1B}	Gastric bypass on obese male rats (10 days).	↑ 39% (ir in PVN)	[262]
5-HT_{2A}	Daily ip injections of (-)-1-(2,5-dimethoxy-4-iodophenyl)-2-aminopropane HCl (DOI; 4 or 7 day treatment).	↓ ~50% (ARG in PVN); ↑ 167% (4 days) or ↑ 191% (7 days) (Westerns on PVN tissue); no effect on mRNA (q-PCR on PVN mRNA).	[281]
α_1- and α_2-adrenoceptors	Salt loading (10 days) or adrenalectomy (sacrificed after 14 days).	Salt loading ↓ in α_1 (43%) and α_2 (50%), while adrenalectomy ↓ (45 %) α_2 but has no effect on α_1 (ARG in PVN)	[56]
α_{1B}-adrenoceptor	Adrenalectomy (sacrificed 1, 3, 7 or 14 days), some received sc CORT pellets (sc for 7 days).	↑ mRNA 7 (173%*) or 14 (193%*) days following adrenalectomy; 10 mg CORT prevented adrenalectomy-induced ↑ in mRNA, and 50 mg further ↓ (42%*) mRNA expression (ISHH in PVN). * compared to sham controls.	[59]
Angiotensin AT_1	24 hour isolation stress or sc infusion of candesartan, a non-competitive AT_1 receptor antagonist, for 14 days.	Isolation stress ↑ (~2-fold) receptor binding, an effect inhibited by candesartan pretreatment (ARG in PVN).	[10]
"	2 week sc administration of PD123319 a AT_2 receptor antagonist.	↑ mRNA (~10%) and protein (40-60%) (ISHH and ARG in PVN).	[196]
"	4 week sc infusion of Angiotensin II (with or without concomitant 4 week icv infusions of MAPK inhibitors or losartan (AT_1 receptor antagonist)).	Angiotensin II ↑ (~1.5-2-fold) mRNA and protein (~1.5-2-fold), an effect blocked by losartan, the p44/42 MAPK inhibitor PD-98059, and the JNK inhibitor SP-600125, but not p38 MAPK inhibitor SB-203580 (q-PCR, and Westerns on PVN tissue).	[319]
"	Adrenalectomy, CORT (in drinking water), dexamethasone injection (SC), and various stress paradigms.	~ 20% ↓ mRNA and protein following adrenalectomy (reversed with CORT or dexamethasone); ~ 20% ↑ mRNA and protein following dexamethasone injection in intact rats; immobilization stress ↑ mRNA (49-66%) and protein (~30%) in intact animals; ip salt injection, water deprivation and salt loading also ↑ mRNA and protein in intact animals; stress ↓ (30%) mRNA in adrenalectomized animals (a stress induced CORT surge is required to ↑ mRNA)(ISHH and ARG in PVN).	[1]
"	Coronary artery ligation-induced heart failure	AT_1 protein ↑ in PVN (Western blots of dissected PVN)	[142]
"	Pharmacological model of acute Na^+ depletion (furosemide injections).	Furosemide induces a rapid and long-lasting ↑ (estimated ~3-4-fold) in pPVN AT_{1A} mRNA (ISHH) and angiotensin II binding sites (ARG).	[42]
Apelin APJ	Acute/chronic restraint stress and/or adrenalectomy.	Acute/chronic restraint ↑ mRNA (↑ 240% acute, ↑ 95% chronic) in pPVN of intact rats; adrenalectomy ↑ mRNA in pPVN (by 301%); restraint in adrenalectomized rats could not ↑ mRNA above that of adrenalectomized controls in pPVN; stress had no effect on mRNA in mPVN although adrenalectomy ↑ 111% mRNA (ISHH in PVN).	[231]
"	24-48 hour salt-loading (2% NaCl in drinking water) or dehydration.	Salt-loading and dehydration ↑ APJ mRNA (salt loading ↑ mRNA by 101% in mPVN, 75% in SON; dehydration ↑ mRNA by 874% in mPVN, 455% in SON); salt-loading ↑ colocalisation of APJ mRNA in VP mRNA- containing neurons (by ~12%) within SON but not mPVN, dehydration had no effect on colocalisation in either mPVN or SON (ISHH).	[232]
Cannabinoid CB_1	Chronic treatment (15 days) with SR 141716A (ip) a selective CB_1 receptor antagonist	↑ 10 % (ARG in PVN)	[39]
Chemokine CXCR4	Long Evans and Brattleboro (VP-deficient) rats	ir-CXCR4 ↓ 60% in the PVN/SON of Brattleboro rats, when compared to Long Evans control rats.	[37]
Chemokine CX_3CR1	Induced chronic heart failure	↑ ~34 % in pPVN and ~28% in mPVN (ir in PVN)	S.T. Yao *et al.*, unpublished data
Cholecystokinin CCK_1 and CCK_2	Salt-loading (various durations)	Large ↑ (~8-10-fold) CCK_2 mRNA and protein in PVN and SON; smaller ↑ CCK_1 mRNA (PVN ↑ ~169%; SON ↑ ~355%)/ protein (PVN ↑ 26%; SON ↑ 50%)(ISHH/ARG).	[116,217]

Supplementary Table 8. Examples of GPCR regulation in the PVN/SON

GPCR	Experimental Conditions	Change in GPCR expression*	Reference
Corticotropin-releasing factor CRF_1	Immobilization stress, dehydration, salt-loading (2% NaCl in drinking water for 12 days), adrenalectomy.	↑ (50-76%) mRNA in PVN following acute and chronic immobilization stress; dehydration (24 or 60 hours) and salt-loading ↑ mRNA in PVN and SON; transient ↑ mRNA (4-5-fold) in PVN 18 hours after adrenalectomy in PVN but no ↑ following long-term adrenalectomy (4-6 days)(ISHH).	[190,191]
"	Leptin infusions into third ventricle (5 days) and/or running stress (60 min)	Running stress ↑ mRNA in PVN (↑ ~4-5-fold) and SON (↑ ~4-5-fold), an effect blunted by leptin (ISHH).	[120]
"	0.1 μg CRF microinjection into the PVN.	↑ (~3-fold) mRNA (ISHH in PVN).	[157]
"	Restraint stress (60 min) on virgin, pregnant or lactating female rats	CRF_1 mRNA ↑ in PVN in response to restraint; restraint response is augmented (estimated ~1.2-fold) in lactation when compared with parturition (ISHH).	[58]
Galanin GAL_1 and GAL_2	4 day salt-loading (2% NaCl in drinking water), dehydration and food-deprivation.	Salt-loading and dehydration ↑ GAL_1 mRNA in mainly mPVN and SON (e.g., SON mRNA: ↑ ~143% in salt-loading, and ↑ ~180% in dehydration)(ISHH)) and ↑ total GAL-binding sites (e.g., SON protein ↑ ~120-130% in salt-loading and water deprivation (ARG); food deprivation ↓ GAL_1 mRNA (~30-45%)(ISHH) but not protein (ARG) in the SON. GAL_2 mRNA expression in pPVN or SON did not change following salt-loading, dehydration or food deprivation (ISHH).	[35]
Ghrelin	48 hour fasting.	No effect on receptor protein (ARG in PVN)	[104]
GPR101 (orphan)	Female virgin vs pregnant or lactating rats	↑ mRNA at the end of gestation (↑ ~75%) and during lactation (↑ ~125%) in SON and throughout lactation in pPVN (↑ ~200%) (ISHH).	[227]
Metabotropic glutamate $mGluR_1$ and $mGluR_3$	Stage 5 amygdala kindling (induction of seizures)	↑ mGluR1 and mGluR3 mRNA (28-61%), but only ↑ mGluR1 protein (↑ ~30%)(ISHH and ir in SON).	[6]
Neuropeptide Y Y_1	Salt-loading (2% NaCl in drinking water for 24-72 hours) or dehydration (48 hours)	~2-fold ↑ number of ir-Y_1 positive cells protein in SON following salt-loading or dehydration (IHC); ~2-3-fold ↑ in Y_1 mRNA in SON after salt-loading (ISHH).	[307]
Neuropeptide Y_1 and Y_5	Comparison of young (8-10 months), presenescent (27-30 months) vs. senescent (27-33 months) Fischer rats	Y_1 and Y_5 mRNA ~2-4-fold higher in young versus older animals; no difference in Y_1 and Y_5 mRNA between presenescent and sensescent (q-PCR in PVN), although number of ir-Y_1-expressing PVN neurons ↑ in presenescent compared with young and senescent rats.	[51]
Prostanoid EP_4	iv LPS/IL-1β, icv PGE_2 (500ng), im injection of turpentine.	~2-fold ↑ EP_4 mRNA in pPVN following LPS; IL-1β ↑ EP_4 mRNA in pPVN (but not SON) ~4-6-fold; PGE_2 ↑ pPVN EP_4 mRNA ~2-3-fold; turpentine ↑ EP_4 mRNA ~2-4-fold in pPVN (ISHH).	[236,340,341]
VIP/PACAP PAC_1	Salt-loading (2% NaCl in drinking water for 5 days)	↑ protein (ir in SON)	[91]
Vasopressin/Oxytocin V_{1A}	1 week of reduced or high water intake.	High water intake ↓ (59%), while reduced water intake ↑ (26%) mRNA (ISHH in the SON). Reduced water intake significantly ↑ (35%) protein levels (ir in the SON).	[122]
Vasopressin/Oxytocin OT	Female virgin vs pregnant or ovariectomised (with progesterone or E2 replacement) rats.	OTR mRNA expression ↑ ~1.5 fold in SON (but not PVN) at parturition (ISHH); OTR binding ↑ mid-late gestation in the PVN/SON (0.5-2.5 fold); E2 (but not progesterone) ↑ binding in SON (but not PVN) ~2-2.5 fold in ovariectomized animals (ARG).	[214,20]

Supplementary Table 8. Examples of GPCR regulation in the PVN and SON

* Change in GPCR protein (ARG), immunoreactivity (ir/Western), or mRNA (ISHH/RT-PCR/quantitative (q)-PCR). All studies were performed on male rats unless otherwise stated. icv, intracerebroventricular injection; im, intramuscular; ip, intraperitoneal injection; iv, intravenous injection; mPVN, magnocellular PVN; pPVN, parvoceullar PVN; sc, subcutaneous injection.

GPCR	Role of GPCRs in regulating PVN/SON activity	References
5-Hydroxytryptamine	5-HT_{1A} inhibits water intake; ↓ GABA synaptic transmission in presympathetic PVN neurons; and ↑ plasma OT and ACTH levels. The 5-$HT_{2A/2C}$ receptor agonist, DOI ((±)1-(2,5-dimethoxy-4-iodophenyl)-2 aminopropane), ↑ c-Fos in PVN neurons and plasma OT, prolactin, ACTH and CORT levels. Administration (sc) of 5-HT_{1A} agonist ↑ expression of phosphorylated ERKs in the PVN.	[64,170,242, 172,337,54]
Acetylcholine	Intra-PVN injection of the muscarinic receptor antagonist, or nicotinic receptor antagonist, blocks saline-stimulated ↑ in plasma VP levels. Icv administration of carbachol (muscarinic and nicotinic receptor agonist) stimulates VP release. Muscarine (muscarinic receptor agonist) ↑ the frequency of phasic bursts by VP neurons in the SON *in vitro*. Iv muscarinic agonist arecoline stimulates ACTH and CORT release *in vivo*, and arecoline ↑ CRF secretion in hypothalamic cells *in vitro* (blocked by atropine). Cholinergic stimulation of PVN ↓ body temperature and ↑ water intake, whereas cholinergic stimulation of SON ↑ body temperature (blocked by muscarinic antagonist).	[254,125,89, 38,297]
Adenosine	Application of the selective adenosine A_{2A} receptor agonist depolarizes SON neurons. Adenosine inhibits SON neurons via presynaptic A_1 receptors. Activation of A_1 ↓ firing activity and hyperpolarizes PVN presympathetic neurons.	[251,238,17 9]
Adrenoceptors	α_2-adrenoceptor agonist (ip) ↑ c-Fos expression in OT but not VP neurons. α_1-adrenoceptor agonist (icv) ↑ CRF mRNA in PVN and plasma ACTH release. Noradrenaline excites both phasic and non-phasic firing SON neurons (putative VP and OT cells, respectively). Noradrenaline microinjected into the PVN ↑ pain threshold via local α-adrenoceptors and NMDA receptors. Noradrenaline ↑ frequency of spontaneous glutamatergic excitatory postsynaptic currents (EPSCs) in PVN and SON magnocellular neurons via presynaptic α_1-adrenoceptors > α_2-adrenoceptors. Hypoxia ↑ noradrenaline and CRF release in the PVN and median eminence: Hypoxia-stimulated release of CRF from median eminence is blocked by α_1-adrenoceptor antagonist but facilitated by α_2-adrenoceptor antagonist. α_1-adrenoceptor agonist ↑ the firing rate of spinally projecting PVN neurons (but not in the presence of $GABA_A$ or ionotropic glutamate receptor antagonists), and also ↑ the frequency of spontaneous EPSCs and ↓ the frequency of spontaneous inhibitory postsynaptic currents (IPSCs). Icv noradrenaline augments TRH release from the PVN and median eminence in response to acute hypoxia, via α_2-adrenoceptors. α_2-adrenoceptor agonist ↓ the amplitude of evoked GABAergic IPSCs and ↓ the frequency of GABAergic miniature IPSCs (blocked by α_2-adrenoceptor antagonist) in spinally-projecting PVN neurons. VP release from HNS explants ↑ following exposure to a α_1-adrenoceptor agonist, while simultaneous exposure to ATP and α_1-adrenoceptor agonist induces a synergistic stimulation of sustained VP and OT release, through activation of multiple α_1-subtypes ($\alpha_{1A,B,D}$). Stimulations of α_1-adrenoceptors ↑ intracellular Ca^{2+} in isolated SON explants. Stimulation of α1/α2 receptors modulate spontaneous IPSCs in mPVN and pPVN neurons: α_{2A} ↓ spontaneous IPSCs whereas α_1 (subtype unknown) ↑ spontaneous IPSCs.	[250,152,33 2,342,28,43, 44,118,178, 143,290,291 ,46]
Anaphylatoxin	Ip administration of a C5a antagonist ↓ LPS-induced c-Fos in CRF neurons.	[53]
Angiotensin	Angiotensin II (ATII) activates the intracellular MAPK and JNK signalling pathways in PVN neurons via AT_1. ATII stimulates VP, OT, ACTH secretion (some effects may be indirect via SFO). Activation of central AT_1 receptors is necessary to mount a full HPA axis response to isolation stress: subcutaneous infusion of an AT_1 antagonist inhibits isolated stress mediated ↑ in pituitary ACTH and adrenal CORT content, an effective glucocorticoid feedback inhibition (a ↓ in PVN CRF mRNA and protein), and an ↑ in AT_1 binding (ARG) in pPVN. AII excites SON OT and VP neurons in *ex vivo* preparations. AII microinjected into the PVN ↑ blood pressure, which is blocked by systemic administration of an AT1 receptor antagonist. AII depolarizes mPVN neurons and ↑ frequency of EPSCs/excitatory postsynaptic potentials via glutamate release. AII depolarizes and ↑ frequency of action potential discharge of PVN neurons that innervate in the rostral ventrolateral medulla via AT_1. AII intra-PVN ↑ renal sympathetic nerve activity responses to electrical stimulation: blocked by intra-PVN AT_1 antagonist. AT_1 antisense oligonucleotides into PVN ↓ resting renal sympathetic nerve activity and normalizes enhanced cardiac sympathetic afferent reflex in males rats with chronic heart failure. AII ↑ intracellular Ca^{2+} in SON neurons.	[319,80,10,2 37,13,168,4 0,344,343,2 83]
Apelin	Apelin depolarizes and ↑ axonal action potential firing in VP (but not OT) SON neurons, while ↓ somatodendritic VP release. APJ KO mouse studies suggest apelin stimulates HPA axis activity via both CRF_1 and VP V_{1B} receptors.	[302,225]
Bombesin	Icv (but not iv) gastrin-releasing peptide (BB_2 agonist) ↑ 5-HT in PVN and plasma ACTH and CORT levels. Gastrin-releasing peptide also ↑ CRF release from isolated hypothalami.	[86,85]
Bradykinin	Bradykinin regulates release of noradrenaline from rat hypothalamic slices.	[305]
Calcitonin	Icv adrenomedullin-5 ↑ c-Fos mRNA in PVN & SON OT neurons and ↑ plasma OT levels through central CGRP or AM receptors. Adrenomedullin excites OT but not VP neurons in SON. icv adrenomedullin 2 and adrenomedullin ↑ plasma OT levels (adrenomedullin 2 > adrenomedullin).	[243,306,10 5]
Cannabinoid	Endocannabinoids mediate fast-feedback action of glucocorticoids on PVN CRF release; presynaptic action mediates □-MSH-induced inhibition of OT cells. Endocannabinoids released from SON magnocellular soma/dendrites ↓ glutamate release and postsynaptic spiking.	[66,271,65]
Chemokine	Chemokine stromal cell derived factor 1 SDF-1/CXCL12 (activates CXCR4) icv blocks plasma VP release induced by icv angiotensin or ip injection of NaCl, but has no effect on basal plasma VP levels. Electrophysiological recordings demonstrate that endogenous SDF-1 has no effect on basal plasma VP levels (basal activity not inhibited by a CXCR4 antagonist), though administration of SDF-1 can blunt the autoregulation of VP neurons.	[36]
Cholecystokinin	CCK ↑ OT neuronal activity and OT release, and ↓ VP neuronal activity and VP release.	[106,269]
Corticotropin-releasing factor	Stress induces CRF_1 expression in pPVN and SON. Urocortin 1 (binds CRF_2 with higher affinity than CRF_1) injected into the SON alters behaviour in open-field test (blocked by CRF_2 antagonists). CRF injection into PVN ↑ CRF_1 mRNA expression in pPVN (blocked by CRF antagonist). CRF ↑ CRF_1 mRNA levels in primary hypothalamic neuron cultures. CRF icv ↑ plasma OT, with no effect on plasma VP levels. Urocortin 2 and 3 (CRF_2 agonists) into lateral ventricle ↑ CRF and VP hnRNA in pPVN and plasma CORT levels; effect attenuated by CRF_2 antagonist. Urocortin 3 into PVN ↑ blood pressure, heart rate and renal sympathetic nerve activity (blocked by CRF_2 antagonist). CRF (icv) ↑ c-Fos and CRF mRNA in the pPVN, an effect blocked by a CRF_1 antagonist. CRF_1 antagonist intra-PVN potentiates the feeding induced by intra-PVN NPY (CRF systems in the PVN exert inhibitory control over NPY-induced food intake).	[126,76,157, 34,206,180, 246,109]
Dopamine	Dopamine acts mainly on D_2 and D_4 to ↑ OT-stimulated penile erection. Dopamine ↑ magnocellular neuron excitability: activation of D_4 ↓ the frequency of miniature IPSCs; D_4 activation reduces GABA release in SON - dopamine facilitation of neurohypophysial hormone release partly results from distribution of magnocellular neurons; presynaptic D_4 activation inhibits glutamate neurotransmission onto SON magnocellular neurons (N.B. when deviating from base line activity the modification of both glutamatergic and GABAergic input is essential to allow for phasic or spontaneous firing of VP or OT neurons, respectively). Dopamine D_2 activation ↑ TRH release. D_4 receptor activation ↑ ERK phosphorylation and c-Fos expression in the PVN.	[293,14,12,2 52,177,25]
Endothelin	ET_A agonists ↑, while ET_B agonists ↓ basal VP release.	[264]

Supplementary Table 9. Some functions of GPCRs in the rat PVN/SON

GPCR	Role of GPCRs in regulating PVN/SON activity	References
E2	E2 ↓ 5-HT-stimulated ACTH release via GPER, independent of ERβ. ER amplifies the naloxone-induced ↑ in OT neuron firing rate in morphine-dependent female rats.	[330,266,32]
Formylpeptide	Formylpeptide works concomitantly with annexin to ↓ VP and CRF release.	[135]
$GABA_B$	Activation of $GABA_B$ ↓ the frequency of spontaneous and miniature IPSCs in pPVN.	[187]
Galanin	Galanin ↓ evoked EPSCs and ↓ eEPSC frequency in VP/OT neurons. Administration of galanin (icv) ↓ hypothalamic and neurohypophysial OT, but has no effect on plasma OT or VP levels in euhydrated rats; icv galanin in salt-loaded rats ↑ VP and OT levels within the hypothalamus and neural lobe and ↓ plasma VP and OT levels. Intra-PVN microinjection of galanin ↑ food intake.	[159,49,162]
Ghrelin	Ghrelin injected into PVN ↑ food intake (inhibited by MC_4 agonists). Icv and iv administration of ghrelin ↑ VP plasma levels. Knockdown of Ghsr1a in the PVN ↓ body weight and plasma ghrelin levels. Ghrelin icv ↑ c-Fos in magnocellular and parvocellular PVN OT neurons. Ghrelin (via Ghsr1a) potentiates miniature EPSCs in approximately 80% of SON magnocellular neurons tested. Ghrelin (100nM) ↑ CRF and VP mRNA levels 2-3 fold (maximum response at 6 hours) in hypothalamic 4B cell line.	[285,128,286,239,335,139]
Glucagon	Secretin ↑ VP release from hypothalamus. Icv glucagon-like peptide-1-(7–36)amide (GLP-1) ↑ VP (though not OT) and CORT release, and ↑ c-Fos expression mainly in CRF neurons of the pPVN and OT neurons of the mPVN/SON.	[47,167]
Histamine	Histamine ↑ PVN and plasma OT levels and modulates OT neuronal activity in the SON via H_2 receptors. In HNS explants histamine depolarizes VP neurons via H_1 receptors. Histamine H_2 receptor activation ↑ TRH release from hypothalamic slices. Histamine H_1 and H_2 antagonists prevents suckling-induced OT release in PVN.	[18,107,287,41,19]
Kisspeptin	Kisspeptin injected into PVN augments plasma LH and testosterone levels.	[247]
Leukotriene	Leukotriene B4 (LTB_4) ↑ CRF release from hypothalamic explants in vitro. Icv LTB_4 (via BLT_1) ↑ PVN CRF mRNA/protein and plasma ACTH/CORT levels in ovalbumin-sensitized animals.	[23,338]
Melanin-concentrating hormone	MCH icv or directly into the PVN ↑ ACTH release; MCH ↑ CRF release from hypothalamic explants; intra-PVN injection of MCH ↑ food intake. MCH ↓ basal ACTH release at end of lights-on period.	[146,265,26]
Melanocortin	Icv melanocortin agonist ↑ CRF transcription in PVN and plasma CORT levels. alpha-melanocyte-stimulating hormone (α-MSH) ↑ OT release from SON dendrites and ↓ OT release from neurohypophysial terminals (via MC4). α-MSH ↑ intracellular Ca^{2+} in isolated SON neurons. Adrenoviral shRNA-MC_4 into PVN ↓ food intake and body mass. α-MSH infused over SON *in vivo*, ↑ c-Fos mRNA expression, though has no effect on VP hnRNA or mRNA. MC_4 agonist into PVN ↓ food intake. Melanocortin MC_4 activation ↑ TRH release from hypothalamic slices.	[188,270,87,145,92,148]
Melatonin	Melatonin significantly ↓ VP secretion in HNS explants; ↓ substance P-stimulated OT and VP release *in vitro;* and ↓ VP and OT (but not CRF) release from the hypothalamus *in vitro*.	[137,138,333]
Metabotropic glutamate	Activation of presynaptic group III mGluRs (includes $mGlu_4$,$mGlu_6$, $mGlu_7$,and $mGlu_8$ although distribution studies suggest that only $mGlu_4$and $mGlu_7$ may be present in the SON) ↓ frequency of miniature EPSCs in SON neurons, and ↓ glutamate/GABA release onto SON neurons. Activation of group I mGluRs ($mGlu_1$ and $mGlu_5$: however only mGlu1 has been shown to be in the SON) ↑ glutamate/GABA release onto SON neurons. Group 1 mGlu agonist injected into PVN ↑ lumbar sympathetic nerve activity (blocked by $mGlu_{1/5}$ antagonists).	[29,277,182]
Motilin	Icv motilin ↑ c-Fos in PVN and SON.	[328]
Neuromedin U	100nM neuromedin U (NMU) binding of NMU2 depolarizes 31% of pPVN neurons, but not magnocellular neurons, via enhancement of hyperpolarization-activated inward current; Neuromedin S (icv), an endogenous ligand for NMU2, ↑ c-Fos in OT neurons in PVN and SON, and OT release. Intra-PVN NMU ↓ food intake and ↑ plasma ACTH and CORT levels. NMU ↑ CRF and VP release from hypothalamic explants.	[255,256,273,326]
Neuropeptide FF/neuropeptide AF	Neuropeptide FF (NPFF) facilitates inhibitory input to mPVN via GABAergic interneurons. Hypervolemia or hyperosmolality-induced ↑ in plasma levels of VP are blunted by NPFF (injected into the lateral ventricle), and hyperosmolality-induced plasma VP is significantly augmented by icv NPFF antibodies. Icv NPFF ↑ c-Fos expression mainly in brainstem-projecting pPVN OT neurons, and a few VP and CRF neurons.	[132,9,334,134]
Neuropeptide S	Icv or intra-PVN neuropeptide S ↓ palatable food intake. Intra-PVN injection of neuropeptide S ↑ plasma ACTH and CORT levels, and neuropeptide S ↑ CRF and VP release from HNS explants.	[77,288]
Neuropeptide W/neuropeptide B	Neuropeptide B (icv) induced increase in ACTH is completely blocked by anti-CRF antibodies with no effect on plasma VP/OT levels. Neuropeptide W (icv) stimulated-rise in plasma CORT is prevented by CRF antagonist without effect on plasma VP/OT levels. Neuropeptide W depolarizes and ↑ spike frequency of PVN neurons.	[274,301]
Neuropeptide Y	Stimulation of HNS explants with NPY potentiates the VP and OT response to phenylephrine, but has no effect on basal VP and OT release; however the Y1-agonist, [Leu31,Pro34]-NPY stimulates OT and VP under resting conditions, with no effect on phenylephrine stimulated release, suggesting alternative roles for the neuropeptide receptors . *In vivo* intra-PVN injections of NPY ↑ feeding, and plasma VP and CORT levels in males. Intra- SON administration of NPY ↑ plasma OT levels in lactating females via Y_1 and also ↑ the OT secretory response to α_1-adrenergic receptor stimulation. Icv NPY ↓ PVN pro-TRH mRNA expression. NPY-induced c-Fos in mPVN blocked by Y_1 and Y_5 antagonists; both Y_1 and Y_5 antagonists required to block feeding. Y1 and Y5 agonists delivered in the cerebrospinal fluid ↓ PVN pro-TRH mRNA expression. NPY ↑ CRF release from hypothalamic explants, and ↑ CRF mRNA in the PVN.	[144,174,322,244,78,140,79,304,294]
Neurotensin	Neurotensin (icv) ↑ plasma ACTH and CORT levels (attenuated by CRF antagonist); icv neurotensin ↑ VP but not CRF in median eminence.	[267]
Opioid	Opioids have complex (and contradictory) effects on ACTH and CORT release: acute dose of morphine (ip) ↑ plasma ACTH and CORT levels; chronic morphine administration (ip) ↓ plasma ACTH and CORT levels; and endomorphin 1 and 2 have no effect on the CORT levels. Sc injection of κ or μ agonists (but not δ) strongly inhibit the release of OT and VP, however only μ agonists ↓ release when given icv. Icv nociceptin ↑ plasma ACTH/CORT levels and ↑ pPVN CRF mRNA (no effect on VP mRNA), an effect blocked by a nociceptin antagonist. Microinjection of δ agonist into the PVN ↑ ethanol intake, while κ agonist ↓ alcohol intake. μ-agonist DAMGO ([d-Ala^2,N-Me-Phe^4,Gly^5-ol]-enkephalin) ↓ K^+-induced OT > VP release. Intra-PVN injection of dynorphin ↑ food intake via κ opioid receptor.	[312,52,308,173,16,241,95]
Orexin	Icv orexin-A ↑ pPVN CRF and VP mRNA levels and plasma ACTH and CORT levels. Orexin A ↑ CRF and NPY release, but not VP from isolated hypothalamic explants, an effect blocked by a neuropeptide Y1 antagonist. Orexin-A depolarizes mPVN and pPVN neurons.	[268,82,2]
P2Y	ATP ↑ Ca^{2+} in SON neurons. $P2Y_1$ activation ↑ Ca^{2+} in HNS SON explants (response blocked by $P2Y_1$-selective antagonist); Responses to UTP (most potent at $P2Y_2$/Y_4 receptors) and UDP (most potent agonist for $P2Y_6$) occurred in fewer SON neurons and produced smaller peak amplitude when compared to a $P2Y_1$ stimulated response.	[73,292]
Platelet-activating factor	Platelet-activating factor ↑ CRF release from hypothalamic explants.	[69]
Parathyroid hormone	Icv tuberoinfundibular peptide of 39 residues (TIP39) (the endogenous PTH2 ligand) ↓ VP release in response to dehydration. TIP39 ↑ the release of CRF and VP from *in vitro* hypothalamic explants. Icv TIP39 ↑ basal ACTH release.	[295,316]

GPCR	Role of GPCRs in regulating PVN/SON activity	References
Prokineticin	Prokineticin 2 (PK2) depolarizes the majority of magnocellular neurons, an effect blocked by kynurenic acid (glutamate antagonist), which suggests involvement of glutamate interneurons. On the other hand, PK2 depolarizes the pre-autonomic and neuroendocrine parvocellular neurons through MAPK signalling.	[336]
Prolactin-releasing peptide (GPR10)	Icv prolactin-releasing peptide ↑ plasma ACTH levels (inhibited by CRF antagonist), ↑ c-Fos expression in neurons of the pPVN and mPVN, and ↑ plasma OT and VP levels in female rats, but only plasma OT levels in male rats.	[211,331,207]
Prostanoid	Prostaglandin E_2 (PGE_2) ↑ the firing rate of rat SON neurons an effect mimicked by an EP_4 agonist (but not by EP_1, EP_2, or EP_3 agonists). PGE2 and EP_3 ↓ the frequency of spontaneous IPSCs in the rat SON (EP_1, EP_2, EP_2 or FP agonists had no significant effects on IPSCs). PGE_2 effects on phasic and non-phasic neurons in SON mostly excitatory. EP_4 levels in the PVN are ↑ following iv IL-1β. Icv PGE_2 ↑ plasma CORT levels.	[123,282,341,278]
Relaxin	Icv relaxin ↑ c-Fos expression in VP and OT neurons of PVN and SON, as well as many pPVN neurons. Relaxin-3 ↑ food intake (via RXFP3) when administered intra-PVN or -SON, and water intake when administered icv (via RXFP1?). Relaxin-3 intra-PVN ↑ plasma luteinizing hormone levels.	[213,299]
Somatostatin	Icv somatostatin (SST) ↑ plasma OT levels in virgin and pregnant rats. Icv SST ↑ OT and VP neuron firing rates and c-Fos expression in SON and PVN (which may be mediated in part by SST_2). Retrodialysis of SST onto ventrally exposed SON ↑ VP neuron firing rate but ↓ OT neuron firing rate - this may indicate that the direct effect of SST on SON OT neurons is inhibitory, and may not contribute to enhanced OT release.	[215,93]
Tachykinin	Hydralazine induced hypotension activates NK_3 signalling in magnocellular neurons to release VP and OT. Icv NK_1 antagonist attenuates the duration of plasma ACTH and CORT response to acute restraint stress. Icv NK_1 antagonists ↓ the activation of c-Fos in the PVN, and the cardiovascular (↑ in mean arterial pressure and heart rate) and behavioural reactions (hind limb grooming/biting) in response to noxious stimuli (sc formalin). NK_3 agonist intra-PVN causes hypertension which is blocked by a VP V_1 antagonist. NK_3 agonist ↑ VP release and substance P ↑ VP and OT release from HNS explants.	[103,131,55,17,298,119,144]
Thyrotropin-releasing hormone	Iv TRH appears to ↑ hypothalamic VP content in young male rats, and ↓ hypothalamic OT content in mature male rats.	[48]
Trace amine	Chronic 10 day delivery of β-phenylethylamine (ip) ↑ CRF mRNA in the PVN, CRF immunoreactivity in the median eminence, and plasma ACTH and CORT levels in response to stress.	[158]
Urotensin	Icv urotensin II ↑ c-Fos immunoreactivity in the PVN, heart rate, and plasma glucose and CORT levels.	[317]
VIP and PACAP	Pituitary adenylate cyclise activating polypeptide (PACAP) excites and ↑ firing rate of both phasic and non-phasic neurons; PACAP stimulates local somatodendritic VP release in SON and ↓ basal glutamate and aspartate release. Icv PACAP ↑ c-Fos in rat PVN and SON. PACAP ↑ VP/OT release from isolated neural lobe. Intra-PVN injection of vasoactive intestinal peptide (VIP) ↑ plasma ACTH and CORT levels, an effect attenuated by pre-treatment with the CRF_1 and/or V_1 receptor antagonists. Peptide histidine isoleucine (PHI) via VIP/PACAP receptors ↑ % c-Fos staining neurons in PVN. PHI icv or intra-PVN ↓ food consumption in overnight food-deprived rats. PACAP ↑ intracellular Ca^{2+} in isolated SON neurons.	[283,91,230,193,4,5,240,60]
Vasopressin and oxytocin	VP effects depend on activity of VP neurons; VP neurons with weak phasic or irregular activity are excited by VP, whereas VP neurons with robust phasic activity or continuous activity are inhibited by VP (N.B. most VP neurons do not display phasic activity under basal conditions). OT excites OT and VP neurons but only OT neurons show spike frequency reduction. Ionotropic glutamate receptor antagonists ↓ the effects of OT on firing rate (consistent with presynaptic loci of OT action). V_{1A} antagonists (concomitantly with CRF antagonists) delivered into the PVN ↑ plasma ACTH levels - thus PVN V_{1A} has an inhibitory effect of on VP-induced HPA activity. V_{1A}/V_2 antagonists ↓ osmotically-stimulated intra-SON VP release. OT and VP stimulate the release of OT and VP, respectively from SON *in vitro*. Infusion of lysine VP intra-SON ↑ basal VP release into extracellular fluid. Intra-PVN OT administration ↓ anxiety-related behaviour in male rats, and ↑ ERK phosphorylation in PVN and SON neurons (some expressing VP) which may be linked to the anxiolytic actions of OT. OT and V_{1A} ↑ intracellular Ca^{2+} in isolated SON neurons. OT intra-PVN exerts anxiolytic effects via OT receptor.	[33,315,324,90,189,325,27,166,97,309]

Supplementary Table 9. Some functions of GPCRs in the rat PVN/SON

Abbreviations: ACTH, adrenocorticotropic hormone; CORT, corticosterone; CRF, corticotropin-releasing factor; EPSCs, excitatory postsynaptic currents; HPA, hypothalamic-pituitary-adrenal; HNS, hypothalamo-neurohypophysial system; IPSCs, inhibitory postsynaptic currents; icv, intracerebroventricular injection; ip, intraperitoneal injection; iv, intravenous injection; pPVN, parvocellular region of the paraventricular nucleus; mPVN, magnocellular region of the paraventricular nucleus; OT, oxytocin; sc, subcutaneous injection; VP, vasopressin; TRH, thyrotropin-releasing hormone.

Appendix IV: References for supplementary data

[1] G. Aguilera, A. Kiss, X. Luo, Increased expression of type 1 angiotensin II receptors in the hypothalamic paraventricular nucleus following stress and glucocorticoid administration, J. Neuroendocrinol. 7 (1995) 775-783.

[2] K.A. Al-Barazanji, S. Wislon, J. Baker, D.S. Jessop, M.S. Harbuz, Central orexin-A activates hypothalamic-pituitary-adrenal axis and stimulates hypothalamic corticotropin releasing factor and arginine vasopressin neurones in conscious rats, J. Neuroendocrinol. 13 (2001) 421-424.

[3] M.J. Alexander, S.E. Leeman, Widespread expression in adult rat forebrain of mRNA encoding high-affinity neurotensin receptor, J. Comp. Neurol. 402 (1998) 475-500.

[4] L.D. Alexander, L.D. Sander, Vasoactive intestinal peptide stimulates ACTH and corticosterone release after injection into the PVN, Regul. Pept. 51 (1994) 221-227.

[5] L.D. Alexander, L.D. Sander, Involvement of vasopressin and corticotropin-releasing hormone in VIP- and PHI-induced secretion of ACTH and corticosterone, Neuropeptides 28 (1995) 167-173.

[6] W.M. Al-Ghoul, R.B. Meeker, R.S. Greenwood, Kindled Seizures Increase Metabotropic Glutamate Receptor Expression and Function in the Rat Supraoptic Nucleus. J. Neurosci. Res. 54 (1998) 412–423.

[7] C. Aoki, C.G. Go, C. Venkatesan, H. Kurose, Perikaryal and synaptic localization of alpha 2A-adrenergic receptor-like immunoreactivity, Brain Res. 650 (1994) 181-204.

[8] N.M. Appel, W.M. Mitchell, R.K. Garlick, R.A. Glennon, M. Teitler, E.B. De Souza, Autoradiographic characterization of (±)-1-(2,5-dimethoxy-4-[125I]iodophenyl)-2-aminopropane (125I]DOI binding to 5-HT2 and 5-HT1C receptors in rat brain, J. Pharmacol. Exp. Ther. 255 (1990) 843-857.

[9] H. Arima, T. Murase, K. Kondo, Y. Iwasaki, Y. Oiso, Centrally administered neuropeptide FF inhibits arginine vasopressin release in conscious rats, Endocrinology 137 (1996) 1523-1529.

[10] I. Armando, S. Volpi, G. Aguilera, J.M. Saavedra, Angiotensin II AT_1 receptor blockade prevents the hypothalamic corticotropin-releasing factor response to isolation stress, Brain Res. 1142 (2007) 92-99.

[11] U. Arvidsson, M. Riedl, S. Chakrabarti, L. Vulchanova, J.H. Lee, A.H. Nakano, X. Lin, H.H. Loh, P.Y. Law, M.W. Wessendorf, R. Elde, The κ-opioid receptor is primarily postsynaptic: combined immunohistochemical localization of the receptor and endogenous opioids, Proc. Natl. Acad. Sci. USA 92 (1995) 5062-5066.

[12] K. Azdad, R. Piet, D.A. Poulain, S.H.R. Oliet, Dopamine D4 receptor-mediated presynaptic inhibition of GABAergic transmission in the rat supraoptic nucleus, J. Neurophysiol. 90 (2003) 559-565.

[13] J.S. Bains, A. Potyok, A.V. Ferguson, Angiotensin II actions in paraventricular nucleus: functional evidence for neurotransmitter role in efferents originating in subfornical organ, Brain Res. 599 (1992) 223-229.

[14] D.V. Balmoukhametova, S.A. Hewitt, C.A. Sank, J.S. Bains, Dopamine modulates use-dependent plasticity of inhibitory synapses, J. Neurosci. 24 (2004) 5162-5171.

[15] G. Banisadr, R.D. Gosselin, P. Mechighel, W. Rostène, P. Kitabgi, S. Mélik Parsadaniantz, Constitutive neuronal expression of CCR2 chemokine receptor and its colocalization with neurotransmitters in normal rat brain: functional effect of MCP-1/CCL2 on calcium mobilization in primary cultured neurons, J. Comp. Neurol. 492 (2005) 178-192.

[16] J.R. Barson, A.J. Carr, J.E. Soun, N.C. Sobhani, P. Rada, S.F. Leibowitz, B.G. Hoebel, Opioids in the hypothalamic paraventricular nucleus stimulate ethanol intake, Alcoholism: Clin. Exp. Res. 34 (2010) 1-9.

[17] J. Baulmann, H. Spitznagel, T. Herdegen, T. Unger, J. Culman, Tachykinin receptor inhibition and c-Fos expression in the rat brain following formalin-induced pain. Neuroscience, 95 (2000) 813-820.

[18] S.L. Bealer, W.R. Crowley, Stimulation of central and systemic oxytocin release by histamine in the paraventricular nucleus: evidence for an interaction with norepinephrine, Endocrinology 140 (1999) 1158-1164.

[19] S.L. Bealer, W.R. Crowley, Histaminergic control of oxytocin release in the paraventricular nucleus during lactation in rats, Exp. Neurol. 171 (2001) 317-322.

[20] S.L. Bealer, D.L. Lipschitz, G. Ramoz, W.R. Crowley, Oxytocin receptor binding in the hypothalamus during gestation in rats, Am. J. Physiol. Regul. Integr. Comp. Physiol. 291 (2006) 53-58.

[21] A. Beaudet, D. Greenspun, J. Raelson, G.S. Tannenbaum, Patterns of expression of SSTR1 and SSTR2 somatostatin receptor subtypes in the hypothalamus of the adult rat: relationship to neuroendocrine function, Neuroscience 65 (1995) 551-561.

[22] C. Becskei, T. Riediger, D. Zünd, P. Wookey, T.A. Lutz, Immunohistochemical mapping of calcitonin receptors in the adult rat brain, Brain Res. 1030 (2004) 221-233.

[23] R. Bernardini, A. Chiarenza, A.E. Calogero, P.W. Gold, G.P. Chrousos GP, Arachidonic acid metabolites modulate rat hypothalamic corticotropin-releasing hormone secretion in vitro, Neuroendocrinology 50 (1989) 708-715.

[24] S. Bischoff, S. Leonhard, N. Reymann, V. Schuler, R. Shigemoto, K. Kaupmann, B. Bettler, Spatial distribution of GABA(B)R1 receptor mRNA and binding sites in the rat brain, J. Comp. Neurol. 412 (1999) 1-16.

[25] R.S. Bitner, A.L. Nikkel, S. Otte, B. Martino, E.H. Barlow, P. Bhatia, A.O. Stewart, J.D. Brioni, M.W. Decker, R.B. Moreland, Dopamine D4 receptor signaling in the rat paraventricular hypothalamic nucleus: Evidence of natural coupling involving immediate early gene induction and mitogen activated protein kinase phosphorylation, Neuropharmacology 50 (2006) 521-531.

[26] M.T. Bluet-Pajot, F. Presse, Z. Voko, C. Hoeger, F. Mounier, J. Epelbaum, J.L. Nahon, Neuropeptide-E-I antagonizes the action of melanin-concentrating hormone on stress-induced release of adrenocorticotropin in the rat, J. Neuroendocrinol. 7 (1995) 297-303.

[27] A. Blume, O.J. Bosch, S. Miklos, L. Torner, L. Wales, M. Waldherr, I.D. Neumann, Oxytocin reduces anxiety via ERK1/2 activation: local effect within the rat hypothalamic paraventricular nucleus, Eur. J. Neurosci. 27 (2008) 1947-1956.

[28] C. Boudaba, S. Di, J.G. Tasker, Presynaptic noradrenergic regulation of glutamate inputs to hypothalamic magnocellular neurons, J. Neuroendocrinol. 15 (2003) 803-810.

[29] C. Boudaba, D.M. Linn, K.C. Halmos, J.G. Tasker, Increased tonic activation of presynaptic metabotropic glutamate receptors in the rat supraoptic nucleus following chronic dehydration, J. Physiol. 551 (2003) 815-823.

[30] M.L. Bouthenet, E. Souil, M.P. Martres, P. Sokoloff, B. Giros, J.C. Schwartz, Localization of dopamine D3 receptor mRNA in the rat brain using in situ hybridization histochemistry: comparison with dopmaine D2 receptor mRNA, Brain Res. 564 (1991) 203-219.

[31] E. Brailoiu, S.L. Dun, G.C. Brailoiu, K. Mizuo, L.A. Sklar, T.I. Oprea, E.R. Prossnitz, N.J. Dun, Distribution and characterization of estrogen receptor G protein-coupled receptor 30 in the rat central nervous system, J. Endocrinol. 193 (2007) 311-321.

[32] C.H. Brown, P.J. Brunton, J.A. Russell, Rapid estradiol-17beta modulation of opioid actions on the electrical and secretory activity of rat oxytocin neurons in vivo, Neurochem. Res. 33 (2008) 614-623.
[33] C.H. Brown, V. Scott, M. Ludwig, G. Leng, C.W. Bourque, Somatodendritic dynorphin release: orchestrating activity patterns of vasopressin release, Biochem. Soc. Trans. 35 (2007) 1236-1242.
[34] T.O. Bruhn, S.W. Sutton, P.M. Plotsky, W.W. Vale, Central administration of corticotropin-releasing factor modulates oxytocin secretion in the rat, Endocrinology 119 (1986) 1558-1563.
[35] T.C.D. Burazin, J.A. Larm, A.L. Gundlach, Regulation by osmotic stimuli of galanin-R1 receptor expression in magnocellular neurones of the paraventricular and supraoptic nuclei of the rat, J. Neuroendocrinol. 13 (2001) 358-370.
[36] C. Callewaere, G. Banisadr, M.G. Desarménien, P. Mechighel, P. Kitabgi, W.H. Rostène, S. Mélik Parsadaniantz, The chemokine SDF-1/CXCL12 modulates the firing pattern of vasopressin neurons and counteracts induced vasopressin release through CXCR4, Proc. Natl. Acad. Sci. USA 103 (2006) 8221-8226.
[37] C. Callewaere, B. Fernette, D. Raison, P. Mechighel, A. Burlet, A. Calas, P. Kitabgi, S.M. Parsadaniantz, W. Rostène, Cellular and subcellular evidence for neuronal interaction between the chemokine stromal cell-derived factor-1/CXCL 12 and vasopressin: regulation in the hypothalamo-neurohypophysial system of the Brattleboro rats, Endocrinology 149 (2008) 310-319.
[38] A.E. Calogero, T.C. Kamilaris, M.T. Gomez, E.O. Johnson, M.E. Tartaglia, P.W. Gold, G.P. Chrousos, The muscarinic cholinergic agonist arecoline stimulates the rat hypothalamic-pituitary-adrenal axis through a centrally-mediated corticotropin-releasing hormone-dependent mechanism, Endocrinology 125 (1989) 2445-2453.
[39] M.P. Castelli, A.P. Piras, T. Melis, S. Succu, F. Sanna, M.R. Melis, S. Collu, M.G. Ennas, G. Diaz, K. Mackie, A. Argiolas, Cannabinoid CB1 receptors in the paraventricular nucleus and central control of penile erection: immunocytochemistry, autoradiography and behavioural studies, Neuroscience 147 (2007) 197-206.
[40] M.J. Cato, G.M. Toney, Angiotensin II excites paraventricular nucleus neurons that innervate the rostral ventrolateral medulla: an in vitro patch-clamp study in brain slices, J. Neurophysiol. 93 (2005) 403-413.
[41] J.L. Charli, P. Joseph-Bravo, J.M. Palacios, C. Kordon, Histamine-induced release of thyrotropin releasing hormone from hypothalamic slices, Eur. J. Pharmacol. 52 (1978) 401-403.
[42] G. Charron, S. Laforest, C. Gagnon, G. Drolet, D. Mouginot, Acute sodium deficit triggers plasticity of the brain angiotensin type 1 receptors, FASEB J. 16 (2002) 610-612.
[43] X.Q. Chen, J.Z. Du, Y.S. Wang, Regulation of hypoxia-induced release of corticotropin-releasing factor in the rat hypothalamus by norepinephrine, Regul. Pept. 119 (2004) 221-228.
[44] Q. Chen, D.P. Li, H.L. Pan, Presynaptic α1 adrenergic receptors differentially regulate synaptic glutamate and GABA release to hypothalamic presympathetic neurons, J. Pharmacol. Exp. Therap. 316 (2006) 733-742.
[45] M.Y. Cheng, C.M. Bullock, C. Li, A.G. Lee, J.C. Bermak, J. Belluzzi, D.R. Weaver, F.M. Leslie, Q.Y. Zhou, Prokinectin 2 transmits the behavioural circadian rhythm of the suprachiasmatic nucleus, Nature 417 (2002) 405-410.
[46] W. Chong, L.H. Li, K. Lee, M.H. Lee, J.B. Park, P.D. Ryu, Subtypes of alpha1- and alpha2-adrenoceptors mediating noradrenergic modulation of spontaneous inhibitory postsynaptic currents in the hypothalamic paraventricular nucleus, J. Neuroendocrinol. 16 (2004) 450-457.
[47] J.Y. Chu, L.T Lee, C.H. Lai, H. Vaudry, Y.S. Chan, W.H. Yung, B.K. Chow, Secretin as a neurohypophyseal factor regulating water homeostasis, Proc. Natl. Acad. Sci. USA 106 (2009) 15961-15966.
[48] J. Ciosek, K. Izdebska, Thyrotropin-releasing hormone modulates vasopressin and oxytocin synthesis and release from the hypothalamo-neurohypophysial system of different age male rats. J. Physiol. Pharmacol. 60 (2009) 63-70.
[49] A. Cisowska-Maciejewska, J. Ciosek, Galanin influences vasopressin and oxytocin release from the hypothalamo-neurohypophysial system of salt-loaded rats, J. Physiol. Pharmacol. 56 (2005) 673-688.
[50] J.E. Cluderay, D.C. Harrison, G.J. Hervieu, Protein distribution of the orexin-2 receptor in the rat central nervous system, Regul. Pept. 104 (2002) 131-144.
[51] J.D. Coppola, B.A. Horwitz, J. Hamilton, R.B. McDonald, Expression of NPY Y1 and Y5 receptors in the hypothalamic paraventricular nucleus of aged Fischer 344 rats, Am. J. Physiol. Regul. Integr. Comp. Physiol. 287 (2004) 69-75.
[52] T.L. Coventry, D.S. Jessop, D.P. Finn, M.D. Crabb, H. Kinoshita, M.S. Harbuz, Endomorphins and activation of the hypothalamo-pituitary-adrenal axis, J. Endocrinol. 169 (2001) 185-193.
[53] J.W. Crane, K.M. Buller, Systemic blockade of complement C5a receptors reduces lipopolysacharride-induced responses in the paraventricular nucleus and the central amygdala, Neurosci. Lett. 424 (2007) 10-15.
[54] J.W. Crane, K. Shimizu, G.A. Carrasco, F. Garcia, C. Jia, N.R. Sullivan, D.N. D'Souza, Y. Zhang, L.D. Van de Kar, N.A. Muma, G. Battaglia, 5-HT1A receptors mediate (+)8-OH-DPAT-stimulation of extracellular signal-regulated kinase (MAP kinase) in vivo in rat hypothalamus: time dependence and regional differences, Brain Res. 1183 (2007) 51-59.
[55] J. Culman, S. Klee, C. Ohlendorf, T. Unger, Effect of tachykinin receptor inhibition in the brain on cardiovascular and behavioural responses to stress, J. Pharmacol. Exp. Ther. 280 (1997) 238-246.
[56] S. Cummings, V. Seybold, Relationship of alpha-1 and alpha-2-adrenergic-binding sites to regions of the paraventricular nucleus of the hypothalamus containing corticotrophin-releasing factor and vasopressin neurons, Neuroendocrinology 47 (1988) 523-532.
[57] A. Czyrak, A. Chocyk, M. Maćkowiak, K. Fijał, K. Wedzony, Distribution of dopamine D1 receptors in the nucleus paraventricularis of the hypothalamus in rats: an immunohistochemical study, Brain Res. Mol. Brain Res. 85 (2000) 209-217.
[58] A.P. da Costa, X. Ma, C.D. Ingram, S.L. Lightman, G. Aguilera, Hypothalamic and amygdaloid corticotropin-releasing hormone (CRH) and CRH receptor-1 mRNA expression in the stress-hyporesponsive late pregnant and early lactating rat, Brain Res. Mol. Brain Res. 91 (2001) 119-130.
[59] H.E.W. Day, S. Campeau, S.J. Watson, H. Akil, Expression of α1b adrenoceptor mRNA in corticotropin-releasing hormone-containing cells of the rat hypothalamus and its regulation by corticosterone, J. Neurosci. 19 (1999) 10098-10106.
[60] G. Dayanithi, N. Sabatier, H. Widmer, Intracellular calcium signalling in magnocellular neurones of the rat supraoptic nucleus: understanding the autoregulatory mechanisms, Exp. Physiol. 85 (2000) 75-84.
[61] M.C. Defagot, E.L. Malchiodi, M.J. Villar, M.C. Antonelli, Distribution of D4 dopamine receptor in rat brain with sequence-specific antibodies, Brain Res. Mol. Brain Res. 45 (1997) 1-12.
[62] B. Depczynski, K. Nichol, Z. Fathi, T. Iismaa, J. Shine, A. Cunningham, Distribution and characterization of the cell types expressing GALR2 mRNA in brain and pituitary gland, Ann. N Y Acad. Sci. 863 (1998) 120-128.
[63] E.B. De Souza, T.R. Insel, M.H. Perrin, J. Rivier, W.W. Vale, M.J. Kuhar, Corticotropin-releasing factor receptors are widely distributed within the rat central nervous system: an autoradiographic study, J. Neurosci. 5 (1995) 3189-3203.
[64] P. de Souza Villa, J.V. Menani, G.M. de Arruda Camargo, L.A. de Arruda Camargo, W.A. Saad, Activation of the serotonergic 5-HT1A receptor in the paraventricular nucleus of the hypothalamus inhibits water intake and increases urinary excretion in water-deprived rats, Regul. Pept. 150 (2008) 14-20.

[65] S. Di, C. Boudaba, I.R. Popescu, F.J. Weng, C. Harris, V.L. Marcheselli, N.G. Bazan, J.G. Tasker, Activity-dependent release and actions of endocannabinoids in the rat hypothalamic supraoptic nucleus. J. Physiol 569 (2005) 751-760.
[66] S. Di, R. Malcher-Lopes, K.C. Halmos, J.G. Tasker JG, Nongenomic glucocorticoid inhibition via endocannabinoid release in the hypothalamus: a fast feedback mechanism, J. Neurosci. 23 (2003) 4850-4857.
[67] Y.Q. Ding, B.Z. Lu, Z.L. Guan, D.S. Wang, J.Q. Xu, J.H. Li, Neurokinin B receptor (NK3)-containing neurons in the paraventricular and supraoptic nuclei of the rat hypothalamus synthesize vasopressin and express fos following intravenous injection of hypertonic saline, Neuroscience 91 (1999) 1077-1085.
[68] A.V. Domyancic, D.A. Morilak, Distribution of alpha1A adrenergic receptor mRNA in the rat brain visualized by in situ hybridization, J. Comp. Neurol. 386 (1997) 358-378.
[69] F. Dray, A. Wisner, M.C. Bommelaer-Bayet, C. Tiberghien, K. Gerozissis, M. Saadi, M.P. Junier, C. Rougeot, Prostaglandin E2, leukotriene C4, and platelet-activating factor receptor sites in the brain. Binding parameters and pharmacological studies, Ann. NY Acad. Sci. 559 (1989) 100-111.
[70] Y. Dumont, R. Quirion, [^{125}I]-GR231118: a high affinity radioligand to investigate neuropeptide Y Y1 and Y4 receptors, Br. J. Pharmacol. 129 (2000) 37-46.
[71] M.M. Durkin, C.A. Gunwaldsen, B. Borowsky, K.A. Jones, T.A. Branchek, An in situ hybridization study of the distribution of the GABAB2 mRNA in the rat CNS, Mol. Brain Res. 71 (1999) 185-200.
[72] T. Eguchi, Y. Takano, T. Hatae, R. Saito, Y. Nakayama, Y. Shigeyoshi, H. Okamura, J.E. Krause, H. Kamiya, Antidiuretic action of tachykinin NK-3 receptor in the rat paraventricular nucleus, Brain Res. 743 (1996) 49-55.
[73] J. Espallergues, O. Solovieva, V. Techer, K. Bauer, G. Alonso, A. Vincent, N. Hussy, Synergistic activation of astrocytes by ATP and norepinephrine in the rat supraoptic nucleus, Neuroscience 148 (2007) 712-723.
[74] N.K. Evanson, D.C. Van Hooren, J.P. Herman, GluR5-mediated glutamate signaling regulates hypothalamo-pituitary-adrenocortical stress responses at the paraventricular nucleus and median eminence, Psychoneuroendocrinology 34 (2009)1370-1379.
[75] A. Fassio, G. Evans, R. Grisshammer, J.P. Bolam, M. Mimmack, P.C. Emson, Distribution of the neurotensin receptor NTS1 in the rat CNS studied using an amino-terminal directed antibody, Neuropharmacology 39 (2000) 1430-1442.
[76] A. Fatima, M.F. Haroon, G. Wolf, M. Engelmann, M.G. Spina, Urocortin 1 administered into the hypothalamic supraoptic nucleus affects open-field behaviour in rats, Amino Acids 38 (2010) 1407-1414.
[77] A. Fedelli, S Braconi, D. Economidou, N. Cannella, M. Kallupi, R. Guerrini, C. Calo, M. Massi, R. Ciccocioppo, The paraventricular nucleus of the hypothalamus is a neuroanatomical substrate for the inhibition of palatable food intake by neuropeptide S, Eur. J. Neurosci. 30 (2009) 1594-1602.
[78] C. Fekete, J. Kelly, E. Mihaly, S. Sarkar, W.M. Rand, G. Legradi, C.H. Emerson, R.M. Lechan, Neuropeptide Y has a central inhibitory action on the hypothalamic-pituitary-thyroid axis, Endocrinology 142 (2001) 2602-2613.
[79] C. Fekete, S. Sarkar, W.M. Rand, J.W. Harney, C.H. Emerson, A.C. Bianco, A. Beck-Sickinger, R.M. Lechan, Neuropeptide Y1 and Y5 receptors mediate the effects of neuropeptide Y on the hypothalamic-pituitary-thyroid axis, Endocrinology 143 (2002) 4513-4519.
[80] A.V. Ferguson, Angiotensinergic regulation of autonomic and neuroendocrine outputs: critical roles for the subfornical organ and paraventricular nucleus, Neuroendocrinology 89 (2009) 370-376.
[81] S.O. Fetissov, J. Kopp, T. Hokfelt, Distribution of NPY receptors in the hypothalamus, Neuropeptides 38 (2004) 175-188.
[82] M.J. Follwell, A.V. Ferguson, Cellular mechanisms of orexin actions on paraventricular nucleus neurones in rat hypothalamus, J. Physiol. 545 (2002) 855-867.
[83] R.T. Fremeau, G.E. Duncan, M.G. Fornaretto, A. Dearry, J.A. Gingrich, G.R. Breese, M.G. Caron, Localization of D1 dopamine receptor mRNA in brain supports a role in cognitive, affective, and neuroendocrine aspects of dopaminergic neurotransmission, Proc. Natl. Acad. Sci. USA 88 (1991) 3772-3776.
[84] S. Fukusumi, H. Yoshida, R. Fujii, M. Maruyama, H. Komatsu, Y. Habata, Y. Shintani, S. Hinuma, M. Fujino, A new peptidic ligand and its receptor regulating adrenal function in rats, J. Biol. Chem. 278 (2003) 46387-46395.
[85] M.M. Garrido, J. Manzanares, J.A. Fuentes, Hypothalamus, anterior pituitary and adrenal gland involvement in the activation of adrenocorticotropin and corticosterone secretion by gastrin-releasing peptide, Brain Res. 828 (1999) 20-26.
[86] M.M. Garrido, S. Martin, E. Ambrosio, J.A. Fuentes, J. Manzanares, Role of corticotropin-releasing hormone in gastrin-releasing peptide-mediated regulation of corticotropin and corticosterone secretion in male rats, Neuroendocrinology 68 (1998) 116-122.
[87] J.C. Garza, C.S. Kim, J. Liu, W. Zhang, X.Y. Lu, Adeno-associated virus-mediated knockdown of melanocortin-4 receptor in the paraventricular nucleus of the hypothalamus promotes high-fat diet-induced hyperphagia and obesity, J. Endocrinol. 197 (2008) 471-482.
[88] S.R. George, R.L. Zastawny, R. Briones-Urbina, R. Cheng, T. Nguyen, M. Heiber, A. Kouvelas, A.S Chan, B.F. O'Dowd. Distinct distributions of mu, delta and kappa opioid receptor mRNA in rat brain. Biochim. Biophys. Res. Commun. 205 (1994) 1438-1444.
[89] M. Ghamari-Langroudi, C.W. Bourque, Muscarinic receptor modulation of slow afterhyperpolarization and phasic firing in rat supraoptic nucleus neurons, J. Neurosci. 24 (2004) 7718-7726.
[90] E.R. Gillard, C.G. Coburn, A. de Leon, E.P. Snissarenko, L.G. Bauce, Q.J. Pittman, B. Hou, M.C. Curras-Collazo, Vasopressin autoreceptors and nitric oxide-dependent glutamate release from rat magnocellular neuroendocrine cells responding to osmotic stimuli, Endocrinology 148 (2007) 479-489.
[91] E.R. Gillard, M. Leon-Olea, S. Mucio-Ramirez, C.G. Coburn, E. Sanchez-Islas, A. de Leo, H. Mussenden, L.G. Bauce, Q.J. Pittman, M.C. Curras-Collazo, A novel role for endogenous pituitary adenylate cyclase activating poplypeptide in the magnocellular neuroendocrine system, Endocrinology 147 (2006) 791-803.
[92] S.Q. Giraudo, C.J. Billington, A.S. Levine, Feeding effects of hypothalamic injection of melanocortin 4 receptor ligands, Brain Res. 809 (1998) 302-306.
[93] M. Goebel, A. Stengel, L. Wang, T. Coskun, J. Alsina-Fernandez, J. Rivier, Y. Taché, Pattern of Fos expression in the brain induced by selective activation of somatostatin receptor 2 in rats, Brain Res. 1351 (2010) 150-164.
[94] R. Goke, P.J. Larsen, J.D. Mikkelsen, S.P. Sheikh, Distribution of GLP-1 binding sites in the rat brain: evidence that exendin-4 is a ligand of brain GLP-1 binding sites, Eur. J. Neurosci. 7 (1995) 2294-2300.
[95] B.A. Gosnell, J.E. Morley, A.S. Levine, Opioid-induced feeding: localization of sensitive brain sites, Brain Res. 369 (1986) 177-184.
[96] C. Gouarderes, I. Quelven, C. Mollereau, H. Mazarguil, S.Q. Rice, J.M. Zajac, Quantitative autoradiographic distribution of NPFF1 neuropeptide FF receptor in the rat brain and comparison with NPFF2 receptor by using [125I]YVP and [125I]EYF as selective radioligands, Neuroscience 115 (2002) 349-361.

[97] L. Gouzénes, N. Sabatier, P. Richard, F.C. Moos, G. Dayanithi, V1a- and V2-type vasopressin receptors mediate vasopressin-induced Ca2+ responses in isolated rat supraoptic neurones, J. Physiol. 517 (1999) 771-779.
[98] X.M. Guan, H. Yu, Q. Jiang, L.H. Van Der Ploeg, Q. Liu, Distribution of neuromedin U receptor subtype 2 mRNA in the rat brain, Brain. Res. Gene. Expr. Patterns 1 (2001) 1–4.
[99] X.M. Guan, H. Yu, O.C. Palyha, K.K. McKee, S.D. Feighner, D.J. Sirinathsinghji, R.G. Smith, L.H. Van der Ploeg, A.D. Howard, Distribution of mRNA encoding the growth hormone secretagogue receptor in brain and peripheral tissues, Brain Res. Mol. Brain Res. 48 (1997) 23-29.
[100] A.L. Gundlach, T.C. Burazin, Galanin-galanin receptor systems in the hypothalamic paraventricular and supraoptic nuclei. Some recent findings and future challenges, Ann. NY Acad. Sci. 863 (1998) 241-251.
[101] E.L. Gustafson, M.M Durkin, J.A. Bard, J. Zgombick, T.A. Branchek, A receptor autoradiographic and in situ hybridization analysis of the distribution of the 5-ht7 receptor in rat brain. Br. J. Pharmacol. 117 (1996) 657-666.
[102] G.E. Haley, F.W. Flynn, Agonist and hypertonic saline-induced trafficking of the NK3-receptors on vasopressin neurons within the paraventricular nucleus of the hypothalamus, Am. J. Physiol. Integr. Comp. Physiol. 290 (2006) 1242-1250.
[103] G.E. Haley, F.W. Flynn, Blockade of NK3R signalling in the PVN decreases vasopressin and oxytocin release and c-fos expression in the magnocellular neurons in response to hypotension, Am. J. Physiol. Regul. Integr. Comp. Physiol. 295 (2008) 1158-1167.
[104] J.A. Harrold, T. Dovey, X.J. Cai, J.C. Halford, J. Pinkney, Autoradiographic analysis of ghrelin receptors in the rat hypothalamus, Brain Res. 1196 (2008) 59-64.
[105] H. Hashimoto, S. Hyodo, M. Kawasaki, M. Shibata, T. Saito, H. Suzuki, H. Otsubo, T. Yokoyama, H. Fujihara, T. Higuchi, Y. Takei, Y. Ueta, Adrenomedullin 2 (AM2)/intermedin is a more potent activator of hypothalamic oxytocin-secreting neurons than AM possibly through an unidentified receptor in rats, Peptides 28 (2007) 1104-1112.
[106] H. Hashimoto, T. Onaka, M. Kawasaki, L. Chen, T. Mera, A. Soya, T. Saito, H. Fujihara, H. Sei, Y. Morita, Y. Ueta, Effects of cholecysokinin (CCK)-8 on hypothalamic oxytocin-secreting neurons in rats lacking CCK-A receptor, Auton. Neurosci. 121 (2005) 16-25.
[107] G.I. Hatton, Q.Z. Yang, Ionotropic histamine receptors and H2 receptors modulate supraoptic oxytocin neuronal excitability and dye coupling, J. Neurosci. 21 (2001) 2974-2982.
[108] G.G. Hazell, S.T.Yao, J.A. Roper, E.R. Prossnitz, A-M. O'Carroll, S.J. Lolait, Localisation of GPR30, a novel G protein-coupled oestrogen receptor, suggests multiple functions in rodent brain and peripheral tissues, J. Endocrinol. 202 (2009) 223-236.
[109] S.C. Heinrichs, F. Menzaghi, E.M. Pich, R.L. Hauger, G.F. Koob, Corticotropin-releasing factor in the paraventricular nucleus modulates feeding induced by neuropeptide Y, Brain Res. 611 (1993) 18-24.
[110] L.K. Heisler, N. Pronchuk, K. Nonogaki, L. Zhou, J. Raber, L. Tung, G.S. Yeo, S. O'Rahilly, W.F. Colmers, J.K. Elmquist, L.H. Tecott, Serotonin activates the hypothalamic-pituitary-adrenal axis via serotonin 2C receptor stimulation, J. Neurosci. 27 (2007) 6956-6964.
[111] M. Herkenham, A.B. Lynn, M.R. Johnson, L.S. Melvin, B.R. de Costa, K.C. Rice, Characterization and localization of cannabinoid receptors in rat brain: a quantitative in vivo autoradiographic study, J. Neurosci. 11 (1991) 563-583.
[112] G.J. Hervieu, J.E. Cluderay, D. Harrison, J. Meakin, P. Maycox, S. Nasir, R.A. Leslie, The distribution of the mRNA and protein products of the melanin-concentrating hormone (MCH) receptor gene, slc-1, in the central nervous system of the rat, Eur. J. Neurosci. 12 (2000) 1194-1216.
[113] G.J. Hervieu, J.E. Cluderay, D.C. Harrison, J.C. Roberts, R.A. Leslie, Gene expression and protein distribution of the orexin-1 receptor in the rat brain and spinal cord, Neuroscience 103 (2001) 777-797.
[114] J.M. Hilton, S.Y. Chai, P.M. Sexton, In vitro autoradiographic localization of the calcitonin receptor isoforms, C1a and C1b, in rat brain, Neuroscience 69 (1995) 1223-1237.
[115] C. Hindmarch, S. Yao, G. Beighton, J. Paton, D. Murphy, A comprehensive description of the transcriptome of the hypothalamoneurohypophyseal system in euhydrated and dehydrated rats, Proc. Natl. Acad. Sci. USA 103 (2006) 1609-1614.
[116] G.L. Hinks, J.A. Poat, J. Hughes, Changes in hypothalamic cholecystokinin A and cholecysotkinin B receptor subtypes and associated neuropeptide expression in response to salt-stress in the rat and mouse, Neuroscience 68 (1995) 765-781.
[117] T. Honda, E. Wada, J.F. Battey, S.A Wank, Differential Gene Expression of CCK(A) and CCK(B) Receptors in the Rat Brain, Mol. Cell. Neurosci. 4 (1993) 143-154.
[118] T.D. Hou, J.Z. Du, Norepinephrine attenuates hypoxia-inhibited thyrotropin-releasing hormone release in median eminence and paraventricular nucleus of rat hypothalamus, Neuro. Endocrinol. Lett. 26 (2005) 43-49.
[119] H.E. Howe, S.J. Somponpon, C.D. Sladek, Role of neurokinin 3 receptors in supraoptic vasopressin and oxytocin neurons, J. Neurosci. 24 (2004) 10103-10110.
[120] Q. Huang, E. Timofeeva, D. Richard, Regulation of corticotropin-releasing factor and its types 1 and 2 receptors by leptin in rats subjected to treadmill running-induced stress, J. Endocrinol. 191 (2006) 179-188.
[121] A. Hurbin, L. Boissin-Agasse, H. Orcel, A. Rabié, N. Joux, MG. Desarménien, P. Richard, F.C. Moos, The V1a and V1b, but not V2, vasopressin receptor genes are expressed in the supraoptic nucleus of the rat hypothalamus, and the transcripts are essentially colocalized in the vasopressinergic magnocellular neurons, Endocrinology 139 (1998) 4701-4707.
[122] A. Hurbin, H. Orcel, G. Alonso, F. Moos, A. Rabié, The vasopressin receptors colocalize with vasopressin in the magnocellular neurons of the rat supraoptic nucleus and are modulated by water balance, Endocrinology 143 (2002) 456-466.
[123] N. Ibrahim, I Shibuya, N. Kabashima, S.V. Sutarmo, Y. Ueta, H. Yamashita H, Prostaglandin E2 inhibits spontaneous inhibitory postsynaptic currents in rat supraoptic neurones via presynaptic EP receptors, J. Neuroendocrinol. 11 (1999) 879-886.
[124] A. Ichimura, A. Hirasawa, T. Hara, G. Tsujimoto, Free fatty acid receptors act as nutrient sensors to regulate energy homeostasis, Prostaglandins Other Lipid Mediat. 89 (2009) 82-88.
[125] K. Iitake, L. Share, Y. Ouchi, J.T. Crofton, D.P. Brooks, Central cholinergic control of vasopressin release in conscious rats, Am. J. Physiol. 251 (1986) 146-150.
[126] T. Imaki, H. Katsumata, S.I. Konishi, Y. Kasagi, S. Minami, Corticotropin-releasing factor type-1 receptor mRNA is not induced in mouse hypothalamus by either stress or osmotic stimulation, J Neuroendocrinology 15 (2003) 916-924.
[127] T. Imaki, H. Katsumata, M. Miyata, M. Naruse, J. Imaki, S. Minami, Expression of corticotropin-releasing hormone type 1 receptor in paraventricular nucleus after acute stress, Neuroendocrinology 73 (2001) 293-301.
[128] S. Ishizaki, T. Murase, Y. Sugimura, S. Kakiya, H. Yokoi, K. Tachikawa, H. Arima, Y. Miura, Y. Oiso, Role of ghrelin in the regulation of vasopressin release in conscious rats, Endocrinology 143 (2002) 1589-1593.
[129] S. Jegou, D. Cartier, C. Dubessy, B.J. Gonzalez, D. Chatenet, H. Tostivint, E. Scalbert, J. Leprince, H. Vaudry, I. Lihrmann, Localization of the urotensin II receptor in the rat central nervous system, J. Comp. Neurol. 495 (2006) 21-36.

[130] C.A. Jennings, D.C. Harrison, P.R. Maycox, B. Crook, D. Smart, G.J. Hervieu, The distribution of the orphan bombesin receptor subtype-3 in the rat CNS, Neuroscience 120 (2003) 309-324.
[131] D.S. Jessop, D. Renshaw, P.J. Larsen, H.S. Chowdrey, M.S. Harbuz, Substance P is involved in terminating the hypothalamo-pituitary-adrenal axis response to acute stress through centrally located neurokinin-1 receptors, Stress 3 (2000) 209-220.
[132] J.H. Jhamandas, D. MacTavish, K.H. Harris, Neuropeptide FF (NPFF) control of magnocellular neurosecretory cells of the rat hypothalamic paraventricular nucleus (PVN), Peptides 27 (2006) 973-979.
[133] M. Jhanwar-Uniyal, C.R. Roland, S.F. Leibowitz SF, Diurnal rhythm of alpha 2-noradrenergic receptors in the paraventricular nucleus and other brain areas: relation to circulating corticosterone and feeding behavior, Life Sci. 38 (1986) 473-482.
[134] J.H. Jjamandas, D. MacTavish, Central administration of neuropeptide FF causes activation of oxytocin paraventricular hypothalamic neurones that project to the brainstem, J. Neuroendocrinol. 15 (2003) 24-32.
[135] C.D. John, F.N. Gavins, N.A. Buss, P.O. Cover, J.C. Buckingham. Annexin A1 and the formyl peptide receptor family: neuroendocrine and metabolic aspects. Curr. Opin. Pharmacol. 8 (2008) 765-776.
[136] K.M. Joo, Y.H. Chung, M.K. Kim, R.H. Nam, B.L. Lee, K.H. Lee, C.I. Cha, Distribution of vasoactive intestinal peptide and pituitary adenylate cyclase-aqctivating polypeptide receptors (VPAC1, VPAC2, and PAC1 receptor) in the rat brain, J. Comp. Neurol. 476 (2004) 388-413.
[137] M. Juszczak, E. Boczek-Leszczyk, B. Stempniak, Effect of melatonin on the vasopressin secretion as influenced by tachykinin NK-1 receptor agonist and antagonists: in vivo and in vitro studies, J. Physiol Pharmacol. 58 (2007) 829-843.
[138] M. Juszczak, B. Stempniak, Melatonin inhibits the substance P-induced secretion of vasopressin and oxytocin from the rat hypothalamo-neurohypophysial system: in vitro studies, Brain Res. Bull. 59 (2003) 393-397.
[139] K. Kageyama, Y. Kumata, K. Akimoto, S. Takayasu, N. Tamasawa, T. Suda, Ghrelin stimulates corticotropin-releasing factor and vasopressin gene expression in rat hypothalamic 4B cells, Stress (2011) In press.
[140] S.P. Kalra, P.S. Kalra, NPY and cohorts in regulating appetite, obesity and metabolic syndrome: beneficial effects of gene therapy, Neuropeptides 38 (2004) 201-211.
[141] J. Kampe, P. Wiedmer, P.T. Pfluger, T.R. Castaneda, L. Burget, H. Mondala, J. Kerr, C. Liaw, B.J. Oldfield, M.H. Tschöp, D. Bagnol, Effect of central administration of QRFP(26) peptide on energy balance and characterization of a second QRFP receptor in rat, Brain Res. 1119 (2006) 133-149.
[142] Y.M. Kang, Y. Ma, C. Elks, J.P. Zheng, Z.M. Yang, J. Francis, Cross-talk between cytokines and renin-angiotensin in hypothalamic paraventricular nucleus in heart failure: role of nuclear factor-kappaB, Cardiovasc. Res. 79 (2008) 671-678.
[143] J.R. Kapoor, C.D. Sladek, Purinergic and adrenergic agonists synergize in stimulating vasopressin and oxytocin release, J. Neurosci. 20 (2000) 8868–8875.
[144] J.R. Kapoor, C.D. Sladek, Substance P and NPY differentially potentiate ATP and adrenergic stimulated vasopressin and oxytocin release, Am. J. Physiol. Regul. Integr. Comp. Physiol. 280 (2001) 69-78.
[145] M. Kawasaki, T.A. Ponzio, C. Yue, R.L. Fields, H. Gainer, Neurotransmitter regulation of c-fos and vasopressin gene expression in the rat supraoptic nucleus, Exp. Neurol. 219 (2009) 212-222.
[146] A.R. Kennedy, J.F. Todd, W.S. Dhillo, L.J. Seal, M.A. Ghatei, C.P. O'Toole, M. Jones, D. Witty, K. Winborne, G. Riley, G. Hervieu, S. Wilson, S.R. Bloom, Effect of direct injection of melanin-concentrating hormone into the paraventricular nucleus: further evidence for a stimulatory role in the adrenal axis via SLC-1, J. Neuroendocrinol. 15 (2003) 268-272.
[147] Z.U. Khan, A. Gutiérrez, R. Martín, A. Peñafiel, A. Rivera, A. de la Calle, Dopamine D5 receptors of rat and human brain, Neuroscience 100 (2000) 689-699.
[148] M.S. Kim, C.J. Small, S.H. Russell, D.G. Morgan, C.R. Abbott, S.H. alAhmed, D.L. Hay, M.A. Ghatei, D.M. Smith, S.R. Bloom, Effects of melanocortin receptor ligands on thyrotropin-releasing hormone release: evidence for the differential roles of melanocortin 3 and 4 receptors, J. Neuroendocrinol. 14 (2002) 276-282.
[149] A. Kinoshita, R. Shigemoto, H. Ohishi, H. van der Putten , N. Mizuno, Immunohistochemical localization of metabotropic glutamate receptors, mGlu7a and mGlu7b, in the central nervous system of the adult rat and mouse: a light and electron microscopic study, J. Comp. Neurol. 393 (1998) 332-352.
[150] J.M. Kinzie, J.A. Saugstad, G.L.Westbrook, T.P. Segerson, Distribution of metabotropic glutamate receptor 7 messenger mRNA in the developing and adult rat brain, Neuroscience 69 (1995) 167-176.
[151] T. Kishi, C.J. Aschkenasi, C.E. Lee, K.G. Mountjoy, C.B. Saper, J.K. Elmquist, Expression of melanocortin 4 receptor mRNA in the central nervous system of the rat, J. Comp. Neurol. 457 (2003) 213-235.
[152] A. Kiss, G. Aguilera, Role of alpha-1-adrenergic receptors in the regulation of corticotropin-releasing hormone mRNA in the paraventricular nucleus of the hypothalamus during stress, Cell Mol. Neurobiol. 20 (2000) 683-694.
[153] R.M Kobayashi, M. Palkovits, R.E. Hruska, R. Rothschild, H.I. Yamamura, Regional distribution of muscarinic cholinergic receptors in rat brain, Brain Res. 154 (1978) 13-23.
[154] K. Kocsis, J. Kiss, T. Görcs, B. Halász, Metabotropic glutamate receptor in vasopressin, CRF and VIP hypothalamic neurones, NeuroReport 9 (1998) 4029–4033.
[155] M. Kohzuki, S.Y. Chai, G. Paxinos, A. Karavas, D.J. Casley, C.I. Johnston, F.A. Mendelsohn, Localization and characterization of endothelin receptor binding sites in the rat brain visualized by in vitro autoradiography, Neuroscience 42 (1991) 245-260.
[156] S. Koirala, G. Corfas, Identification of novel glial genes by single-cell transcriptional profiling of Bergmann glial cells from mouse cerebellum, PLoS One 5 (2010) e9198.
[157] S.I. Konishi, Y. Kasagi, H. Katsumata, S. Minami, T. Imaki, Regulation of corticotropin-releasing factor (CRF) type 1 receptor gene expression by CRF in the hypothalamus, Endocr. J. 50 (2003) 21-36.
[158] E. Kosa, A. Marcilhac-Flouriot, M.P. Fache, P. Siaud, Effects of β-phenylethylamine on the hypothalamo-pituitary-adrenal axis in the male rat, Pharmacol. Biochem. Behav. 67 (2000) 527-535.
[159] M.G. Kozoriz, J.B. Kuzmiski, M. Hirasawa, Q.J. Pittman, Galanin modulates neuronal and synaptic properties in the rat supraoptic nucleus in a use and state dependent manner, J. Neurophysiol. 96 (2006) 154-164.
[160] U. Kumar, Colocalization of somatostatin receptor subtypes (SSTR1-5) with somatostatin, NADPH-diaphorase (NADP-d), and tyrosine hydroxylase in the rat hypothalamus, J. Comp. Neurol. 504 (2007) 185-205.
[161] K. Kurokawa, H. Yamada, J. Ochi, Topographical distribution of neurons containing endothelin type A receptor in the rat brain, J. Comp. Neurol. 389 (1997) 348-360.
[162] S.E. Kyrkouli, B.G. Stanley, R.D. Seirafi, S.F. Leibowitz, Stimulation of feeding by galanin: anatomical localization and behavioral specificity of this peptide's effects in the brain, Peptides 11 (1990) 995-1001.
[163] E.E. Ladenheim, R.T. Jensen, S.A. Mantey, T.H. Moran, Distinct distributions of two bombesin receptor subtypes in the rat central nervous system, Brain Res. 593 (1992) 168-178.

[196] M. Macova, J. Pavel, J.M. Saavedra, A peripherally administered, centrally acting angiotensin II AT2 antagonist selectively increases brain AT1 receptors and decreases brain tyrosine hydroxylase transcription, pituitary vasopressin and ACTH, Brain Res. 1250 (2009) 130-140.

[197] H. Maeno, H. Kiyama, M. Tohyama, Distribution of the substance P receptor (NK-1 receptor) in the central nervous system, Brain Res. Mol. Brain Res. 18 (1993) 43-58.

[198] I.G. Makarenko, M.M Meguid, M.V Ugrumov, Distribution of serotonin 5-hydroxytriptamine 1B (5-HT1B) receptors in the normal rat hypothalamus, Neurosci. Lett. 328 (2002) 155–159.

[199] A. Mansour, C.A. Fox, S. Burke, H. Akil, S.J. Watson, Immunohistochemical localization of the cloned μ opioid receptor in the rat CNS, J. Chem. Neuroanat. 8 (1995) 283-305.

[200] A. Mansour, C.A. Fox, S. Burke, F. Meng, R.C. Thompson, H. Akil, S.J. Watson, Mu, delta, and kappa opioid receptor mRNA expression in the rat CNS: an in situ hybridization study. J. Comp. Neurol. 350 (1994) 412-438.

[201] A. Mansour, H. Khachaturian, M.E. Lewis, H. Akil, S.J. Watson, Autoradiographic differentiation of mu, delta, and kappa opioid receptors in the rat forebrain and midbrain, J. Neurosci. 7 (1987) 2445-2464.

[202] J.N. Marcus, C.J. Aschkenasi, C.E. Lee, R.M. Chemelli, C.B. Saper, M. Yanagisawa, J.K. Elmquist, Differential expression of orexin receptors 1 and 2 in the rat brain, J. Comp. Neurol. 435 (2001) 6-25.

[203] M. Margeta-Mitrovic, I. Mitrovic, R.C. Riley, L.Y. Jan, A.I. Basbaum, Immunohistochemical localization of GABA(B) receptors in the rat central nervous system, J. Comp. Neurol. 405 (1999) 299-321.

[204] S.S. Marroni, F.N. Nakano, C.D.C. Gati, J.A.C. Oliveira, J. Antunes-Rodrigues, N. Garcia-Cairasco, Neuroanatomical and cellular substrates of hypergrooming induced by microinjection of oxytocin in central nucleus of amygdala, an experimental model of compulsive behaviour, Mol. Psychiatry. 12 (2007) 1103-1117.

[205] J.L. Martin, M.M. Dieti, P.R. Hof, J.M. Palacios, P.J. Magistretti, Autoradiographic mapping of [mono[125I]iodo-Tyr10, MetO17] vasoactive intestinal peptide binding sites in the rat brain, Neuroscience 23 (1987) 539-565.

[206] H. Maruyama, S. Makino, T. Noguchi, T. Nishioka, K. Hashimoto, Central type 2 corticotropin-releasing hormone receptor mediates hypothalamic-pituitary-adrenocortical axis activation in the rat, Neuroendocrinology 86 (2007) 1-16.

[207] M. Maruyama, H. Matsumoto, K. Fujiwara, J. Noguchi, C. Kitada, S. Hinuma, H. Onda, O. Nishimura, M. Fujino, T. Higuchi, K. Inoue, Central administration of prolactin-releasing peptide stimulates oxytocin release in rats, Neurosci. Lett. 276 (1999) 193-196.

[208] Y. Masuo, T. Ohtaki, Y. Masuda, M. Tsuda, M. Fujino, Binding sites for pituitary adenylate cyclase activating polypeptide (PACAP): comparison with vasoactive intestinal polypeptide (VIP) binding site localization in rat brain sections, Brain Res. 575 (1992) 113-123.

[209] L.A. Matsuda, T.I. Bonner, S.J. Lolait, Localization of cannabinoid receptor mRNA in rat brain, J. Comp. Neurol. 327 (1993) 535-550.

[210] M. Matsumoto, S. Beltaifa, C.S. Weickert, M.M. Herman, T.M. Hyde, R.C. Saunders, B.K. Lipska, D.R. Weinberger, J.E. Kleinman, A conserved mRNA expression of SREB2 (GPR85) in adult human, monkey, and rat forebrain, Brain Res. Mol. Brain Res. 138 (2005) 58-69.

[211] M. Matsumoto, M. Maruyama, J. Noguchi, Y. Horikoshi, K. Fujiwara, C. Kitada, S. Hinuma, H. Onda, O. Nishimura, K. Inoue, M. Fujino, Stimulation of corticotropin-releasing hormone-mediated adrenocorticotropin secretion by central administration of prolactin-releasing peptide in rats, Neurosci. Lett. 285 (2000) 234-238.

[212] Y. Matsuoka, T. Furuyashiki, H. Bito, F. Ushikubi, Y. Tanaka, T. Kobayashi, S. Muro, N. Satoh, T. Kayahara, M. Higashi, A. Mizoguchi, H. Shichi, Y. Fukuda, K. Nakao, S. Narumiya, Impaired adrenocorticotropic hormone response to bacterial endotoxin in mice deficient in prostaglandin E receptor EP1 and EP3 subtypes, Proc. Natl. Acad. Sci. USA 100 (2003) 4132-4137.

[213] M.J. McKinley, P. Burns, L.M. Covill, B.J. Oldfield, J.D. Wade, R.S. Weisinger, G.W. Tregear, Distribution of fos immunoreactivity in the lamina terminalis and hypothalamus induced by centrally administered relaxin in conscious rats, J. Neuroendocrinol. 9 (1997) 431-437.

[214] S.L. Meddle, V.R. Bishop, E. Gkoumassi, F.W. van Leeuwen, A.J Douglas, Dynamic changes in oxytocin receptor expression and activation at parturition in the rat brain, Endocrinology 148 (2007) 5095-5104.

[215] S.L. Meddle, P.M. Bull, G.L. Leng, J.A. Russell, M. Ludwig, Somatostatin actions on rat supraoptic nucleus oxytocin and vasopressin neurons, J. Neuroendocrinol. 22 (2010) 438-445.

[216] A.D. Medhurst, C.A. Jennings, M.J. Robbins, R.P. Davis, C. Ellis, K.Y. Winborn, K.W. Lawrie, G. Hervieu, G. Riley, J.E. Bolaky, N.C. Herrity, P. Murdock, J.G. Darker, Pharmacological and immunohistochemical characterization of the APJ receptor and its endogenous ligand apelin, J. Neurochem. 84 (2003) 1162-1172.

[217] B. Meister, C. Broberger, M.J. Villar, T. Hökfelt, Cholecystokinin B receptor gene expression in hypothalamic neurosecretory neurons after experimental manipulations, Neuroendocrinology 60 (1994) 458-469.

[218] F. Mennicken, C. Hoffert, M. Pelletier, S. Ahmad, D. O'Donnell, Distribution of galanin receptor 3 (GalR3) mRNA in the adult rat central nervous system, J. Chem. Neuroanat. 24 (2002) 257-268.

[219] I. Merchenthaler, M. Lane, P. Shughrue, Distribution of Pre-Pro-Glucagon and Glucagon-Like Peptide-1 Receptor Messenger RNAs in the Rat Central Nervous System, J. Comp. Neurol. 403 (1999) 261-280.

[220] T. Mitsuma, N. Rhue, M. Kayama, Y. Mori, K. Adachi, Y. Yokoi, J. Ping, T. Nogimori, Y. Hirooka, Distribution of calcium sensing receptor in rats: an immunohistochemical study, Endocr. Regul. 33 (1999) 55-59.

[221] S.M. Molineaux, T.M. Jessell, R. Axel, D. Julius, 5-HT1c receptor is a prominent serotonin receptor subtype in the central nervous system, Proc. Natl. Acad. Sci. USA 86 (1989) 6793-6797.

[222] K. Nakamura, T. Kaneko, Y. Yamashita, H. Hasegawa, H. Katoh, M. Negishi, Immunohistochemical localization of prostaglandin EP3 receptor in the rat nervous system, J. Comp. Neurol. 421 (2000) 543-569.

[223] C.R. Neal, A. Mansour, R. Reinscheid, H-P. Nothacker, O. Civelli, H. Akil, S.J. Watson, Opioid receptor-like (ORL) receptor distribution in the rat central nervous system: comparison of OLR1 receptor mRNA expression with 125I[14Tyr]-orphanin FQ binding, J. Comp. Neurol. 412 (1999) 563-605.

[224] L. Negri, R. Lattanzi, E. Giannini, M. De Felice, A. Colucci, P. Melchiorri, Bv8, the amphibian homologue of the mammalian prokineticins, modulates ingestive behaviour in rats, Br. J. Pharmacol. 142 (2004) 181-191.

[225] M.J. Newson, E.M. Roberts, G.R. Pope, S.J. Lolait, A-M. O'Carroll, The effects of apelin on hypothalamic-pituitary-adrenal axis neuroendocrine function are mediated through corticotrophin-releasing factor- and vasopressin-dependent mechanisms, J. Endocrinol. 202 (2009) 123-129.

[226] A. Nicot, A. Berod, D. Gully, W. Rowe, R. Quirion, E.R. de Kloet, W. Rostene, Blockade of neurotensin binding in the rat hypothalamus and of the central action of neurotensin on the hypothalamic-pituitary-adrenal axis with non-peptide receptor antagonists, Neuroendocrinology 59 (1994) 572-578.
[227] K.N. Nilaweera, D. Wilson, L. Bell, J.G. Mercer, P.J. Morgan, P. Barrett, G protein-coupled receptor 101 mRNA expression in supraoptic and paraventricular nuclei in rat hypothalamus is altered by pregnancy and lactation, Brain Res. 1193 (2008) 76-83.
[228] C.M. Niswender, P.J. Conn, Metabotropic glutamate receptors: physiology, pharmacology, and disease, Annu. Rev. Pharmacol. Toxicol. 50 (2010) 295-322.
[229] M. Nomura, Y. Ueta, R. Serino, N. Kabashima, I. Shibuya, H. Yamashita, Pacap type I receptor gene expression in the paraventricular and supraoptic nuclei of rats, NeuroReport 8 (1996) 67-70.
[230] M. Nomura, Y. Ueta, R. Serino, Y. Yamamoto, I. Shibuya, H. Yamashita, Effects of centrally administered pituitary adenylate cyclase-activating polypeptide on c-fos gene expression and heteronuclear RNA for vasopressin in rat paraventricular and supraoptic nuclei, Neuroendocrinology 69 (1999) 167-180.
[231] A-M O'Carroll, A.L. Don, S.J. Lolait, APJ receptor mRNA expression in the rat hypothalamic paraventricular nucleus: regulation by stress and glucocorticoids, J. Neuroendocrinol. 15 (2003) 1095-1101.
[232] A-M O'Carroll, S.J. Lolait, Regulation of rat APJ receptor messenger ribonucleic acid expression in magnocellular neurones of the paraventricular and supraopric nuclei by osmotic stimuli, J. Neuroendocrinol. 15 (2003) 661-666.
[233] A-M. O'Carroll, T.L. Selby, M. Palkovits, S.J. Lolait, Distribution of mRNA encoding B78/apj, the rat homologue of the human APJ receptor, and its endogenous ligand apelin in brain and peripheral tissues, Biochim. Biophys. Acta. 1492 (2000) 72-80.
[234] B.F. O'Dowd, D.K. Lee, W. Huang, T. Nguyen, R. Cheng, Y. Liu, B. Wang, M.C. Gershengorn, S.R. George, TRH-R2 exhibits similar binding and acute signalling but distinct regulation and anatomic distribution compared with TRH-R1, Mol. Endo. 14 (2000) 183-193.
[235] H. Ohishi, R. Shigemoto, S. Nakanishi, N. Mizuno, Distribution of the mRNA for a metabotropic glutamate receptor (mGluR3) in the rat brain: an *in situ* hybridization study, J. Comp. Neurol. 335 (1993) 252-266.
[236] T. Oka, K. Oka, T.E. Scammell, C. Lee, J.F. Kelly, F. Nantel, J.K. Elmquist, C.B. Saper. Relationship of EP1-4 prostaglandin receptors with rat hypothalamic cell groups involved in lipopolysaccharide fever responses. J. Comp. Neurol. 428 (2000) 20-32.
[237] S. Okuya, K. Inenaga, T. Kaneko, H. Yamashita, Angiotensin II sensitive neurons in the supraoptic nucleus, subfornical organ and anteroventral third ventricle of rats in vitro, Brain Res. 402 (1987) 58-67.
[238] S.H. Oliet, D.A. Poulain, Adenosine-induced presynaptic inhibition of IPSCs and EPSCs in rat hypothalamic nucleus neurons, J. Physiol. 520 (1999) 815-825.
[239] P.K. Olszewski, E.M. Bomberg, A. Martell, M.K. Grace, A.S. Levine, Intraventricular ghrelin activates oxytocin neurons: implications in feeding behavior, Neuroreport. 18 (2007) 499-503.
[240] P.K. Olszewski, M.M. Wirth, T.J. Shaw, M.K. Grace, A.S. Levine, Peptides that regulate food intake: effect of peptide histidine isoleucine on consummatory behavior in rats, Am. J. Physiol. Regul. Integr. Comp. Physiol. 284 (2003) 1445-1453.
[241] S.I. Ortiz-Miranda, G. Dayanithi, V. Coccia, E.E. Custer, S. Alphandery, E. Mazuc, S. Treistman, J.R. Lemos, mu-Opioid receptor modulates peptide release from rat neurohypophysial terminals by inhibiting Ca(2+) influx, J. Neuroendocrinol. 15 (2003) 888-894.
[242] P. Osei-Owusu, A. James, J. Crane, K.E. Scrogin, 5-Hydroxytryptamine 1A receptors in the paraventricular nucleus of the hypothalamus mediate oxytocin and adrenocorticotropin hormone release and some behavioral components of the serotonin syndrome, J. Pharmacol. Exp. Ther. 313 (2005) 1324-1330.
[243] H. Otsubo, S. Hyodo, H. Hashimoto, M. Kawasaki, H. Suzuki, T. Saito, T. Ohbuchi, T. Yokoyama, H. Fujihara, T. Matsumoto, Y. Takei, Y. Ueta, Centrally administered adrenomedullin 5 activates oxytocin-secreting neurons in the hypothalamus and elevates plasma oxytocin level in rats, J. Endocrinol. 202 (2009) 237-247.
[244] S.L. Parker, W.R. Crowley, Central stimulation of oxytocin release in the lactating rat: interaction of neuropeptide Y with alpha-1-adrenergic mechanisms, Endocrinology 132 (1993) 658-666.
[245] R.M.C. Parker, H. Herzog, Regional distribution of Y-receptor subtype mRNAs in rat brain, Eur. J. Neurosci. 11 (1999) 1431–1448.
[246] D. Parkes, S. Rivest, S. Lee, C. Rivier, W. Vale W, Corticotropin-releasing factor activates c-fos, NGFI-B, and corticotropin-releasing factor gene expression within the paraventricular nucleus of the rat hypothalamus, Mol. Endo. 7 (1993) 1357-1367.
[247] M. Patterson, K.G. Murphy, E.L. Thompson, S. Patel, M.A. Ghatei, S.R. Bloom, Administration of kisspeptin-54 into discrete regions of the hypothalamus potently increases plasma luteinizing hormone and testosterone in male adult rats, J. Neuroendocrinol. 18 (2006) 349-354.
[248] J. Pfister, C. Spengler, E. Grouzmann, M.K. Raizada, D. Felix, H. Imboden, Intracellular staining of angiotensin receptors in the PVN and SON of the rat, Brain Res. 754 (1997) 307–310.
[249] C. Pillot, A. Heron, V. Cochois, J. Tardivel-Lacombe, X. Ligneau, J.C. Schwartz, J.M. Arrang, A detailed mapping of the histamine H(3) receptor and its gene transcripts in rat brain, Neuroscience 114 (2002) 173-193.
[250] Z. Pirnik, D. Jezova, J.D. Mikkelsen, A. Kiss, Xylazine activates oxytocinergic but not vasopressinergic hypothalamic neurons under normal and hyperosmotic conditions in rats, Neurochem. Int. 47 (2005) 458-465.
[251] T.A. Ponzio, Y-F. Wang, G.I. Hatton, Activation of adenosine A2A receptors alters postsynaptic currents and depolarises neurons of the supraoptic nucleus, Am. J. Physiol. Regul. Integr. Comp. Physiol. 291 (2006) 359-366.
[252] C.J. Price, Q.J. Pittman, Dopamine D4 receptor activation inhibits presynaptically glutamatergic neurotransmission in the rat supraoptic nucleus, J. Neurophysiol. 86 (2001) 1149-1155.
[253] F. Qadri, EC Schwartz, W. Häuser, O. Jöhren, W. Müller-Esterl, P. Dominiak, Kinin B2 receptor localization and expression in the hypothalamo–pituitary–adrenal axis of spontaneously hypertensive rats, Int. Immunopharmacol. 3 (2003) 285–292.
[254] F. Qadri, T. Waldmann, A. Wolf, S. Hohle, W. Rascher, T. Unger, Differential contribution of angiotensinergic and cholinergic receptors in the hypothalamic paraventricular nucleus to osmotically induced AVP release, J. Pharmacol. Exp. Ther. 285 (1998) 1012-1018.
[255] D.L. Qiu, C.P. Chu, T. Shirasaka, T. Nabekura, T. Kunitake, K. Kato, M. Nakazato, T. Katoh, H. Kannan, Neuromedin U depolarises rat hypothalamic paraventricular nucleus neurons in vitro by enhancing I_H channel activity, J. Neurophysiol. 90 (2003) 843-850.
[256] D.L. Qiu, C.P. Chu, H. Tsukino, T. Shirasaka, H. Nakao, K. Kato, T. Kunitake, T. Katoh, H. Kannan, Neuromedin U receptor subtype -2 mRNA and HCN channels mRNA expression NMU-sensitive neurons in rat hypothalamic paraventricular nucleus, Neurosci. Lett. 374 (2005) 69-72.
[257] D.S. Richards, R.M. Villalba, F.J Alvarez, J.E. Stern, Expression of GABAB receptors in magnocellular neurosecretory cells of male, virgin female and lactating rats, J. Neuroendocrinol. 17 (2005) 413-423.

[258] M. Rigby, R. O'Donnell, N.M. Rupniak, Species differences in tachykinin receptor distribution: further evidence that the substance P (NK1) receptor predominates in human brain, J. Comp. Neurol.490 (2005) 335-353.
[259] S.A. Rivkees, S.L. Price, F.C. Zhou, Immunohistochemical detection of A 1 adenosine receptors in rat brain with emphasis; on localization in the hippocampal formation, cerebral cortex, cerebellum, and basal ganglia, Brain Res. 677 (1995) 193-203.
[260] K.V. Rogers, C.K. Dunn, S.C. Hebert, E.M. Brown, Localization of calcium receptor mRNA in the adult rat central nervous system by in situ hybridization, Brain Res. 744 (1997) 47-56.
[261] B.L. Roland, S.W. Sutton, S.J. Wilson, L. Luo, J. Pyati, R. Huvar, M.G. Erlander, T.W. Lovenberg, Anatomical distribution of prolactin-releasing peptide and its receptor suggests additional functions in the central nervous system and periphery, Endocrinology 140 (1999) 5736-5745.
[262] I.V. Romanova, E.J. Ramos, Y. Xu, R. Quinn, C. Chen, Z.M. George, A. Inui, U. Das, M.M Meguid, Neurobiologic Changes in the Hypothalamus Associated with Weight Loss after Gastric Bypass, J. Am. Coll. Surg. 199 (2004) 887-895.
[263] D.L. Rosin, A. Robeva, R.L. Woodward, P.G. Guyenet, J. Linden, Immunohistochemical localization of adenosine A2A receptors in the rat central nervous system, J. Comp. Neurol. 401 (1998) 163-186.
[264] N.F. Rossi, Regulation of vasopressin secretion by ETA and ETB receptors in compartmentalized rat hypothalamo-neurohypophysial explants, Am. J. Physiol. Endocrinol. Metab. 286 (2004) 535-541.
[265] M. Rossi, S.A. Beak, S.J. Choi, C.J. Small, D.G. Morgan, M.A. Ghatei, D.M. Smith, S.R. Bloom, Investigation of the feeding effects of melanin concentrating hormone on food intake – action independent of galanin and the melanocortin receptors, Brain Res. 846 (1999) 164-170.
[266] D.V. Rossi, Y. Dai, P. Thomas, G.A. Carrasco, L.L. DonCarlos, N.A. Muma, Q. Li, Estradiol-induced desensitization of 5-HT1A receptor signaling in the paraventricular nucleus of the hypothalamus is independent of estrogen receptor-beta, Psychoneuroendocrinology 7 (2010) 1023-1033.
[267] W. Rowe, V. Viau, M.J. Meaney, R. Quirion, Stimulation of CRF-mediated ACTH secretion by central administration of neurotensin: evidence for the participation of the paraventricular nucleus, J. Neuroendocrinol. 7 (1995) 109-117.
[268] S.H. Russell, C.J. Small, C.L. Dakin, C.R. Abbott, D.G. Morgan, M.A. Ghatei, S.R. Bloom, The central effects of orexin-A in the hypothalamic-pituitary-adrenal axis in vivo and in vitro in male rats, J. Neuroendocrinol. 13 (2001) 561-566.
[269] N. Sabatier, C.H. Brown, M. Ludwig, G. Leng, Phasic spike patterning in rat supraoptic neurones in vivo and in vitro, J. Physiol. 558 (2004) 161-180.
[270] N. Sabatier, C. Caquineau, G. Dayanithi, P. Bull, A.J. Douglas, X.M. Guan, M. Jiang, L. Van der Ploeg, G. Leng, □-Melanocyte-stimulating hormone stimulates oxytocin release from the dendrites of hypothalamic neurons while inhibiting oxytocin release from their terminals in the neurohypophysis, J. Neurosci. 23 (2003) 10351-10358.
[271] N. Sabatier, G. Leng, Presynaptic action of endocannabinoids mediate □-MSH-induced inhibition of oxytocin cells, Am. J. Physio. Integr. Comp. Physiol. 290 (2006) 577-584.
[272] R. Sah, L.M. Pritchard, N.M. Richtand, R. Ahlbrand, K. Eaton, F.R. Sallee, J.P. Herman, Expression of the glucocorticoid-induced receptor mRNA in rat brain, Neuroscience 133 (2005) 281-292.
[273] T. Sakamoto, K. Mori, M. Miyazato, K. Kangawa, H. Sameshima, K. Nakahara, N. Murakami, Involvement of neuromedin S in the oxytocin release response to suckling stimulus, Biochem. Biophys. Res. Comm. 375 (2008) 49-53.
[274] W.K. Samson, J.R. Baker, C.K. Samson, H. Samson, M.M Taylor, Central neuropeptide B administration activates stress hormone secretion and stimulates feeding in male rats, J. Neuroendocrinol. 16 (2004) 842-849.
[275] S.A. Sands, D.A. Morilak, Expression of alpha1D adrenergic receptor messenger RNA in oxytocin- and corticotropin-releasing hormone-synthesizing neurons in the rat paraventricular nucleus, Neuroscience 91 (1999) 639–649.
[276] K. Sango, H. Yanagisawa, E. Kawakami, S. Takaku, K. Ajiki, K. Watabe, Spontaneously immortalized Schwann cells from adult Fischer rat as a valuable tool for exploring neuron-Schwann cell interactions, J. Neurosci. Res (2011) In Press.
[277] L.A. Schrader, J.G. Tasker, Presynaptic modulation by metabotropic glutamate receptors of excitatory and inhibitory synaptic inputs to hypothalamic magnocellular neurons, J. Neurophysiol. 77 (1997) 527-536.
[278] V.S. Setiadji, I. Shibuya, N. Kabashima, N. Ibrahim, N. Harayama, Y. Ueta, H. Yamashita, Actions of prostaglandin E2 on rat supraoptic neurons, J. Neuroendocrinol. 10 (1998) 927-936.
[279] S.G. Shelat, L.P. Reagan, J.L. King, S.J. Fluharty, L.M. Flanagan-Cato, Analysis of angiotensin type 2 receptors in vasopressinergic neurons and pituitary in the rat, Regul. Pept. 73 (1998) 103-112.
[280] W.J. Sheward, E.M. Lutz, A.J. Harmar, The expression of the calcitonin receptor gene in the brain and pituitary gland of the rat, Neurosci. Lett. 181 (1994) 31-34.
[281] J. Shi, M. Landry, G.A. Carrasco, G. Battaglia, N.A. Muma, Sustained treatment with a 5-HT2A receptor agonist causes functional desensitisation and reductions in agonist-labeled 5-HT2A receptors despite increases in receptor protein levels in rats, Neuropharmacology 55 (2008) 687-692.
[282] I. Shibuya, S.V. Setiadji, N. Ibrahim, N. Harayama, T. Maruyama, Y. Ueta, H. Yamashita, Involvement of postsynaptic EP4 and presynaptic EP3 receptors in actions of prostaglandin E2 in rat supraoptic nucleus, J. Neuroendocrinol. 14 (2002) 64-72.
[283] N. Shibuya, N. Kabashima, K. Tanaka, S. Setiadji, J. Noguchi, N. Harayama, Y. Ueta, H. Yamashita, Patch-clamp analysis of the mechanism of PACAP-induced excitation in rat supraoptic neurons, J. Neuroendocrinol. 10 (1998) 759-768.
[284] R. Shigemoto, S. Nakanishi, N. Mizuno, Distribution of the mRNA for a metabotropic glutamate receptor (mGluR1) in the central nervous system: an in situ hybridization study in adult and developing rat, J. Comp. Neurol. 322 (1992) 121-135.
[285] Y.B. Shrestha, K. Wickwire, S. Giraudo, Action of MT-II on ghrelin-induced feeding in the paraventricular nucleus of the hypothalamus, NeuroReport 15 (2004) 1365-1367.
[286] Y.B. Shrestha, K. Wickwire, S. Giraudo, Effect of reducing ghrelin receptor gene expression on energy balance, Peptides 30 (2009) 1336-1341.
[287] B.N. Smith, W.E. Armstrong, The ionic dependence of the histamine-induced depolarization of vasopressin neurones in the rat supraoptic nucleus, J. Physiol. 495 (1996) 465-478.
[288] K.L. Smith, M. Patterson, W.S. Dhillo, S.R. Patel, N.M Semjonous, J.V. Gardiner, M.A. Ghatei, S.R. Bloom, Neuropeptide S stimulates the hypothalamo-pituitary-adrenal axis and inhibits food intake, Endocrinology 147 (2006) 3510-3518.
[289] Z. Song, D.A. Gomes, W. Stevens, Role of purinergic P2Y1 receptors in regulation of vasopressin and oxytocin secretion, Am. J. Physiol. Regul. Integr. Comp. Physiol. 297 (2009) 478-484.
[290] Z. Song, D.A. Gomes, W. Stevens, C.D. Sladek, Multiple α1 adrenergic receptor subtypes support synergistic stimulation of vasopressin and oxytocin release by ATP and phenylephrine, Am. J. Physiol. Regul. Integr. Comp. Physiol. 299 (2010) 1529-1537.
[291] Z. Song, S. Vijayaraghavan, C.D. Sladek, Simultaneous exposure to ATP and phenylephrine induces a sustained elevation in the intracellular calcium concentration in supraoptic neurons, Am. J. Physiol. Regul. Integr. Comp. Physiol. 291 (2006) 37-45.

[292] Z. Song, S. Vijayaraghavan, C.D. Sladek, ATP increases intracellular calcium in supraoptic neurons by activation of both P2X and P2Y purinergic receptors, Am. J. Physiol. Regul. Integr. Comp. Physiol. 292 (2007) 423-431.
[293] S. Succu, F. Sanna, T. Melis, A. Boi, A. Argiolas, M.R. Melis, Stimulation of dopamine receptors in the paraventricular nucleus of the hypothalamus of male rats induces penile erection and increases extra-cellular dopamine in the nucleus accumbens: involvement of central oxytocin, Neuropharmacology 52 (2007) 1034-1043.
[294] T. Suda, F. Tozawa, I. Iwai, Y. Sato, T. Sumitomo, Y. Nakano, M. Yamada, H. Demura, Neuropeptide Y increases the corticotropin-releasing factor messenger ribonucleic acid level in the rat hypothalamus, Brain Res. Mol. Brain Res. 18 (1993) 311-315.
[295] Y. Sugimura, T. Murase, S. Ishizaki, K. Tachikawa, H. Arima, Y. Miura, T.B. Usdin, Y. Oiso, Centrally administered tuberoinfundibular peptide 39 residues inhibits arginine vasopressin release in conscious rats, Endocrinology 144 (2003) 2791-2796.
[296] S.W. Sutton, P. Bonaventure, C. Kuei, B. Roland, J. Chen, D. Nepomuceno, T.W. Lovenberg, C. Liu, Distribution of G-protein-coupled receptor (GPCR) 135 binding sites and receptor mRNA in the rat brain suggests a role for relaxin-3 in neuroendocrine and sensory processing, Neuroendocrinology 80 (2004) 296-307.
[297] A. Takahashi, H. Ishimaru, Y. Ikarashi, E. Kishi, Y. Maruyama, Opposite regulation of body temperature by cholinergic input to the paraventricular nucleus and supraoptic nucleus in rats, Brain Res. 909 (2001) 102-111.
[298] Y. Takano, Y. Nakayama, T. Matsumoto, R. Saito, H.O. Kamiya, The mechanism of central pressor actions of tachykinin NK-3 receptor in the paraventricular nucleus of the hypothalamus in rats, Regul. Peptides. 46 (1993) 360-363.
[299] M. Tanaka, Relaxin-3/insulin-like peptide 7, a neuropeptide involved in the stress response and food intake, FEBS J. 277 (2010) 4990-4997
[300] J.B. Tatro, M.L. Entwistle, Heterogeneity of brain mealnocortin receptors suggested by diferential ligand binding in situ, Brain Res. 635 (1994) 148-158.
[301] M.M. Taylor, E.A. Yuill, J.R. Baker, C.C. Ferri, A.V. Ferguson, W.K. Samson, Actions of neuropeptide W in paraventricular hypothalamus: implications for the control of stress hormone secretion, Am. J. Physiol. Regul. Integr. Comp. Physiol. 288 (2005) 270-275.
[302] V.A. Tobin, P.M. Bull, S. Arunachalam, A-M. O'Carroll, Y. Ueta, M. Ludwig, The Effects of Apelin on the Electrical Activity of Hypothalamic Magnocellular Vasopressin and Oxytocin Neurons and Somatodendritic Peptide Release, Endocrinology 149 (2008) 6136–6145.
[303] P. Trivedi, H. Yu, D.J. MacNeil, L.H. Van der Ploeg, X.M. Guan, Distribution of orexin receptor mRNA in the rat brain, FEBS Lett. 438 (1998) 71-75.
[304] S. Tsagarakis, L.H. Rees, G.M. Besser, A. Grossman, Neuropeptide-Y stimulates CRF-41 release from rat hypothalami in vitro, Brain Res. 502 (1989) 167-170.
[305] K. Tsuda, S. Tsuda, I. Nishio, Y. Masuyama, M. Goldstein, Synergistic effects of Bay K8644 and bradykinin on norepinephrine release in the hypothalamus of spontaneously hypertensive rats, Clin. Exp. Pharmacol. Physiol. Suppl. 22 (1995) 54-57.
[306] Y. Ueta, R. Serino, I. Shibuya, K. Kitamura, K. Kangawa, J.A. Russell, H. Yamashita, A physiological role for adenomedullin in rats: a potent hypotensive peptide in the hypothalamo-neurohypophysial system, Exp. Physiol. 85 (2000) 163-169.
[307] J.H. Urban, R.J. Leitermann, M.R. DeJoseph, S.J. Somponpun, M.L. Wolak, C.D. Sladek, Influence of Dehydration on the Expression of Neuropeptide Y Y1 Receptors in Hypothalamic Magnocellular Neurons, Endocrinology 147 (2006) 4122–4131.
[308] B.J. Van de Heijning, I. Koehhoek-Van den Herik, T.B. Van Wimersma Greidanus, The opioid receptor subtypes mu and kappa, but not delta, are involved in the control of the vasopressin and oxytocin release in the rat, Eur. J. Pharmacol. 17 (1991) 199-206.
[309] E.H. van den Burg, I.D. Neumann, Bridging the Gap between GPCR activation and behaviour: oxytocin and prolactin signalling in the hypothalamus, J. Mol. Neurosci. 43 (2011) 200-208.
[310] K. Van Pett, V. Viau, J.C. Bittencourt, R.K. Chan, H.Y. Li, C. Arias, G.S. Prins, M. Perrin, W. Vale, P.E. Sawchenko, Distribution of mRNAs encoding CRF receptors in brain and pituitary of rat and mouse, J. Comp. Neurol. 428 (2000) 191-212.
[311] P. Vertongen, S.N. Schiffmann, P. Gourlet, P. Robberecht, Autoradiographic visualization of the receptor subclasses for vasoactive intestinal polypeptide (VIP) in rat brain, Peptides 18 (1997) 1547-1554.
[312] C. Vuong, S.H. Van Uum, L.E. O'Dell, K. Lutfy, T.C. Friedman, The effects of opioids and opioid analogs on animal and human endocrine systems, Endocr. Rev. 31 (2010) 98-132.
[313] E. Wada, J. Way, H. Shapira, K. Kusano, A.M. Lebacq-Verheyden, D. Coy, R. Jensen, J. Battery, cDNA cloning, characterization, and brain region-specific expression of a neuromedin-B-preferring bombesin receptor, Neuron 6 (1991) 421-430.
[314] T. Wang, M. Palkovits, M. Rusnak, E. Mezey, T.B. Usdin, Distribution of parathyroid hormone 2 receptor-like immunoreactivity and messenger mRNA in the rat nervous system, Neuroscience 100 (2000) 629-649.
[315] Y.F. Wang, T.A. Ponzio, G.I. Hatton, Autofeedback effects of progressively rising oxytocin concentrations on supraoptic oxytocin neuronal activity in slices from lactating rats, Am. J. Physiol. Regul. Integr. Comp. Physiol. 290 (2006) 1191-1198.
[316] H.L. Ward, C.J. Small, K.G. Murphy, A.R. Kennedy, M.A. Ghatie, S.R. Bloom, The actions of tuberoinfundibular peptide on the hypothalamo-pituitary axes, Endocrinology 142 (2001) 3451-3456.
[317] A.M. Watson, M.J. McKinley, C.N. May, Effect of central urotensin II on the heart rate, blood pressure and brain fos immunoreactivity in conscious rats, Neuroscience 155 (2008) 241-249.
[318] D.R.Weaver, J.D Deeds, K. Lee, G.V.Segre, Localization of parathyroid hormone-related peptide (PTHrP) and PTH/PTHrP receptor mRNAs in rat brain, Mol. Brain. Res. 28 (1995) 296-310.
[319] S.G. Wei, Y. Yu, Z.H. Zhang, R.B. Felder, Angiotensin II upregulates hypothalamic AT1 receptor expression in rats via the mitogen-activated protein kinase pathway, Am. J. Physiol. Heart Circ. Physiol. 296 (2009) 1425-1433.
[320] D.M. Weiner, A.I. Levey, R.K. Sunahara, H.B. Niznik, B.F. O'Dowd, P. Seeman, M.R. Brann, D1 and D2 dopamine receptor mRNA in rat brain, Proc. Natl. Acad. Sci. USA 88 (1991) 1859-1863.
[321] A.M. Williams, D.A. Morilak, alpha1B adrenoceptors in rat paraventricular nucleus overlap with, but do not mediate, the induction of c-Fos expression by osmotic or restraint stress, Neuroscience 76 (1997) 901-913.
[322] J.O. Willoughby, W.W. Blessing, Neuropeptide Y injected into the supraoptic nucleus causes secretion of vasopressin in the unanesthetized rat, Neurosci. Lett. 75 (1987) 17-22.
[323] M.L. Wolak, M.R. deJoseph, A.D. Cator, A.S. Mokashi, M.S. Brownfield, J.H. Urban, Comparative distribution of neuropeptide Y Y1 and Y5 receptors in the rat brain by using immunohistochemistry, J. Comp. Neurol. 464 (2003) 285-311.
[324] C.T. Wotjak, M. Kubota, G. Liebsch, A. Montkowski, F. Holsboer, I. Neumann, R. Landgraf, Release of vasopressin within the rat paraventricular nucleus in response to emotional stress: a novel mechanism or regulating adrenocorticotropin hormone secretion, J. Neurosci. 16 (1996) 7725-7732.

[325] C.T. Wotjak, M. Ludwig, R. Langraf, Vasopressin facilitates its own release within the rat supraoptic nucleus in vivo, Neuroreport 5 (1994) 1181-1184.
[326] A.M. Wren, C.J. Small, C.R. Abbott, P.H. Jethwa, A.R. Kennedy, K.G. Murphy, S.A. Stanley, A.N. Zollner, M.A. Ghatei and S.R. Bloom, Hypothalamic Actions of Neuromedin U, Endocrinology 143 (2002) 4227-4234.
[327] D.E. Wright, K.B. Seroogy, K.H. Lundgren, B.M. Davis, L. Jennes, Comparative localization of serotonin 1A, 1C, and 2 receptor subtype mRNAs in rat brain, J. Comp. Neurol. 351 (2004) 357-373.
[328] M. Wu, M. Tang, D. Adriaensen, I. Depoortere, T.L. Peeters, J.P. Timmermans, Central, but not peripheral application of motilin increases c-Fos expression in hypothalamic nuclei in the rat brain, Histochem. Cell Biol. 123 (2005) 139-145.
[329] Y.L. Xu, C.M. Gall, V.R. Jackson, O. Civelli, R.K Reinscheid, Distribution of Neuropeptide S Receptor mRNA and Neurochemical Characteristics of Neuropeptide S Expressing Neurons in the Rat Brain, J. Comp. Neurol. 500 (2007) 84-102.
[330] H. Xu, S. Qin, G.A. Carrasco, Y. Dai, E.J. Filardo, E.R. Prossnitz, G. Battaglia, L.L. Doncarlos, N.A. Muma, Extra-nuclear estrogen receptor GPR30 regulates serotonin function in rat hypothalamus, Neuroscience 158 (2009) 1599-1607.
[331] T. Yamada, A. Mochiduki, Y. Sugimoto, Y. Suzuki, K. Itoi, K. Inoue, Prolactin-releasing peptide regulates the cardiovascular system via corticotrophin-releasing hormone, J. Neuroendocrinol. 21 (2009) 586-593.
[332] H. Yamashita, K. Inenaga, H. Kannan, Depolarizing effect of noradrenaline on neurons of the rat supraoptic nucleus in vitro, Brain Res. 405 (1987) 348-352.
[333] S.A. Yasin, A. Costa, G.M. Besser, D. Hucks, A. Grossman, M.L. Forsling, Melatonin and its analogs inhibit the basal and stimulated release of hypothalamic vasopressin and oxytocin in vitro, Endocrinology 132 (1993) 1329-1336.
[334] H. Yokoi, H. Arima, K. Kondo, T. Murase, Y. Iwasaki, H.Y. Yang, Y. Oiso, Antiserum against neuropeptide FF augments vasopressin release in conscious rats, Peptides 19 (1998) 393-395.
[335] T. Yokoyama, T. Saito, T. Ohbuchi, H. Suzuki, H. Otsubo, T. Okamoto,H. Fujihara, T. Nagatomo, Y. Ueta, Ghrelin potentiates miniature excitatory postsynaptic currents in supraoptic magnocellular neurons, J. Neuroendocrinol. 21 (2009) 910-920.
[336] E.A. Yuill, T.D. Hoyda, C.C. Ferri, Q.Y. Zhou, A.V. Ferguson, Prokineticin 2 depolarizes paraventricular nucleus magnocellular and parvocellular neurons, Eur. J. Neurosci. 25 (2007) 425-434.
[337] Y. Zhang, KJ Damjanoska, G.A. Carrasco, B. Dudas, D.N. D'Souza, J. Tetzlaff, F. Garcia, N.R. Hanley, K. Scripathirathan, B.R. Petersen, T.S. Gray, G. Battaglia, N.A. Muma, L.D. Van de Kar, Evidence that 5-HT2A receptors in the hypothalamic paraventricular nucleus mediate neuroendocrine responses to (-)DOI, J. Neurosci. 22 (2002) 9635-9642.
[338] S.J. Zhang, Y.M. Deng, Y.L. Zhu, X.W. Dong, J.X. Jiang, Q.M. Xie, Intracerebroventricular injection of leukotriene B4 attenuates antigen-induced asthmatic response via BLT1 receptor stimulating HPA-axis in sensitized rats, Respir. Res. 11 (2010) 39-47.
[339] Y. Zhang, T.S. Gray, D.N. D'Souza, G.A. Carrasco, K.J. Damjanosk, B. Dudas, F. Garcia, G.M. Zainelli, N.R. Sullivan Hanley, G. Battaglia, N.A. Muma, L.D.Van de Kar, Desensitization of 5-HT1A receptors by 5-HT2A receptors in neuroendocrine neurons in vivo, J. Pharmacol. Exp. Ther. 310 (2004) 59-66.
[340] J Zhang, S. Rivest, Distribution, regulation and colocalization of the genes encoding the EP2- and EP4-PGE2 receptors in the rat brain and neuronal responses to systemic inflammation, Eur. J. Neurosci. 11 (1999) 2651-2668.
[341] J. Zhang, S. Rivest, A functional analysis of EP4 receptor expressing neurons in mediating the action of prostaglandin E2 within specific nuclei of the brain in response to circulating interleukin-1β, J. Neurochem. 74 (2000) 2134-2145.
[342] X.J. Zhou, J. Yang, F.L. Yan, D.X. Wang, X.Y. Li, X.Q. Fan, F. Hao, X.Q. Yan, X.P. Li, H. Li, W.Y. Liu, B.C. Lin, Norepinephrine plays an important role in antinociceptive modulation of hypothalamic paraventricular nucleus in the rat, Int. J. Neurosci. 120 (2010) 428-438.
[343] G.Q. Zhu, L. Gao, Y. Li, K.P. Patel, I. H. Zucker, W. Wang, AT1 receptor mRNA antisense normalizes enhanced cardiac sympathetic afferent reflex in rats with chronic heart failure, Am. J. Physiol. Heart Circ. Physiol. 287 (2004) 1828-1835.
[344] G.Q. Zhu, K.P. Patel, I.H. Zucker, W. Wang, Microinjection of ANG II into paraventricular nucleus enhances cardiac sympathetic afferent reflex in rats, Am. J. Physiol. Heart Circ. Physiol. 282 (2002) 2039-2045.
[345] J.M. Zigman, J.E. Jones, C.E. Lee, C.B. Saper, J.K. Elmquist, Expression of the ghrelin receptor mRNA in the rat and the mouse brain, J. Comp. Neurol. 494 (2006) 528-548.

Appendix V: Published Work and Presentations

Publications

G.G. Hazell, C.C. Hindmarch, G.R. Pope, J.A. Roper, S.L. Lightman, D. Murphy, A.M. O'Carroll, S.J. Lolait, G protein-coupled receptors in the hypothalamic paraventricular and supraoptic nuclei - Serpentine gateways to neuroendocrine homeostasis, Front. Neuroendocrinol. (2011) doi:10.1016/j.yfrne.2011.07.002.

C.C. Hindmarch, M. Fry, P.M. Smith, S.T. Yao, G.G. Hazell, S.J. Lolait, J.F. Paton, A.V. Ferguson, D. Murphy, The transcriptome of the medullary area postrema: The thirsty rat, the hungry rat and the hypertensive rat, Exp. Physiol. 96 (2011) 495-504.

G.G Hazell, S.T. Yao, J.A. Roper, E.R. Prossnitz, A.M. O'Carroll, S.J. Lolait, Localisation of GPR30, a novel G protein-coupled oestrogen receptor, suggests multiple functions in rodent brain and peripheral tissues, J. Endocrinol. 202 (2009) 223-236.

G.G. Hazell, J.A. Roper, A.M. O'Carroll, S.J. Lolait, The effects of oestrogen on oxytocin synthesis and release and oxytocin receptor expression, Handbook of Oxytocin Research: Synthesis, Storage and Release, Actions and Drug Forms, Jastrow H and Feuerbach D, Nova publishers 1st edition (2009) 127-154.

Oral communications

Winter Neuropeptide Conference, Colorado, Jan 2009: "The novel G protein-coupled oestrogen receptor GPR30 in neuroendocrine systems."

The Dorothy Hodgkin building Brambles seminar, University of Bristol. Feb 2009: "GPR30, a G-coupled oestrogen receptor."

Poster presentations

Poster presented at the British Society for Neuroendocrinology meeting Bristol, Sep 2008: "GRP30 a novel G protein-coupled oestrogen receptor is present in the hypothalamic paraventricular and supraoptic nuclei, and multiple peripheral tissues."

Poster presented at the North and South Bristol Clinical Sciences PhD day, Dec 2009: "Localisation of GPER, a novel G protein-coupled oestrogen receptor, suggests multiple functions in rodent brain and peripheral tissues."